COMPILATION REPORT

on the

WILLIAMS SOUTH PROJECT

in the CARMACKS COPPER-GOLD BELT,

Yukon Territory

WS 1 – 82	YC53521 - 602
WS 83 – 156	YC53748 - 821
WS 157 – 196	YC53993 - 4032
WS 197 – 208	YC91789 - Y800
BC 35 – 50, 65 – 144	YC60218 - 233, 248 - 327
ICE 1 – 41	YC46784 - 87, YC54407 - 443
SLEEP 13 – 18	YC60134 - YC60139

NTS: 115I/7

UTM NAD 83 Zone 8: 416500m E and 6912000m N

Latitude 62°19'N Longitude 136°38'W

Whitehorse Mining District

Work completed between January 2 and 20, 2016
Site visits on September 27 and 29, 2015

For
BCGold Corp.
Suite 520 - 800 West Pender St.
Vancouver, British Columbia
Canada V6C

By:
Jean Pautler, P.Geo.
JP Exploration Services Inc.
#103-108 Elliott Street
Whitehorse, Yukon
Y1A 6C4

January 20, 2016

1.0 Executive Summary

The 7300 hectare Williams South Project, NTS map sheet 115I/7, is located within the Yukon Plateau, approximately 32 km northwest of Carmacks, which is 175 km by paved highway north of Whitehorse, Yukon Territory. The property is situated in the Whitehorse Mining District centered at a latitude of 62°19'N and a longitude of 136°38'W. Road access exists to the property via the Freegold and Williams Creek roads. The Williams South Project comprises 351 claims (the WS, BC, ICE, and SLEEP) registered to BCGold Corp., which owns 100% of the Project and funded the January 2016 program, the subject of this report. This report is a compilation, integration and summary of all work conducted by BCGold Corp. on the Williams South Project in order to document and make recommendations for the next stage of exploration.

The Williams South Project lies within the southern portion of the Carmacks copper-gold belt, a 180 km by 60 km-wide north-northwest trending mineralized belt of similar intrusion-hosted copper-gold mineralization. The belt includes the Carmacks Copper deposit (Williams Creek) of Copper North Mining Corp. (3-10 km northwest of the Williams South Project), the Minto Mine of Capstone Mining Corporation (45 km to the northwest), and the STU drilled prospect (15 km northwest), all hosted by Minto suite plutonic rocks of the Granite Mountain Batholith. Carmacks Copper contains a resource (to NI 43-101 standards) of 12.0 million tonnes of copper oxide ore grading 1.07% Cu (0.86% oxide Cu), 0.46 g/t Au and 4.6 g/t Ag, using a cutoff grade of 0.25% Cu *(Huss et al., 2012).* Minto is a 3,850 tonne per day copper-gold-silver mine, in production since 2007 *(www.capstonemining.com)*. The above reserve and resource information has not been verified by the author and is not necessarily indicative of the mineralization on the Williams South Project which is the subject of this report.

The Williams South Project is primarily underlain by Early Jurassic intrusive rocks of the Granite Mountain Batholith (Minto suite) which intrude the Paleozoic metamorphic basement rocks of the Yukon-Tanana terrane, and locally volcanic rocks of the Povoas Formation of Stikinia to the east, and are overlain by younger volcanic rocks, and intruded by related dykes, of the Late Cretaceous Carmacks Group. Foliated biotite ±hornblende granodiorite occurs in a 0.5 by 4 km northwest trending band across the WS grid from the north end of Merrice Lake to the northwest property boundary, and as a northeasterly (?) 150m by 1 km band at the BCIce showing; the latter particularly limited by poor exposure. Mineralization within the Carmacks copper-gold belt is associated with more foliated to gneissic zones within the batholith. The granodiorite is unconformably overlain by minor younger basalt flows of the Cretaceous Carmacks Group.

The deposit model for the Carmacks copper-gold belt is controversial and has ranged from digested red-bed copper, to aborted and deformed porphyry, to iron oxide copper gold. The author believes the deposit model to be consistent with that of a calc-alkaline porphyry copper-gold model such as at the Kemess Mine and the Kemess North deposit in central British Columbia, but formed at deeper crustal levels.

There are three Minfile occurrences within the Williams South Project; Bishi (now moved and renamed BCIce), Taslar (now moved and renamed WS), and Merrice, as documented by the Yukon Geological Survey *(Deklerk, 2009)*. The Bishi and Taslar were staked in the

early 1970's on aeromagnetic anomalies, but no mineralization was found. The Merrice showing covers copper bearing quartz veins of probable orogenic type. The BCIce showing was originally discovered by United Keno Hill Mines Ltd. in1982, consisting of two zones of copper oxide mineralization in foliated granodiorite, but was not followed up. The WS showing covers significant mineralization intersected in drilling, and other showings and anomalies, discovered by BCGold Corp. on the WS grid, which covers the strike extension of mineralized zones on the adjoining Carmacks Copper Project.

Exploration by BCGold Corp. since the granting of the option from Shawn Ryan in March, 2007 has involved a property wide airborne magnetic and radiometric geophysical survey, approximately 3,551 MMI and 317 conventional grid soil samples from 5 grids, 62.4 line km of induced polarization geophysics from 3 grid areas, a 1.26 km high resolution multi-array induced polarization survey, property wide geological mapping and prospecting with concurrent geochemical sampling, a structural analysis, a 660 sample biogeochemical survey, trenching on BCIce, WS and Copper Hill showings, 2,659m of diamond drilling in 14 holes (2 holes totaling 67.7m were lost and re-drilled), and infrared spectroscopy and petrography on the 2008 drill core.

BCGold's drill program intersected 0.17% Cu over 63.1m in drill hole WS08-09B, 1 km along strike from Copper North's Zone 14; Zone 14 returned 0.23% Cu over 79.7m in hole WC07-141 *(Western Copper news release November 22, 2007)*. Trend appears to be northwest, dipping 25 to 45°NE. This intersection has not been followed up along strike or down dip. WS-08-08 intersected a copper anomalous interval of 0.04% Cu over 25m, including two narrow zones of mineralization (0.10% Cu over 3.9m and 0.12% Cu over 2.0m), which could reflect proximity to the strike extent of Copper North's Zone 12. An infrared spectrographic survey of WS-08-11 (500m southwest of WS-08-08 but drilled to the northeast, sub-parallel to the dip of most mineralization in the area) displays a continuous chlorite spectral signature at the bottom, suggesting it may represent a halo to mineralization *(Fonseca, 2009a)*. Consequently there is good potential to intersect the extension of Copper North's Zone 12 between drill holes WS-08-08 and -11. In addition a coincident VLF-electromagnetic conductor and a strong copper-silver-nickel-tungsten biogeochemical anomaly occur between drill holes WS-08-08 and -11, with a proximal induced polarization chargeability high to the west.

WS-07-07 intersected a series of weakly mineralized zones of copper oxide mineralization throughout the entire hole length, with limited sampling returning 0.67% Cu over 1.0m, 0.38% Cu over 1.2m and 0.20% Cu over 4.0m. The presence of malachite throughout the hole suggests proximity to the possible strike extensions of Copper North's Zone 12. Grab samples from a trench about 300m northwest of the collar of WS-07-07 returned 0.71, 1.87 and 2.83% Cu and coincide with a 700m long, northwest trending VLF-electromagnetic conductor, which is open to the north and coincident with a strong tungsten-antimony-cerium-chromium and weak copper-molybdenum-nickel-silver biogeochemical anomaly. These lie uphill and just west of a significant copper MMI soil anomaly and the three 2007 WS holes, including WS-07-07. To the north the VLF-electromagnetic conductor merges with an induced polarization chargeability trend which extends for a further 4.5 km to the northwest. The anomalies lie along the margins of a northwest trending aeromagnetic vertical gradient high anomaly, which is characteristic of mineralization within the Carmacks Copper camp.

Copper oxide mineralization is exposed at the BCIce showing, seven km southwest of mineralized zones at the Carmacks Copper deposit. The main zone (ICE) covers a discontinuously exposed 20m x 100m zone of moderately foliated granodiorite with malachite trending 294°/20°NE. Chip samples from the ICE zone returned 0.48% Cu over 0.8m, 0.45% Cu over 0.85m and 0.30% Cu over 2.0m. A similar zone occurs 200m south-southwest of the ICE with 0.39% Cu and 0.38 ppb Au in a grab sample. Anomalous soil samples (maximum 935 ppm Cu) occur 200m further to the southwest.

Drilling of the ICE zone encountered two narrow, relatively flat-lying mineralized horizons in ICE 07-2 and -4. The upper and lower horizons returned 0.48% Cu over 4.8m and 0.15% Cu over 3.7m in ICE 07-2 and 0.39% Cu over 5.5m and 0.25% Cu over 0.7m in ICE 07-4, respectively. This style of mineralization commonly occurs distal to larger zones so may have potential along strike or down dip to the northeast. ICE 07-1, 400m west-northwest of the ICE zone, intersected anomalous mineralization, with 0.04% Cu over 24.4m, despite being drilled along, as opposed to perpendicular to, the mineralized trend.

Mineralized intervals in drilling are commonly associated with enhanced gold with a maximum of 190 ppb Au from ICE-07-04. In a study of the 2008 core *(Fonseca, 2009a)* an enrichment in calcium, iron, molybdenum, thallium, tellurium, mafic-associated elements (magnesium, nickel, cobalt), tin, and sphalerite associated elements (zinc, selenium, cadmium, vanadium) was noted. The elements potassium, sodium, lanthanum, and cerium were found to be enriched in the footwall and hangingwall of mineralized zones, suggesting that ore associated mineral alteration assemblage immediately outside ore zones may be propylitic, and possibly overprinting potassic.

Other untested copper showings occur on the Williams South Project, as well as numerous geophysical and geochemical anomalies. The 20m by 5m Copper Hill showing, on the southwestern WS grid approximately 2.5 km southeast generally along trend of Zones 5, 6 and 8 of the Carmacks Copper Project, consists of copper oxides and chalcocite mineralization with values of 0.85% Cu and 0.42 g/t Au from a grab sample, 0.19% Cu and 0.08 g/t Au across 1.5m and 0.4% Cu over 0.5m. A 600m by generally 100m wide copper MMI soil anomaly lies 150m upslope of the showing coincident with an induced polarization chargeability high – resistivity anomaly. The Copper Float showing consists of a malachite stained foliated granodiorite float boulder on the WS grid, which returned 0.94% Cu and 0.26 g/t Au. The float appears isolated but generally occurs within an area of poor exposure with some exposures of foliated granodiorite, approximately 2 km southeast along trend of Zones 12-13 of the Carmacks Copper Project.

The Williams South Project constitutes a property of merit based on significant drill intercepts from limited drilling, the presence of untested copper showings, northwest trending induced polarization chargeabilty, VLF-electromagnetic, ± proximal copper MMI soil anomalies, in part underlain by foliated to gneissic granodiorite, coincident with the margins of linear magnetic high features, similar to and directly along trend from the adjoining Carmacks Copper Project of Copper North Mining Corporation.

A seven hole, 2,400m diamond drill program is recommended on the Williams South Project to follow up on the significant drill intercept in DDH WS-08-9B and to test coincident geophysical and geochemical anomalies, with preliminary groundtruthing of proposed drill sites, examination of the WS trenches and about 40 line km of detailed magnetic surveying proposed prior to drilling. The program is expected to cost $1,000,000.

Table of Contents

Page

1.0 Executive Summary.....i
2.0 Introduction And Terms of Reference 1
2.1 Qualified Person and Participating Personnel..... 1
2.2 Terms, Definitions and Units 2
2.3 Source Documents..... 2
2.4 Limitations, Restrictions and Assumptions..... 3
3.0 Reliance on Other Experts 3
4.0 Property Description And Location 4
4.1 Location..... 4
4.2 Land Tenure 4
5.0 Accessibility, Climate, Local Resources, Infrastructure & Physiography 7
5.1 Access, Local Resources and Infrastructure 7
5.2 Physiography, Climate and Infrastructure 7
6.0 History..... 8
7.0 Geological Setting..... 10
7.1 Regional Geology..... 10
7.2 Property Geology 13
7.3 Mineralization..... 14
8.0 Deposit Type 21
9.0 Exploration 22
9.1 Geochemistry..... 23
9.1.1 Grid Soil Geochemistry 23
9.1.2 Reconnaissance Geochemistry 26
9.1.3 Biogeochemistry 27
9.1.4 Trenching 28
9.2 Geophysics 28
10.0 Drilling..... 34
10.1 Drill Sampling Method and Approach 41
11.0 Sample Preparation, Analyses And Security 41
12.0 Data Verification..... 43
13.0 Mineral Processing And Metallurgical Testing 43
14.0 Mineral Resource Estimates..... 43
15.0 Adjacent Properties..... 43
16.0 Other Relevant Data And Information..... 44
17.0 Interpretation And Conclusions 44
18.0 Recommendations..... 48
18.1 Budget..... 49
19.0 Signature Page..... 50
20.0 References..... 51
21.0 Certification, Date And Signature..... 55
22.0 Appendices..... 56

List of Illustrations

		Page
Figure 1:	Location Map	3
Figure 2:	Claim Map	6
Figure 3:	Geological Setting.	11
Figure 4:	Property Geology Map	12
Figure 5:	ICE Zone trenches	19
Figure 6:	BCIce Showing	20
Figure 7:	Copper MMI Soils	25
Figure 8:	Compilation over Magnetic Map	31
Figure 9:	eTh/K Map	32
Figure 10:	WS Showing	33
Figure 11:	Section through WS-08-08 to -11	37
Figure 12:	Section through WS-07-07	38
Figure 13:	Section through ICE-07-01 to -03	39
Figure 14:	Section through ICE-07-04	40
Figure 15:	Compilation over Geology	43

List of Tables

Table 1:	Claim data	5
Table 2:	Drill hole specifications	34
Table 3:	Significant drill hole intersections	35
Table 4:	Proposed drill hole specifications	49

List of Photographs

Photo 1:	ICE Zone	15
Photo 2:	Copper Hill showing	17
Photo 3:	Mineralized “gneissic” zone at Minto	18

List of Appendices

Appendix I	Statement of Expenditures
Appendix II	Sample Descriptions
Appendix III	Geology of the ICE copper-gold deposit *(Fage, 2008)*
Appendix IV	Structural and Geology Reports *(Devine 2009a & b)*
Appendix V	Field Examination Report (*Cardinal, D., 2009)*
Appendix VI	MMI Orientation Report *(Lustig, 2009)*
Appendix VII	Infrared Spectroscopy Report *(Fonseca, 2009a)*
Appendix VIII	Petrographic Report *(Fonseca, 2009b)*
Appendix IX	Strip logs
Appendix X	Drill Database in Access on CD
Appendix XI	MMI Data on CD *(Ryanwood, 2008)*

2.0 INTRODUCTION AND TERMS OF REFERENCE

2.1 Qualified Person and Participating Personnel

Ms. Jean M. Pautler, P.Geo. was commissioned by BCGold Corp. of Vancouver, British Columbia to compile, integrate and summarize all work conducted by BCGold Corp. on the Williams South Project, situated within the Carmacks copper-gold belt, in order to document and make recommendations for the next stage of exploration. Approval for the submittal of a compilation report for assessment credits, and qualification for double assessment if filed by February 1, 2016, was obtained from the chief mining recorder on December 22, 2015. The Williams South Project consists of 351 Yukon Quartz Mining claims covering an area of approximately 7300 hectares in the Whitehorse Mining District.

Exploration by BCGold Corp. since the granting of the option from Shawn Ryan in March, 2007 has involved a property wide airborne magnetic and radiometric geophysical survey (by Aeroquest Surveys, Toronto, Ontario), approximately 3,551 MMI and 317 conventional grid soil samples, 62.4 line km of induced polarization geophysics (by Aurora Geosciences Ltd. of Whitehorse Yukon Territory), a 1.26 km high resolution multi-array induced polarization survey, property wide geological mapping and prospecting with concurrent geochemical sampling, a structural analysis, with select detailed mapping by Fionnuala Devine, P.Geo., M.Sc., a 660 sample biogeochemical survey on WS by Kory Dumas, trenching on BCIce, WS and Copper Hill showings, 2,659m of diamond drilling in 14 holes, and infrared spectroscopy and petrography on the 2008 drill core by Anna Fonseca, P.Geo., M.Sc.

All soil samples were collected in 2007 and 2008 by Ryanwood Exploration Inc. of Dawson City, Yukon (a company owned by the original vendor of the property, Shawn Ryan). GroundTruth Exploration Inc. conducted the 1.26 km high resolution multi-array induced polarization survey.

Mapping and prospecting with concurrent geochemical sampling was completed by Don Coolidge, Adam Fage, Ann Doyle, Peter Ledwidge, and the author, and prospecting with concurrent geochemical sampling by Ken Galambos, P.Eng. (with extensive experience in the Yukon) and Ralph Keefe. Dan Cardinal, P.Geo., and Dave Heino completed a preliminary field examination in 2009. Don Coolidge, Ralph Keefe and Dave Heino are well known prospectors with extensive experience, and Ann Doyle and Peter Ledwidge are geologists with significant experience in the Yukon.

2.2 Terms, Definitions and Units

All costs contained in this report are denominated in Canadian dollars. Distances are reported in metres (m) and kilometres (km). GPS refers to global positioning system with co-ordinates reported in UTM grid, Zone 8, Nad 83 projection. The annotation 060º/70ºSE refers to an azimuth of 060 degrees, dipping 70 degrees to the southeast, Ma refers to million years, and °C refers to temperature in degrees Celsius. Minfile showing refers to documented mineral occurrences on file with the Yukon Geological Survey. DDH refers to diamond drill hole. IP refers to an induced polarization type of geophysical survey useful in detecting the presence of conductive disseminated sulphides. VLF-EM refers to an electromagnetic type of geophysical survey useful in detecting conductors, commonly related to structures. MMI soil sampling refers to soil samples collected in a specific manner and analyzed by a process that measures mobile metal ions, useful in detecting mineralization beneath younger cover rocks and thick glacial till.

The term ppm refers to parts per million, which is equivalent to grams per metric tonne (g/t) and ppb refers to parts per billion. The abbreviation oz/ton and oz/t refers to troy ounces per imperial short ton. The symbol % refers to weight percent unless otherwise stated.

Elemental abbreviations used in this report include: gold (Au), silver (Ag), copper (Cu), iron (Fe), arsenic (As), bismuth (Bi), manganese (Mn), sulphide (S) and oxide (O). K-spar refers to potassium feldspar. Minerals found in the Carmacks copper-gold belt include pyrite (iron sulphide), magnetite and hematite (iron oxides), malachite and azurite (both hydrous copper carbonates), and chalcopyrite, chalcocite and bornite (copper sulphides).

2.3 Source Documents

Sources of information are detailed below and include available public domain information and private company data.

- Research of the Minfile data available for the area at http://data.geology.gov.yk.ca/ on January 4, 2016.
- Research of mineral titles at http://apps.gov.yk.ca/pls/apex40p/f?p=116:1:2534937475277042 and http://mapservices.gov.yk.ca/YGS/ on January 4, 2016.
- Review of company reports and annual assessment reports filed with the government at http://199.247.132.58:8000/cgi-bin/gw/chameleon.
- Review of geological maps and reports completed by the Yukon Geological Survey or its predecessors.
- Review of published scientific papers on the geology and mineral deposits of the region and on mineral deposit types.
- Company data and reports of BCGold Corp.

- Discussions with Dr. Maurice Colpron and Dr. Patrick Sack of the Yukon Geological Survey and Dr. Jim Mortenson of the University of British Columbia, all with considerable experience within the belt.
- The author has recent previous independent experience and knowledge of the Carmacks copper-gold belt having worked on the privately owned STU drilled prospect between 2006 and 2015, on the Carmacks copper-gold belt properties of Northern Tiger Resources in 2010 and 2011, and on the Carmacks Copper-Gold Project for BCGold Corp. in 2008 and 2009.
- Site visits by the author on September 27 and 29, 2015 and April 20, 2012, and work on the property by the author on June 10-14, 2009 and June 2-11, 2008 and a review of the entire 2007-2013 work programs.
- A review of pertinent news releases of BCGold Corp. and of other companies conducting work in the regional area.

2.4 Limitations, Restrictions and Assumptions

The author has relied in part upon work and reports completed by others in previous years in the preparation of this report as identified under section 2.3, “Source Documents” and section 20.0, “References”. Thorough checks to confirm the results of such work and reports have not been done, but the author has no reason to doubt the correctness of such work and reports. All exploration assessment reports, listed in Section 20.0, “References”, were completed by competent professionals and have been accepted by the Mining Recorder. The work undertaken between 2007 and 2013 was completed by or under the direction of BCGold Corp. by reputable personnel and contractors.

3.0 RELIANCE ON OTHER EXPERTS

While title documents and option agreements were reviewed for this study as identified under section 2.3, “Source Documents”, this report does not constitute nor is it intended to represent a legal, or any other, opinion as to the validity of the title. Data concerning the location and status of mineral claims was obtained from the Whitehorse District Mining Recorder. The title information was relied upon to describe the ownership of the property and claim summary in Section 4.2, “Land Tenure”.

4.0 PROPERTY DESCRIPTION AND LOCATION

4.1 Location (Figures 1 and 2)

The Williams South Project, NTS map sheet 115I/7, lies within the southern Merrice Creek drainage, 5-10 km southwest of the Yukon River, approximately 32 km northwest of Carmacks, Yukon Territory. Carmacks is 175 km by paved highway north of Whitehorse, Yukon Territory *(Figures 1 and 2)*. The property is centered at a latitude of 62°19'N and a longitude of 136°38'W *(Figure 2)*.

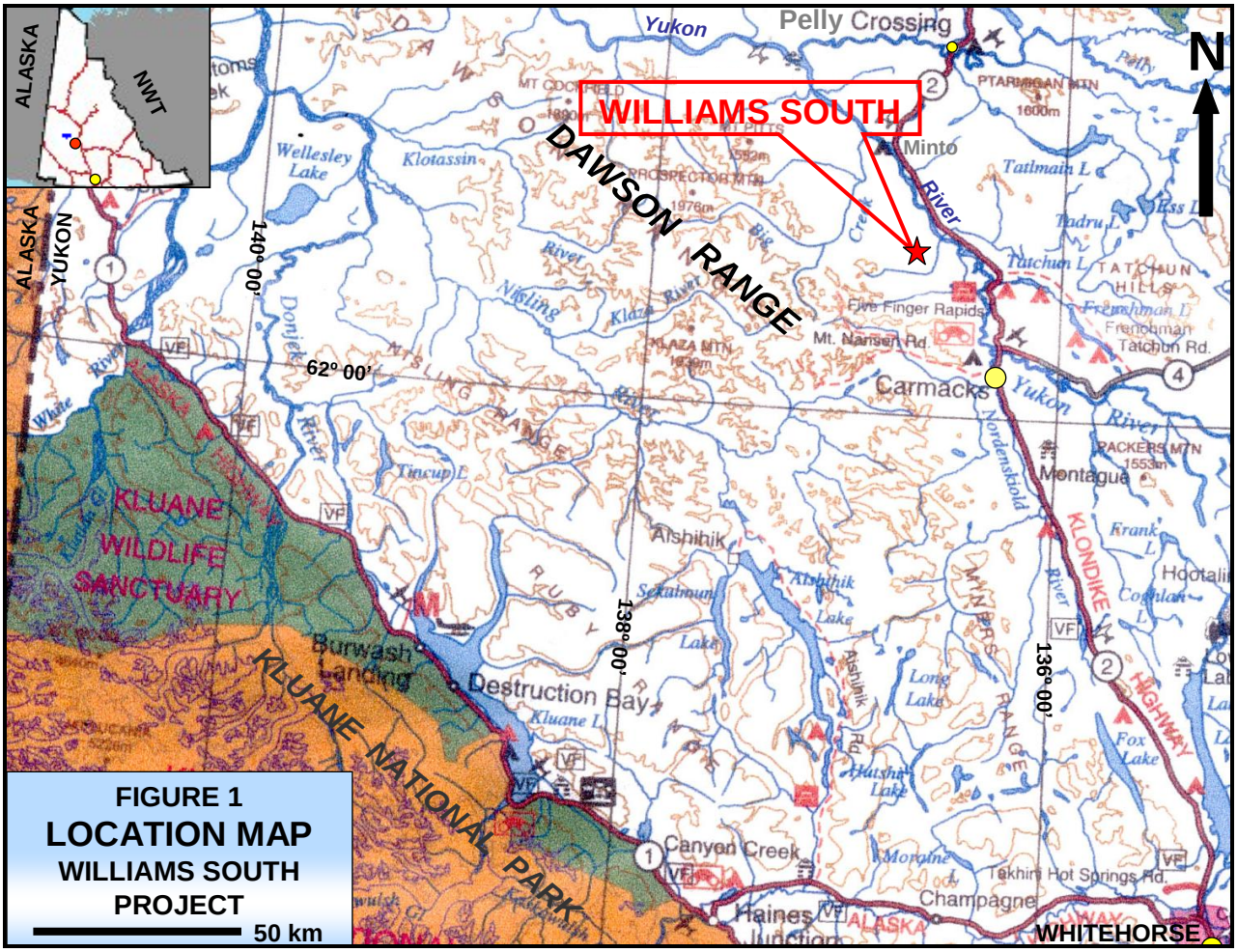

4.2 Land Tenure (Figures 2 and 3)

The Williams South Project consists of 351 Yukon Quartz Mining claims covering an area of approximately 7300 hectares in the Whitehorse Mining District *(Figure 2)*. The area is approximate since claim boundaries have not been legally surveyed. The mineral claims were located by GPS and compass and staked in accordance with the

Yukon Quartz Mining Act on claim sheet 115I/7, available for viewing in the Whitehorse Mining Recorder's Office. A table summarizing pertinent claim data follows.

TABLE 1: Claim data

Claim Name	Grant No.	No. of Claims	Expiry Date	New Expiry Date*
WS 1 – 82	YC53521 - 602	82	4/2/2016	4/2/2017
WS 83 – 156	YC53748 - 821	74	4/2/2016	4/2/2017
WS 157 – 196	YC53993 - 4032	40	4/2/2016	4/2/2017
WS 197 – 208	YC91789 - Y800	12	4/2/2016	4/2/2017
BC 35 – 50, 65 – 144	YC60218 - 233, 248 - 327	96	4/2/2016	4/2/2017
ICE 1 – 4	YC46784 - 87	4	4/12/2016	4/12/2017
ICE 5 – 41	YC54407 - 443	37	4/2/2016	4/2/2017
SLEEP 13 – 18	YC60134 - YC60139	6	4/2/2016	4/2/2017
TOTAL		**351**		

***** new expiry date based on acceptance of this report for assessment

The registered owner of the claims is BCGold Corp. of Vancouver, British Columbia, which holds 100% interest, subject to a 1.75% underlying net smelter royalty (NSR), of which 1.25% may be purchased for $1,500,000.

The claims are located within the Traditional Territories of the Selkirk First Nation and the Little Salmon/Carmacks First Nation, which have a land claim settlement agreement under the Yukon Umbrella Final Agreement. A Little Salmon/Carmacks land parcel (surface and subsurface rights) is located approximately 3 km northwest of the property and another (surface rights only) 2 km to the east. The land in which the mineral claims are situated is Crown Land and the mineral claims fall under the jurisdiction of the Yukon Government. Surface rights would have to be obtained from the government if the property were to go into development.

A mineral claim holder is required to perform assessment work and is required to document this work to maintain the title as outlined in the regulations of the Yukon Quartz Mining Act. The amount of work required is equivalent to $100.00 of assessment work per quartz claim unit per year. Alternatively, the claim holder may pay the equivalent amount per claim unit per year to the Yukon Government as "Cash in Lieu" to maintain title to the claims.

Preliminary exploration activities do not require permitting, but significant drilling, trenching, blasting, cut lines, and excavating may require a Mining Land Use Permit that must be approved under the Yukon Environmental Socioeconomic Assessment Act (YESSA). To the author's knowledge, the Williams South Project area is not subject to any environmental liability.

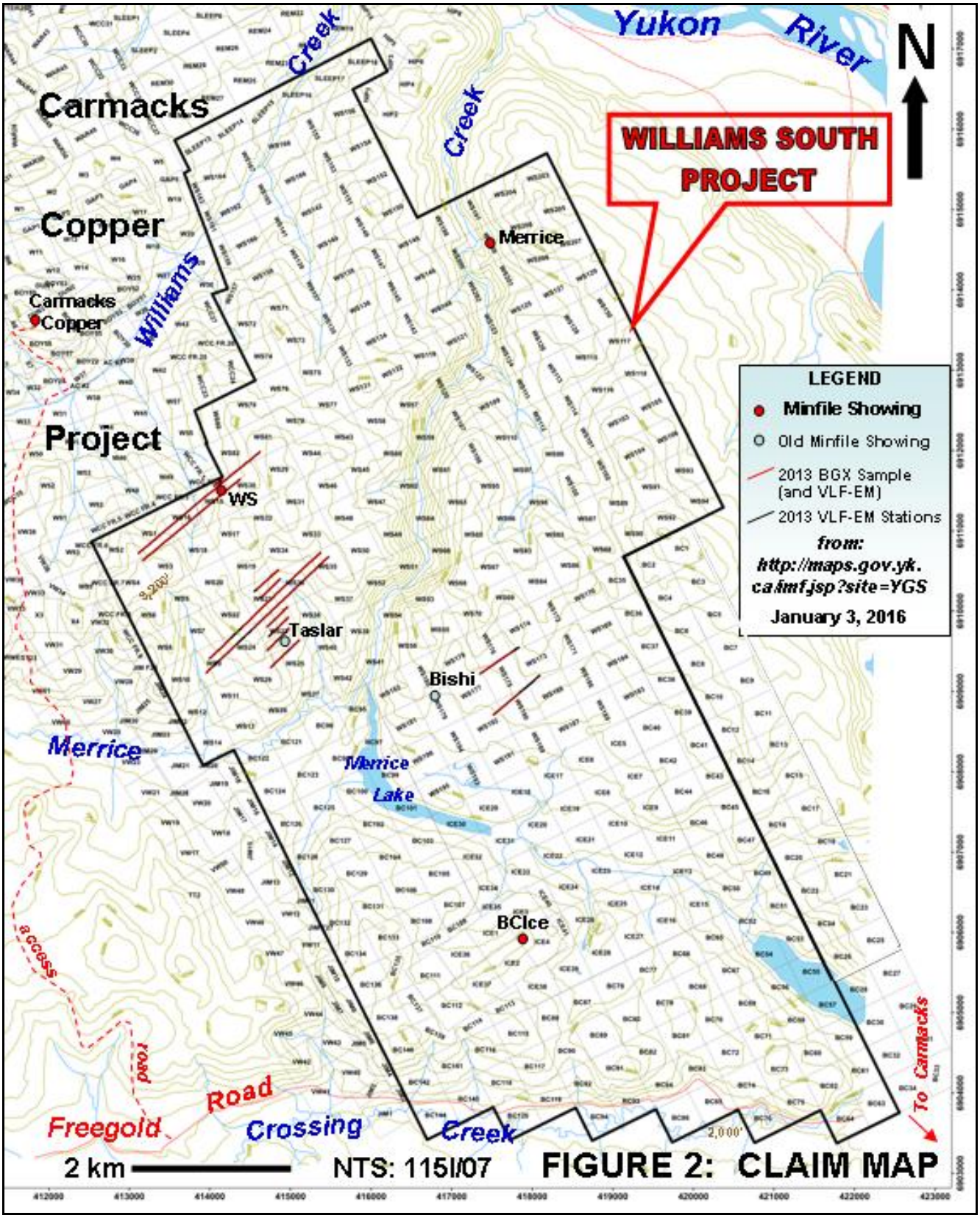
Yukon River
N
Creek
Carmacks
Copper
Project
Williams Creek
WILLIAMS SOUTH PROJECT
Merrice
Carmacks Copper
WS
Taslar
Bishi
Merrice Lake
BCIce
Access road
Freegold Road
Crossing Creek
To Carmacks
2,000'
LEGEND
Minfile Showing
Old Minfile Showing
2013 BGX Sample (and VLF-EM)
2013 VLF-EM Stations
from: http://maps.gov.yk.ca/imf.jsp?site=YGS
January 3, 2016
2 km
NTS: 115I/07
FIGURE 2: CLAIM MAP

5.0 ACCESSIBILITY, CLIMATE, LOCAL RESOURCES, INFRASTRUCTURE AND PHYSIOGRAPHY

5.1 Access, Local Resources and Infrastructure

The Williams South Project is accessible from Carmacks via the Freegold Road *(Figure 2)*, a year round government maintained gravel road, which traverses the southern property area from approximately 25 to 31 km. The western property area can be accessed by 4WD road and ATV trails heading east from the 12 km access road to the Carmacks Copper Project camp, located at 412013mE, 6912697mN, Zone 8, Nad 83 projection. The eastern property area is only accessible by foot or helicopter.

Carmacks is the closest town of significant size, with a population of approximately 500, a gravel airstrip, suitable for medium sized aircraft, and a seasonal helicopter base (Trans North Helicopters). Facilities include a grocery store, nursing station, police station, two service stations, accommodation, a restaurant and a café. Some heavy equipment is available for contract mining work. Complete services are available in Whitehorse, less than two hours by all-weather highway, 175 km south of Carmacks *(Figure 1)*.

5.2 Physiography, Climate and Infrastructure

The Williams South Project is located along the northeastern flank of the Dawson Range within the Yukon Plateau, covering moderate rolling hills, 5-10 km southwest of the Yukon River *(Figures 1 and 2)*. Southern Merrice Creek transects the property, which is also drained by northerly flowing tributaries of Williams Creek to the north and southerly flowing tributaries of Crossing Creek in the south. Elevation ranges from about 1980 feet along Crossing Creek in the southeastern property area to 3240 feet along the northeast trending ridge in the northern property area *(Figure 2)*.

Vegetation consists of pine occasionally broken by poplar stands. On north facing slopes black spruce predominates with permafrost. Muskeg, thick willow and alder cover low swampy ground in the eastern property area. Volcanic ash, which deadens and dilutes soil geochemical responses, was encountered in the property area.

The area has a northern interior climate characterized by a wide temperature range with warm summers, long cold winters and light precipitation. Summers are moderately cool to hot, with daily highs of 15°C to 30°C. Winters are cold, with temperatures of -30°C to -40°C common. The exploration season lasts from mid May until October.

Although there do not appear to be any topographic or physiographic impediments, and suitable lands appear to be available for a potential mine, including mill, tailings storage, heap leach and waste disposal sites, engineering studies have not been undertaken and there is no guarantee that such areas will be available within the subject property. The nearest source of power is the transmission line northwest of Carmacks, approximately 10-20 km away.

6.0 HISTORY

The first claims were staked in the Carmacks Copper area in 1898 to cover copper showings associated with quartz veins located in Williams Creek and Merrice Creek Canyons, east of the present Carmacks Copper deposit. The Merrice showing, which lies on the northeastern Williams South Project area, is one of these. In the late 1960's the discovery of the Casino porphyry copper deposit, 104 km to the northwest, sparked a staking rush that led to the staking of the Williams Creek (now Carmacks Copper) property in 1970.

The area covered by the Williams South Project saw some prior reconnaissance exploration work as part of the work around the Williams Creek deposit. Four old trenches were encountered on the northern WS claims in 2008 *(Pautler, 2008)* but no mineralization was observed, although exposure is limited. There are three Minfile occurrences within the Williams South Project; Bishi (Minfile Number 115I 006) (now moved and renamed BCIce), Taslar (Minfile Number 115I 007) (now moved and renamed WS), and Merrice (Minfile Number 115I 009), as documented by the Yukon Geological Survey *(Deklerk, 2009)*. The Bishi and Taslar were staked in the early 1970's on aeromagnetic anomalies, but no mineralization was discovered. Previous work by United Keno Hill Mines Ltd. in the ICE claim area resulted in the discovery of the Poon showing *(Canam, 1982)*, now referred to as BCIce. Old placer workings are evident at the north end of Merrice Lake.

The Williams South Project area of BCGold Corp's Carmacks Copper-Gold Project was staked by prospector Shawn Ryan in 2006, following up magnetic high anomalies on trend with known mineralization at the Carmacks Copper deposit, located 3-10 km northwest of the Williams South Project *(Figure 2)*. BCGold Corp. was granted an option on the project area from Shawn Ryan in March, 2007 and acquired 100% ownership of the claims in July, 2010.

The following is a record of the known work history on the Williams South Project.

1902-8 Easterly trending quartz veins with chalcopyrite and bornite, 0.3-1.4m wide and dipping 50°N, were staked by prospectors (Merrice showing), who explored with a 47.2m adit *(Deklerk, 2009)*.

1970 Geological mapping and soil sampling on the BF claims (WS property, northeast of Merrice Lake) by Mitsubishi Metal Mining Co. Ltd. did not uncover mineralization or significant soil anomalies *(Kikuchi, 1970)*.

1971-3 Geochemical sampling, prospecting and road building was carried out on the Taslar (WS property, northwest of Merrice Lake) by Taseko Mining Ltd. and LaRonge Mining Ltd. The Wet claims were staked to the southwest (WS property, west of north end of Merrice Lake) and explored by grid soil sampling in 1972 and a ground magnetic survey in 1973 by Minto Mining Ltd. Outlining a number of small but distinct copper anomalies and magnetic low anomalies *(Guardia, 1972 and Mullin, 1974)*.

1974 Geological mapping and a small geochemical survey by Asarco on Merrice showing *(Deklerk, 2009)*.

1982 Discovery of Poon (now called BCIce) showing, consisting of two zones of foliated granodiorite with malachite staining, by United Keno Hill Mines Ltd. Trenching was recommended but soil geochemistry suggested limited extent *(Canam, 1982)*.

2006 Staked by Shawn Ryan to cover favourable geology and government regional airborne magnetic and stream sediment anomalies considered prospective for Carmacks copper-gold belt mineralization. Minor prospecting and geochemical sampling relocated the Poon (BCIce) showing *(Ryan, 2007)*.

2007 A 3,295 line km airborne magnetic and radiometric geophysical survey was funded by BCGold Corp. over their Carmacks Copper-Gold Project, which included the Williams South Project, under option from Ryan *(Aeroquest International, 2008).* BCGold Corp. also completed MMI grid soil sampling on WS claims (1618 samples) and MMI and conventional grid soils on ICE claims (603 samples), mapping, prospecting and rock sampling (21 samples), trenching on ICE, and 1360m of diamond drilling in 7 holes on ICE and WS *(partially in Doherty, 2008a-d)*.

2007-8 A winter 14 line km induced polarization geophysical survey was completed by Aurora Geosciences for BCGold Corp. on the ICE claims

2008 A 22.1 line km induced polarization geophysical survey was completed by Aurora Geosciences for BCGold Corp. delineating several anomalies which suggest the extension of Zone 12 at Carmacks Copper onto the northern portion of the WS claims covered by geophysical lines L162N and L159N *(Barrios and Newton, 2009)*. BCGold Corp. also conducted mapping, prospecting and sampling *(Pautler, 2008 and Galambos, 2008),* 1646 MMI soils, a 133 sample MMI/conventional soil geochemical orientation survey over the Carmacks Copper deposit, with permission *(Lustig, 2009)*, 1,300m of diamond drilling in 7 holes on WS (2 holes totaling 67.7m were lost and re-drilled).

2009 BCGold Corp. completed mapping, prospecting and sampling *(Pautler, 2009 and Cardinal, 2009)*, trenching on WS (7) and ICE (2-3), 26.3 line km of induced polarization geophysical surveys on the northeast WS claims and infill over the ICE-WS claim boundary *(Sidhu, 2010)*, detailed mapping on western WS and structural interpretation *(Devine 2009a)*, and infrared spectroscopy and petrography on WS *(Fonseca, 2009a and b)*. The induced polarization survey outlined open ended high chargeability zones coincident with MMI soil anomalies *(Sidhu, 2010d)*.

2012 BCGold Corp completed a biogeochemical orientation survey, consisting of 116 biogeochemcal samples at 10m spacings on two lines along the drill trace of hole WS08-09B, which intersected Cu mineralization. The survey appeared to detect the mineralization encountered in the drill hole *(Dumas, 2013)*.

2013 A small VLF survey, biogeochemistry (550 samples at 20m spacings on 12 lines) and a 1.26 km high resolution multi-array induced polarization survey was done on the WS claims for BCGold Corp. Proximal VLF-EM conductors and geochemical anomalies were obtained *(Dumas, 2014)*.

Details and results of the work completed and funded by BCGold Corp., undertaken from 2007 to 2013, with complete results will be discussed under section 9.0, “Exploration”.

7.0 GEOLOGICAL SETTING

7.1 Regional Geology (Figure 3)

The regional geology of the area is primarily summarized from Hood et. al. (2009), Gordey and Makepeace (2000), Mortensen and Tafti (2003) and Tafti (2005).

The Williams South Project lies within the southern portion of the Carmacks copper-gold belt, a 180 km by 60 km-wide north-northwest trending mineralized belt of similar intrusion-hosted copper-gold mineralization. The belt includes the Minto Mine (Minfile 115I 021) of Capstone Mining Corporation (formerly Sherwood Copper Corp.), the Carmacks Copper deposit (Minfile 115I 008) and the STU drilled prospect (Minfile 115I 011).

The regional area of the Carmacks copper-gold belt *(Figure 3)* is underlain by intermediate to felsic intrusive and meta-intrusive rocks of the Early Jurassic Minto plutonic suite intruding Paleozoic metaplutonic rocks and locally metavolcanic rocks of the Yukon-Tanana terrane, near the boundary with upper Triassic and/or older mafic volcanic rocks of Stikinia/Quesnellia terranes to the east. The above lithologies are overlain by younger basaltic volcanic rock units of the Late Cretaceous Carmacks Group and the Quaternary Selkirk Group.

The northwest trending Hoochekoo Fault, which trends along the northeast side of STU and Carmacks Copper, parallel to the regional strike slip Teslin Fault, separates the Granite Mountain Batholith (GMB) from Upper Triassic mafic volcanic rocks of the Lewes River Group (basal Povoas Formation) which are in turn overlain by Jurassic Laberge Group sedimentary rocks. At the south end of the belt the Granite Mountain Batholith is in normal fault contact with Carmacks Group basalts.

The area has been glaciated with overall northwesterly ice directions and local southeast ice directions, particularly in the west.

The Carmacks Copper (formerly Williams Creek) deposit of Copper North Mining Corporation (formerly Western Copper) is located approximately 3-10 km northwest of the Williams South Project. Carmacks Copper contains a resource of 12.0 million tonnes of copper oxide ore grading 1.07% Cu (0.86% oxide Cu), 0.46 g/t Au and 4.6 g/t Ag, using a cutoff grade of 0.25% Cu *(Huss et al., 2012).* The above reserve information has not been verified by the author and is not necessarily indicative of the mineralization on the Williams South Project which is the subject of this report. The 3,850 tonne per day producing Minto Mine, lies 45 km northwest of the Williams South Project (*www.capstonemining.com*).

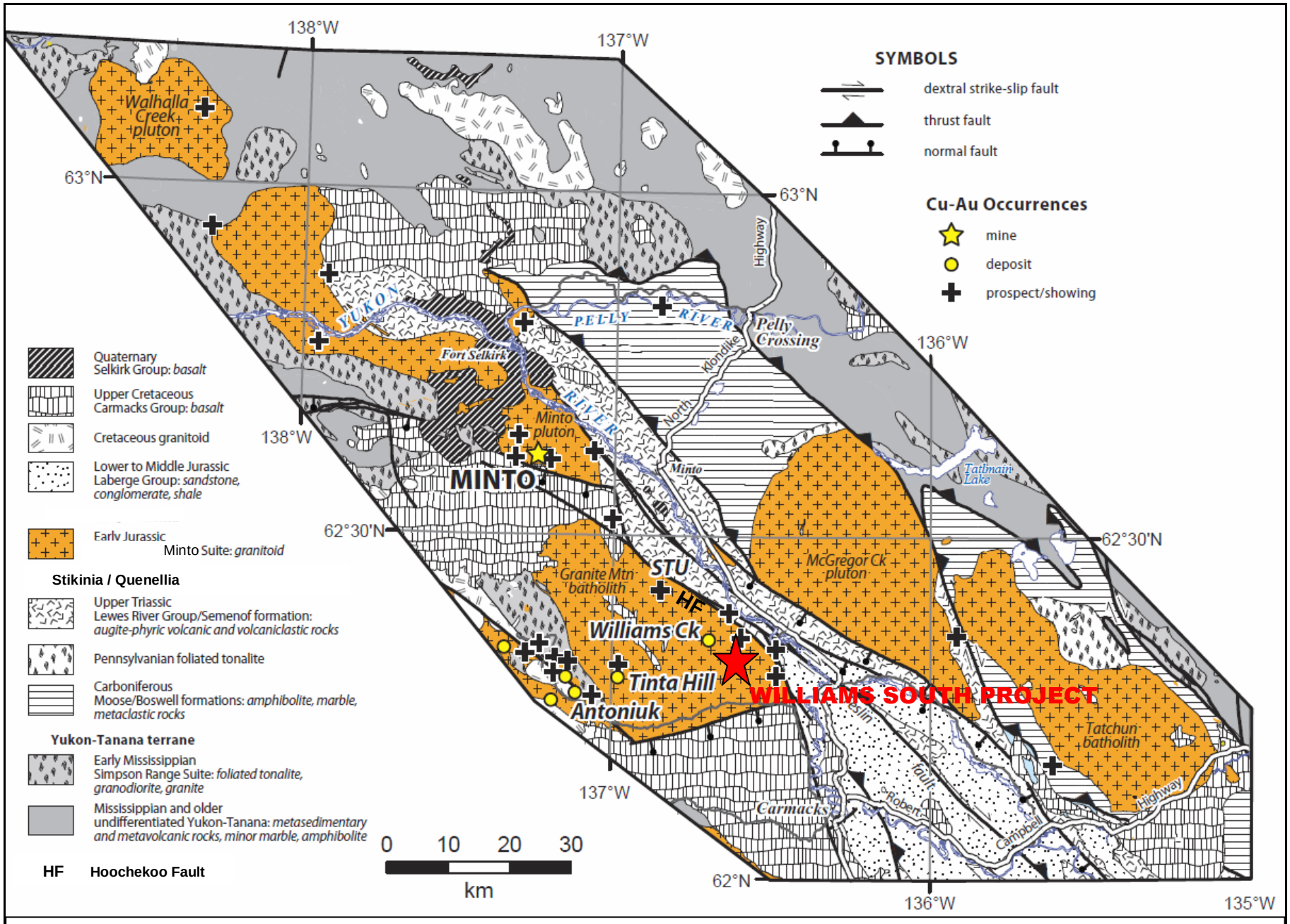

FIGURE 3: GEOLOGICAL SETTING *from Hood et al., 2009*

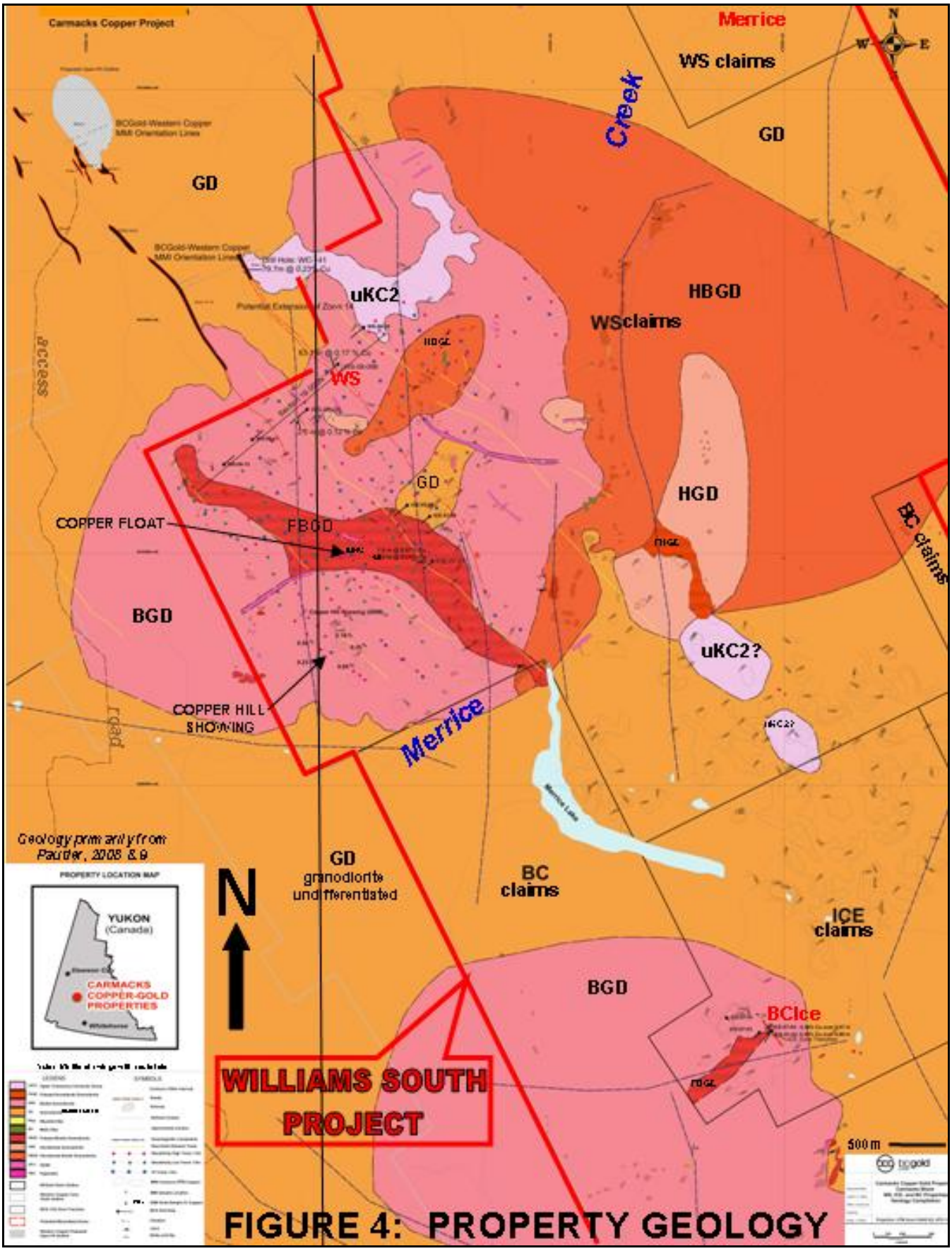

FIGURE 4: PROPERTY GEOLOGY

7.2 Property Geology (Figure 4)

Property scale mapping was primarily completed by Don Coolidge and the author in 2008 and 2009, and Adam Fage as well in 2008, with some preliminary mapping by Ann Doyle, Peter Ledwidge and Adam Fage in 2007. Mapping, petrography, geochemical analysis and genesis of the ICE zone were the subject of a B.Sc. thesis by Adam Fage in 2007 *(Fage, 2007)*. Infrared spectroscopy and petrography on the 2008 drill core was completed by Anna Fonseca in 2009 *(Fonseca, 2009a & b)*. Later in 2009 a structural analysis with select detailed mapping was completed by Fionnuala Devine *(Devine, 2009a & b)*; and Dan Cardinal, P.Geo., and Dave Heino (prospector) completed a preliminary field examination *(*Cardinal*, 2009)*. The above-referenced reports are enclosed as appendices in this report.

The Williams South Project is primarily underlain by Early Jurassic intrusive rocks of the Granite Mountain Batholith (Minto suite) which intrude the Paleozoic metamorphic basement rocks of the Yukon-Tanana terrane, and locally volcanic rocks of the Povoas Formation of Stikinia to the east, and are overlain by younger volcanic rocks, and intruded by related dykes, of the Late Cretaceous Carmacks Group. Numerous aplite, felsite and pegmatite dykes, slightly younger than the main batholith, intrude the Granite Mountain Batholith (GMB). Outcrop is limited on the property, comprising less than 5%, and generally confined to ridge lines and the canyon of Merrice Creek. A Table of Formations follows.

Table of Formations:

***Upper Cretaceous*:**			
	Carmacks Group:	**volcanic rocks (uKv)**	andesite-basalt flows and tuff breccia
		mafic dykes	diorite and gabbro
***Early Jurassic*:**			
	slightly post GMB:	**felsic dykes**	aplite, felsite, pegmatite
	Minto suite:	**GMB**	primarily Kspar megacrystic biotite ±hornblende granodiorite grading to gneiss

The intrusive rocks of the Granite Mountain Batholith (GMB) consist of several different phases that include potassium feldspar megacrystic biotite ±hornblende granodiorite that grades to foliated biotite, biotite ±hornblende gneiss and locally biotite ±hornblende schist, quartz-phyric granodiorite to monzogranite, and minor diorite to quartz diorite and hornblendite. Foliation of the granodiorite, where present, trends northwest and varies from very weak to moderate to locally strong to gneissic; the latter particularly in mineralized zones. It should be noted that within the Carmacks copper-gold belt (i.e. Minto, Carmacks Copper, STU) mineralization is typically associated with foliated to gneissic granodiorite, more mafic phases and often finer grained variants of the granodiorite.

Areas marked “GD” on Figure 4 are undifferentiated granodiorite, since they either lie outside of mapped areas and/or insufficient exposure is available to subdivide the phases. Much of the mapping is based on small outcrop exposures, subcrop and float. The main phase of the Granite Mountain Batholith, a massive coarse grained biotite-hornblende granodiorite with 5-15% mafic minerals and potassium feldspar megacrysts,

is exposed throughout most of the property. Overall, more biotite dominant granodiorite is exposed in the western and southern property areas and more hornblende rich biotite granodiorite in an area north of Merrice Lake and east of a line just west of the Merrice Creek canyon, wrapping further northwest in the northern property area *(Figure 4)*. A 0.5 by 1.5 km pod of more hornblende rich biotite granodiorite is exposed in the northeastern WS grid area and was intersected in DDH WS-08-09B and -08. Localized more hornblende dominant granodiorite occurs within or proximal to the areas underlain by the more hornblende rich biotite granodiorite phase.

Foliated biotite ±hornblende granodiorite occurs in a 0.5 by 4 km northwest trending band across the WS grid from the north end of Merrice Lake to the northwest property boundary, and as a northeasterly (?) 150m by 1 km band at the BCIce showing; the latter particularly limited by poor exposure.

Aplite dykes, which trend northwesterly and easterly to northeasterly, are more abundant in the WS grid area and further north, possibly partly due to more detailed mapping and/or better exposure in the area.

Basalt flows of the Late Cretaceous Carmacks Group overlie the granodiorite in the area just north of the northeast WS grid area and have been interpreted from magnetic signature and geochemistry in the north-central ICE grid on the southern WS claims near the claim boundary. Minor northerly trending rhyolite quartz feldspar porphyry dykes, probably of the Late Cretaceous Prospector Mountain (Casino) suite, were identified in the southern and western property areas. Similar dykes and related stocks are known to host gold ±copper mineralization within the Freegold camp to the west.

A number of northerly trending lineaments, defined by airborne magnetic low anomalies, bisect the WS claims and are suggestive of structures *(Figure 4)*. An easterly trending airborne magnetic low feature is evident through the BCIce showing area *(Figure 4)*.

7.3 MINERALIZATION (Figures 4-7)

Mineralization within the Carmacks copper-gold belt consists of chalcopyrite and bornite with minor chalcocite as disseminations, irregular grains, aggregates and stringers, associated with more foliated to gneissic, finer grained and more mafic rich zones with biotite, silicification hematite, epidote, chlorite and locally sericite alteration. Supergene alteration has produced secondary copper minerals such as chalcocite, azurite and malachite. Mineralization at Minto is flat lying but mineralization at Carmacks Copper and alignment of mineralized zones within the entire belt generally trend 315-340º.

There are three Minfile occurrences within the Williams South Project; Bishi (115I 006) (now moved and renamed BCIce), Taslar (115I 007) (now moved and renamed WS), and Merrice (115I 009), as documented by the Yukon Geological Survey *(Deklerk, 2009)*. The Bishi and Taslar were staked in the early 1970's on aeromagnetic anomalies. Geological and geochemical surveys on the BF claims (WS property, northeast of Merrice Lake) by Mitsubishi Metal Mining Co. Ltd. outlined the presence of granodiorite and diorite, cut by aplite and pegmatite dykes, in an area of very poor

exposure, and only a few spot copper soil anomalies up to 50 ppm *(Kikuchi, 1970*). No mineralization was found on the Taslar, but grid soil sampling and a ground magnetic survey in 1972-73 to the southwest on the Wet claims (WS property, west of north end of Merrice Lake) by Minto Mining Ltd, outlined a number of small but distinct copper anomalies and magnetic low anomalies *(Guardia, 1972 and Mullin, 1974)*.

The Merrice showing was located in 2009 at 417439mE, 6914656mN, Nad 83, Zone 8 projection. Several quartz veins with malachite, minor chalcopyrite and locally high concentrations of bornite hosted by hornblende rich diorite to hornblendite were found to trend 290°/55°N and 320°/85°NE. Malachite and trace chalcopyrite were observed within the host rock 3m into the footwall of the main vein, which was explored by an adit, now caved. The main vein explored by the adit returned 0.52% Cu over the 1.5m vein. The diorite footwall with malachite and trace chalcopyrite, 3m south of the vein carried 0.14% Cu. A grab sample from a bornite rich 0.5m vein south of the adit returned 2.52% Cu, 0.51 g/t Au and 42 g/t Ag *(Pautler, 2009)*.

Previous work by United Keno Hill Mines Ltd. in the ICE claim area resulted in the discovery of the Poon showing, consisting of two zones of foliated granodiorite with malachite *(Canam, 1982)*, now referred to as BCIce in Minfile. The main zone (now called ICE) was reported to cover a discontinuously exposed 20m x 100m zone of moderately foliated granodiorite with malachite trending 294°/20°NE *(Photo 1)* with a second 5 by 10m zone 300m to the west *(Canam, 1982)*.



Photo 1: ICE zone, BCIce showing: shallowly dipping foliated granodiorite with malachite overlying massive granodiorite (0.48% Cu over 0.8m)

MMI and conventional soil sampling (614 samples), 60m of trenching in 3 trenches, 859m of diamond drilling in 4 holes and one north-northeast trending IP line was completed by BCGold Corp. in 2007 over the BCIce showing area *(Figure 5)*. Both malachite bearing zones *(Figure 6)* are associated with a bulls-eye aeromagnetic high feature, measuring approximately 1,000 by 700m in size *(Ryan, 2007)*. Grab samples from the showing in 2007 returned maximum values of 1.83% Cu and 0.41 g/t Au. Outcrop and trench chip samples returned, 0.48% Cu over 0.8m, 0.45% Cu over 0.85m and 0.30% Cu over 2.0m *(Figure 5)*. Mineralization consists of malachite, associated with secondary biotite (potassic) alteration.

A prospecting sample, 200m south-southwest of the ICE zone returned 0.39% Cu with 0.38 ppb Au from foliated granodiorite in 2007 *(Figure 6)*. A trench was excavated here in late 2009 with reported grab samples of 0.32 and 0.10% Cu. This may correspond to the second zone, described as being 300m west of the main (ICE) zone, in Canam (1982). Two conventional soil samples collected 200m further to the southwest in 2006 by Ryan returned 281 and 935 ppm Cu *(Figure 6) (Ryan, 2007)*.

Mapping, petrography, geochemical analysis and genesis of the ICE zone were the subject of a B.Sc. thesis by Adam Fage in 2007, completed prior to drilling and the IP line *(Appendix III)*. The following description of the ICE zone is summarized from Fage (2008) The ICE zone contains malachite and other copper oxides in pores and fractures, (previously occupied by sulphides) and small irregular particles of native silver hosted within variably sheared and altered hornblende-biotite granodiorite. Disseminated magnetite, partially oxidized to hematite (martite) accounts for the relatively high magnetic susceptibility of the rocks, but does not account for the magnetic high anomaly. Fabrics and recrystallized quartz veinlets suggest that hydrothermal mineralization preceded deformation.

Drilling of the ICE zone encountered two narrow, relatively flat-lying mineralized horizons in ICE 07-2 and -4. The upper and lower horizons returned 0.48% Cu over 4.8m and 0.15% Cu over 3.7m in ICE 07-2 and 0.39% Cu over 5.5m and 0.25% Cu over 0.7m in ICE 07-4, respectively. The upper horizon is described as foliated megacrystic biotite rich granodiorite with 5-10% malachite on fractures and along the foliation. The lower horizon is characterized by 5% malachite on fractures and along foliation planes. This style of mineralization commonly occurs distal to larger zones so may have potential along strike and/or down dip, further to the northeast.

The most significant copper mineralization encountered on the Williams South Project was intersected in drill hole WS08-09B, targeting a weak copper MMI anomaly coincident with a pronounced 2 km long linear induced polarization geophysical anomaly, 1 km along strike from Copper North's Zone 14; Zone 14 returned 0.23% Cu over 79.7m in hole WC07-141 *(Western Copper news release November 22, 2007)*.

Mineralization in WS08-09B occurs in two discrete and relatively homogenous intervals of foliated hornblende schist within a white megacrystic potassium feldspar granodiorite. Mineralization in the upper interval, which averages 0.13% Cu over 20.0m from 46.0 to 66.0m, consists primarily of pyrite and chalcopyrite intermixed in foliated schist. Massive

chalcopyrite occurs along the edges of carbonate stringers and malachite occurs along fractures. Chalcopyrite mineralization occurs in a similar fashion in the lower interval from 85.5 to 109.1m, averaging 0.34% copper over 23.6m. Chalcopyrite and fracture controlled malachite occur intermixed with pyrite in foliated hornblende schist. Massive chalcopyrite rims carbonate stringers and larger chalcopyrite grains display red oxidized rims. Propylitic (chlorite, epidote, carbonate, and sericite) alteration with secondary hematite and weak potassium feldspar alteration predominates.

The Copper Hill showing *(Photo 2)* was discovered in 2008 on the southwestern WS grid at 6909150mN, 414100mE, Nad 83, Zone 8 projection on L144N at 10335E, approximately 2.5 km southeast generally along trend of Zones 5, 6 and 8 of the Carmacks Copper Project *(Figure 7)*. The showing consists of malachite, lesser chrysocolla, minor azurite, and chalcocite mineralization, primarily hosted by more mafic zones of quartz diorite to diorite composition (varying from fine to very coarse grained and locally moderately foliated) within coarse grained granodiorite. Exposure consists of a small 1.5 by 3m outcrop, scattered subcrop and local float. Mineralization appears to follow the foliation, which trends 315º/80E, and can be discontinuously traced for 20m along strike and 3-5m in width, limited only by exposure. A 330º/70ºE trending joint set cuts the foliation. Alteration includes abundant epidote as fracture fillings and along foliation, local concentrations of limonite, and local magnetite-silica with clots of magnetite and quartz flooding and veinlets.



Photo 2: Copper Hill showing

Samples from the Copper Hill showing in 2008 returned maximum values of 0.85% Cu and 0.42 g/t Au from a grab sample and 0.19% Cu and 0.08 g/t Au across 1.5m from the same location. A 600m by generally 100m wide copper MMI soil anomaly lies 150m

upslope of the showing coincident with an induced polarization chargeability high – resistivity anomaly.

A 30 by 25 cm rounded float boulder (Copper Float) of foliated biotite-hornblende granodiorite with malachite staining centred within a 2 cm more biotite rich, more foliated section with secondary magnetite and trace bornite, was discovered in 2007 on the WS grid at 414311mE, 6909970mN *(Figures 4 and 7)*. It should be noted that the intrusive rock commonly weathers rounded. A grab sample of the float returned 0.94% Cu and 0.26 g/t Au. The float appears isolated but generally occurs within an area of poor exposure with some exposures of foliated granodiorite approximately 2 km southeast along trend of Zone 12-13 of the Carmacks Copper Project.

For comparison, at the Minto mine copper mineralization occurs within 13 horizontally stacked “gneissic” zones from 1-50m wide which vary in consistency and grade. At the Carmacks Copper deposit not all of the zones are near vertical nor are they all consistent at depth. Zone 4 is bowl-shaped and the southern half of the No. 1, No. 7 and 7A zones are interrupted and offset by faults. Generally the more gneissic material and number of gneissic zones in an area, the better the grade. In addition, contacts are sharp between mineralized and unmineralized rock with little obvious alteration *(Photo 3)*. Consequently, there can be difficulty in correlating between wider spaced drill holes and in intersecting the irregular, discrete zones.



Photo 3: Mineralized “gneissic” zone at Minto within massive granodiorite

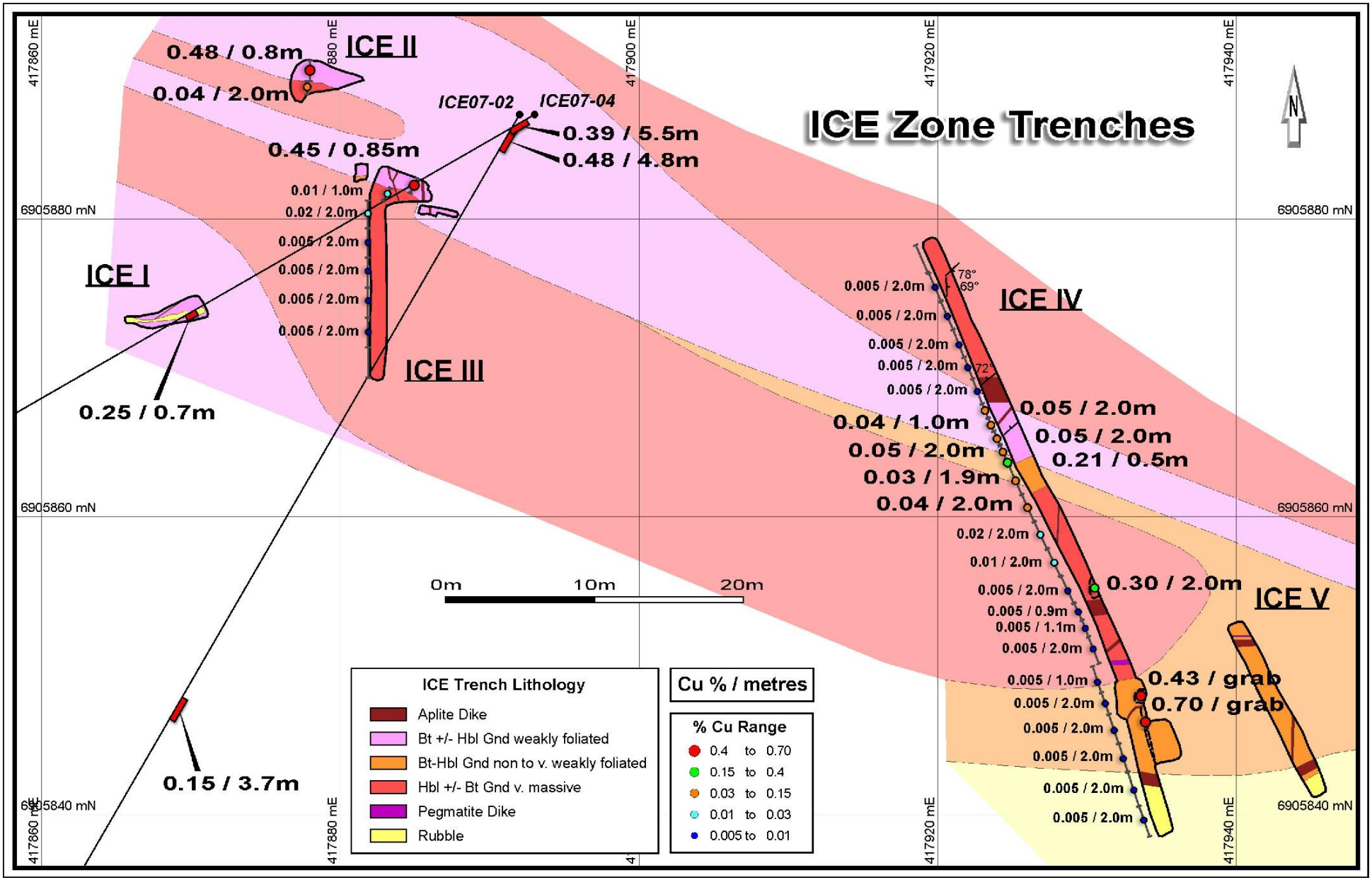

Figure 5: ICE Zone trenches at the BCIce Showing

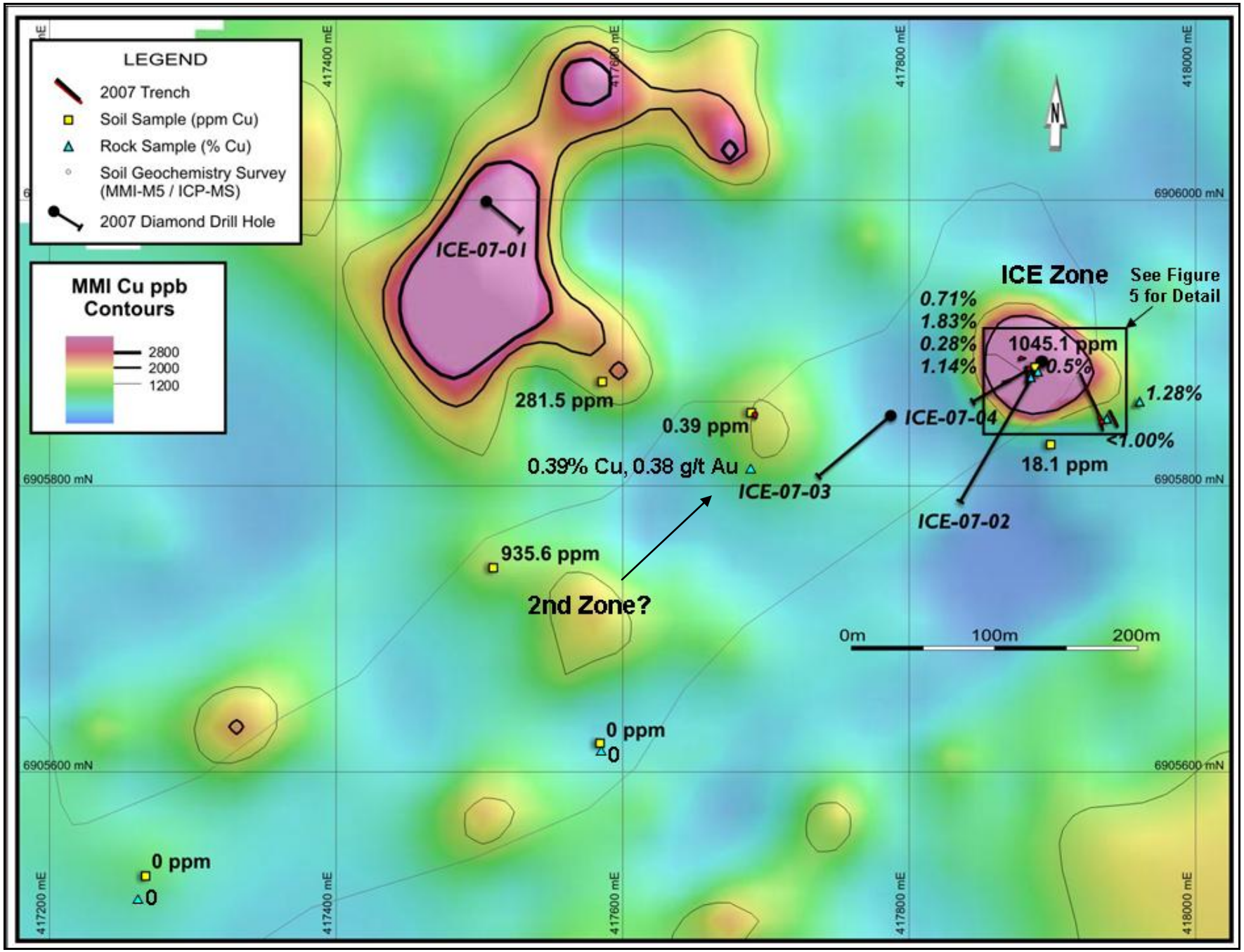

Figure 6: BCIce Showing

8.0 DEPOSIT TYPE

The Williams South Project lies within the southern portion of the Carmacks copper-gold belt, a 180 km by 60 km-wide north-northwest trending mineralized belt of similar intrusion-hosted copper-gold mineralization that includes the Minto Mine of Capstone Mining Corporation and the Carmacks Copper deposit of Western Copper Corporation (9 km southeast of the Williams South Project). Mineralization within the belt appears to fit a variant on the copper-gold porphyry deposit model as proposed by Tafti and Mortensen (2004) and Pearson and Clark (1979) for the two deposits. Several variations have been proposed including metamorphosed, deformed, and stalled porphyry models *(Tafti and Mortensen, 2004, Tafti, 2005 and Mortensen, 2014)*. The deposit model for mineralization within the Carmacks copper-gold belt remains controversial and has ranged from digested red-bed copper, to aborted and deformed porphyry, to iron oxide copper gold *(Hood et. al, 2009)*.

In the “stalled porphyry” model, Mortensen suggests that the porphyry style mineralization formed at a depth of less than 9 km with copper and gold exsolved from sulphide veins *(Mortensen, 2014)*. This was followed by active faulting, crustal thickening (resulting in the formation of shears, and burial to depths of 20 km, which stalled the system), followed by rapid uplift. The system was short lived (from 203-195 Ma), which is similar in age to the porphyry deposits (e.g. Kemess) of the Quesnel Trough, British Columbia. The alkaline porphyry deposits within Quesnellia in British Columbia formed at 204 Ma.

Mineralization on the Williams South Project has strong similarities to both Minto and Carmacks Copper, hosted by the same rock units with similar alteration (secondary biotite, magnetite-silica) and mineralization (gold-bornite association). It has been documented that the Minto and Carmacks Copper deposits are hosted by variably deformed plutonic rocks that occur as pendants and schlieren within slightly younger less deformed intermediate intrusive rocks of the Minto suite *(Tafti and Mortensen, 2004)*. Schlieren are fragile, usually elongate concentrations of mafic material within some intrusions. Genesis may be due to shearing of heterogeneities (enclaves or xenoliths), crystal sorting during convective or magmatic flow, or crystal settling. Petrographic and field studies of the more gneissic host rocks from Minto and Carmacks Copper show that they represent strongly deformed and metamorphosed intrusive rocks (orthogneiss), with the excess amount of biotite representing secondary (hydrothermal) biotite associated with strong hypogene potassic alteration *(Tafti and Mortensen, 2004)*.

Hornblende geochemical studies of plutonic and meta-plutonic host rocks at Minto and Carmacks Copper indicate that they formed in a continental magmatic arc setting *(Tafti and Mortensen, 2004)*. The setting, timing of mineralization and petrographic and field observations of the host rocks, mineralization and alteration led Tafti and Mortensen (2004) to conclude that the two deposits represent variations on typical copper (-gold) porphyry deposits.

It has been suggested that the highly foliated rocks controlling economic mineralization at the Carmacks Copper deposit are rafts and lenses (xenoliths) of augite-phyric volcanic rocks of the Povoas Formation within the Granite Mountain Batholith *(Hood et. al, 2009)*. The Povoas Formation occurs at the base of the Triassic aged Lewes River Group, part of Stikinia, and is exposed to the northeast of the Granite Mountain Batholith *(see Figure 3)*. Similarly mineralization at the Minto deposit has been described as being hosted by zones of strongly developed penetrative foliation, interpreted as shears or as rafts of volcanic rock within the granodiorite host.

Calc-alkaline porphyry copper-gold mineralization at the Kemess Mine (Kemess South deposit) and the Kemess North deposit in central British Columbia is hosted by Jurassic granodiorite intrusions and adjacent Upper Triassic augite-phyric flows of the Takla Group, indicating similar chemistry, age and deposit characteristics to mineralization within the Carmacks copper-gold belt. The main difference is the lack of foliated rocks associated with the mineralization.

Similarities exist between the Williams South Project and the Minto and Carmacks Copper deposits. The presence of ubiquitous magmatic epidote has been reported at Minto, Carmacks Copper and STU, suggesting depths of formation of 18 to 20 km, which far exceeds typical depths of formation for porphyry style deposits *(Hood et. al, 2009)*.

Based on the above discussion, the author believes that mineralization within the Carmacks copper - gold belt is hosted by schlieren zones (probably formed by crystal sorting or settling during magmatic flow) within Jurassic granodiorite and is consistent with a calc-alkaline porphyry copper-gold model (with similarities to the Kemess Mine and Kemess North deposit), but formed (or was buried) at a deep crustal level.

9.0 EXPLORATION (Figures 4-15)

Exploration by BCGold Corp. since the granting of the option from Shawn Ryan in March, 2007 has involved a property wide airborne magnetic and radiometric geophysical survey, approximately 3,551 MMI and 317 conventional grid soil samples from 5 grids, 62.4 line km of induced polarization geophysics from 3 grid areas, a 1.26 km high resolution multi-array induced polarization survey, property wide geological mapping and prospecting with concurrent geochemical sampling (33 rock, 10 soil and 6 stream sediment samples), a structural analysis, a 660 sample biogeochemical survey on WS, trenching on BCIce, WS and Copper Hill showings, 2,659m of diamond drilling in 14 holes (2 holes totaling 67.7m were lost and re-drilled), and infrared spectroscopy and petrography on the 2008 drill core.

9.1 Geochemistry (Figures 5 to 8)

9.1.1 Grid Soil Geochemistry (Figures 7 to 8)

A total of 3,551 grid MMI soil samples (3,264 on the WS claims and 287 from the ICE claims) and 317 conventional grid soils for comparison purposes (316 on ICE and 1 on WS), including quality assurance and quality control samples, were collected from the Williams South Project by BCGold Corp. The samples were collected from 5 grids, a large grid (WS) in the western property area to cover a 7 km extent of the projected southeastern strike extension of mineralization on the adjoining Carmacks Copper Project of Copper North Mining Ltd., a small grid to cover the BCIce showing, and 3 small grids on the north to northeast WS claims (NEWS, NE and NW). Grid locations are shown on Figure 7. All samples were collected by Ryanwood Exploration Inc. of Dawson City, Yukon (a company owned by the original vendor of the property, Shawn Ryan) in 2007 and 2008. A total of 57 blank and 100 field duplicate samples were submitted for quality control in the soil surveys.

The MMI soil samples were collected at a 50m sample spacing, primarily along 050º trending lines, generally 100m apart with the 3 isolated grids in the north to northeast property area 200m apart and the central portion of the BCIce grid at a 50m line spacing, covering approximately 35% of the Williams South property. MMI sampling is an analytical process that measures mobile metal ions reported to be useful in detecting mineralization beneath younger cover rocks and thick glacial till. The samples were collected using 1m soil augers and mattocks, whichever was appropriate depending on vegetative cover and the thickness of the organic horizon. Generally samples were collected 10-25 cm below the base of the organic horizon, were placed in plastic zip-lock bags and then into pre-numbered Kraft soil bags. The auger or mattock was cleaned after each sample with a J-cloth to avoid contamination.

Conventional soil samples were collected from the B-C horizons, irrespective of depth, with one meter soil augers, or with a mattock where necessary, depending on vegetative cover and the thickness of the organic horizon. Approximately 400-500 grams of soil were collected and placed in well marked pre-numbered Kraft soil bags. Both MMI and conventional soils were collected over a 1 km by 1 km grid over the ICE showing for comparison purposes, along northwest trending lines.

At each soil sample location, a GPS reading was taken using the pre-numbered soil sample bag for reference. Sample sites were marked in the field with pink flagging and a three inch aluminum tag with sample number, and locations recorded by GPS using UTM coordinates, Nad 83 datum, Zone 8 projection.

The conventional soils were sent to, and processed at, Acme Analytical Laboratories Ltd., Vancouver, British Columbia. Acme was an IS0 9001 accredited facility. Soil preparation (SS80) involved drying at 60°C and sieving to -80 mesh. Samples were analyzed for Al, Sb, As, Ba, Bi, B, Cd, Ca, Cr, Co, Cu, Ga, Au, Fe, La, Pb, Mg, Mn, Hg, Mo, Na, Ni, P, Ag, K, Sc, Sr, S, Tl, Th, Ti, Sn, W, U, V and Zn using Acme's Group 1DX-

MS(15) analysis, a 36 element ICP package which involves a nitric-aqua regia digestion on a 15g sample.

MMI samples were sent to, and processed at, SGS Mineral Services in Toronto, an ISO/IEC 17025 accredited facility where they were analyzed using a weak acid leach. Response ratios were calculated by determining the average value of the sample population, then dividing each sample value by the sample average. Response ratios are then plotted using percentile ranges to indicate anomalous areas. Contoured copper MMI soil results are shown in Figure 7 and overlain on the airborne vertical magnetic gradient contours Figure 8, with IP chargeability highs shown.

The 1 km by 1 km grid over the ICE showing, sampled by both methods, produced coincident anomalies with the conventional ICP anomaly slightly displaced down slope to the southeast, probably related to down slope dispersion. The coincident anomalies indicate the effectiveness of the MMI sampling method in detecting mineralized zones in this environment. The MMI survey outlined a copper MMI anomaly over the ICE zone and a 350 by 100m copper anomaly 400m to the west-southwest of the ICE zone *(Figure 6)*.

A northwest trending MMI soil anomaly was outlined on the WS grid along the projected southeastern strike extension of Zone 12 from the adjoining Carmacks Copper Project of Copper North Mining Ltd. The anomaly appears to “blow out” in the central grid area on lines 144 to 149N, generally correlates with the exposure of a northwest trending band of foliated granodiorite, and was tested by drill holes WS-07-05 to -07 *(Figure 7)*. Another discontinuous northwest trending anomaly occurs in the western WS grid on trend of Copper North’s Zone 8. It consists of highs in the extreme northwest corner of the claims, and trends northwest from the western end of L139N through lines 141 and 144N, proximal to the Copper Hill showing *(Figure 7)*.

An extensive area of anomalous copper in MMI soils occurs west of Merrice Lake in an area of limited exposure *(Figure 7)*, and is thought to be related to swampy terrain, similar to the response of conventional soils in swamps. However, within this area there is an exposure of a more favourable mafic intrusion of hornblendite to diorite along a low ridge in the old Bishi Minfile area, near the centre of L124N. The area of anomalous copper in MMI soils on the NEWS grid appears to be devoid of rock exposure and, although not swampy is poorly drained, which may explain the anomalies. However, more favourable mafic intrusive units have been mapped along trend of the anomalies.

Very little exposure is evident on the two grids on the northern WS claims. An old trench was found at 415200E, 6913600N, Nad 83, zone 8, but no mineralization, alteration or foliation was evident.

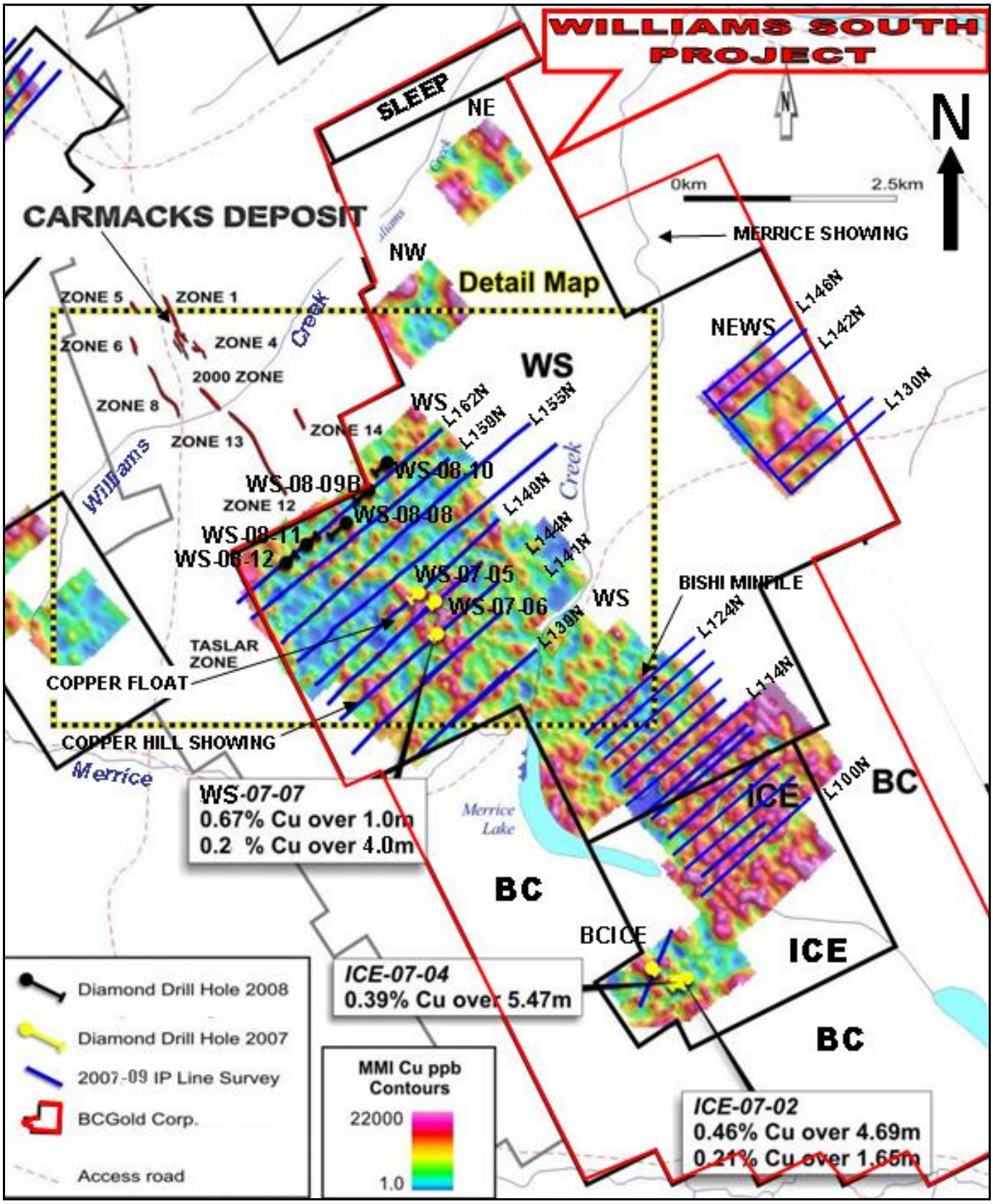

Figure 7: Copper MMI Soils

9.1.2 Reconnaissance Geochemistry (Figures 4 to 7)

During the process of geological mapping and prospecting on the Williams South Project in 2007 to 2009, 33 rock, 10 soil and 6 stream sediment samples were collected. Four days of mapping and prospecting, primarily in the BCIce showing, area were completed by Peter Ledwidge, Ann Doyle and Adam Fage in 2007, a 7 day prospecting program was conducted by Ken Galambos and Ralph Keefe in the fall of 2008, and 11 days of property scale mapping and prospecting were completed by Jean Pautler and Don Coolidge in the spring of 2008 and 2009, also with Adam Fage in 2008.

The rock samples primarily consisted of grab samples, and chip samples where possible, of rusty, foliated and or malachite stained granodiorite, with copper bearing quartz veins sampled at the Merrice showing. The soil samples were collected from rusty zones in areas of foliated granodiorite. Stream sediment samples consisted of silts and moss mats collected along Merrice Creek, with one sample collected from a small creek draining the BCIce showing. Rock samples were placed in clear plastic sample bags and soils and stream sediments in waterproof Kraft bags. All samples were located and recorded by GPS using UTM coordinates, Nad 83 datum, Zone 8 projection, numbered and secured in the field.

The 2008 and 2009 samples were sent to Eco Tech Laboratory Limited (Alex Stewart Geochemical, now ALS Minerals) for gold and ICP analysis. Details are discussed under section 11.0, “Sample Preparation, Analysis And Security”. Sample descriptions, locations and results are documented in Appendix II with select anomalous results plotted on Figure 4. The 2007 samples were assayed for gold and copper only, the same as for trench samples. Reconnaissance grab samples (3) collected from the BCIce showing area in 2007 will be discussed under section 9.1.4, “Trenching”, below.

Significant results were obtained from three areas, Copper Hill, Copper Float and the Merrice Minfile showing *(Figures 4 and 7)*. The showings are discussed in detail under section 7.3, “Mineralization”.

The Copper Hill showing discovered in 2008 *(Galambos, 2008)* on the southwestern WS grid at 6909150mN, 414100mE on L144N at 10335E, 2.5 km southeast generally along trend of Zones 5, 6 and 8 of the Carmacks Copper Project, consists of malachite, lesser chrysocolla, minor azurite, and chalcocite mineralization, primarily hosted by more mafic intrusive phases. Results of 0.85% Cu, 0.42 g/t Au and 5.3 g/t Ag from a grab sample and 0.19% Cu and 0.08 g/t Au across 1.5m from the same location were obtained. Mineralization appears to follow the foliation at 315º/80E, and was discontinuously traced for 20m along strike and 3-5m in width, limited only by exposure. Alteration consists of epidote, limonite, magnetite and quartz flooding and veinlets.

The Copper Float showing consists of a 30 by 25 cm rounded float boulder of malachite stained foliated biotite-hornblende granodiorite with secondary magnetite and trace bornite discovered in 2007 on the WS grid at 414311mE, 6909970mN. A grab sample of the float returned 0.94% Cu and 0.26 g/t Au. It occurs within an area of foliated

granodiorite along trend of Zone 12-13 of the Carmacks Copper Project. Mineralization at the Merrice showing (417439mE, 6914656mN) is confined to quartz veins and adjacent wallrock. The main vein, explored by the adit returned 0.52% Cu over the 1.5m vein. The diorite footwall with malachite and trace chalcopyrite, 3m south of the vein carried 0.14% Cu. A grab sample from a bornite rich 0.5m vein south of the now caved adit returned 2.52% Cu, 0.51 g/t Au and 42 g/t Ag.

A deep orange coloured soil exposed along an old cat trail in the northern WS grid area returned an anomalous value of 28 ppm Cu proximal to weakly foliated granodiorite. The sample is also proximal to exposures of the overlying Carmacks basalt unit, which could account for the elevated copper response.

One copper anomalous stream sediment sample, returning 23 ppm Cu, was obtained from Merrice Creek, just upstream of its intersection with the tributary draining Merrice Lake. This area corresponds to where the northwest trending band of foliated granodiorite crosses the creek. Fine gold has also been panned from this section of the creek and an old placer camp is situated at the north end of Merrice Lake.

9.1.3 Biogeochemical sampling (Figures 8 and 15)

In 2012 BCGold Corp completed a biogeochemical orientation survey, consisting of 116 black spruce bark/twig/needle and labrador tea samples at 10m spacings on two lines 20m apart, parallel to the drill trace of hole WS08-09B, which intersected significant copper mineralization. The survey, especially the spruce twig and labrador tea, appeared to detect the mineralization encountered in the drill hole (Dumas, 2013) In 2013 550 twig samples (including 28 duplicate samples) were collected from 12 lines at 20m spacings, primarily from the WS (WS West) grid, with 2 lines on the northern ICE grid *(Dumas, 2014)*. A strong copper-silver-nickel-tungsten biogeochemical anomaly occurs between drill holes WS-08-08 and -11 and lies directly on trend of Zone 12 on the Carmacks Copper Project. Further south a strong tungsten-antimony-cerium-chromium and weak copper-molybdenum-nickel-silver anomaly occur just uphill of the area tested by the 2007 WS drilling. The anomalies are summarized in Figures 8 and 15.

The following procedure is summarized from Dumas (2013 and 2014). In the orientation survey approximately 50g of outer bark for the bark samples was scraped around the entire trunk approximately 4 - 5 feet off the ground from a selection of about 2-3 similar sized trees using a plastic paint scraper into a large poly sample bag, then transferred to a paper bag. The twig and needle samples were collected by clipping the ends of small branches (approximately 200g) from about 2-3 similar sized trees approximately 6 inches in length. Labrador tea foliage was collected by plucking approximately 200g of leaves by hand from the bushes. All samples were collected from healthy specimens within 1 or 2m of the sample site and placed in labeled paper bags. In the 2013 survey the twig samples were collected by clipping approximately 15 cm off the ends of small branches) from similar sized trees showing new growth (with a target tree height of 5m) and placing approximately 250g in 5x7 Hubco bags.

9.1.4 Trenching (Figures 5, 6, 8 and 15)

In 2007 approximately 60m of trenching in 3 trenches was undertaken on the ICE zone, excavated intermittently over an 80m strike length. A total of 45 rock samples, including 2 gold standards for quality control, were collected from the trenches and outcrop exposures. Outcrop and trench chip samples returned 0.48% Cu over 0.8m, 0.45% Cu over 0.85m and 0.30% Cu over 2.0m *(Figure 5)*. Copper and gold grades from grab samples ranged up to 1.83% Cu, 0.25 g/t Au and 1.28% Cu, 0.41 g/t Au. Mineralization consists of malachite which is primarily associated with discrete zones of weak to moderate foliation dipping 25-30°NE, with the foliation defined by secondary biotite (potassic) alteration. Sample descriptions, locations and results are documented in Appendix II with results plotted on Figure 5. The samples were assayed for gold and copper only, as described under section 11.0, “Sample Preparation, Analysis And Security”.

Three grab samples were also collected from the BCIce showing area in 2007 during reconnaissance mapping and prospecting. One sample, 200m south-southwest of the ICE zone returned 0.39% Cu with 0.38 ppb Au from foliated granodiorite *(Figure 6)*. This may correspond to the second zone, about 300m west of the main (ICE) zone, in Canam (1982).

Seven trenches were apparently excavated on the WS in the fall of 2009. A trench was excavated at the projected surface extent of mineralization intersected in DDH WS-08-09B. No samples were collected due to the predominance of permafrost. The Copper Hill showing was also trenched, with results of 0.40% Cu over 0.5m. Two additional trenches were excavated upslope of the showing over a copper MMI soil anomaly. The trenches may have intersected permafrost as no samples are plotted. Three trenches were excavated over an induced polarization chargeability anomaly between 147N and 151N, on trend of mineralization encountered in WS-07-07. Grab samples of 0.71, 1.87 and 2.83% Cu are reported from the southern trench at 414700E/6910100N. Two or three additional trenches appear to have been excavated on the BCIce showing. Grab samples of 0.32 and 0.10% Cu are reported 200m west of the main zone. This zone may correspond to the second zone from Canam (1982). No other data or information could be found regarding the trenching program.

9.2 Geophysics (Figures 8 to 10)

In 2007 a 3,295 line km airborne magnetic and radiometric geophysical survey, with a 200m line spacing was flown by Aeroquest Surveys, Mississauga, Ontario for BCGold Corp. over their Carmacks Copper-Gold Project which included the Williams South Project. The vertical gradient magnetic map is shown as a base in Figure 8. The airborne vertical gradient magnetic signature shows strong linear northwest magnetic high trends on strike of those related to mineralized zones on the adjoining Carmacks Copper Project *(Figure 8)*. The airborne radiometric survey also shows that most of the

Williams South Project is underlain by a similar thorium/potassium signature to that of the Carmacks Copper deposit *(Figure 9)*. The northeast trending thorium/potassium low through the central WS claims corresponds to Merrice Creek.

A total of 62.4 line km of pole-dipole induced polarization was conducted over the Williams South Project in 3 grids (WS West, ICE, and NEWS), with one line at the BCIce showing, between 2007 and 2009 by Aurora Geosciences Ltd. for BCGold Corp. The surveys were undertaken along northeast trending lines (primarily 050° with the BCIce line at 020°). The grid lines were cut by Coureur des Bois Ltd. of Whitehorse, Yukon Territory. A modified pole-dipole array was used with 100m dipole spacing, reading to the 6th dipole separation *(Figures 8 and 15)*. Aurora Geosciences Ltd. performed 2D IP inversions and 3D IP inversions were performed by Mira Geosciences on the WS West grid. The data between the winter survey (modified due to extreme cold) and summer surveys were not consistent for either the resistivity or the chargeability suggesting significantly different current paths between the two geometries of the surveys *(Hildes, 2008)*.

The WS West tested magnetic and linear copper MMI soil anomalies, and two new copper showings along trend of the Carmacks Copper deposit. The NEWS grid tests a strong copper MMI anomaly in an area of no exposure, and the ICE grid tests strong copper MMI anomalies in an area of poor exposure, with a more favourable mafic intrusion at the north end.

The following interpretation of the WS West survey is summarized from Hildes (2008). An orientation survey across L4400 on the adjoining Carmacks Copper Project of Copper North Mining Corp. (formerly Western Copper) showed reasonably good correlation between the elevated chargeability and intersected sulphides in Zones 13 and 12. There was not a strong resistivity signature. In the survey across BCGold's WS West grid open ended high chargeability zones were outlined coincident with copper MMI soil anomalies, suggesting the extension of Zone 12 onto the northern portion of the WS claims through the central sections of lines 162N and 159N, with the best signature on L159N. In addition a subtle resistivity low centered at approximately station 11500E corresponds with slightly elevated copper MMI soil results. A southwest directed hole from L159N/11550E was proposed *(Hildes, 2008)*. A resistive feature continues from L62N/12000E 159N, passing through approximately L155N/11800E, with the most prominent feature the elevated chargeability coupled with reduced resistivity on the far eastern parts of the lines.

Elevated chargeabilities occur on Lines 149, 147, 144 and 141N around station 10600E (in the 2D but not 3D inversions), particularly distinct on lines 141N (stronger IP) and 144N (more consistent IP, stronger MMI) and coincident with elevated copper MMI values. A steeply east dipping hole is recommended at station 10650E on L144N *(Hildes, 2008)*. A resistive feature (possibly continued from L152N) runs from about L149N/11200E through to L141N/11000E, with elevated MMI west of this feature.

Broadly elevated chargeability occurs on L135, strongest at 10800E, coincident with elevated copper MMI soil results, with significantly higher copper MMI results further to the east

The following interpretation of the ICE and NEWS surveys are summarized from Dziuba (2009). On the ICE grid two chargeability zones were outlined, one 300m wide from L124N to L120N, centered near station 13000E at an approximate 80 to 150m depth, coincident with a total magnetic field high, elevated copper soil, open to the north where foliated granodiorite is interpreted to occur. The second chargeable zone, which occurs on L118N at a depth of 130m is much broader, but has poorer resolution, and occurs proximal to a larger MMI anomaly and a total field magnetic high. The magnetic high is, however, interpreted as being underlain by basaltic volcanic rocks of the Upper Cretaceous Carmacks Group, based on magnetic signature and MMI soil geochemistry.

On the northwestern NEWS grid, a north-northwest trending vertical gradient magnetic lineament may explain the sharp contrast in resistivities and chargeabilities, generally with low resistivity and chargeability in the southwest and higher values in the northeast. There are three chargeability anomalies occurring at an approximate 80 to 120m depth and identified as NEWS 1, 2 and 3. NEWS 1, proximal to a total magnetic field high and elevated copper MMI, occurs on L142 and 144N at 16350E and 146N/16750E, NEWS 2 (lines 132 and 134N/16550E) is proximal to elevated copper MMI and a magnetic lineament and NEWS 3 (lines 132 and 130N/15900E) is coincident with a total magnetic field high. NEWS 2 has higher chargeability values than NEWS 1 and 3.

In 2013 a high resolution induced polarization survey, consisting of one long traverse 1260m in length, was run along standard IP L162N, which covers drill holes WS08-08, -09B and -11. Several arrays were tested with the optimum being inverse schlumberger (using 121 electrode, 600m Hz length) and extended dipole-dipole (using 252 electrode, 1260m Hz length). The survey shows mineralization in WS-08-09 to be related to a resistivity low feature below a resistivity high feature and just northeast of and above a chargeability high feature. Overall a dip of -45°NE is suggestive. *(Refer to Fage, 2013.)*

A small VLF electromagnetic survey (readings at 20m spacings on 12 lines) outlined VLF-EM conductors proximal to biogeochemical anomalies on the WS West grid *(Dumas, 2014)*. VLF-EM interpretation suggests that there is a northwest trending conductor approximately 100m west of the surface extent of known mineralization in WS-08-09, which is in fact coincident with a stronger geochemical signature than that shown over the known mineralization. This new target, defined by a strong copper-silver-nickel-tungsten biogeochemical anomaly, occurs between WS-08-08 and -11 and lies directly on trend of Zone 12 on the Carmacks Copper Project. Further south, in the vicinity of the 2007 drilling, VLF-EM interpretation shows a northwest trending conductor which can be traced for 700m and remains open to the north. This conductor, which lies uphill and just west of the 2007 WS holes, is coincident with a strong tungsten-antimony-cerium-chromium and weak copper-molybdenum-nickel-silver anomaly. *(Refer to Figures 8 and 15.)*

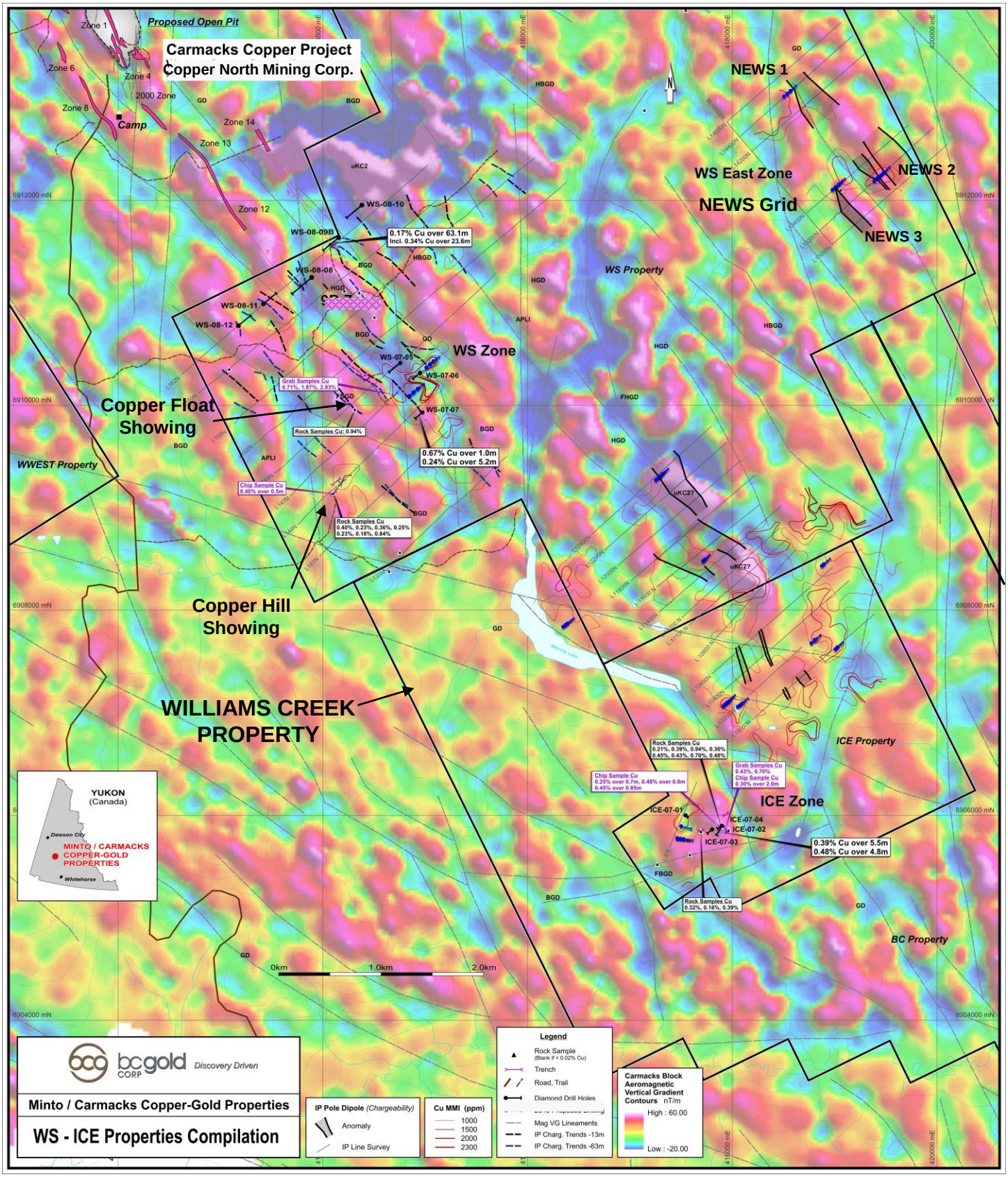

Figure 8: Compilation Map over Vertical Gradient Magnetics (to be printed at 11” by 17”)

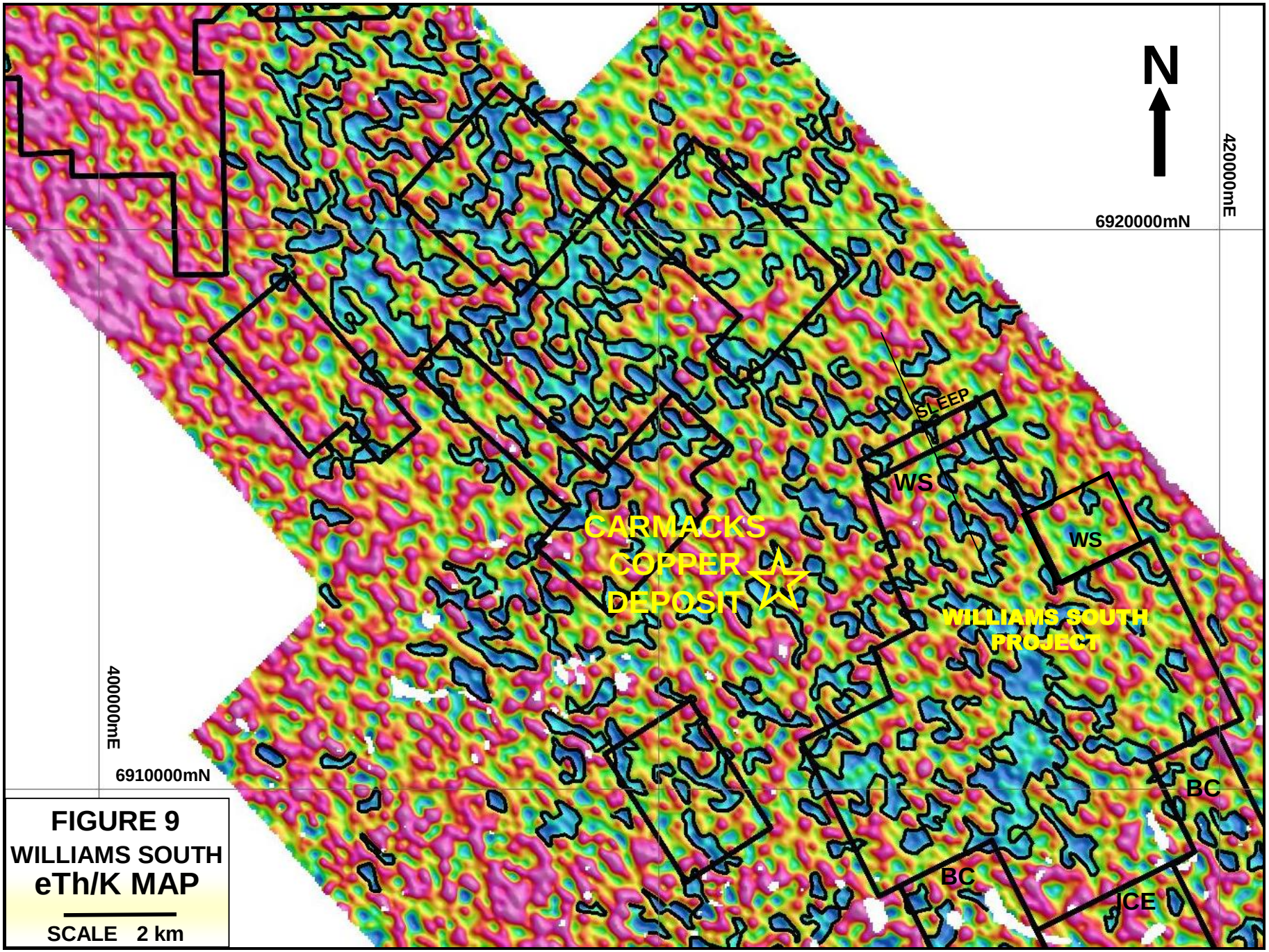
N
420000mE
6920000mN
SLEEP
WS
WS
CARMACKS
COPPER
DEPOSIT
WILLIAMS SOUTH
PROJECT
BC
BC
CE
400000mE
6910000mN
FIGURE 9
WILLIAMS SOUTH
eTh/K MAP
SCALE 2 km

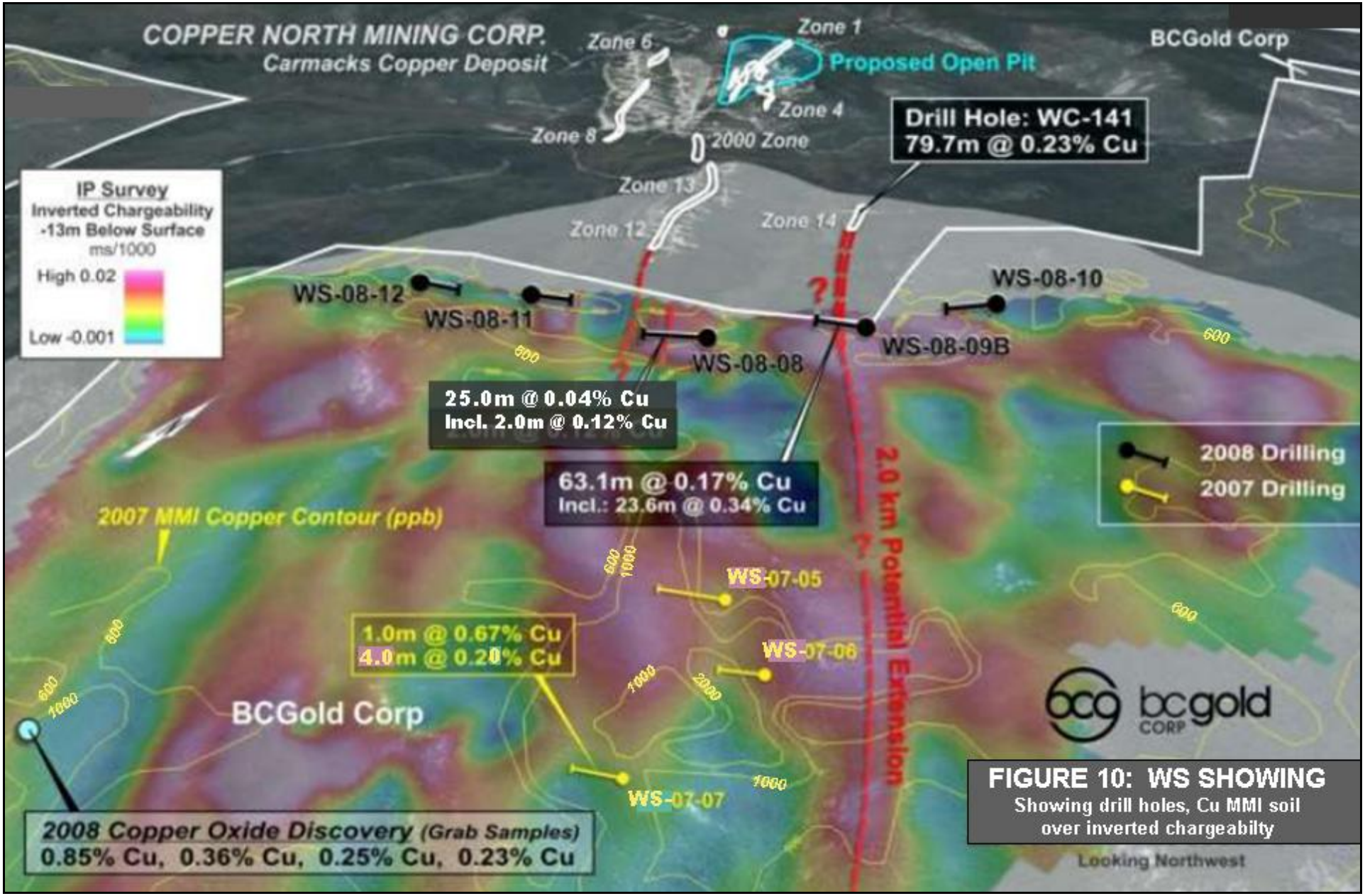

FIGURE 10: WS SHOWING
Showing drill holes, Cu MMI soil over inverted chargeabilty

10.0 DRILLING Figures 6-7 and 11-14

The only known drilling on the Williams South Project is 2,659.4m of diamond drilling in 14 holes, completed by BCGold Corp. in 2007 and 2008 (2 holes totaling 67.7m were lost and re-drilled). A total of 1360m in 7 holes were drilled in 2007 and 1299.4m in 7 holes in 2008. There is no record or evidence of any previous drilling in the project area. The diamond drilling was carried out by Kluane Drilling Ltd. of Whitehorse, Yukon Territory utilizing a KDHT 600 drill with NTW thin-walled wireline tools. The drilling was helicopter supported by Trans North Helicopters Ltd., from their seasonal base in Carmacks, Yukon.

The drill holes were surveyed in using a hand held GPS unit and a Brunton compass. In the 2008 drilling a FlexIt MultiSmart survey tool was utilized for down hole surveys. Single Shot down hole surveys were completed after every shift and multi shot surveys were completed at the end of the hole.

The 2007 drill core is stored at the collars for ICE07-02 and -04 at 417890mE, 6908728mN beside a good helipad at 417883mE, 6905881mN, Nad 83, Zone 8 projection. The 2008 drill core is stored at Carmacks Core Storage (Mona Garvice), 108 Garvice road, Carmacks, Yukon on the northwest side of the warehouse. Select core boxes containing mineralized intercepts from the 2007 program are stored at the office of Aurum Geological Consultants Inc., Whitehorse and from the 2008 program at the office of BCGold. A number of the drill sites and select core intervals have been inspected by the author. Drill collars are shown in Figure 7, with a detail of the ICE drill holes in Figure 6 and a detail of the WS drill holes in Figure 10. Cross sections are shown in Figures 11 to 14. Diamond drill hole specifications are summarized in Table 2, below. Strip logs are enclosed in Appendix IX.

Table 2: Diamond drill hole specifications

Drill Hole Number	Easting Nad 83	Northing Zone 8	Elev (m)	Az. (°)	Dip (°)	Length (m)	Samples	
							No.	QAQC
ICE-07-01	417505	6905999	770	130	-80	181.36	25	1S, 1B
ICE-07-02	417892	6905887	825	210	-65	267.61	23	1S, 1B
ICE-07-03	417787	6905849	826	230	-70	192.33	13	1S, 1B
ICE-07-04	417893	6905887	825	240	-75	217.93	22	1S, 1B
WS-07-05	414753	6910415	857	230	-50	217.93	4	0
WS-07-06	414947	6910319	833	230	-50	141.12	0	0
WS-07-07	414970	6909932	846	230	-50	141.73	16	?
WS-08-08	413890	6911242	855	230	-50	292.60	132	8S,8B,7D
WS-08-09	414156	6911632	850	230	-50	33.86	0	lost hole
WS-08-09A	414156	6911632	850	230	-53	33.86	0	lost hole
WS-08-09B	414156	6911632	850	230	-60	294.13	84	5S,5B,5D
WS-08-10	414378	6911949	892	230	-60	224.94	14	1D, 1B
WS-08-11	413419	6910982	921	50	-50	188.98	4	1S
WS-08-12	413174	6910768	952	50	-50	231.04	0	0
TOTAL						**2659.42**	**337**	**49**

Drill holes ICE-07-01 to -04 (859.23m) targeted the BCICE showing and copper MMI soil anomalies in the area, with 83 samples submitted for analysis. An additional 500.78m in 3 holes were drilled in 2007 as ICE-07-05 to -07 and are marked as such on

earlier maps, but are now referred to as WS-07-05 to -07. These holes targeted copper MMI soil anomalies on the WS grid, approximately 2 to 2.5 km along trend of Copper North's Zone 12, with 20 samples submitted for analysis. The 1300m in 7 holes drilled in 2008 (WS-08-09 and -09A were lost near surface), with 234 samples submitted for analysis, targeted five discrete induced polarization geophysical and/or copper MMI soil anomalies along or proximal to L162N near the northern WS claim boundary, approximately 0.5 to 1 km along strike from Copper North's Zones 12 and 14. A total of 337 samples of drill core were submitted for analysis in the 2007 and 2008 drill programs with an additional 49 samples submitted for quality assurance and quality control. Significant intersections are tabulated below.

TABLE 3: Significant drill hole results

DDH No.	From (m)	To (m)	Length (m)	Cu (%)
ICE-07-01	16.13	39.11	24.4	0.04
ICE-07-02	3.25	8.08	4.8	0.48
and	107.80	111.48	3.68	0.15
ICE-07-04	2.78	8.25	5.47	0.39
and	103.82	104.47	0.65	0.26
WS-07-07	51.75	52.75	1.0	0.67
and	104.0	105.2	1.2	0.38
and	107.8	111.8	4.0	0.20
WS-08-8	238.0	263.0	25.0	0.04*
incl.	246.5	250.0	3.5	0.10
and	261.0	263.0	2.0	0.12
WS08-09B	**46.0**	**109.1**	**63.1**	**0.17***
incl.	46.0	66.0	20.0	0.13
and	**85.5**	**109.1**	**23.6**	**0.34**

** using value of 0 for 3 unsampled intervals*
NB lengths are thought to approximate true widths (except for in ICE-07-01 where true width is not known), but due to limited drilling have not been determined.

The most significant copper mineralization was intersected in drill hole WS08-09B, targeting a weak copper MMI anomaly coincident with a pronounced 2 km long linear induced polarization chargeability high geophysical anomaly *(Figure 10)*, 1 km along strike from Copper North's Zone 14; Zone 14 returned 0.23% Cu over 79.7m in hole WC07-141 *(Western Copper news release November 22, 2007)*.

Mineralization in WS08-09B *(Figure 11)* occurs in two discrete and relatively homogenous intervals of foliated hornblende granodiorite (hornblende schist) within a white megacrystic alkali feldspar granodiorite. Mineralization in the upper interval, which averages 0.13% Cu over 20.0m from 46.0 to 66.0m, consists primarily of pyrite and chalcopyrite intermixed in foliated schist. Massive chalcopyrite occurs along the edges of carbonate stringers and malachite occurs along fractures. Chalcopyrite mineralization occurs in a similar fashion in the lower interval from 85.5 to 109.1m, averaging 0.34% copper over 23.6m. Chalcopyrite and fracture controlled malachite occur intermixed with pyrite in foliated hornblende schist. Massive chalcopyrite rims carbonate stringers and larger chalcopyrite grains display red oxidized rims. Propylitic (chlorite, epidote, carbonate, and sericite) alteration with secondary hematite and weak alkali feldspar alteration predominates.

Drill holes WS-08-10 to -12 did not intersect significant mineralization *(Figure 11)*. Holes WS-08-11 and -12 were drilled northeasterly, generally sub-parallel to the dip direction

of mineralization in the area. WS-08-10 would not have been drilled deep enough to intersect the mineralized horizons in WS08-09B, which appears to have a dip of 25 to 45°NE based on induced polarization geophysics, and the proximal Zone 13 on the adjoining Copper North's Carmacks Copper property tends to steepen with depth *(Copper North's website at www.coppernorthmining.com)*.

It is highly possible that Zone 12 extends between holes WS-08-08 and -11 *(Figure 10)*. A copper anomalous interval was intersected in WS-08-08 returning 0.04% Cu over 25m from 238 to 263m, including two narrow zones of mineralization (0.10% Cu over 3.9m and 0.12% Cu over 2.0m), which could reflect proximity to the strike extent of Zone 12. An infrared spectrographic survey of WS-08-11 (500m southwest of WS-08-08 but drilled to the northeast, sub-parallel to the dip of most mineralization in the area) displays a continuous chlorite spectral signature at the bottom, suggesting it may represent a halo to mineralization *(Fonseca, 2009a)*. Consequently there is good potential to intersect the extension of Copper North's Zone 12 between drill holes WS-08-08 and -11. In addition a coincident VLF-electromagnetic conductor and a strong copper-silver-nickel-tungsten biogeochemical anomaly occur between drill holes WS-08-08 and -11, with a proximal induced polarization chargeability high to the west.

WS-07-07 targeted a >5000 ppb Cu MMI soil anomaly and intersected a series of weakly mineralized zones of copper oxide (malachite) mineralization throughout the entire hole length, with 5-10% malachite on fractures and foliation planes *(Figure 12)*. Only 16 samples were collected from the hole, with mineralized intervals listed in Table 3 limited by sampling. The presence of malachite throughout the hole suggests proximity to the possible strike extensions of Zones 12 and/or 14.

Drilling of the main (ICE) zone at the BCIce showing (chip samples include 0.48% Cu over 0.8m, and 0.30% Cu over 2.0m) encountered two narrow, relatively flat-lying mineralized horizons in ICE 07-2 and -4 *(Figure 13)*. The upper and lower horizons returned 0.48% Cu over 4.8m and 0.15% Cu over 3.7m in ICE 07-2 and 0.39% Cu over 5.5m and 0.25% Cu over 0.7m in ICE 07-4, respectively. The upper horizon is described as foliated megacrystic biotite rich granodiorite with 5-10% malachite on fractures and along the foliation. The lower horizon is characterized by 5% malachite on fractures and along foliation planes. Both of the mineralized zones in Hole ICE-07-02 contain discreet grains of magnetite. This style of commonly occurs distal to larger zones so may have potential along strike or down dip to the northeast.

ICE 07-1, 400m west-northwest of the ICE zone *(Figure 6)*, intersected anomalous mineralization, with 0.04% Cu over 24.4m, despite being drilled along, as opposed to perpendicular to, the mineralized trend *(Figure 14)*.

Mineralized intervals in drilling are commonly associated with enhanced gold with a maximum of 190 ppb Au from ICE-07-04. In a study of the 2008 core *(Fonseca, 2009a)* an enrichment in calcium, iron, molybdenum, thallium, tellurium, mafic-associated elements (magnesium, nickel, cobalt), tin, and sphalerite associated elements (zinc, selenium, cadmium, vanadium) was noted. The elements potassium, sodium, lanthanum, and cerium were found to be enriched in the footwall and hangingwall of mineralized zones, suggesting that ore associated mineral alteration assemblage immediately outside ore zones may be propylitic, and possibly overprinting potassic.

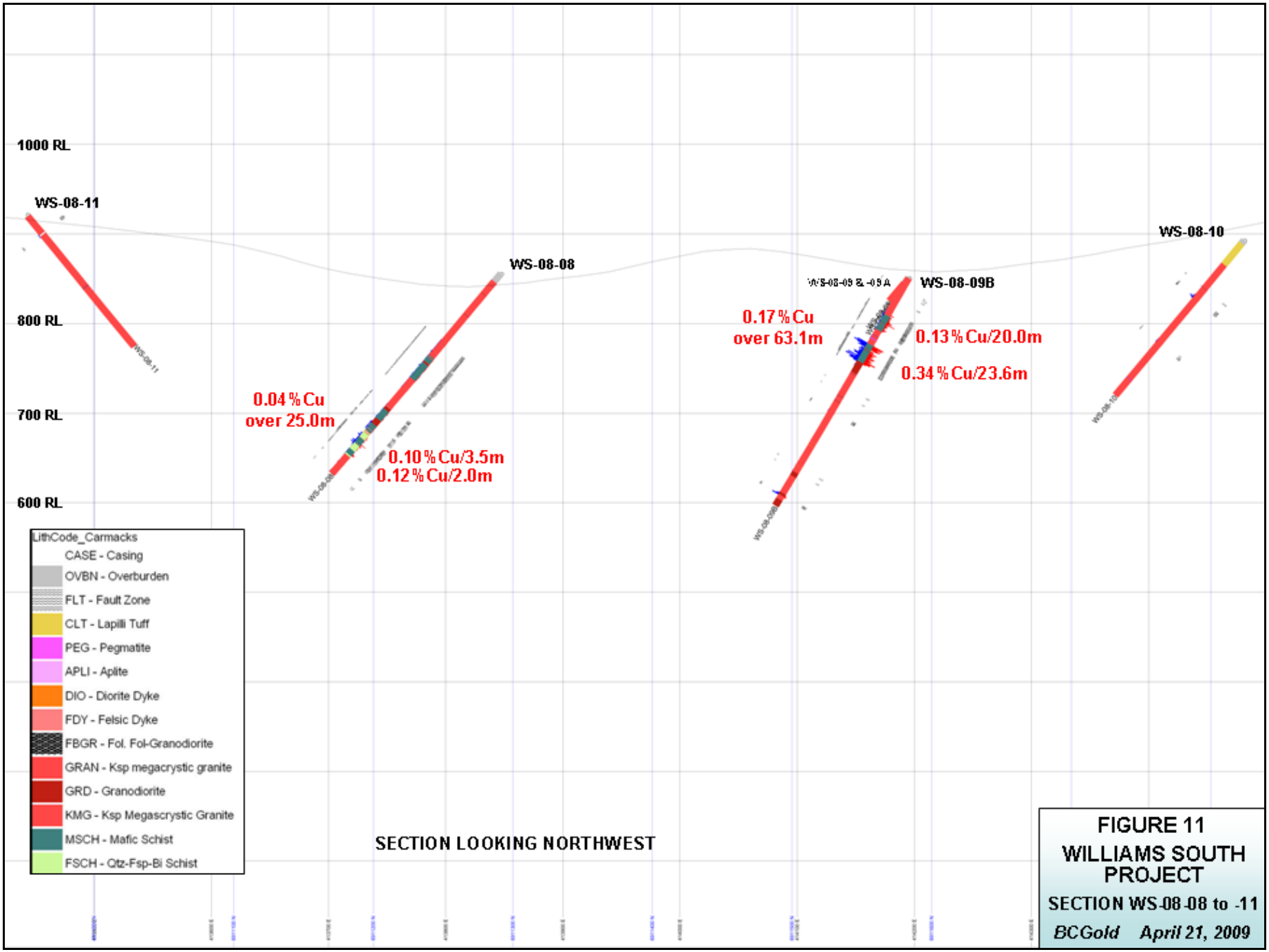
1000 RL
800 RL
700 RL
600 RL
WS-08-11
WS-08-08
WS-08-09 & -09A
WS-08-09B
WS-08-10
0.04 % Cu
over 25.0m
0.10 % Cu/3.5m
0.12 % Cu/2.0m
0.17 % Cu
over 63.1m
0.13 % Cu/20.0m
0.34 % Cu/23.6m
LithCode_Carmacks
CASE - Casing
OVBN - Overburden
FLT - Fault Zone
CLT - Lapilli Tuff
PEG - Pegmatite
APLI - Aplite
DIO - Diorite Dyke
FDY - Felsic Dyke
FBGR - Fol. Fol-Granodiorite
GRAN - Ksp megacrystic granite
GRD - Granodiorite
KMG - Ksp Megascrystic Granite
MSCH - Mafic Schist
FSCH - Qtz-Fsp-Bi Schist
SECTION LOOKING NORTHWEST
FIGURE 11
WILLIAMS SOUTH PROJECT
SECTION WS-08-08 to -11
BCGold April 21, 2009

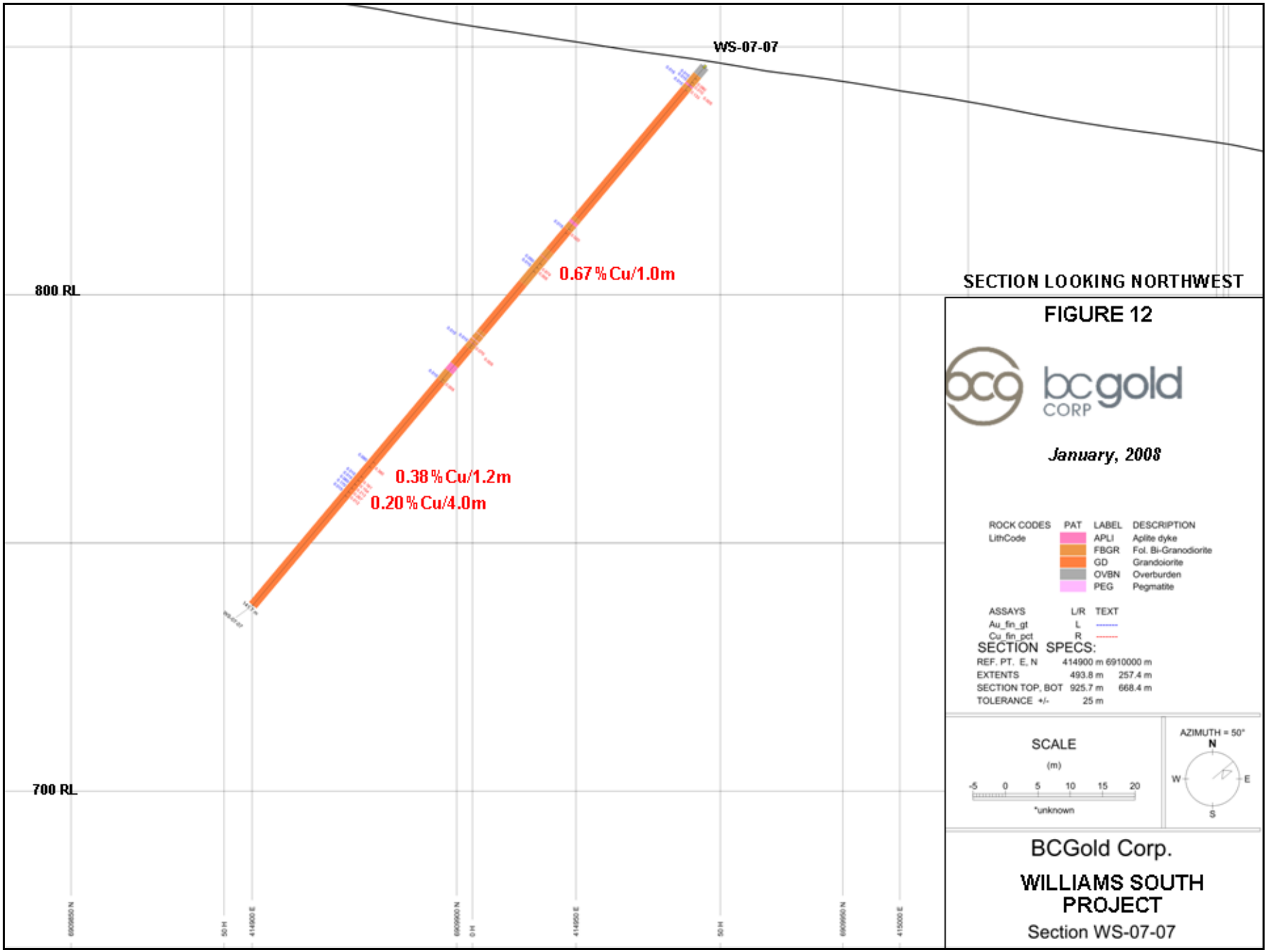
WS-07-07
0.67 % Cu/1.0m
0.38 % Cu/1.2m
0.20 % Cu/4.0m
800 RL
700 RL
SECTION LOOKING NORTHWEST
FIGURE 12
bcgold CORP
January, 2008
ROCK CODES PAT LABEL DESCRIPTION
LithCode
APLI Aplite dyke
FBGR Fol. Bi-Granodiorite
GD Grandoiorite
OVBN Overburden
PEG Pegmatite
ASSAYS L/R TEXT
Au_fin_gt L
Cu_fin_pct R
SECTION SPECS:
REF. PT. E, N 414900 m 6910000 m
EXTENTS 493.8 m 257.4 m
SECTION TOP, BOT 925.7 m 668.4 m
TOLERANCE +/- 25 m
SCALE
(m)
-5 0 5 10 15 20
*unknown
AZIMUTH = 50°
N
W
E
S
BCGold Corp.
WILLIAMS SOUTH PROJECT
Section WS-07-07

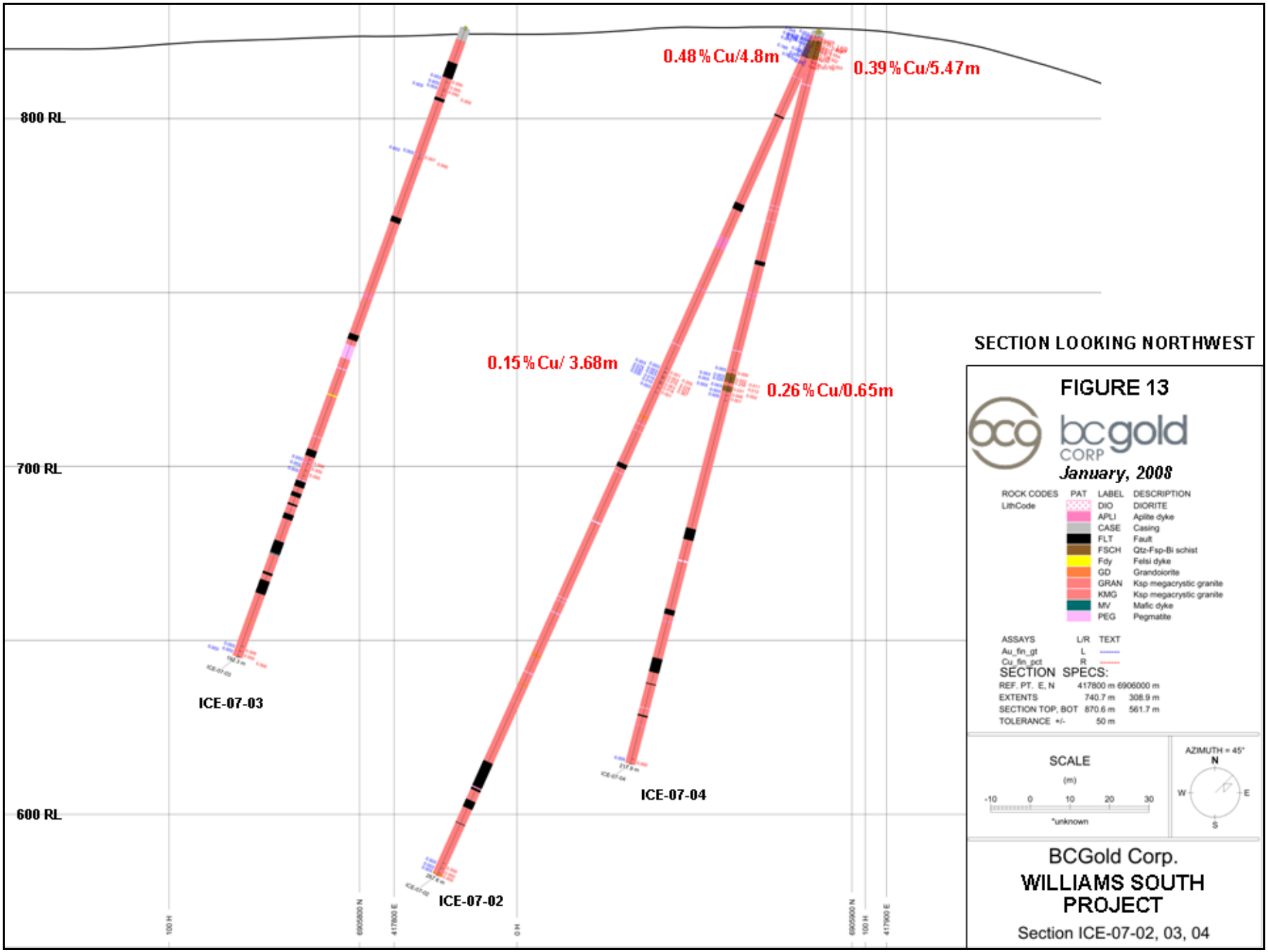
800 RL
700 RL
600 RL
0.48 % Cu/4.8m
0.39 % Cu/5.47m
0.15 % Cu/ 3.68m
0.26 % Cu/0.65m
ICE-07-03
ICE-07-02
ICE-07-04
SECTION LOOKING NORTHWEST
FIGURE 13
bcgold CORP
January, 2008
ROCK CODES LithCode
PAT LABEL DESCRIPTION
DIO DIORITE
APLI Aplite dyke
CASE Casing
FLT Fault
FSCH Qtz-Fsp-Bi schist
Fdy Felsi dyke
GD Grandiorite
GRAN Ksp megacrystic granite
KMG Ksp megacrystic granite
MV Matic dyke
PEG Pegmatite
ASSAYS L/R TEXT
Au_fin_gt L
Cu_fin_pct R
SECTION SPECS:
REF. PT. E, N 417800 m 6906000 m
EXTENTS 740.7 m 308.9 m
SECTION TOP, BOT 870.6 m 561.7 m
TOLERANCE +/- 50 m
SCALE
(m)
-10 0 10 20 30
*unknown
AZIMUTH = 45°
N
W
E
S
BCGold Corp.
WILLIAMS SOUTH PROJECT
Section ICE-07-02, 03, 04

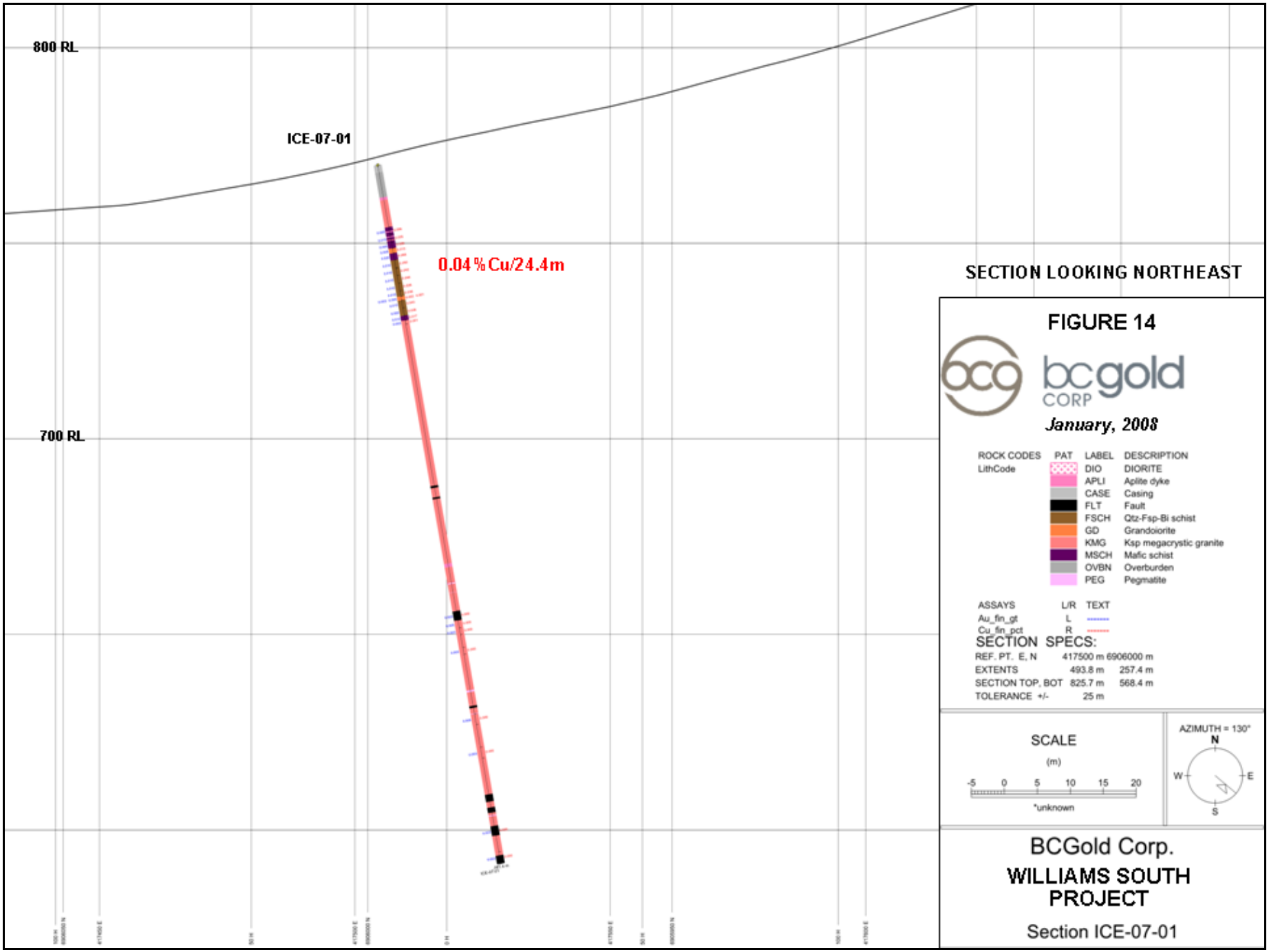
800 RL
ICE-07-01
0.04 % Cu/24.4m
700 RL
SECTION LOOKING NORTHEAST
FIGURE 14
bcgold CORP
January, 2008
ROCK CODES LithCode
PAT LABEL DESCRIPTION
DIO DIORITE
APLI Aplite dyke
CASE Casing
FLT Fault
FSCH Qtz-Fsp-Bi schist
GD Grandoiorite
KMG Ksp megacrystic granite
MSCH Mafic schist
OVBN Overburden
PEG Pegmatite
ASSAYS L/R TEXT
Au_fin_gt L
Cu_fin_pct R
SECTION SPECS:
REF. PT. E, N 417500 m 6906000 m
EXTENTS 493.8 m 257.4 m
SECTION TOP, BOT 825.7 m 568.4 m
TOLERANCE +/- 25 m
SCALE
(m)
-5 0 5 10 15 20
*unknown
AZIMUTH = 130°
N
W
E
S
BCGold Corp.
WILLIAMS SOUTH PROJECT
Section ICE-07-01

10.1 Drill Sampling Method and Approach

The core was delivered to the core processing site. Block markers in imperial units were first converted into metric units and the core was then metered with a black marker or yellow grease pencil. Interval lengths and descriptions of lithology, alteration, structure, mineralization, and sample intervals were all entered. Lithological units less than 0.3m were generally not noted unless of specific interest. The 2007 core logging and sampling was completed by R. Al Doherty and Joanna Ettlinger (Hodge) of Aurum Geological Consultants Inc., and in 2008 by Geoff Newton and Gary Sidhu of BCGold Corp. Core boxes were labeled with aluminum tags and core was photographed.

After logging, intervals for geochemical analysis were selected for sampling, primarily chosen for their potential to contain copper and gold, but also based on alteration, lithology, and to characterize background values for some rock units (for example dykes). The selected core samples were marked both on the core and on the core box in red grease pencil. Sample lengths varied between 0.14 and 3.05m and were generally 1.0m in length. A total of 337 samples of drill core were submitted for analysis with 49 additional QAQC samples. Drill core samples were split, and one half of the core replaced in the core box for future reference, and the other half bagged in numbered plastic bags, placed in rice bags and sealed for shipping. The field duplicates consisted of quartering the remaining half core. Core samples were tracked by three-part sample tag books. One part was placed in the core box at the end of the assay interval, one tag went with the sample for assay and the last tag was kept as a record.

11.0 SAMPLE PREPARATION, ANALYSIS AND SECURITY

All 2007 to 2009 core and rock, stream sediment and reconnaissance soil samples were placed in rice bags in the field, secured and delivered to the sample preparation laboratory of Eco Tech Laboratory Limited (now ALS Minerals) in Whitehorse for preparation. Samples were then internally sent directly to Eco Tech's facility in Kamloops, British Columbia for analysis.

All 2008 and 2009 rock samples were analyzed by Eco Tech Laboratory Limited for a multi-element ICP package which involves a nitric-aqua regia digestion. Gold was analyzed by fire assay with an atomic absorption finish on a 30 gram split. A multi-element ICP-MS package, including gold, was utilized for soil and stream sediment samples on a 15 gram split. Eco Tech was an ISO 9001:2000 accredited facility.

All 2008 drill core was analyzed by Eco Tech Laboratories Ltd. in Kamloops, a subsidiary of the global Alex Stewart Group, BC Certified Assayers and an ISO 9001-2000 certified laboratory. All samples were analyzed for 45 elements including copper by induction coupled plasma mass spectroscopy (ICP-MS) and for gold by fire assay on a 30g sample with atomic absorption spectroscopy (AAS) determination. Samples returning greater than 1 g/t gold were re-assayed by fire assay with a gravimetric measurement.

The 2007 drill core, trench and reconnaissance rock samples were analyzed for gold by fire assay with an atomic absorption finish ("FA-AA") on a 30 gram split, and for copper by induction coupled plasma emission spectroscopy (ICP-AES) following an aqua-regia digestion. Copper values over 1% were assayed by atomic absorption spectroscopy (AAS) following an aqua regia digestion. The 2008 drill core was analyzed for gold by fire assay with an atomic absorption finish ("FA-AA") on a 30 gram split, and for 46 elements by ICP which involves a nitric-aqua regia digestion.

At least 49 samples from the 2007 and 2008 drill programs were submitted by BCGold for quality assurance and quality control, consisting of 18 standards, 18 blanks and 13 field duplicates. Standards used were CGS-15 and CM-1. All standards returned results within acceptable limits for copper and gold. The duplicates and blanks indicated that the analytical results had an acceptable degree of precision and were free from contamination during sample preparation. In addition quality control procedures were implemented at the laboratory, involving the regular insertion of blanks and standards and repeat analyses of at least 25% of the samples, with re-analyses being performed for one sample in each batch on the original sample prior to splitting (resplit).

MMI samples were sent to, and processed at, SGS Mineral Services in Toronto, an ISO/IEC 17025 accredited facility. Samples are subjected to a weak leach resulting in dissolution of only the mobile metal ions in the soil, allowing the detection of deeply buried mineralization. A total of 57 blank and 100 field duplicate samples were submitted for quality control in the soil surveys. The conventional soils were sent to, and processed at, Acme Analytical Laboratories Ltd., Vancouver, British Columbia. Acme was an IS0 9001 accredited facility. Soil preparation (SS80) involved drying at 60°C and sieving to -80 mesh. Samples were analyzed for Al, Sb, As, Ba, Bi, B, Cd, Ca, Cr, Co, Cu, Ga, Au, Fe, La, Pb, Mg, Mn, Hg, Mo, Na, Ni, P, Ag, K, Sc, Sr, S, Tl, Th, Ti, Sn, W, U, V and Zn using Acme's Group 1DX-MS(15) analysis, a 36 element ICP package which involves a nitric-aqua regia digestion on a 15g sample.

The following procedure is summarized from Dumas (2013 and 2014). All 2012 biogeochemical samples were sent to Acme Laboratories in Vancouver. Samples were dried (the twig and needle samples were separated at this point), and macerated to a -100 mesh prior to analysis. Samples were then digested using a 1g split, digested first in HNO3 followed by aqua-regia. This was then analyzed using Acme's Group 1VE-MS ultratrace analysis, which is an ICP-mass spectrometry analysis which returns results for 53 elements: Au, Ag, Al, As, B, Ba, Bi, Ca, Cd, Co, Cr, Cu, Fe, Ga, Hg, K, La, Mg, Mn, Mo, Na, Ni, P, Pb, S, Sb, Sc, Se, Sr, Te, Th, Ti, Tl, U, V, W, Zn, Be, Ce, Cs, Ge, Hf, In, Li, Nb, Rb, Re, Sn, Ta, Y, Zr, Pt, Pd. The 2013 samples were analyzed at Activation Laboratories' Kamloops lab. Twig samples were dried, after which the needles were separated and discarded. The remaining twig material was then macerated and digested in an acid mixture composed of HCl with trace HF. Following digestion, a 250 mg sample was analyzed using a high resolution ICP-MS, with assay results returned for 63 elements. (Activation Lab codes: Prep – B2; Analysis – 2F).

There is no evidence of any tampering with the samples during collection, shipping, analytical preparation or analysis. All sample preparation was conducted by the laboratories. Sample preparation, security and analytical procedures appear to be adequate.

A sampling protocol should be implemented, involving the routine and regular insertion of blanks, standards and duplicates sent to the primary laboratory, and re-assaying of selected mineralized pulps at a second independent laboratory in the recommended drill program on the project.

12.0 DATA VERIFICATION

The geochemical data was verified by sourcing original analytical certificates and digital data. Analytical data quality assurance and quality control was indicated by the favourable reproducibility obtained in laboratory standards, blanks and duplicates, and in field blanks and duplicates for the MMI survey. Quality control procedures are documented in section 11.0, “Sample Preparation, Analysis And Security”.

There does not appear to have been any tampering with or contamination of the samples during collection, shipping, analytical preparation or analysis. In the author’s opinion, the data provided in this technical report is adequately reliable for its purposes.

13.0 MINERAL PROCESSING AND METALLURGICAL TESTING

The Williams South Project is at an early exploration stage and no mineral processing or metallurgical testing has been carried out. However, mineralization would be expected to be similar to that at the Carmacks Copper deposit to the northwest.

14.0 RESOURCE AND MINERAL RESERVE ESTIMATES

There has not been sufficient work on the Williams South Project to undertake a resource calculation.

15.0 ADJACENT PROPERTIES (Figure 2)

The Williams South Project adjoins the Carmacks Copper (Minfile 115I 008) property of Copper North Mining Corporation to the northwest *(Figure 2)*, which is discussed under section 8.0, “Deposit Type”.

16.0 OTHER RELEVANT DATA AND INFORMATION

To the author's knowledge, there is no additional information or explanation necessary to make this technical report understandable and not misleading.

17.0 INTERPRETATION AND CONCLUSIONS

The Williams South Project constitutes a property of merit based on significant drill intercepts from limited drilling, the presence of untested copper showings, northwest trending induced polarization chargeabilty, VLF-electromagnetic, ± proximal copper MMI soil anomalies, in part underlain by foliated to gneissic granodiorite, coincident with the margins of linear magnetic high features, similar to and directly along trend from the adjoining Carmacks Copper Project of Copper North Mining Corporation (*Figures 8 and 15)*.

The Williams South Project of BCGold Corp. lies less than 1km southeast along trend of the potential target of 7-9 million tonnes with a range of about 0.3 to 0.7% Cu (not a 43-101 resource) estimated by Copper North following their 2015 Phase 2 drilling program *(Copper North news release January 11, 2016)*

Only 2,659.4m of diamond drilling in 14 holes (including 67.7m in 2 holes that were lost in drilling) has been completed by BCGold Corp. on the property. The most significant copper mineralization, 0.17% Cu over 63.1m, was intersected from 46 to 109.1m in drill hole WS08-09B, targeting a weak copper MMI anomaly coincident with a pronounced 2 km long linear induced polarization geophysical anomaly, 1 km along strike from Copper North's Zone 14; Zone 14 returned 0.23% Cu over 79.7m in hole WC07-141 *(Western Copper news release November 22, 2007)*. Mineralization in WS08-09B occurs in two discrete and relatively homogenous intervals of foliated hornblende granodiorite (hornblende schist) with chalcopyrite, pyrite and malachite and an apparent dip of 25 to 45°NE. Alteration consist of propylitic (chlorite, epidote, carbonate, and sericite) with secondary hematite and weak alkali feldspar. This intersection has not been followed up along strike or down dip.

WS-08-08 intersected a copper anomalous interval of 0.04% Cu over 25m from 238 to 263m, including two narrow zones of mineralization (0.10% Cu over 3.9m and 0.12% Cu over 2.0m), which could reflect proximity to the strike extent of Copper North's Zone 12. WS-08-08 lies almost 600m southeast along trend of Zone 12, which is 275m northwest of the Williams South Project boundary. An infrared spectrographic survey of WS-08-11 (500m southwest of WS-08-08 but drilled to the northeast, sub-parallel to the dip of most mineralization in the area) displays a continuous chlorite spectral signature at the bottom, suggesting it may represent a halo to mineralization *(Fonseca, 2009a)*. Consequently there is good potential to intersect the extension of Copper North's Zone 12 between drill holes WS-08-08 and -11. In addition a coincident VLF-electromagnetic

conductor and a strong copper-silver-nickel-tungsten biogeochemical anomaly occur between drill holes WS-08-08 and -11, with a proximal induced polarization chargeability high to the west *(Figures 8 and 15)*.

WS-07-07 targeted a >5000 ppb Cu MMI soil anomaly and intersected a series of weakly mineralized zones of copper oxide (malachite) mineralization throughout the entire hole length, with 5-10% malachite on fractures and foliation planes. Only 16 samples were collected from the hole, with mineralized intervals of 0.67% Cu over 1.0m, 0.38% Cu over 1.2m and 0.20% Cu over 4.0m limited by sampling. The presence of malachite throughout the hole suggests proximity to the possible strike extensions of Copper North's Zone 12. Grab samples from a trench about 300m northwest of the collar of WS-07-07 returned 0.71, 1.87 and 2.83% Cu, and coincide with a 700m long, northwest trending VLF-electromagnetic conductor, which is open to the north and coincident with a strong tungsten-antimony-cerium-chromium and weak copper-molybdenum-nickel-silver biogeochemical anomaly. These lie uphill and just west of a significant copper MMI soil anomaly and the three 2007 WS holes, including WS-07-07. To the north the VLF-electromagnetic conductor merges with an induced polarization chargeability trend which extends for a further 4.5 km to the northwest. The anomalies lie along the margins of a northwest trending aeromagnetic vertical gradient high anomaly, which is characteristic of mineralization within the Carmacks Copper camp. *(Refer to Figures 8 and 15.)*

Copper oxide mineralization is exposed at the BCIce showing, seven km southwest of mineralized zones at the Carmacks Copper deposit. The main zone (now called ICE) was reported to cover a discontinuously exposed 20m x 100m zone of moderately foliated granodiorite with malachite trending 294°/20°NE with a second 5 by 10m zone 300m to the west *(Canam, 1982)*. Chip samples from the ICE zone, which is associated with a 1045.1 ppm Cu soil anomaly, returned 0.48% Cu over 0.8m, 0.45% Cu over 0.85m and 0.30% Cu over 2.0m. A prospecting sample, 200m south-southwest of the ICE zone returned 0.39% Cu with 0.38 ppb Au from foliated granodiorite in 2007 *(Figure 6)*. A trench was excavated here in late 2009 with reported grab samples of 0.32 and 0.10% Cu. This may correspond to the second zone, described as being 300m west of the main (ICE) zone, in Canam (1982). Two conventional soil samples collected 200m further to the southwest in 2006 by Ryan returned 281 and 935 ppm Cu *(Figure 6)* *(Ryan, 2007)*.

Drilling of the ICE zone encountered two narrow, relatively flat-lying mineralized horizons in ICE 07-2 and -4. The upper and lower horizons returned 0.48% Cu over 4.8m and 0.15% Cu over 3.7m in ICE 07-2 and 0.39% Cu over 5.5m and 0.25% Cu over 0.7m in ICE 07-4, respectively. This style of commonly occurs distal to larger zones so may have potential along strike or down dip to the northeast. ICE 07-1, 400m west-northwest of the ICE zone, intersected anomalous mineralization, with 0.04% Cu over 24.4m, despite being drilled along, as opposed to perpendicular to, the mineralized trend.

Mineralized intervals in drilling are commonly associated with enhanced gold with a maximum of 190 ppb Au from ICE-07-04. In a study of the 2008 core *(Fonseca, 2009a)* an enrichment in calcium, iron, molybdenum, thallium, tellurium, mafic-associated elements (magnesium, nickel, cobalt), tin, and sphalerite associated elements (zinc, selenium, cadmium, vanadium) was noted. The elements potassium, sodium, lanthanum, and cerium were found to be enriched in the footwall and hangingwall of mineralized zones, suggesting that ore associated mineral alteration assemblage immediately outside ore zones may be propylitic, and possibly overprinting potassic.

Other untested copper showings occur on the Williams South Project. The 20m by 5m Copper Hill showing, on the southwestern WS grid approximately 2.5 km southeast generally along trend of Zones 5, 6 and 8 of the Carmacks Copper Project, consists of copper oxides and chalcocite mineralization, primarily hosted by more mafic and foliated zones within the granodiorite. Alteration includes abundant epidote as fracture fillings and along foliation, local concentrations of limonite, and local magnetite-silica with clots of magnetite and quartz flooding and veinlets. Samples returned values of 0.85% Cu and 0.42 g/t Au from a grab sample, 0.19% Cu and 0.08 g/t Au across 1.5m and 0.4% Cu over 0.5m. A 600m by generally 100m wide copper MMI soil anomaly lies 150m upslope of the showing coincident with an induced polarization chargeability high – resistivity anomaly. The Copper Float showing consists of a malachite stained foliated granodiorite 30 by 25 cm float boulder on the WS grid, which returned 0.94% Cu and 0.26 g/t Au. The float appears isolated but generally occurs within an area of poor exposure with some exposures of foliated granodiorite approximately 2 km southeast along trend of Zones 12-13 of the Carmacks Copper Project *(Figure 15)*.

Foliated biotite ±hornblende granodiorite occurs in a 0.5 by 4 km northwest trending band across the WS grid from the north end of Merrice Lake to the northwest property boundary, and as a northeasterly (?) 150m by 1 km band at the BCIce showing; the latter particularly limited by poor exposure *(Figure 15)*. It should be noted that within the Carmacks copper-gold belt (i.e. Minto, Carmacks Copper, STU) mineralization is typically associated with foliated to gneissic granodiorite, more mafic phases and often finer grained variants of the granodiorite. Exploration in the Williams South Project area has been hampered by lack of exposure, overburden cover, and presence of a locally thick ash layer.

In conclusion the Williams South Project has potential to host mineralization similar to that within the Carmacks copper-gold belt such as at the Minto and Carmacks Copper deposits. The 2007 to 2013 programs were successful in intersecting significant copper mineralization from limited drilling, discovering surface copper showings despite limited exposure and delineating northwest trending induced polarization chargeabilty, VLF-electromagnetic, ± proximal copper MMI soil anomalies, in part underlain by foliated to gneissic granodiorite, coincident with the margins of linear magnetic high features, similar to and directly along trend from the adjoining Carmacks Copper Project of Copper North Mining Corporation.

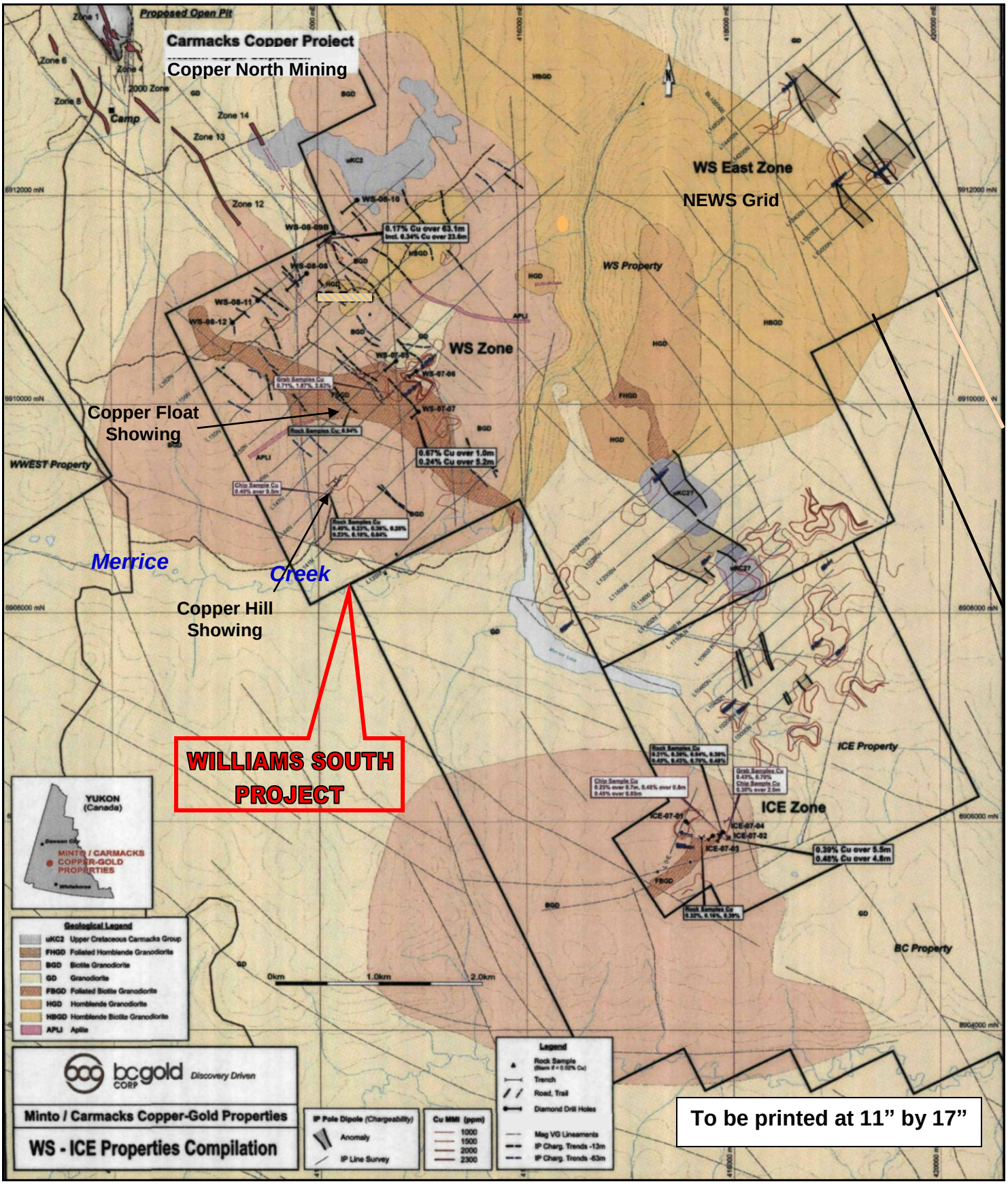

Figure 15: Compilation Map over Geology

18.0 RECOMMENDATIONS AND BUDGET

Based, on significant drill intercepts from limited drilling, the presence of untested copper showings, northwest trending induced polarization chargeabilty, VLF-electromagnetic, ± proximal copper MMI soil anomalies, in part underlain by foliated to gneissic granodiorite, coincident with the margins of linear magnetic high features, similar to and directly along trend from the adjoining Carmacks Copper Project of Copper North Mining Corporation further work is recommended on the Williams South Project.

A seven hole, 2,400m diamond drill program is recommended to follow up on the significant drill intercept in DDH WS-08-9B and to test coincident geophysical and geochemical anomalies for Carmacks Copper belt type copper and gold mineralization. Proposed drill specifications, based on the integration of the geological information with the airborne magnetic, VLF-electromagnetic, and induced polarization geophysics surveys, copper MMI soil and biogeochemical anomalies, are outlined in Table 4. Groundtruthing of proposed drill sites and examination of the WS trenches is recommended prior to drilling. A detailed ground magnetic survey could de done at this time to aid in final determination of the drill sites. This has been a useful targeting method on the adjoining Carmacks Copper Project. Examination of additional anomalies that exist across the property can be done during the recommended drill program.

Top priority for drilling are the strike extensions of Zones 12-14 onto the northern WS grid from the adjacent Carmacks Copper Project of Copper North Mining Corp. WS-A and-B are proposed to test the southeastern strike and down dip extent of mineralization intersected in WS-08-9B. The southeastern strike extent coincides with a chargeability anomaly along the margins of a vertical gradient magnetic anomaly. WS-C targets the southeastern strike extent of Copper North's Zone 12 between WS-08-08 and -11, coincident with a chargeability anomaly, a VLF-electromagnetic conductor and a biogeochemical anomaly along the margins of a vertical gradient magnetic anomaly. WS-08-08 intersected a copper anomalous interval of 0.04% Cu over 25m from 238 to 263m, including two narrow zones of mineralization (0.10% Cu over 3.9m and 0.12% Cu over 2.0m), which could reflect proximity to mineralization. An infrared spectrographic survey of WS-08-11 (500m southwest of WS-08-08 but drilled to the northeast, sub-parallel to the dip of most mineralization in the area) displays a continuous chlorite spectral signature at the bottom, suggesting it may represent a halo to mineralization *(Fonseca, 2009a)*.

Also of high priority are the uphill, probable source areas, of the highest copper MMI soil anomalies on the grid, just west and uphill of WS-07-06 and -07. Proposed DDH WS-D targets a VLF-electromagnetic conductor and biogeochemical anomaly along the margins of a vertical gradient magnetic anomaly, still within a copper MMI soil anomaly, uphill of anomalous intersections in WS-07-07. WS-E targets a copper showing with grab sample results of up to 2.83% Cu, coincident with a VLF-electromagnetic conductor and biogeochemical anomaly along the margins of a vertical gradient

magnetic anomaly, and still within a copper MMI soil anomaly. If results are favourable another hole (WS-F) should be drilled 200m to the northeast.

WS-G targets the Copper Hill showing (results of 0.85% Cu, 0.42 g/t Au and 5.3 g/t Ag from a grab sample and 0.19% Cu and 0.08 g/t Au across 1.5m) and a copper MMI soil anomaly, uphill, along the margins of a vertical gradient magnetic anomaly.

Tentative proposed drill hole specifications are tabulated below in Table 4, but should be modified based on field locations and ground conditions, and preliminary drill results during the program.

TABLE 4: Proposed drill hole specifications

DDH	Nad 83 Zone 8		Az.	Dip	Depth	Target
No.	Easting	Northing	(°)	(°)	(m)	
WS-A	414470	6911460	230	-55	350	SE strike extent of WS-08-09B intercept, chg high, mag high margin
WS-B	414340	6911760	230	-55	300	down dip extent of WS-08-09B
WS-C	413680	6911200	230	-55	350	Strike extent of Zone 12 between WS-08-08 & -11, chg high, VLF-EM, mag margin
WS-D	414870	6909910	230	-55	350	VLF-EM, biogc, chg high, Cu MMI
WS-E	414820	6910210	230	-55	350	Cu in trench, VLF-EM conductor, biogc, chg high, Cu MMI
WS-F	414600	6910290	230	-55	350	If hit in E drill 200m NW along strike
WS-G	414230	6909320	230	-55	350	Cu Hill showing, Cu MMI
TOTAL					**2400**	

chg = chargeability; mag = vertical gradient magnetic; biogc = biogeochemical anomaly

18.1 Budget:

Based on the above recommendations, the following exploration program with corresponding budget is proposed:

• detailed magnetic survey (40-45 line km)	25,000
• diamond drilling (2,400m @ $300/m all in)	720,000
• wages (geologist, core splitter, supervision)	50,000
• helicopter	50,000
• accommodation/camp	10,000
• groceries and meals	5,000
• field supplies, communication	5,000
• geochemistry (625 rocks @ $40/ea)	25,000
• preparation, report and drafting	10,000
• contingency	100,000
TOTAL:	**$1,000,000**

19.0 SIGNATURE PAGE

Respectfully submitted,
"Signed and Sealed"

Effective Date: January 20, 2016

"Jean Pautler"
Jean Pautler, P.Geo.

Signing Date: January 20, 2016

The signed and sealed copy of this Signature page has been delivered to BCGold Corp.

20.0 REFERENCES

Aeroquest International, 2008. Report on a helicopter-borne magnetic gradiometer and gamma ray spectrometer survey, Aeroquest Job # 08010, Minto and Williams Creek properties, Minto Area, Yukon, NTS 115I01, 02, 06, 07, 08, 11, 12, 14, For: BCGold Corp.

Arsenault, G. and Casselman, S., December, 2007. Resource estimate of the No. 1, No. 4, and No. 7 zones Carmacks deposit, Yukon Territory. Prepared For Western Copper Corporation by Waldrop Engineering Inc.

Barrios, A. and Newton, G., 2009. 2008 geophysical report on the WS claim group. Report for BCGold Corporation. Yukon assessment report # 095221.

BCGold Corp., January, 2016, Website at www.bcgoldcorp.com.

Canam, T. W., 1982 and Geochemical report on the Poon Claim Group for United Keno Hill Mines Limited. Assessment report # 091087.

Capstone Mining Corp., 2010. Website at www.capstonemining.com.

Cardinal, D., 2009. A preliminary field examination, observations and interpretation of the South Block claims – Carmacks Copper Project. Interoffice Memorandum for BCGold Corp.

Copper North Mining Corp. Website at http://www.coppernorthmining.com.

Deklerk, R., 2009. The MINFILE Manual. Yukon Geological Survey, CD-ROM.

Devine, F. 2009b. WS property area geology. Interoffice Memorandum for BCGold Corp.

2009a. Carmacks Copper Project: Preliminary structural interpretation on the South Block of claims with detail on the WS property. Interoffice Memorandum for BCGold Corp.

Doherty, R.A. 2008d. Assessment report on the ICE claims, Carmacks area, Yukon. Report by Aurum Geological Consultants Inc. for BCGold Corp. Yukon assessment report #095008.

2008c. Report on the ICE claims: target evaluation program, Carmacks area, Yukon. Report by Aurum Geological Consultants Inc. for BCGold Corp. Report YEIP 2007-026.

2008b. Assessment report on the WS TOTAL claims, target evaluation program, Carmacks area, Yukon. Report by Aurum Geological Consultants Inc. for BCGold Corp. Yukon assessment report #094984.

2008a. Yukon mining incentive program report on the WS TOTAL claims, target evaluation program, Carmacks area, Yukon. Report by Aurum Geological Consultants Inc. for BCGold Corp. Report YEIP 2007-027.

Drury, I. and Kramar, S., 2008. Induced polarization survey preliminary field report. Report by Aurora Geosciences Ltd. for BCGold Corp.

Dumas, K. 2014. 2013 geochemical and geophysical report on the WS property, Yukon. Yukon assessment report # 096561.

2013. Geochemical report on the WS property. Report for BCGold Corp.

Dzuibia, Frank. 2009. Memorandum: Carmacks 2009 IP Surveys. December 15, 2009. Report by Aurora Geosciences Ltd. for BCGold Corp. *In* Sidhu, 2010d, Yukon assessment report #095185.

Fage, A. 2008. Geology of the ICE copper-gold deposit, Yukon. Unpublished Bachelor of Sciences Thesis for Department of Earth Sciences, Dalhousie University, Halifax, Nova Scotia.

Fage, I. 2013. Geophysical survey report: high resolution resistivity and induced polarization Williams South Project. Report by GroundTruth Exploration Inc. for BCGold Corp. *In* Dumas, 2014, Yukon assessment report # 096561.

Fisher, J, 1981: Diamond drilling, STU property, United Keno Hill Mines Ltd., Hoochekoo Creek area, Yukon. Yukon assessment report # 090729.

Fonseca, A., 2009b. Summary report on the petrographic survey of drill core samples from the Carmacks Copper Project, Yukon Territory. Prepared for BCGold Corp.

2009a. Infrared spectroscopy survey of diamond drill core from the Carmacks Copper-Gold Project, Yukon, Canada. Prepared for BCGold Corp.

Guardia, F., 1972. Report on a geochemical survey on the Wet claims, Carmacks, Yukon Territory. For Minto Mining Limited. Yukon Assessment Report #060137.

Galambos, K., 2008. Geological report on the Carmacks Project, WS, ICE and WWest claims. Report for BCGold Corp.

Gordey, S.P. and Makepeace, A.J., (compilers), 2000. Yukon Digital Geology; Exploration and Geological Services Division (EGSD), Yukon Region, Indian and Northern Affairs Canada (DIAND) EGSD Open File 1999-1(D).

Government of Yukon, 2015. Minfile. Yukon Geological Survey. Website at http://data.geology.gov.yk.ca/.

Hester, M.G., Oliver, T.S., Hanks, J.T., Arsenault, G., Cornett, D.D., Hull, J.A., May, 2007. Carmacks Copper Project copper mine and process plant N1 43-101 technical report feasibility study Volume 1 executive summary near Carmacks, Yukon Territory Canada. Prepared For Western Copper Corporation by M3 Engineering & Technology Corporation.

Hildes, Dave, 2008. Memorandum: BCG 2008 IP survey - Interpretation supplement. Report by Aurora Geosciences Ltd. for BCGold Corp. *In* Barrios, A. and Newton, G., 2009, Yukon assessment report # 095221.

Hood, S., Hickey, K., Colpron, M. and Mercer, B., 2009. High-grade hydrothermal copper-gold mineralization in foliated granitoids at the Minto mine, central Yukon. In: Yukon Exploration and Geology 2008, L.H. Weston, L.R. Blackburn and L.L. Lewis (eds.), Yukon Geological Survey, p. 137-146.

Huss, C. Drielick, T.L., Roth D., Hull, J., Hester, M.G., and Arseneau, G., 2012. Carmacks Copper Project, NI 43-101 technical report, feasibility study, Vol. 1, Yukon Territory, Canada. Report for Copper North. Available at www.sedar.com.

Kikuchi, T., 1970. Geological and geochemical report on the BF mineral claims group, Merrice Lake area, Yukon Territory. Report for Mitsubishi Metal Mining Co. Ltd. Yukon assessment report # 060204.

Lustig, G. N., 2009. Carmacks Copper deposit geochemical orientation survey, Yukon. Report for BCGold Corp.

McNaughton, K. 1994. Carmacks Copper Project 1994 Exploration Program. Report for Western Copper Holdings Limited. Report YMIP 94-029.

Mortensen, J. K., 2014. Minto and Williams Creek (Carmacks Copper) as examples of "stalled" Early Jurassic Cu-Au porphyry deposits. Talk presented at Technical Meeting of the Yukon - Alaska Metallogeny Project, Mineral Deposit Research Unit, University of British Columbia, Dawson City, Yukon, August 5, 2014.

Mortensen, J. K. and Tafti, R., 2003. Nature and origin of copper-gold mineralization at the Minto and Williams Creek deposits, west-central Yukon: Preliminary investigations. In Yukon Exploration and Geology 2002, D. S. Emond and L. L. Lewis (eds.), Exploration and Geological Services Division, Yukon Region, Indian and Northern Affairs Canada, p. 165-174.

Mullin, A.W., 1974. Report on the magnetometer survey of the Wet claim group Whitehorse Mining Division, Yukon Territory. For Minto Mining Limited. Yukon Assessment Report #060927.

Pautler, J.M., 2009. Carmacks Copper-Gold Project evaluation and recommendations. Interoffice Memorandum for BCGold Corp.

2008. Carmacks Copper-Gold Project evaluation and recommendations. Interoffice Memorandum for BCGold Corp.

Pearson, W. N. and Clark, A. H., 1979. The Minto copper deposit, Yukon Territory: a metamorphosed orebody in the Yukon Crystalline Terrane. Economic Geology, vol. 74, p.1577-1599.

Ryan, S., 2007. Geochemical report ICE 1-4. Yukon Assessment Report #094841.

Sherwood Copper Corp., June, 2009. Minto mine project, Yukon. Website at www.sherwoodcopper.com .

Sidhu, Gary., 2010d. 2009 geophysical report on the WS property. Report by BCGold Corp. Yukon assessment report #095185.

2010c. Technical report for ICE claims: target evaluation program, Carmacks area, Yukon. Report by BCGold Corp. Yukon Mining Incentives Program, YEIP 2009-168.

2010b. Technical report for BC claims: target evaluation program, Carmacks area, Yukon. Report by BCGold Corp. Yukon Mining Incentives Program, YEIP 2009-167

2010a. Technical report for WS claims: target evaluation program, Carmacks area, Yukon. Report by BCGold Corp. Yukon Mining Incentives Program, YEIP 2009-163.

2009. Technical report for WS claims: target evaluation program, Carmacks area, Yukon. Report by BCGold Corp. Yukon Mining Incentives Program, YEIP 2008-035.

Sinclair, W.D., 1977. Geology and mineral deposits of the Minto area, Yukon Territory. In: Yukon Mineral Industry Report 1977, Geology Section, Yukon Region, Indian and Northern Affairs, Canada, pp 68-82.

Tafti, R., 2005. Nature and origin of the Early Jurassic copper (-gold) deposits at Minto and Williams Creek, Carmacks Copper Belt, western Yukon: examples of deformed porphyry deposits. Unpublished Master of Sciences Thesis for Department of Earth Sciences, University of British Columbia, Vancouver, British Columbia.

Tafti, R. and Mortensen, J. K., 2004. Early Jurassic porphyry (?) copper (-gold) deposits at Minto and Williams Creek, Carmacks Copper Belt, western Yukon. In Yukon Exploration and Geology 2003, Exploration and Geological Services Division, Yukon Region, Indian and Northern Affairs Canada, p. 289-303.

Tempelman-Kluit, D. J., 1984. Geology of the Laberge and Carmacks map sheets. Geological Survey of Canada Open File 1101.

Verweerd, A. and Killin, K., 2010. Report on a Quantec Titan-24 geophysical survey over the Minto Mine, central Yukon. Quantec Geoscience Ltd. Preface by M. Colpron (Yukon Geological Survey) and B. Mercer (Capstone Mining Corp.). YGS OF 2010-19 Minto Titan 24.

Western Copper Corporation, April, 2010. Carmacks Copper project, Yukon. Website at www.westerncoppercorp.com. Now posted on sedar.

21.0 CERTIFICATE, DATE AND SIGNATURE

1) I, Jean Marie Pautler of 103-108 Elliott Street, Whitehorse, Yukon Territory am self-employed as a consultant geologist, authored and am responsible for all sections of this report entitled “Compilation report on the Williams South Project, within the Carmacks copper-gold belt”, dated January 20, 2016.

2) I am a graduate of Laurentian University, Sudbury, Ontario with an Honours B.Sc. degree in geology (May, 1980) with 30 years mineral exploration experience in the North American Cordillera. Pertinent experience includes the acquisition and delineation of the Tsacha epithermal gold deposit, British Columbia and the evaluation of various deposit types including porphyry for Teck Exploration Limited, drilling the Brenda gold-copper porphyry property in the Kemess Camp for Northgate Exploration Limited, work throughout the Dawson Range and White Gold District including the Freegold Project of Northern Freegold Resources Limited and work on the STU prospect and properties of Northern Tiger Resources Inc. within the Carmacks copper-gold belt.

3) I am a registered member of the Association of Professional Engineers and Geoscientists of British Columbia, registration number 19804.

4) I have visited the subject mining property of this report and am a “Qualified Person” in the context of and have read and understand National Instrument 43-101 and the Companion Policy to NI 43-101.

5) This report is based upon work on the property by the author for BCGold Corp. in 2008 and 2009, a property examination on April 20, 2012, a review of the entire 2007 to 2013 work programs, the author’s personal knowledge of the region, and a review of pertinent data.

6) As stated in this report, in my professional opinion the property is of potential merit and further exploration work is justified.

7) At the effective date of the technical report, to the best of my knowledge, information, and belief, the technical report contains all scientific and technical information that is required to be disclosed to make the technical report not misleading.

8) I am entirely independent, as defined in section 1.5 of National Instrument 43-101, of BCGold Corp. and any associated companies. I do not have any agreement, arrangement or understanding with BCGold Corp. and any affiliated company to be or become an insider, associate or employee. I do not own securities in BCGold Corp. or any affiliated companies and my professional relationship is at arm’s length as an independent consultant, and I have no expectation that the relationship will change. I am also entirely independent, as defined in section 1.5 of National Instrument 43-101, of BCGold Corp., Shawn Ryan and the Williams South property.

Dated at Carcross, Yukon Territory this 20th day of January, 2016,

“Signed and Sealed”

“Jean Pautler”

Jean Pautler, P.Geo. (APEGBC Reg. No. 19804)
JP Exploration Services Inc.
#103-108 Elliott St.
Whitehorse, Yukon Y1A 6C4

The signed and sealed copy of this Certificate, Date and Signature page has been delivered to BCGold Corp.

22.0 APPENDICES

APPENDIX I: Statement of Expenditures

Compilation report:	J. Pautler between Jan 2-20, 2016 15 days @ 700.00/day	**$10,500.00**
Map and data preparation:	BCGold Corp. between Jan 6-20, 2016	**5,800.00**
Assembly, Plotting, Copying, Printing:		**1,250.00**
GRAND TOTAL:		**$17,550.00**

APPENDIX II: SAMPLE DESCRIPTIONS

Sample	Sampler	LOCATION	EASTING	NORTHING	TYPE	GEOLOGY	Cu	Au	Ag	Al	As	Ba	Bi	Cat	Cd	Co	Cr	Fe
2008							ppm	ppb	ppm	%	ppm	ppm	ppm	%	ppm	ppm	ppm	%
526101	DC	Merrice Canyon	416611	6912518	0.3m chip	Foliated granite (336/76) zone 40cm wide. Weak epidote, calcite, and sericite altered	3	2.5	0.1	0.56	10	80	20	0.57	1	5	79	1.54
526102	DC	Merrice Canyon	416611	6912519	0.15m chip	Taken from foot wall of joint (276/82) in granite above previous sample. 1mm seam chlorite (green) carb alteration.	3	2.5	0.1	0.64	20	65	20	1.04	1	6	63	1.67
526104	DC	Merrice Canyon	417070	6912928	0.5m chip	Biotite granidiorite in fault zone. Foliated, moderate fractues. 0.5m chip across zone.	4	2.5	0.1	0.35	20	70	3	1.39	1	3	66	1.14
526203	JP	ICE South	418439	6904857	grab	biotite hornblende granodiorite, very weakly foliated with epidote, chlorite, hematite on fractures, 060/80 SE	3	5	0.1	0.82	15	70	15	0.81	1	8	74	2.03
526209	JP	WS	414210	6911135	0.5m chip	very weakly foliated biotite-hb granodiorite, previous 1.02 g/t Au reported but was a mistake - standard	4	2.5	0.1	0.63	10	70	10	0.47	1	6	99	1.46
526212	JP	WS	416859	6912815	grab	weak clay-sericite altered well fractured biotite hornblende granodiorite with limonite, 35/60E	2	2.5	0.1	0.24	3	450	20	3.75	1	5	67	2.32
526213	JP	WS	416444	6911870	grab	hornblende-biotite granodiorite with silica-hematite veinlets and epidote-chlorite on fractures, well fractured	3	2.5	0.1	0.78	15	80	20	2.24	1	8	71	2.13
526214	JP	WS	419885	6910850	grab	composite of rhyolite quartz feldspar porphyry, limonite fractures and specifications after pyrite?, local clay alteration, AF	4	2.5	0.1	0.32	10	175	15	0.03	1	3	81	0.74
526220	JP	Merrice Creek	415977	6909635	1m chip	weak foliated zone in granodiorite, 100/60S, chlorite-epidote-magnetite in intrusion and hematite on fractures	4	2.5	0.1	1.02	20	85	20	1.03	1	8	69	1.94
2009							**Cu**	**Au**	**Ag**	**Al**	**As**	**Ba**	**Bi**	**Ca**	**Cd**	**Ce**	**Co**	**Cr**
							ppm	ppb	ppm	%	ppm	ppm	ppm	%	ppm	ppm	ppm	ppm
253024	JP	Copper Hill	414100	6909149	grab	chalcocite rich, heavy, malachite stained fine grained mafic rich granodiorite with fine quartz stringers, epidote alteration	4022.0	115	1.6	5.87	4.0	135.5	2.26	9.66	1.04	15.14	49.6	126.0
253025	JP	Copper Hill	414100	6909149	grab	boulder beside 253024 of diorite to quartz diorite phase with chrysocolla and minor chalcocite	2319.0	215	4.3	6.81	3.7	184.0	3.74	6.76	1.07	97.96	48.4	170.0
253027	JP	WS- Merrrice N	417141	6912893	grab	sheared looking granodiorite with 3-4 cm rusty fractures (055-60/20E), quartz-carbonate and limonite veinlets, E side Merrice Ck	15.3	20	0.1	6.32	3.8	689.5	0.06	7.90	0.19	19.02	18.4	38.0
253029	JP	WS NE	417544	6913868	grab	mafic diorite phase ungulfed in pegmatite and granodiorite, with 315/85W hematitic fractures, magnetite, epidote, heavy	124.0	15	0.1	9.06	25.9	1508.0	0.08	3.98	0.08	39.56	20.2	48.5
253030	JP	Merrice showing	417450	6914647	grab	weakly foliated (315/steep) diorite footwall of main Merrice Vein with malachite, trace chalcopyrite	1377.0	30	1.2	6.70	5.1	331.0	0.40	8.34	0.10	31.08	49.7	133.5
253104	DC	Merrice showing	417455	6914651	1.5m chip	Composite chip of Main Merrice vein above adit, rusty with 3-4 % patchy malachite, 1% azurite, <0.5% chalcopyrite.	5206.0	15	0.7	0.63	1.7	40.0	0.04	0.19	0.03	2.02	6.9	266.5
253105	DC	Merrice showing	417436	6914650	select	High grade from strained 0.5x 1m quartz vein zone below adit of 5-6% bornite with malachite	2.51%	505	41.8	0.29	2.2	84.5	16.14	0.37	0.11	15.48	2.1	224.0
2008							**Cu**	**Au**	**Ag**	**Al**	**As**	**Ba**	**Bi**	**Ca**	**Cd**	**Ce**	**Co**	**Cr**
230001	KG	WS	414750	6908574	grab	Fine grained biotite-granodiorite with magnetite and trace sulphides(?)	19.9	10	0.1	>10	6.9	1860.0	0.06	5.28	0.14	69.75	11.6	97.0
230002	KG	Copper Hill	414100	6909149	grab	Foliated biotite-granodiorite with malachite clots and coatings (grab)	8492.0	415	5.3	6.38	6.6	80.5	4.58	9.02	0.60	12.70	56.8	242.5
230003	KG	Copper Hill	414100	6909149	1.5m chip	Foliated biotite-granodiorite with malachite from same area as 230002	1860.0	80	1.1	8.05	6.1	348.5	1.56	8.31	0.39	30.51	25.9	190.5
230004	KG	Copper Hill	414100	6909149	grab	Foliated biotite-granodiorite with malachite (grab)	2514.0	95	0.8	>10	7.7	183.0	3.66	9.29	0.43	25.27	16.3	150.0
230005	KG	Copper Hill	414100	6909149	grab	Near massive foliated biotite with 5-10% malachite (grab of 40cm float boulder? 3m along strike and downhill of sample 230002)	3610.0	15	0.4	6.18	5.8	322.0	0.88	8.22	1.10	13.09	31.6	193.0
230006	KG	Copper Hill	414100	6909149	1.5m chip	Foliated biotite-granodiorite with malachite (1.5m chip perpendicular to sample 230003	2311.0	120	1.9	8.14	6.5	154.0	2.10	>10	0.57	20.55	34.1	191.0
230007	KG	Copper Hill	414100	6909149	grab	Massive biotite with forest green olivine(?) tinge	676.2	5	0.2	6.92	8.9	48.5	1.04	>10	0.60	23.98	13.2	210.5
230008	KG	WS	414645	6908390	grab	Foliated biotite-granodiorite with light green tinge (epidote?)	60.6	2.5	0.1	7.84	7.5	98.5	1.20	>10	0.17	34.93	13.1	137.0
230009	KG	WS	419059	6912111	grab	Weathered biotite-granodiorite from tree roots	12.1	2.5	0.1	8.83	3.3	2601.0	0.06	1.92	0.06	23.03	3.4	127.0
230010	KG	WS	412441	6909062	grab	Potassic altered biotite-granodiorite with stringers and masses of epidote	4.1	2.5	0.1	>10	6.5	503.5	0.02	5.30	0.02	37.07	4.4	126.0

Sample	La	Mg	Mn	Mo	Nat	Ni	P	Pb	Sb	Sn	Sr	Ti	U	V	W	Y	Zn	Pb	Rb	Re	S	Sb	Sc	Se	Sn	Sr	Ta	Te	Th	Ti	Tl	U	V	W	Zn	Zr
2008	ppm	%	ppm	ppm	%	ppm	ppm	ppm	ppm	ppm	ppm	%	ppm	ppm	ppm	ppm	ppm	ppm	ppm	ppm	%	ppm	ppm	ppm	ppm	ppm	ppm	ppm	ppm	%	ppm	ppm	ppm	ppm	ppm	ppm
526101	1	0.38	360	2	0.05	4	490	12	5	10	33	0.04	1	32	1	2	41																			
526102	10	0.42	404	1	0.04	4	510	16	3	10	31	0.02	1	31	1	8	44																			
526104	10	0.13	296	1	0.05	2	400	10	3	10	25	0.02	1	20	1	6	26																			
526203	1	0.65	365	1	0.07	2	810	18	5	10	43	0.09	1	52	1	1	38																			
526209	1	0.34	284	1	0.08	3	860	14	3	10	51	0.07	1	39	1	1	27																			
526212	1	0.16	1007	1	0.02	4	350	8	3	10	79	0.03	1	43	1	13	60																			
526213	1	0.60	498	2	0.05	5	690	18	10	10	51	0.04	1	55	1	5	46																			
526214	1	0.01	525	1	0.02	2	70	14	3	10	39	0.02	1	6	1	11	18																			
526220	1	0.53	412	1	0.06	3	740	24	5	10	91	0.09	1	48	1	1	39																			
2009	Cs	Fe%	Ga	Ge	Hf	Hg	Ir	K%	La	Li	Mg%	Mn	Mo	Na%	Nb	Ni	P	Pb	Rb	Re	S	Sb	Sc	Se	Sn	Sr	Ta	Te	Th	Ti	Tl	U	V	W	Zn	Zr
	ppm	%	ppm	ppm	ppm	ppb	ppm	ppm	ppm	ppm	ppm	%	ppm	%	ppm	ppm	ppm	ppm	ppm	ppm	%	ppm	ppm	ppm	ppm	ppm	ppm	ppm	ppm	%	ppm	ppm	ppm	ppm	ppm	ppm
253024	0.18	10.31	17.1	15.6	1.18	<5	0.64	0.53	10.5	5.5	2.64	2903	15.22	1.421	2.38	20.7	2154	6.48	7.1	0.013	0.14	0.46	12.5	0.8	1.4	634.5	0.35	1.60	1.7	0.278	0.06	3.2	164	1.2	280.3	22.20
253025	0.18	11.34	28.6	17.8	1.56	10	0.36	0.94	51.5	7.6	3.06	2818	3.84	2.238	23.16	24.8	2136	5.42	7.7	0.003	0.16	0.20	29.1	2.3	3.1	497.5	2.80	3.50	9.0	0.604	0.06	2.4	336	1.0	248.9	19.65
253027	0.62	4.39	16.6	6.4	0.42	<5	0.02	0.83	10.5	9.5	1.64	1813	0.54	2.757	3.38	5.7	383	9.11	23.3	0.002	0.14	0.16	5.5	0.4	0.6	369.0	0.35	0.10	1.3	0.103	0.12	0.5	60	0.4	181.8	8.58
253029	1.28	4.80	24.6	7.5	0.90	40	0.04	2.13	24.0	27.6	1.23	918	0.38	4.390	5.52	2.8	1547	8.52	57.1	0.002	0.16	0.32	10.0	0.7	0.9	1033.0	0.50	0.34	3.6	0.308	0.36	1.3	148	0.3	85.0	15.40
253030	0.42	7.89	19.7	11.0	1.76	5	0.06	0.90	18.5	7.9	3.47	1209	1.22	1.559	4.94	31.9	1854	6.13	21.8	0.002	0.16	0.18	29.9	0.8	1.1	820.0	0.55	0.46	4.1	0.446	0.14	1.9	292	0.4	78.4	30.86
253104	0.24	1.17	2.4	1.6	0.04	<5	<0.02	0.20	1.0	9.1	0.29	118	1.07	0.151	0.20	8.3	127	1.86	6.0	0.002	0.14	0.06	2.8	1.2	0.3	52.5	<0.05	0.06	<0.1	0.034	0.04	0.2	40	0.1	17.0	0.83
253105	0.06	0.78	1.1	1.1	0.04	30	<0.02	0.07	9.0	2.3	0.06	46	0.60	0.206	0.18	5.4	31	2.61	1.7	0.002	0.38	0.04	1.1	14.4	0.2	19.0	<0.05	5.58	0.6	0.011	0.02	1.2	38	<0.1	10.0	1.47
2008	Cs	Fe	Ga	Ge	Hf			K	La	Li	Mg	Mn	Mo	Na	Nb	Ni	P	Pb	Rb	Re	S	Sb	Sc	Se	Sn	Sr	Ta	Te	Th	Ti	Tl	U	V	W	Zn	Zr
230001	0.62	5.15	28.5	25.1	2.60			1.45	35.0	4.3	1.58	1708	0.53	4.421	24.10	4.1	2756	15.63	24.4	0.002	0.14	0.10	13.6	1.2	2.2	1352.0	0.30	0.40	7.6	0.360	0.16	3.4	130	0.3	102.7	183.5
230002	0.24	13.91	18.3	48.5	1.14			0.68	8.5	4.1	2.14	3257	1.07	1.384	4.44	35.6	1995	12.75	6.9	0.001	0.18	0.20	16.1	1.7	1.8	584.5	0.05	3.80	2.3	0.233	0.06	2.8	220	1.1	230.0	83.08
230003	0.42	8.91	21.4	31.4	1.00			0.76	18.0	4.5	2.00	2468	5.31	2.762	8.40	21.2	1705	17.56	10.4	0.004	0.18	0.44	18.8	1.1	1.8	785.5	0.10	0.80	2.3	0.305	0.08	3.1	204	1.3	164.9	77.02
230004	0.40	7.31	25.8	27.1	1.68			0.70	12.0	3.9	1.72	1919	1.53	3.823	8.32	12.9	2235	13.81	8.9	0.001	0.18	0.44	24.0	1.3	1.7	1050.0	0.30	1.26	2.9	0.407	0.06	2.8	286	1.5	140.7	99.82
230005	0.30	9.19	17.4	30.8	0.70			0.67	7.0	5.3	2.43	3144	41.86	2.079	4.44	16.9	1210	15.99	9.9	0.025	0.16	0.82	15.8	0.7	1.4	568.5	0.05	0.18	1.1	0.226	0.08	3.2	146	1.0	250.6	58.32
230006	0.42	10.83	23.0	36.6	1.86			0.77	11.0	5.6	2.79	3331	6.04	2.357	11.36	24.3	1863	13.16	13.4	0.007	0.16	0.60	26.2	1.4	2.2	822.5	0.35	1.52	2.0	0.422	0.06	2.6	268	1.5	207.9	107.7
230007	0.28	9.71	21.4	30.3	1.72			0.39	16.0	3.8	2.64	2924	1.44	0.970	4.64	16.0	2539	14.98	5.5	0.003	0.12	0.92	19.7	0.8	2.3	831.5	0.10	0.22	2.1	0.301	0.04	6.4	220	1.8	145.9	113.7
230008	0.34	8.43	24.7	49.0	1.06			0.41	16.5	4.5	1.79	2050	3.31	2.306	9.72	7.9	1908	18.66	7.0	0.003	0.14	1.18	23.0	1.0	3.7	866.0	0.30	0.24	1.5	0.421	0.04	6.8	252	2.1	83.7	83.96
230009	0.94	1.76	21.3	8.6	1.24			1.75	9.5	5.9	0.38	496	0.54	4.040	11.14	4.3	469	18.49	41.0	0.002	0.14	0.06	4.7	0.5	0.9	905.5	0.10	0.16	2.8	0.104	0.30	1.0	54	0.2	37.3	81.78
230010	0.32	3.50	26.6	14.6	0.78			0.87	19.0	2.8	0.46	721	0.55	5.108	7.70	4.7	978	28.25	21.6	0.002	0.16	0.12	7.4	0.6	0.9	1876.0	0.10	0.44	2.8	0.175	0.14	0.3	96	0.4	33.1	61.42

APPENDIX II: SAMPLE DESCRIPTIONS

	SAMPLE	EAST	NORTH	Au (g/t)	Cu (%)	TYPE	LITHOLOGY	MINERALOGY	
Ice	78851	417267	6905527	<0.03	<0.01	subcrop grab	Non-foliated biotite granodiorite		RECCE
Ice	78852	417584	6905620	<0.03	<0.01	comp grab	Non-foliated biotite granodiorite		
Ice	78853	417690	6905851	0.38	0.39	comp grab	Biotite-granodiorite, weakly foliated	1-2% malachite	
WS	78854	413087	6910364	<0.03	<0.01	grab	Biotite-hornblende granodiorite	trace pyrite, trace hematite staining	
WS	78855	414311	6909970	0.26	0.94	subcrop grab	Biotite granodiorite, weakly foliated	<1% malachite, locally up to 15%	
WS	398001			1.02	<0.01	STANDARD		STANDARD	
WS	398002	414354	6911108	<0.03	<0.01	grab	Granodiorite, strongly magnetic	possible very fine-grained malachite	
WS	398003	414503	6910871	<0.03	<0.01	grab	Granodiorite, epidote and k-spar	possible trace malachite	
Ice	398101	417887	6905894	<0.03	0.48	chip 0.80m	Foliated granodiorite		ICE SHOWING TRENCH SAMPLES
Ice	398102	417887	6905894	<0.03	0.04	chip 2m	Non-foliated biotite-hornblende granodiorite		
Ice	398103	417887	6905894	<0.03	0.01	chip 1m	Non-foliated biotite-hornblende granodiorite		
Ice	398104	417887	6905894	0.05	0.45	chip 0.85m	Biotite granodiorite, well foliated	trace to 2% malachite	
Ice	398105	417887	6905894	<0.03	0.02	chip 2m	Non-foliated biotite-hornblende granodiorite		
Ice	398106	417887	6905894	<0.03	<0.01	chip 2m	Non-foliated biotite-hornblende granodiorite		
Ice	398107	417887	6905894	0.04	<0.01	chip 2m	Non-foliated biotite-hornblende granodiorite		
Ice	398108	417887	6905894	<0.03	<0.01	chip 2m	Non-foliated biotite-hornblende granodiorite		
Ice	398109	417887	6905894	<0.03	<0.01	chip 2m	Non-foliated biotite-hornblende granodiorite		
Ice	398110	417887	6905894	<0.03	<0.01	chip 2m	Non-foliated biotite-hornblende granodiorite		
Ice	398111	417887	6905894	<0.03	<0.01	chip 2m	Non-foliated biotite-hornblende granodiorite		
Ice	398112	417887	6905894	<0.03	<0.01	chip 2m	Non-foliated biotite-hornblende granodiorite		
Ice	398113	417887	6905894	<0.03	<0.01	chip 2m	Non-foliated biotite-hornblende granodiorite		
Ice	398114	417887	6905894	<0.03	<0.01	chip 1.5m	Aplite dyke, 2-3% biotite		
Ice	398115	417887	6905894	<0.03	0.05	chip 1m	Biotite- hornblende granodiorite, weakly foliated	local trace malachite	
Ice	398116	417887	6905894	<0.03	0.04	chip 1m	Biotite- hornblende granodiorite, weakly foliated	local trace malachite	
Ice	398117	417887	6905894	<0.03	0.05	chip 1m	Biotite- hornblende granodiorite, weakly foliated	local trace malachite	
Ice	398118	417887	6905894	<0.03	0.05	chip 1m	Biotite- hornblende granodiorite, weakly foliated	local trace malachite	
Ice	398119	417887	6905894	<0.03	0.21	chip 0.5m	Biotite- hornblende granodiorite, weakly foliated	local trace malachite	
	398120			1.02	<0.01	STANDARD			
Ice	398121	417887	6905894	<0.03	0.03	chip 1.9m	Non-foliated biotite-hornblende granodiorite		
Ice	398122	417887	6905894	<0.03	0.04	chip 2m	Non-foliated biotite-hornblende granodiorite		
Ice	398123	417887	6905894	<0.03	0.02	chip 2m	Non-foliated biotite-hornblende granodiorite		
Ice	398124	417887	6905894	0.03	0.01	chip 2m	Non-foliated biotite-hornblende granodiorite		
Ice	398125	417887	6905894	<0.03	<0.01	chip 2m	Non-foliated biotite-hornblende granodiorite		
Ice	398126	417887	6905894	0.09	0.30	chip 2m	Non-foliated biotite-hornblende granodiorite		
Ice	398127	417887	6905894	<0.03	<0.01	chip 0.9m	Aplite dyke		
Ice	398128	417887	6905894	<0.03	<0.01	chip 1.1m	Non-foliated biotite-hornblende granodiorite		
Ice	398129	417887	6905894	<0.03	<0.01	chip 2m	Non-foliated biotite-hornblende granodiorite		
Ice	398130	417887	6905894	<0.03	<0.01	chip 1m	Non-foliated biotite-hornblende granodiorite		
Ice	398131	417887	6905894	<0.03	<0.01	chip 2m	Non-foliated biotite-hornblende granodiorite		
Ice	398132	417887	6905894	<0.03	0.43	grab	fault	malachite	
Ice	398133	417887	6905894	<0.03	<0.01	chip 2m	Non-foliated biotite-hornblende granodiorite		
Ice	398134	417887	6905894	<0.03	<0.01	chip 2m	Non-foliated biotite-hornblende granodiorite		
Ice	398135	417887	6905894	<0.03	0.70	comp grab	fault zone	malachite	
Ice	398136	417887	6905894	<0.03	<0.01	chip 2m	Aplite dyke, 2-3% biotite		
Ice	398137	417887	6905894	0.03	<0.01	chip 2m	Non-foliated biotite-hornblende granodiorite		
Ice	398138	417693	6905847	<0.03	0.16	chip 1m	Biotite- hornblende granodiorite		
Ice	398139	417693	6905847	<0.03	0.01	chip 2m	Biotite- hornblende granodiorite		
	398140			1.05	<0.01	STANDARD			
Ice	398141	417693	6905847	0.08	0.32	subcrop grab	Non-foliated biotite granodiorite		

APPENDIX II: SAMPLE DESCRIPTIONS

Sample	Sampler	LOCATION	EASTING	NORTHING	TYPE	GEOLOGY	Au	Ag	As	Ba	Bi	Ca	Cd	Co	Cr	Cu	Fe
2008							**ppb**	**ppm**	**ppm**	**ppm**	**ppm**	**%**	**ppm**	**ppm**	**ppm**	**ppm**	**%**
526103	DC	Merrice Creek	416599	6911397	silt	Coarse, light brown sand, granitoid parent rock. West side of creak in small 3x0.25m sand bar.	2.5	0.1	1.11	9.5	143.5	0.08	0.92	0.09	6.2	9.5	8.50
526201	JP	ICE South	418373	6905502	silt	medium sand, granodiorite particles from bar, slow flow, 1m wide	2.5	0.1	0.47	6.9	50.5	0.08	0.47	0.03	3.6	9.0	4.85
526204	JP	ICE South	418448	6904774	soil	red C horizon from hematitic fractures 060/steep	2.5	0.1	2.02	7.6	414.0	0.02	1.37	0.04	10.1	9.5	5.04
526205	JP	WS	414621	6910677	soil	reddish brown B, granodiorite subcrop	2.5	0.1	1.71	6.0	269.0	0.06	0.42	0.04	6.6	13.5	4.44
526206	JP	WS	413793	6909988	silt	fine sand-silt, very slow flow, swampy, boulders to 30 cm, aplite, granodiorite, volcanic breccia float	2.5	0.1	0.69	6.0	229.0	0.08	0.91	0.04	5.4	7.0	5.75
526207	JP	WS	413566	6909425	soil	medium orange brown B, biotite granodiorite subcrop, some foliated	2.5	0.1	1.75	6.3	266.0	0.08	0.41	0.03	6.6	13.5	4.42
526208	JP	WS	415065	6911772	soil	deep orange brown B, cat trail, area of granodiorite	2.5	0.1	3.13	12.8	229.0	0.12	0.25	0.09	10.8	28.0	20.81
526210	JP	WS	416923	6912910	soil	talus fines from hornblende-biotite granodiorite with ep/hem on fractures, well fractured	2.5	0.1	1.71	9.9	142.0	<0.02	2.77	0.04	9.5	2.0	19.87
526211	JP	WS	416863	6912843	soil	rusty orange talus fines from hornblende-biotite granodiorite with ep/hem on fractures, well fractured, clay-sericite altered	2.5	0.1	0.67	10.9	271.5	0.04	2.50	0.04	10.9	4.5	15.90
526219	JP	Merrice Creek	416004	6909420	moss mat	good silt in moss on rocks in creek, moderate flow, 3m wide	2.5	0.4	0.77	10.1	139.0	0.22	0.83	0.16	7.5	28.0	10.60
526221	JP	Merrice Creek	416027	6909720	soil	reddish talus fines from hematite-chlorite altered hornblende granodiorite outcrop	2.5	0.1	1.35	7.2	181.0	<0.02	2.22	0.02	4.8	24.5	1.17
526222	JP	Merrice Creek	415719	6908964	soil	pink-rusty talus fines from hematite-chlorite-epidote altered hornblende granodiorite outcrop	2.5	0.1	1.71	6.4	83.5	<0.02	3.15	0.02	3.0	1.5	0.48
526223	JP	Merrice Creek	415731	6908886	soil	pink-rusty talus fines from hornblende granodiorite outcropwith dark hematite on fractures with slickensides, N/85E	2.5	0.1	2.97	9.9	103.5	<0.02	5.75	0.04	6.6	32.0	1.34
526224	JP	Merrice Creek	415836	6909100	moss mat	good silt in moss on boulders in creek, moderate flow, 2.5m wide	2.5	0.1	0.69	9.1	107.0	0.06	0.71	0.07	6.4	23.0	7.37
2009							**Au**	**Ag**	**As**	**Ba**	**Bi**	**Ca %**	**Cd**	**Co**	**Cr**	**Cu**	**Fe %**
S253026	JP	Merrrice E	416489	6909340	soil	medium orange-brown B, exposed by windfall, from area of MMI anomalies near Bishi Minfile	<5	0.2	5	150	<5	0.51	2	10	17	9	3.38
L253028	JP	Merrrice N	417445	6913130	silt	black sand from bar in fast westerly flowing tributary creek of Merrice Creek, 0.5-1m wide	15	<0.2	<5	110	<5	1.04	1	11	15	75	2.59

Sample	Ga	Hg	K	La	Mg	Mn	Mo	Na	Nim	P	Pb	S	Sb	Sc	Se	Sr	Te	Th	Ti	Tl	U	V	W	Zn
2008	ppm	ppm	%	ppm	%	ppm	ppm	%	ppm	ppm	ppm	%	ppm	ppm	ppm	ppm	ppm	ppm	%	ppm	ppm	ppm	ppm	ppm
526103	1.98	4.9	0.07	7.5	0.50	831	0.26	0.050	6.8	654	13.10	0.06	0.12	2.5	0.2	63.0	<0.02	1.1	0.037	0.08	0.4	40	0.05	50.1
526201	1.26	2.2	0.03	6.0	0.28	149	0.19	0.048	6.3	600	12.08	0.04	0.10	1.5	0.1	26.0	<0.02	1.2	0.028	0.06	0.2	32	0.05	29.7
526204	3.45	10.7	0.47	21.5	1.06	563	0.09	0.048	4.1	1866	10.13	0.06	0.06	4.3	0.3	62.5	<0.02	1.7	0.030	0.08	0.3	60	0.05	88.3
526205	2.77	7.3	0.19	5.0	0.64	386	0.30	0.042	7.5	1061	10.26	0.04	0.14	2.3	0.1	27.0	<0.02	1.2	0.119	0.12	0.2	54	0.05	74.1
526206	2.15	3.9	0.14	8.5	0.40	346	0.24	0.044	3.9	1125	10.79	0.06	0.10	2.3	0.6	66.5	<0.02	0.7	0.045	0.10	0.5	48	0.05	40.0
526207	2.74	7.3	0.19	5.0	0.64	386	0.28	0.043	7.4	1091	10.68	0.04	0.16	2.3	0.1	27.0	<0.02	1.2	0.119	0.12	0.2	54	0.05	74.0
526208	3.59	8.9	0.12	6.0	0.82	409	0.70	0.044	17.6	568	14.22	0.06	0.36	3.0	0.2	21.5	<0.02	1.6	0.086	0.10	0.3	82	0.05	71.4
526210	2.17	7.6	0.12	9.0	0.95	646	0.10	0.048	3.0	1118	11.51	0.06	0.04	2.5	0.2	82.0	<0.02	0.6	0.029	0.04	0.2	50	0.05	62.4
526211	3.74	6.2	0.19	32.5	0.47	1188	0.43	0.037	4.5	1150	10.99	0.04	0.12	7.1	0.8	67.5	<0.02	3.0	0.016	0.06	0.5	66	0.05	109.1
526219	5.36	5.2	0.05	10.5	0.40	1079	0.45	0.050	9.1	1122	13.89	0.06	0.22	2.5	0.3	50.5	<0.02	1.6	0.042	0.06	0.5	136	0.05	64.1
526221	1.36	6.2	0.04	7.5	0.56	543	0.06	0.039	6.2	547	10.72	0.04	0.06	2.2	0.2	67.0	<0.02	0.9	0.014	<0.02	0.2	30	0.05	38.0
526222	0.92	6.9	0.07	4.0	0.39	347	0.02	0.038	1.0	526	9.90	0.02	0.06	1.4	0.1	85.5	<0.02	0.5	0.007	<0.02	0.1	16	0.05	30.1
526223	2.70	14.2	0.13	10.0	0.89	801	0.51	0.064	12.5	1404	13.06	0.04	0.04	6.2	0.2	169.5	<0.02	1.3	0.102	0.02	0.3	62	0.05	67.4
526224	4.17	4.6	0.05	11.5	0.38	667	0.29	0.049	8.2	1113	11.59	0.04	0.20	2.3	0.3	37.0	<0.02	2.0	0.044	0.06	0.4	108	0.05	41.1

2009	La	Mg %	Mn	Mo	Na %	Ni	P	Pb	Sb	Sn	Sr	Ti %	U	V	W	Y	Zn	Al %
S253026	<10	0.64	298	1	0.02	9	1910	10	<5	<20	24	0.07	<10	69	<10	3	66	1.85
L253028	<10	0.72	344	<1	<0.01	9	2760	6	<5	<20	58	0.08	<10	78	<10	5	31	0.87

Appendix III:

GEOLOGY OF THE ICE COPPER-GOLD DEPOSIT, YUKON

Adam Fage
Supervisor: Dr. Marcos Zentilli

© Adam Fage

Submitted in Partial Fulfilment of the Requirements
For the Degree of Bachelor of Sciences, Honours
Department of Earth Sciences
Dalhousie University, Halifax, Nova Scotia
March 2008

DALHOUSIE UNIVERSITY
Inspiring Minds

Department of Earth Sciences
Halifax, Nova Scotia
Canada B3H 4J1
(902) 494-2358
FAX (902) 494-6889

DATE: April 24, 2008

AUTHOR: Adam Fage

TITLE: Geology of the Ice Copper-Gold Deposit, Yukon

Degree: BSc (honours) Convocation: May Year: 2008

Permission is herewith granted to Dalhousie University to circulate and to have copied for non-commercial purposes, at its discretion, the above title upon the request of individuals or institutions.

Adam Fage
Signature of Author

THE AUTHOR RESERVES OTHER PUBLICATION RIGHTS, AND NEITHER THE THESIS NOR EXTENSIVE EXTRACTS FROM IT MAY BE PRINTED OR OTHERWISE REPRODUCED WITHOUT THE AUTHOR'S WRITTEN PERMISSION.

THE AUTHOR ATTESTS THAT PERMISSION HAS BEEN OBTAINED FOR THE USE OF ANY COPYRIGHTED MATERIAL APPEARING IN THIS THESIS (OTHER THAN BRIEF EXCERPTS REQUIRING ONLY PROPER ACKNOWLEDGEMENT IN SCHOLARLY WRITING) AND THAT ALL SUCH USE IS CLEARLY ACKNOWLEDGED.

Table of Contents

Copyright Page……...ii

Table of Contents……iii

List of Figures…….....v

Abstract……...……...vii

Acknowledgements……..……viii

Chapter 1. Introduction

1.1 General statement……..…1
1.2 Mineral deposits of the Carmacks Copper Belt……....1
1.3 Background of the Ice Property……....4
1.4 Questions to be answered……..…4
1.5 Objectives…….....5
1.6 Methodology…….....5
1.7 Organization of the Thesis……....6

Chapter 2. Regional Geology

2.1 Tectonic Framework……..…7
2.2 Stratigraphy……..…7
2.3 Structural Geology……....8
2.4 Igneous History…….....8
2.5 Metamorphic History……....9
2.6 Metallogeny……..…..……...……..…9
2.7 Geomorphology……..10

Chapter 3. The Ice Property

3.1 History of the Project……..13
3.2 Geophysics……..13
3.3 Geochemistry……..14
3.4 Field Geology……..17

Chapter 4. Geology of the Ice Property

4.1 Field Work……..18
4.2 Structural Geology……..20

Chapter 5. Igneous Petrology of the Ice Property

5.1 Macroscopic……22
5.2 Microscopic……24

5.3 Geochemistry……..25
5.4 Hornblende Geobarometry and Two-Feldspar Geothermometry……..27
5.5 Interpretations…….30

Chapter 6. Mineralogy of Alteration and Ores

6.1 Thin Section Descriptions……...32
6.2 Electron Microprobe……...33
6.3 X-ray Diffraction……37
6.4 Interpretations…….37

Chapter 7. Genetic Model for the Ice Property

7.1 Model for Minto and Williams Creek…….39
7.2 Exotic Deposits……...40
7.3 Porphyry Copper Deposits……..41
7.4 Model for the Ice deposit……43

Chapter 8. Conclusions and Recommendations for Future Work

8.1 Discussion ……...46
8.2 Suggestions for Future Work……...47
8.3 Conclusions……..47

Appendix 1 Rock sample Descriptions……..49
Appendix 2 Magnetic Susceptibility……..53
Appendix 3 XRF Geochemistry…….54
Appendix 4a Silicate Microprobe data……...55
Appendix 4b Geobarometry / Geothermometry Microprobe data……...59

References……..61

List of Figures

Figure 1.1 Location Map of the Ice property……...2

Figure 1.2 Regional Geology……3

Figure 2.1 Plutonic rocks of the Ice property plotted on a QAP diagram…….9

Figure 2.2 Hypothetical paleodrainage of the southern Yukon……...11

Figure 2.3 Maximum extent of continental ice during the last glaciation……...12

Figure 3.1 Aeromagnetic map of the Ice property and surrounding area……14

Figure 3.2 Copper MMI contours of the Ice property and surrounding area……..…15

Figure 3.3 Copper MMI contours of the Ice property…….16

Figure 3.4 Detailed geological map of the Ice property……..17

Figure 4.1 Ice trench #4……...18

Figure 5.1 Mineralized outcrop at the Ice property…….23

Figure 5.2 Photo of hand sample AFI-14A…….23

Figure 5.3 Oxidized magnetite grain……...24

Figure 5.4 Biotite grains defining a foliation……..25

Figure 5.5 Granitoid discrimination diagrams……26

Figure 5.6 Rock classification diagrams…….26

Figure 5.7 LogCu vs. K_2O and LogCu vs. Rb…….27

Figure 6.1 Rimmed malachite in sample AFI-05……32

Figure 6.2 Backscatter electron image of sample AFI-14b……34

Figure 6.3 Elemental map from the electron microprobe……...35

Figure 6.4 Ice feldspars plotted on an An-Ab-Or diagram…….36

Figure 6.5 Classification of Ice biotites……...36

Figure 6.6 X-Ray Diffraction plot for malachite…….37

Figure 7.1 Exotic copper deposit……41

Figure 7.2 Porphyry copper deposit……43

Figure 7.3 Simplified tectonic deformation……45

ABSTRACT

The Ice copper-gold deposit is located in the Carmacks copper belt, UTM zone 08V, 417935E, 6905900N, Yukon. First staked in the early 1970s, it is currently being explored by BC Gold Corporation of Vancouver, British Columbia. Exploration has focused on the eastern edge of a bulls-eye positive aeromagnetic anomaly, measuring roughly 1000 m by 700 m. The Carmacks copper belt contains economic porphyry-type copper type deposits, such as the Minto and the Carmacks Copper. This study is based on field mapping, petrography, ore microscopy, microprobe analyses and rock geochemistry. It reviews exploration history in the context of genetic models and the known geology of other deposits in the region.

The Ice surficial rocks studied so far contain malachite and other copper oxides in pores and fractures, probably previously occupied by sulphides. Small irregular particles of native silver are present. Disseminated magnetite, partially oxidized to hematite (martite) accounts for the relatively high magnetic susceptibility of the rocks; however the association of copper with a magnetic anomaly seems to be fortuitous. The low-grade copper is hosted within variably sheared and altered hornblende-biotite granodiorite phases of the early Jurassic Granite Mountain Batholith. Fabrics and recrystallized quartz veinlets suggest that hydrothermal mineralization preceded deformation. It is suggested that, as previously established for the Minto and Carmacks Copper, the Ice deposit formed in the Jurassic at considerable depth (> 5 km) in a porphyry copper system, and that tectonic deformation (ductile shearing) followed the main mineralization event. Exhumation and extensive weathering occurred in the Cenozoic.

The positive correlation of copper values with potassium and rubidium is compatible with a primary association of copper with potassic alteration in a porphyry system; the occurrence of remnants of iron and native silver in vugs occupied by copper oxides suggests that these were occupied by hypogene minerals. The preferred model envisages a porphyry system sheared into a tabular foliated granodiorite body; structural mapping and radiometric surveys could be useful exploration tools. It is possible that some of the oxide mineralization has been displaced from its hypogene source by migrating groundwaters during the Cenozoic, making it an exotic (displaced, secondary) copper deposit.

Acknowledgments

I would like to thank BCGold Corp. and Brian Fowler for the opportunity to study this deposit; Shawn Ryan and Cathy Wood of Ryan-Wood Exploration for the great opportunity to work in the Yukon and for suggesting this project; Peter and Anne Ledwidge for instruction in the field.

Lexie Arnott for the help with geobarometry and geothermometry; Gordon Brown for preparing my thin and polished sections; Patricia Stoffyn for instruction on microprobe analyses; Patrick Ryall for guidance and suggestions on early drafts of the thesis; Keith Taylor for help with XRD analyses.

My family has given me a great deal of support throughout my undergraduate degree. Thank you Mom, Dad, Jill, Monique, Isaac, Cecille and Orion.

Finally, thank you to Dr. Marcos Zentilli, your countless hours of assistance made this project possible.

Financial assistance was given by BCGold Corporation and NSERC Discovery Grant No. 9036 to Dr. Marcos Zentilli.

Chapter 1

Introduction

1.1 General statement

The Ice copper-gold deposit is a prospect known since the early 1970s, situated in the Carmacks Copper Belt where two economic deposits are located. This thesis is a case study of the exploration activities at the Ice deposit, in which the author participated. This study includes field descriptions, petrography, analysis of available geochemical data, and evaluates various genetic models for the genesis of the Ice deposit. A comparison with the larger Minto and Williams Creek deposits allows the conclusion that the Ice deposit is potentially economic.

It is concluded that the deposit was formed either as a deformed porphyry copper type deposit or is an exotic copper deposit. Tectonic deformation, burial and exhumation appear to have followed the main mineralization event. Porphyry type deposits are large, low to medium grade deposits in which primary ore minerals are deposited within felsic to intermediate porphyritic intrusions (Eckstrand et al. 1995). Exotic deposits are secondary deposits that occur in paleodrainage networks leading away from primary porphyry deposits that have undergone supergene enrichment; during supergene enrichment, acid-oxidizing copper-bearing fluids escape the supergene enrichment system into the surrounding drainage network and flow downhill to sites where precipitation of copper oxides occurs (Mote et al. 2001).

1.2 Mineral deposits of the Carmacks Copper Belt

Figure 1.1 shows the location of the Ice property in the Yukon. The nature and origin of deposits in the Carmacks Copper Belt are poorly known because they are

deformed, metamorphosed, deeply weathered, variably oxidized and poorly exposed (Tafti and Mortenson, 2004). Figure 1.2 shows the two main deposits of the Carmacks Copper Belt as well as the Ice property superimposed on the regional geology.



Figure 1.1: Location map of the Ice property (and the Carmacks Copper Belt). The Ice is located at UTM zone 08V, 417935E, 6905900N.

1.2.1 Minto

The Minto project (Fig. 1.2), owned by the Sherwood Copper Corporation is located 240 km north of Whitehorse, Yukon Territory and 50 km northwest of the Ice property. The main zone of the Minto deposit contains measured and indicated resources

of about 8 million tones grading 1.89% Cu, 0.66 g/t Au and 7.7 g/t Ag (Dessureault et al. 2006). Copper is contained primarily in bornite and minor chalcopyrite.

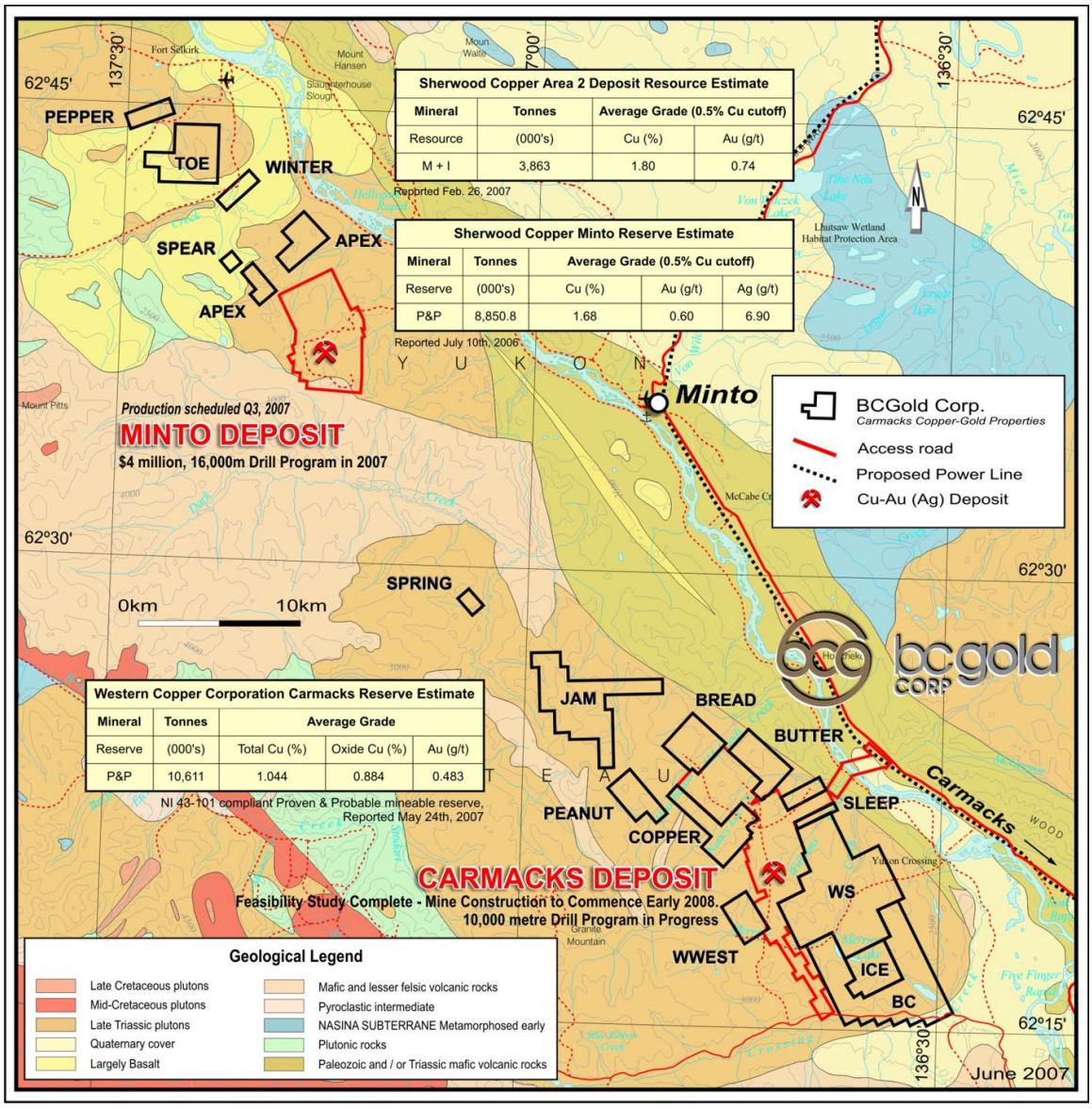

Figure 1.2: Location map of the Ice property on top of the regional geology. Also shown are the locations of the Minto and Williams Creek (Carmacks) deposits. (From http://www.bcgoldcorp.com/main/?carmacksmaps)

1.2.2 Williams Creek

The Williams Creek project (Fig 1.2), owned by Western Copper Corporation is located 200km north of Whitehorse, Yukon Territory, 40km southeast of the Minto

deposit and 10km northwest of the Ice property. The main zone of the Williams Creek deposit contains measured and indicated resources of about 10 million tones grading 1.044% Cu, 0.483 g/t Au, and 4.62 g/t Ag. (Robinson and Casselman, 2007)

1.3 Background of the Ice Property

The first report of copper in this region was made by Dr. G.M. Dawson (son of Sir William Dawson, after whom The Dawson Geology Club was named) in 1887 (Robinson and Casselman, 2007) concerning copper occurrences at Hoochekoo Bluff, located to the north of the property on the Yukon River. The first claims were staked in 1898 to cover copper showings that were associated with copper bearing quartz veins located in Williams Creek Canyon, 10km north of the property and Merrice Creek Canyon, 4 km north of the property.

In the spring of 2006, the Ice property was staked by Ryan-Wood Exploration Ltd. The property was named Ice after Merrice Lake (The last three letters of Merrice were taken), located 1.5km to the north of the property. In late 2006, the property was sold to BC Gold Corporation.

1.4 Questions to be answered

This thesis addressed some important questions such as:

- What are the Cu and Au bearing minerals in the Ice property?
- This area has not been glacially eroded; what implications does this have?
- What is the nature of hydrothermal alteration?
- Why is the mineralization associated with a positive magnetic anomaly?
- Was the mineralization pre- or post- regional deformation/metamorphism?

- Is the mineralization of porphyry copper type or something else?
- Are the Igneous Host rocks the same as at Minto and Williams Creek?
- Is the Ice at the same structural level/phase of the batholith as the other deposits?
- Was the Cu mineralization associated in any way with the magnetite; was the magnetite part of the ore suite or just a spatial coincidence?
- Is the oxidized copper replacing pre-existing sulphides in situ, or have the copper oxides been transported from elsewhere, making Ice an exotic deposit?

1.5 Objectives

1. To understand the correlation (or non-correlation) between magnetic anomalies and mineralization in the Ice area.
2. To determine the relative timing of mineralization and regional deformation/metamorphism.
3. A comparison of the mineralogy of alteration (feldspars and biotite)
4. To determine similarities/differences between the Ice and Minto/Williams Creek deposits.
5. To generate a genetic deposit model for the Ice deposit.

1.6 Methodology

In June 2007, geological mapping, trench mapping, geochemical sampling and rock sampling were done by the author under supervision of geologists Peter and Anne Ledwidge. Soil samples for ICP-MS (Inductively coupled plasma mass spectrometry) and MMI (Mobile Metal Ion) analysis were taken at 50 m station spacings trending north-

south along lines spaced 100 m apart. In September 2007, the rocks were photographed, described, and cut into slabs in the Department of Earth Sciences, Dalhousie University. Magnetic susceptibility of all of the rocks was measured. The slabs were photographed and thin sections made for petrography. Polished sections were created for ore petrography. Whole rock geochemical analyses, electron microprobe analyses, and X-ray diffraction identifications were done. Geochemical data were analyzed with statistical programs.

1.7 Organization of the Thesis

This thesis is divided into 8 chapters. Chapter 2 gives an overview of the regional geology around the study area. Chapter 3 gives an overview of the history of the Ice property, as well as the geophysics, geochemistry, and the field geology of the property. Chapter 4 describes the field work done at the Ice property, as well as the stratigraphy and structural geology of the area. Chapter 5 deals with the igneous petrology of the Ice property. Chapter 6 deals with the mineralogy of alteration and ores at the Ice property. Chapter 7 gives a genetic model for the Ice property. Chapter 8 presents the conclusion of the thesis and recommendations for future work. Appendices follow that contain sample descriptions, microprobe data, geochemical data, and methodologies.

Chapter 2

Regional Geology

2.1 Tectonic Framework

The Carmacks Copper Belt lies within the Yukon-Tanana Terrane of western Canada. The metamorphic rocks in central-eastern Yukon and central western Alaska have also been described as being part of the Yukon Crystalline Terrane by Tempelman-Kluit (1976).

Tafti and Mortenson (2004) concluded that the Minto and Williams Creek deposits formed during a major period of 'vertical tectonics' that affected the region. Regional-scale uplift from mid-crustal to shallow depths at ~186 Ma was deduced from field and U-Pb dating studies of the Aishihik batholith and Lang Lake plutonic suite intrusions 70km to the southwest (Tafti and Mortenson, 2004). There is also evidence for crustal scale thickening throughout large portions of the Yukon-Tanana terrane in western Yukon and eastern Alaska between ~195 to 185 Ma, which could coincide with the burial of the mineralizing systems at Minto and Williams creek (Tafti and Mortenson, 2004). The crustal thickening, burial, and uplift of the region must have occurred within an active continental arc setting, since Tafti and Mortenson (2004) recognized that the geochemical signature of the intrusives is indicative of a continental magmatic arc.

2.2 Stratigraphy

The porphyritic granodiorite is ascribed into the Granite Mountain batholith, interpreted to be intruded into the Yukon- Tanana Terrane. The batholithic rocks are in fault with, or intruded into an unnamed package of altered mafic volcanic rocks to the

northeast and are unconformably overlain by sedimentary rocks and volcanics of the Late Cretaceous Tantalus Formation and Late Cretaceous Carmacks Group, respectively (Tafti and Mortenson, 2004).

2.3 Structural Geology

Tafti and Mortenson (2004) have described the structural geology of the area, although the regional structure is poorly understood because outcrop is very sparse (<1%) and the area is unglaciated and deeply weathered. They found that generalized alignment of K-feldspar phenocrysts in the porphyritic granodiorite indicate magmatic flow. Post-mineralization deformation includes brittle faults with several orientations, including the DEF fault which forms the northern boundary of the main zone at Minto (Tafti and Mortenson, 2004). There is also evidence of block rotation, evidenced by the tilting of younger sedimentary units. This block rotation may account for anomalously shallow dips of the dominant foliations in gneissic host rocks at Minto (Tafti and Mortenson, 2004).

2.4 Igneous History

The rocks of the Ice property are entirely made up of granodiorites of the Granite Mountain Batholith which has been dated by Tafti and Mortenson (2004) to be Early Jurassic (~194 Ma). Post-mineralization granite pegmatite and aplite dykes are widespread in the area. The Ice rocks are plotted on a QAP (Quartz-Alkali Feldspar-Plagioclase) diagram in figure 2.1.

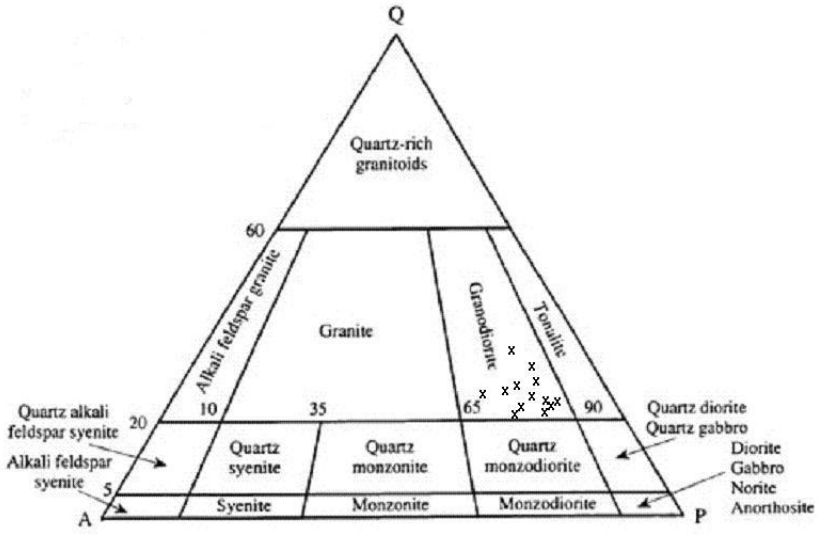

Figure 2.1: Plutonic rocks from the Ice property plotted onto a QAP diagram, from petrographic analysis by the author.

2.5 Metamorphic History

The area has not undergone regional metamorphism, but rafts of host rock within the granodiorite body are locally contact metamorphosed. There are no metamorphic rocks at the Ice property, but Tafti and Mortenson (2004) have described amphibolite/biotite-schist as xenoliths at Williams Creek.

2.6 Metallogeny

At Minto and Williams Creek, the main host rocks for the deposits are variably deformed plutonic rocks. The following description is based on Tafti and Mortenson (2004). Mineralization at Minto is hosted within foliated biotite and quartzofeldspathic orthogneiss, with a lesser amount contained within a banded, relatively quartz-rich rock. The ore zones are enclosed within massive to weakly foliated granodiorite. The host rock for the Williams Creek deposit is foliated intrusive rock of dioritic to quartz dioritic composition, also enclosed within massive to weakly foliated granodiorite. At both

deposits, chalcopyrite, bornite and lesser pyrite are disseminated and occur as stringers (Tafti and Mortenson, 2004).

At the Ice property, mineralization has only been observed as malachite in weakly to strongly foliated granodiorite. Mineralization is interpreted to have occurred prior to the pervasive structural deformation that has affected the host units. No primary sulfide minerals were encountered.

2.7 Geomorphology

Tempelman-Kluit (1980) has given a good synthesis of the evolution of the physiography and paleodrainage of the southern Yukon from the Miocene to present. Before the rapid rise of the St. Elias Mountains, uplift of the Pelly Range and other ranges in southern Yukon and the formation of the Tintina Trench in the Pliocene, southern Yukon had comparatively low relief. The southwestern barrier of the St. Elias Mountains (Fig 2.3) did not exist at this time, which may have allowed water to drain directly to the Pacific via a now abandoned southwesterly route. This deserted drainage hypothesis can explain inconsistencies in relative maturity of parts of valleys, for example, the Takhini and Dezadeash Rivers are small for the valley that they occupy; this valley is considered to be the outlet to the coast of the abandoned drainage. The Yukon River valley in the area of the Klondike is small for its present stream, and the White Channel Gravels and equivalents from the old alluvial surface slope to the southeast in this area, opposite to the gradient of present streams. Figure 2.2 shows the hypothetical paleodrainage as well as the current drainage (Tempelman-Kluit, 1980).

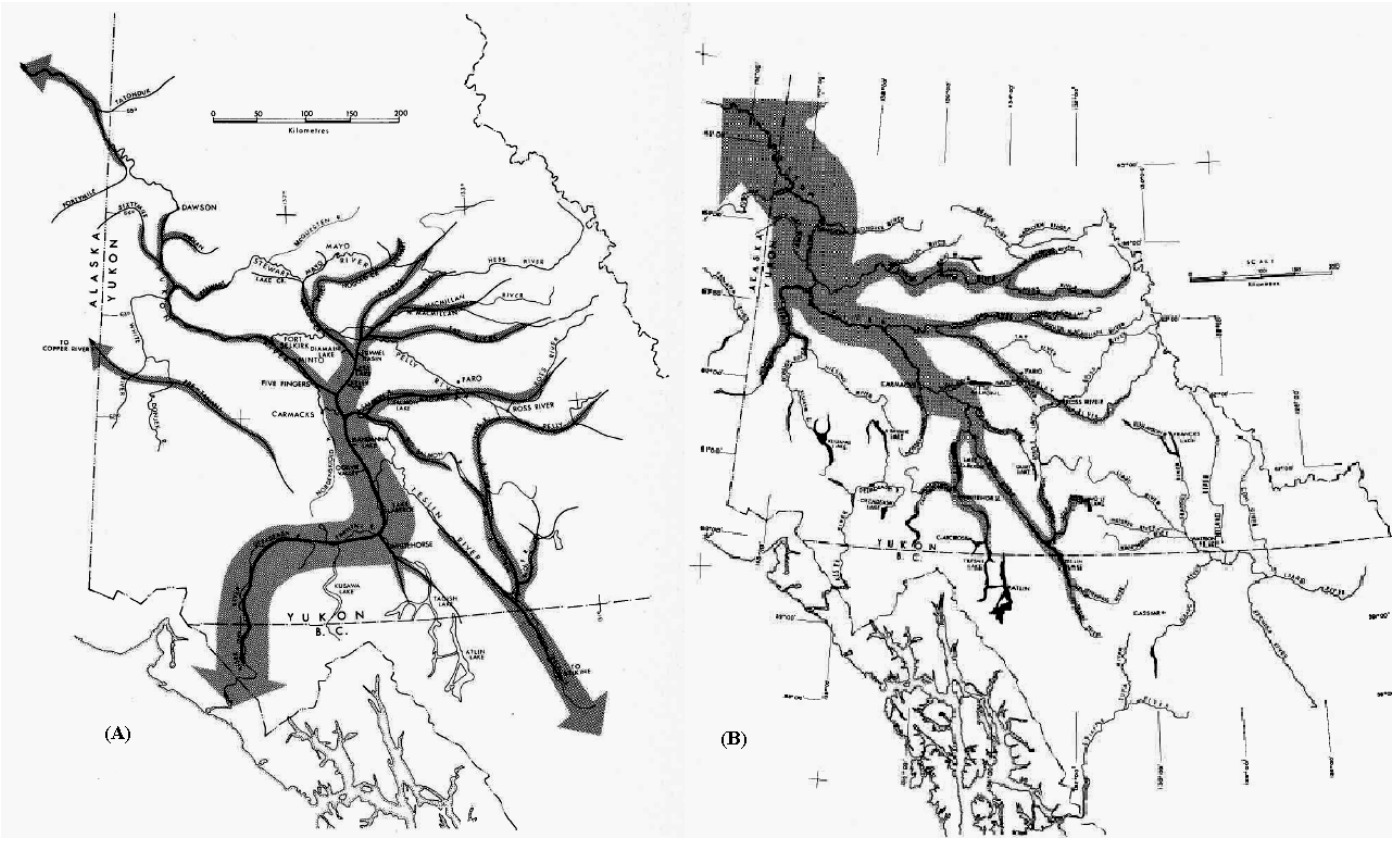

Figure 2.2: A) Hypothetical southwest-flowing drainage (gray arrows) of southern Yukon that probably existed during the Miocene and Pliocene. Water probably drained directly to the Pacific through the valley of the Takhini-Dezadeash Rivers via the ancestral Stikine River. B) The modern, northwest-flowing drainage is shown for comparison. (After Tempelman-Kluit, 1980)

Rerouting of the direct southwesterly drainage to the present northwesterly course probably occurred during the Pleistocene due to damming by glacial Ice in the St. Elias Mountains. When deglaciation began, ice melted in the interior but remained in the St. Elias Mountains preventing drainage to the coast via the old route and initiating rerouting of the drainage to its present route (Tempelman-Kluit, 1980).

The newer drainage is a long and circuitous route in comparison to the old route; for example, Lake Laberge, near Whitehorse, at about 600m above sea level drains to the Pacific through about 2500km of Yukon River, while along the Takhini-Dezadeash route the distance to the Pacific is only 300km (Tempelman-Kluit, 1980).

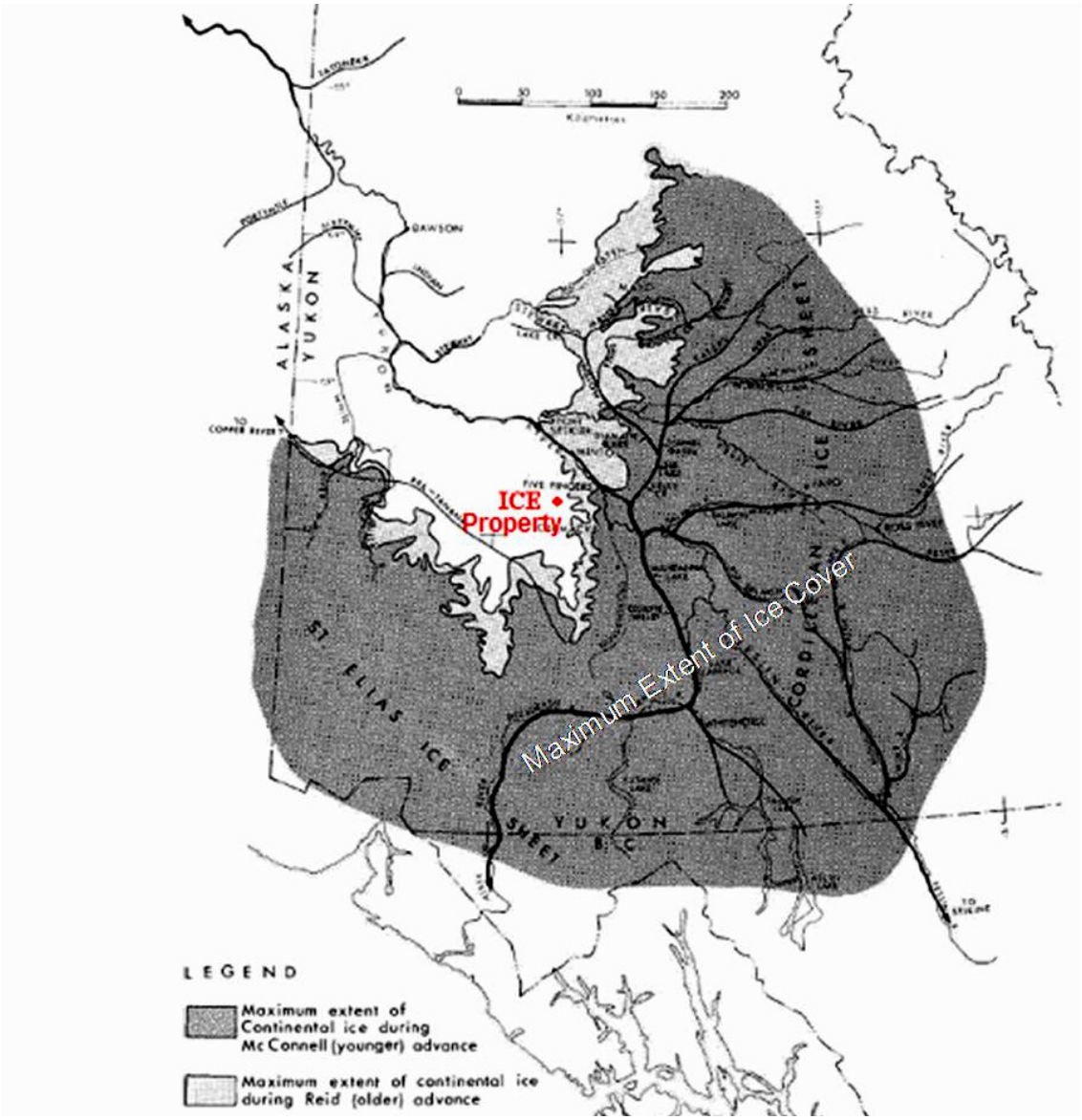

Figure 2.3: Extent of continental ice during the two latest glacial advances of the Pleistocene. Hypothetical Drainage is shown on top of current drainage for reference. The St. Elias Mountains are located in south-western Yukon in the area of the St. Elias Ice Sheet. Darker areas denote glaciation (After Tempelman-Kluit, 1980).

Figure 2.3 shows the extent of continental ice during the two latest advances of continental ice sheets during the Pleistocene. If the deeply weathered rocks of the Ice property had been affected by a glaciation, they would have been easily broken up and transported away by the continental ice sheet, probably removing any evidence of the deposit.

Chapter 3

The Ice Property

3.1 History of the Project

The first report of copper in this region was made by Dr. G.M. Dawson in 1887 concerning copper occurrences at Hoochekoo Bluff, located to the north of the property on the Yukon River. The first claims in the region were staked in 1898 to cover copper showings that were associated with copper-bearing quartz veins located in Williams Creek Canyon, 10km north of the Ice property, and Merrice Creek Canyon, 4km north of the property (Robinson and Casselman, 2007).

In the spring of 2006, the Ice property and the surrounding Williams South property was staked by Ryan-Wood Exploration Ltd. of Dawson City, YT. The Ice property was named after nearby Merrice Lake (From the last three letters of Merrice). In late 2006, the Ice and Williams South properties were sold to BC Gold Corporation of Vancouver, BC. In June 2007, prospecting, geological mapping, sampling, trenching and grid installation started on the Ice property and surrounding Williams South Property. A 1,400m diamond drill program started on the Ice and Williams South Properties in August 2007(Fowler, 2007).

3.2 Geophysics

In July 2007, Aeroquest Ltd. completed a 3,295 line kilometre airborne magnetometer and radiometric survey over BC Gold's Ice and surrounding properties (Fowler, 2007). Figure 3.1 shows the aeromagnetic data. The Ice zone occurs on a bull's-eye shaped magnetic high. Magnetic susceptibility data for rock samples collected at the Ice are presented in Appendix 2.

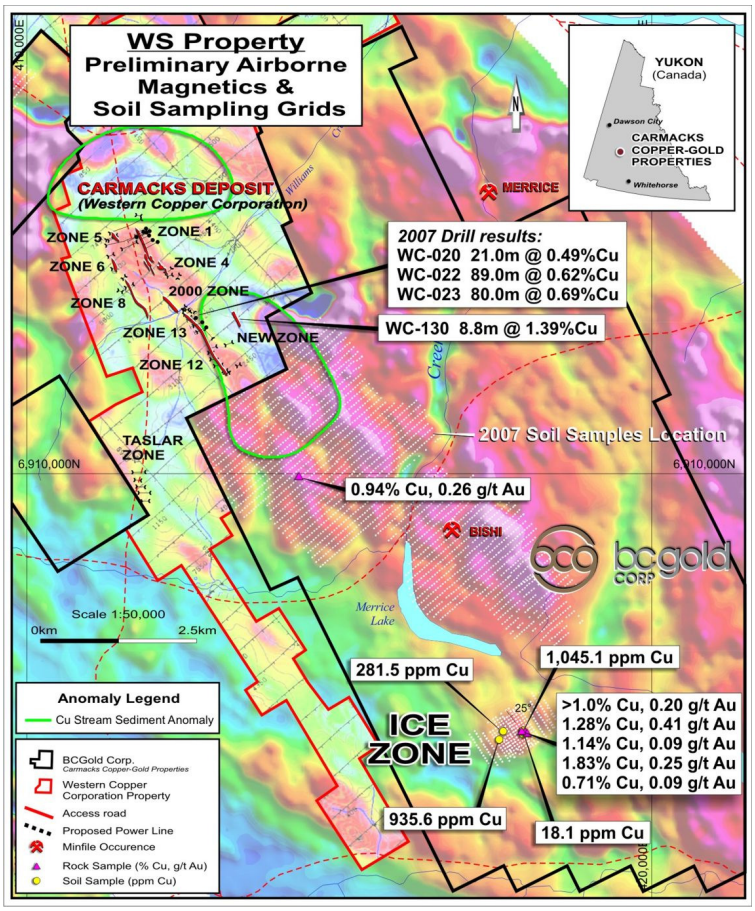

Figure 3.1: Aeromagnetic map of the Ice property and surrounding Williams South Property. Pink-purple is a magnetic high while light blue is a magnetic low. The Ice is located at UTM zone 08V, 417935E, 6905900N.
(After http://www.bcgoldcorp.com/main/?carmacksmaps)

3.3 Geochemistry

In July 2007, over 4,000 MMI (Mobile Metal Ion) soil samples were taken at 50m spacings along lines 100m apart at BC Gold's Carmacks properties (Fowler, 2007). Figures 3.2 and 3.3 show the contoured Cu values from the overall MMI survey in the Ice zone. Over 300 soil samples for ICP analysis were taken over the Ice zone as well. Several grab rock samples were taken at the Ice showing which have copper grades up to 1.83% and gold grades up to 0.41 g/t (Fowler, 2007).

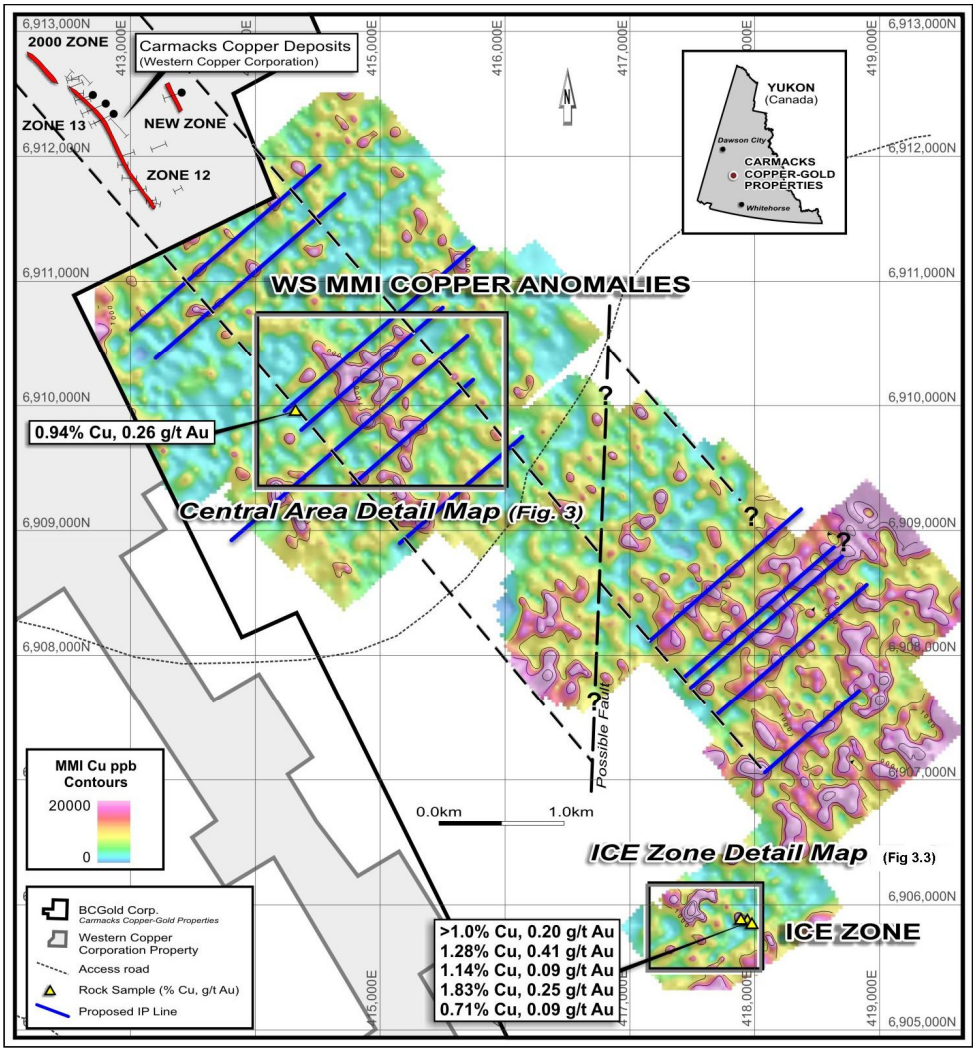

Figure 3.2: Copper MMI contours in the Ice and Williams South zones.
(After http://www.bcgoldcorp.com/main/?carmacksmaps)

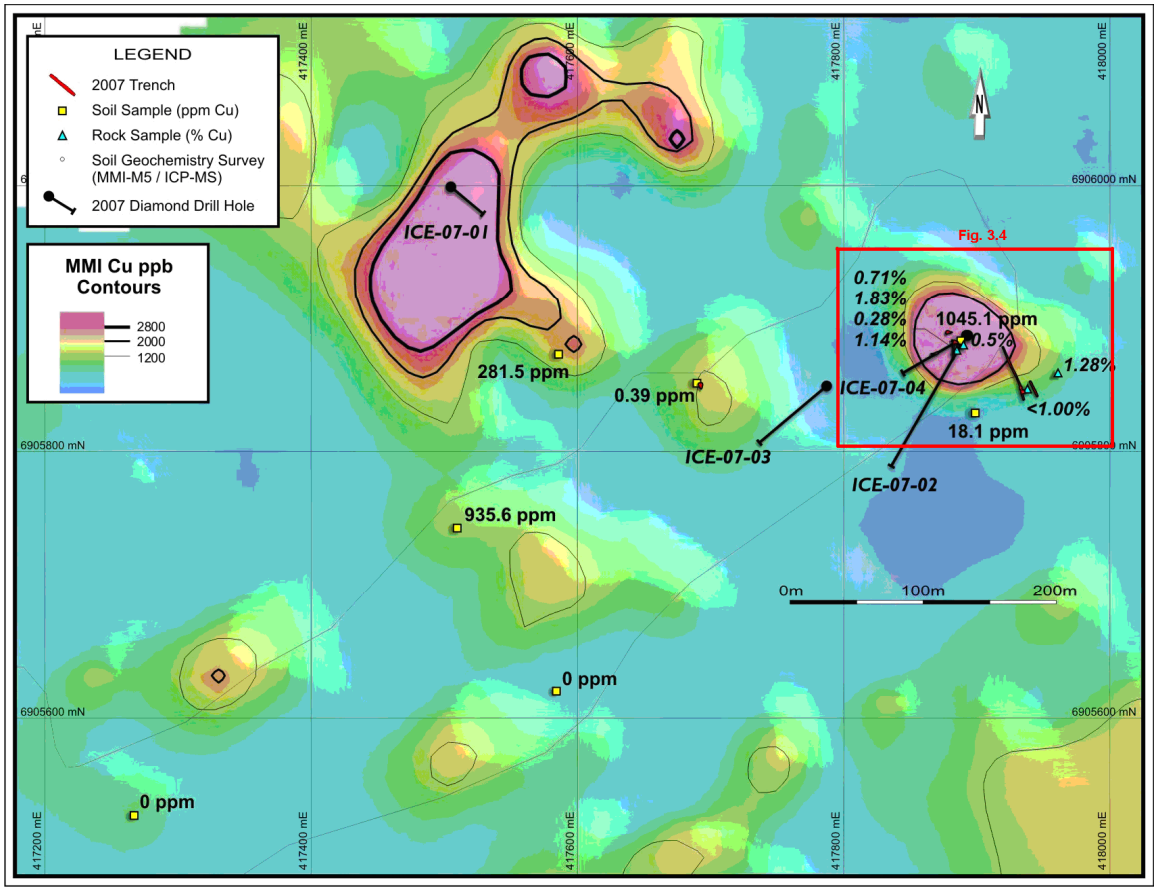

Figure 3.3: Copper MMI contours at the Ice zone. Locations of 2007 diamond drill holes are also indicated. (After http://www.bcgoldcorp.com/main/?carmacksmaps)

A geochemical study by Tafti and Mortenson (2004) indicates that most intrusive rocks in the adjacent Williams Creek deposit are subalkaline, and weakly to moderately peraluminous. Concentrations of immobile trace, high field-strength and rare-earth elements are consistent with generation in a continental magmatic arc and indicate that intrusive rocks in this area are geochemically very similar to other Late Triassic and Early Jurassic intrusive rocks elsewhere in the Yukon-Tanana Terrane in Yukon and eastern Alaska as described by Mortensen et al. (2000) and Tafti and Mortenson, (2004).

3.4 Field Geology

The rocks at the Ice and Williams South properties consist of intermediate to felsic intrusive and meta-intrusive rocks of the early Mesozoic Granite Mountain Batholith. The area is unglaciated and deeply weathered, outcrop is very sparse (<1%), and regional structure is poorly understood. The area is overlain by 1-5cm of volcanic ash from a distal source. The rocks at the Ice zone range from foliated biotite granodiorite to biotite +/- hornblende granodiorite to hornblende granodiorite. The rocks also range from non-magnetic to strongly magnetic. Felsic aplite dykes ranging from 1-40cm in thickness are present as well as pegmatitic dykes ranging from 1-20cm in thickness. Rocks that contain malachite mineralization contain biotite and are also weakly to strongly foliated. Figure 3.4 shows the detailed geology of the Ice property.

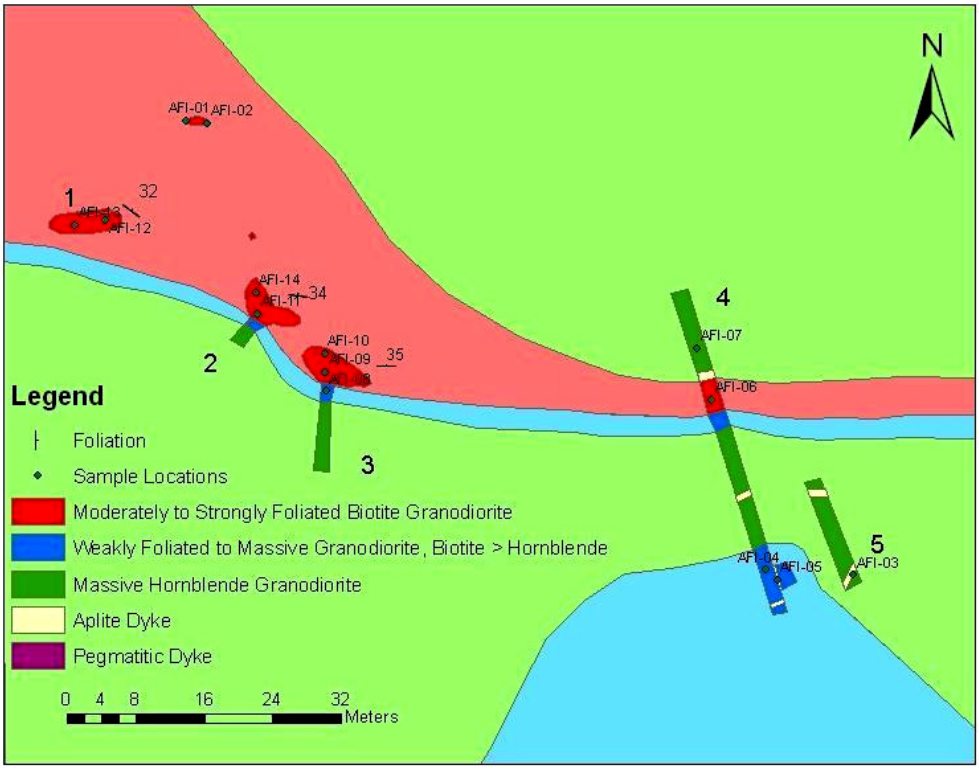

Figure 3.4: Detailed geology of the outcrops and five trenches of the Ice property. Darker colours denote outcrop and trenches; lighter colors are inferred bedrock geology. Copper mineralization is found primarily in the moderately to strongly foliated biotite granodiorite unit.

Chapter 4

Geology of the Ice Property

4.1 Field Work

In June 2007, the author participated in a regional mapping project of the properties surrounding the Ice, and created a detailed map of the outcrops and trenches at the mineralized zone of the Ice property. 14 Rock samples collected by the author were grab samples selected to study differences in mineralogy in both mineralized and unmineralized phases of the granodiorite. Five trenches were dug over an aera approximately 100mx75m on top and down the southwest side of a hill (Fig. 3.4) to increase bedrock exposure, as exposure is sparse in the area (<1%), using a lightweight backhoe which could be transported to the site via helicopter. Structural measurements are reported using the right hand rule.

Trench #1, dug next to mineralized subcrop, is approximately 8m x 2m, and is entirely composed of magnetic, mineralized (1-3% malachite), weakly foliated biotite granodiorite. Trench #1 has a foliation of 306/32 NE and contains a 2-5 cm thick pegmatite dyke with a strike of 240/65 N. About 10m to the north of trench #1, there is subcrop of weakly magnetic, foliated, mineralized biotite granodiorite.

Trench #2 was dug at the base of a 5 m^2 outcrop of magnetic, mineralized (1-3% malachite), foliated biotite granodiorite with a foliation of 276/34 N. Trench #2 is approximately 5m long and 1m wide, at the base of the outcrop there is a sharp contact between the magnetic, mineralized, foliated biotite granodiorite and massive, weakly magnetic biotite granodiorite which grades into massive hornblende granodiorite over 1m past the contact into the trench.



Figure 4.1: View from the bottom of Ice trench #4, Rock hammer for scale.

Trench #3 was dug at the base of a 5x3m outcrop of magnetic, mineralized (1-3% malachite), foliated biotite granodiorite with a foliation of 270/35 N. As in trench #2, at the base of the outcrop there is a sharp contact between the magnetic, mineralized, foliated biotite granodiorite and massive, weakly magnetic biotite granodiorite which grades into massive hornblende granodiorite over 1-2m past the contact into the trench. Trench #3 is about 12m long and contains no copper mineralization.

Trench #4 (Figure 4.1) is approximately 40m long and 1m wide, it was dug in proximity to several pieces of mineralized float on the side of the hill. From the top (north end) of the trench there is about 10m of weakly magnetic massive hornblende granodiorite. At approximately 10m there is a near vertical 1m thick aplite dyke trending

towards 062. Past the aplite dyke, the granodiorite is deeply weathered but chunks of magnetic, mineralized, weakly foliated biotite granodiorite were recovered from the trench wall over a distance of about 5 m. At approximately 15 m down the trench, the biotite granodiorite grades to hornblende granodiorite over about 1.5 m. At 15 m down the trench, there is copper mineralization present within a fracture with a strike of 078/36 S; 1 m past this there is an aplite dyke 90 cm thick with a strike of 066/56. At 31 m down the trench, the mineralogy changes back to biotite granodiorite and a mineralized aplite dyke with a strike of 127/60 SW appears, and is visible for 5m in the trench; it is displaced after 1m by a group of fractures over 50 cm trending 028/67 E with a sinistral sense.

Trench #5 was dug in proximity to mineralized float on the side of the hill but is composed entirely of hornblende granodiorite and contains no copper mineralization. Trench #5 is about 12m long and 1m wide. From the top (north end) of the trench, at 1m there is a 50cm thick aplite dyke with a strike of 063/43 S. At 11m there is a near vertical 60cm thick aplite dyke trending at 245.

4.2 Structural Geology

Petrographic studies by Tafti and Mortenson (2004) have shown that the intrusive rocks at Minto and Williams Creek have been affected by at least two distinct phases of foliation development. Feldspar phenocrysts (dominantly plagioclase) at Williams Creek are typically strongly recrystallised in both the massive and foliated phases. In moderately to strongly foliated phases, quartz and plagioclase grains show strong recrystallisation and strain (Tafti and Mortenson, 2004). Field relationships at Williams Creek show that this foliation is cut by massive to weakly foliated intrusive phases and

several generations of aplitic dykes (Tafti and Mortenson, 2004). Ductile deformation has also affected some of the late dykes that cut massive intrusive rocks at Williams Creek (Tafti and Mortenson, 2004). Post-mineralization brittle faulting has also been observed in the area, in some cases forming conjugate fault sets. The young brittle faults have facilitated deep circulation of meteoric water and the oxidation of hypogene sulphide minerals and their host rocks (Tafti and Mortenson, 2004).

Chapter 5

Igneous Petrology of the Ice Property

5.1 Macroscopic Igneous Petrography

The rocks of the Ice Property are porphyritic granodiorite in composition and range from strongly foliated to massive and biotite-rich to hornblende-rich. Several aplitic and pegmatitic dykes cut the granodiorite. The granodiorite is variably magnetic with no clear correlation between copper mineralization and magnetism at outcrop scale; mineralized rocks are commonly magnetic, but so are unmineralized rocks. Copper mineralization correlates with rocks being rich in biotite and commonly correlates with a medium to strong foliation. Rocks grade from being rich in biotite to rich in hornblende over 1-3 m away from copper mineralization. There is a sharp contact from foliated to massive granodiorite (Fig. 5.1). No sulphides are visible and all copper minerals appear to be oxides or silicates. The heavily weathered, foliated rocks contain rusty vugs which may have previously been occupied by sulphides (Fig 5.2).



Figure 5.1: Outcrop at the top of trench #3 at the Ice property. A clear contact is visible between foliated, mineralized granodiorite (upper) and massive unmineralized granodiorite (lower). Sample AFI-14 was taken from the foliated section of this outcrop.



Figure 5.2: Hand specimen of sample AFI-14A. Copper oxide is visible in the rock as well as rusty vugs (scale bar is in cm).

5.2 Microscopic Igneous Petrography

Thin sections were prepared for 12 samples and polished sections were prepared for 10 samples at Dalhousie University in the fall of 2007. Thin section descriptions are given in Appendix 1. Polished sections were analyzed with the electron microprobe at Dalhousie University's Robert Mackay Laboratory. Figure 5.3 shows a grain of magnetite partially oxidized to hematite (martite). The rocks at the Ice property are heavily weathered and oxidized.

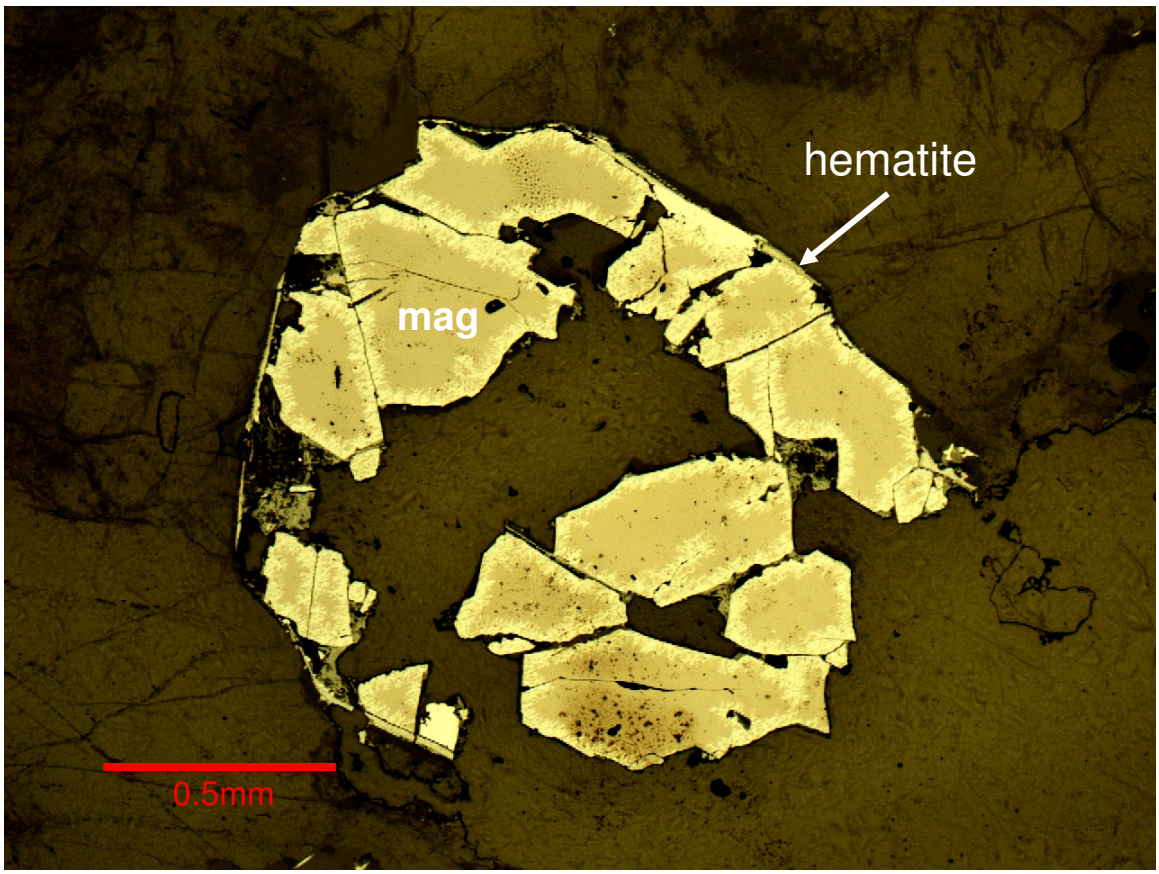

Figure 5.3: Polished section picture (Sample AFI-14b) showing a magnetite grain partially oxidized to hematite (martite).

The foliation of the foliated granodiorite is defined by grains of biotite; figure 5.4 shows biotite grains defining a foliation in sample AFI-13.

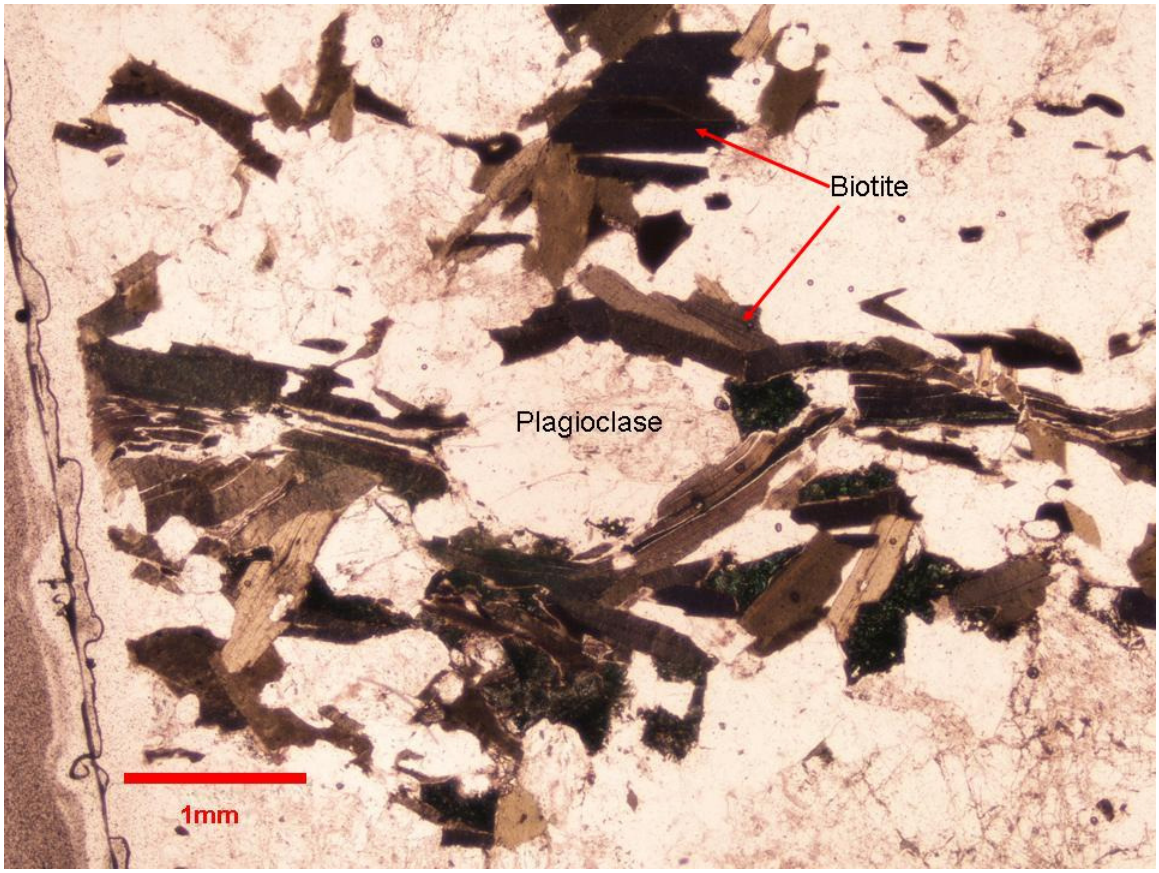

Figure 5.4: Biotite grains defining a foliation in sample AFI-13. The foliation is a secondary feature related to tectonic deformation and wraps around a plagioclase grain.

Recrystallized quartz veinlets are visible in thin section which indicates that the rocks have undergone tectonic strain.

5.3 Geochemistry

Ten samples were analyzed by Geo Labs in Sudbury, ON for whole-rock major and trace elements and ferrous iron (FeO) using X-ray fluorescence spectrometry (XRF). Appendix 3 shows these analyses. FeO analyses have not yet been returned by the lab (March 11, 2008).

Increased copper values correlate with an increase in As, Sn, Rb, Pb, Ba, and K_2O and a decrease in Na_2O, and LOI (Loss on ignition).

A plot of Nb vs. Y and a plot of Rb versus Y+Nb (Fig 5.5) indicates a volcanic arc setting for the intrusive rocks of the Ice property (Pearce et al., 1984) which agrees with Tafti and Mortenson's (2004) findings.

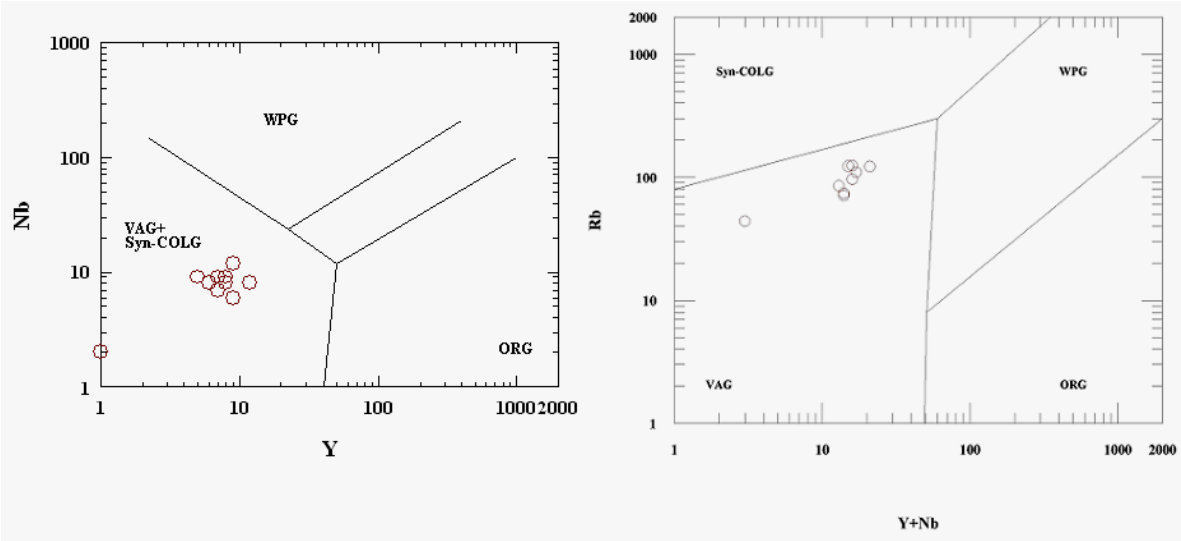

Figure 5.5: A logarithmic plot of Nb vs. Y indicates that the Ice granodiorites were formed within a syn-collisional or volcanic arc setting; a logarithmic plot of Rb vs Y+Nb for the Ice indicates that the igneous rocks formed in a volcanic arc setting (VAG = Volcanic Arc Granite, Syn-ColG = Syn-Collisional Granite). (After Pearce and Cann, 1973).

Figure 5.6 shows the Ice rocks classified based on geochemical data.

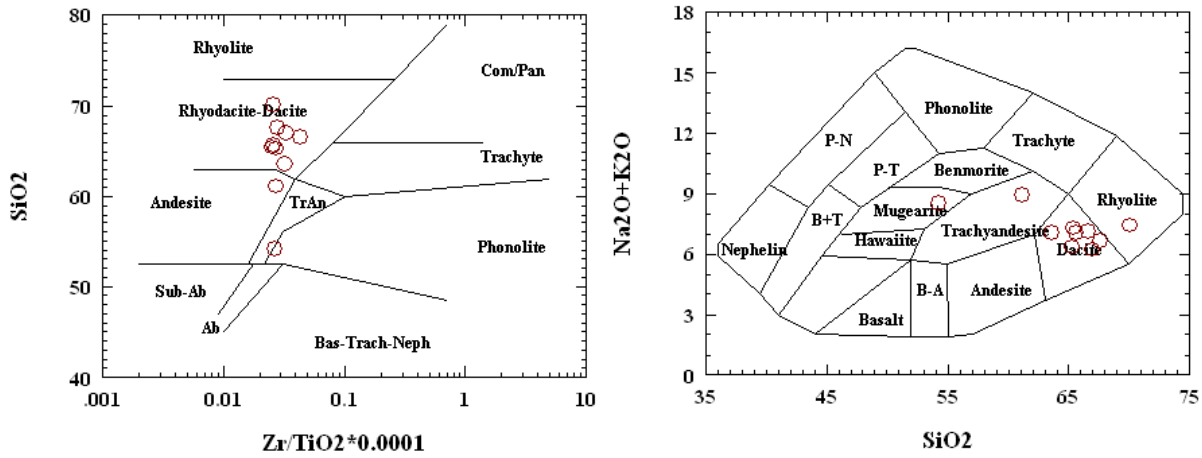

Figure 5.6: Two different rock classification diagrams illustrating that the rocks from the Ice property primarily fall under the granodiorite category (Dacite is the volcanic equivalent of Granodiorite). (After Winchester and Floyd, 1977).

A plot of logCu vs. K_2O indicates that higher copper values correspond to increased levels of potassium in the rocks, which is most probably due to potassic alteration, rather than a different intrusive body. Rubidium often substitutes for potassium, and a plot of logCu vs. Rb also shows a positive correlation which helps to validate this observation. These plots are shown in figure 5.7.

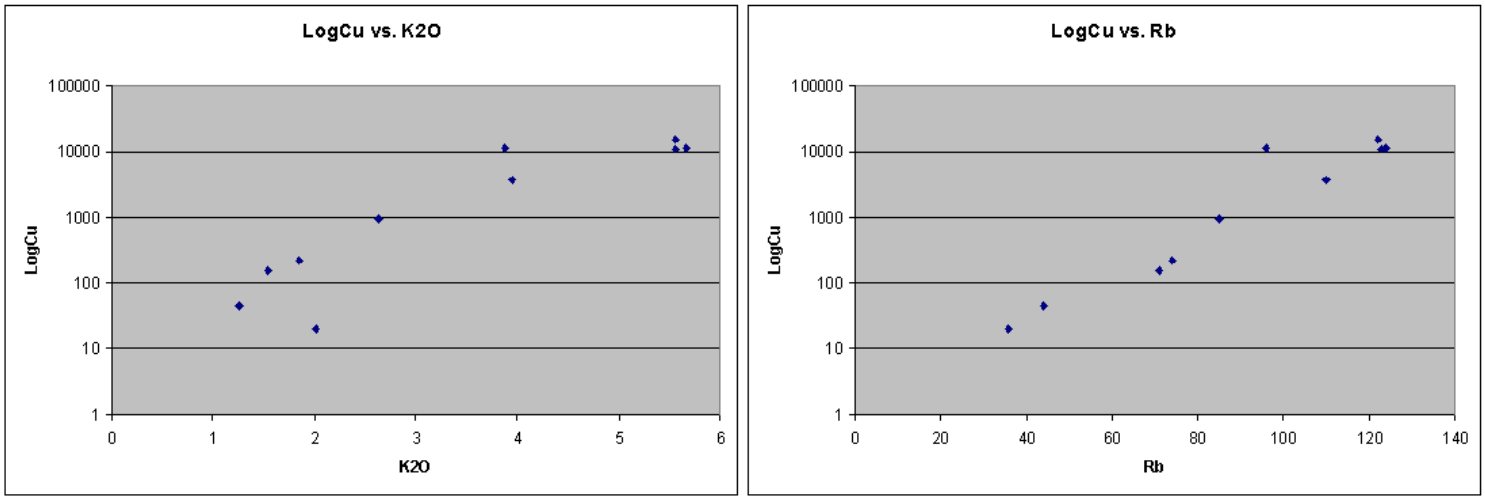

Figure 5.7: Plots of logCu vs. K_2O and logCu vs. Rb show a positive correlation which suggests that high copper values correspond to potassic alteration of the igneous rocks in a porphyry copper setting.

5.4 Hornblende Geobarometry and Two-Feldspar Geothermometry

The amphiboles used in this experiment have been classified as magnesian hastingsitic hornblende using Hawthorne (1981)'s classification system.

There are enough thermodynamic constraints on the composition of hornblende that the total aluminum values in the rims of hornblende of calc-alkaline rocks may be used to calculate the pressure of crystallization (Hammarstrom and Zen, 1986; Hollister et al. 1987; Schmidt, 1992). The requirements to constrain the degrees of freedom and make the Al-content of hornblende a valid geobarometer are the following (Hammarstrom and Zen, 1986; Hollister et al. 1987):

1) The rocks should be calc-alkaline;

2) An assemblage of plagioclase-quartz-hornblende-biotite-orthoclase-magnetite-titanite must have crystallized together;

3) To constrain temperature, only the compositions of the rims of the hornblende should be determined (the rims were the only part of the grains that could have crystallized with the other phases in the final melt);

4) The plagioclase rim compositions should be between An_{25} and $An_{35;}$

5) The pressure has to have been >2 kbars (the limit of the experiment).

Schmidt (1992) gives the following equation to calculate the pressure:

$$P\ (\pm\ 0.6\ \text{kbar}) = -3.01 + 4.76Al^{tot} \qquad (5.1)$$

Where P is the pressure in kilobars and Al^{tot} is the total aluminum in the hornblende in apfu (atoms per formula unit). Microprobe data for hornblendes are found in appendix 4b. The values for mass percent of aluminum range from 10.652 to 11.983 with a mean of 11.423. The apfu for all elements were calculated for all microprobe analyses and were found to be very similar. Table 5.1 shows the data for analysis AFI-07-32 calculated to apfu, assuming that all of the Fe is ferric.

Using Schmidt (1992)'s equation a value of 6.40 kbar is found for the pressure of solidification of this hornblende.

Oxygens per formula =		23.000						
Oxide	**GFW**	**FeO only Wt.%**	**Fe2O3 only Wt.%**	**Mole Units**	**Oxygen Units**	**Normaliz. Ox Units**	**Atom Units**	
SiO2	60.084	40.9131	40.913	0.681	1.362	12.000	6.000	**Si**
TiO2	79.866	0.8727	0.873	0.011	0.022	0.193	0.096	**Ti**
Al2O3	101.961	11.4373	11.437	0.112	0.337	2.965	1.977	**Al**
Fe2O3	159.688		21.967	0.138	0.413	3.637	2.424	**Fe+3**
FeO	71.844	19.7662					0.000	**Fe+2**
MnO	70.937	0.6631	0.663	0.009	0.009	0.082	0.082	**Mn**
MgO	40.304	8.8618	8.862	0.220	0.220	1.937	1.937	**Mg**
CaO	56.077	11.6663	11.666	0.208	0.208	1.833	1.833	**Ca**
Na2O	61.979	1.5049	1.505	0.024	0.024	0.214	0.428	**Na**
K2O	94.196	1.4774	1.477	0.016	0.016	0.138	0.276	**K**
H2O	18.015						2.000	**H**
Totals		97.2173	99.364	1.419	2.610	23.000	17.055	

Table 5.1: Microprobe analysis AFI-07-32 of a hornblende used in hornblende geobarometry calculations. This analysis was chosen as it has median numbers in all elements (Table after Leake et al., 1997).

The following equation is a two-feldspar geothermometer as given by Haselton et al. (1983):

$$T_K = \frac{(X^{AF}_{Or})^2(18810+17030X^{AF}_{Ab}+0.364P) - (X^{Pl}_{An})^2(28230-39520X^{Pl}_{Ab})}{10.3(X^{AF}_{Or})^2+8.3143\ln\left\{\frac{(X^{Pl}_{Ab})^2(2-X^{Pl}_{Ab})}{X^{AF}_{Ab}}\right\}} \quad (5.3)$$

Where T_K is temperature in degrees Kelvin, X= the mole fraction for the feldspars and P is the pressure in bars. No error is given for this calculation.

Using the pressure from equation 5.1 and the average feldspar values of Or_{82} and An_{30}, a value of 657°C is calculated (the increase in pressure to account for temperature used in the following paragraph increased the calculated temperature to 660°C which is a negligible increase).

Anderson and Smith (1995) have added to the hornblende geobarometry equation to account for the effects of temperature on the Al-in-hornblende geobarometer; the revised equation is:

$$P\ (\pm 0.6\ \text{kbar}) = 4.76Al^{tot}\text{-}3.01\text{-}[(T\text{-}675)/85)]\ [0.530Al^{tot} + 0.005294(T\text{-}675)] \quad (5.2)$$

Where P is the pressure in kilobars, Al^{tot} is the total aluminum in the hornblende in apfu (atoms per formula unit) and T is temperature in °C. Using the temperature value calculated in the next section, the pressure of solidification for this hornblende is calculated to be 6.60 kbar.

5.5 Interpretations

The foliation observed in hand sample and thin section scales is a secondary feature related to tectonic deformation. Potassic alteration correlates to higher copper grades, and the foliation defining the higher grade areas are defined by biotite. The geochemistry of the Ice rocks indicates that they are granodiorites formed in a volcanic arc setting.

Using the Al-in-hornblende geobarometer, Tafti and Mortenson (2004) have found that the latest intrusive phases at Minto and Williams Creek formed at depths greater than 9km and have given a value of <6 kbar. Using amphibole-plagioclase thermometry, they have calculated the crystallization temperature at 720ºC to 840ºC which is low for intrusive rocks with granodioritic to dioritic composition (Tafti and Mortenson, 2004).

The Al-in-hornblende geobarometry values of 6.4-6.6 ±0.6 kbar correlate to depths of 18-20km and agree with Tafti and Mortenson (2003)'s findings. The calculated crystallization temperature of about 660°C is lower than Tafti and Mortenson's, but with

the amount of error involved in geothermometry calculations, they may actually be in the same range.

The geobarometric calculations are tentative, and completed mainly to compare with similar work by other authors. The rocks at Ice do not qualify as calc-alkaline, but nor did those used by Tafti and Mortenson (2003). Also, without determination of the valency state of the Fe in the hornblende, which is out of the scope of this study, the uncertainty of the pressure calculation is considerable. Nevertheless, the results are consistent with crystallization of the rocks at several kilometres depth, such as is considered common for porphyry copper type systems (e.g. Lowell and Guilbert, 1970).

Chapter 6

Mineralogy of Alteration and Ores

6.1 Thin section descriptions

Thin section descriptions are in Appendix 1. From thin section analysis, the rocks were confirmed to be granodiorite. Strong foliations are visible in some samples, as well as recrystallised quartz, plagioclase and alkali feldspar grains. Foliated granodiorite from sample AFI-05, foliation defined by biotite, with a carbonate rim is shown in figure 6.1.

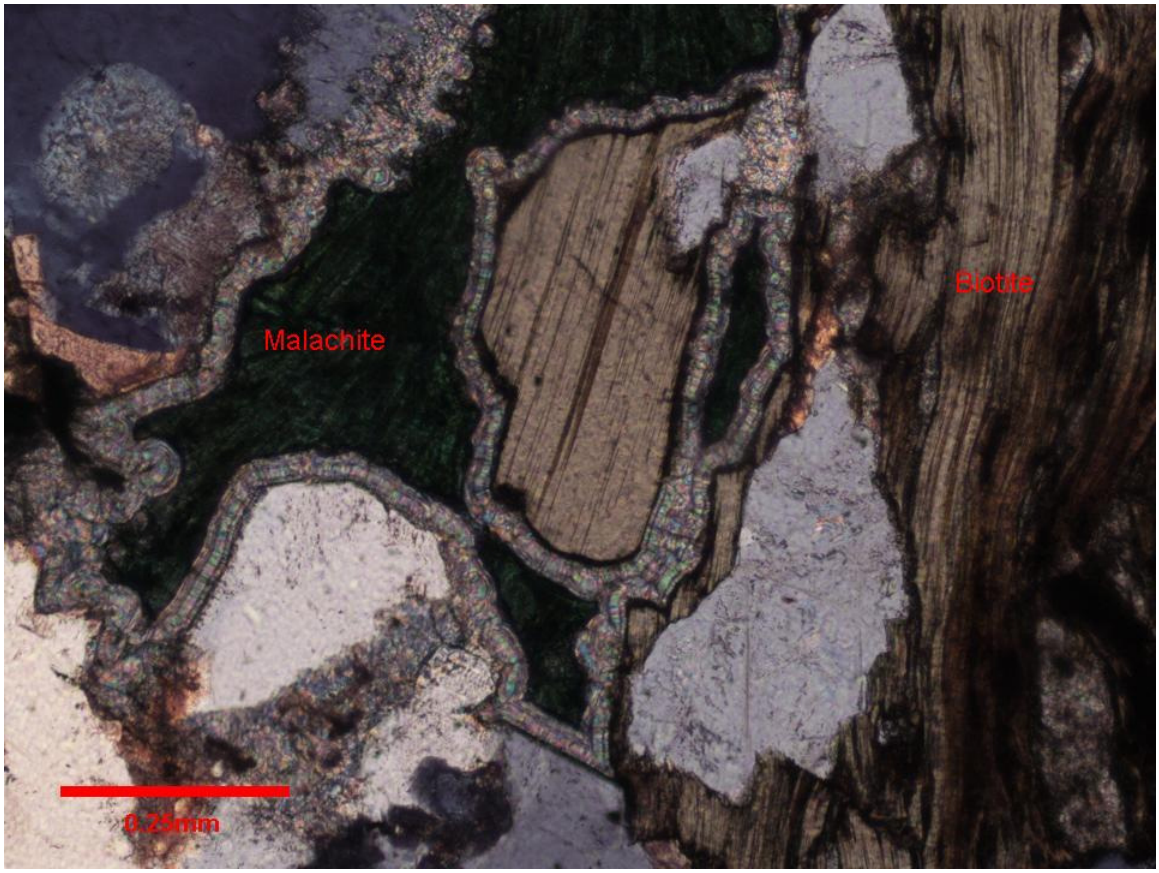

Figure 6.1: Sample AFI05, a carbonate (highly birefringent, probably calcite) rim is visible around malachite grains; some iron oxide-hydroxide is responsible for the reddish staining (e.g. near the scale bar in the figure). Sample AFI-05 is the only sample containing malachite rims. A strong foliation is defined by biotite.

From thin section analysis, the rocks containing copper mineralization can be described as porphyritic, foliated biotite granodiorite with a mineral assemblage of

plagioclase, quartz, potassium feldspar, biotite, magnetite, hematite, malachite and minor amounts of opaque minerals; one sample contains rimmed malachite. The rocks with no copper mineralization can be described as porphyritic hornblende ±biotite granodiorite with a mineral assemblage of plagioclase, quartz, potassium feldspar, hornblende, biotite, magnetite, hematite and minor amounts of opaque minerals.

Recrystallized quartz grains as well as undulose extinction in quartz grains are visible in all samples, indicating that these rocks have undergone strain. The rims of magnetite grains are partially oxidized to hematite during weathering.

6.2 Electron Microprobe

The electron microprobe analyses were done at Dalhousie University's Robert Mackay Laboratory. Microprobe analysis was used to confirm the identification of phases for petrography and to study variations in the mineral chemistry. A JEOL 733 electron microprobe with four wavelength dispersive spectrometers and an Oxford Link eXL energy dispersive system was used. The resolution of the energy dispersive detector was 137 V at 5.9 KV. Each spectrum was acquired for 40 seconds, with an acceleration voltage of 15 Kv and a beam current of 15 nA. Probe spot size was approximately 1 µm in diameter. Geological standards were used for controls. Analyses were carried out under the supervision of Dr. Patricia Stoffyn.

Electron microprobe analyses are given in Appendix 4. No sulphides were encountered in the thin or polished sections. Figure 6.2 shows an electron backscatter image of the common assemblage of minerals in the foliated, mineralized samples from the Ice property (sample 14b).

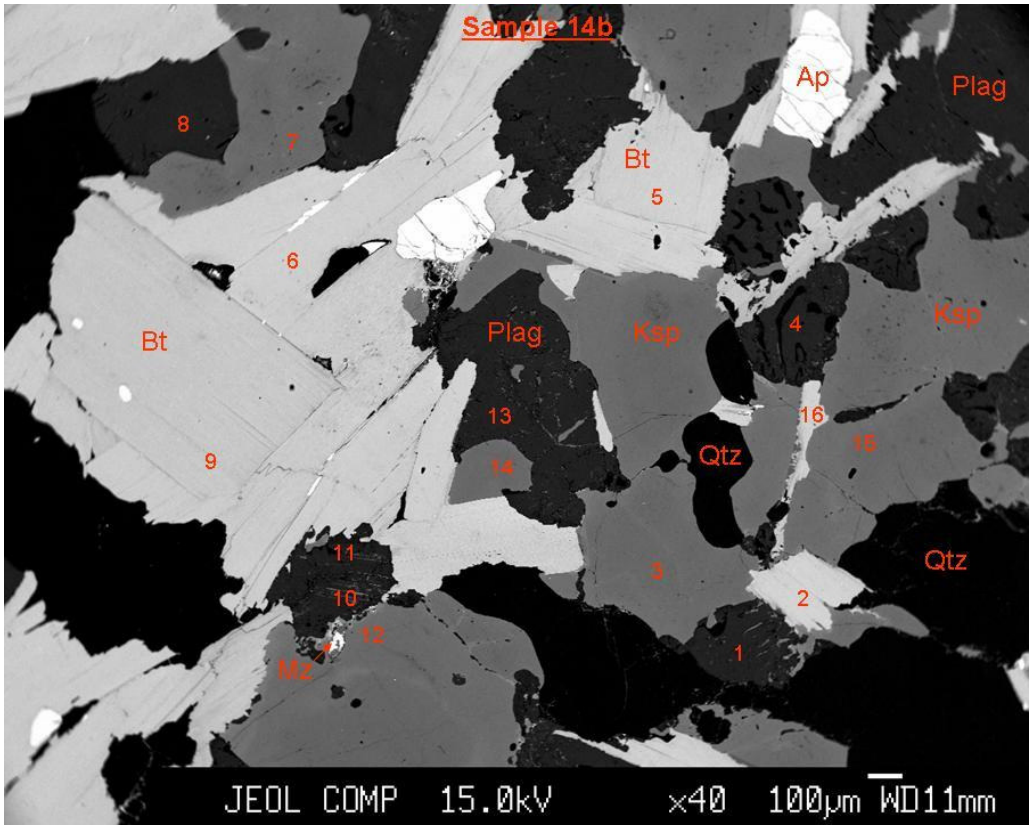

Figure 6.2: Backscatter electron image of sample 14b. Ap=Apatite, Bt=Biotite, Qtz=Quartz, Plag=Plagioclase, Ksp=Alkali feldspar, Mz=Monazite. Numbers refer to electron microprobe measurements located in appendix 4a (beginning with AFI-14b-1). 1=Plagioclase, 2=Biotite, 3=Alkali feldspar, 4=Plagioclase, 5=Biotite, 6=Biotite, 7=Alkali feldspar, 8=Plagioclase, 9=Biotite, 10=Plagioclase, 11=Quartz in Plagioclase, 12=Alkali feldspar, 13=Plagioclase, 14=Alkali feldspar, 15= Alkali feldspar, 16=Biotite.

Figure 6.3 shows an element map generated with the electron microprobe of S, Fe, Na, Si, and Cu to illustrate that there is no sulfur in the rocks of the Ice property. Copper minerals in the Ice samples come in at least two species, a Cu-Si-Fe bearing species (possibly chrysocolla) and a Cu species (probably malachite, as O and C are not analyzed for in the microprobe). From XRD analysis, the dominant copper mineral is confirmed to be malachite; chrysocolla is amorphous and generally yields no recognizable crystalline pattern in XRD.

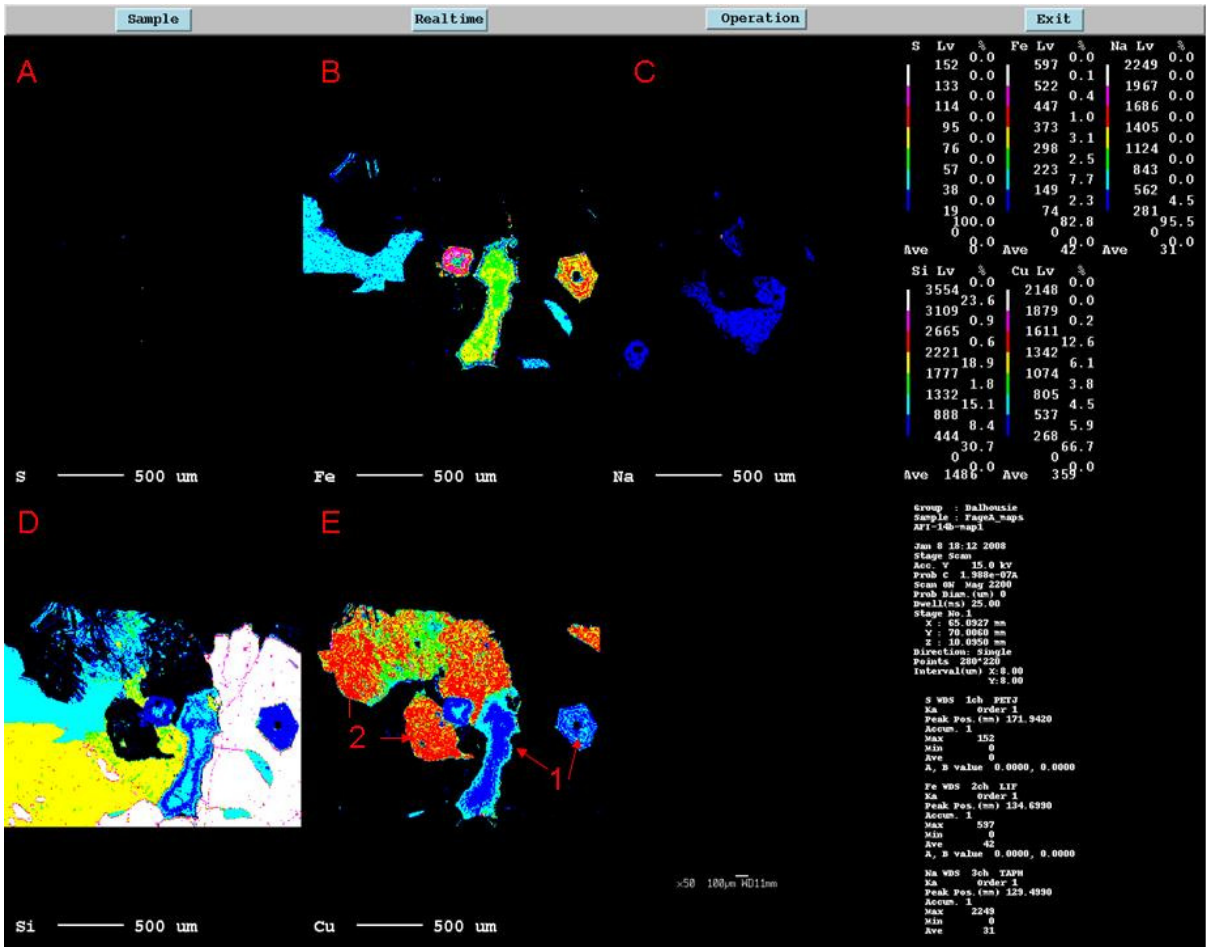

Figure 6.3: Element map from the electron microprobe. A-Sulfur, B-Iron, C-Sodium, D-Silicon, E-Copper. 1-Copper Silicate, 2-Copper Oxide. The copper minerals do not contain sulfur, and no sulphides were encountered in any microprobe analysis of Ice samples. The occurrence of remnant Fe associated with the Cu suggests that the copper oxides may be the oxidised equivalent of pre-existing sulphides (Sample AFI-14b)

Analyses of feldspars from the Ice samples, plotted on an Orthoclase-Albite-Anorthite diagram in figure 6.4, shows that the majority of k-feldspars are Or_{80-85}, and the majority of plagioclase are oligoclase, An_{30}. There are also a number of pure albite grains in the rocks.

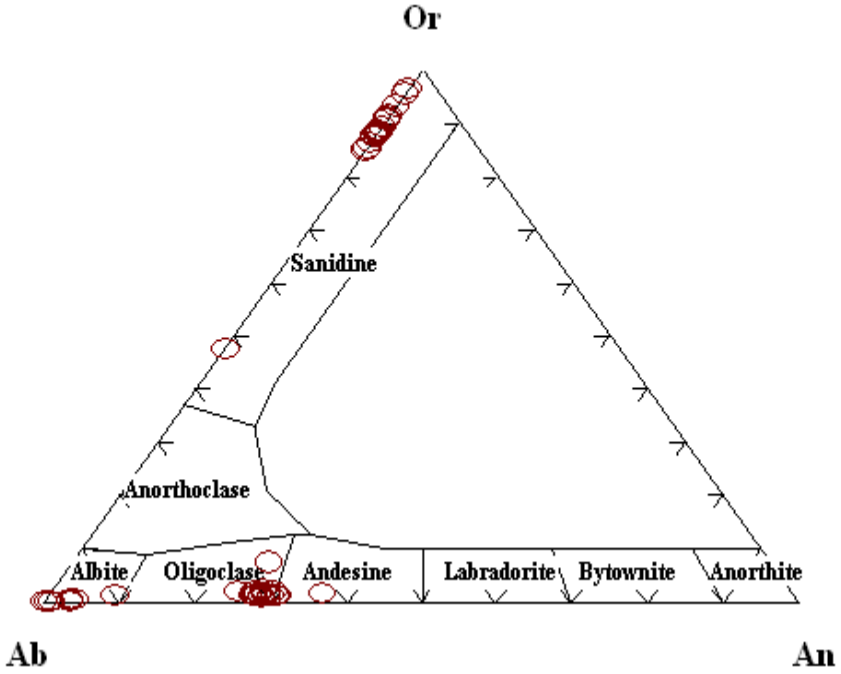

Figure 6.4: Analyses of feldspar grains from Ice samples plotted on an Orthoclase-Albite-Anorthite diagram.

A classification of the biotites analyzed with the electron microprobe is shown in figure 6.5.

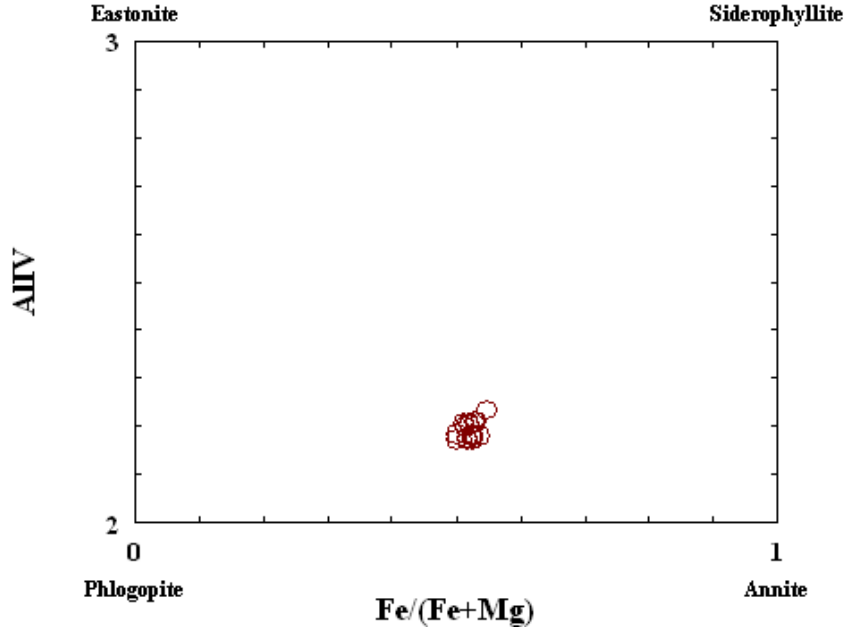

Figure 6.5: Classification of biotites as of intermediate composition from microprobe analyses.

6.3 X-ray Diffraction

Three samples from the Ice property were measured using X-ray diffraction to determine the identity of the green 'copper oxide' minerals. From the electron microprobe it is evident that there are at least two copper bearing phases, a Cu-Fe-Si bearing phase and a Cu-bearing phase (C and O are not analyzed for but are assumed to be present). From the X-ray diffraction analyses, the green mineral has been identified as malachite [$Cu_2(CO_3)(OH)_2$]. In samples AFI-05 and AFI-06 there was some contamination from other minerals (quartz and feldspars) in the diffractogram, but sample AFI-14 (Fig. 6.6) clearly shows the diffractogram for malachite.

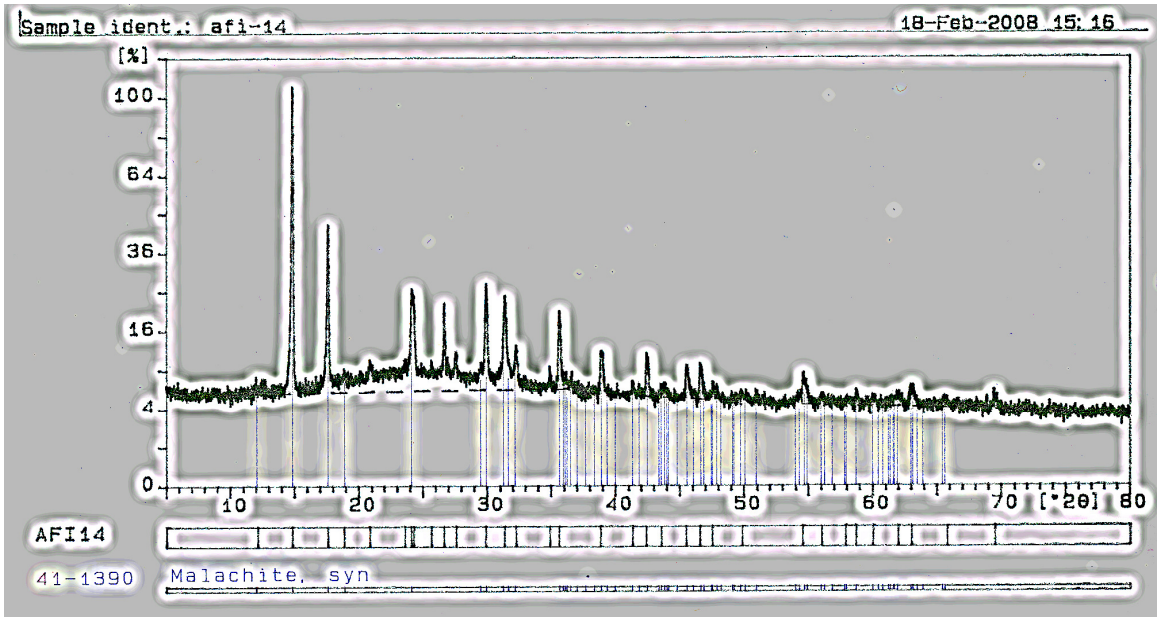

Figure 6.6: X-Ray Diffraction plot from sample AFI-14 showing the major peaks for malachite.

6.4 Interpretations

From thin section description, the Ice rocks are granodiorites, and from the textures observed, they have undergone strain and have been oxidized and weathered. Sulphides are not present in the Ice rock samples. Feldspars analysed in the Ice samples are sanidine with Or_{80-85}, Oligoclase and Albite. There are at least two copper minerals in

the Ice rocks, but malachite is the dominant copper mineral, whereas some indication of Chrysocolla (Cu silicate) was obtained though the microprobe.

Chapter 7

Genetic Model for the Ice Property

7.1 Model for Minto and Williams Creek

Previous workers have assigned the deposits of the Carmacks Copper Belt to various different deposit types, including metamorphosed volcanogenic massive sulphide deposits, metamorphosed redbed copper deposits and deformed copper-gold porphyries (Pearson and Clark, 1979). Tafti and Mortenson (2004) reported that the ore and alteration assemblages closely resemble those associated with early stages of mineralization in typical copper (-gold) porphyry deposits as well as some iron-oxide-copper-gold-type (IOCG) deposits. Supergene effects at Minto and Williams Creek are characterized by the presence of abundant secondary copper oxide minerals and less abundant secondary copper sulphide minerals and by the local presence of hematite and clays. Nearly all of the copper contained at the No. 1 zone at Williams Creek appears to occur in the form of secondary copper oxide minerals, and there is little evidence that significant amounts of hypogene sulphide minerals were ever present in the rocks (Tafti and Mortenson, 2004). They proposed a simple ‘arrested porphyry’ deposit model has been where the deposit formed as a porphyry system which stopped developing at some point. The extent of supergene enrichment at the Williams Creek suggests that it was the product of secondary oxide-mineral enrichment, and is not hypogene ore that has oxidized in place.

7.2 Exotic Deposits

Because the Ice mineralization has some characteristics of a transported or exotic copper deposit, the concept is introduced here. Exotic copper deposits are formed in association with the supergene oxidation and enrichment of porphyry copper deposits. Supergene alteration commonly involves vertical solution movement, but can also involve a horizontal component when copper-rich acidic solutions can migrate laterally. Depending on Eh and pH conditions, copper may be transported through paleodrainage networks over several kilometres from source and produce continuous copper mineralization. This copper mineralization is primarily deposited in oxide form but secondary sulphide copper may also be present close to the source (Munchmeyer, 1996).

Geomorphologic conditions and the chemical reactivity of host rocks and sediments influence the size and shape of exotic deposits. Exotic deposits mainly consist of oxidized copper minerals (silicates, chlorides, oxides, and carbonates) deposited into gravels and underlying bedrock of paleodrainages which carry the copper-bearing solutions. Copper may also precipitate as chalcocite on pyrite close to the source. In the Andean porphyry systems, exotic deposits were created in arid to semi-arid conditions (Munchmeyer, 1996). Figure 7.1 shows a schematic model of an exotic system.

For example, the Exotica deposit in Chile is located within a paleochannel that begins at the head of a paleodrainage located over the central portion of the Chuquicamata porphyry deposit and extends southward with a slope of 3 to 7 degrees over 6.5km. Its northern end is found within the Chuquicamata mine and its southern end is found beneath 200 m of gravels. The copper minerals are deposited within the base of the paleochannel and are composed of chrysocolla, copper wad (a copper-rich Mn-Fe oxide) and atacamite (Munchmeyer, 1996).

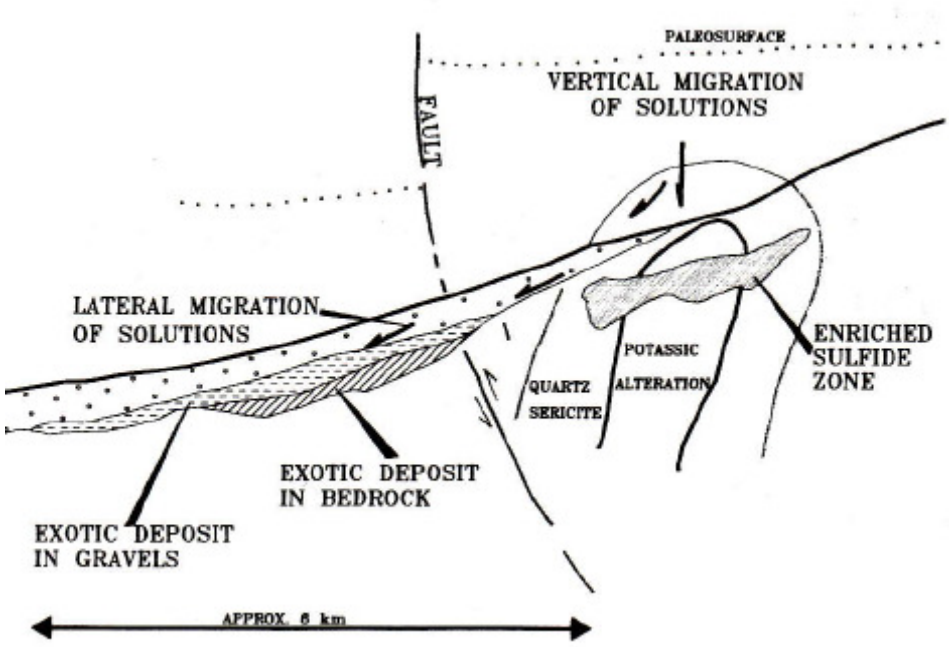

Figure 7.1: Representation of an exotic copper deposit and its relation to a porphyry copper deposit undergoing supergene enrichment (After Munchmeyer, 1996).

7.3 Porphyry Copper Deposits

Porphyry deposits are large, low to medium grade deposits where hypogene ore minerals are spatially and genetically related to felsic to intermediate porphyry intrusions and are often structurally controlled (Eckstrand et al. 1995). Porphyry copper deposits are associated with subduction of oceanic crust in both island arcs (Philippines) and at continental margins (North and South Cordillera). Supergene enrichment may occur by weathering of primary sulphides, creating zones of much higher copper grades, enhancing the possibility of economic exploitation (Eckstrand et al. 1995). Porphyry copper deposits range in size from tens of millions of tones of ore to billions of tones; with copper grades ranging from 0.2% to more than 1%.

The sequence of events that generates a porphyry deposit can be paraphrased as an intrusion followed by early marginal crystallization, producing a solid shell which

later ruptures to produce porphyritic-aphanitic textures in the crystallized rocks (Lowell and Guilbert, 1970). Volatiles are released due to quenching and migrate outward through stockwork and brecciated zones in the cool margins where alteration and mineralization occurs (Lowell and Guilbert, 1970).

Porphyry copper deposits are commonly rich in sulphur, with copper contained in chalcopyrite ($CuFeS_2$) and are associated with pyrite (FeS_2). Some porphyry copper deposits, however, contain much lower amounts of sulphur with the copper being contained primarily in bornite (Cu_5FeS_4) which has a lower S/(Fe+Cu) ratio.

A geologic report of the San Manuel-Kalamazoo deposit, Arizona, by Lowell and Guilbert (1970) illustrates the alteration and mineralization zoning found in porphyry deposits shown in figure 7.2. A potassic zone, near the centre of the deposit, is characterized by replacement of primary minerals by secondary biotite, K-feldspar, quartz, sericite, and to a lesser extent anhydrite. The potassic zone is characterized by a 1:2 pyrite:chalcopyrite ratio with about 0.5% copper; surrounding the potassic zone is an ore shell with a pyrite:chalcopyrite ratio of about 1:1 and 0.5-1% Cu. The phyllic zone is characterized by alteration minerals including quartz, sericite, pyrite, hydrous micas and minor chlorite and rutile. The argillic zone is characterized by pyrite and the alteration of plagioclase to clay minerals. Mineralization in the phyllic and argillic zones consists of a zone on the periphery of the ore shell with a 10:1 pyrite:chalcopyrite ratio with 0.1-0.5% Cu grading into a pyrite shell which contains 6-25% pyrite by weight. The propylitic zone is characterized by plagioclase either fresh or rimmed with clay minerals, biotite replaced by chlorite and carbonate, and minor epidote and calcite are also present (Lowell and Guilbert, 1970).

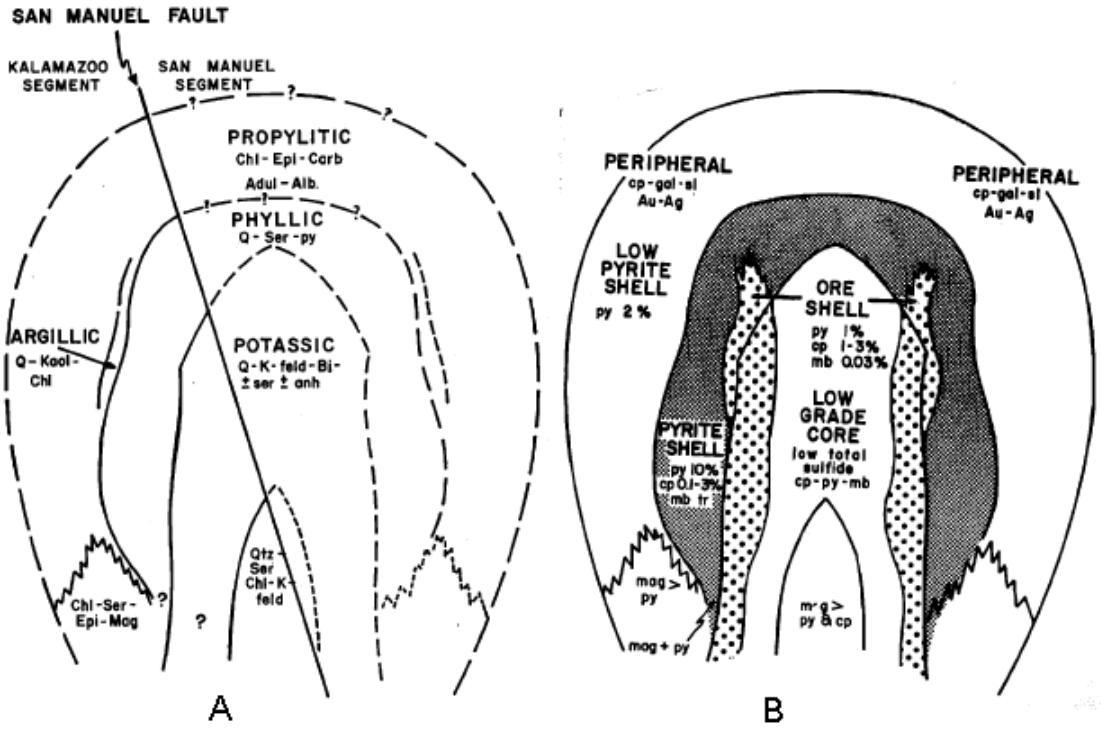

Figure 7.2: Concentric mineralization zones at the San Manuel-Kalamazoo Porphyry deposit. (A) Alteration zones. (B) Mineralization zones: py=pyrite, cp=chalcopyrite, mb=molybdenum, mag=magnetite, gal=galena (After Lowell and Guilbert, 1970).

7.4 Model for the Ice deposit

On the basis of observations at Ice, it seems that the deposit has properties of a porphyry type deposit, but the mineralization shows some characteristics of being transported from another place (exotic).

The Ice may be an exotic deposit because the rocks of the Ice contain no sulphur or obvious remnants of sulphides; all of the copper minerals are oxides or carbonates such as malachite and chrysocolla, which are both Cu minerals common in exotic deposits. The base of the deposit occurs as a coherent layer which may represent a paleo-water table. The deposit contains gold, up to 0.4 g/t, which cannot be mobilized into the

water table as easily as copper, and the potassic alteration in the ore zone is not part of the exotic deposit model.

Although the Ice contains no copper sulphides, the Cu carbonates and silicates in the mineralized vugs seem to contain remnants of Fe (Fig 6.3). The mineralized vugs may represent a dissolved hypogene mineral, which could well have been a sulphide of Fe and Cu. Ice also contains gold grades up to 0.4 g/t which are approaching the threshold between copper porphyry and copper-gold porphyry. The high copper grades and lack of sulphides at the Ice could represent in situ supergene enrichment at the top of an exposed porphyry copper deposit. The potassic alteration correlation with higher copper grades is a property of porphyry copper deposits, and is unlikely to be associated with an exotic deposit; an explanation why surface transported Cu would predominantly precipitate in the K_2O and Rb rich rocks is not forthcoming; not all exposed rocks containing biotite, or magnetite are mineralized.

The deposit model chosen by the writer for this deposit is a ‘deformed porphyry’ similar to the model proposed by Tafti and Mortenson (2004) for Minto and Williams Creek. The deposit was formed in a porphyry system which was later subjected to tectonic deformation, changing the shape of the orebody into a coherent layer as in the simplified process shown in figure 7.3.

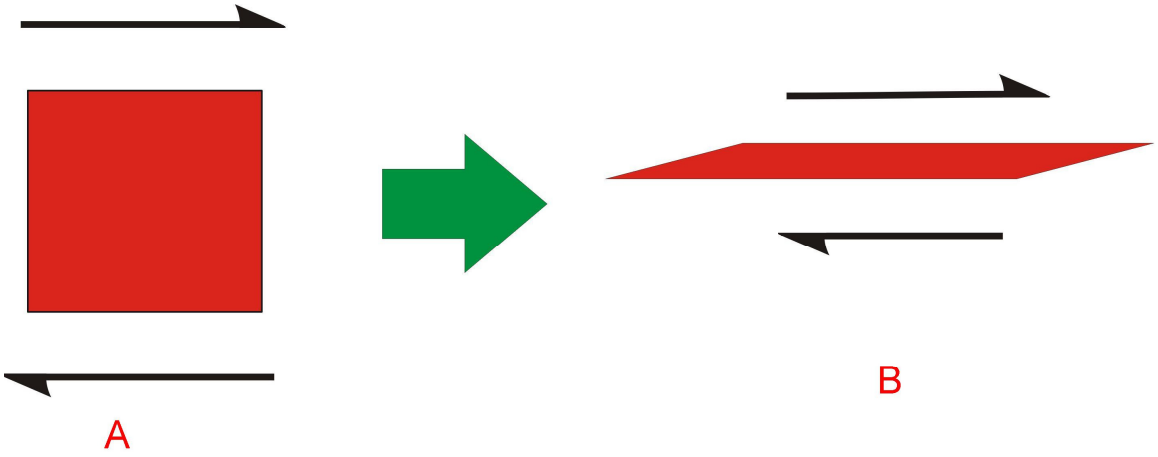

Figure 7.3: Simplified diagram (cross-section view) showing an orebody undergoing tectonic deformation.

It is proposed that the malachite and chrysocolla (?) found in the Ice rocks are found in situ; inhabiting the same space as sulphides before they were oxidized. The primary deposit is probably a low sulphur porphyry copper deposit with bornite being the major sulphide (much like Minto).

Chapter 8

Conclusions and Recommendations for Future Work

8.1 Discussion

If the Ice were formed as an exotic deposit, the Williams Creek deposit could be a candidate for the primary deposit because of its proximity to the ICE, but there are doubts whether it ever contained primary sulphide minerals as well (Tafti and Mortenson, 2004). The primary porphyry deposit could also be an undiscovered deposit buried below the surface or could have already been eroded away and destroyed. To explore for more exotic deposits in the area, it would be necessary to reconstruct the Tertiary paleotopography of a stream system and groundwater table connecting the Minto, Williams Creek and Ice.

It is concluded that the granodiorites of the Ice property have undergone tectonic strain and were crystallized at depths of >9km. Whatever the irregular shape of the original Cu-rich, K-feldspar and biotite porphyry, during deformation it has been transposed into a tabular body. To explore for more porphyry-type mineralization, it is suggested that airborne radiometric detection of potassium could be useful.

8.2 Suggestions for Future Work

1. Study of the vugs containing Cu minerals to deduce the pre-existing mineral dissolved to create the vug. It is suggested that microprobe maps of 50 or more vugs would give enough information to ascertain whether the dissolved minerals were Cu sulphides, pyrite or some other mineral phase.
2. Study of weathering surfaces and distribution of Cu as they may relate to a Tertiary paleosurface.

3. Sulphides should be found up or down foliation from the outcropping copper oxides. Mapping the structure of the area is recommended for future workers.
4. The results of the drilling and ICP/MMI soil geochemistry (valuable exploration tools) are not available to the author at this time, so these cannot be commented on in the context of exploration.
5. A radiometric survey to identify areas with elevated zones of potassium and rubidium.

8.3 Conclusions

The objectives of the thesis laid out in 1.5 have been met to some extent; comments follow.

1. To understand the correlation (or non-correlation) between magnetic anomalies and mineralization in the Ice area. Although there is abundant magnetite in various parts of the Ice deposit, no direct correlation exists with copper mineralization. It is possible that magnetite is more abundant in the biotite rich granodiorite, but magnetic anomalies do not necessarily correlate with higher copper grades.

2. To determine the relative timing of mineralization and regional deformation/metamorphism. This study concurs with previous authors that mineralization preceded deformation. The data are compatible with sulphide mineralization and potassic alteration having been formed at several kilometres depth and subsequently sheared, to be later exposed and oxidized by weathering near the surface.

3. A comparison of the mineralogy of alteration (feldspars and biotite). Due to the intense structural deformation, it was not possible to differentiate what is magmatic K-feldspar and magmatic biotite from (potassic) alteration equivalents in the rocks.

However, feldspar and biotite appear to be identical to those described at Minto and Williams Creek by other workers (Tafti and Mortenson, 2004).

4. To determine similarities/differences between the ICE and Minto/Williams Creek deposits. Ice has no sulphides, which is similar to Williams Creek, whereas Minto has remnants of Cu sulphides and pyrite. The deposits have a similar origin and Ice seems to have more analogies with Williams Creek.

5. To generate a genetic deposit model for the Ice deposit. The preferred model for Ice is formation of a porphyry type deposits with Cu and Au at several kilometres depth, accompanied by potassic alteration. Subsequently, shearing transformed the irregular deposit into tabular foliated bodies. Exposure to the surface during Tertiary exhumation may have eliminated many mineralized areas due to erosion, but also allowed the remnant copper and gold minerals to be weathered and oxidized. Lack of glaciation in the immediate area prevented the oxidized, possibly in part exotic copper minerals from being eroded.

Appendix 1
Rock Sample Descriptions

Samples with high copper concentrations are AFI-02 (11269ppm), AFI-5 (11126ppm), AFI-6 (14904ppm), and AFI-14 (10689ppm) which are above the upper limit level for XRF (10000ppm).

AFI-01
Granodiorite
Foliated
Porphyritic
Malachite ~ 1%
Plagioclase
Quartz (recrystallized?)
Potassium Feldspar
Biotite
Magnetite and Hematite

AFI-02
Granodiorite
Foliated
Porphyritic
0.5 cm pegmatitic vein cuts across sample
Malachite ~1%
Plagioclase
Quartz
Potassium Feldspar (Large phenocrysts 1-4cm)
Biotite
Magnetite and Hematite

AFI-03
Aplite Dyke
Aphanitic
3cm pegmatitic vein cuts across sample
Plagioclase >60%
Quartz
Potassium Feldspar
Biotite

AFI-04
Granodiorite
Massive
Porphyritic
Coarse grained (0.2-1cm)
Plagioclase
Quartz
Potassium Feldspar (Low Amounts)
Hornblende>>Biotite

AFI-05
Granodiorite
Foliated
Porphyritic
Malachite ~2%
Plagioclase
Potassium Feldspar
Plagioclase
Quartz
Biotite
Magnetite and Hematite

AFI-06
Granodiorite
Weakly foliated
Porphyritic
Pegmatitic
Malachite >2%
Potassium Feldspar
Plagioclase
Quartz
Magnetite and Hematite

AFI-07
Granodiorite
Massive
Porphyritic
Plagioclase
Quartz
Potassium Feldspar
Hornblende>Biotite
Magnetite and Hematite

AFI-08
Granodiorite
Possible weak foliation
Porphyritic
Plagioclase
Quartz
Potassium Feldspar
Biotite
Magnetite and Hematite

AFI-09
Granodiorite
Strongly Foliated
Porphyritic

Malachite >1%
Plagioclase
Potassium Feldspar
Quartz
Biotite
Magnetite and Hematite

AFI-10
Granodiorite
Foliated
Porphyritic
Plagioclase
Quartz
Potassium Feldspar
Biotite

AFI-11
Granodiorite
Porphyritic
Pegmatitic
Malachite<1%
Plagioclase
Quartz
Potassium Feldspar
Biotite
Magnetite and Hematite

AFI-12
Granodiorite
Strongly Foliated
Porphyritic
Malachite ~1%
Plagioclase
Quartz
Potassium Feldspar
Biotite
Magnetite and Hematite

AFI-13
Granodiorite
Strongly Foliated
Porphyritic
Malachite <1%
Plagioclase
Quartz
Potassium Feldspar
Biotite
Magnetite and Hematite

AFI-14
Granodiorite
Strongly Foliated
Porphyritic
Malachite 1-2%
Plagioclase
Potassium Feldspar
Quartz
Biotite
Magnetite and Hematite

Samples from Minto

AFI-15
From the oxidized zone above the Minto Deposit
Consists of recrystallized fine grained Plagioclase and Quartz
Malachite and Azurite infilling cracks 2-3%
Hematite

AFI-16, AFI-17, AFI-18
Ore from Minto
Foliated
Bornite and Chalcopyrite 15-30%
Plagioclase
Quartz
Potassium Feldspar
Biotite

Appendix 2
Magnetic Susceptibility
Based on 10 readings taken on each sample.

Sample ID	Max	Min	Mean
AFI-01	0.11	0.01	0.03
AFI-02	0.23	0.03	0.08
AFI-03	0.38	0.21	0.29
AFI-04	1.3	0.12	0.75
AFI-05	1.6	1.2	1.3
AFI-06	0.87	0.18	0.56
AFI-07	0.92	0.31	0.56
AFI-08	0.75	0.05	0.31
AFI-09	0.14	0.01	0.06
AFI-10	0.07	0.01	0.03
AFI-11	0.81	0.24	0.56
AFI-12	0.19	0.02	0.09
AFI-13	0.23	0.01	0.11
AFI-14	1.1	0.27	0.53

Appendix 3
XRF Geochemistry
Major elements

Sample ID	Al2O3	CaO	Fe2O3	K2O	LOI	MgO	MnO	Na2O	P2O5	SiO2	TiO2	Total
Units	wt%	wt%	wt%	wt%	wt%	wt%	wt%	wt%	wt%	wt%	wt%	wt%
Detect Limit	0.01	0.01	0.01	0.01	0.05	0.01	0.01	0.01	0.01	0.01	0.01	
AFI-2	15.04	2.27	4.17	3.88	1.41	1.47	0.06	3.18	0.24	65.65	0.37	97.75
AFI-3	18.92	3.66	2.37	1.26	0.47	0.8	0.04	5.83	0.09	66.58	0.31	100.3
AFI-4	16.69	3.79	4.23	1.54	0.57	1.43	0.07	4.64	0.21	67.01	0.42	100.6
AFI-5	16.54	1.89	5.44	5.67	1.93	1.78	0.09	3.26	0.28	61.15	0.52	98.55
AFI-6	18.6	3.1	5.35	5.56	4.81	1.94	0.09	2.94	0.26	54.22	0.55	97.42
AFI-7	17.77	4.56	3.95	2.02	2.34	1.32	0.09	5	0.19	63.57	0.38	101.2
AFI-8	16.74	3.66	4.89	1.85	1.19	1.71	0.08	4.48	0.32	65.3	0.48	100.7
AFI-10	16.2	3.21	4.05	2.63	0.53	1.72	0.06	4.02	0.27	67.59	0.45	100.7
AFI-12	16.09	2.48	4.88	3.95	1.46	1.7	0.07	3.32	0.24	65.43	0.43	100.1
AFI-14	12.58	1.27	4.19	5.56	1.03	1.32	0.06	1.86	0.21	70.13	0.34	98.55

Trace Elements

Sample ID	Ag	As	Ba	Bi	Co	Cr	Cu	Mo	Nb	Ni	Pb	Rb
units	ppm	ppm	ppm	ppm	ppm	ppm	ppm	ppm	ppm	ppm	ppm	ppm
AFI-2	0	2	2234	0	11	26	11269	12	8	0	6	96
AFI-3	0	0	560	0	0	12	45	1	2	2	0	44
AFI-4	0	0	548	0	11	18	153	1	9	4	3	71
AFI-5	0	5	4822	0	29	20	11126	2	9	3	11	124
AFI-6	7	13	3148	0	22	10	14904	3	12	0	10	122
AFI-7	0	0	1657	0	8	17	20	1	8	3	4	36
AFI-8	0	1	638	0	11	17	222	0	8	4	3	74
AFI-10	0	0	1638	0	7	17	956	1	7	3	4	85
AFI-12	0	3	2169	0	15	17	3739	5	9	3	6	110
AFI-14	5	2	4650	0	11	20	10689	2	6	0	8	123

Sample ID	Sn	Sr	Th	U	V	Y	Zn	Zr
units	ppm	ppm	ppm	ppm	ppm	ppm	ppm	ppm
AFI-2	5	665	8	0	76	8	102	97
AFI-3	0	1226	7	0	34	1	44	131
AFI-4	0	766	8	0	76	5	64	138
AFI-5	5	756	7	0	112	7	99	144
AFI-6	5	723	7	0	99	9	101	148
AFI-7	0	946	4	0	66	12	55	121
AFI-8	0	783	9	0	92	6	84	131
AFI-10	0	783	7	0	85	7	74	126
AFI-12	0	655	8	0	85	8	102	110
AFI-14	7	592	5	0	74	9	69	90

Appendix 4a: Silicate Microprobe data (Mass Percent).

ID	Mineral	K2O	Cr2O3	Na2O	Al2O3	MnO	CaO	TiO2	MgO	SiO2	FeO	Total
AFI03b-01	Magnetite (core)	0.0643	0.2747	0	0.1356	0.3053	0.0784	0.2498	0.0182	0.0922	91.9954	93.214
AFI03b-2	Magnetite (rim)	0.0834	0.2447	0.002	0.113	0.1893	0.0609	0.2596	0	0.1072	88.5438	89.604
AFI03b-3	Plagioclase	0.3667	0	8.0637	24.5034	0	5.5181	0	0	60.9405	0.0565	99.449
AFI03b-4	K Feldspar	15.3117	0	0.4554	18.9799	0	0.0293	0.0295	0	62.9226	0.0345	97.763
AFI03b-5	Plagioclase(core)	0.3802	0	8.3108	24.4593	0	5.098	0	0	61.8417	0.074	100.1639
AFI03b-6	Plagioclase (rim)	0.2401	0	8.4001	24.5278	0	5.1297	0	0	62.1241	0.044	100.4657
AFI03b-7	K Feldspar	14.4075	0.0055	0.882	18.344	0	0	0.0913	0	58.4504	0.0474	92.2282
AFI03b-8	Biotite	9.1751	0.0546	0.1014	15.3892	0.3967	0.0414	3.0592	9.898	35.2244	19.6907	93.0308
AFI03b-9	Titano-magnetite	0.1376	0.2095	0.0595	2.4159	0.1196	0.3209	5.9015	0.8594	4.365	74.9205	89.3095
AFI03b-10	Biotite	8.6243	0.0538	0.0912	15.6303	0.3925	0.1252	2.5464	10.8515	35.7319	19.2861	93.3333
AFI03b-12	Plagioclase	0.2451	0	8.1044	23.8201	0	5.4913	0	0	58.8764	0.0515	96.5889
AFI04-01	K Feldspar	14.3548	0.0177	1.1009	18.8057	0	0.0432	0.0269	0	61.9443	0.0349	96.3285
AFI04-2	Plagioclase	0.1309	0	10.0544	20.4136	0	0.5537	0	0	67.897	0	99.0497
AFI04-3	Biotite	0.1987	0.0399	0.0062	17.4266	0.6096	0.2421	0.44	14.181	27.5949	24.4938	85.2328
AFI04-6	Biotite	0.0308	0.0484	0.0116	17.6431	0.652	0.0422	0.0537	14.683	27.0921	25.5961	85.8531
AFI04-7	Rutile	0.2534	0.1156	0.0526	1.7646	0.0525	0.6745	75.6768	0.138	8.5395	2.6911	89.9587
AFI04-8	K Feldspar	13.8094	0	1.4054	18.578	0	0.0153	0.0431	0	60.9429	0.0195	94.8137
AFI04-9	Plagioclase	0.1201	0	10.0239	20.2372	0	0.6802	0	0	67.3491	0	98.4106
AFI04-10	Plagioclase	0.0473	0	10.312	19.7348	0	0.0177	0	0	67.5835	0	97.6954
AFI04-12	Biotite	0.0686	0.0291	0.0075	16.8687	0.606	0.7927	1.2882	13.1432	26.0244	23.5256	82.3541
AFI04-13	Biotite	3.2039	0.0514	0.0463	15.2815	0.4311	0.1723	2.244	12.0104	28.6855	21.3187	83.4452
AFI04-14	Biotite	0.0483	0.031	0.0158	17.8004	0.6204	0.1918	0.3474	13.627	26.4251	24.7575	83.8648
AFI11-03	Biotite	8.8087	0	0.092	15.9479	0.4637	0.0239	2.877	10.7306	36.4496	20.5126	95.9061
AFI11-4	K Feldspar	0.0155	0	0.0148	0.0188	0	0	0	0.0129	97.2498	0	97.3119
AFI11-5	K Feldspar	14.3273	0	1.2186	19.2693	0	0.0082	0	0	63.7539	0.0225	98.5999
AFI11-6	K Feldspar	14.0619	0	1.2737	19.3067	0	0.0226	0.0006	0.0067	63.1632	0.0235	97.8589
AFI11-7	K Feldspar	14.09	0	1.2212	19.3161	0	0.0049	0.0413	0	63.3824	0.0304	98.0864
AFI11-8	Biotite	8.787	0	0.0803	15.4593	0.4906	0.0376	2.926	10.3644	36.1973	20.3776	94.7202
AFI11-9	Plagioclase	0.224	0	7.4703	24.5229	0	5.2244	0	0.0104	60.1377	0.019	97.6087
AFI11-10	Plagioclase	1.6951	0	8.6549	21.1979	0	1.5409	0	0	66.2942	0	99.383

ID	Mineral	K2O	Cr2O3	Na2O	Al2O3	MnO	CaO	TiO2	MgO	SiO2	FeO	Total
AFI11-11	Plagioclase	0.336	0	7.6689	25.3742	0	5.9169	0	0	60.7824	0.053	100.1313
AFI11-12	Plagioclase	0.3168	0	7.8729	25.5915	0	5.8487	0	0	61.1577	0.0465	100.834
AFI11-13	K Feldspar	14.5586	0	0.9677	19.3852	0	0.0017	0.0569	0.0041	63.5635	0.0354	98.5732
AFI16-2	Chlorite	8.8519	0.0256	0.1333	15.9711	0.3854	0.0803	2.3536	9.4307	36.1107	21.4817	94.8243
AFI16-3	K Feldspar	14.4853	0	0.825	19.3005	0	0.0152	0.05	0	62.4088	0.0225	97.1074
AFI16-4	K Feldspar	14.1916	0	0.9028	19.4515	0	0.0165	0.1364	0.0069	62.0636	0.005	96.7743
AFI-04A-1	Plagioclase	0.2058	0	7.8325	23.6689	0	6.0029	0	0	57.5954	0.0806	95.3861
AFI-04A-2	K Feldspar	14.3211	0	0.3483	18.145	0	0.0042	0.0737	0	60.585	0	93.4773
AFI-04A-4	Biotite	9.1836	0.0423	0.107	15.7487	0.4656	0.0235	2.8893	10.9461	36.5025	19.6084	95.5171
AFI-04A-5	Plagioclase	0.1764	0	8.093	24.8834	0	5.9025	0	0	60.8707	0.1997	100.1256
AFI-04A-6	K Feldspar	14.4816	0	0.8879	19.0502	0	0	0.0347	0	63.397	0.1265	97.978
AFI-04A-7	Biotite	8.8647	0.0123	0.0899	15.8106	0.46	0.0952	3.1528	10.4593	36.2205	19.8156	94.9809
AFI-04A-8	Biotite	9.0395	0	0.0656	15.6353	0.4886	0.0186	2.9325	10.5596	36.3708	20.1121	95.2227
AFI-04A-9	Plagioclase	0.1461	0	8.1461	25.071	0	5.8128	0	0	61.3819	0.0737	100.6315
AFI-04A-10	K Feldspar	14.3052	0.0035	0.9451	19.0353	0	0	0.0254	0	63.6248	0.0227	97.9621
AFI-04A-11	Plagioclase (rim)	0.2423	0	7.8922	25.4191	0	6.241	0	0	60.7882	0.13	100.7127
AFI-04A-12	Plagioclase(core)	3.8846	0	5.4069	22.6867	0	4.0336	0	1.5741	51.6056	2.9157	92.1073
AFI-04A-13	Biotite	9.1977	0.0314	0.0813	15.3789	0.4673	0.0041	2.8515	10.2542	35.9885	19.9941	94.2491
AFI-04A-14	Biotite	9.0966	0.0529	0.127	15.5252	0.5343	0.0644	2.8485	10.2857	36.5432	20.6223	95.7002
AFI-04A-15	Plagioclase	0.2842	0	7.13	26.4069	0	7.5176	0	0	58.7881	0.0574	100.1842
AFI-04A-16	Plagioclase	0.3992	0	7.9953	25.0089	0	5.8294	0	0	61.2737	0.087	100.5934
AFI-04A-17	K Feldspar	14.8135	0	0.6979	19.1631	0	0.0065	0.0669	0	63.2337	0.0543	98.0359
AFI-04A-18	K Feldspar	14.4642	0	0.9228	19.1792	0	0	0.0656	0	63.5129	0.0375	98.1823
AFI-05b-1	Plagioclase	0.0439	0	10.9671	19.9042	0	0.1585	0	0	68.0952	0.0054	99.1744
AFI-05b-2	K Feldspar	13.8037	0	1.2893	19.1882	0	0.0368	0.0631	0	63.0699	0.0375	97.4886
AFI-05b-3	K Feldspar	13.7309	0	1.4131	19.0274	0	0.0194	0.0916	0	63.1927	0.0193	97.4945
AFI-05b-4	Biotite	9.1138	0.0392	0.1383	15.951	0.5229	0.0063	3.1202	10.5482	36.3374	19.6682	95.4455
AFI-05b-5	K Feldspar	13.2363	0	1.5387	19.0805	0	0.0221	0.068	0	63.5155	0.038	97.4992
AFI-05b-6	K Feldspar	13.8192	0	1.3639	19.1736	0	0.0171	0.0514	0	63.1901	0.0445	97.6599
AFI-05b-7	Biotite	9.3311	0.0468	0.098	15.7647	0.4662	0.0133	3.0899	9.9207	36.1171	21.4993	96.3472
AFI-05b-8	K Feldspar	13.9843	0	1.218	19.0028	0	0	0.0607	0	63.366	0.0459	97.6778
AFI-05b-9	K Feldspar	13.9898	0	1.1719	19.1663	0	0.0153	0.0489	0	63.5951	0.0331	98.0205

ID	Mineral	K2O	Cr2O3	Na2O	Al2O3	MnO	CaO	TiO2	MgO	SiO2	FeO	Total
AFI-05b-10	Biotite	2.3145	0.0078	0.0406	16.6659	0.5752	0.0826	0.9841	13.9882	30.5006	22.0338	87.1934
AFI-05b-11	K Feldspar	13.5029	0	1.4987	19.1754	0	0.0331	0.0557	0	63.1898	0.0494	97.5051
AFI-05b-12	K Feldspar	14.0476	0	1.2185	19.2476	0	0.0409	0.0551	0	63.6381	0.0158	98.2637
AFI-05b-13	Plagioclase	0.0443	0	11.1342	19.6793	0	0.108	0	0	68.8501	0	99.8159
AFI-05b-14	Plagioclase	0.0168	0	11.1774	19.922	0	0.0229	0	0	68.8159	0	99.9551
AFI-05b-15	Biotite	9.1437	0.0123	0.0949	15.4333	0.4893	0.0089	3.1337	10.5606	35.9673	19.5258	94.3699
AFI-05b-16	K Feldspar	13.8621	0	1.2726	19.0357	0	0.0295	0.0309	0	63.3935	0.0415	97.6658
AFI-05b-17	Plagioclase	0.03	0	10.8896	19.7588	0	0.1773	0	0	67.6876	0	98.5434
AFI-05b-18	K Feldspar	13.8529	0	1.2797	18.9899	0	0.0171	0.0563	0	63.0118	0.2241	97.4319
AFI-05b-19	Biotite	2.9971	0.0138	0.0528	16.6301	0.5944	0.0722	1.8853	13.792	31.4396	21.8574	89.3348
AFI-14b-1	Plagioclase	0.2658	0.0276	8.0065	24.5719	0	5.7173	0	0.0009	62.4087	0.0932	101.0919
AFI-14b-2	Biotite	9.4101	0.0956	0.0779	15.7992	0.4657	0.0362	2.5666	10.3965	36.4556	20.9865	96.29
AFI-14b-3	K Feldspar	13.9093	0.0572	1.2446	19.067	0.0117	0.0096	0.0881	0.0033	62.9119	0.0728	97.3756
AFI-14b-4	Plagioclase	0.2245	0.0012	8.065	24.7155	0	5.8024	0	0	60.8401	0.1656	99.8144
AFI-14b-5	Biotite	9.1869	0.0978	0.0794	15.9179	0.471	0.0233	2.7455	10.0376	36.3644	20.6373	95.5611
AFI-14b-6	Biotite	9.3585	0.0911	0.0934	16.067	0.4795	0.0057	2.9323	10.453	36.4919	20.186	96.1585
AFI-14b-7	K Feldspar	13.969	0.0397	1.2468	18.9471	0.0165	0	0.0887	0.0063	63.1836	0.0644	97.5621
AFI-14b-8	Plagioclase	0.2365	0.0174	7.8182	25.3025	0	6.3131	0	0	60.5181	0.0902	100.2959
AFI-14b-9	Biotite	9.11	0.0693	0.1168	15.5873	0.4462	0.0242	2.8458	10.4744	35.9889	20.2608	94.9238
AFI-14b-10	Plagioclase	0.2739	0.0109	8.159	24.4421	0	5.6158	0	0	61.124	0.1026	99.7284
AFI-14b-11	Quartz	0.0296	0	0.0091	0.0166	0	0.0067	0	0.0009	97.5949	0.0525	97.7104
AFI-14b-12	K Feldspar	13.9218	0.0188	1.205	19.1089	0.0149	0.0294	0.0906	0.0111	62.9645	0.0738	97.4389
AFI-14b-13	Plagioclase	0.2456	0	8.0113	24.7363	0	5.9983	0	0	60.9092	0.0917	99.9924
AFI-14b-14	K Feldspar	14.0415	0.0549	1.1695	18.8479	0.0186	0.016	0.0949	0.0039	63.156	0.0832	97.4865
AFI-14b-15	K Feldspar	13.9327	0.0216	1.2889	18.8609	0.0106	0.0096	0.059	0.0089	63.6263	0.0713	97.8899
AFI-14b-16	Biotite	9.5128	0.094	0.1042	15.9766	0.4618	0.0145	2.4696	10.4749	36.5964	20.549	96.2539
AFI-14b-17	K Feldspar	14.0674	0.0244	1.1947	18.8968	0.0117	0.0404	0.0999	0.0087	63.0061	0.0763	97.4265
AFI-14b-18	Plagioclase	0.0188	0	0.0231	0	0	0	0	0.0133	97.4568	0.0005	97.5126
AFI-17b-1	K Feldspar	14.6454	0.0605	0.6809	18.9432	0.0096	0.0091	0.0795	0	63.1086	0.059	97.5959
AFI-17b-2	Plagioclase	0.2858	0	8.6989	23.7777	0.0005	4.6886	0	0	62.4789	0.0912	100.0216
AFI-17b-3	Biotite	9.0899	0.1228	0.0746	16.3714	0.5549	0.0643	2.7645	9.3806	36.3132	20.9476	95.6839
AFI-17b-4	Biotite	8.8542	0.0936	0.0782	16.7348	0.4608	0.0414	2.2487	9.4698	36.543	21.3998	95.9244

ID	Mineral	K2O	Cr2O3	Na2O	Al2O3	MnO	CaO	TiO2	MgO	SiO2	FeO	Total
AFI-17b-5	Biotite	9.3138	0.079	0.0851	16.2775	0.4785	0.0242	2.3293	9.9012	35.4323	20.9665	94.8875
AFI-17b-6	Plagioclase	0.2214	0.0031	8.3785	24.3068	0	5.2133	0	0	61.4392	0.053	99.6154
AFI-17b-7	Plagioclase	0.3002	0	8.8662	23.1793	0.0069	4.5034	0	0	62.9023	0.0822	99.8406
AFI-17b-8	K Feldspar	14.2017	0.0077	1.1121	18.8778	0.0101	0.0234	0.0663	0.0013	63.3557	0.0218	97.6779
AFI-17b-9	K Feldspar	14.5376	0.0216	1.0796	18.6358	0.0053	0	0.0347	0.0063	64.2458	0.049	98.6158
AFI-17b-12	Biotite	3.4739	0.0949	0.053	17.1752	0.3885	0.1005	1.8092	10.8021	31.7968	26.2075	91.9016
AFI-17b-13	Plagioclase	0.6164	0.0095	7.6859	25.1774	0	3.8321	0	0.0185	61.4386	0.105	98.8835
AFI-17b-14	K Feldspar	14.3712	0.0345	0.8649	19.0084	0.0069	0.0123	0.0862	0.0028	63.142	0.0688	97.5981
AFI-18-1	Biotite	8.9743	0.0977	0.1103	15.9998	0.5608	0.1507	2.8032	9.6052	35.5843	20.1813	94.0677
AFI-18-2	Biotite	9.2573	0.0998	0.1051	16.0821	0.5504	0.0136	2.8751	9.6118	36.2058	20.7296	95.5306
AFI-18-3	Plagioclase	0.238	0.0017	8.5209	24.0692	0	4.997	0	0	61.8723	0.2144	99.9136
AFI-18-4	Plagioclase	0.2914	0	8.5099	23.9247	0	4.8542	0	0	62.189	0.0946	99.8638
AFI-18-5	K Feldspar	0.4076	0.0044	8.5996	23.6887	0.0053	4.5675	0	0	62.3391	0.1228	99.7351
AFI-18-6	Plagioclase	0.0279	0	0	0	0	0	0	0.0248	96.3286	0.011	96.3923
AFI-18-7	K Feldspar	0.1747	0.0155	8.437	24.0559	0	4.651	0	0	62.2876	0.1203	99.7421
AFI-18-8	K Feldspar	0.1608	0.004	8.6229	24.036	0	4.87	0	0	61.6369	0.1416	99.4723
AFI-18-9	Plagioclase	0.3118	0.0123	8.2729	24.3165	0	4.9109	0.0043	0	62.9636	0.1748	100.967
AFI-18-10	Biotite	9.078	0.1042	0.1122	16.1236	0.5871	0.0526	3.1603	9.4716	36.1051	20.5702	95.3649
AFI-18-11	Biotite	9.1112	0.0957	0.125	16.0948	0.5894	0.0302	2.8817	9.7212	35.9979	20.0832	94.7303
AFI-18-12	Biotite	8.7219	0.0839	0.1674	16.0128	0.5796	0.042	2.9206	9.7162	35.7742	20.042	94.0607
AFI-18-13	Biotite	9.0581	0.1042	0.1489	16.1415	0.5865	0.0314	3.0316	9.6481	36.2102	20.7888	95.7494
AFI-18-14	Plagioclase	0.3364	0.0119	8.5851	23.8984	0.009	4.5467	0	0	62.4362	0.1079	99.9317

ID	Mineral	K2O	Cr2O3	Na2O	Al2O3	MnO	CaO	TiO2	MgO	SiO2	FeO	CuO	Total
AFI-05b-20	Cu Silicate	0.0922	0	0.0646	3.1349	0.0061	1.0068	0.056	0.1992	30.0635	0.4632	43.6159	78.7024
AFI-05b-21	Cu Silicate	0.0891	0.0084	0.0969	4.838	0	1.1266	0.0902	0.327	42.0093	0.5396	44.2088	93.334

Appendix 4b: Microprobe data for geobarometry and Geothermometry (Mass Percent)

ID	Mineral	SiO2	TiO2	Al2O3	Cr2O3	FeO	MnO	MgO	CaO	Na2O	K2O	Total
AFI07-1	Hornblende	38.9853	0.7378	11.0786	0	16.7526	0.775	8.4188	9.2744	1.4767	1.0816	88.5809
AFI07-2	Hornblende	41.5823	0.7916	11.1768	0.0526	19.5543	0.6295	8.869	11.649	1.5176	1.372	97.1947
AFI07-3	Plagioclase	62.2732	0	23.0281	0	0.3439	0	0	5.0781	7.3154	1.4687	99.5075
AFI07-4	Plagioclase	61.4329	0	23.725	0	0.1618	0	0	5.7203	8.3957	0.2284	99.6642
AFI07-5	Plagioclase	64.1809	0	23.0166	0	0.0309	0	0	3.3453	7.6086	0.5688	98.7512
AFI07-6	Plagioclase	62.3548	0	24.1027	0	0.1309	0	0	5.7121	8.2686	0.3145	100.8835
AFI07-7	Hornblende	41.4231	0.8167	11.1545	0.0516	19.437	0.6933	8.8425	11.7558	1.402	1.39	96.9665
AFI07-8	Hornblende	40.9219	0.8116	11.6761	0.0459	19.794	0.6791	8.805	11.6476	1.5178	1.5146	97.4137
AFI07-9	Plagioclase	61.9124	0	23.5481	0	0.166	0.0028	0	5.4578	8.5452	0.1446	99.777
AFI07-11	Plagioclase	61.9682	0	23.7164	0	0.041	0	0	5.6189	8.4001	0.1595	99.9042
AFI07-12	Hornblende	41.6392	0.7953	11.3346	0.0196	19.4018	0.6869	9.032	11.5952	1.5399	1.4381	97.4827
AFI07-13	Hornblende	40.6924	0.9383	14.3734	0.0253	17.8439	1.3139	7.2719	8.7908	1.209	1.312	93.771
AFI07-14	Hornblende	41.5018	0.8004	11.4925	0.0305	19.4899	0.6701	8.7606	11.8835	1.4189	1.337	97.3853
AFI07-15	Plagioclase	61.9068	0	23.7386	0	0.1272	0	0	5.3558	8.5733	0.2724	99.9742
AFI07-16	Hornblende	41.7363	1.2677	11.9831	0.0527	18.9018	0.6455	8.9359	11.8417	1.4869	1.4064	98.2581
AFI07-17	Plagioclase	62.0568	0	24.0041	0	0.1491	0	0	5.2422	8.4208	0.1959	100.0688
AFI07-18	Hornblende	40.5883	0.9038	11.7061	0.0422	20.1063	0.6977	8.7765	11.6742	1.5721	1.6094	97.6767
AFI07-19	Hornblende	40.4636	0.8678	11.8166	0.0426	19.7744	0.7061	8.5297	11.5026	1.6692	1.626	96.9986
AFI07-20	Hornblende	37.5557	0.8927	10.8207	0.0538	20.0687	0.703	8.5048	11.5113	1.4953	1.5454	93.1515
AFI07-21	Hornblende	40.7297	0.8279	11.3804	0.0408	19.8758	0.6431	8.73	11.7619	1.4153	1.3567	96.7617
AFI07-24	Plagioclase	59.6623	0	23.3384	0	0.3609	0	0.02	5.2906	7.6239	0.5096	96.8058
AFI07-25	Hornblende	41.0899	0.8885	10.9058	0.0352	19.3436	0.6191	9.2919	11.7708	1.4151	1.2924	96.6524
AFI07-26	Hornblende	41.8919	0.7714	11.9489	0.0578	19.5104	0.656	8.4573	11.8948	1.2939	1.4647	97.9472
AFI07-27	Hornblende	40.7096	0.4205	13.2581	0.0041	19.249	0.521	9.2996	8.1672	0.9187	1.169	93.7169
AFI07-28	Plagioclase	61.5185	0	23.8841	0	0.0772	0	0	5.6489	8.3567	0.2182	99.7037
AFI07-29	Plagioclase	61.8415	0	23.7203	0	0.1673	0	0	5.5382	8.4776	0.1688	99.9137
AFI07-30	Hornblende	42.2584	0.8203	11.1522	0.0202	18.9533	0.6168	9.3726	11.7355	1.4952	1.3353	97.7599
AFI07-31	Hornblende	41.1114	0.9107	11.5402	0.0239	19.5676	0.676	8.9551	11.7893	1.5305	1.5187	97.6235
AFI07-32	Hornblende	40.9131	0.8727	11.4373	0.0544	19.7662	0.6631	8.8618	11.6663	1.5049	1.4774	97.2173
AFI07-33	Plagioclase	62.1057	0	23.6349	0	0.1847	0	0	5.1732	8.5902	0.2301	99.9189

ID	Mineral	SiO2	TiO2	Al2O3	Cr2O3	FeO	MnO	MgO	CaO	Na2O	K2O	Total
AFI07-34	Plagioclase	61.4358	0	23.8121	0	0.0724	0.0068	0	5.7306	8.3283	0.1923	99.5784
AFI07-35	Plagioclase	61.266	0	23.3882	0	0.148	0.0017	0	5.4044	8.3194	0.1705	98.6983
AFI07-36	Hornblende	40.323	0.8198	11.6133	0.0567	20.0835	0.6829	8.5696	11.6674	1.4948	1.4619	96.773
AFI07-37	Hornblende	41.0713	0.8522	11.5274	0.0351	19.6513	0.6955	8.7843	11.8298	1.5151	1.4295	97.3916
AFI07-38	Hornblende	41.064	0.6436	11.1124	0.0219	20.4014	0.6982	8.6662	11.9885	1.3253	1.2919	97.2134
AFI07-42	Plagioclase	61.5888	0.029	23.3974	0.0637	0.1506	0.0277	0	5.6131	8.4733	0.1057	99.4493
AFI07-43	Plagioclase	63.281	0.1406	18.1418	0.0593	0.1579	0.0367	0	0	1.0843	14.3652	97.2669
AFI07-44	Hornblende	41.2297	0.9797	11.0544	0.1583	19.2137	0.6861	9.2614	11.6495	1.5105	1.3691	97.1124
AFI07-45	Hornblende	40.9228	0.8895	10.652	0.1298	19.8134	0.7018	9.1273	11.7805	1.4646	1.3162	96.798
AFI07-46	Hornblende	42.9734	0.9338	11.4645	0.1168	18.0156	0.7206	9.3971	11.739	1.3435	1.1992	97.9036
AFI07-47	Hornblende	42.1964	1.0175	11.7591	0.1542	18.0979	0.6167	9.4316	11.8442	1.5369	1.3344	97.989

References

Anderson, J.L., and Smith, D.R. 1995. The effects of temperature and fO2 on the Al-in-hornblende barometer, American Mineralogist, v. 80, p. 549-559.

Colpron, M., Nelson, J.L., Murphy, D.C. 2007. Northern Cordilleran terranes and their interactions through time. GSA Today: v. 17, no. 4/5.pp. 4-10.

Dessureault, Y., Watson, K., Giroux, G., Lee, C., Trimble, R., Barratt, D., Doherty, A., The, H., Stibbard, J. 2006. Technical Report (NI 43-101) for the Minto Project, Hatch, Sherwood Mining Corp. – Minto Project.

Eckstrand, O.R., Sinclair, W.D., Thorpe, R.I. 1995. Geology of Canadian Mineral Deposit Types, Geological Survey of Canada, Geology of Canada, no. 8, Ch. 19, p. 421-446.

Fowler, B. 2007. Interim Management Discussion and Analysis for BCGold Corp. www.sedar.com (System for Electronic Document Analysis and Retrieval for the Canadian Securities Administrators).

Hammarstrom, J.M. and Zen, E., 1986. Aluminum in hornblende: An empirical igneous geobarometer, American Mineralogist, v. 71, p. 1297-1313.

Haselton, H.T., Hovis, G.L., Hemingway, B.S., Robie, R.A. 1983. Calorimetric investigation of the excess entropy of mixing in analbite-sanidine solid solutions: lack of evidence for Na,K short-range order and implications for two-feldspar thermometry, American Mineralogist, v. 68, p. 298-413.

Hawthorne, F. 1981. Crystal chemistry of the amphiboles. Mineralogical Society of America. Reviews in Mineralogy, v. 9A, P. 1-102.

Hollister, L.S., Grissom, G.C., Peters, E.K., Stowell, H.H., and Sisson, V.B., 1987. Confirmation of the empirical correlation of Al in hornblende with pressure of solidification of calc-alkaline plutons, American Mineralogist, v.72, p. 231-239.

Leake, B.E., Woolley, A.R., Arps, C.E.S., Birch, W.D., Gilbert, M.C., Grice, J.D., Hawthorne, F.C., Kato, A., Kisch, H.J., Krivovichev, V.G. and others. 1997. Nomenclature of amphiboles; Report of the Subcommittee on Amphiboles of the International Mineralogical Association, Commission on New Minerals and Mineral Names, American Mineralogist, v. 82, no. 910, p. 1019-1037.

Lowell, J.D., and Guilbert, J.M. 1970, Lateral and Vertical Alteration-Mineralization Zoning in Porphyry Ore Deposits, Economic Geology, v. 65, P. 373-408.

Mortensen, J.K., Emon, K., Johnston, S.T. and Hart, C.J.R., 2000. Age, geochemistry, paleotectonic setting and metallogeny of Late Triassic- Early Jurassic intrusions in the Yukon and eastern Alaska: A preliminary report. In: Yukon Exploration and Geology

1999, D.S. Emond and L.H. Weston (eds.), Exploration and Geological ServICEs Division, Yukon, Indian and Northern Affairs Canada, p. 139-144.

Mortensen, J.K. and Tafti, R., 2003. Nature and origin of copper-gold mineralization at the Minto and Williams Creek deposits, west-central Yukon: Preliminary investigations. *In*: Yukon Exploration and Geology 2003, D.S. Emond and L.L. Lewis (eds.), Exploration and Geological ServICEs Division, Yukon Region, Indian and Northern Affairs Canada, p. 175-182.

Mote, T.I., Brimhall, G.H., Tidy-Finch, E., Muller, G., Carrasco, P. 2001. Application of Mass-Balance Modeling of Sources, Pathways, and Sinks of Supergene Enrichment to Exploration and Discovery of the Quebrada Turquesa Exotic Copper Orebody, El Salvador District, Chile, Economic Geology, v. 96, p. 367-386.

Munchmeyer, C. 1996. Exotic Deposits – Products of Lateral Migration of Supergene Solutions from Porphyry Copper Deposits. *In* "Andean copper deposits: new discoveries, mineralization, styles and metallogeny", Society of Economic Geologists Special Publication No. 5, p. 43-58.

Pearce, J.A., Cann, J.R. 1973. Tectonic setting of basic volcanic rocks determined using trace element analysis. Earth and Planetary Science Letters, v. 19, p. 290-300.

Pearce, J.A., Harris, N.B.W., Tindle, A.G. 1984. Trace Element Discrimination Diagrams for the Tectonic Interpretation of Granitic Rocks. Journal of Petrology, v. 25, p. 956-983.

Pearson, W.N. and Clark, A.H., 1979. The Minto Copper Deposit, Yukon Territory: A Metamorphosed Orebody in the Yukon Crystalline Terrane. Economic Geology, vol. 74, p. 1577-1599.

Robinson, R.J., Casselman, S.G. 2007. Technical Report on the Mineral Resource Estimate For the Carmacks Copper Project. Aurora Geosciences Ltd.

Schmidt, M.W., 1992. Amphibole composition in tonalite as a function of pressure: an experimental calibration of the Al-in hornblende barometer, Contributions to Mineralogy and Petrology, v. 110, p. 304-310.

Tafti, R. and Mortensen, J.K., 2004. Early Jurassic porphyry(?) copper (-gold) deposits at Minto and Williams Creek, Carmacks Copper Belt, western Yukon. *In:* Yukon Exploration and Geology 2003, D.S. Emond and L.L. Lewis (eds.), Yukon Geological Survey, p. 289-303.

Tempelman-Kluit, D.J. 1976. The Yukon Crystalline terrane; Enigma in the Canadian Cordillera, Bulletin of the Geological Society of America, v. 87, p. 1343-1357.

Tempelman-Kluit, D. 1980. Evolution of physiography and drainage in southern Yukon. Canadian Journal of Earth Sciences, v. 17, p. 1189-1203.

Winchester, J.A., and Floyd, P.A. 1977. Geochemical discrimination of different magma series and their differentiation products using immobile elements. Chemical Geology, v. 20, p. 325-343.

Maps taken from http://www.bcgoldcorp.com/main/?carmacksmaps

APPENDIX IV:
Structural and Geology Reports
(Devine 2009a & b)

Interoffice MEMO

To:	Brian Fowler, BCGold Corp.
Cc:	Geoff Newton, BCGold Corp
From:	Fionnuala Devine
Subject:	**Carmacks Copper Project** **Preliminary Structural Interpretation on the South Block of Claims, with detail on the WS Property**
Date:	July 26, 2009

SUMMARY

This preliminary report summarizes the results to-date of a structural study on the BCGold Carmacks Block of claims in the Carmacks area, central Yukon. The region is underlain by the Jurassic Granite Mountain batholith and is prospective for Cu-Au "Carmacks-type" deposits. The findings in this report include a regional lineament and geological analysis from regional aeromagnetic data, as well a detailed study and structural interpretation on the WS property. The WS property is the target of current exploration work including trenching. The data and ideas presented in this report are aimed at providing direction to the current program on the WS property.

CONTENTS

1. METHODS OF STRUCTURAL AND GEOLOGICAL INTERPRETATION
   1.1. Availability of Data ad Methods of Use
   1.2. The use of Aerial And Satellite Imagery
   1.3. Future Directions of Study

2. DISCUSSION OF REGIONAL FEATURES
   2.1. Regional Faults
   2.2. Carmacks Group basalt

3. WS PROPERTY
   2.3. WS Property Faults
   2.4. WS Property Foliations and Mineralization Trends

4. REFERENCES

1. METHODS OF STRUCTURAL AND GEOLOGICAL INTERPRETATION

1.1 Availability of Data and Methods of Use

For the purposes of this report, the authour conducted a review of all available data on the Carmacks block of claims owned by BCGold. With the exception of numerous assessment reports, the data has been compiled by BCGold into a series of MapInfo .tab files and other formats for use in GIS. Use of these data, as well as other available public data listed below, form the basis for the analysis presented in this report.

- The **regional aeromagnetic survey** flown in 2007 is a good regional data set that has continuity across all properties and across areas of interest in between.
    - The *Vertical Magnetic Gradient map* is very useful in identifying relatively young, brittle structures as the vertical gradient above a vertical fault is zero (Aryamanesh, 2009). These linear "lows" show up well in the data. The vertical gradient data also shows variations in lithology, particularly close to surface.
    - The *Total Magnetic Field map* highlights regional lithological variation and trends; the data is generally a representation of deeper and more regional variations and changes than the vertical gradient data (NRCAN-website).

- **IP surveys** have been conducted on selected areas in the Carmacks Block; over the northern part of the WS claim, the Peanut, and a section of the Copper claim. The WS Claim data has been analyzed in detail for this study.
    - On the WS Claim, *IP chargeability* highs generally seem to follow the 315° foliation in the granodioritic rocks (J.Paulter field maps), and potentially highlight areas of alteration and sulphide mineralization in mafic domains of the batholith. The trends match the orientation of the mineralized zones along strike at the Carmacks Copper Deposit.
    - *IP resistivity models* show highs that correlate with predicted faults generated from the vertical gradient magnetic data.
- A **geological map of the Carmacks Copper Deposit** is presented in the mineral resource estimate for the Carmacks Copper deposit (Robinson and Casselman, 2007). The map is generalized but does show the outline of several ore zones and simplified structure in the area. The orientation of these structures was compared to the compilation created from the geophysics interpretation and found to be a good match, confirming regional continuity of structural style.

- **Regional geological maps** available include:
  - *Tempelman-Kluit, 1984* – includes a geological compilation of the Carmacks 115I 1:250,000 sheet.
  - *Colpron et al, 2007* – a geological compilation of the northern Whitehorse trough. This map shows major faults that trend into the Carmacks Block of claims area. The major, through-going structures can be traced in the aeromagnetic data up the eastern side of the claim block.

1.2 The Use of Aerial and Satellite Imagery

A Landsat 7 mosaic of the Carmacks sheet is available for free download from Yukon Geomatics. However, the resolution is poor for the level of detail that is required for property-scale ground work or even regional lineament analysis.

The authour investigated the availability of high-resolution satellite imagery for the area – SPOT5, IKONOS, or QuickBird. There is SPOT5 data available over the Carmacks Block of claims, however the photos have up to 25% cloud cover and are not an economical option, at least for the quality of product obtained in this case.

The availability of QuickBird and IKONOS imagery is still under investigation.

There are no airphotos available for the WS property area.

1.3 Future Directions of Study

1. There is potential with the aeromagnetic data to identify different lithological domains using their magnetic signatures. This would allow for general mapping, or at least theorizing of the geology under covered terrain. A characterization of the units that comprise the Granite Mountain batholith using a magnetic susceptibility meter is currently underway (G.Newton, pers. comm.)

2. Detailed structural mapping along the 315° trends where possible on the WS property to:

   a. Confirm the structural model (ie/ the brittle faults) presented herein.
   b. To establish detailed outcrop and structural control around potential mineralized zones.
   c. To establish the trend of regional foliations, ie' are there regional fold patterns outlined by folded foliation? Are there kinks and bends in the foliation?

3. Expand on Jean Pautler's prospecting and mapping to develop a summary of the geologic history for this section of the Granite Mountain batholith.

2. DISCUSSION OF FEATURES

2.1 Regional Faults

Regional structures display a dominant northwest trend with younger north-trending cross faults, and few east-west (normal?) faults (Figure 1). The belt has a protracted deformational history that is evident in the abundance and complexity of the faults and fault patterns.

NW-trending strike-slip faults
The youngest faults are brittle and show up most prominently in the aeromagnetic data. The Teslin fault, the Braeburn fault, and the Hoochekoo fault are some of the named regional through-going structures with post-Late Cretaceous movement that occur along the northeastern boundary of the Granite Mountain Batholith. Most-recent movement on these structures is *right-lateral*; they offset major, regionally continuous lithological and tectonic domains. Minor, synchronous structures parallel these major brittle faults along the eastern side of the block.

Along the southwestern margin of the Carmacks Block of claims northwest-trending structures are also dominant, also with post-Late Cretaceous movement. These faults form a > 6km wide zone of northwest-trending parallel structures, seen along the southwestern limit of the aeromagnetic survey. All lithological units are affected by these structures, including the Carmacks Group basalt.

N-NNW-trending structures
The central region of the Carmacks Block of claims is a more coherent section of the Granite Mountain batholith that also displays a NW trend to local structures, but with younger cross-cutting north- to NNW-trending faults that offset the NW-faults. Although with some normal component of displacement, the N-NNW-trending faults in the northern part of the block display *right-lateral* displacement, while the same orientation of faults in the southern part of the block (and under the WS property) display *left-lateral* sense of displacement, as based on offset of major lithological domains outlined in the total field magnetic data (Figure 1).

NE-trending faults
There is some evidence of northeast-trending faults, particularly in the northern section of the Block, but this area needs to be studied in more detail and compared with mapped geology to ensure that the pattern is not an artifact of processing the magnetic data.

The southern boundary of the Granite Mountain batholith – the "Miller Fault"
There is little evidence found in the geophysical data of the 'Miller Fault', a south-dipping normal fault inferred to trend across the southern boundary of the Carmacks

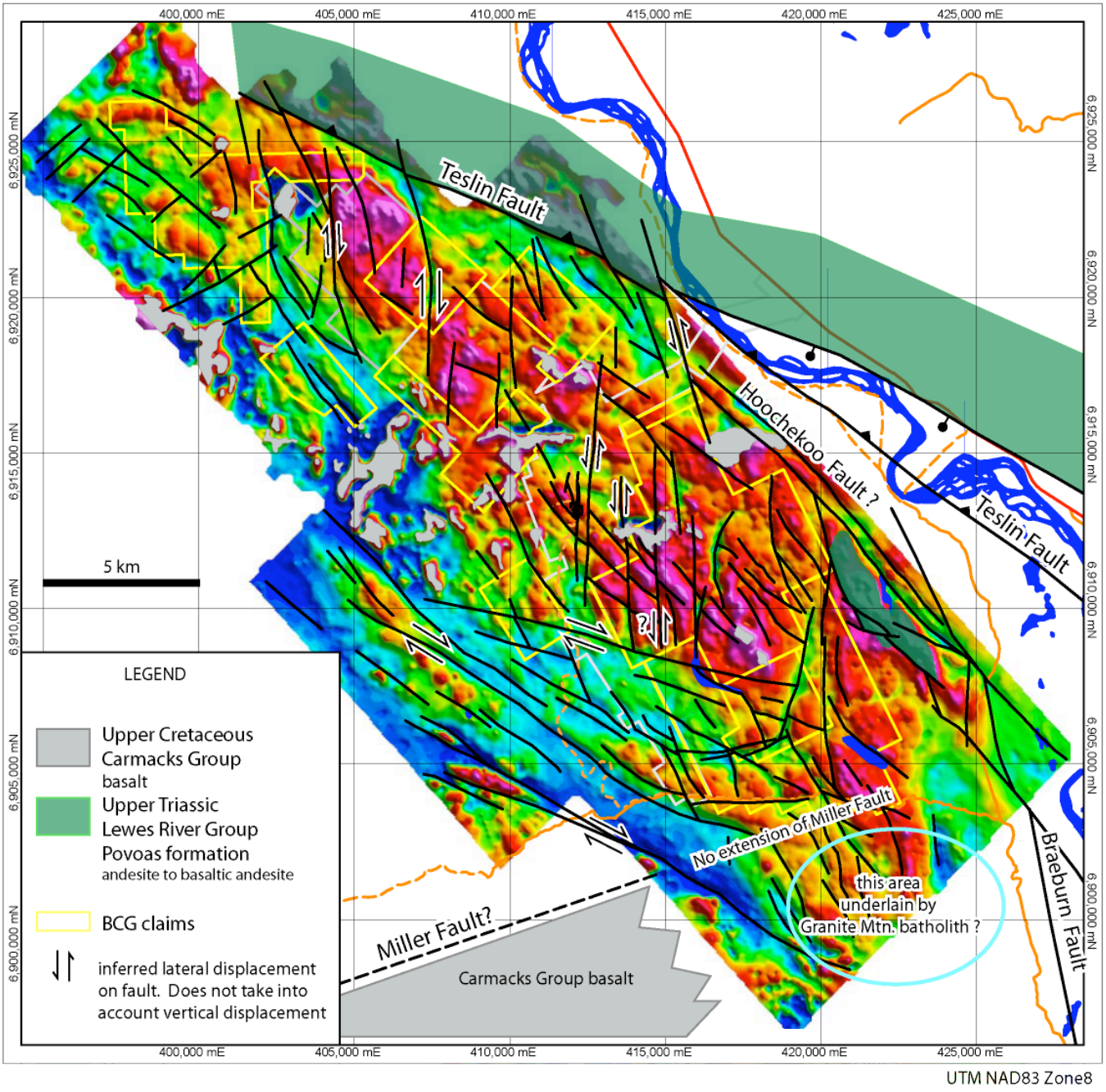

Figure 1. *The regional structural interpretation overlain on the regional total magnetic field data. Black lines show lineaments in the magnetic data interpreted to be brittle faults. The extents of the geological units shown are interpreted from distinct aeromagnetic responses. Most of the area covered by the BCGold claims is underlain by various phases of the Granite Mountain batholith; although perhaps possible, the individual phases have not yet been distinguished using the geophysical data.*

Block of claims, along Crossing Creek (Figure 1, mapped by Tempelman-Kluit, 1984). There is one section of Crossing Creek that may preserve a section of this fault, but it is cross-cut and offset by younger northwest-trending structures. This is significant because the Miller fault is interpreted be the southern boundary of the Granite Mountain batholith exposure in the area, with Carmacks Group basalt occurring south of the fault on the down-dropped side. There may, in fact, be more un-staked ground to the south of the southern Block of claims that is underlain by Granite Mountain batholith, prospective host rocks for a "Carmacks-type" deposit.

2.2 Carmacks Group Basalt (Upper Cretaceous)

Throughout the southern Block of claims isolated remnants of the basalt occur only locally across the region (Figure 1). However, its location is important as the basalt is younger than the Granite Mountain batholith and the included ~198-197 Ma copper mineralization. Remnants of the basalt flows cover ridges and hilltops and obscure the geophysical response of the Granite Mountain batholith, other structures, and the potential zones of mineralization beneath.

3. WS PROPERTY

3.1 WS Property Faults

Evidence in the data of fault orientations on the WS property was examined in detail, particularly because fault offsets are important considerations in following mineralized zones at the property scale. To the north, at the Carmacks Copper deposit, fault offsets clearly create offsets of the mineralized zones in the map pattern (Figure 2). Similar offset of mineralized zones along young, brittle structures is also reported at the Minto mine (Hood et al., 2008).

Two main orientations of young, brittle faults affect the rocks on the west side of the WS property. The IP resistivity data and the vertical gradient magnetic data both support the fault model (Figure 3). An early NW-trending set of subvertical(?) faults spaced at 600-800 metres are cut and offset by a second set of N-trending steep faults. The magnitude and direction of vertical displacement is not yet established for either set of faults. However, the horizontal component to the N-trending set is left-lateral, on the order of 20 metres for some faults, and up to 500 metres for others, based on offset of the earlier NW set and offset of domains with similar magnetic signatures (Figure 4).

The NW set of faults run slightly oblique to the trend of mineralized zones on at the Carmacks Copper deposit immediately to the north. Direction and magnitude of displacement of mineralized zones is challenging to determine along this fault set. The N-trending set cut across the trend of mineralized zones at an angle of up to 45 degrees. With the better constraints on displacement early-stage estimates can be made for the offset of potential extensions of mineralized zones. Figure 5 is a first-pass summary

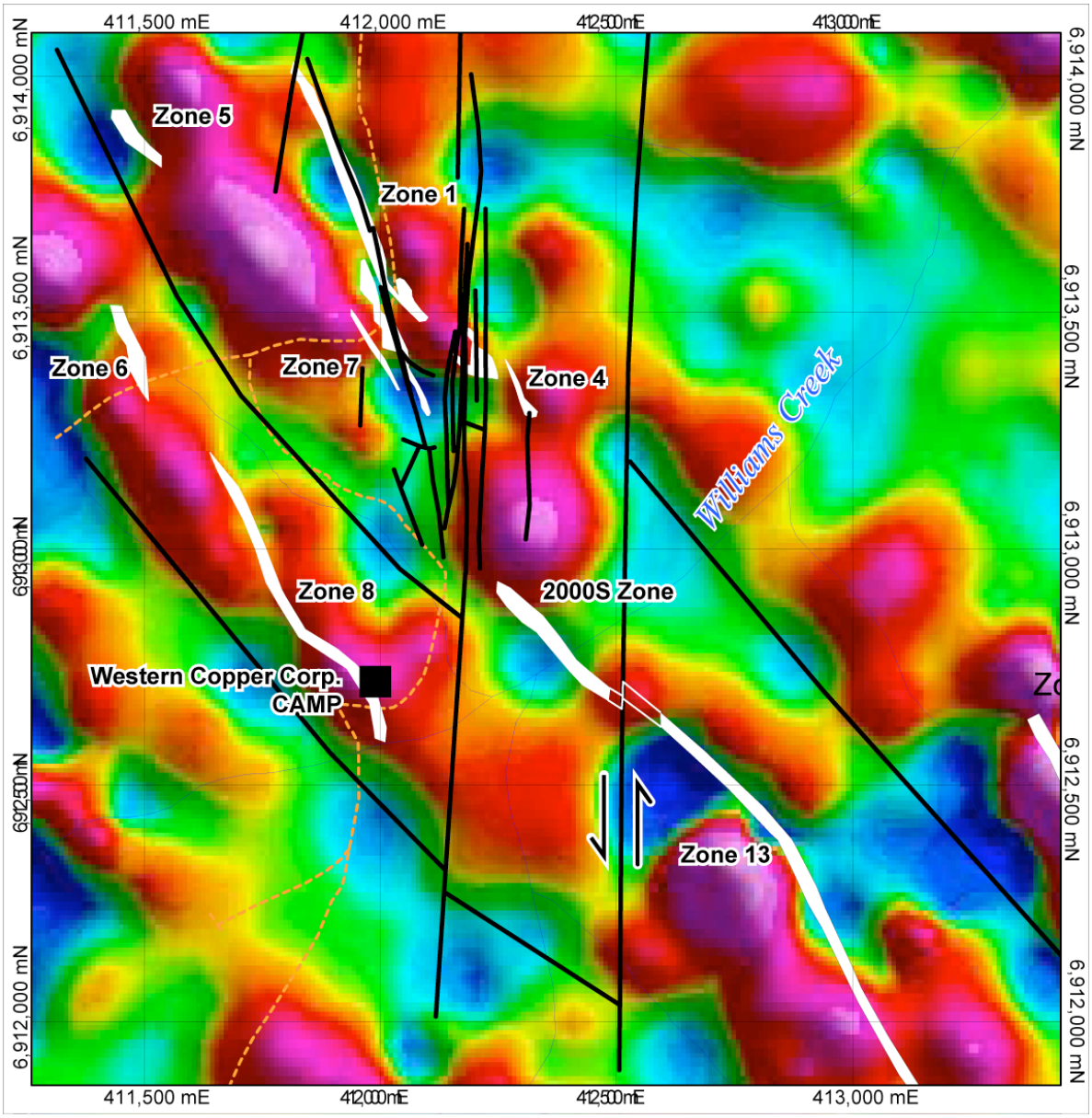

Figure 2. *Map of the Carmacks Copper deposit (from the 2008 mineral resource estimate, Robinson and Casselman, 2007; and Casselman, 2008) with interpretation of brittle structures and offset of mineralized zones. The style and orientations of structures and mineralized zones are also evident along the western wide of the WS property to the southeast.*

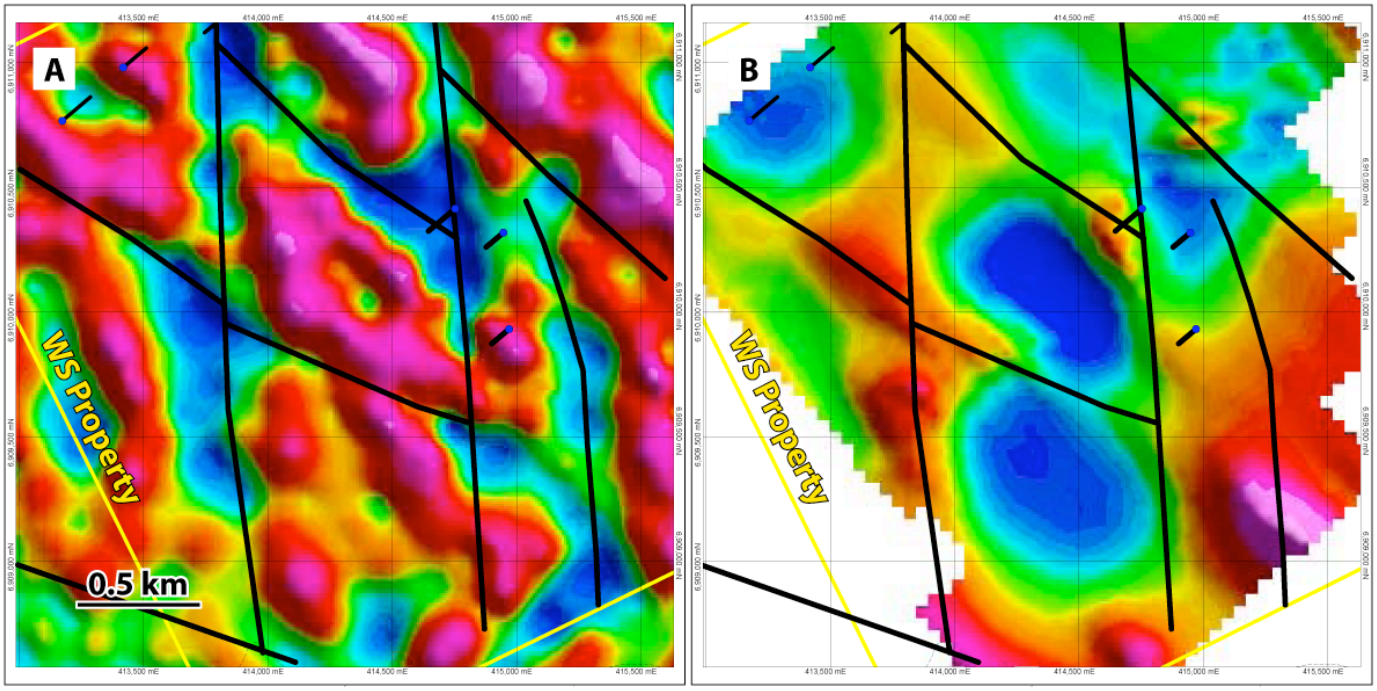

Figure 3. *Interpreted model for young brittle structures along the west side of the WS property.* **(A)** *The vertical magnetic gradient data show magnetic "low" lineaments along the faults, while* **(B)** *the IP resistivity model (-163m) shows resistive zones along the interpreted faults.*

of offsets along these structures and zones of high potential for the occurrence of mineralized zones. Further work in the field will confirm the orientation and displacement along these faults.

1.5 WS Property foliations and mineralization trends

Foliation of the intrusive units and trends of mineralized bodies in the granodiorite on the WS property are interpreted from the *IP chargeability data*. Trends in the chargeability data match orientations of measured foliations on the WS property (J. Pautler field maps). In several instances the chargeability highs also correlate with MMI Cu anomalous zones, these areas have been targeted for trenching in the 2009 season (G. Newton and G. Lustig correspondence).

Establishing the location and orientation of these zones is the focus of the upcoming field work.

3. REFERENCES

Aryamanesh, 2009. Aeromagnetic Data Interpr8-197etation to Locate Buried Faults in Yazd Province – Iran. World Applied Sciences Journal 6 (10). p.1429-1432.

Casselman, S.G., 2008. Map of the Carmacks Copper Project 2007 IP Survey Grid. For Western Copper Corporation, June 20, 2008, by Aurora Geosciences.

Colpron, M., Gordey, S.P., Lowey, G.W., White, D. and Piercey, S.J., 2007. Geology of the northern Whitehorse trough, Yukon (NTS 105E/12,13, and parts of 11 and 14; 105L/4 and parts of 3 and 5; parts of 115H/9 and 16; 115I/1 and part of 8)(1:150,000 scale). Yukon Geological Survey, Open File 2007-6.

Hood, S., Hickey, K., Colpron, M. and Mercer, B., 2009. High-grade hydrothermal copper-gold mineralization in foliated granitoids at the Minto mine, central Yukon. In: Yukon Exploration and Geology2008, L.H. Weston, L.R. Blackburn and L.L. Lewis (eds.), Yukon Geological Survey, p. 137-146.

Robinson, R.J. and Casselman, S.G. 2007. Mineral Resource Estimate For the Carmacks Copper Project. For Western Copper Corporation, January 2007. By Aurora Geosciences Ltd.

Tafti, R. and Mortensen, J.K., 2004. Early Jurassic porphyry(?) copper(-gold) deposits at Minto and Williams Creek, Carmacks Copper Belt, western Yukon. In: Yukon Exploration and Geology 2003, D.S. Emond and L.L. Lewis (eds.), Yukon Geological Survey, p. 289-303.

Tempelman-Kluit, D.J., 1984. Geology, Laberge (105E) and Carmacks (115I), Yukon Territory. Geological Survey of Canada, Open File Report 1101 (two 1:250,000 scale maps and legend).

Natural Resources Canada, Earth Sciences Sector, Geoscience Data Repositories:
Aeromagnetic and Electromagnetic data
First vertical derivative of residual total magnetic field 200 m grid of Canada
http://gdr.nrcan.gc.ca/aeromag/can200m_vg_e.php

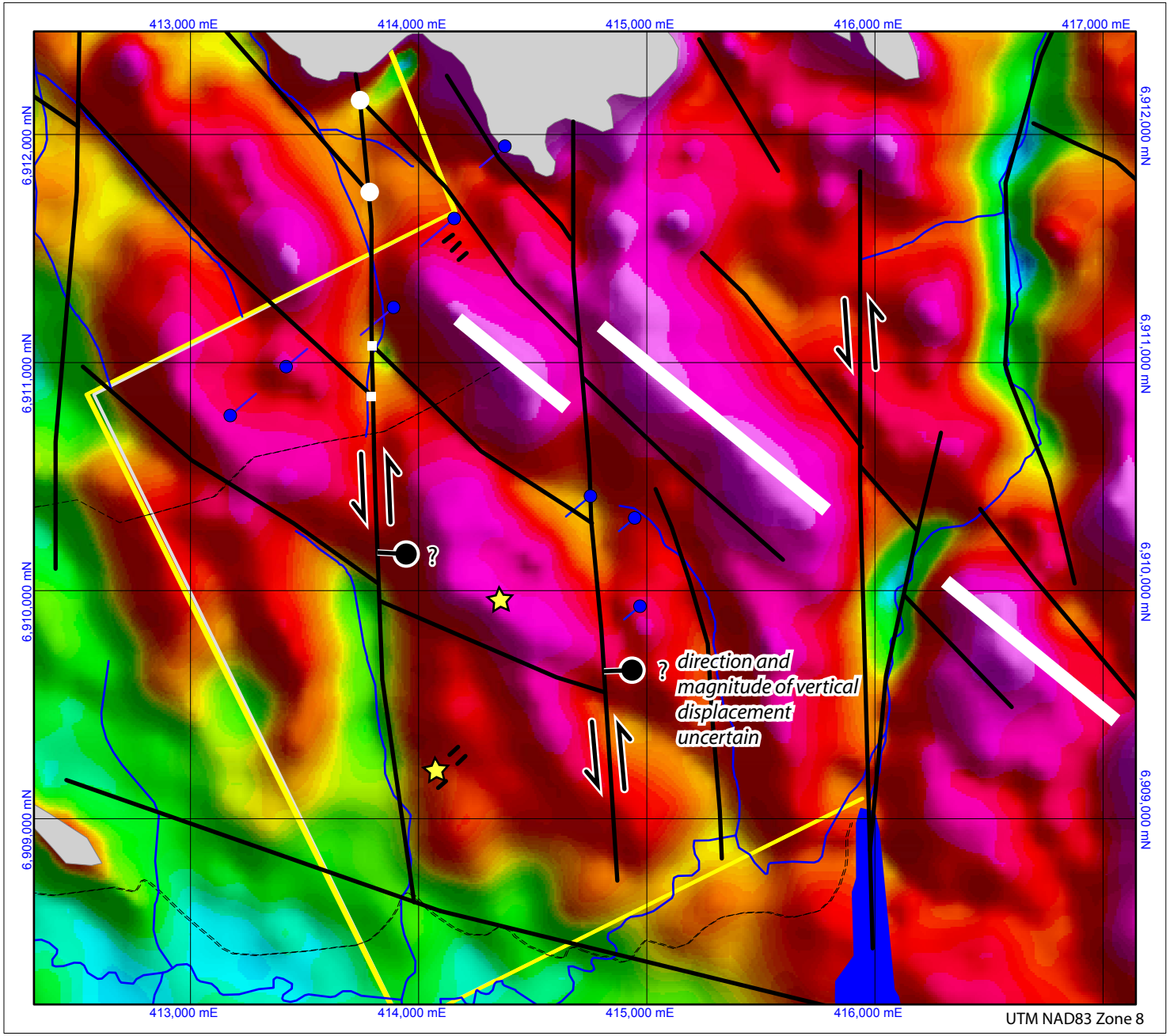

Figure 4. Direction and estimates of horizontal displacement on brittle structures on the WS property overlain on the total magnetic field data. White shapes show piercing points along the faults and lithological zones used to infer horizontal displacement direction. See following figure (Figure 5) for legend.

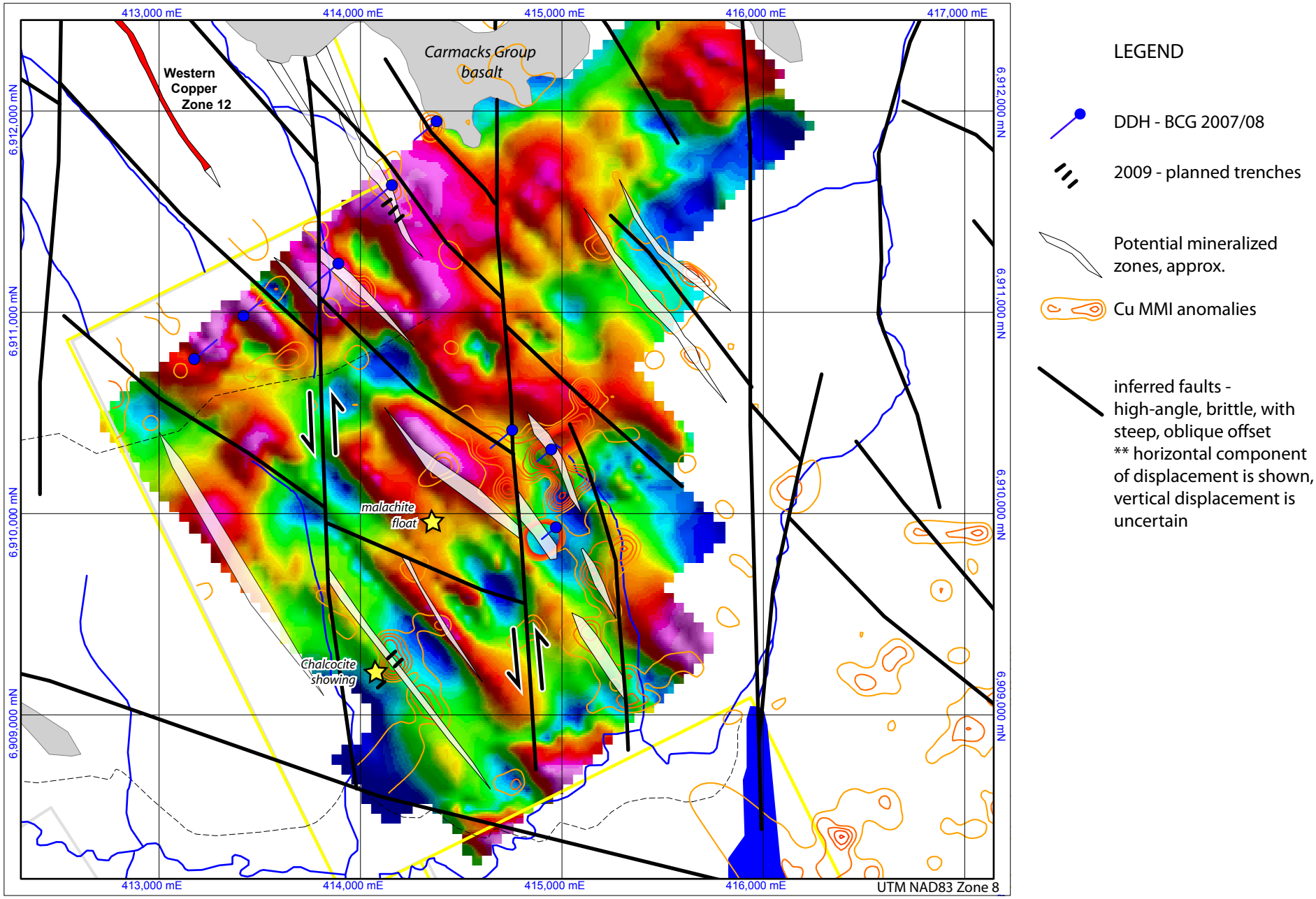

Figure 5. A summary of the structural interpretation on the west side of the WS property, overlain on the IP chargeability model (-63m). Zones of potential mineralization zones are shown, and offsets along inferred structures are shown. The data are correlated with the MMI Cu anomalies in the area.
*** This map is presented as a summary of ideas – note that the zones of mineralization shown are 'potential zones' and are shown to highlight trend and location of potential mineralized bodies. The model is to be tested in the field during a future site visit.

Interoffice MEMO

To:	Brian Fowler, BCGold Corp.
Cc:	Geoff Newton, BCGold Corp
From:	Fionnuala Devine
Subject:	**WS PROPERTY AREA GEOLOGY**
Date:	August 8, 2009

SUMMARY

- Geological relationships and rocks types in the WS property area are presented as:
  1) Photos of rock types divided into pre- and post-mineralization phases.
  2) Summary graphic logs compiled for drill holes on the Carmacks Deposit to the north, along strike of the WS property.

- Structural relationships and models for evolution of the geology in each the drill hole logged are presented following each graphic log.

- Local relationships suggest two possible models for the occurrence and relationships surrounding mineralization on the property, and at other properties in the South Block. These are:

  - Mineralized zones occur in localized shear zones within early to middle Granite Mountain batholith granodioritic rocks. The shear zone *boundaries are defined by progressively increasing strain*. Late Granite Mountain batholith granodioritic intrusions cut across the mineralized shear zones and are themselves only weakly foliated.

  - Mineralized zones occur in localized shear zones within early to middle Granite Mountain batholith granodioritic intrusive rocks. Rafts and screens of early to middle Granite Mountain intrusions with local mineralized shear zones are engulfed and surrounded by late-stage Granite Mountain batholith intrusive rocks. *Boundaries of the mineralized zones will be defined by intrusive contacts.*

- The exploration implications for each model are presented.

INTRODUCTION

This report is prepared as an update of ideas on the geology of the WS Property area in Central Yukon following a five-day field visit to the property. The WS property area has been the focus of field studies to-date, but ideas and geological interpretation on the southern Carmacks Copper Belt are also presented. Publications on the geology of the Minto Mine, in the northern part of the Belt provide some of the most detailed geological information on the "Minto-type" deposits due to access through mine development, and these models are also used as a guide for exploration in the southern part of the belt.

BCGold Corp. is currently exploring for "Minto-type" copper-gold deposits and holds properties along the length of the Carmacks Copper Belt, focused in two areas: 1) the South Block, including properties which broadly surround Western Copper Resources' Carmacks Copper Deposit, and 2) the North Block, including properties to the north and along trend of the Minto Mine.

The WS Property sits immediately to the south of the Carmacks Copper Deposit, along trend from the mineralized zones. Access is via the Western Copper road to the deposit, and by ATV trail and helicopter to the more remote parts of the property. Resistant ridge shoulders with outcrop and drill core provide the best exposure to rock on the property, while a regional aeromagnetic survey and property IP surveys provide sub-surface information.

WORK COMPLETED

During a 5-day field visit, in order to gain an understanding of the local rock types and relationships and to guide future exploration, the following was accomplished:

- Mapping (1:1000 scale) of the east-side of the WWest Property (immediately to the west of the WS Property)
- Mapping (1:1000 scale) of sections of the west-side of the WS Property, following up on Jean Pautler's identification of foliated granodioritic rocks, and including the 'Copper Hill' showing area.
- Graphic summary logging of available drill core (presented here-in)
- Development of a field compilation system for the WS property on a standardized compilation map to be used to organize new data gathered on the property. G Sidhu to follow up on maintaining this system.
- Development of a summary geological chronology for the WS property area, to be added to and developed during the course of continuing exploration.

GEOLOGICAL SUMMARY

The western side of the WS Property is underlain by various phases of the Granite Mountain batholith. The area is immediately south, along strike from the Carmacks Copper Deposit. The rocks types, structural fabric, geophysical trends, and MMI geochemical anomalies all indicate that the mineralized zones at Carmacks Copper likely continue onto the WS Property.

Rocks types range from fine –grained, sugary textured, biotite-amphibole rocks, to well foliated biotite-amphibole gneissic rocks, up thorugh various granodiorite to quartz-monzonite intrusions and granitic pegmatite dykes.

Figure 1 on the following page shows a summary of the rock types and their inferred chronological relationships based on field and drill core observations. Early, well foliated, gneissic and schistose rocks may be incorporated supracrustal rocks and/or earliest phases of the Granite Mountain batholith (Figures 2 and 3). Well-foliated granodioitic rocks cut the fine-grained rocks and are themselves incorporated into the strongly foliated zones. The relationships suggest progressive ductile deformation contemporaneous with igneous intrusion. Other phases and compositions of intrusion, commonly quartz-diorite also intrude the fine-grained rocks and are moderately foliated to well-foliated (Figure 4). These early intrusions also commonly display fine to medium-grained, equigranular texture, with higher concentrations of mafc minerals – biotite and amphibole. The may have experienced a higher degree of metamorphism than later intrusions, or perhaps been altered during the follosing mineralization event.

Chalcopyrite and bornite mineralization occurs in both the fine-grained rocks, and also the well foliated intrusions. The sulphides are fine grained and disseminated in the fine-grained rocks (Figure 2a), but vary to disseminated with coarse blebs and patches in the fine to medium-grained intrusive rocks (Figure 3). Mineralization is incorporated into the foliation indicating that is occurred either pre-ductile deformation, or more likely, syn-ductile deformation. Some patches of mineralization show an affinity for amphibole (Figure 3), while in other areas there are indications that sulphides may be replacing biotite (Figures 5 and 6). There is a biotite phase that is silver to brass-coloured, occurring locally in the mineralized zone. Textures show that the sulphides appear to be surrounding grained of amphibole and feldspar, taking the place of biotite (Figure 6). The relationship of biotite and amphiboe to mineralization needs to be studied in more detail.

Also important for mineralization is the orientation of the penetrative foliation affecting the host rocks. In drill core it was observed that mineralization occurred where the foliations were steep relative to the core axis. The pattern that developed out of the logging is summarized in Figure 11, it shows that mineralization is concentrated in high-strain bands within a ductile shear zone. Whether the mineralization is related to a developing porphyry system, or to an IOCG system is uncertain. The models for mineralization, orientation of the ductile shear zone, and the relationship to surrounding intrusive units are presented in Figure 9 and 11.

Following mineralization there are several intrusive units that occur in both drill core and in outcrop. They include medium- to coarse-grained granodiorites to monzonites, locally with pink K-feldpsar phenocrysts up to 4 cm long, and round clear grey quartz phenocrysts up to 2 cm wide (Figure 7). Dykes of these units were observed to crosscut mineralized units in core. The latest stages of intrusion are fine grained aplite, medium grained granitic dykes, and pegmatitic granitic dykes all commonly <5 metres wide, more commonly 10cm to 1 metre wide (Figure 8).

Two models for the geological relationship around mineralized zones in the WS property area are presented in Figure 9.

GRAPHIC CORE LOGS

Diamond drill core from two holes was studied at and summary graphic logged. Figures 10 through 13 summarize the logging. Notes associated with the logs point out interesting patterns and outstanding questions.

Highlights include:

WC-002

WC-002 includes over 200 metres of discontinuously mineralized core, including one section of 130 metres of continuous mineralization broken only by narrow post-mineralization dykes (Figure 10). The oldest rocks types include the fine-grained, feldspar-amphibole-biotite rock and well segregated amphibole-biotite gneiss. Medium-grained granodiorite to dioritic intrusions are interfoliated with the gneisses. These units are locally mineralized with disseminated chalcopyrite and bornite. The dominant factor on sulphide deposition appears to be the orientation of the penetrative ductile foliation. Where the foliation orientation is near the core axis, mineralization is strongest, and it dies off where the angle-to-core-axis is greater.

Post minerlalization intrusions cut out mineralization in sections of the hole, and only locally display a weak penetrative foliation, which is both a penetrative strain fabric, but also and igneous mineral alignment fabric.

Figure 11 is a reconstruction of the hole where all post mineralization intrusions have been removed, to give a clear picture of the relationships during mineralization. The relationship of mineralization to a steep foliation orientation is clear. A model for the orientation of high-strain zones being the loci of mineralization is proposed.

WC-027

This hole records a history of progressive emplacement of intrusive phases into a ductile shear zone (Figure 12). The oldest rock type present is a fine-grained, well-foliated, locally gneissic rock that may have either a supracrustal protolith (metavolcanic?), or an early intrusive protolith. Sucessive intrusive phases include, in order of intrusion: medium grained quartz-diorite, K-feldspar porphyritic granodiorite, and medium grained, locally K-feldspar porphyritic granodiorite. The earlier quartz-diorite cuts the fine, gneissic foliation, but is itself moderately foliated. The later K-feldspar porphyritic unit is also locally well foliated in a localized, relatively late shear zone (~85-92 m).

Disseminated chalcopyrite mineralization is hosted the fine-grained genissic rocks as well as the earliest intrusive phases (quartz-diorites). The mineralizing event occured during ductile deformation, as deformation also affects the units that cut mineralization (the K-feldspar porphyritic unit). Alteration related to mineralization is not very obvious, but may include pervasive biotite alteration. Epidote-chlorite replacement of mafics occurs in the post-mineral K-feldpsar porphyritic unit.

Late brittle faults are from 1 cm to 2 metres wide, and reactivate ductile shear zone boundaries and foliation planes.

Figure 13 is a summary of the progressive development of the geology of WC-027. It shows timeslices of the geology from early to late intrusive rocks emplacement and ductile shearing. It shows that the location of shearing changed over the evolution of the geology, focusing in the K-feldspar porphyritic unit late in the geological development.

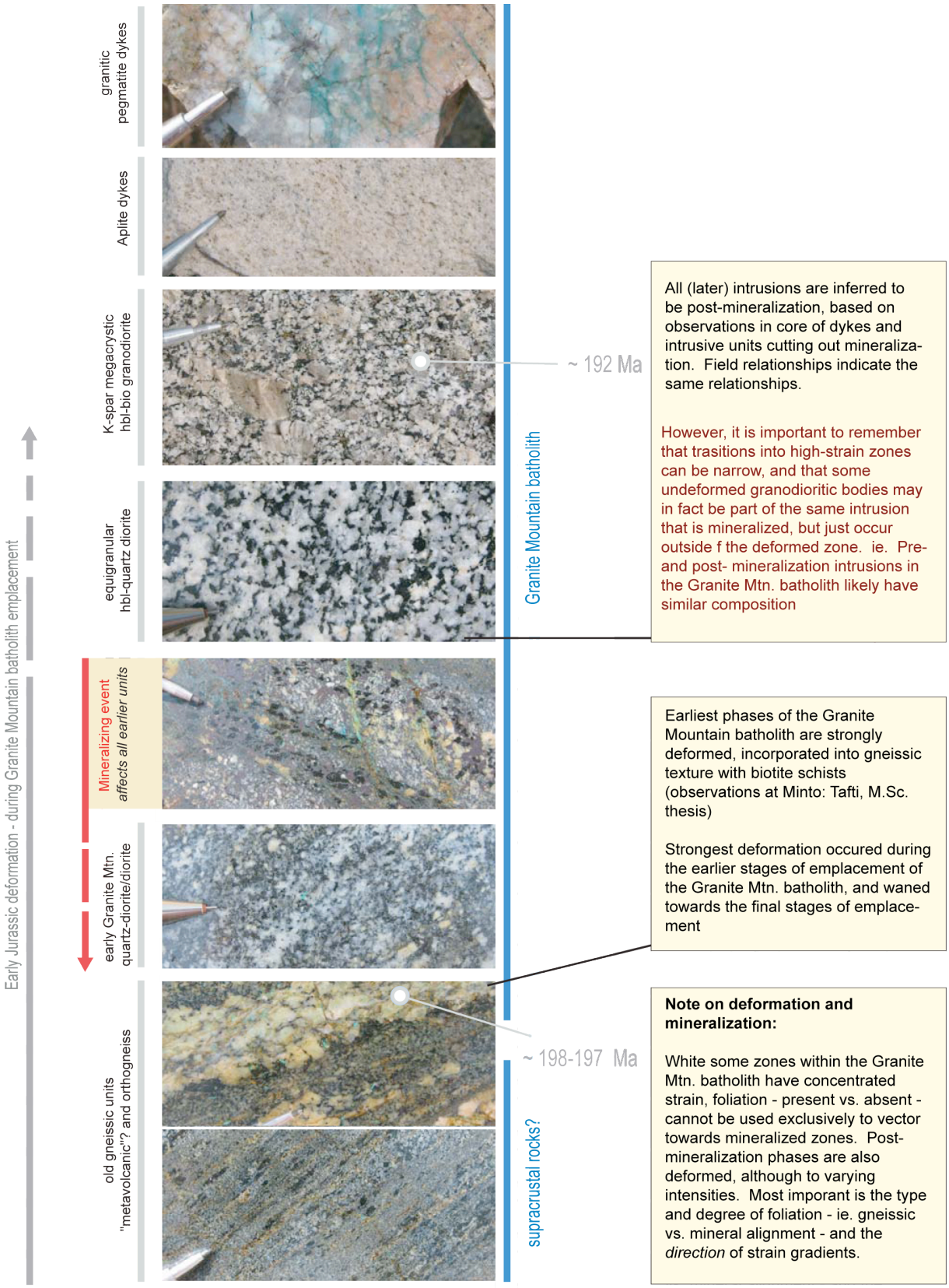

Figure 1. Photo-chronology of the rocks in the WS property area. Rocks types are shown in order of oldest to youngest (bottom to top) based on cross cutting field relationships. No rocks above the "mineralizing event" contain sulphide copper mineralization and are presumed to be post-mineralization phases. Dates shown are zircon U-Pb ages from Tafti (M.Sc. thesis) for rocks at both Minto and Carmacks Copper.

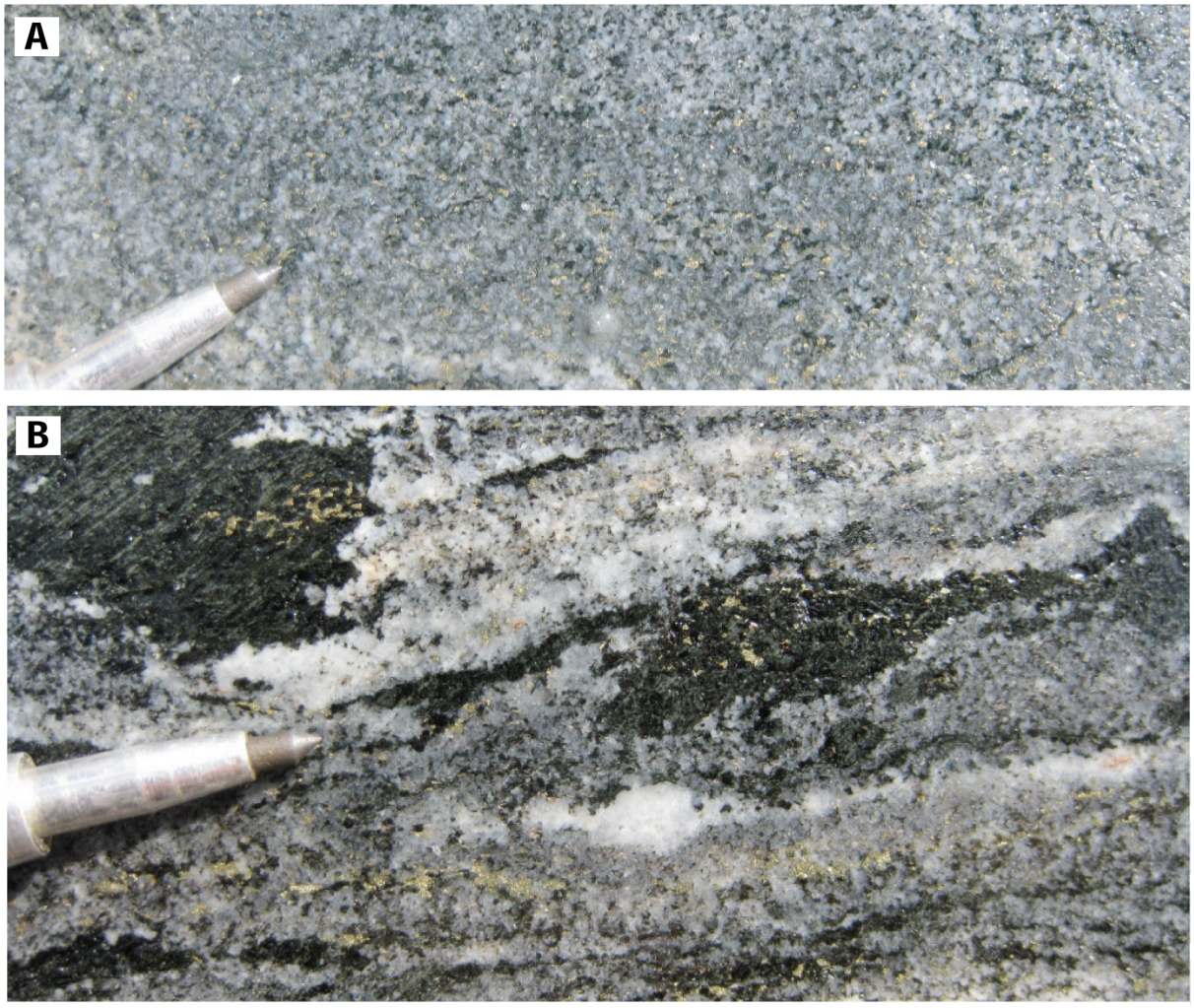

Figure 2. Disseminated chalcopyrite and bornite mineralization in fine-grained and gneissic rocks. **(A)** Fine-grained, granular textured domains, and **(B)** well-banded, segregated domains. Mineralization occurs in both melanocratic and leucocratic sections of the unit. Orientation of the gneissic, ductile fabric is an important trap for mineralization (see graphic log diagrams)

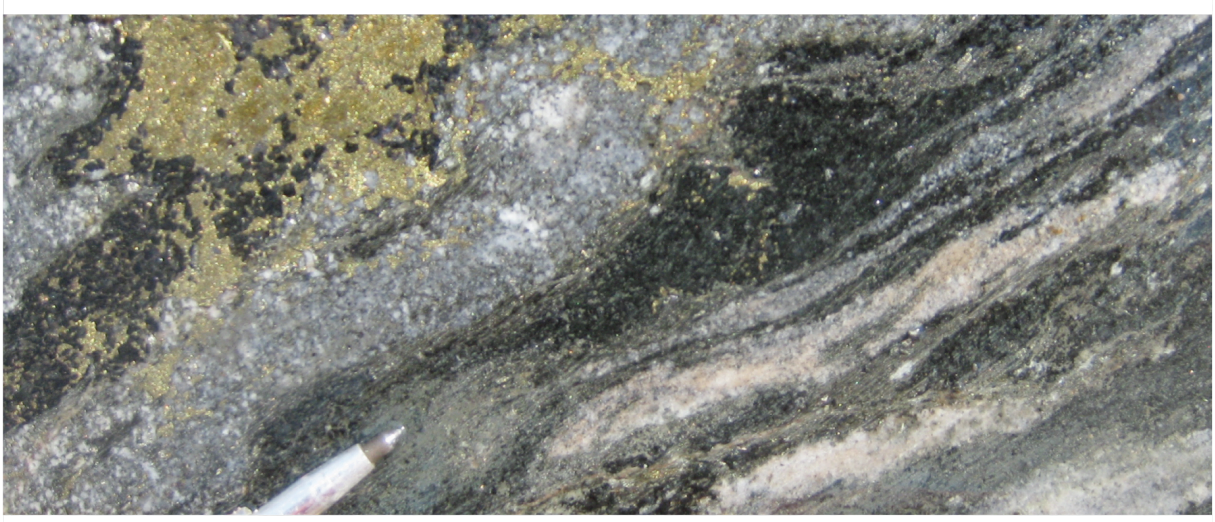

Figure 3. Disseminated and patchy chalcopyrite mineralization in biotite-amphibole gneiss. Chalcopyrite mineralization is intergrown with amphibole (left side of photo) and extends across the foliation – evidence that mineralization was synchronous with the development of the pervasive foliation.

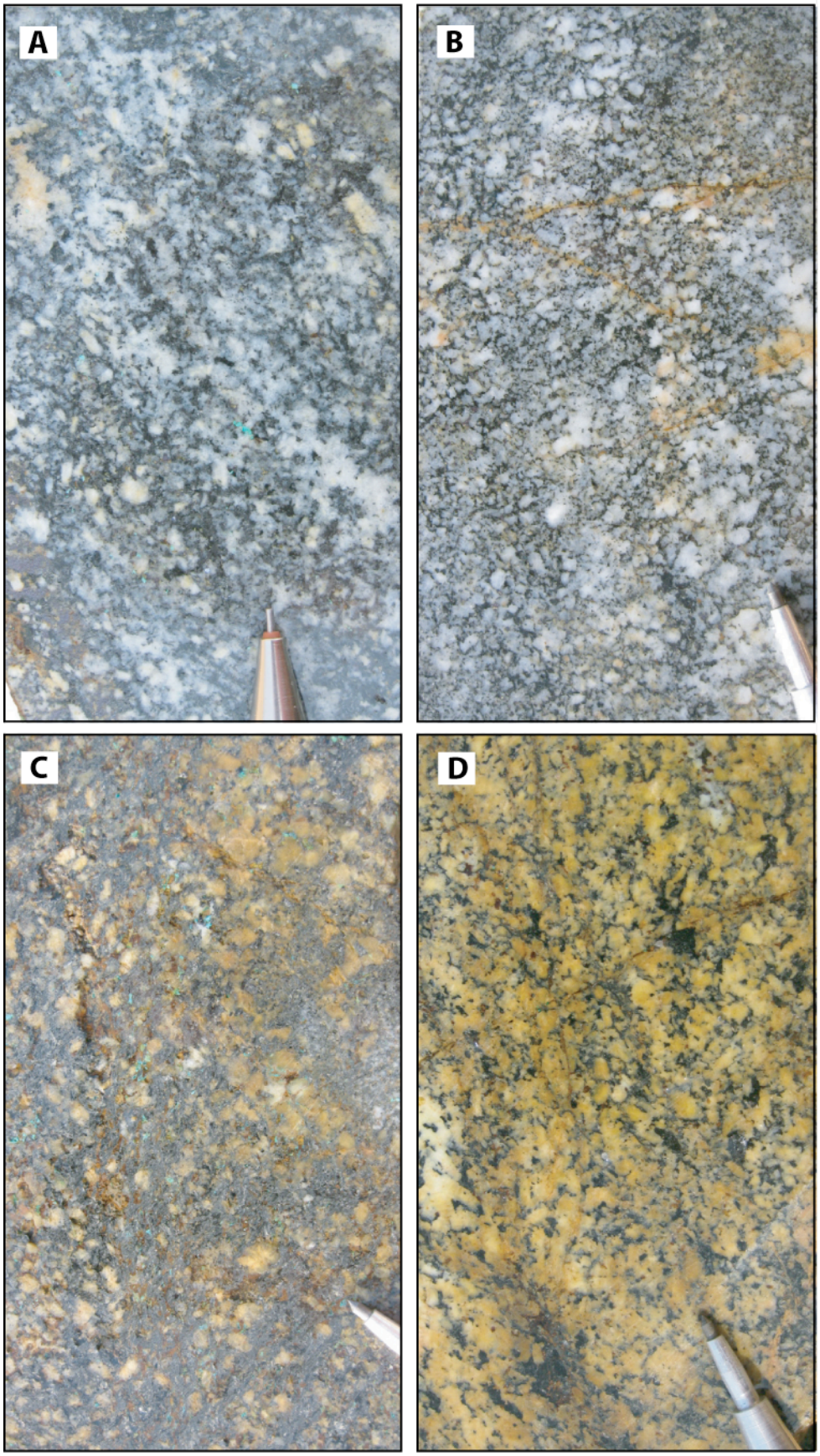

Figure 4. Pre-mineralization intrusions – granodiorite to diorite. Medium-grained equigranular, with weak to strong penetrative foliation (ductile) and amphibole and biotite alteration /metamorphic minerals.

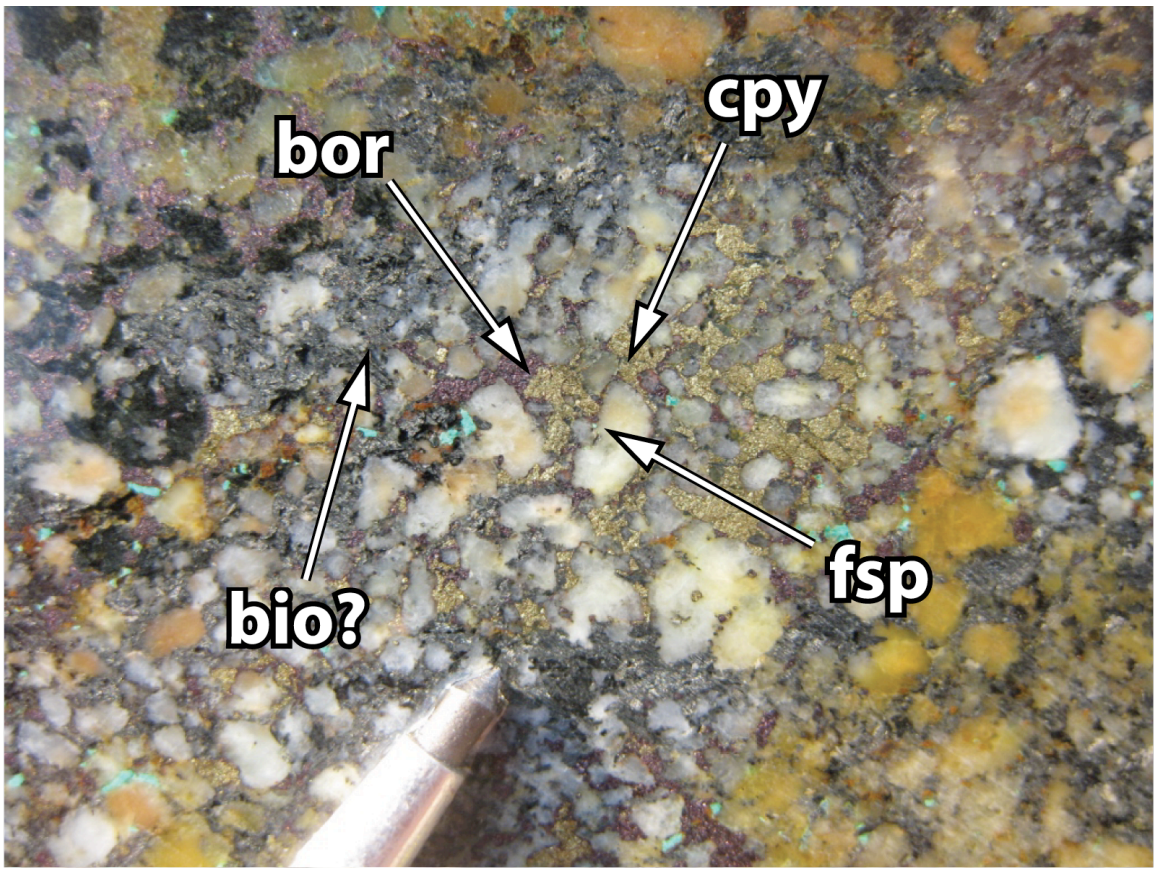

Figure 5. Chalcopyrite and bornite mineralization interstitial to feldspar domains in gneissic rocks. Chalcopyrite and bornite occupy the same textural sites as biotite (silver-coloured biotite – is this biotite?), indicating that replacement of biotite is a potential mechanism of copper deposition.

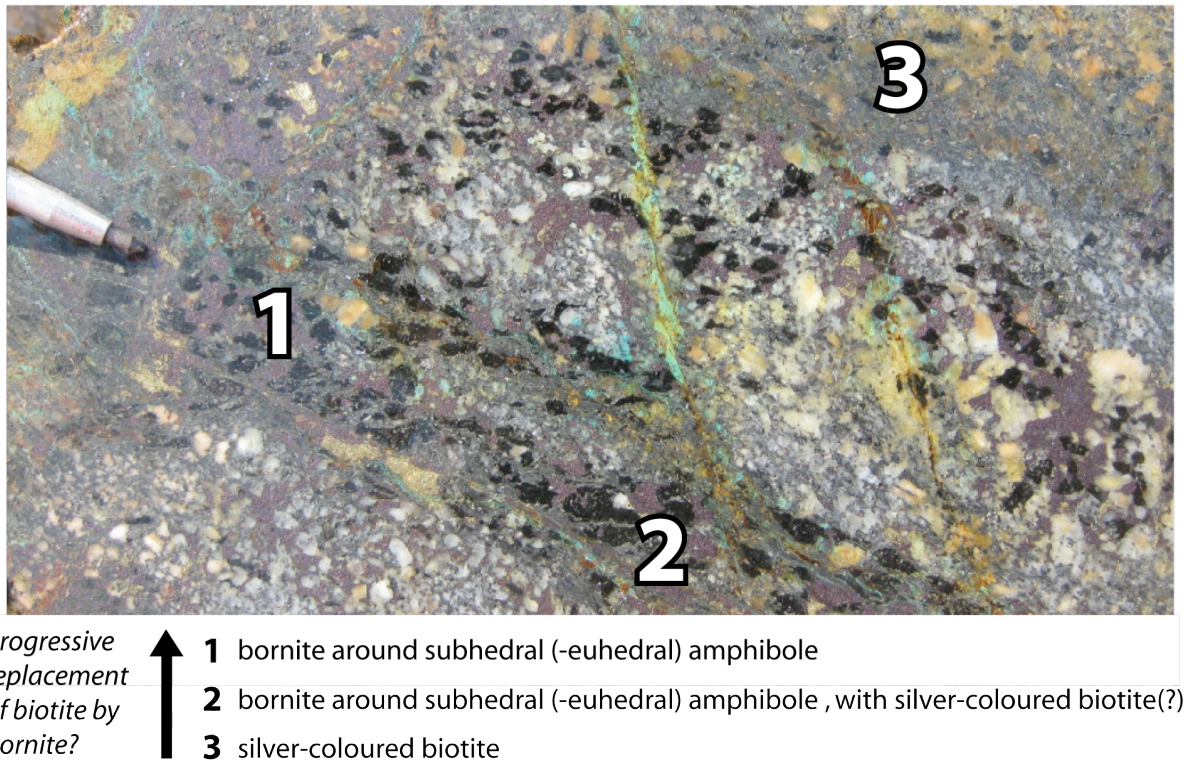

Figure 6. Chalcopyrite and bornite mineralization in metaigneous rocks with late Cu-oxide veinlets along fractures. Bornite shows the same replacement of biotite around relict feldspars and amphibole as in Figure 5.

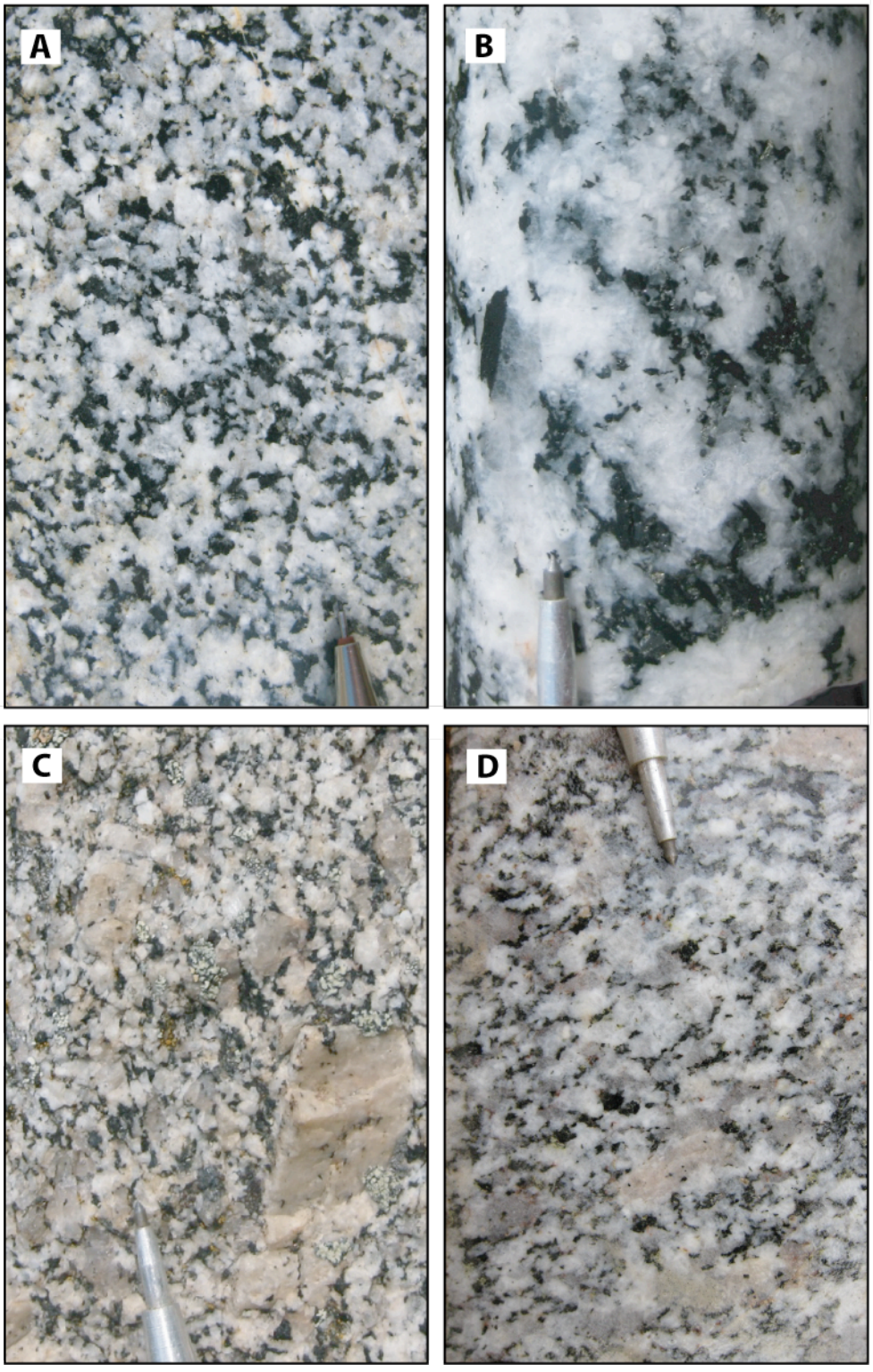

Figure 7. Post-mineralization intrusions – granodiorites, quartz-monzonites, and quartz-diorites, medium to coarse-grained, equigranular to locally K-feldspar and quartz-porphyritic.

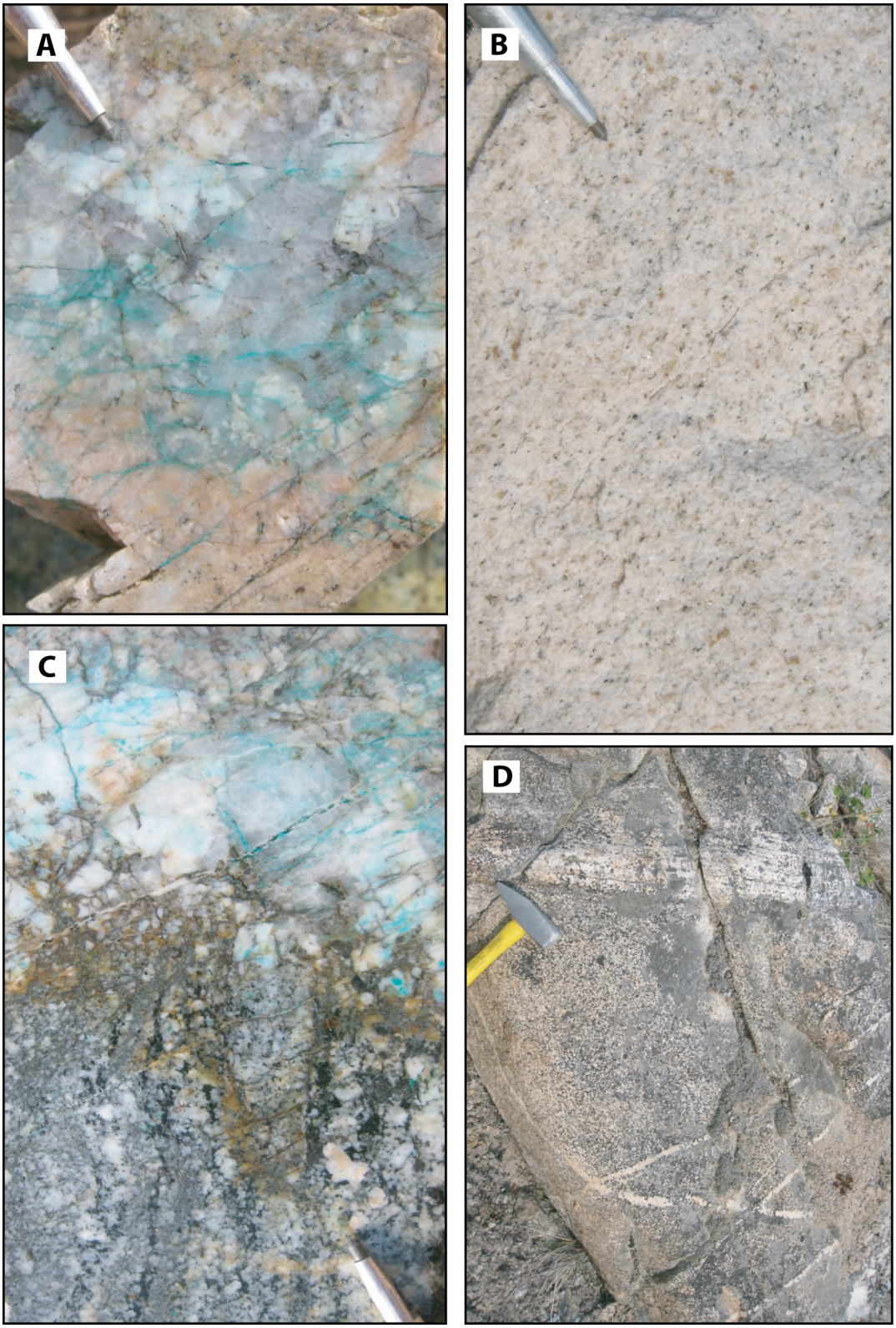

Figure 8. Late granitic pegmatite and aplite dykes, locally with Cu-oxide-lined fractures. These dykes are young, and relatively late. They are not penetratively ductile-deformed, but are locally flow-banded (aplite). They range from 1 cm to 5 metres wide, most commonly <1 metre wide, and follow the pre-existing ductile foliation anisotropy.

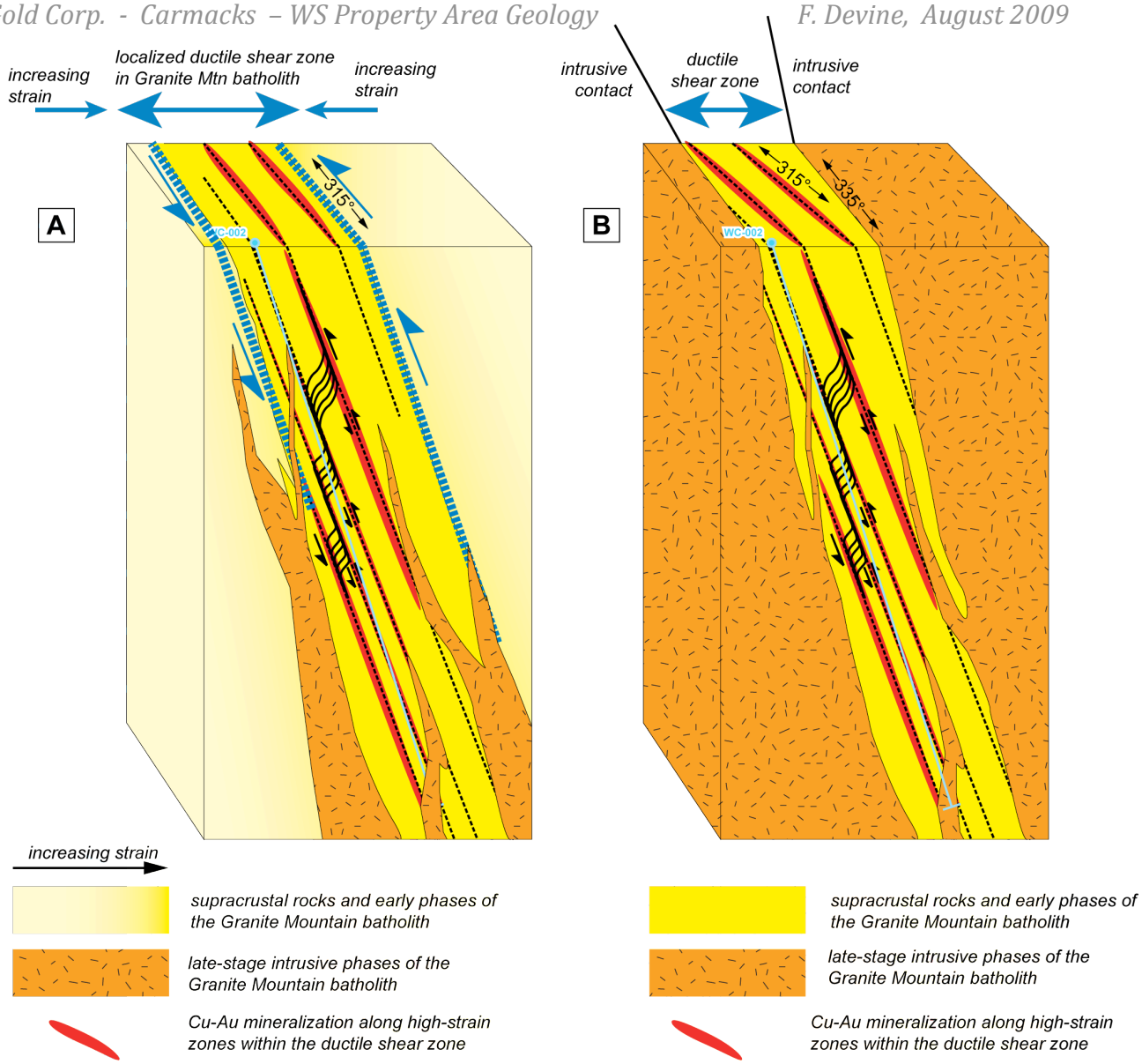

Exploration Implications:

- Shear zones (mineralized zones) could have excellent lateral continuity and depth
- A pattern for the orientation of ductile shear zones could guide exploration
- Ductile deformation intensity gradients could be used as a vector to mineralized zones
- If an alteration pattern is defined, there is the possibility to vector to mineralization using alteration intensity

Questions:

- Do relationships along mineralized zones show these relationships? At Carmacks Copper, the mineralized zones are bounded by post-mineralization intrusions. What about Minto?

Exploration Implications:

- Much of the Granite Mtn. batholith could include post-mineralization intrusive phases
- Mineralized zones are isolated pendants and screens, occurring in groups, but also randomly
- There will be no alteration halo to use in vectoring, contacts with mineralized zones will be sharp

Questions:

- Then why the lateral continuity of Minto? Up to 1.5 km of continuity of individual (<50m wide) zones (Hood, et atl., 2008)

Figure 9. Two models for the occurrence of mineralized zones in the Granite Mountain batholith. **(A)** Mineralized zones occur along localized shear zones within early phases of the batholith, and are only partly engulfed by late-shearing post-mineralization intrusions. **(B)** Mineralized zones occur as pendants and screens of ductile deformed, early intrusive phases within late-stage intrusive phases that are only weakly deformed.

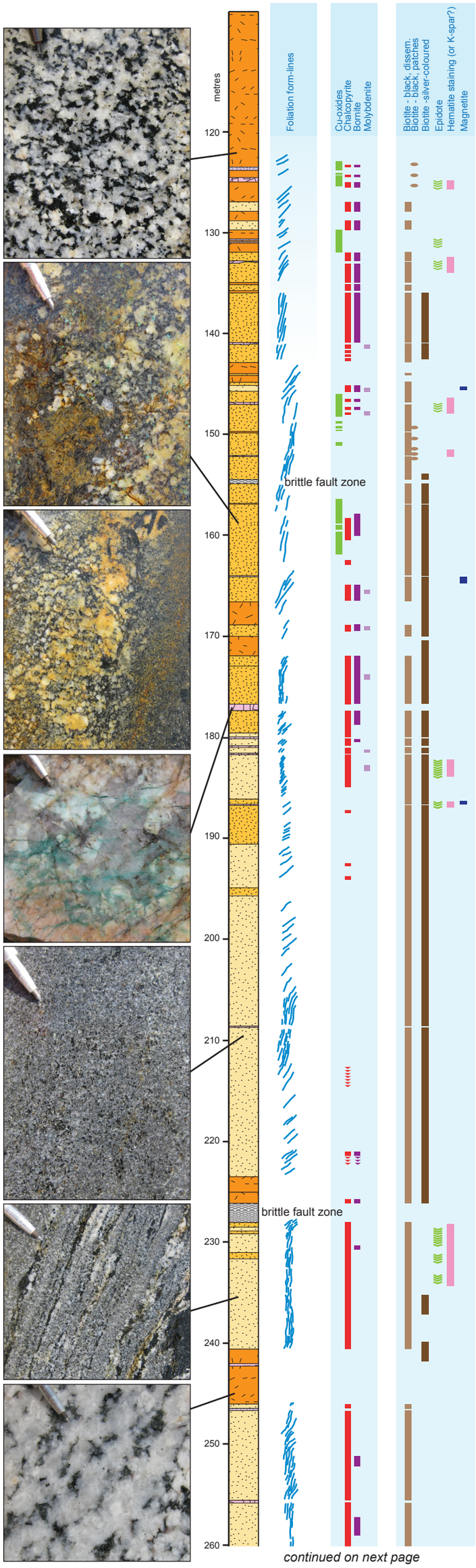

continued on next page

LEGEND

LITHOLOGY

Jurassic Granite Mountain batholith

Granitic pegmatite dykes - quartz, feldspars, biotite, muscovite?, in dkes <1 m wide

"aplite" dykes - fine grained quartz + feldspar. <1% fine grained mafics.

Biotite-hornblende granodiorite - medium to coarse grained; equigranular; 5-10% porphyritic, clear grey quartz;

Biotite-hornblende qtz-diorite - medium grained; equigranular; white-black coloured, 20-50% mafics (alteration?), acicular hornblende to 1cm locally.

Earliest Unit
early Granite Mtn batholith intrusions?
or metamorphosed supracrustal rocks?

Granular rock, well foliated. Fine to medium grained rock, feldspar-mafics, up to 60% mafic content locally, although highly variable. Well foliated with gneissic texture common.

ALTERATION

Biotite ?alteration? metamorphic? Disseminated biotite, recrystalized in igneous mafic sites

Biotite ?alteration? metamorphic? Patches of coarse, black biotite, follow foliation.

Biotite ?alteration? silver- to brassy-coloured biotite, finely disseminated to coarse textured patches. Occurs over several unit types.

Epidote disseminated, and vein. occurs disseminated near zones of pegmatite dykes, commonly with pervasive pick (hematite?) wash. Some veins are epidote, pink hematite? or K-feldspar?, and locally with coarse magnetite.

Pink wash - hematite staining? pink staining along fractures, and pervasive discolouration of feldspars. Locally may be pink K-feldspar?

Magnetite coarse patches (<1cm) of magnetite, occur only locally. Some associated with epidote veins.

MINERALIZATION

Cu-oxides veins and fracture fillings, locally disseminated as pits after disseminated sulphides

Chalcopyrite dissminated as <2mm grains, also as <5mm patches within mafic foliations (triangle symbol). Rarely wtih epidote veins - remobilized?

Bornite dissminated as <2mm grains, also as <5mm patches within mafic foliations (triangle symbol). Shows a textural pattern indicating replacement of biotite?

Molybdenite Occurs only locally as <2mm grains with cpy and bornite.

STRUCTURE

Foliation formlines. Lines follow orientation of foliation relative to the core axis.

Summary orientation of foliation

Carmacks Copper
Zone 1

DDH WC-002

065deg., -72deg., 446m

Figure 10. Graphic log summary for DDH WC-002 from 110 to 400 metres.

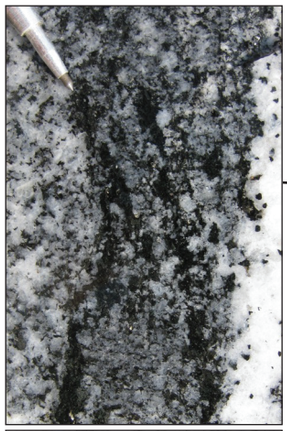









continued from next page

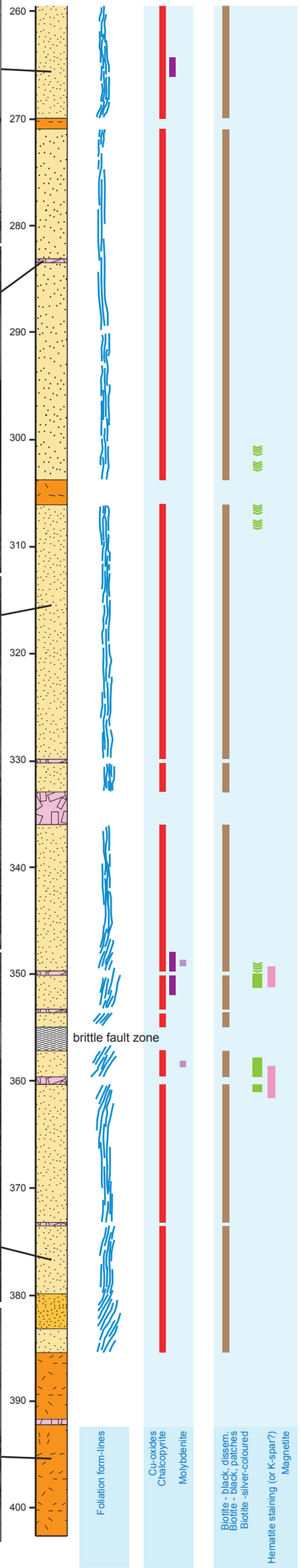

epidote veining around late-stage granodiorite dyke.

epidote veining around late-stage granitic pegmatite dyke

LEGEND

LITHOLOGY

Jurassic Granite Mountain batholith

Granitic pegmatite dykes - quartz, feldspars, biotite, muscovite?, in dkes <1 m wide

"aplite" dykes - fine grained quartz + feldspar. <1% fine grained mafics.

Biotite-hornblende granodiorite - medium to coarse grained; equigranular; 5-10% porphyritic, clear grey quartz;

Biotite-hornblende qtz-diorite - medium grained; equigranular; white-black coloured, 20-50% mafics (alteration?), acicular hornblende to 1cm locally.

Earliest Unit
early Granite Mtn batholith intrusions?
or metamorphosed supracrustal rocks?

Granular rock, well foliated. Fine to medium grained rock, feldspar-mafics, up to 60% mafic content locally, although highly variable. Well foliated with gneissic texture common.

ALTERATION

Biotite ?alteration? metamorphic? Disseminated biotite, recrystalized in igneous mafic sites

Biotite ?alteration? metamorphic? Patches of coarse, black biotite, follow foliation.

Biotite ?alteration? silver- to brassy-coloured biotite, finely disseminated to coarse textured patches. Occurs over several unit types.

Epidote disseminated, and vein. occurs disseminated near zones of pegmatite dykes, commonly with pervasive pick (hematite?) wash. Some veins are epidote, pink hematite? or K-feldspar?, and locally with coarse magnetite.

Pink wash - hematite staining? pink staining along fractures, and pervasive discolouration of feldspars. Locally may be pink K-feldspar?

Magnetite coarse patches (<1cm) of magnetite, occur only locally. Some associated with epidote veins.

MINERALIZATION

Cu-oxides veins and fracture fillings, locally disseminated as pits after disseminated sulphides

Chalcopyrite dissminated as <2mm grains, also as <5mm patches within mafic foliations (triangle symbol). Rarely wtih epidote veins - remobilized?

Bornite dissminated as <2mm grains, also as <5mm patches within mafic foliations (triangle symbol). Shows a textural pattern indicating replacement of biotite?

Molybdenite Occurs only locally as <2mm grains with cpy and bornite.

STRUCTURE

Foliation formlines. Lines follow orientation of foliation relative to the core axis.

Summary orientation of foliation

Carmacks Copper
Zone 1

DDH WC-002

065deg., -72deg., 446m

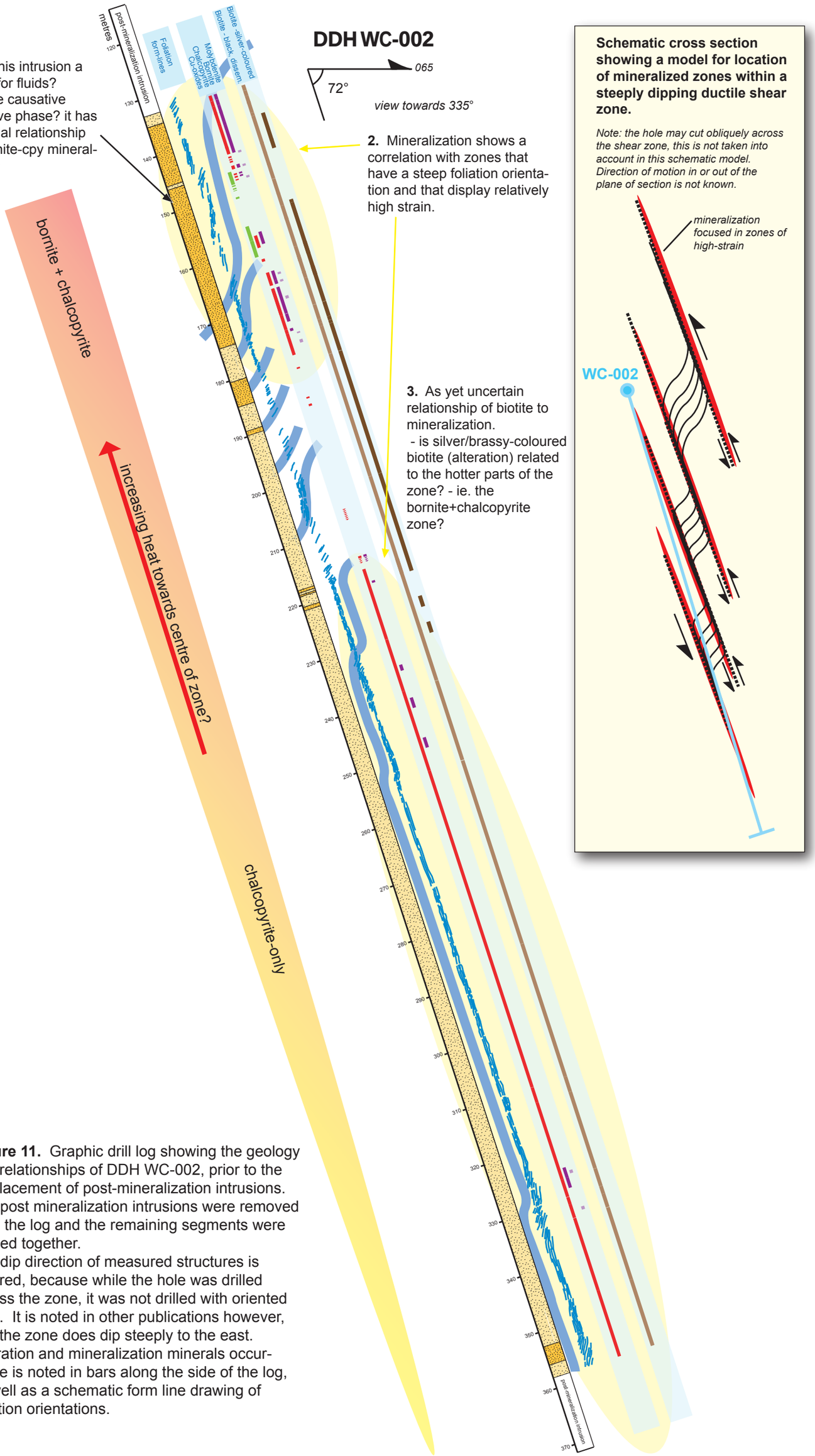

Figure 11. Graphic drill log showing the geology and relationships of DDH WC-002, prior to the emplacement of post-mineralization intrusions. The post mineralization intrusions were removed from the log and the remaining segments were spliced together.
The dip direction of measured structures is inferred, because while the hole was drilled across the zone, it was not drilled with oriented core. It is noted in other publications however, that the zone does dip steeply to the east.
Alteration and mineralization minerals occurrence is noted in bars along the side of the log, as well as a schematic form line drawing of foliation orientations.

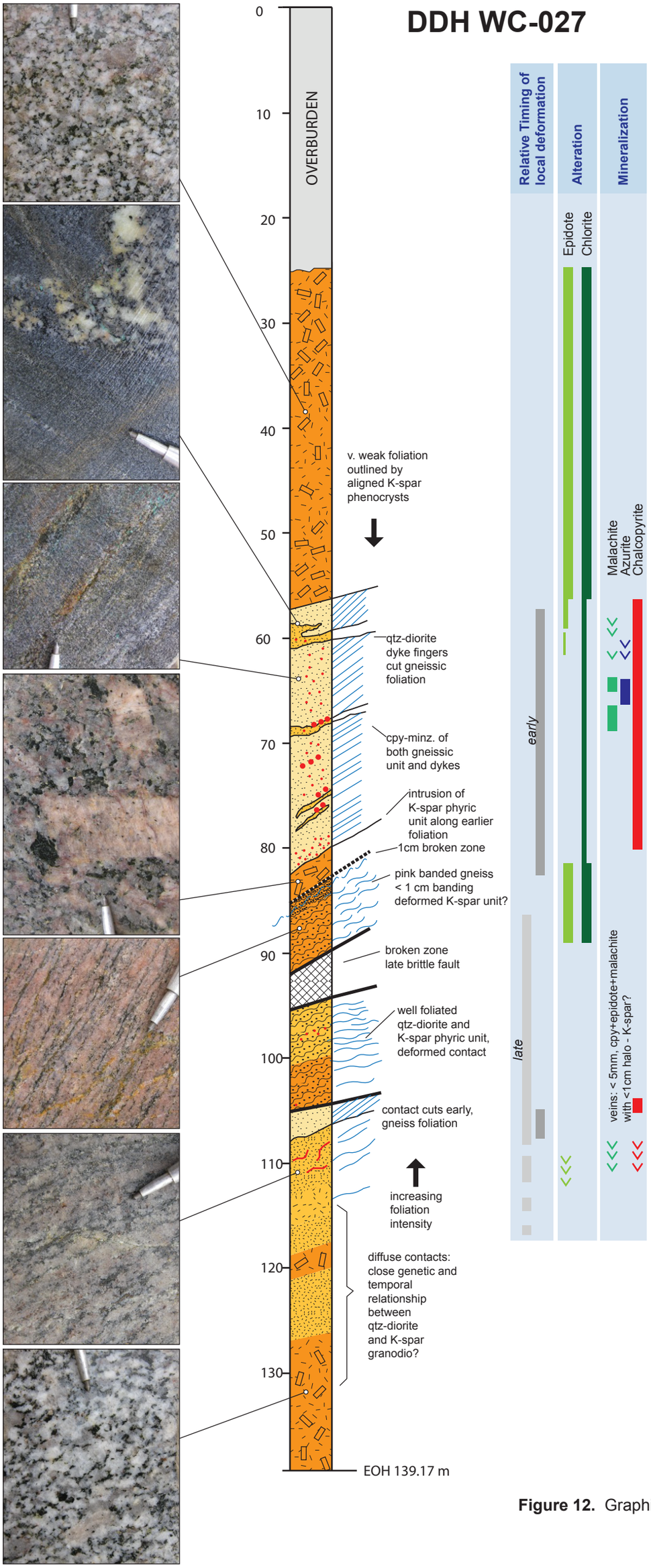

SUMMARY

This hole records a history of progressive emplacement of intrusive phases into a ductile shear zone. The oldest rock type present is a fine grained, well foliated, locally gneissic rock that may have either a supracrustal protolith (metavolcanic?), or an early intrusive protolith. Sucessive intrusive phases include, in order of intrusion: medium grained quartz-diorite, K-feldspar porphyritic granodiorite, and medium grained, locally K-feldspar porphyritic granodiorite. The earlier qtz-diorite cuts the fine, gneissic foliation, but is itself moderately foliated. The later K-feldspar megacrystic unit is also locally well foliated in a localized, relatively late shear zone (~85-92 m).

Disseminated chalcopyrite mineralization is hosted the fine grained genissic rocks as well as the earliest intrusive phases (quartz-diorites). The mineralizing event also occured during ductile deformation, as deformation also affects the units that cut mineralization (the K-feldspar porphyritic unit). Alteration related to mineralization is not very obvious, but may include pervasive biotite alteration. Epidote-chlorite replacement of mafics occurs in the *post*-mineral K-feldpsar porphyritic unit.

Late brittle faults are from 1 cm to 2 metres wide, and reactivate ductile shear zone boundaries and foliation planes.

Figure 12. Graphic log summary of DDH WC-027.

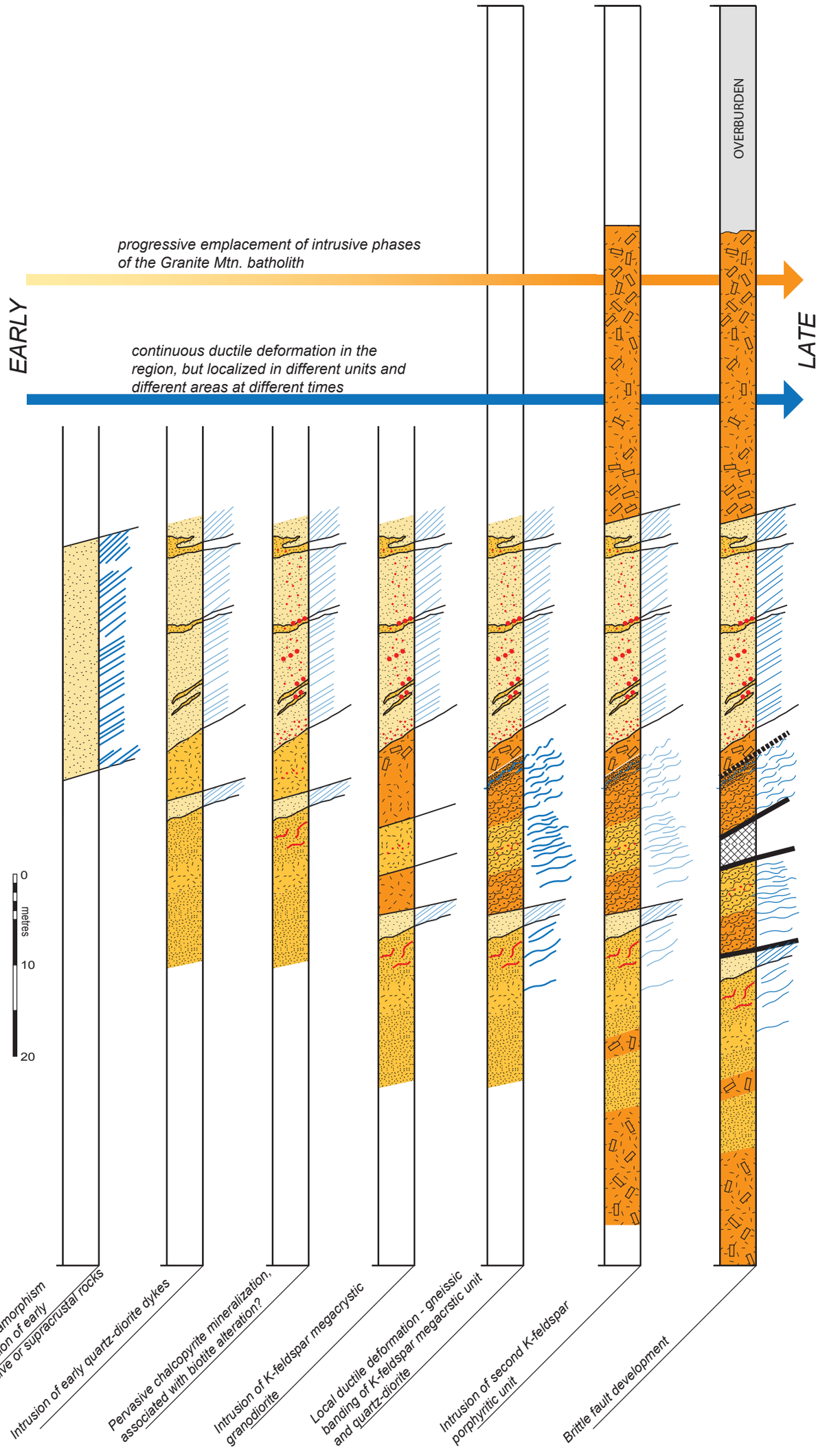

Figure 13. Schematic chronological summary of DDH WC-027. Timeslices show the devleopment of the geological relationships in the hole with respect to mineralization and structural deformation events.

APPENDIX V:
Field Examination Report
(Cardinal, 2009)

Interoffice MEMO

To:	***Brian Fowler, P.Geo., Pres., CEO, BCGold Corp.***
Cc:	***Geoff Newton, Project Geologist, BCGold Corp.***
From:	***Dan Cardinal, P. Geo.***
Subject:	***A Preliminary Field Examination, Observations and Intrepretation of the South Block claims – Carmacks Copper Project***
Date:	***September 5, 2009***

Introduction:

Megascopic observations and conclusions outlined in this memo are based on 9 days of field examinations of the South Block claims – Carmacks Copper project. Based on field evidence, structural settings conducive to potentially hosting copper (gold) mineralization in the granite exist.

Procedures and Objectives:

At the company's request, I and Dave Heino (prospector) examined and prospected a number of the claims that make up the South Block, located some 33 road kilometres northwest of the community of Carmacks, Yukon, a project known as the 'Carmacks Copper Project'. We arrived at the Carmacks camp site the afternoon of August 14th with property examinations conducted between the dates: August 15th to 23rd. I left on the 24th to Whitehorse and returned to Vancouver the 25th. Dave stayed to assist Geoff Newton (Project Geologist) with the trenching. Permitting was actually finalized and approved to build a road to the trench sites on August 24th, once some archeological concerns were addressed. A backhoe, 250 Cat, was already at the site and rehabbing parts of the existing access road.

Reconnaissance mapping and prospecting at a scale of 1:10,000 had already been conducted by Jean Pautler and prospector assistant. I found this work to be of high quality with practically every outcrop visible mapped and indentified. I found no reason for this work to be duplicated and therefore focused my time on searching for certain glues such as subtle alteration features (i.e. potassic, silicification, epidotization, etc.) and structural fabrics (schistose/foliation, second-third order fault-shears, etc.), field evidence that could be utilized as vectoring tools in search for a Williams type copper (gold) deposit. Fionnuala Devine's views and structural intrepretation of the South Block

setting, in terms of structure and mineral controls, were of great assistance. Dave's efforts were focused on panning of certain creeks and obtaining pan cons for possible gold colours, not placer type, but for gold morphology that may indicate gold originating from the system(s) with the South Block. Usually the pan cons were examined in detail in camp with a field binocular microscope. Gold flake morphology and population in terms of size, texure coarseness and number of colours were noted as well as other heavies in the pan including alteration minerals: magnetite, epidote, chalcopyrite and other related sulphide minerals. Dave then collects representative con samples for future lab analyses.

During my stay we were able to examine-prospect WS claim including Merrice and Copper Hill showings as well as the Ice, Copper and Peanut claims and a tour of the Williams deposit, trenches and Copper Hog prospect. Both Ice, Peanut and Merrice showing were with the aide of a helicopter. The other sites were accessible via ATV.

At least 4 days were spent covering parts of the WS as Merrice canyon affords an excellent section of the southeastern domain of the WS claim. As well, old placer workings identified on the northern of end of Merrice Lake offered an intriguing possibility for the provenance of the gold. During this time pan cons were obtained from parts of Merrice creek as well as a small tributary which originates from the sites of several MMI isolated highs previously tested by limited drilling.

Observations:

My observations are as follows:

(i) Copper Hill Showing: Localized malachite staining can be observed on a small rock outcrop. The exposed bedrock is limited to a few square metres and is composed predominately of dark, fine grain, foliated amphibolite intruded by quartz diorite (Photo 1). The amphibolite is cut by narrow (1-2cm) quartz veins which host minor chalcopyrite, lesser bornite and magnetite. On surface the mineralization appears to be limited to the quartz veining, however trenching should determine the extent of the mineralization and structural fabric.

(ii) Merrice Creek: Merrice canyon displays an excellent view of the various phases of the Granite Mountain Batholith. The canyon extends from the creek crossing and northward beyond Merrice Showing for some 8-10 kilometres. Part of the ridge running along the west side of Merrice Lake also affords good rock exposure. Within this southeastern domain of WS claim the predominate underlying bedrock is of intermediate composition characterisically - a massive, medium to coarse grain, pink K-spar (orthoclase phenocrysts) prophyritic-megacrystic, hornblende granodiorite / biotite granodiorite to localized phases of more mafic composition quartz diorite with lesser syenitic phases. Occassionally only minor sporadic potassic and epidote veining was observed these alterations are not believed to be related to a mineralized event. Structural fabric is generally weak to nonfoliated. Just west of the Merrice creek crossing an

outcrop just north of the old road (mapped by Jean) is a granodiorite hosting mafic-rich, schistose zenolith/boudinage lenses (Photo 2). Further (approximately 100m) to the southwest along the creek is a well exposed section of the same rock but hosts large lensoid fragments and zenoliths of mafic-rich bodies incorporated within the granodiorite. No sulphides or alteration minerals were observed.

(iii) Merrice Copper-Quartz Vein Showing: This showing is in somewhat of different geological setting. The vein which is well exposed just 25 metres above the old portal, is about 1.5 metres wide striking 342 degrees - dipping 40 degrees westerly and is hosted within a medium grain quartz diorite to dioritic intrusive. It bears little to no resemblance of Williams type mineralization and appears to be structurally controlled and suggests more of mesothermal origin. The footwall rock is altered to amphibolitic phase grading to more dioritic composition a few metres away. The hanging wall consists of unaltered quartz diorite. Copper mineralization includes malachite along fractures, lesser chalcopyrite and bornite associated with minor pyrrhotite occurring as blebs and fine seams in the quartz.

Four rock types were noted within the general area of the vein. To the southeast is a thick sequence of meta-volcanic/andesitic greenstone of probable Carmacks Group. In the area of the vein are various phases of micro-diorite to medium grain quartz diorite. To the north is an outcrop of intensely sheared, fragmented and in part mylonitic, fault-shear slices of meta-volcanic, chloritic granodiorite and quartz diorite. This section of Merrice canyon experienced intense brittle deformation and fault movement. Southwest of the portal and near valley bottom is a mafic-rich, medium grain alkalic-syenitic compostion localized stock or plug. It appears to be the youngest of the intrusive phases in this area.

(iv) Ice: The Ice claim covers the 'Ice Showing' which includes 2 small (approx. 1.5m by 2m) naturally exposed, localized, malachite stained outcrops. This area was subsequently drill tested based on trench results, MMI anomaly and IP response, meeting with limited success. The 2 outcrops are approximately 25 metres apart. Surface weathering has taken place between the outcrops suggesting that a larger zone of mineralized bedrock probably existed prior to erosion. Erosional remnants of malachite mineralization is hosted in well foliated biotite granodiorite approximately 0.5m thick immediately underlain by massive, unmineralized, biotite granodiorite. Foliation dips are shallow (25 degrees) northerly and suggests a zone of ductile deformation (Photo 3 & 3a). It is the first evidence where copper mineralization was observed to be directly hosted in granite (Photo 4) without any spatial relationship to mafic-rich, foliated bodies as observed at the Williams deposit. Either the Williams type mineralization has been eroded away leaving some copper mineral remnants or, that a slightly different genetic pattern of mineralization, possibly more of disseminated/porphyritic origin, occurs to the southeast. The population of MMI elevated copper values tend to coincidentally increase through part of this domain and may reflect a zone of mineralization at depth. Unfortunately there is little to no bedrock outcropping further to the south and southeast with the MMI values occurring along recessive terrain in areas of more bog type vegetation.

(v) Copper Claim-Copper Hog: Although this claim is covered mostly by overburden a small creek know as 'Nancy Lee' cutting the northern portion of the claim was panned tested. Pan cons showed at least 2 very fine colours suggesting possible source further to the west – probably on First Nation Land. The Copper Hog on Western Copper's ground was examined. Majority of the copper mineralization occurs along a natural hog back-like ridge (Photo 5). Here the host rock is massive, coarse to medium grain, hornblende quartz diorite carrying disseminated malachite as fracture fillings and interstitial between mineral grains. Approximately 100 metres westerly is a large, mafic-rich, highly foliated well mineralized schist engulfed within the mineralized quartz diorite. The mineralized quartz diorite offers an intriguing possibility that more then one mineral event – not just islolated to Williams type mineralization – could occur along the Carmacks copper-gold trend. This observation is further supported in the case of the Copper Hog showing, where structural fabric within the quartz diorite is not evident, suggesting that foliation and type of host rock (i.e. mafic-rich schists) may not be a pre-requisite to a mineral event – along some sections of the Carmacks trend.

(vi) Peanut: Much of the Peanut claim appears to have experienced ductile deformation and is predominately underlain by well foliated, schistosic, biotite granodiorite with strained ortho-spar minerals. The meta-granodiorite shows some evidence of gneissosity expressing some higher degree of deformation. A traverse conducted for about 2 kilometres along northwesterly trend follows a ridge with well exposed areas of rock outcrop. Bedrock foliation tends to vary along the ridge from about 310 degrees with dips of 23 degrees along the southeast rotating to about 335-40 degrees and vertical along the northeast, this would suggest some possible fold structures along strike and to depth. This folding is coincidental with the localized I.P. signature which is consistent to depth and may reflect a zone of copper mineralization possibly hosted along one of the fold limbs. Also, the foliation is very similar to the mineralized foliation observed at the Ice copper showing.

Conclusion:

The WS claim extending southeast of the Copper Hill showing in the area of Merrice canyon and southeasterly along the Merrice Lake, is underlain predominately by homogeneous, massive, K-spar megacrystic, biotite to hornblende granodiorite with occassional remnants of mafic-rich, schistosic zenoliths. Only minor, localized epidote and lesser potassic alteration was noted and is not believed to be vectoring to any potential copper mineralized event.

Trending further to the southeast to the Ice claim the structural nature of the granodiorite appears to change from more massive to isolated sections experiencing ductile deformation, hosting copper mineralization such as that preserved at the Ice showing. As well, the number of elevated MMI copper values coincidentally increase in population southeastward and may reflect an underlying foliated granodiorite, possibly preserving a larger section of Ice-like mineralization.

The Peanut is positioned some 5-6 kilometres northwest of Williams deposit and is underlain by well foliated granodiorite and appears to occur along a zone of strong ductile deformation. Foliated open folds observed on Peanut with a strong coincidental I.P. signature could host Ice-like mineralization at depth.

Additionally, based on observations of the Copper Hog, here a body of massive (nonfoliated) quartz diorite is well mineralized - other Copper Hog-like mineralized zones hosted in granitic bodies need to be considered along the Carmacks copper-gold trend. The implication of tensional block faulting along this trend also needs to be considered. It is possible that within the Merrice granitic domain exposure is of higher level versus Ice domain further to southeast where a shift downward could explain preservation of the Ice mineralization and the increase in MMI copper anomalies. Based on the Copper Hog and Ice showings, both non-ductile and ductile respectively need to be considered as hosts to granitic mineralization.

Trending southeastward from the Copper Hill showing on to the Ice and into the BC claims, rocks and structural fabric hosting copper mineralization appears to pass from the mafic-rich, highly foliated schists hosted along zones of brittle deformation (i.e. Williams type) into zones of mineralization hosted in well foliated granites along zones of ductile deformation. Copper Hill may represent an up lifted block and possibly the structural terminus of the southeastern extension of the Williams deposit.

Based on field observations there is sound structural evidence to suggest that portions of the Granite Mountain Batholith have experienced zones of ductile deformation hosting mobile belts conducive to copper-gold mineralization. Peanut, Ice and BC claims may overlie or partly overlie such a belt(s). It is also possible that some of the fine gold colours panned from sections of Merrice creek originate from such a mineralized structures.



Photo 1

Copper Hill: showing mafic-rich, fine grain, foliated amphbolite. Mineralization is associated with quartz veining including minor chalcopyrite, lesser bornite and magnetite.



Photo 2

Near Merrice creek crossing: outcrop displaying mafic-rich zenoliths engulfed in medium grain, hornblende quartz diorite (near the possible structural terminus of the Williams type mineralizaion).

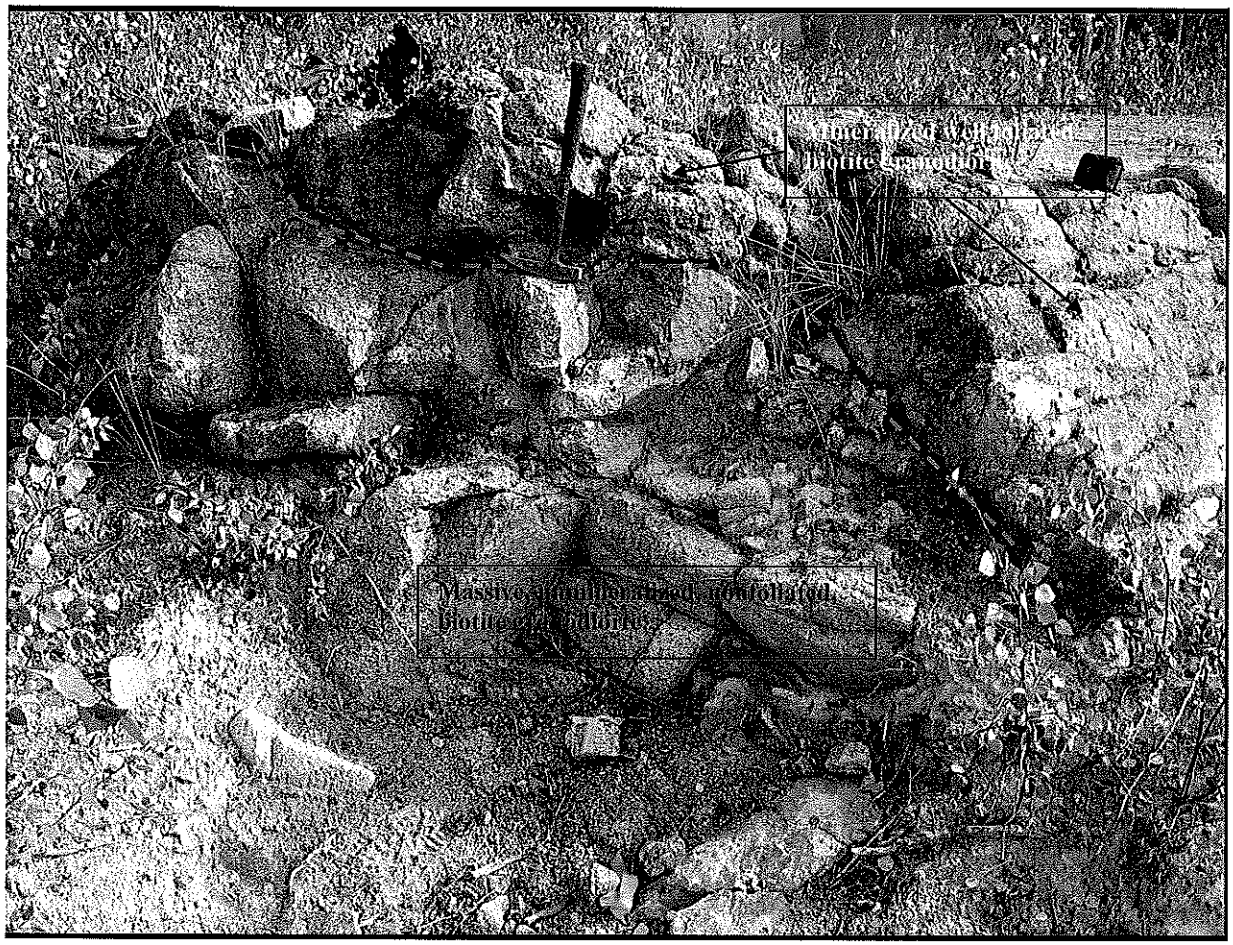

Photo 3

Ice Copper Showing: with exposed remnant (approximately 0.5m thick) of well foliated, mineralized, biotite granodiorite underlain by more massive, unmineralized, nonfoliated biotite granodiorite.

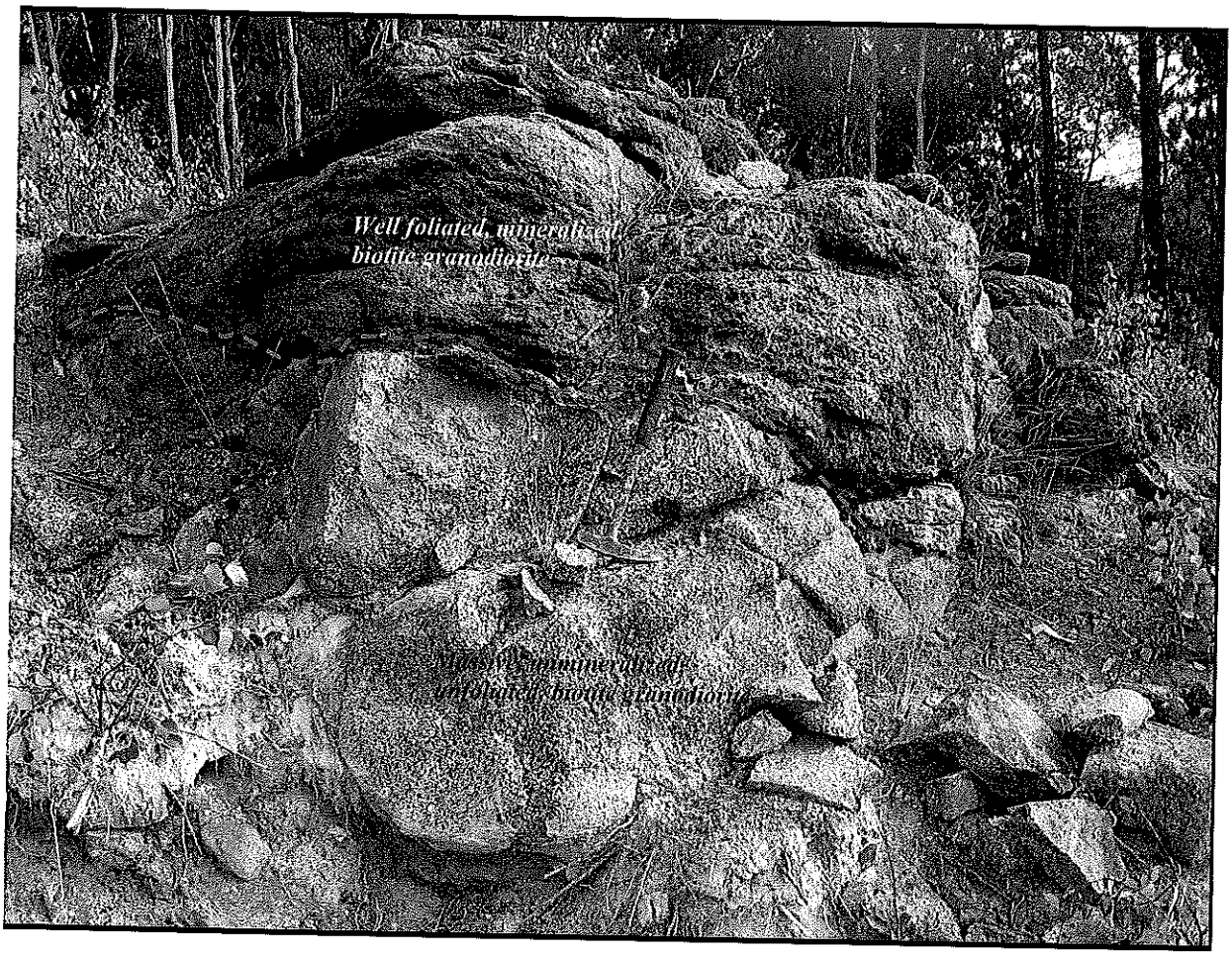

Photo 3a

Ice copper showing: exposed remnant of second outcrop approximately 25m east of outcrop one on Photo 3.



Photo 4

Ice Copper Showing: close-up of disseminated mineralized, nonfoliated megacrystic K-spar, coarse grain, biotite granodiorite. The mineralization zone occurs along the contact immediately below the mineralized foliated granodiorite, with copper mineralization penetrating several centimeters into the underlying massive, unmineralized granodiorite (in part it resembles the Copper Hog mineralization – see photo 5)

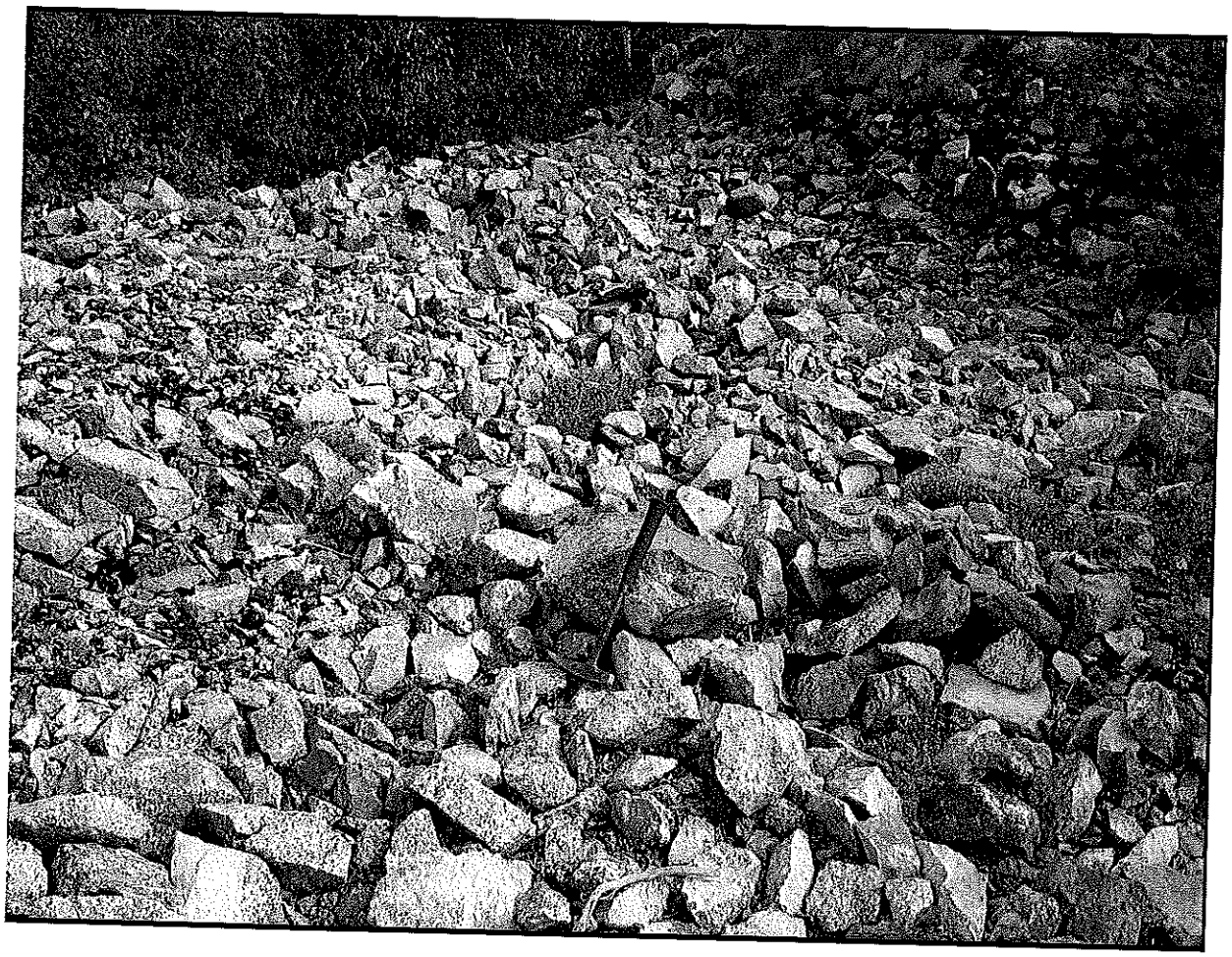

Photo 5

Copper Hog: showing massive, nonfoliated, disseminated mineralization hosted within hornblende granodiorite. Malachite mineralization occurs as fracture fillings and interstitially between mineral grains of the granodiorite.

APPENDIX VI:
MMI Orientation Report
(Lustig, 2009)

Carmacks Copper Deposit
Geochemical Orientation Survey
Yukon

Prepared for

BCGold Corp.

February 2009

Gary Lustig, MSc, PGeo

G. N. LUSTIG CONSULTING LTD.

TABLE OF CONTENTS

LIST OF FIGURES II
LIST OF APPENDICES III
1 INTRODUCTION 1
2 MMI™ BACKGROUND/PRINCIPALS 1
3 SAMPLING METHODOLOGY 1
3.1 SURFICIAL DEPOSITS 1
3.2 MINERALIZATION 3
4 ANALYSES 3
5 RESULTS 4
5.1 STATISTICS 4
5.1.1 Multivariate Analyses 4
5.2 PROFILES 8
5.2.1 Zone-1 8
5.2.2 Zones 13 and 14 (12E) 11
6 CONCLUSIONS 16
7 REFERENCES 17

LIST OF FIGURES

FIGURE 1 LOCATION MAP 2
FIGURE 2 BOX AND WHISKER PLOT - MMI™ LEACH ANALYSES 5
FIGURE 3 BOX AND WHISKER PLOT, AQUA REGIA DIGESTION ANALYSES 5
FIGURE 4 DENDOGRAM - MMI™ CLUSTER ANALYSES BASED ON PEARSON CORRELATION AND COMPLETE LINKAGE 7
FIGURE 5 AQUA REGIA CLUSTER ANALYSES BASED ON PEARSON CORRELATION AND COMPLETE LINKAGE 7
FIGURE 6 PROFILE ZONE 1 NORTH, MMI™ COPPER AND GOLD 9
FIGURE 7 ZONE 1 NORTH PROFILE, COPPER AQUA REGIA AND MMI. THE RED AQUA REGIA PROFILE CORRESPONDS WITH THE RED SCALE ON THE RIGHT AND ARE SAMPLES TAKEN BENEATH THE ASH LAYER. 9
FIGURE 8 AQUA REGIA AND MMI™ ALUMINUM PROFILES ALONG THE ZONE 1 NORTH PROFILE 10
FIGURE 9 MMI™ RARE EARTH ELEMENT (REE) ZONE 1, NORTH PROFILE. RED LINES ARE LREE (LIGHT) AND BLUE LINES ARE HREE (HEAVY) 10
FIGURE 10 ZONE 1, SOUTH PROFILE, MMI™ COPPER AND GOLD 11
FIGURE 11 ZONE 1 SOUTH PROFILE, COPPER AQUA REGIA AND MMI 12
FIGURE 12 PROFILE ZONE 1 SOUTH, MMI™ RARE EARTH ELEMENT (REE) ZONE 1, NORTH PROFILE. RED LINES ARE LREE (LIGHT) AND BLUE LINES ARE HREE (HEAVY) 12
FIGURE 13 PROFILE ZONE 13-14 LINE 4400S, NORTH, MMI™ COPPER AND GOLD 13
FIGURE 14 PROFILE ZONE 13-14 LINE 4400S, NORTH COPPER AQUA REGIA AND MMI 13
FIGURE 15 PROFILE ZONE 13-14 LINE 4400S, NORTH, MMI™ RARE EARTH ELEMENT (REE) ,RED LINES ARE LREE (LIGHT) AND BLUE LINES ARE HREE (HEAVY) 13
FIGURE 16 PROFILE ZONE 13-14 LINE 4400S, SOUTH, MMI™ COPPER AND GOLD 14
FIGURE 17 PROFILE ZONE 13-14 LINE 4400S, SOUTH COPPER AQUA REGIA AND MMI 15
FIGURE 18 PROFILE ZONE 13-14 LINE 4400S, SOUTH, MMI™ RARE EARTH ELEMENT (REE), RED LINES ARE LREE (LIGHT) AND BLUE LINES ARE HREE (HEAVY) 15

FIGURE 19 PROFILE ZONE 13-14 LINE 4400S, SOUTH, MMI™ RARE EARTH ELEMENT (REE). PLOT INCLUDES JUST THE MATCHING PAIRS OF AR-MMI ELEMENTS. NOTE THE RELATIONSHIP WITH MINERALIZATION IN THE MMI DATA THAT IS ABSENT IN THE AQUA REGIA DATA. 16

List of Appendices

Appendix I Descriptive Statistics
Appendix II Correlation Coefficients
Appendix III Factor Analyses
Appendix IV MMI™ Copper-Gold Pro MMI™ files
Appendix V MMI™-Aqua Regia Profile Plots
Appendix VI MMI™-Aqua Regia Scatter Plots

1 Introduction

As part of information exchange with Western Copper Corporation, BCGold Corp. was provided with access to the Carmacks property to perform a geochemical orientation survey over the deposits. As part of this program 133 MMI™ samples were collected from the prescribed depth of 10 to 25 cm below the top of mineral soil. To compare the MMI™ results with the bulk composition of the soil, the samples were also analysed by ICP-MS following an aqua regia digestion. The sampling program was designed by and supervised by Shawn Ryan.

2 MMI™ Background/Principals

'Mobile Metal Ion' or MMI™ is an analytical method based on a very weak leach that only dissolves ions weakly of loosely attached to surface soil particles. It is similar to a number of weak or partial extractions that have been developed to detect deposits buried beneath exotic cover. The developers of MMI™ indicate that the presence of ligands in the leach solution allows the MMI™ method to keep the metal ions in solution long enough to be analysed. The exact chemistry of the leach solution is proprietary and used exclusively by SGS. As proposed by Allan Mann, the developer of MMI™ and confirmed by the CAMIRO "Deep Penetrating Geochemistry Project" (Coker, 2005), the depth of sampling is critical, regardless of soil horizons. The zone of metal accumulation is ~ 10 to 25 cm beneath any surface organic layers.

3 Sampling Methodology

Sampling was completed along four profiles; two across Zone 1 and two across Zones 13 and 14 (Fig. 1). Samples were collected where the surface environment was least disturbed, so sampling was generally done adjacent to the main grid lines. Samples were taken at depths ranging from 20 cm to 50 cm with a median depth of 30 cm, regardless of soil horizon or surficial material. This may be a bit deeper than optimal, but no depth profiles were sampled to determine the best sampling depth.

Sixteen additional samples were collected immediately over the projected mineralized zones, beneath the ash layers where present and within the b-horizon where absent.

3.1 Surficial Deposits

There was no detailed study of the surficial deposits as part of this survey. Data collected included slope, depth of sample (to nearest 10 cm), quality, soil horizon, vegetation and ground cover. The presence or absence of a volcanic ash layer was

indicated in notes attached to the sample record, and was converted to a “true/false’ field.

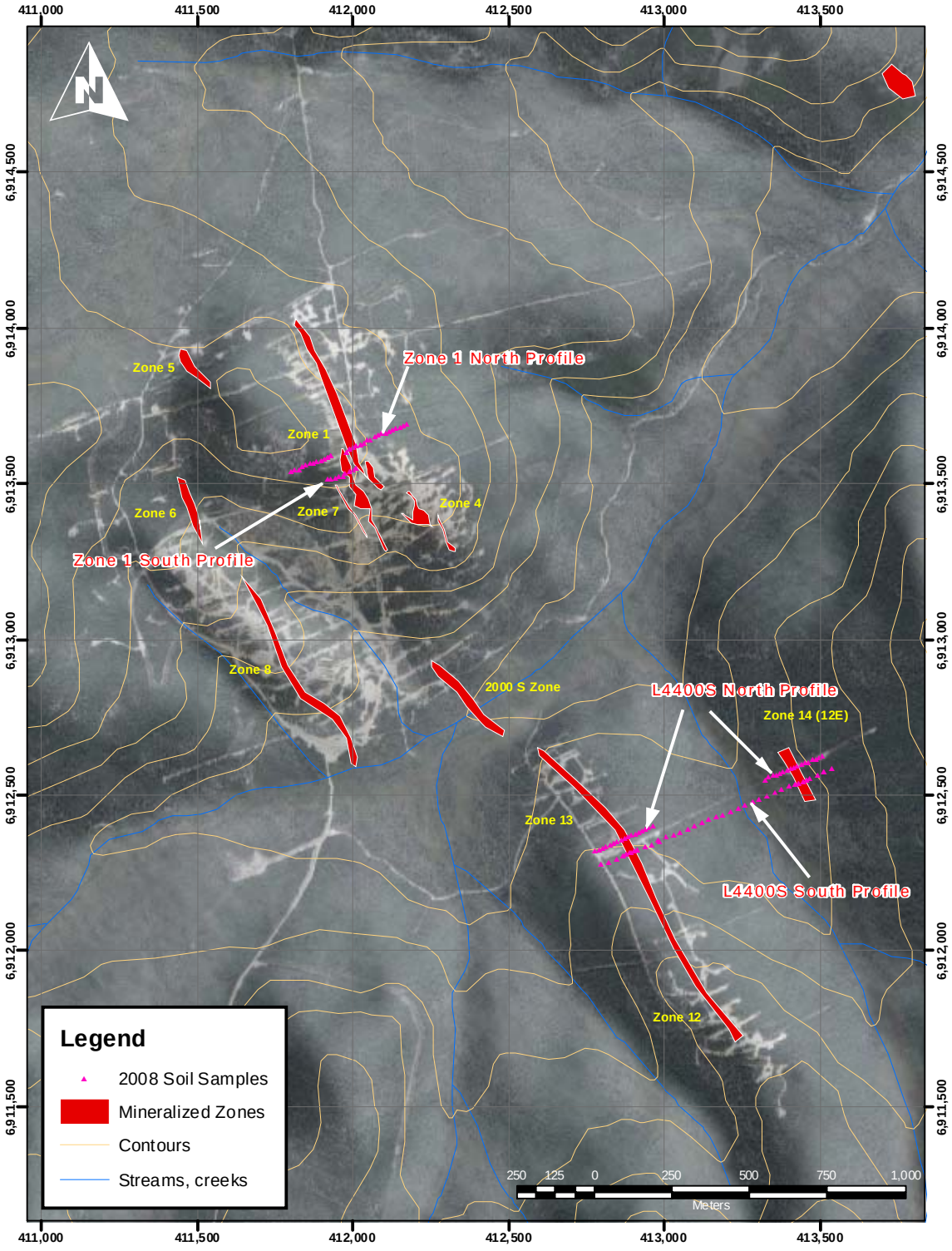

Figure 1 Location Map

The Carmacks deposits haves been covered to varying degrees by the White River Ash deposited by the eruption of Mount Churchill in Alaska, ~1200 years ago. The ash is a white to beige-coloured rhyodacitic tephra that ranges in thickness from 5 cm to 20 cm in the vicinity of the Carmacks deposits (Arseneau and Casselman, 2008).

Allan Mann, the developer of MMI™, has indicated that 1200 years is approximately the amount of time required to create an MMI™ anomaly (pers. comm.). The plots of MMI™ results include an indication of which samples were collected from ash and which were conventional soil to determine if this pattern affects the MMI™ results.

Glacial deposits occur irregularly within the area and consist of ~1 m thick till. There are thicker till and colluvium deposits in the valleys. In the unglaciated areas the ash is underlain by 10 cm of organics or peat and 10-50 cm of soil (Arseneau and Casselman, 2008).

3.2 Mineralization

Primary copper mineralization consists of chalcopyrite and bornite. At the No.1 Zone, there is a 230 m deep zone of oxidation extending below the surface. In this oxidized zone pyrite is virtually absent and pyrrhotite is completely absent and the majority of the copper consists of malachite, cuprite, azurite and tenorite (Oliver *et al*, 2007). The Zone 13 and 14 (12E) deposits are predominantly primary sulphide.

4 Analyses

Samples were shipped to SGS in Toronto, where the samples were split producing two separate samples; one for MMI™ analyses and the other for ICP-OES/MS analyses following an aqua regia digestion. The specific leach used in this test survey was "MMI-M", which is a multi-element package including Cu, Cd, Pb, Zn, Au, Ag, Pd, Co, Ni, U, Rb, Y, Ba, LA, Ta, Ce, Pr, Nb, Sm Tb, Er, Yb, Ti, Zr, Ca, Mg, Al, Sc, Th, Li, Fe, As, Sb, Bi, Ti, W, Sn, Mo, Te, Cr, Nd and Sr. The ICP-OES/MS analyses following aqua regia (HNO_3 + HCl) digestion included B, Ba, Ca, Cr, Cu, Fe, K, Li, Mg, Mn, Na, Ni, P, S, Sr, Ti, V, Zn, Ag, Zr, As, Be, Bi, Cd, Ce, Co, Cs, Ga, Ge, Hf, Hg, In, La, Lu, Mo, Nb, Pb, Rb, Sb, Sc, Se, Sn, Ta, Tb, Te, Th, Tl, U, W, Y and Yb.

The sixteen samples of conventional b-horizon/beneath ash material were analysed by ICP-MS following aqua regia digestion at Acme Labs in Vancouver.

5 Results

As there is a large number of elements analysed, a variety of methods were employed to examine inter-element relations including correlation coefficients, cluster analyses and factor analyses. Because of the large number of variables not all are presented in profile plots. Copper and gold for all four profiles as well as pairs of MMI™ and aqua regia copper analyses are presented in the following text. Profile plots of the all elements that were analysed by both methods can be found in Appendix V.

5.1 Statistics

Statistical analyses include descriptive statistics, correlation coefficients, cluster analyses and factor analyses. The general distribution of the data is presented in tables in Appendix I as well as graphically as a series of box and whisker plots. (Figs. 2 and 3 for MMI™ and aqua regia analyses respectively). The box and whisker plot indicates the median as the horizontal line within the box, the first and third quartile are represented by the extent of the box and the extreme range is indicated by the whiskers. Individual outliers are indicated as symbols.

Scatter plots for all of the MMI™-aqua regia pairs are in Appendix VI.

5.1.1 Multivariate Analyses

5.1.1.1 Data Treatment

Prior to analyses, data was log transformed if the transformed variable had less skewness than the untransformed variable. A filter was applied excluding all variables where the mean was less than three times the detection limit for that variable. Analyses less than the detection limit were replaced with values of half the detection limit.

5.1.1.2 Correlation

Both Pearson and Spearman (Rank) correlation coefficients are presented in tables in Appendix II for MMI™ and aqua regia. The tables are colour coded with strong positive correlations in red and strong negative correlations in blue, with varying shades in between. In the MMI™ data, copper correlates moderately with cobalt (0.506). Gold was not included due to the large number of values near or below the detection limit. Strongest correlations are among the rare earth elements.

The aqua regia correlations are unusual in that there are a large number of elements that correlate positively with each other. The main exceptions to this is silver that

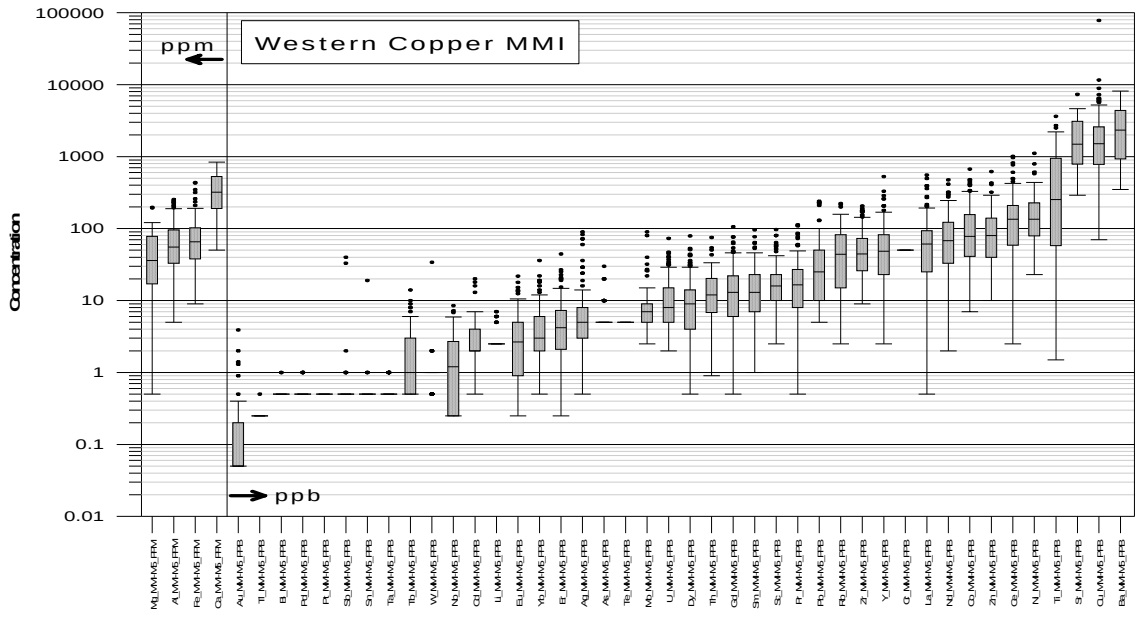

Figure 2 Box and whisker plot - MMI™ leach analyses

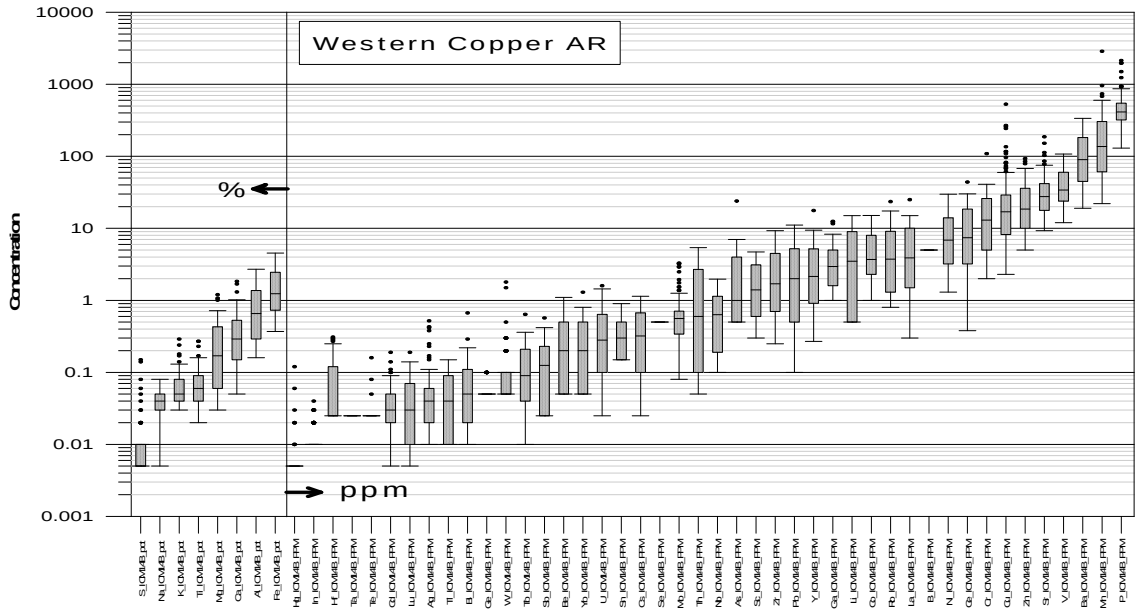

Figure 3 Box and whisker plot, aqua regia digestion analyses

correlates weakly with most elements with the exception of copper, molybdenum and bismuth, and sodium which have a negative correlation with all elements.

5.1.1.3 Cluster Analyses

To provide additional insight into the inter-element associations, dendograms were produced using agglomerative hierarchical clustering (AHC). Agglomerative hierarchical clustering is a bottom-up clustering method where clusters have sub-clusters, which in turn have sub-clusters, etc. Successive clustering operations produce a binary clustering tree (dendrogram), whose root is the class that contains all the observations. This dendrogram represents a hierarchy of partitions.

The MMI™ dendrogram based on the Pearson correlation indicates that Cu is weakly correlated with Cd, Co and Fe Fig. 4). The strongest correlations indicated by the shortest linkages are between the REEs + Sc, Th, Y.

The dendrogram produced for the aqua regia (Fig. 5), groups Cu and Mo, with a weaker linkage to a largest group including REE's. Other groups, containing Zr, K, Ti, V, Zn, Co, Fe, and P, Sr, Ca form separate clusters. It is speculated that some of this clustering is due to the presence or absence of ash.

5.1.1.4 Factor Analyses

Due to the large number of variables, a factor analyses was run on the data to reduce the number of variables and to investigate commonalities between the variables. Factor analysis is a statistical technique applied to a single set of variables to discover which sets of variables in the set form coherent subsets that are relatively independent of one another. Variables that are correlated with one another which are also largely independent of other subsets of variables are combined into factors. Factors which are generated are thought to be representative of the underlying processes that have created the correlations among variables. Although factor analysis is commonly applied to geochemical data, particularly as a method of reducing the large number of variables produced by modern multi-element analysis, it should be used with caution. An excellent review of the use of factor analysis in geochemical data is presented by Reimann et al (2002), from which the following is quoted:

> *"Complex polypopulational regional geochemical (or environmental) data are not really suited for factor analysis. In nature the chemical elements show neither a normal nor a log-normal distribution. Different geochemical processes can govern the regional distribution of one and the same factor. It is not sufficient to use just one method of factor analysis with one set of elements to explain the inherent information of a whole data set. Different choices of parameters result in a multitude of results — some may be useful, others cannot be interpreted. The fact that single elements do not enter any of the factors does not mean that the regional distribution of these elements is uninteresting — for an interpretation these may be the most interesting elements of all."*

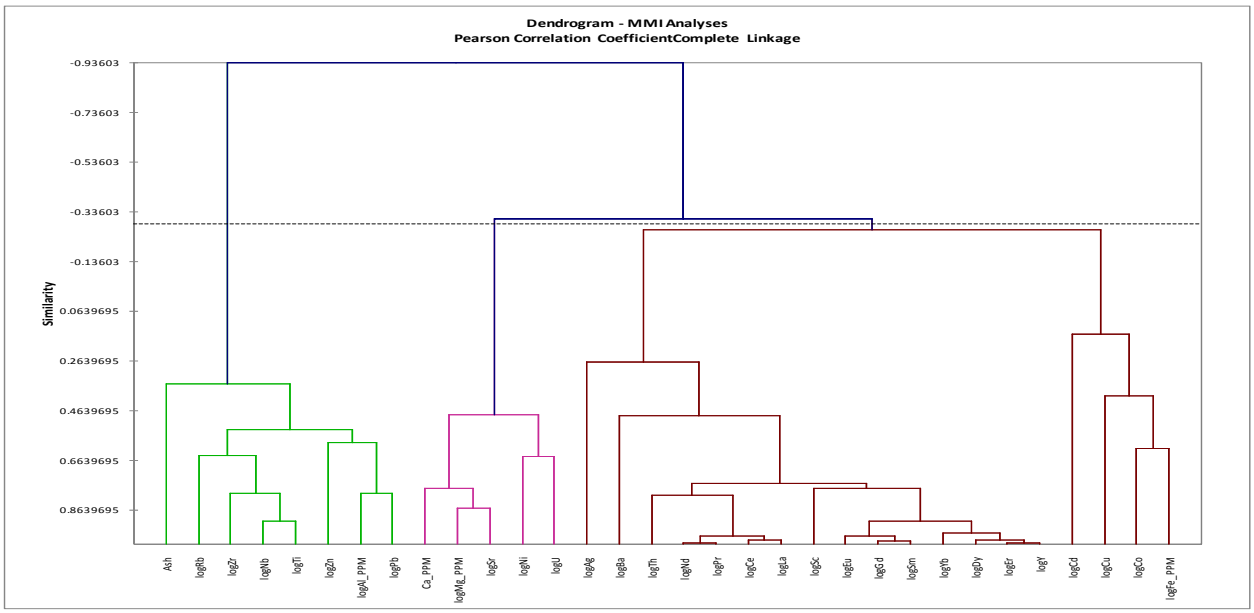

Figure 4 Dendogram - MMI™ cluster analyses based on Pearson correlation and complete linkage

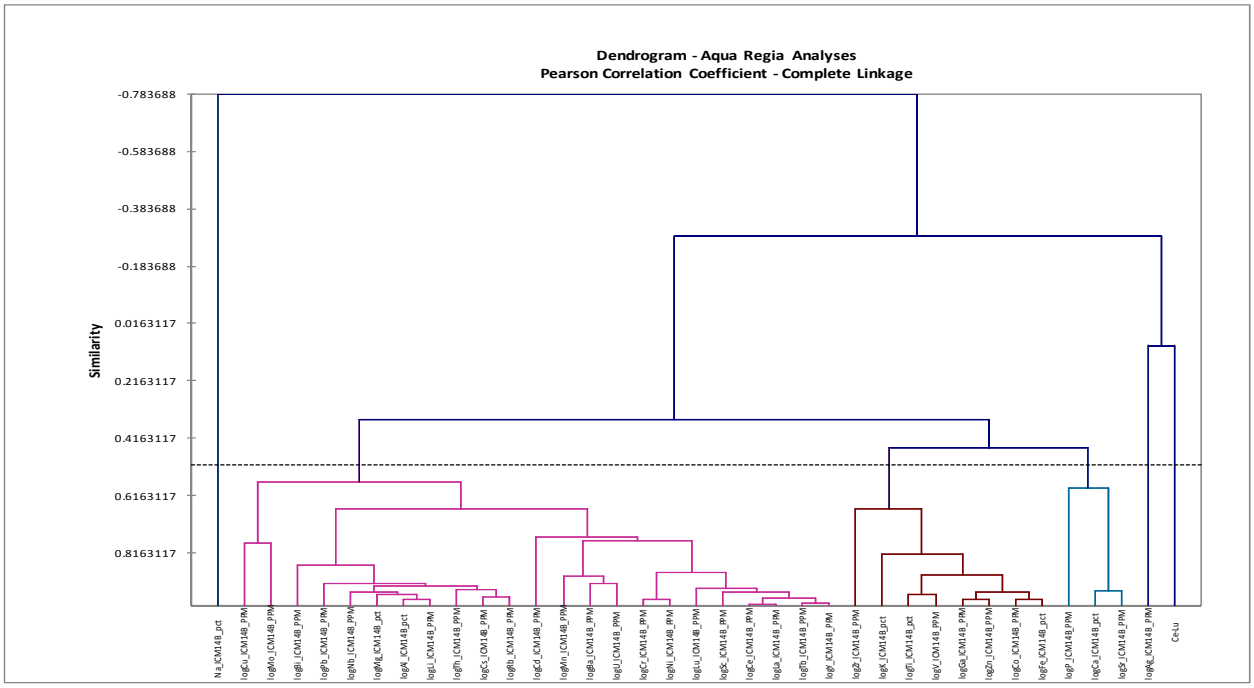

Figure 5 Aqua regia cluster analyses based on Pearson correlation and complete linkage

Results of the factor analyses are shown in Appendix III, for MMI™ data followed by aqua regia results. For the MMI™ data four factors were extracted. The 'factor patterns' or loadings are the correlation coefficients between the factors and the variables. Factor 1 is dominated by REE's, Th, Ba, with moderate to low loadings for

Cu and Ag. Factor 2 has high loadings for Ti, Nb, Rb, Al, Zn, Pb and Ash. Factor 3 has high loadings for Fe, Co, Ni and Cu. Factor 4 has highest loadings for Ba, Sr and Pb.

The factor analyses was not particularly successful in outlining mineralization, with the best indication being a single peak on the north profile over Zone 1 from a sample taken where ash was absent. The pattern indicated by the factor analyses is likely most strongly influenced by the presence or absence of ash.

5.2 Profiles

The primary commodities of interest, copper and gold, are presented in a series of profile plots (Profile 1-4) with the UTM easting as the x-axis. Known mineralized zones are indicated as red bars along the lower x-axis. Additional profiles are presented to demonstrate specific features. Complete sets of profiles can be found in the appendices at the end of the report.

5.2.1 Zone-1

5.2.1.1 North Profile

Zone 1, which is underlain by more deeply oxidized mineralization, has a strong response from both Cu and Au (Fig. 6). The gold response is a single anomalous sample, with a lower peak at the eastern end of the mineralization. Copper shows more of a 'rabbit ear' response, although this could be a result of the multiple zones rather than the presence of a 'redox cell'. There is an isolated copper and gold response ~110 m east of the mineralized zones. It is not known if there is mineralization associated with this anomaly; it may be an extension of the 'Zone 4' structure. The yellow symbols indicate the presence of ash and the brown symbol is the absence of ash. Note the two samples with the same easting at 412 010mE, where two samples have been collected; one in ash at 20 cm depth and the other beneath the ash at 50 cm depth. Results for copper are significantly higher in the sample beneath the ash than the sample in ash.

In comparing the MMI™ leach results to the aqua regia digestion results (Fig. 7), the patterns are similar, with a similar contrast of anomaly to background. The aqua regia analyses provides a generally lower response in ash, and probably would not have provided a significant anomaly if it were not for the single anomalous sample taken below the ash. The MMI™ on the other hand has significant anomalous values both in ash and non-ash soil.

The red symbols indicate the copper response from deep samples, generally 60 to 70 cm deep. The peak value over mineralization is 6837.6 ppm copper, with the sample immediately to the west returning 2530.5 ppm copper. This sampling

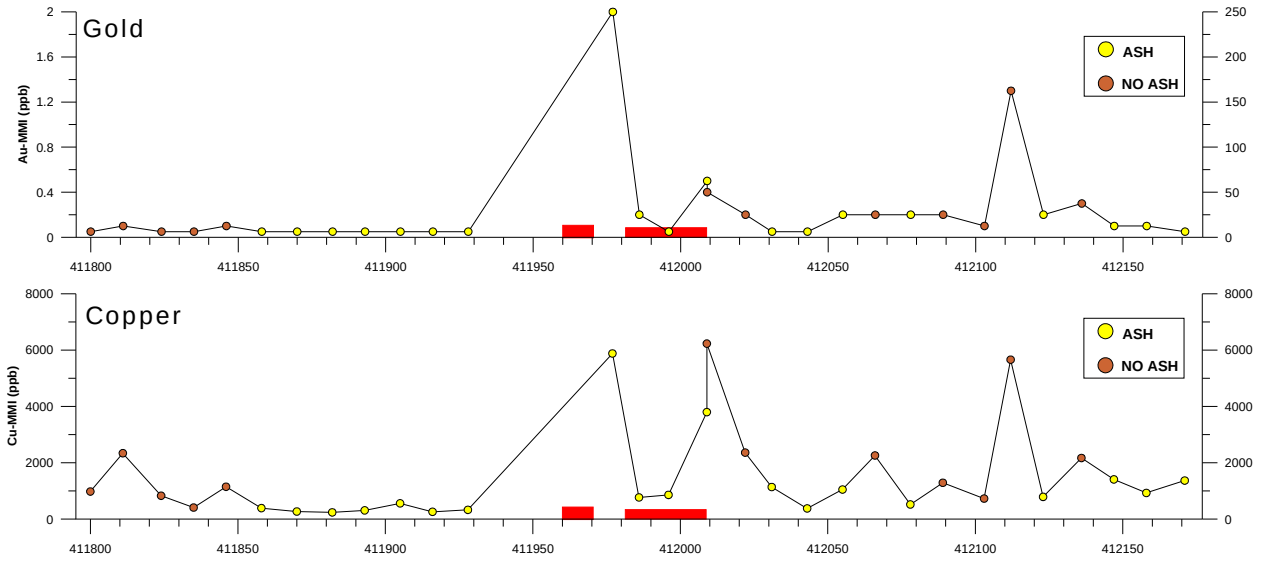

Figure 6 Profile Zone 1 North, MMI™ copper and gold

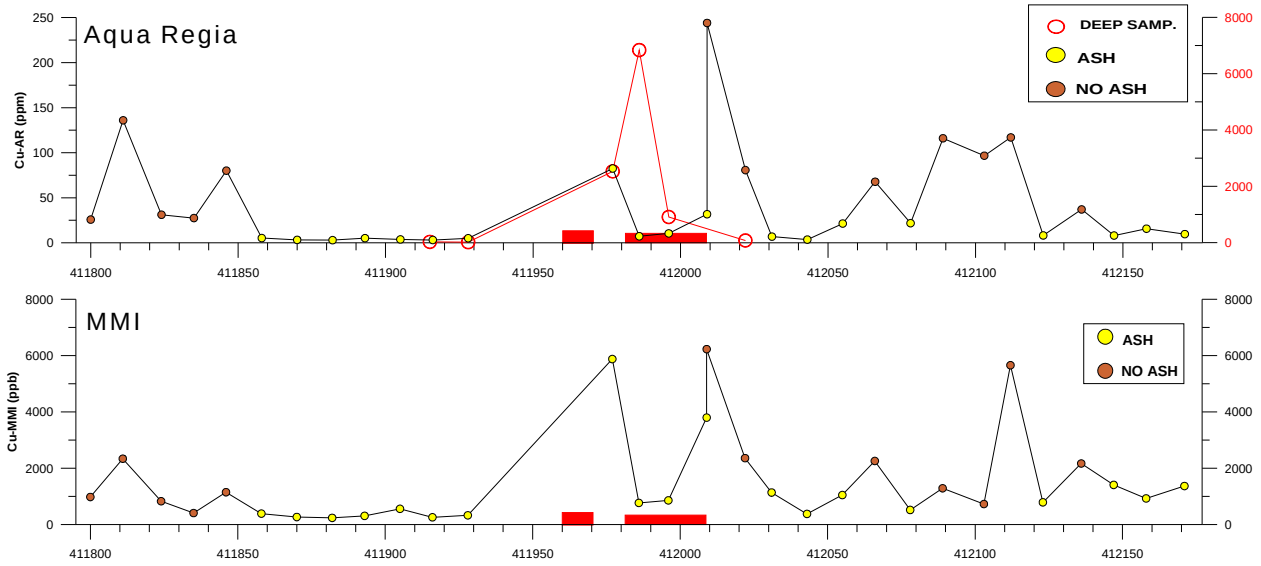

Figure 7 Zone 1 North profile, copper aqua regia and MMI. The red aqua regia profile corresponds with the red scale on the right and are samples taken beneath the ash layer.

demonstrates dramatically the masking effect of the White River Ash when using strong acid digestions.

Although both MMI™ and AR (aqua regia) results were anomalous, it appears that MMI™ is more successful at detecting copper anomalies through the young ash layer. Clearly the best results would be sampling deep material beneath the ash within the residual soil.

The aluminum aqua regia profile (Fig. 8) displays a pattern that is repeated with many elements including As, Ba, Co, Cr, Fe, Li, Mg, Nb, Ni, Pb, Sc, Th, U, Zn and in a

more subdued form by Ca, Rb, Sr, Ti, and Zr and REEs. The high values within this group are for the most part from samples taken from non-ash soil. It is likely that this pattern reflects the bulk chemistry of the normal soil compared to the volcanic ash.

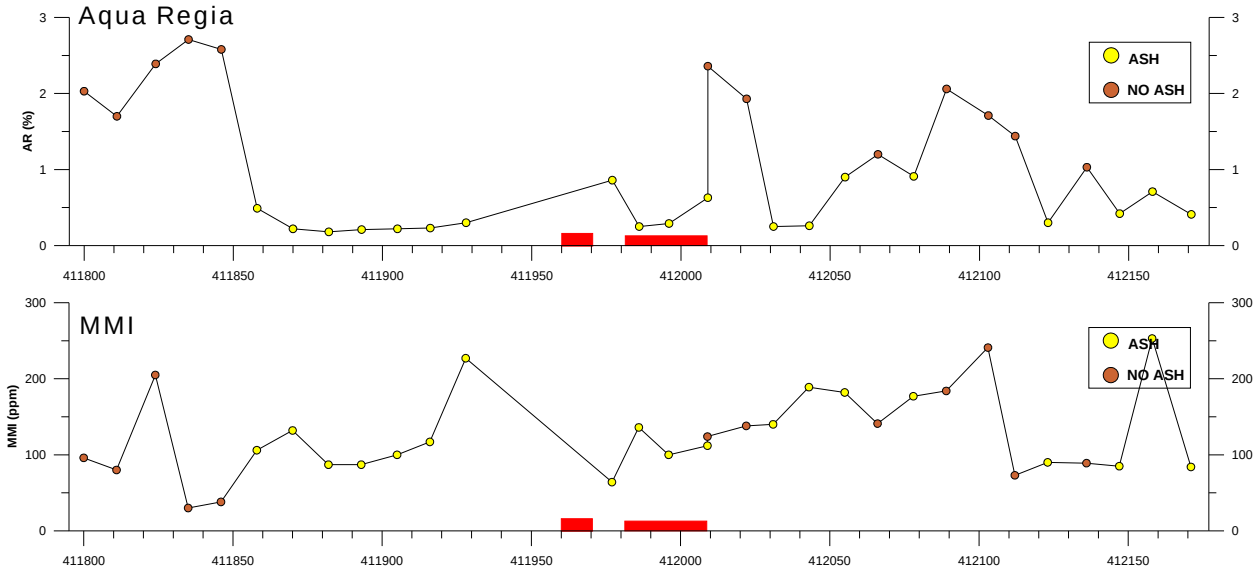

Figure 8 Aqua regia and MMI™ aluminum profiles along the Zone 1 North Profile.

Most of the MMI™ profiles have patterns quite independent of the aqua regia pattern, indicating some independence of the MMI™ results from the bulk composition of the soils (Appendix V). Barium is an exception, with a pattern mimicking the MMI™ pattern. Cobalt and silver have patterns similar to copper, and iron has a single sample peak adjacent to the mineralized zone on the east.

Rare earth elements (Fig. 9) do not show distinctive patterns relative to mineralization on this profile.

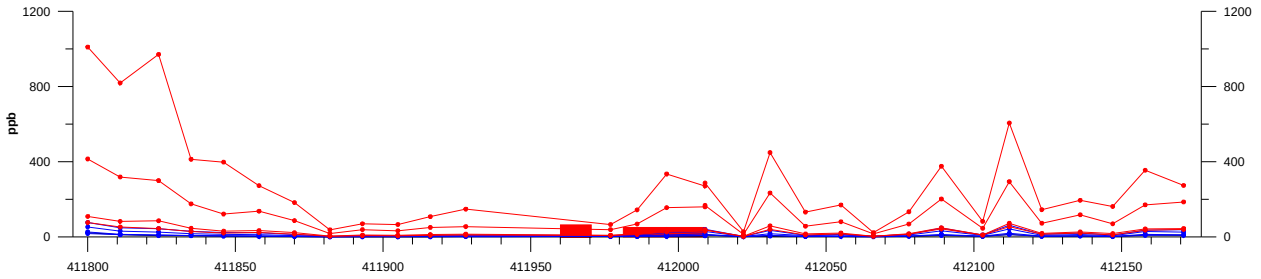

Figure 9 MMI™ Rare earth element (REE) Zone 1, North profile. Red lines are LREE (light) and blue lines are HREE (heavy)

5.2.1.2 South Profile

The south profile at Zone 1 is relatively short, with all of the samples consisting of ash (Fig. 10). The copper and gold MMI™ profiles both have a single sample anomaly ~15 m east of the surface projection of the mineralized zone. The gold value is 4 ppb and copper is ~8000 ppb, so it can be considered a very strong anomaly, particularly compared with the other profiles.

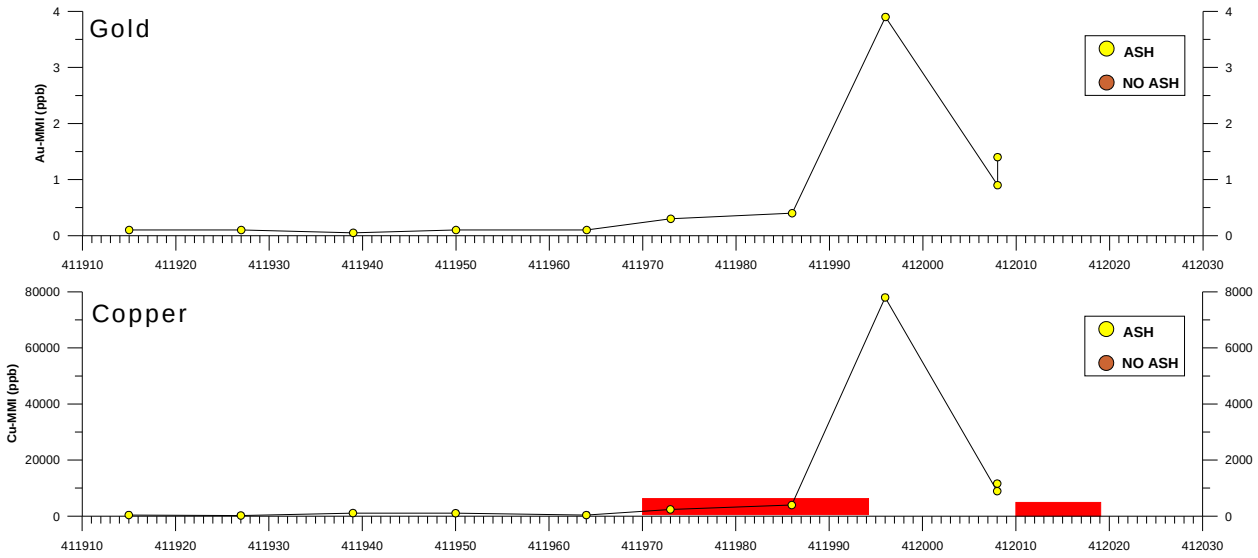

Figure 10 Zone 1, South profile, MMI™ copper and gold

The aqua regia copper anomaly (Fig. 11) peak is a bit displaced from the MMI™ peak, but has a strong contrast over the relatively low background. The easternmost sample is a duplicate which indicates a considerable variability in the bulk copper values which could indicate some contamination or mixing during sampling.

The MMI™ REE results indicate an increasing gradient towards the east with peak values coinciding with the copper peak (Fig. 12).

5.2.2 Zones 13 and 14 (12E)

5.2.2.1 North Profile

Sampling on a profile north of Line 4400S consisted of two shorter segments, each ~150 m long. They provide information on the immediate vicinity of the deposits, with a limited extension into background.

The copper MMI™ response to Zone 13 (west) is a noisy multiple peak anomaly with highest values approaching 7000 ppm (Fig. 13). There is a relative low immediately over the deposit, flanked by higher values that could indicate a 'rabbit ear' type

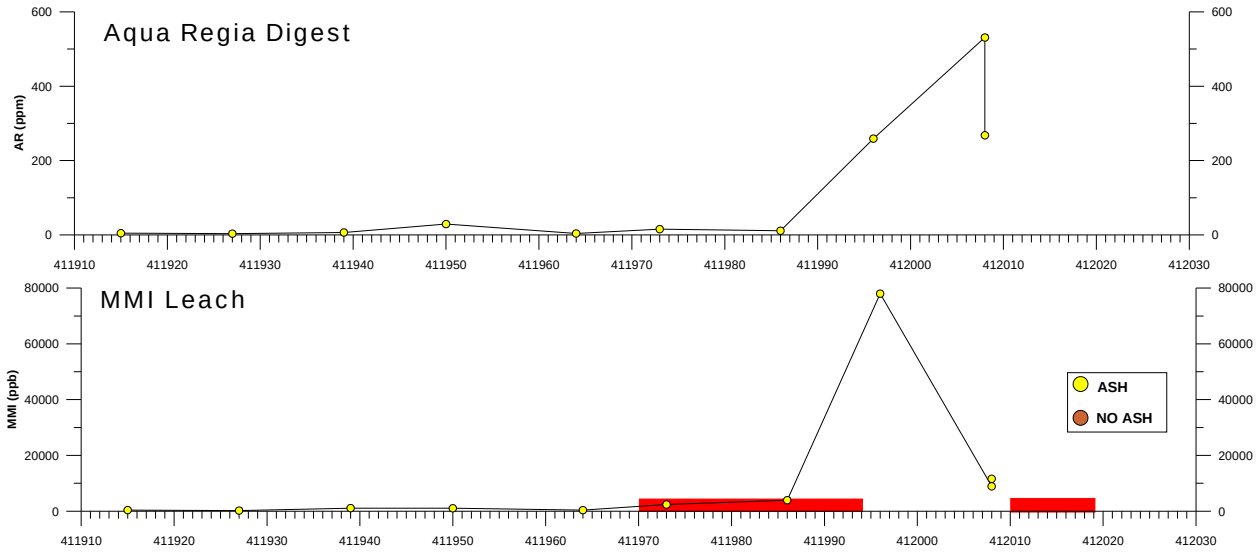

Figure 11 Zone 1 South profile, copper aqua regia and MMI

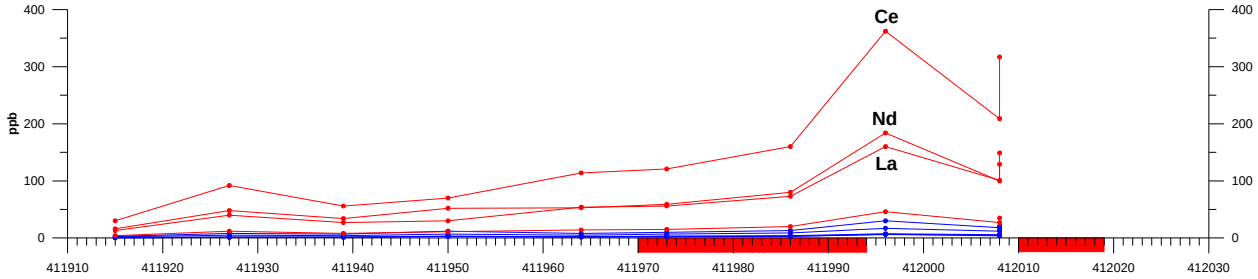

Figure 12 Profile Zone 1 South, MMI™ Rare earth element (REE) Zone 1, North profile. Red lines are LREE (light) and blue lines are HREE (heavy)

response. The response to the eastern Zone 14 is clearly anomalous with values ~6000 ppm, but is relatively noisy with three distinctive peaks.

There is a clear MMI™ gold anomaly over Zone 13 (east) consisting of two samples of 0.2 and 0.3 ppm above a background that is less than the detection limit of 0.1 ppb. This is a relatively low value compared to values encountered over Zone 1 of up to 2 ppb. All but one of the samples is within ash with the highest gold analyses coming from a sample without ash. The profile over Zone 14 is primarily in material without ash and gives noisy results with no defined anomaly.

The aqua regia response for copper actually provides better anomaly contrast than MMI™ (Fig. 14). The aqua regia copper response over Zone 13 is relatively low compared to the Zone 1 profiles and even the profile just south of L4400S.

The REE's in MMI™ profile over Zone 13 (Fig. 15) emphasize the 'rabbit ear' pattern seen with the MMI™ copper results, with a fairly broad low zone above mineralization. The REE's in MMI™ over the eastern segment provides a very strong single sample anomaly immediately east of the surface projection of the Zone 13.

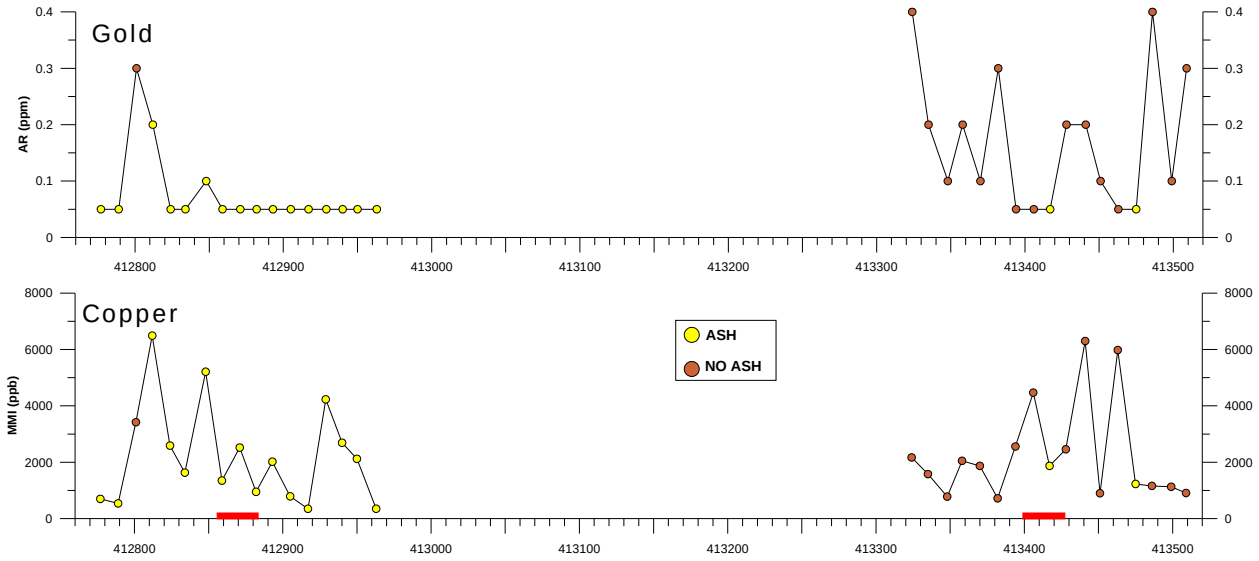

Figure 13 Profile Zone 13-14 Line 4400S, North, MMI™ copper and gold

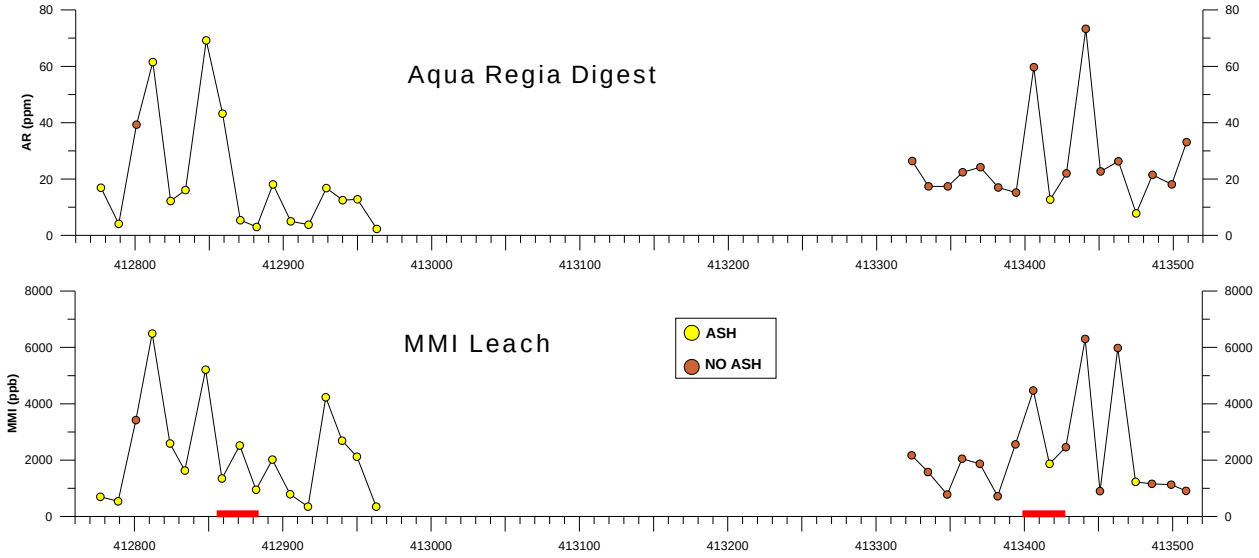

Figure 14 Profile Zone 13-14 Line 4400S, North copper aqua regia and MMI

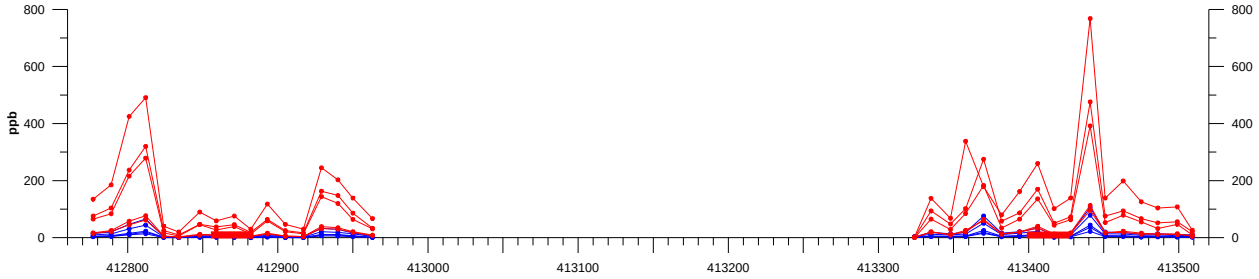

Figure 15 Profile Zone 13-14 Line 4400S, North, MMI™ Rare earth element (REE) ,red lines are LREE (light) and blue lines are HREE (heavy)

5.2.2.2 South Profile

A long continuous profile was sampled just south of line 4400S across Zones 13 and 14 (Figs. 1 and 16). In contrast to Zone 1, mineralization at Zone 13 and 14 is primarily sulphide. Zone 14 is covered by a younger flood basalt layer and does not extend to surface.

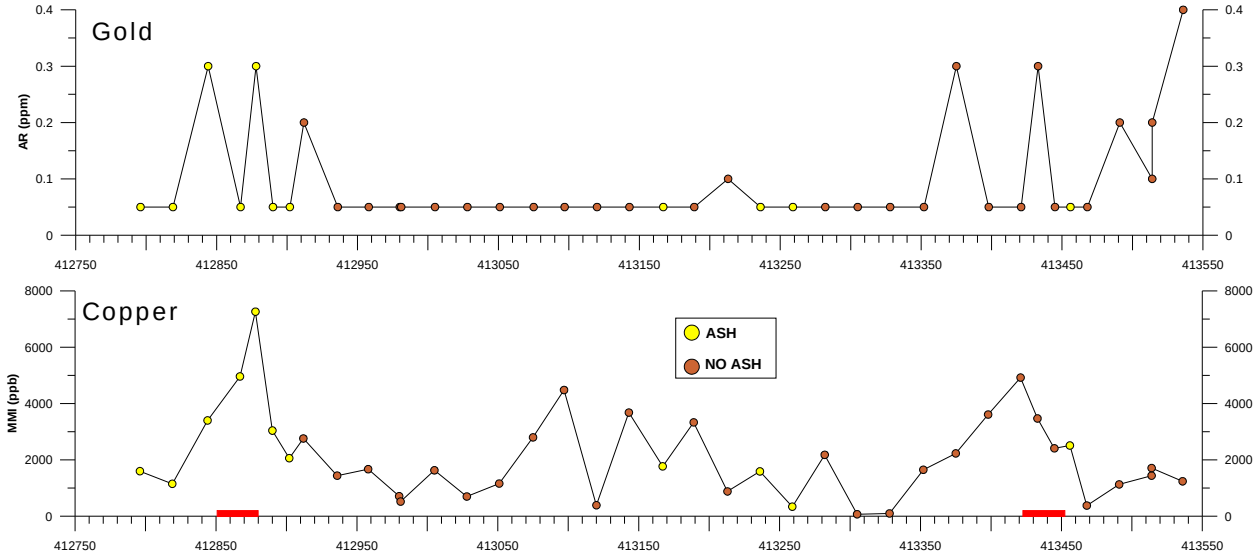

Figure 16 Profile Zone 13-14 Line 4400S, South, MMI™ copper and gold

The copper results over Zone 13 indicate a strong 'apical' peak over the known mineralization. These samples were from ash indicating again the ability of MMI™ to detect mineralization through the relatively young cover. The eastern Zone 14, where ash was for the most part absent, also showed a broader peak, with a lower absolute value at ~5000 ppm compared to ~8000 at zone 12. The profile is generally noisy with numerous anomalous samples between the zones, with the anomaly contrast being somewhat less than at Zone 1.

The gold profile does indicate some peaks associated with mineralized zones, but the samples are all close to the detection limit.

Comparing the aqua regia digest copper results with MMI™ (Fig. 17), the aqua regia profile provides a stronger anomaly contrast than MMI. This may indicate that there is probably some mixing of soil and ash. The aqua regia profile has no significant response to the eastern Zone 14, so this may be a success for MMI™ in detecting mineralization under cover.

Of particular note are the anomalies associated with both zones in the rare earth elements (Fig. 18). The light rare earths are in red and the heavy rare earths are in blue. Although the scale suppresses the results of the HREE's, all of the REE's have similar anomaly contrast. A comparison of the limited set of REE's with the

comparable elements from the MMI™ data (Fig. 19) does not provide coherent anomalies that can be correlated with the mineralized zones.

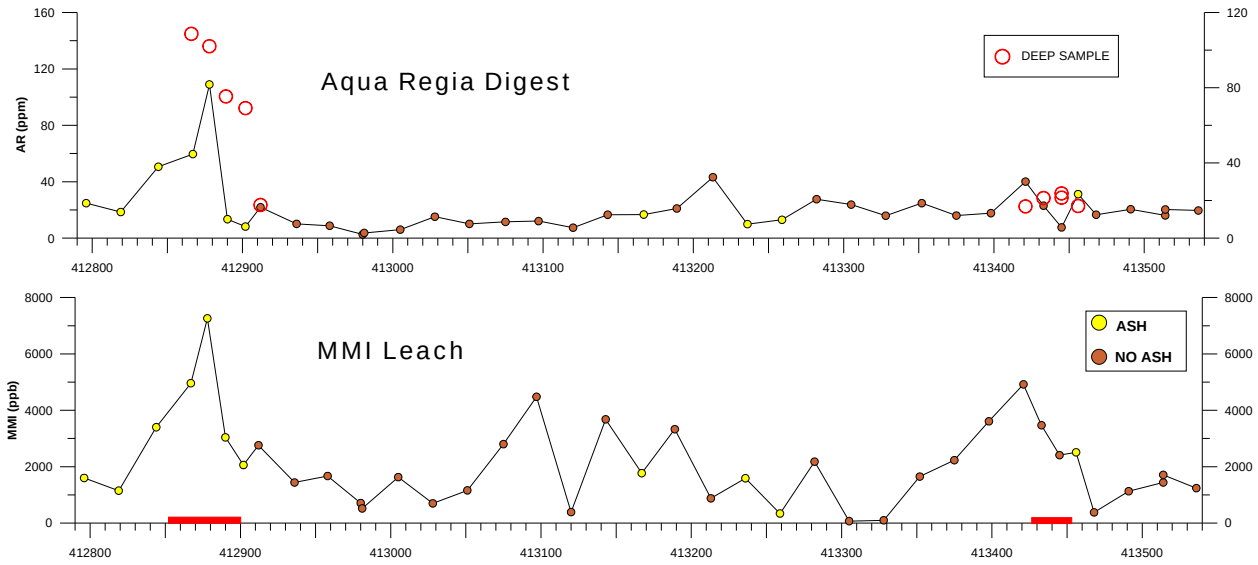

Figure 17 Profile Zone 13-14 Line 4400S, South copper aqua regia and MMI

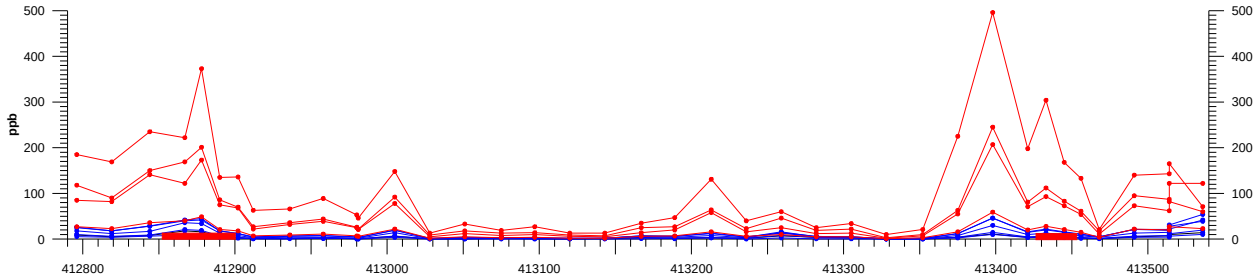

Figure 18 Profile Zone 13-14 Line 4400S, South, MMI™ rare earth element (REE), red lines are LREE (light) and blue lines are HREE (heavy)

Mo, Ag, Cd have aqua regia anomalies associated with Zone 14 but generally do not provide distinctive contrast from other 'false' anomalies of similar amplitude. REE's generally provide the best anomaly contrast and anomaly definition on this profile.

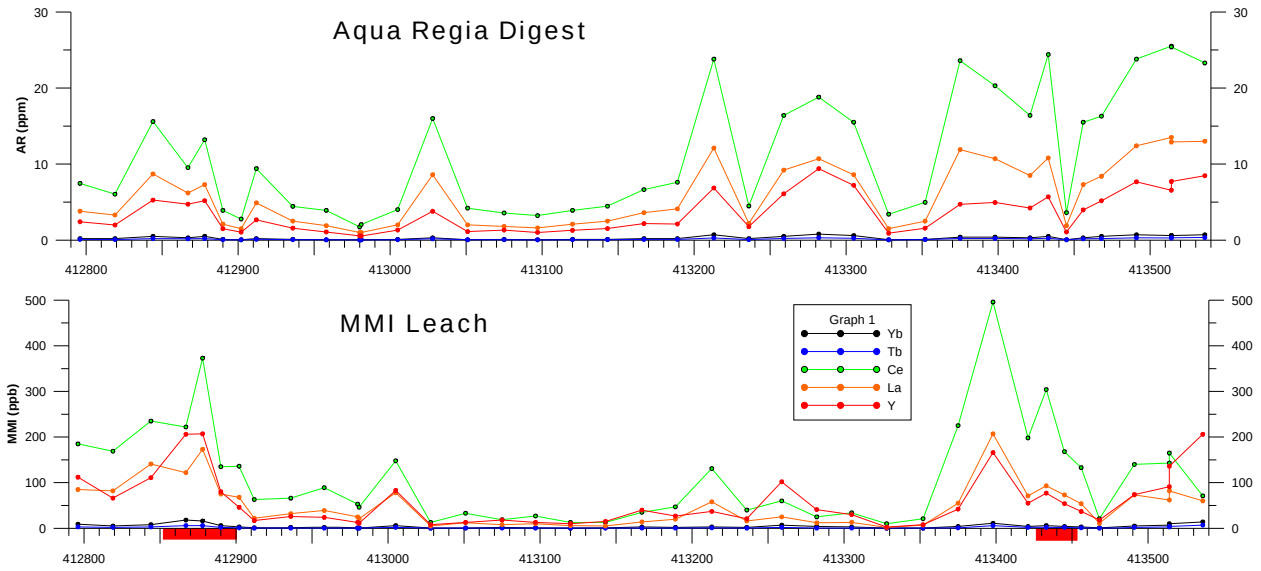

Figure 19 Profile Zone 13-14 Line 4400S, South, MMI™ Rare earth element (REE). Plot includes just the matching pairs of AR-MMI elements. Note the relationship with mineralization in the MMI data that is absent in the aqua regia data.

6 Conclusions

Two conclusions can be drawn from the sampling over the Carmacks deposits. One is that the surficial geochemistry is strongly influenced by the presence or absence of relatively thin deposits of rhyodacitic volcanic ash (White River Ash). The other conclusion is that MMI™ sampling and analysis has been able to provide indications of copper mineralization where conventional soil sampling of 'B' horizon is not possible. The strongest response to the soil sampling was from the few deep samples taken beneath ash, within residual soil directly overlying the deposit.

The presence of a copper MMI™ anomaly above the 14 zone is particularly significant as this zone is blind at a depth of 100 m below surface, with ~50 m of Carmacks Group plateau basalt cover. There is a relatively weak copper response from the aqua regia analyses on the profile north of line 4400S and no indications of mineralization in the aqua regia data on the south profile. The rare earths have provided the best anomaly contrast over the southern profile.

The test work has indicated that in the Carmacks area the MMI™ analyses of soils can detect copper and gold in all situations where conventional soils indicate an anomaly. In addition, the method indicated significant anomalies where the aqua regia conventional analyses were unsuccessful.

As partial extraction, weak leach geochemistry can be difficult to interpret. It is always useful to have conventional soil analyses as a reference, although this would result in an increased analytical cost. If only one method is used, the MMI™ would be the most effective method, particularly where there is ash or other exotic cover.

7 References

Arsenau, G., and Casselmann, S., 2008, Resource Estimate of the No. 1, No. 4, and No. 7 Zones, Carmacks Deposit, Yukon Territory, Ni 43-101 Technical Report

Coker, W., 2005, Three Dimensional Surface Geochemistry, CAMIRO Project 02E01 and OMET Project P01-02-002, Overall project review and executive summary, unpublished CAMIRO project report.

Oliver, T., Hanks, J., Arseneau, G., Hester, M., Cornett, D., Hull, J., (2007) Carmacks Copper Project, Coppermine and Process Plant, Ni 43-101 Technical Report, Feasibility Study Volume I

Reimann, C., Filzmoser, P and Garrett, R, 1002, Factor analysis applied to regional geochemical data: problems and possibilities, Applied Geochemistry, v 17, Pages 185-206

Certificate of Qualified Person

I, Gary Norman Lustig hereby certify that:

1. I reside at 1637 Springhaven Place, Kamloops, BC, Canada V2E 1C7;

2. I am a geologist employed by G. N. Lustig Consulting Ltd. with offices at 1637 Springhaven Place, Kamloops, BC, Canada V2E 1C7;

3. I have a Bachelor of Science (Advanced) Degree in Geology from the University of Saskatchewan, Saskatoon, Saskatchewan, Canada and a Master of Science Degree from the University of Manitoba, Winnipeg, Manitoba, Canada;

4. I have practiced my profession continuously since 1973, with the exception of 2 years in which I was in full-time graduate studies. I have worked on a variety of mining and exploration projects in Canada, United States, Mexico, Spain, Australia, Papua New Guinea, Indonesia, South Africa and Chile.

5. I am registered with the following statutory professional organizations:
   - Professional Geoscientist with The Association of Professional Engineers and Geoscientists of the Province of British Columbia as Member - Reg. No. 20462
   - Professional Geologist with the Association of Professional Engineers, Geologists and Geoscientists of the Northwest Territories as Licensee - Reg. No. L908
   - Professional Engineer with The Association of Professional Engineers and Geoscientists of Saskatchewan as Member - Cert. No. 4392

6. I am a member of the following professional societies:
   - Geological Association of Canada
   - Canadian Institute of Mining and Metallurgy
   - Society of Economic Geologists
   - Association of Applied Geochemists

7. I have read the definition of “qualified person” set out in National Instrument 43-101 (“NI 43-101”) and certify that by reason of my education, affiliation with a professional association (as defined in NI 43-101) and past relevant work experience, I fulfill the requirements to be a “qualified person” for the purposes of NI 43-101. This report is not a Technical Report as defined in NI 43-101 and does not follow the guidelines for a complete property technical report.

8. I have not visited the Carmacks Copper project.

9. I am independent of BCGold Corp. applying all of the tests of Section 1.5 of National Instrument 43-101.

Dated on February 13, 2009

_____

Gary Lustig, MSc, PGeo

Appendix I
Descriptive Statistics

Aqua Regia Analyses

Statistic	Al_ICM14B_pct	B_ICM14B_PPM	Ba_ICM14B_PPM	Ca_ICM14B_pct	Cr_ICM14B_PPM	Cu_ICM14B_PPM	Fe_ICM14B_pct	K_ICM14B_pct	Li_ICM14B_PPM	Mg_ICM14B_pct
No. of observations	114	114	114	114	114	114	114	114	114	114
No. of missing values	0	0	0	0	0	0	0	0	0	0
Minimum	0.160	5.000	19.000	0.050	2.000	2.300	0.370	0.030	0.500	0.030
Maximum	2.710	5.000	338.000	1.840	109.000	531.000	4.540	0.290	15.000	1.200
Freq. of minimum	2	114	1	2	1	1	1	21	32	8
Range	2.550	0.000	319.000	1.790	107.000	528.700	4.170	0.260	14.500	1.170
1st Quartile	0.290	5.000	45.250	0.150	5.000	8.350	0.730	0.040	0.500	0.060
Median	0.655	5.000	90.000	0.290	13.000	16.950	1.235	0.050	3.500	0.170
3rd Quartile	1.360	5.000	181.500	0.530	26.000	28.725	2.438	0.080	9.000	0.428
Mean	0.864	5.000	116.421	0.379	16.596	35.636	1.578	0.065	4.895	0.256
Variance (n-1)	0.415	0.000	6342.441	0.092	207.960	4279.108	0.941	0.002	19.476	0.058
Standard deviation (n-1)	0.644	0.000	79.639	0.304	14.421	65.415	0.970	0.043	4.413	0.242
Variation coefficient	0.742	0.000	0.681	0.798	0.865	1.828	0.612	0.648	0.898	0.941
Skewness (Pearson)	0.729		0.545	2.005	2.485	4.960	0.855	2.358	0.598	1.300
Kurtosis (Pearson)	-0.408		-0.845	6.310	12.741	30.051	-0.035	7.801	-0.950	1.909
Standard error of the mean	0.060	0.000	7.459	0.028	1.351	6.127	0.091	0.004	0.413	0.023
Lower bound on mean (95%)	0.745	5.000	101.644	0.323	13.921	23.498	1.398	0.057	4.076	0.211
Upper bound on mean (95%)	0.984	5.000	131.199	0.435	19.272	47.774	1.758	0.073	5.714	0.301

Statistic	Mn_ICM14B_PPM	Na_ICM14B_pct	Ni_ICM14B_PPM	P_ICM14B_PPM	S_ICM14B_pct	Sr_ICM14B_PPM	Ti_ICM14B_pct	V_ICM14B_PPM	Zn_ICM14B_PPM	Ag_ICM14B_PPM
No. of observations	114	114	114	114	114	114	114	114	114	114
No. of missing values	0	0	0	0	0	0	0	0	0	0
Minimum	22.000	0.005	1.300	130.000	0.005	9.300	0.020	12.000	5.000	0.010
Maximum	2880.000	0.080	29.800	2140.000	0.150	187.000	0.270	108.000	93.000	0.520
Freq. of minimum	1	1	1	1	85	1	2	1	1	5
Range	2858.000	0.075	28.500	2010.000	0.145	177.700	0.250	96.000	88.000	0.510
1st Quartile	61.500	0.030	3.200	320.000	0.005	17.825	0.040	24.000	10.000	0.020
Median	137.000	0.040	6.850	415.000	0.005	27.650	0.060	34.000	18.500	0.040
3rd Quartile	304.000	0.050	13.950	550.000	0.009	41.775	0.090	59.750	35.750	0.060
Mean	219.254	0.042	8.817	500.702	0.011	33.996	0.071	41.588	24.465	0.061
Variance (n-1)	93450.616	0.000	41.374	107461.450	0.000	695.679	0.002	430.421	315.844	0.007
Standard deviation (n-1)	305.697	0.016	6.432	327.813	0.021	26.376	0.044	20.747	17.772	0.083
Variation coefficient	1.388	0.385	0.726	0.652	1.855	0.772	0.613	0.497	0.723	1.350
Skewness (Pearson)	6.076	0.365	0.766	3.075	5.107	2.999	2.292	0.885	1.412	3.719
Kurtosis (Pearson)	48.796	-0.343	-0.228	11.113	28.036	12.261	7.218	0.326	2.288	14.586
Standard error of the mean	28.631	0.002	0.602	30.703	0.002	2.470	0.004	1.943	1.665	0.008
Lower bound on mean (95%)	162.531	0.039	7.623	439.875	0.007	29.101	0.063	37.738	21.167	0.046
Upper bound on mean (95%)	275.978	0.045	10.010	561.529	0.015	38.890	0.079	45.437	27.763	0.076

Statistic	Zr_ICM14B_PPM	As_ICM14B_PPM	Be_ICM14B_PPM	Bi_ICM14B_PPM	Cd_ICM14B_PPM	Ce_ICM14B_PPM	Co_ICM14B_PPM	Cs_ICM14B_PPM	Ga_ICM14B_PPM	Ge_ICM14B_PPM
No. of observations	114	114	114	114	114	114	114	114	114	114
No. of missing values	0	0	0	0	0	0	0	0	0	0
Minimum	0.250	0.500	0.050	0.010	0.005	0.380	1.000	0.025	1.000	0.050
Maximum	9.300	24.000	1.100	0.670	0.190	44.000	15.100	1.140	12.500	0.100
Freq. of minimum	14	51	38	28	16	1	1	1	1	103
Range	9.050	23.500	1.050	0.660	0.185	43.620	14.100	1.115	11.500	0.050
1st Quartile	0.700	0.500	0.050	0.020	0.020	3.205	2.300	0.100	1.600	0.050
Median	1.700	1.000	0.200	0.050	0.030	7.405	3.700	0.320	2.950	0.050
3rd Quartile	4.450	4.000	0.500	0.110	0.050	18.375	8.000	0.670	4.975	0.050
Mean	2.796	2.575	0.268	0.073	0.037	10.986	5.182	0.410	3.596	0.055
Variance (n-1)	7.048	9.373	0.057	0.006	0.001	86.326	11.977	0.108	5.607	0.000
Standard deviation (n-1)	2.655	3.061	0.239	0.079	0.029	9.291	3.461	0.328	2.368	0.015
Variation coefficient	0.945	1.184	0.888	1.080	0.790	0.842	0.665	0.797	0.656	0.269
Skewness (Pearson)	1.082	3.322	0.988	4.022	1.923	0.784	0.831	0.485	1.316	2.733
Kurtosis (Pearson)	0.035	19.086	0.409	26.620	6.323	-0.160	-0.236	-1.159	2.321	5.470
Standard error of the mean	0.249	0.287	0.022	0.007	0.003	0.870	0.324	0.031	0.222	0.001
Lower bound on mean (95%)	2.303	2.006	0.223	0.058	0.032	9.262	4.539	0.349	3.156	0.052
Upper bound on mean (95%)	3.288	3.143	0.312	0.088	0.042	12.711	5.824	0.471	4.035	0.058

Statistic	Hf_ICM14B_PPM	Hg_ICM14B_PPM	In_ICM14B_PPM	La_ICM14B_PPM	Lu_ICM14B_PPM	Mo_ICM14B_PPM	Nb_ICM14B_PPM	Pb_ICM14B_PPM	Rb_ICM14B_PPM	Sb_ICM14B_PPM
No. of observations	114	114	114	114	114	114	114	114	114	114
No. of missing values	0	0	0	0	0	0	0	0	0	0
Minimum	0.025	0.005	0.010	0.300	0.005	0.080	0.100	0.100	0.800	0.025
Maximum	0.310	0.120	0.040	25.000	0.190	3.280	1.970	11.100	23.500	0.570
Freq. of minimum	60	106	90	1	25	2	1	10	5	35
Range	0.285	0.115	0.030	24.700	0.185	3.200	1.870	11.000	22.700	0.545
1st Quartile	0.025	0.005	0.010	1.525	0.010	0.340	0.190	0.500	1.300	0.025
Median	0.025	0.005	0.010	3.900	0.030	0.560	0.635	2.000	3.750	0.125
3rd Quartile	0.118	0.005	0.010	9.925	0.070	0.710	1.140	5.150	9.050	0.230
Mean	0.078	0.007	0.013	5.848	0.041	0.700	0.706	2.844	5.396	0.138
Variance (n-1)	0.006	0.000	0.000	24.339	0.001	0.422	0.279	6.921	21.620	0.012
Standard deviation (n-1)	0.075	0.012	0.006	4.933	0.037	0.649	0.528	2.631	4.650	0.108
Variation coefficient	0.952	1.700	0.457	0.840	0.898	0.924	0.744	0.921	0.858	0.780
Skewness (Pearson)	1.416	7.672	2.284	0.852	1.139	2.567	0.482	0.672	0.984	0.850
Kurtosis (Pearson)	1.112	63.678	5.087	0.326	1.217	6.749	-1.032	-0.613	0.681	0.774
Standard error of the mean	0.007	0.001	0.001	0.462	0.003	0.061	0.049	0.246	0.435	0.010
Lower bound on mean (95%)	0.065	0.005	0.012	4.933	0.034	0.579	0.608	2.356	4.533	0.118
Upper bound on mean (95%)	0.092	0.009	0.014	6.764	0.047	0.820	0.804	3.332	6.258	0.159

Statistic	Sc_ICM14B_PPM	Se_ICM14B_PPM	Sn_ICM14B_PPM	Ta_ICM14B_PPM	Tb_ICM14B_PPM	Te_ICM14B_PPM	Th_ICM14B_PPM	Tl_ICM14B_PPM	U_ICM14B_PPM	W_ICM14B_PPM
No. of observations	114	114	114	114	114	114	114	114	114	114
No. of missing values	0	0	0	0	0	0	0	0	0	0
Minimum	0.300	0.500	0.150	0.025	0.010	0.025	0.050	0.010	0.025	0.050
Maximum	4.700	0.500	0.900	0.025	0.640	0.160	5.400	0.150	1.600	1.800
Freq. of minimum	12	114	54	114	6	111	7	46	2	74
Range	4.400	0.000	0.750	0.000	0.630	0.135	5.350	0.140	1.575	1.750
1st Quartile	0.600	0.500	0.150	0.025	0.040	0.025	0.100	0.010	0.105	0.050
Median	1.400	0.500	0.300	0.025	0.090	0.025	0.600	0.040	0.280	0.050
3rd Quartile	3.075	0.500	0.500	0.025	0.210	0.025	2.700	0.090	0.635	0.100
Mean	1.816	0.500	0.331	0.025	0.130	0.027	1.419	0.051	0.389	0.118
Variance (n-1)	1.962	0.000	0.039	0.000	0.012	0.000	2.266	0.002	0.106	0.049
Standard deviation (n-1)	1.401	0.000	0.198	0.000	0.109	0.014	1.505	0.041	0.326	0.220
Variation coefficient	0.768	0.000	0.597	0.000	0.835	0.510	1.056	0.810	0.836	1.853
Skewness (Pearson)	0.538		0.629		1.267	8.553	0.836	0.474	1.033	6.199
Kurtosis (Pearson)	-1.175		-0.766		2.565	76.692	-0.613	-1.137	0.849	41.192
Standard error of the mean	0.131	0.000	0.019	0.000	0.010	0.001	0.141	0.004	0.031	0.021
Lower bound on mean (95%)	1.556	0.500	0.294	0.025	0.110	0.024	1.140	0.043	0.328	0.078
Upper bound on mean (95%)	2.076	0.500	0.368	0.025	0.150	0.029	1.698	0.058	0.449	0.159

Statistic	Y_ICM14B_PPM	Yb_ICM14B_PPM
No. of observations	114	114
No. of missing values	0	0
Minimum	0.270	0.050
Maximum	17.700	1.300
Freq. of minimum	1	37
Range	17.430	1.250
1st Quartile	0.925	0.050
Median	2.145	0.200
3rd Quartile	5.178	0.500
Mean	3.160	0.264
Variance (n-1)	8.053	0.057
Standard deviation (n-1)	2.838	0.238
Variation coefficient	0.894	0.898
Skewness (Pearson)	1.595	1.191
Kurtosis (Pearson)	4.419	1.638
Standard error of the mean	0.266	0.022
Lower bound on mean (95%)	2.634	0.219
Upper bound on mean (95%)	3.687	0.308

MMI Analyses

Statistic	Ag_MMI-M5_PPB	Al_MMI-M5_PPM	As_MMI-M5_PPB	Au_MMI-M5_PPB	Ba_MMI-M5_PPB	Bi_MMI-M5_PPB	Ca_MMI-M5_PPM	Cd_MMI-M5_PPB	Ce_MMI-M5_PPB	Co_MMI-M5_PPB
No. of observations	114	114	114	114	114	114	114	114	114	114
No. of missing values	0	0	0	0	0	0	0	0	0	0
Minimum	0.500	5.000	5.000	0.050	350.000	0.500	50.000	0.500	2.500	7.000
Maximum	90.000	253.000	30.000	3.900	8160.000	1.000	840.000	20.000	1010.000	670.000
Freq. of minimum	8	1	100	63	1	112	3	10	1	1
Range	89.500	248.000	25.000	3.850	7810.000	0.500	790.000	19.500	1007.500	663.000
1st Quartile	3.000	33.000	5.000	0.050	930.000	0.500	192.500	2.000	59.250	41.000
Median	5.000	55.500	5.000	0.050	2330.000	0.500	320.000	2.000	134.500	78.000
3rd Quartile	8.000	95.000	5.000	0.200	4350.000	0.500	527.500	3.750	207.500	156.000
Mean	9.395	73.649	6.053	0.197	2732.807	0.509	364.561	3.044	176.373	121.667
Variance (n-1)	245.976	3309.752	12.599	0.195	4136754.883	0.004	47030.337	9.011	34202.995	14860.507
Standard deviation (n-1)	15.684	57.530	3.550	0.442	2033.901	0.066	216.865	3.002	184.941	121.904
Variation coefficient	1.662	0.778	0.584	2.232	0.741	0.129	0.592	0.982	1.044	0.998
Skewness (Pearson)	3.622	1.262	4.447	6.191	0.697	7.350	0.328	3.708	2.373	1.876
Kurtosis (Pearson)	13.237	1.021	22.026	44.576	-0.485	52.018	-1.000	15.922	6.674	3.782
Standard error of the mean	1.469	5.388	0.332	0.041	190.492	0.006	20.311	0.281	17.321	11.417
Lower bound on mean (95%)	6.485	62.974	5.394	0.115	2355.407	0.497	324.321	2.487	142.056	99.047
Upper bound on mean (95%)	12.305	84.324	6.711	0.279	3110.207	0.521	404.802	3.601	210.689	144.286

Statistic	Cr_MMI-M5_PPB	Cu_MMI-M5_PPB	Dy_MMI-M5_PPB	Er_MMI-M5_PPB	Eu_MMI-M5_PPB	Fe_MMI-M5_PPM	Gd_MMI-M5_PPB	La_MMI-M5_PPB	Li_MMI-M5_PPB	Mg_MMI-M5_PPM
No. of observations	114	114	114	114	114	114	114	114	114	114
No. of missing values	0	0	0	0	0	0	0	0	0	0
Minimum	50.000	70.000	0.500	0.250	0.250	9.000	0.500	0.500	2.500	0.500
Maximum	50.000	78000.000	79.000	44.400	21.800	435.000	106.000	554.000	7.000	197.000
Freq. of minimum	114	1	2	1	18	2	1	1	106	1
Range	0.000	77930.000	78.500	44.150	21.550	426.000	105.500	553.500	4.500	196.500
1st Quartile	50.000	782.500	4.000	2.125	0.925	38.250	6.000	25.500	2.500	17.250
Median	50.000	1510.000	9.000	4.200	2.650	65.500	13.000	61.000	2.500	36.000
3rd Quartile	50.000	2582.500	14.000	7.300	4.950	101.000	21.750	92.000	2.500	77.500
Mean	50.000	2754.561	12.588	6.259	3.882	83.184	18.496	85.355	2.737	46.803
Variance (n-1)	0.000	54390147.151	160.452	42.758	16.269	5474.736	326.374	9417.370	0.793	1507.078
Standard deviation (n-1)	0.000	7374.968	12.667	6.539	4.033	73.991	18.066	97.043	0.890	38.821
Variation coefficient	0.000	2.666	1.002	1.040	1.035	0.886	0.972	1.132	0.324	0.826
Skewness (Pearson)		9.458	2.312	2.709	1.816	2.741	2.040	2.553	3.683	1.139
Kurtosis (Pearson)		93.775	6.875	10.137	3.774	9.016	5.189	7.589	12.332	1.855
Standard error of the mean	0.000	690.729	1.186	0.612	0.378	6.930	1.692	9.089	0.083	3.636
Lower bound on mean (95%)	50.000	1386.103	10.237	5.046	3.133	69.455	15.143	67.348	2.572	39.599
Upper bound on mean (95%)	50.000	4123.020	14.938	7.473	4.630	96.914	21.848	103.362	2.902	54.006

Statistic	Mo_MMI-M5_PPB	Nb_MMI-M5_PPB	Nd_MMI-M5_PPB	Ni_MMI-M5_PPB	Pb_MMI-M5_PPB	Pd_MMI-M5_PPB	Pr_MMI-M5_PPB	Pt_MMI-M5_PPB	Rb_MMI-M5_PPB	Sb_MMI-M5_PPB
No. of observations	114	114	114	114	114	114	114	114	114	114
No. of missing values	0	0	0	0	0	0	0	0	0	0
Minimum	2.500	0.250	2.000	23.000	5.000	0.500	0.500	0.500	2.500	0.500
Maximum	90.000	8.500	476.000	1110.000	240.000	1.000	113.000	0.500	223.000	40.000
Freq. of minimum	28	35	1	1	21	109	1	114	4	107
Range	87.500	8.250	474.000	1087.000	235.000	0.500	112.500	0.000	220.500	39.500
1st Quartile	5.000	0.250	33.000	79.000	10.000	0.500	8.250	0.500	15.000	0.500
Median	7.000	1.200	68.000	134.500	25.000	0.500	16.500	0.500	44.000	0.500
3rd Quartile	8.750	2.675	121.000	225.250	50.000	0.500	27.000	0.500	81.750	0.500
Mean	9.105	1.775	92.272	172.158	41.272	0.522	22.662	0.500	55.044	1.162
Variance (n-1)	141.290	3.129	7574.324	22968.258	2374.695	0.011	468.790	0.000	2213.308	22.741
Standard deviation (n-1)	11.887	1.769	87.031	151.553	48.731	0.103	21.652	0.000	47.046	4.769
Variation coefficient	1.300	0.992	0.939	0.876	1.176	0.196	0.951	0.000	0.851	4.085
Skewness (Pearson)	4.956	1.409	1.881	3.126	2.533	4.455	1.956		1.210	7.444
Kurtosis (Pearson)	28.140	1.692	4.108	14.007	6.782	17.846	4.312		1.537	54.015
Standard error of the mean	1.113	0.166	8.151	14.194	4.564	0.010	2.028	0.000	4.406	0.447
Lower bound on mean (95%)	6.900	1.447	76.123	144.037	32.230	0.503	18.645	0.500	46.314	0.277
Upper bound on mean (95%)	11.311	2.103	108.421	200.279	50.314	0.541	26.680	0.500	63.773	2.047

Statistic	Sc_MMI-M5_PPB	Sm_MMI-M5_PPB	Sn_MMI-M5_PPB	Sr_MMI-M5_PPB	Ta_MMI-M5_PPB	Tb_MMI-M5_PPB	Te_MMI-M5_PPB	Th_MMI-M5_PPB	Ti_MMI-M5_PPB	Tl_MMI-M5_PPB
No. of observations	114	114	114	114	114	114	114	114	114	114
No. of missing values	0	0	0	0	0	0	0	0	0	0
Minimum	2.500	1.000	0.500	290.000	0.500	0.500	5.000	0.900	1.500	0.250
Maximum	97.000	96.000	19.000	7320.000	1.000	14.000	5.000	75.300	3630.000	0.500
Freq. of minimum	4	1	110	1	104	43	114	1	1	113
Range	94.500	95.000	18.500	7030.000	0.500	13.500	0.000	74.400	3628.500	0.250
1st Quartile	10.000	7.000	0.500	790.000	0.500	0.500	5.000	6.850	58.000	0.250
Median	16.000	13.000	0.500	1485.000	0.500	1.000	5.000	12.000	253.500	0.250
3rd Quartile	23.000	22.750	0.500	3095.000	0.500	2.750	5.000	20.300	928.250	0.250
Mean	20.325	18.368	0.675	1959.211	0.544	2.154	5.000	15.048	572.075	0.252
Variance (n-1)	271.026	278.642	3.004	1828832.115	0.020	5.487	0.000	139.791	485559.598	0.001
Standard deviation (n-1)	16.463	16.693	1.733	1352.343	0.142	2.342	0.000	11.823	696.821	0.023
Variation coefficient	0.806	0.905	2.555	0.687	0.260	1.083	0.000	0.782	1.213	0.092
Skewness (Pearson)	2.249	1.881	10.502	0.849	2.915	2.231		1.900	1.642	10.536
Kurtosis (Pearson)	5.881	4.403	108.528	0.567	6.496	6.057		5.710	2.878	109.009
Standard error of the mean	1.542	1.563	0.162	126.659	0.013	0.219	0.000	1.107	65.263	0.002
Lower bound on mean (95%)	17.270	15.271	0.354	1708.277	0.517	1.719	5.000	12.854	442.776	0.248
Upper bound on mean (95%)	23.379	21.466	0.997	2210.144	0.570	2.588	5.000	17.242	701.373	0.257

Statistic	U_MMI-M5_PPB	W_MMI-M5_PPB	Y_MMI-M5_PPB	Yb_MMI-M5_PPB	Zn_MMI-M5_PPB	Zr_MMI-M5_PPB
No. of observations	114	114	114	114	114	114
No. of missing values	0	0	0	0	0	0
Minimum	2.000	0.500	2.500	0.500	10.000	9.000
Maximum	73.000	34.000	528.000	36.000	620.000	206.000
Freq. of minimum	3	28	1	10	6	2
Range	71.000	33.500	525.500	35.500	610.000	197.000
1st Quartile	5.000	1.000	23.250	2.000	40.000	26.000
Median	8.000	1.000	48.500	3.000	80.000	44.500
3rd Quartile	14.750	1.000	82.000	6.000	140.000	71.500
Mean	12.544	1.211	72.338	5.000	105.526	58.132
Variance (n-1)	132.817	9.699	5898.153	27.128	8444.411	2128.292
Standard deviation (n-1)	11.525	3.114	76.799	5.208	91.893	46.133
Variation coefficient	0.915	2.561	1.057	1.037	0.867	0.790
Skewness (Pearson)	2.264	10.372	2.782	2.790	2.425	1.446
Kurtosis (Pearson)	6.480	106.715	10.858	11.032	9.008	1.315
Standard error of the mean	1.079	0.292	7.193	0.488	8.607	4.321
Lower bound on mean (95%)	10.405	0.633	58.087	4.034	88.475	49.571
Upper bound on mean (95%)	14.682	1.788	86.588	5.966	122.578	66.692

Appendix II
Correlation Coefficients

MMI

Proximity matrix (Pearson correlation coefficient):

	Ag	Al	Ba	Ca	Cd	Ce	Co	Cu	Dy	Er	Eu	Fe	Gd	La	Mg	Nb	Nd	Ni	Pb	Pr	Rb	Sc	Sm	Sr	Th	Ti	U	Y	Yb	Zn	Zr
Ag	1	0.301	0.276	-0.232	0.020	0.437	0.012	0.305	0.364	0.315	0.420	-0.146	0.414	0.443	-0.275	0.212	0.430	-0.259	0.438	0.431	0.305	0.376	0.419	-0.113	0.375	0.212	-0.079	0.312	0.268	0.213	0.496
Al	0.301	1	-0.088	-0.759	0.184	0.269	-0.081	0.014	0.063	0.016	0.123	0.379	0.085	0.283	-0.567	0.684	0.201	-0.417	0.797	0.240	0.684	0.392	0.126	-0.540	0.009	0.813	-0.412	0.019	-0.002	0.647	0.717
Ba	0.276	-0.088	1	0.389	-0.265	0.499	0.328	0.238	0.624	0.634	0.669	0.003	0.603	0.483	0.523	-0.366	0.525	0.230	0.173	0.506	-0.457	0.515	0.578	0.638	0.682	-0.272	0.405	0.622	0.625	-0.256	0.061
Ca	-0.232	-0.759	0.389	1	-0.188	-0.171	0.220	0.101	0.061	0.110	0.025	-0.300	0.027	-0.193	0.776	-0.878	-0.099	0.644	-0.595	-0.142	-0.842	-0.264	-0.020	0.854	0.036	-0.936	0.536	0.117	0.126	-0.682	-0.743
Cd	0.020	0.184	-0.265	-0.188	1	-0.002	0.157	0.250	0.042	0.076	-0.017	0.260	0.053	0.009	-0.247	0.224	0.040	0.121	0.139	0.035	0.227	0.127	0.041	-0.308	-0.110	0.173	-0.160	0.076	0.048	0.499	0.172
Ce	0.437	0.269	0.499	-0.171	-0.002	1	0.316	0.318	0.835	0.799	0.892	0.225	0.889	0.986	-0.027	0.191	0.970	-0.061	0.475	0.981	0.110	0.759	0.927	-0.046	0.815	0.287	0.281	0.809	0.764	0.145	0.598
Co	0.012	-0.081	0.328	0.220	0.157	0.316	1	0.506	0.332	0.390	0.323	0.618	0.294	0.258	0.279	-0.182	0.292	0.601	-0.074	0.299	-0.310	0.381	0.299	0.257	0.276	-0.130	0.503	0.385	0.456	-0.210	-0.020
Cu	0.305	0.014	0.238	0.101	0.250	0.318	0.506	1	0.388	0.436	0.352	0.404	0.369	0.305	0.135	-0.075	0.348	0.371	0.056	0.348	-0.120	0.405	0.367	0.092	0.273	-0.065	0.319	0.430	0.458	-0.036	0.109
Dy	0.364	0.063	0.624	0.061	0.042	0.835	0.332	0.388	1	0.987	0.953	0.158	0.980	0.851	0.209	-0.030	0.913	0.232	0.345	0.894	-0.172	0.822	0.967	0.179	0.833	0.010	0.515	0.984	0.956	0.022	0.408
Er	0.315	0.016	0.634	0.110	0.076	0.799	0.390	0.436	0.987	1	0.937	0.198	0.968	0.815	0.267	-0.084	0.885	0.310	0.296	0.865	-0.233	0.818	0.946	0.217	0.820	-0.038	0.544	0.996	0.978	-0.004	0.348
Eu	0.420	0.123	0.669	0.025	-0.017	0.892	0.323	0.352	0.953	0.937	1	0.152	0.970	0.897	0.155	-0.005	0.943	0.138	0.385	0.930	-0.110	0.776	0.972	0.167	0.837	0.056	0.451	0.938	0.914	0.036	0.452
Fe	-0.146	0.379	0.003	-0.300	0.260	0.225	0.618	0.404	0.158	0.198	0.152	1	0.119	0.214	-0.070	0.335	0.188	0.184	0.247	0.217	0.128	0.456	0.146	-0.228	0.105	0.419	0.152	0.191	0.272	0.222	0.301
Gd	0.414	0.085	0.603	0.027	0.053	0.889	0.294	0.369	0.980	0.968	0.970	0.119	1	0.905	0.149	0.001	0.956	0.163	0.370	0.940	-0.106	0.795	0.990	0.132	0.839	0.050	0.438	0.971	0.928	0.050	0.448
La	0.443	0.283	0.483	-0.193	0.009	0.986	0.258	0.305	0.851	0.815	0.897	0.214	0.905	1	-0.046	0.204	0.983	-0.084	0.490	0.990	0.126	0.763	0.939	-0.075	0.804	0.301	0.255	0.828	0.773	0.191	0.607
Mg	-0.275	-0.567	0.523	0.776	-0.247	-0.027	0.279	0.135	0.209	0.267	0.155	-0.070	0.149	-0.046	1	-0.752	0.023	0.554	-0.327	-0.009	-0.758	0.000	0.104	0.856	0.166	-0.670	0.494	0.271	0.289	-0.516	-0.630
Nb	0.212	0.684	-0.366	-0.878	0.224	0.191	-0.182	-0.075	-0.030	-0.084	-0.005	0.335	0.001	0.204	-0.752	1	0.120	-0.589	0.581	0.159	0.777	0.278	0.047	-0.828	0.044	0.909	-0.431	-0.098	-0.101	0.615	0.795
Nd	0.430	0.201	0.525	-0.099	0.040	0.970	0.292	0.348	0.913	0.885	0.943	0.188	0.956	0.983	0.023	0.120	1	0.027	0.433	0.997	0.044	0.770	0.981	0.003	0.818	0.197	0.340	0.897	0.844	0.134	0.547
Ni	-0.259	-0.417	0.230	0.644	0.121	-0.061	0.601	0.371	0.232	0.310	0.138	0.184	0.163	-0.084	0.554	-0.589	0.027	1	-0.377	0.003	-0.632	0.074	0.115	0.586	0.001	-0.611	0.650	0.318	0.355	-0.415	-0.503
Pb	0.438	0.797	0.173	-0.595	0.139	0.475	-0.074	0.056	0.345	0.296	0.385	0.247	0.370	0.490	-0.327	0.581	0.433	-0.377	1	0.454	0.568	0.565	0.393	-0.315	0.280	0.714	-0.337	0.300	0.241	0.594	0.741
Pr	0.431	0.240	0.506	-0.142	0.035	0.981	0.299	0.348	0.894	0.865	0.930	0.217	0.940	0.990	-0.009	0.159	0.997	0.003	0.454	1	0.078	0.776	0.970	-0.031	0.813	0.243	0.323	0.876	0.826	0.156	0.577
Rb	0.305	0.684	-0.457	-0.842	0.227	0.110	-0.310	-0.120	-0.172	-0.233	-0.110	0.128	-0.106	0.126	-0.758	0.777	0.044	-0.632	0.568	0.078	1	0.069	-0.050	-0.790	-0.156	0.815	-0.586	-0.226	-0.274	0.593	0.646
Sc	0.376	0.392	0.515	-0.264	0.127	0.759	0.381	0.405	0.822	0.818	0.776	0.456	0.795	0.763	0.000	0.278	0.770	0.074	0.565	0.776	0.069	1	0.790	-0.060	0.770	0.364	0.319	0.800	0.801	0.242	0.642
Sm	0.419	0.126	0.578	-0.020	0.041	0.927	0.299	0.367	0.967	0.946	0.972	0.146	0.990	0.939	0.104	0.047	0.981	0.115	0.393	0.970	-0.050	0.790	1	0.086	0.836	0.103	0.422	0.952	0.908	0.081	0.489
Sr	-0.113	-0.540	0.638	0.854	-0.308	-0.046	0.257	0.092	0.179	0.217	0.167	-0.228	0.132	-0.075	0.856	-0.828	0.003	0.586	-0.315	-0.031	-0.790	-0.060	0.086	1	0.126	-0.761	0.481	0.225	0.228	-0.553	-0.627
Th	0.375	0.009	0.682	0.036	-0.110	0.815	0.276	0.273	0.833	0.820	0.837	0.105	0.839	0.804	0.166	0.044	0.818	0.001	0.280	0.813	-0.156	0.770	0.836	0.126	1	0.059	0.420	0.802	0.786	-0.065	0.493
Ti	0.212	0.813	-0.272	-0.936	0.173	0.287	-0.130	-0.065	0.010	-0.038	0.056	0.419	0.050	0.301	-0.670	0.909	0.197	-0.611	0.714	0.243	0.815	0.364	0.103	-0.761	0.059	1	-0.498	-0.041	-0.055	0.693	0.796
U	-0.079	-0.412	0.405	0.536	-0.160	0.281	0.503	0.319	0.515	0.544	0.451	0.152	0.438	0.255	0.494	-0.431	0.340	0.650	-0.337	0.323	-0.586	0.319	0.422	0.481	0.420	-0.498	1	0.530	0.595	-0.410	-0.204
Y	0.312	0.019	0.622	0.117	0.076	0.809	0.385	0.430	0.984	0.996	0.938	0.191	0.971	0.828	0.271	-0.098	0.897	0.318	0.300	0.876	-0.226	0.800	0.952	0.225	0.802	-0.041	0.530	1	0.971	-0.005	0.333

MMI

Proximity matrix (Spearman correlation coefficient):

	Ag	Al	Ba	Ca	Cd	Ce	Co	Cu	Dy	Er	Eu	Fe	Gd	La	Mg	Nb	Nd	Ni	Pb	Pr	Rb	Sc	Sm	Sr	Th	Ti	U	Y	Yb	Zn	Zr
Ag	1	0.303	0.341	-0.177	0.017	0.431	0.042	0.194	0.351	0.311	0.407	-0.139	0.392	0.446	-0.071	0.139	0.420	-0.182	0.405	0.424	0.249	0.381	0.402	0.039	0.306	0.197	-0.049	0.312	0.265	0.230	0.398
Al	0.303	1	-0.047	-0.747	0.185	0.210	-0.130	-0.078	0.055	0.012	0.102	0.279	0.072	0.236	-0.570	0.683	0.149	-0.428	0.808	0.185	0.662	0.426	0.110	-0.511	-0.017	0.792	-0.413	0.007	-0.012	0.621	0.716
Ba	0.341	-0.047	1	0.332	-0.301	0.546	0.337	0.207	0.656	0.669	0.681	0.053	0.641	0.529	0.617	-0.328	0.575	0.225	0.179	0.549	-0.452	0.567	0.608	0.633	0.726	-0.189	0.412	0.653	0.651	-0.247	0.077
Ca	-0.177	-0.747	0.332	1	-0.227	-0.148	0.256	0.177	0.068	0.111	0.035	-0.204	0.042	-0.188	0.833	-0.897	-0.078	0.671	-0.608	-0.124	-0.860	-0.289	-0.017	0.868	0.057	-0.937	0.508	0.120	0.127	-0.695	-0.773
Cd	0.017	0.185	-0.301	-0.227	1	0.011	0.132	0.190	0.013	0.024	-0.017	0.228	0.007	0.036	-0.377	0.279	0.033	0.028	0.114	0.045	0.269	0.108	0.020	-0.359	-0.158	0.192	-0.176	0.025	0.028	0.517	0.190
Ce	0.431	0.210	0.546	-0.148	0.011	1	0.342	0.328	0.871	0.833	0.914	0.239	0.909	0.982	0.121	0.177	0.965	-0.013	0.453	0.974	0.041	0.757	0.936	0.024	0.793	0.257	0.332	0.839	0.809	0.086	0.572
Co	0.042	-0.130	0.337	0.256	0.132	0.342	1	0.586	0.327	0.374	0.316	0.638	0.299	0.293	0.304	-0.202	0.311	0.608	-0.132	0.313	-0.363	0.398	0.305	0.279	0.296	-0.190	0.533	0.366	0.413	-0.262	-0.036
Cu	0.194	-0.078	0.207	0.177	0.190	0.328	0.586	1	0.356	0.395	0.338	0.498	0.329	0.309	0.185	-0.137	0.339	0.470	-0.015	0.338	-0.234	0.399	0.339	0.145	0.248	-0.141	0.424	0.389	0.427	-0.115	0.026
Dy	0.351	0.055	0.656	0.068	0.013	0.871	0.327	0.356	1	0.990	0.981	0.188	0.988	0.884	0.343	-0.047	0.944	0.240	0.310	0.925	-0.199	0.763	0.975	0.230	0.820	0.022	0.544	0.990	0.971	0.002	0.366
Er	0.311	0.012	0.669	0.111	0.024	0.833	0.374	0.395	0.990	1	0.961	0.229	0.969	0.846	0.387	-0.089	0.912	0.302	0.270	0.891	-0.260	0.767	0.950	0.266	0.815	-0.020	0.582	0.995	0.986	-0.024	0.313
Eu	0.407	0.102	0.681	0.035	-0.017	0.914	0.316	0.338	0.981	0.961	1	0.170	0.994	0.927	0.312	-0.023	0.974	0.167	0.356	0.959	-0.151	0.757	0.991	0.226	0.821	0.066	0.474	0.965	0.935	0.004	0.409
Fe	-0.139	0.279	0.053	-0.204	0.228	0.239	0.638	0.498	0.188	0.229	0.170	1	0.153	0.229	-0.102	0.287	0.199	0.246	0.220	0.223	-0.004	0.516	0.180	-0.178	0.141	0.310	0.247	0.222	0.288	0.138	0.279
Gd	0.392	0.072	0.641	0.042	0.007	0.909	0.299	0.329	0.988	0.969	0.994	0.153	1	0.924	0.306	-0.021	0.974	0.179	0.333	0.959	-0.150	0.737	0.994	0.205	0.814	0.053	0.488	0.974	0.944	0.010	0.399
La	0.446	0.236	0.529	-0.188	0.036	0.982	0.293	0.309	0.884	0.846	0.927	0.229	0.924	1	0.085	0.203	0.979	-0.036	0.473	0.989	0.065	0.763	0.950	-0.011	0.770	0.290	0.303	0.852	0.819	0.140	0.592
Mg	-0.071	-0.570	0.617	0.833	-0.377	0.121	0.304	0.185	0.343	0.387	0.312	-0.102	0.306	0.085	1	-0.808	0.183	0.587	-0.349	0.138	-0.842	0.050	0.246	0.909	0.331	-0.733	0.577	0.385	0.390	-0.609	-0.572
Nb	0.139	0.683	-0.328	-0.897	0.279	0.177	-0.202	-0.137	-0.047	-0.089	-0.023	0.287	-0.021	0.203	-0.808	1	0.105	-0.620	0.603	0.150	0.800	0.288	0.039	-0.833	0.009	0.934	-0.408	-0.100	-0.097	0.639	0.808
Nd	0.420	0.149	0.575	-0.078	0.033	0.965	0.311	0.339	0.944	0.912	0.974	0.199	0.974	0.979	0.183	0.105	1	0.073	0.397	0.997	-0.028	0.750	0.990	0.084	0.797	0.179	0.404	0.918	0.887	0.067	0.508
Ni	-0.182	-0.428	0.225	0.671	0.028	-0.013	0.608	0.470	0.240	0.302	0.167	0.246	0.179	-0.036	0.587	-0.620	0.073	1	-0.431	0.042	-0.666	0.059	0.131	0.601	0.062	-0.651	0.666	0.311	0.343	-0.461	-0.525
Pb	0.405	0.808	0.179	-0.608	0.114	0.453	-0.132	-0.015	0.310	0.270	0.356	0.220	0.333	0.473	-0.349	0.603	0.397	-0.431	1	0.423	0.565	0.570	0.365	-0.344	0.229	0.727	-0.342	0.269	0.227	0.598	0.778
Pr	0.424	0.185	0.549	-0.124	0.045	0.974	0.313	0.338	0.925	0.891	0.959	0.223	0.959	0.989	0.138	0.150	0.997	0.042	0.423	1	0.010	0.760	0.980	0.040	0.787	0.225	0.373	0.898	0.867	0.101	0.546
Rb	0.249	0.662	-0.452	-0.860	0.269	0.041	-0.363	-0.234	-0.199	-0.260	-0.151	-0.004	-0.150	0.065	-0.842	0.800	-0.028	-0.666	0.565	0.010	1	0.069	-0.091	-0.804	-0.208	0.812	-0.586	-0.259	-0.288	0.647	0.659
Sc	0.381	0.426	0.567	-0.289	0.108	0.757	0.398	0.399	0.763	0.767	0.757	0.516	0.737	0.763	0.050	0.288	0.750	0.059	0.570	0.760	0.069	1	0.752	-0.040	0.735	0.392	0.327	0.750	0.772	0.258	0.632
Sm	0.402	0.110	0.608	-0.017	0.020	0.936	0.305	0.339	0.975	0.950	0.991	0.180	0.994	0.950	0.246	0.039	0.990	0.131	0.365	0.980	-0.091	0.752	1	0.143	0.813	0.113	0.456	0.955	0.925	0.041	0.455
Sr	0.039	-0.511	0.633	0.868	-0.359	0.024	0.279	0.145	0.230	0.266	0.226	-0.178	0.205	-0.011	0.909	-0.833	0.084	0.601	-0.344	0.040	-0.804	-0.040	0.143	1	0.214	-0.766	0.480	0.270	0.266	-0.565	-0.596
Th	0.306	-0.017	0.726	0.057	-0.158	0.793	0.296	0.248	0.820	0.815	0.821	0.141	0.814	0.770	0.331	0.009	0.797	0.062	0.229	0.787	-0.208	0.735	0.813	0.214	1	0.058	0.515	0.796	0.805	-0.111	0.408
Ti	0.197	0.792	-0.189	-0.937	0.192	0.257	-0.190	-0.141	0.022	-0.020	0.066	0.310	0.053	0.290	-0.733	0.934	0.179	-0.651	0.727	0.225	0.812	0.392	0.113	-0.766	0.058	1	-0.471	-0.029	-0.033	0.675	0.840
U	-0.049	-0.413	0.412	0.508	-0.176	0.332	0.533	0.424	0.544	0.582	0.474	0.247	0.488	0.303	0.577	-0.408	0.404	0.666	-0.342	0.373	-0.586	0.327	0.456	0.480	0.515	-0.471	1	0.568	0.617	-0.448	-0.217
Y	0.312	0.007	0.653	0.120	0.025	0.839	0.366	0.389	0.990	0.995	0.965	0.222	0.974	0.852	0.385	-0.100	0.918	0.311	0.269	0.898	-0.259	0.750	0.955	0.270	0.796	-0.029	0.568	1	0.983	-0.026	0.301
Yb	0.265	-0.012	0.651	0.127	0.028	0.809	0.413	0.427	0.971	0.986	0.935	0.288	0.944	0.819	0.390	-0.097	0.887	0.343	0.227	0.867	-0.288	0.772	0.925	0.266	0.805	-0.033	0.617	0.983	1	-0.038	0.279
Zn	0.230	0.621	-0.247	-0.695	0.517	0.086	-0.262	-0.115	0.002	-0.024	0.004	0.138	0.010	0.140	-0.609	0.639	0.067	-0.461	0.598	0.101	0.647	0.258	0.041	-0.565	-0.111	0.675	-0.448	-0.026	-0.038	1	0.574
Zr	0.398	0.716	0.077	-0.773	0.190	0.572	-0.036	0.026	0.366	0.313	0.409	0.279	0.399	0.592	-0.572	0.808	0.508	-0.525	0.778	0.546	0.659	0.632	0.455	-0.596	0.408	0.840	-0.217	0.301	0.279	0.574	1

Aqua Regia Digest

Proximity matrix (Pearson correlation coefficient):

	Ag	Al	Ba	Bi	Ca	Cd	Ce	Co	Cr	Cs	Cu	Fe	Ga	K	La	Li	Lu	Mg	Mn	Mo	Nb	Ni	P	Pb	Rb	Sc	Sr	Tb	Th	Ti	U	V	Y	Zn	Zr	Na
Ag	1	0.285	0.257	0.460	-0.104	0.147	0.123	0.224	0.185	0.274	0.614	0.201	0.280	0.165	0.147	0.281	0.109	0.223	0.147	0.448	0.237	0.193	0.074	0.264	0.298	0.134	-0.018	0.123	0.206	0.195	0.123	0.180	0.105	0.276	0.193	-0.316
Al	0.285	1	0.928	0.898	0.594	0.706	0.921	0.950	0.894	0.955	0.710	0.952	0.978	0.845	0.936	0.979	0.875	0.971	0.843	0.664	0.958	0.902	0.614	0.943	0.961	0.925	0.600	0.881	0.951	0.887	0.878	0.915	0.877	0.948	0.752	-0.769
Ba	0.257	0.928	1	0.846	0.719	0.772	0.902	0.917	0.844	0.889	0.686	0.875	0.879	0.752	0.914	0.905	0.877	0.914	0.912	0.670	0.898	0.886	0.606	0.902	0.865	0.860	0.744	0.874	0.876	0.748	0.923	0.805	0.879	0.853	0.716	-0.627
Bi	0.460	0.898	0.846	1	0.496	0.709	0.826	0.833	0.826	0.895	0.813	0.831	0.864	0.652	0.834	0.913	0.754	0.871	0.761	0.760	0.889	0.822	0.472	0.891	0.871	0.809	0.482	0.790	0.856	0.749	0.798	0.783	0.762	0.841	0.661	-0.716
Ca	-0.104	0.594	0.719	0.496	1	0.717	0.752	0.684	0.622	0.567	0.350	0.620	0.537	0.530	0.736	0.599	0.804	0.706	0.826	0.383	0.640	0.700	0.604	0.622	0.538	0.697	0.946	0.777	0.606	0.473	0.827	0.543	0.793	0.564	0.506	-0.136
Cd	0.147	0.706	0.772	0.709	0.717	1	0.810	0.743	0.770	0.732	0.596	0.683	0.675	0.470	0.802	0.712	0.805	0.736	0.774	0.694	0.752	0.811	0.450	0.784	0.668	0.762	0.654	0.815	0.662	0.551	0.827	0.619	0.806	0.693	0.389	-0.360
Ce	0.123	0.921	0.902	0.826	0.752	0.810	1	0.933	0.912	0.916	0.622	0.906	0.896	0.770	0.996	0.927	0.950	0.942	0.867	0.618	0.932	0.930	0.596	0.920	0.898	0.955	0.689	0.984	0.928	0.819	0.946	0.864	0.972	0.885	0.688	-0.610
Co	0.224	0.950	0.917	0.833	0.684	0.743	0.933	1	0.874	0.903	0.659	0.976	0.952	0.840	0.940	0.926	0.896	0.955	0.911	0.606	0.921	0.901	0.665	0.886	0.917	0.938	0.687	0.905	0.917	0.891	0.891	0.942	0.908	0.960	0.725	-0.688
Cr	0.185	0.894	0.844	0.826	0.622	0.770	0.912	0.874	1	0.905	0.627	0.873	0.859	0.738	0.916	0.907	0.883	0.885	0.775	0.737	0.891	0.976	0.494	0.902	0.882	0.916	0.581	0.902	0.873	0.766	0.864	0.835	0.897	0.851	0.653	-0.643
Cs	0.274	0.955	0.889	0.895	0.567	0.732	0.916	0.903	0.905	1	0.690	0.906	0.926	0.788	0.927	0.961	0.861	0.935	0.799	0.683	0.944	0.901	0.493	0.963	0.970	0.928	0.537	0.889	0.944	0.815	0.860	0.855	0.872	0.901	0.703	-0.762
Cu	0.614	0.710	0.686	0.813	0.350	0.596	0.622	0.659	0.627	0.690	1	0.640	0.693	0.455	0.637	0.703	0.584	0.694	0.589	0.780	0.672	0.656	0.443	0.679	0.680	0.604	0.361	0.607	0.632	0.612	0.613	0.623	0.587	0.684	0.462	-0.489
Fe	0.201	0.952	0.875	0.831	0.620	0.683	0.906	0.976	0.873	0.906	0.640	1	0.965	0.857	0.916	0.931	0.864	0.951	0.860	0.593	0.916	0.881	0.659	0.870	0.930	0.932	0.623	0.871	0.926	0.923	0.848	0.973	0.872	0.972	0.738	-0.735
Ga	0.280	0.978	0.879	0.864	0.537	0.675	0.896	0.952	0.859	0.926	0.693	0.965	1	0.848	0.912	0.957	0.839	0.951	0.813	0.631	0.942	0.857	0.653	0.902	0.950	0.913	0.534	0.849	0.930	0.945	0.822	0.952	0.845	0.976	0.713	-0.778
K	0.165	0.845	0.752	0.652	0.530	0.470	0.770	0.840	0.738	0.788	0.455	0.857	0.848	1	0.785	0.806	0.747	0.850	0.740	0.385	0.755	0.743	0.601	0.738	0.880	0.796	0.572	0.737	0.836	0.821	0.710	0.825	0.750	0.842	0.777	-0.672
La	0.147	0.936	0.914	0.834	0.736	0.802	0.996	0.940	0.916	0.927	0.637	0.916	0.912	0.785	1	0.940	0.958	0.949	0.868	0.623	0.942	0.933	0.601	0.929	0.912	0.960	0.682	0.982	0.934	0.833	0.945	0.873	0.976	0.899	0.694	-0.635
Li	0.281	0.979	0.905	0.913	0.599	0.712	0.927	0.926	0.907	0.961	0.703	0.931	0.957	0.806	0.940	1	0.884	0.960	0.824	0.670	0.962	0.905	0.596	0.951	0.956	0.929	0.573	0.894	0.952	0.862	0.867	0.889	0.884	0.931	0.738	-0.743
Lu	0.109	0.875	0.877	0.754	0.804	0.805	0.950	0.896	0.883	0.861	0.584	0.864	0.839	0.747	0.958	0.884	1	0.905	0.864	0.570	0.893	0.917	0.606	0.880	0.844	0.940	0.750	0.963	0.871	0.760	0.936	0.810	0.984	0.840	0.660	-0.512
Mg	0.223	0.971	0.914	0.871	0.706	0.736	0.942	0.955	0.885	0.935	0.694	0.951	0.951	0.850	0.949	0.960	0.905	1	0.885	0.642	0.952	0.906	0.679	0.925	0.950	0.942	0.699	0.912	0.950	0.879	0.912	0.910	0.906	0.946	0.755	-0.684
Mn	0.147	0.843	0.912	0.761	0.826	0.774	0.867	0.911	0.775	0.799	0.589	0.860	0.813	0.740	0.868	0.824	0.864	0.885	1	0.583	0.833	0.826	0.670	0.827	0.793	0.841	0.820	0.854	0.814	0.710	0.898	0.775	0.864	0.824	0.672	-0.474
Mo	0.448	0.664	0.670	0.760	0.383	0.694	0.618	0.606	0.737	0.683	0.780	0.593	0.631	0.385	0.623	0.670	0.570	0.642	0.583	1	0.645	0.728	0.406	0.698	0.624	0.585	0.366	0.603	0.582	0.494	0.629	0.544	0.573	0.617	0.368	-0.405
Nb	0.237	0.958	0.898	0.889	0.640	0.752	0.932	0.921	0.891	0.944	0.672	0.916	0.942	0.755	0.942	0.962	0.893	0.952	0.833	0.645	1	0.891	0.556	0.950	0.929	0.941	0.608	0.901	0.936	0.858	0.893	0.881	0.893	0.915	0.682	-0.723
Ni	0.193	0.902	0.886	0.822	0.700	0.811	0.930	0.901	0.976	0.901	0.656	0.881	0.857	0.743	0.933	0.905	0.917	0.906	0.826	0.728	0.891	1	0.527	0.902	0.872	0.929	0.672	0.927	0.872	0.754	0.909	0.840	0.927	0.856	0.670	-0.609
P	0.074	0.614	0.606	0.472	0.604	0.450	0.596	0.665	0.494	0.493	0.443	0.659	0.653	0.601	0.601	0.596	0.606	0.679	0.670	0.406	0.556	0.527	1	0.520	0.556	0.571	0.589	0.560	0.556	0.664	0.580	0.645	0.576	0.681	0.450	-0.316
Pb	0.264	0.943	0.902	0.891	0.622	0.784	0.920	0.886	0.902	0.963	0.679	0.870	0.902	0.738	0.929	0.951	0.880	0.925	0.827	0.698	0.950	0.902	0.520	1	0.923	0.912	0.577	0.892	0.926	0.775	0.888	0.810	0.881	0.866	0.684	-0.691
Rb	0.298	0.961	0.865	0.871	0.538	0.668	0.898	0.917	0.882	0.970	0.680	0.930	0.950	0.880	0.912	0.956	0.844	0.950	0.793	0.624	0.929	0.872	0.556	0.923	1	0.921	0.535	0.867	0.952	0.866	0.827	0.887	0.855	0.932	0.746	-0.784
Sc	0.134	0.925	0.860	0.809	0.697	0.762	0.955	0.938	0.916	0.928	0.604	0.932	0.913	0.796	0.960	0.929	0.940	0.942	0.841	0.585	0.941	0.929	0.571	0.912	0.921	1	0.647	0.951	0.926	0.844	0.892	0.898	0.952	0.911	0.679	-0.655
Sr	-0.018	0.600	0.744	0.482	0.946	0.654	0.689	0.687	0.581	0.537	0.361	0.623	0.534	0.572	0.682	0.573	0.750	0.699	0.820	0.366	0.608	0.672	0.589	0.577	0.535	0.647	1	0.707	0.579	0.450	0.807	0.535	0.733	0.560	0.540	-0.183
Tb	0.123	0.881	0.874	0.790	0.777	0.815	0.984	0.905	0.902	0.889	0.607	0.871	0.849	0.737	0.982	0.894	0.963	0.912	0.854	0.603	0.901	0.927	0.560	0.892	0.867	0.951	0.707	1	0.894	0.766	0.941	0.820	0.989	0.846	0.651	-0.548
Th	0.206	0.951	0.876	0.856	0.606	0.662	0.928	0.917	0.873	0.944	0.632	0.926	0.930	0.836	0.934	0.952	0.871	0.950	0.814	0.582	0.936	0.872	0.556	0.926	0.952	0.926	0.579	0.894	1	0.860	0.864	0.887	0.881	0.903	0.819	-0.725
Ti	0.195	0.887	0.748	0.749	0.473	0.551	0.819	0.891	0.766	0.815	0.612	0.923	0.945	0.821	0.833	0.862	0.760	0.879	0.710	0.494	0.858	0.754	0.664	0.775	0.866	0.844	0.450	0.766	0.860	1	0.718	0.959	0.763	0.945	0.663	-0.717
U	0.123	0.878	0.923	0.798	0.827	0.827	0.946	0.891	0.864	0.860	0.613	0.848	0.822	0.710	0.945	0.867	0.936	0.912	0.898	0.629	0.893	0.909	0.580	0.888	0.827	0.892	0.807	0.941	0.864	0.718	1	0.779	0.945	0.816	0.667	-0.539
V	0.180	0.915	0.805	0.783	0.543	0.619	0.864	0.942	0.835	0.855	0.623	0.973	0.952	0.825	0.873	0.889	0.810	0.910	0.775	0.544	0.881	0.840	0.645	0.810	0.887	0.898	0.535	0.820	0.887	0.959	0.779	1	0.818	0.961	0.698	-0.733
Y	0.105	0.877	0.879	0.762	0.793	0.806	0.972	0.908	0.897	0.872	0.587	0.872	0.845	0.750	0.976	0.884	0.984	0.906	0.864	0.573	0.893	0.927	0.576	0.881	0.855	0.952	0.733	0.989	0.881	0.763	0.945	0.818	1	0.842	0.654	-0.533
Zn	0.276	0.948	0.853	0.841	0.564	0.693	0.885	0.960	0.851	0.901	0.684	0.972	0.976	0.842	0.899	0.931	0.840	0.946	0.824	0.617	0.915	0.856	0.681	0.866	0.932	0.911	0.560	0.846	0.903	0.945	0.816	0.961	0.842	1	0.689	-0.754
Zr	0.193	0.752	0.716	0.661	0.506	0.389	0.688	0.725	0.653	0.703	0.462	0.738	0.713	0.777	0.694	0.738	0.660	0.755	0.672	0.368	0.682	0.670	0.450	0.684	0.746	0.679	0.540	0.651	0.819	0.663	0.667	0.698	0.654	0.689	1	-0.597
Na	-0.316	-0.769	-0.627	-0.716	-0.136	-0.360	-0.610	-0.688	-0.643	-0.762	-0.489	-0.735	-0.778	-0.672	-0.635	-0.743	-0.512	-0.684	-0.474	-0.405	-0.723	-0.609	-0.316	-0.691	-0.784	-0.655	-0.183	-0.548	-0.725	-0.717	-0.539	-0.733	-0.533	-0.754	-0.597	1

Aqya Regia Digest

Proximity matrix (Spearman correlation coefficient):

	Ag	Al	Ba	Bi	Ca	Cd	Ce	Co	Cr	Cs	Cu	Fe	Ga	K	La	Li	Lu	Mg	Mn	Mo	Nb	Ni	P	Pb	Rb	Sc	Sr	Tb	Th	Ti	U	V	Y	Zn	Zr	Na	Ce-Lu
Ag	1	0.396	0.421	0.517	0.049	0.315	0.286	0.380	0.284	0.351	0.578	0.325	0.393	0.332	0.304	0.377	0.268	0.306	0.274	0.448	0.366	0.308	0.165	0.376	0.371	0.259	0.127	0.286	0.296	0.315	0.273	0.305	0.273	0.373	0.250	-0.373	0.077
Al	0.396	1	0.926	0.860	0.623	0.705	0.920	0.934	0.895	0.934	0.794	0.932	0.962	0.845	0.926	0.975	0.870	0.957	0.858	0.709	0.926	0.891	0.607	0.939	0.924	0.893	0.678	0.883	0.935	0.895	0.867	0.898	0.868	0.925	0.760	-0.794	0.085
Ba	0.421	0.926	1	0.823	0.716	0.777	0.894	0.920	0.836	0.868	0.782	0.858	0.876	0.774	0.899	0.901	0.872	0.898	0.914	0.724	0.890	0.866	0.635	0.901	0.832	0.842	0.770	0.882	0.850	0.789	0.902	0.808	0.872	0.853	0.710	-0.691	0.033
Bi	0.517	0.860	0.823	1	0.458	0.706	0.794	0.813	0.806	0.859	0.822	0.802	0.852	0.694	0.788	0.864	0.704	0.828	0.740	0.780	0.845	0.791	0.481	0.887	0.815	0.754	0.500	0.762	0.807	0.798	0.752	0.776	0.723	0.821	0.657	-0.754	0.231
Ca	0.049	0.623	0.716	0.458	1	0.689	0.747	0.688	0.642	0.581	0.452	0.602	0.540	0.512	0.742	0.619	0.810	0.723	0.814	0.404	0.675	0.696	0.656	0.626	0.542	0.715	0.958	0.776	0.619	0.496	0.824	0.549	0.796	0.566	0.526	-0.239	-0.272
Cd	0.315	0.705	0.777	0.706	0.689	1	0.767	0.765	0.761	0.716	0.643	0.688	0.685	0.547	0.754	0.692	0.767	0.731	0.770	0.692	0.772	0.794	0.515	0.769	0.644	0.740	0.694	0.783	0.622	0.610	0.804	0.640	0.780	0.704	0.440	-0.459	-0.059
Ce	0.286	0.920	0.894	0.794	0.747	0.767	1	0.927	0.920	0.912	0.714	0.899	0.893	0.814	0.995	0.930	0.955	0.947	0.882	0.649	0.919	0.930	0.608	0.924	0.896	0.952	0.761	0.980	0.936	0.860	0.932	0.866	0.966	0.886	0.735	-0.702	0.031
Co	0.380	0.934	0.920	0.813	0.688	0.765	0.927	1	0.878	0.882	0.785	0.964	0.941	0.815	0.932	0.926	0.903	0.941	0.918	0.700	0.907	0.897	0.662	0.895	0.878	0.925	0.731	0.912	0.892	0.897	0.877	0.934	0.905	0.953	0.705	-0.719	0.025
Cr	0.284	0.895	0.836	0.806	0.642	0.761	0.920	0.878	1	0.919	0.697	0.880	0.872	0.791	0.910	0.900	0.880	0.903	0.800	0.745	0.872	0.980	0.539	0.917	0.876	0.917	0.675	0.911	0.877	0.828	0.855	0.853	0.897	0.863	0.704	-0.698	0.045
Cs	0.351	0.934	0.868	0.859	0.581	0.716	0.912	0.882	0.919	1	0.735	0.893	0.911	0.827	0.906	0.939	0.845	0.918	0.801	0.706	0.891	0.897	0.498	0.960	0.957	0.895	0.617	0.885	0.930	0.845	0.841	0.850	0.856	0.889	0.742	-0.793	0.143
Cu	0.578	0.794	0.782	0.822	0.452	0.643	0.714	0.785	0.697	0.735	1	0.739	0.772	0.604	0.724	0.771	0.682	0.765	0.699	0.779	0.759	0.724	0.530	0.740	0.729	0.687	0.501	0.699	0.695	0.723	0.693	0.722	0.688	0.753	0.530	-0.585	0.068
Fe	0.325	0.932	0.858	0.802	0.602	0.688	0.899	0.964	0.880	0.893	0.739	1	0.960	0.835	0.904	0.936	0.865	0.932	0.844	0.669	0.882	0.873	0.638	0.875	0.898	0.916	0.655	0.874	0.910	0.939	0.817	0.976	0.864	0.970	0.731	-0.772	0.054
Ga	0.393	0.962	0.876	0.852	0.540	0.685	0.893	0.941	0.872	0.911	0.772	0.960	1	0.829	0.902	0.955	0.834	0.925	0.819	0.691	0.918	0.857	0.588	0.912	0.916	0.896	0.594	0.855	0.910	0.948	0.800	0.946	0.838	0.965	0.717	-0.819	0.133
K	0.332	0.845	0.774	0.694	0.512	0.547	0.814	0.815	0.791	0.827	0.604	0.835	0.829	1	0.815	0.844	0.785	0.844	0.760	0.552	0.762	0.783	0.515	0.797	0.892	0.805	0.620	0.791	0.859	0.802	0.740	0.804	0.774	0.833	0.802	-0.756	0.067
La	0.304	0.926	0.899	0.788	0.742	0.754	0.995	0.932	0.910	0.906	0.724	0.904	0.902	0.815	1	0.937	0.960	0.950	0.883	0.647	0.922	0.921	0.618	0.916	0.899	0.951	0.756	0.980	0.936	0.865	0.928	0.872	0.970	0.894	0.727	-0.698	0.009
Li	0.377	0.975	0.901	0.864	0.619	0.692	0.930	0.926	0.900	0.939	0.771	0.936	0.955	0.844	0.937	1	0.874	0.963	0.838	0.696	0.927	0.890	0.619	0.938	0.931	0.904	0.663	0.892	0.945	0.908	0.846	0.907	0.873	0.934	0.772	-0.789	0.104
Lu	0.268	0.870	0.872	0.704	0.810	0.767	0.955	0.903	0.880	0.845	0.682	0.865	0.834	0.785	0.960	0.874	1	0.906	0.879	0.592	0.882	0.906	0.628	0.863	0.835	0.943	0.825	0.981	0.870	0.796	0.927	0.818	0.989	0.846	0.695	-0.592	-0.234
Mg	0.306	0.957	0.898	0.828	0.723	0.731	0.947	0.941	0.903	0.918	0.765	0.932	0.925	0.844	0.950	0.963	0.906	1	0.897	0.689	0.922	0.903	0.693	0.918	0.917	0.932	0.757	0.919	0.941	0.893	0.900	0.902	0.908	0.933	0.762	-0.719	0.056
Mn	0.274	0.858	0.914	0.740	0.814	0.770	0.882	0.918	0.800	0.801	0.699	0.844	0.819	0.760	0.883	0.838	0.879	0.897	1	0.649	0.845	0.836	0.687	0.833	0.785	0.853	0.834	0.877	0.826	0.760	0.900	0.801	0.876	0.833	0.698	-0.574	-0.027
Mo	0.448	0.709	0.724	0.780	0.404	0.692	0.649	0.700	0.745	0.706	0.779	0.669	0.691	0.552	0.647	0.696	0.592	0.689	0.649	1	0.696	0.748	0.456	0.731	0.652	0.623	0.424	0.627	0.612	0.629	0.657	0.633	0.606	0.680	0.465	-0.525	0.156
Nb	0.366	0.926	0.890	0.845	0.675	0.772	0.919	0.907	0.872	0.891	0.759	0.882	0.918	0.762	0.922	0.927	0.882	0.922	0.845	0.696	1	0.872	0.556	0.927	0.872	0.904	0.700	0.898	0.886	0.891	0.877	0.868	0.884	0.893	0.668	-0.742	0.041
Ni	0.308	0.891	0.866	0.791	0.696	0.794	0.930	0.897	0.980	0.897	0.724	0.873	0.857	0.783	0.921	0.890	0.906	0.903	0.836	0.748	0.872	1	0.569	0.901	0.851	0.919	0.733	0.928	0.858	0.807	0.889	0.847	0.919	0.855	0.690	-0.665	-0.021
P	0.165	0.607	0.635	0.481	0.656	0.515	0.608	0.662	0.539	0.498	0.530	0.638	0.588	0.515	0.618	0.619	0.628	0.693	0.687	0.456	0.556	0.569	1	0.527	0.509	0.587	0.659	0.594	0.558	0.577	0.617	0.616	0.605	0.644	0.456	-0.351	-0.123
Pb	0.376	0.939	0.901	0.887	0.626	0.769	0.924	0.895	0.917	0.960	0.740	0.875	0.912	0.797	0.916	0.938	0.863	0.918	0.833	0.731	0.927	0.901	0.527	1	0.907	0.891	0.654	0.898	0.910	0.839	0.875	0.834	0.871	0.879	0.722	-0.772	0.114
Rb	0.371	0.924	0.832	0.815	0.542	0.644	0.896	0.878	0.876	0.957	0.729	0.898	0.916	0.892	0.899	0.931	0.835	0.917	0.785	0.652	0.872	0.851	0.509	0.907	1	0.885	0.592	0.865	0.940	0.862	0.805	0.860	0.841	0.902	0.758	-0.797	0.140
Sc	0.259	0.893	0.842	0.754	0.715	0.740	0.952	0.925	0.917	0.895	0.687	0.916	0.896	0.805	0.951	0.904	0.943	0.932	0.853	0.623	0.904	0.919	0.587	0.891	0.885	1	0.734	0.956	0.907	0.867	0.876	0.894	0.952	0.907	0.694	-0.676	-0.045
Sr	0.127	0.678	0.770	0.500	0.958	0.694	0.761	0.731	0.675	0.617	0.501	0.655	0.594	0.620	0.756	0.663	0.825	0.757	0.834	0.424	0.700	0.733	0.659	0.654	0.592	0.734	1	0.788	0.658	0.557	0.843	0.610	0.803	0.623	0.601	-0.333	-0.254
Tb	0.286	0.883	0.882	0.762	0.776	0.783	0.980	0.912	0.911	0.885	0.699	0.874	0.855	0.791	0.980	0.892	0.981	0.919	0.877	0.627	0.898	0.928	0.594	0.898	0.865	0.956	0.788	1	0.898	0.813	0.940	0.831	0.994	0.859	0.704	-0.641	-0.085
Th	0.296	0.935	0.850	0.807	0.619	0.622	0.936	0.892	0.877	0.930	0.695	0.910	0.910	0.859	0.936	0.945	0.870	0.941	0.826	0.612	0.886	0.858	0.558	0.910	0.940	0.907	0.658	0.898	1	0.884	0.855	0.882	0.875	0.891	0.836	-0.762	0.125
Ti	0.315	0.895	0.789	0.798	0.496	0.610	0.860	0.897	0.828	0.845	0.723	0.939	0.948	0.802	0.865	0.908	0.796	0.893	0.760	0.629	0.891	0.807	0.577	0.839	0.862	0.867	0.557	0.813	0.884	1	0.747	0.964	0.795	0.943	0.706	-0.784	0.125
U	0.273	0.867	0.902	0.752	0.824	0.804	0.932	0.877	0.855	0.841	0.693	0.817	0.800	0.740	0.928	0.846	0.927	0.900	0.900	0.657	0.877	0.889	0.617	0.875	0.805	0.876	0.843	0.940	0.855	0.747	1	0.765	0.933	0.807	0.689	-0.608	-0.072
V	0.305	0.898	0.808	0.776	0.549	0.640	0.866	0.934	0.853	0.850	0.722	0.976	0.946	0.804	0.872	0.907	0.818	0.902	0.801	0.633	0.868	0.847	0.616	0.834	0.860	0.894	0.610	0.831	0.882	0.964	0.765	1	0.818	0.955	0.708	-0.772	0.089
Y	0.273	0.868	0.872	0.723	0.796	0.780	0.966	0.905	0.897	0.856	0.688	0.864	0.838	0.774	0.970	0.873	0.989	0.908	0.876	0.606	0.884	0.919	0.605	0.871	0.841	0.952	0.803	0.994	0.875	0.795	0.933	0.818	1	0.845	0.679	-0.600	-0.147
Zn	0.373	0.925	0.853	0.821	0.566	0.704	0.886	0.953	0.863	0.889	0.753	0.970	0.965	0.833	0.894	0.934	0.846	0.933	0.833	0.680	0.893	0.855	0.644	0.879	0.902	0.907	0.623	0.859	0.891	0.943	0.807	0.955	0.845	1	0.699	-0.791	0.072
Zr	0.250	0.760	0.710	0.657	0.526	0.440	0.735	0.705	0.704	0.742	0.530	0.731	0.717	0.802	0.727	0.772	0.695	0.762	0.698	0.465	0.668	0.690	0.456	0.722	0.758	0.694	0.601	0.704	0.836	0.706	0.689	0.708	0.679	0.699	1	-0.655	0.084
Na	-0.373	-0.794	-0.691	-0.754	-0.239	-0.459	-0.702	-0.719	-0.698	-0.793	-0.585	-0.772	-0.819	-0.756	-0.698	-0.789	-0.592	-0.719	-0.574	-0.525	-0.742	-0.665	-0.351	-0.772	-0.797	-0.676	-0.333	-0.641	-0.762	-0.784	-0.608	-0.772	-0.600	-0.791	-0.655	1	-0.292
Ce-Lu	0.077	0.085	0.033	0.231	-0.272	-0.059	0.031	0.025	0.045	0.143	0.068	0.054	0.133	0.067	0.009	0.104	-0.234	0.056	-0.027	0.156	0.041	-0.021	-0.123	0.114	0.140	-0.045	-0.254	-0.085	0.125	0.125	-0.072	0.089	-0.147	0.072	0.084	-0.292	1

Appendix III
Factor Analyses

MMI

Factor pattern after Varimax rotation:

	D1	D2	D3	D4
Ash	0.017	0.651	-0.075	-0.280
logAg	0.426	0.292	-0.180	0.077
logAl_PPM	0.096	0.818	0.157	0.281
logBa	0.609	-0.373	0.003	0.559
Ca_PPM	0.006	-0.950	-0.012	0.039
logCd	0.015	0.265	0.326	-0.323
logCe	0.914	0.201	0.013	0.080
logCo	0.308	-0.241	0.708	0.003
logCu	0.373	-0.084	0.453	-0.087
logDy	0.972	-0.073	0.093	0.022
logEr	0.954	-0.130	0.171	0.004
logEu	0.973	-0.019	0.025	0.092
logFe_PPM	0.127	0.289	0.828	0.066
logGd	0.993	-0.021	0.015	-0.010
logLa	0.926	0.224	-0.017	0.057
logMg_PPM	0.120	-0.800	0.130	0.317
logNb	0.025	0.905	0.051	-0.066
logNd	0.970	0.126	0.004	-0.001
logNi	0.118	-0.668	0.549	-0.134
logPb	0.364	0.687	0.030	0.400
logPr	0.957	0.167	0.021	0.013
logRb	-0.087	0.882	-0.121	-0.089
logSc	0.798	0.255	0.331	0.218
logSm	0.996	0.031	0.012	-0.013
logSr	0.107	-0.848	0.019	0.421
logTh	0.864	-0.034	-0.042	0.172
logTi	0.068	0.955	0.106	0.132
logU	0.441	-0.579	0.301	-0.089
logY	0.955	-0.133	0.161	-0.003
logYb	0.916	-0.161	0.253	0.005
logZn	0.047	0.719	0.072	-0.050
logZr	0.483	0.805	0.000	0.068

Factor 1		Factor 2		Factor 3		Factor 4	
logSm	0.996	**logTi**	0.955	**logFe_PPM**	0.828	**logBa**	0.559
logGd	0.993	**logNb**	0.905	**logCo**	0.708	**logSr**	0.421
logEu	0.973	**logRb**	0.882	**logNi**	0.549	**logPb**	0.400
logDy	0.972	**logAl_PPM**	0.818	**logCu**	0.453	**logMg_PPM**	0.317
logNd	0.970	**logZr**	0.805	**logSc**	0.331	logAl_PPM	0.281
logPr	0.957	**logZn**	0.719	**logCd**	0.326	logSc	0.218
logY	0.955	**logPb**	0.687	**logU**	0.301	logTh	0.172
logEr	0.954	Ash	0.651	logYb	0.253	logTi	0.132
logLa	0.926	logAg	0.292	logEr	0.171	logEu	0.092
logYb	0.916	logFe_PPM	0.289	logY	0.161	logCe	0.080
logCe	0.914	logCd	0.265	logAl_PPM	0.157	logAg	0.077
logTh	0.864	logSc	0.255	logMg_PPM	0.130	logZr	0.068
logSc	0.798	logLa	0.224	logTi	0.106	logFe_PPM	0.066
logBa	0.609	logCe	0.201	logDy	0.093	logLa	0.057
logZr	0.483	logPr	0.167	logZn	0.072	Ca_PPM	0.039
logU	0.441	logNd	0.126	logNb	0.051	logDy	0.022
logAg	0.426	logSm	0.031	logPb	0.030	logPr	0.013
logCu	0.373	logEu	-0.019	logEu	0.025	logYb	0.005
logPb	0.364	logGd	-0.021	logPr	0.021	logEr	0.004
logCo	0.308	logTh	-0.034	logSr	0.019	logCo	0.003
logFe_PPM	0.127	logDy	-0.073	logGd	0.015	logNd	-0.001
logMg_PPM	0.120	logCu	-0.084	logCe	0.013	logY	-0.003
logNi	0.118	logEr	-0.130	logSm	0.012	logGd	-0.010
logSr	0.107	logY	-0.133	logNd	0.004	logSm	-0.013
logAl_PPM	0.096	logYb	-0.161	logBa	0.003	logZn	-0.050
logTi	0.068	logCo	-0.241	logZr	0.000	logNb	-0.066
logZn	0.047	logBa	-0.373	Ca_PPM	-0.012	logCu	-0.087
logNb	0.025	logU	-0.579	logLa	-0.017	logRb	-0.089
Ash	0.017	logNi	-0.668	logTh	-0.042	logU	-0.089
logCd	0.015	logMg_PPM	-0.800	Ash	-0.075	logNi	-0.134
Ca_PPM	0.006	logSr	-0.848	logRb	-0.121	Ash	-0.280
logRb	-0.087	Ca_PPM	-0.950	logAg	-0.180	logCd	-0.323

Aqua Regia

Factor pattern after Varimax rotation:

	D1	D2	D3
logAg_ICM	0.199	-0.180	0.561
logAl_ICM1	0.843	0.402	0.328
logBa_ICM	0.658	0.576	0.360
logBi_ICM1	0.688	0.296	0.602
logCa_ICM	0.251	0.941	0.017
logCd_ICM	0.349	0.671	0.466
logCe_ICM	0.708	0.615	0.266
logCo_ICM	0.801	0.510	0.229
logCr_ICM1	0.681	0.504	0.380
logCs_ICM1	0.793	0.387	0.396
logCu_ICM	0.466	0.207	0.707
logFe_ICM	0.862	0.426	0.188
logGa_ICM	0.889	0.329	0.277
logK_ICM1	0.837	0.340	-0.020
logLa_ICM1	0.726	0.601	0.272
logLi_ICM1	0.815	0.412	0.356
logLu_ICM	0.608	0.736	0.205
logMg_ICM	0.796	0.518	0.267
logMn_ICM	0.579	0.691	0.221
logMo_ICM	0.347	0.299	0.764
logNb_ICM	0.774	0.465	0.340
logNi_ICM1	0.646	0.592	0.377
logP_ICM1	0.487	0.447	0.036
logPb_ICM	0.716	0.469	0.424
logRb_ICM	0.865	0.336	0.304
logSc_ICM1	0.758	0.558	0.218
logSr_ICM1	0.281	0.853	0.020
logTb_ICM	0.639	0.670	0.268
logTh_ICM	0.844	0.410	0.234
logTi_ICM1	0.890	0.257	0.121
logU_ICM1	0.576	0.725	0.291
logV_ICM1	0.880	0.339	0.148
logY_ICM1	0.627	0.709	0.220
logZn_ICM	0.864	0.362	0.253
logZr_ICM1	0.698	0.315	0.073
Na_ICM14I	-0.843	0.073	-0.234
Ce-Lu	0.188	-0.357	0.174

	D1		D2		D3
logTi_ICM1	0.890	logCa_ICM	0.941	logMo_ICM	0.764
logGa_ICM	0.889	logSr_ICM1	0.853	logCu_ICM	0.707
logV_ICM1	0.880	logLu_ICM1	0.736	logBi_ICM1	0.602
logRb_ICM	0.865	logU_ICM1	0.725	logAg_ICM	0.561
logZn_ICM	0.864	logY_ICM1	0.709	logCd_ICM	0.466
logFe_ICM	0.862	logMn_ICM	0.691	logPb_ICM	0.424
logTh_ICM	0.844	logCd_ICM	0.671	logCs_ICM1	0.396
logAl_ICM1	0.843	logTb_ICM	0.670	logCr_ICM1	0.380
logK_ICM1	0.837	logCe_ICM	0.615	logNi_ICM1	0.377
logLi_ICM1	0.815	logLa_ICM1	0.601	logBa_ICM	0.360
logCo_ICM	0.801	logNi_ICM1	0.592	logLi_ICM1	0.356
logMg_ICM	0.796	logBa_ICM	0.576	logNb_ICM	0.340
logCs_ICM1	0.793	logSc_ICM1	0.558	logAl_ICM1	0.328
logNb_ICM	0.774	logMg_ICM	0.518	logRb_ICM	0.304
logSc_ICM1	0.758	logCo_ICM	0.510	logU_ICM1	0.291
logLa_ICM1	0.726	logCr_ICM1	0.504	logGa_ICM	0.277
logPb_ICM	0.716	logPb_ICM	0.469	logLa_ICM1	0.272
logCe_ICM	0.708	logNb_ICM	0.465	logTb_ICM	0.268
logZr_ICM1	0.698	logP_ICM1	0.447	logMg_ICM	0.267
logBi_ICM1	0.688	logFe_ICM	0.426	logCe_ICM	0.266
logCr_ICM1	0.681	logLi_ICM1	0.412	logZn_ICM	0.253
logBa_ICM	0.658	logTh_ICM	0.410	logTh_ICM	0.234
logNi_ICM1	0.646	logAl_ICM1	0.402	logCo_ICM	0.229
logTb_ICM	0.639	logCs_ICM1	0.387	logMn_ICM	0.221
logY_ICM1	0.627	logZn_ICM	0.362	logY_ICM1	0.220
logLu_ICM1	0.608	logK_ICM1	0.340	logSc_ICM1	0.218
logMn_ICM	0.579	logV_ICM1	0.339	logLu_ICM1	0.205
logU_ICM1	0.576	logRb_ICM	0.336	logFe_ICM	0.188
logP_ICM1	0.487	logGa_ICM	0.329	Ce-Lu	0.174
logCu_ICM	0.466	logZr_ICM1	0.315	logV_ICM1	0.148
logCd_ICM	0.349	logMo_ICM	0.299	logTi_ICM1	0.121
logMo_ICM	0.347	logBi_ICM1	0.296	logZr_ICM1	0.073
logSr_ICM1	0.281	logTi_ICM1	0.257	logP_ICM1	0.036
logCa_ICM	0.251	logCu_ICM	0.207	logSr_ICM1	0.020
logAg_ICM	0.199	Na_ICM14I	0.073	logCa_ICM	0.017
Ce-Lu	0.188	logAg_ICM	-0.180	logK_ICM1	-0.020
Na_ICM14I	-0.843	Ce-Lu	-0.357	Na_ICM14I	-0.234

Western Copper MMI Test
Zone 1 - North Profile

Factor Scores

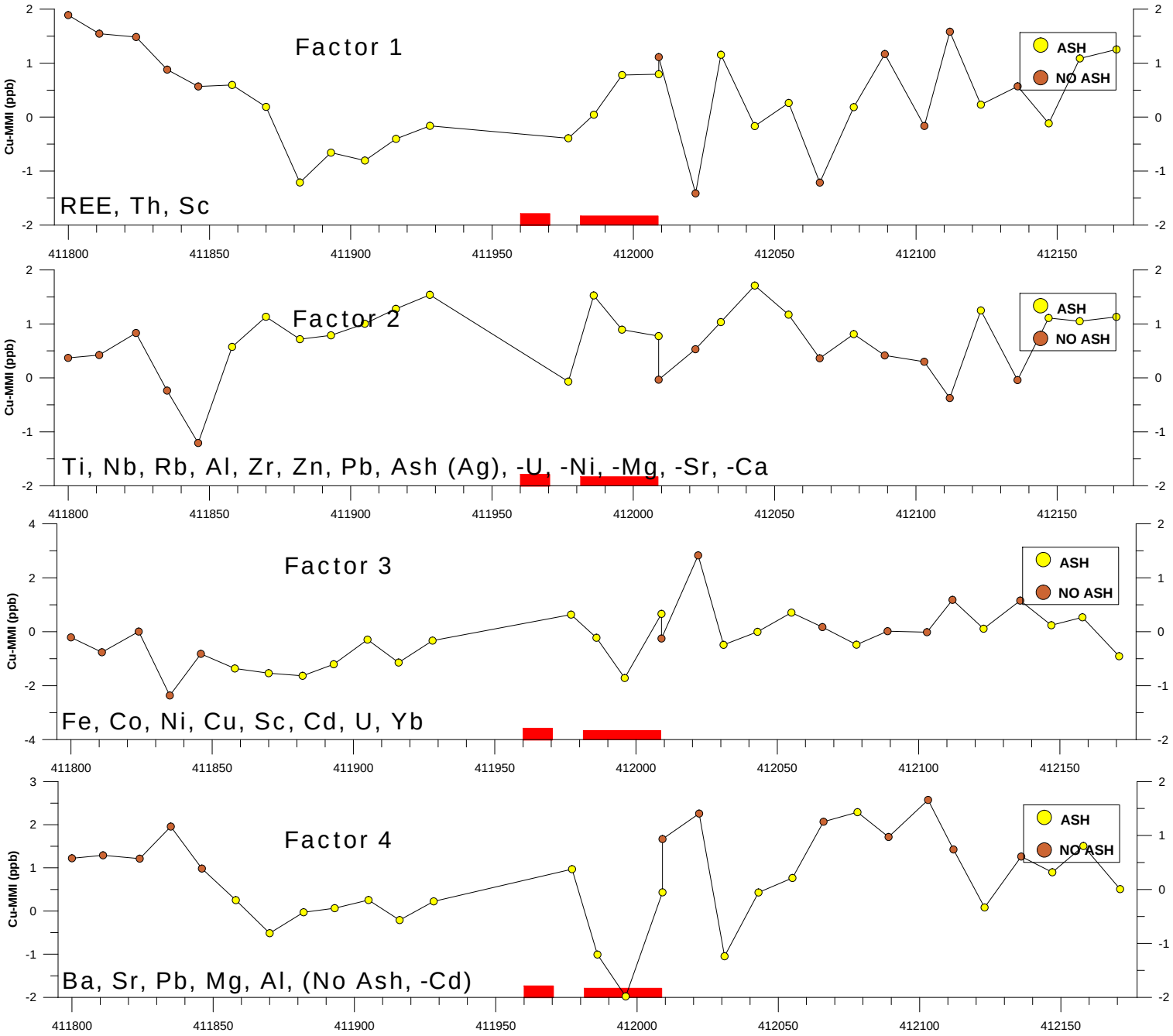

G. N. LUSTIG CONSULTING LTD.- December 27, 2008

Western Copper MMI Test
Zone 1 - South Profile

Factor Scores

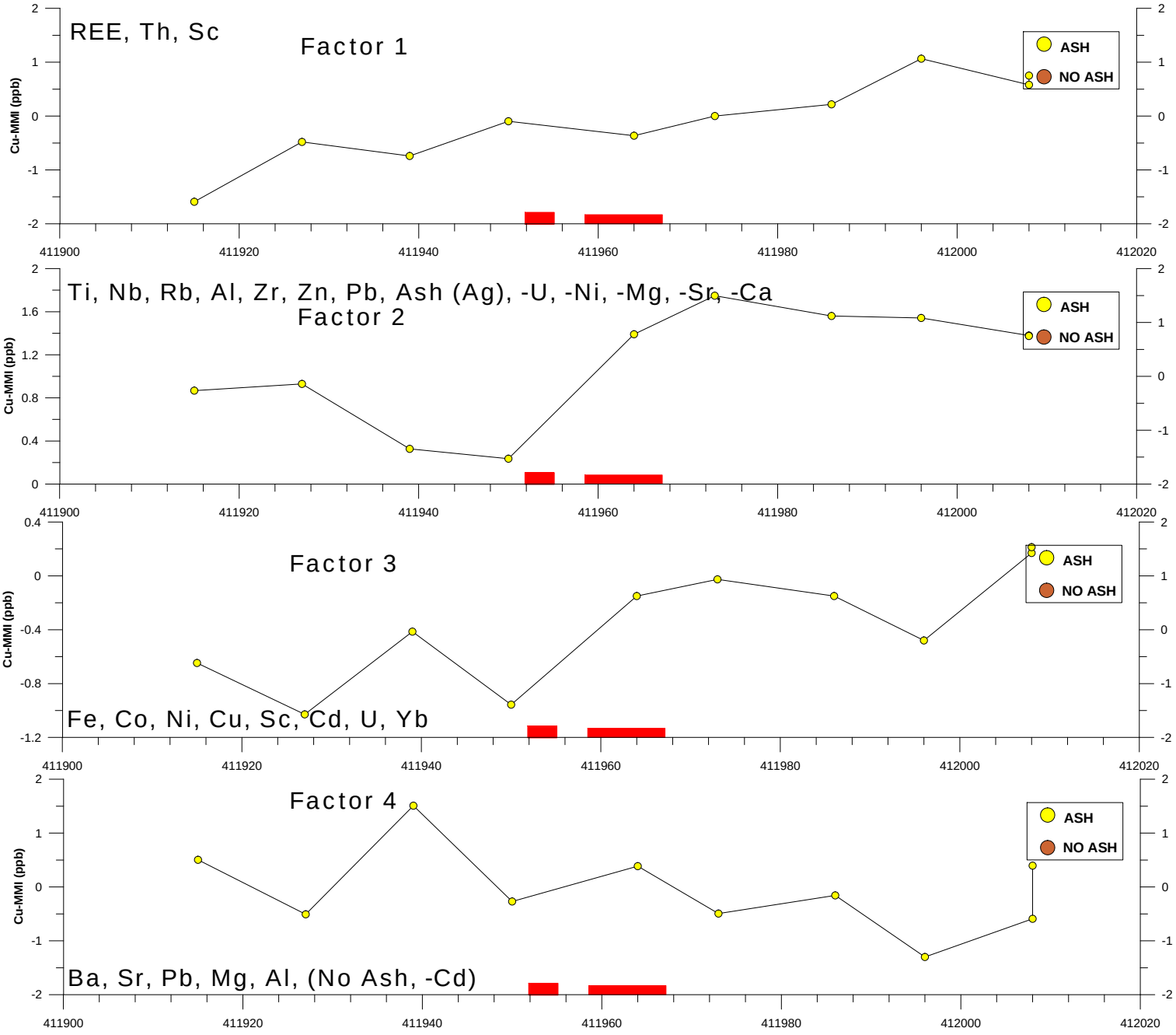

G. N. LUSTIG CONSULTING LTD.- December 27, 2008

Western Copper MMI Test
Line 4400S - 30 m North

Factor Scores

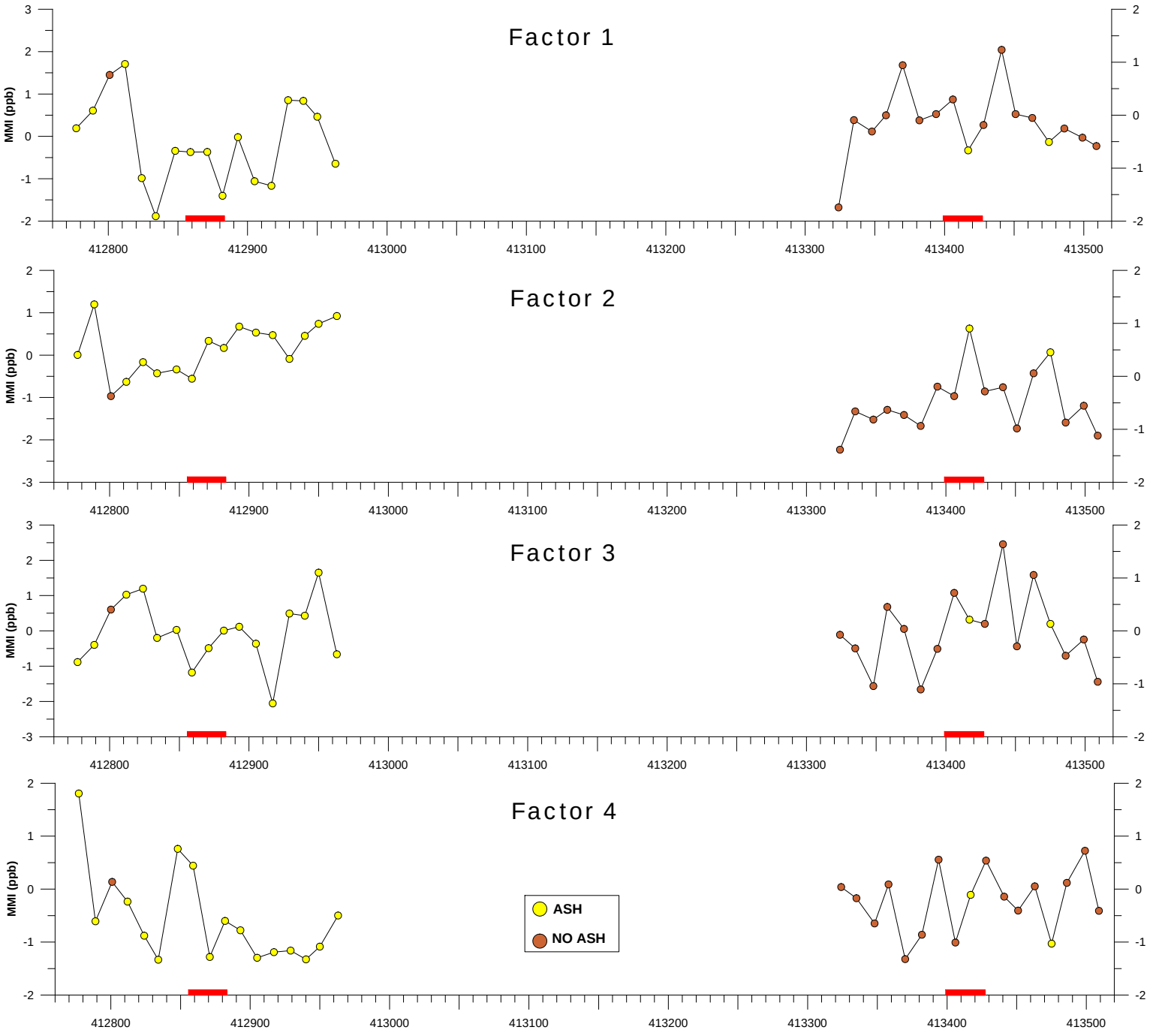

G. N. LUSTIG CONSULTING LTD.- December 11, 2008

Western Copper MMI Test
Line 4400S - 25 m South

Factor Scores

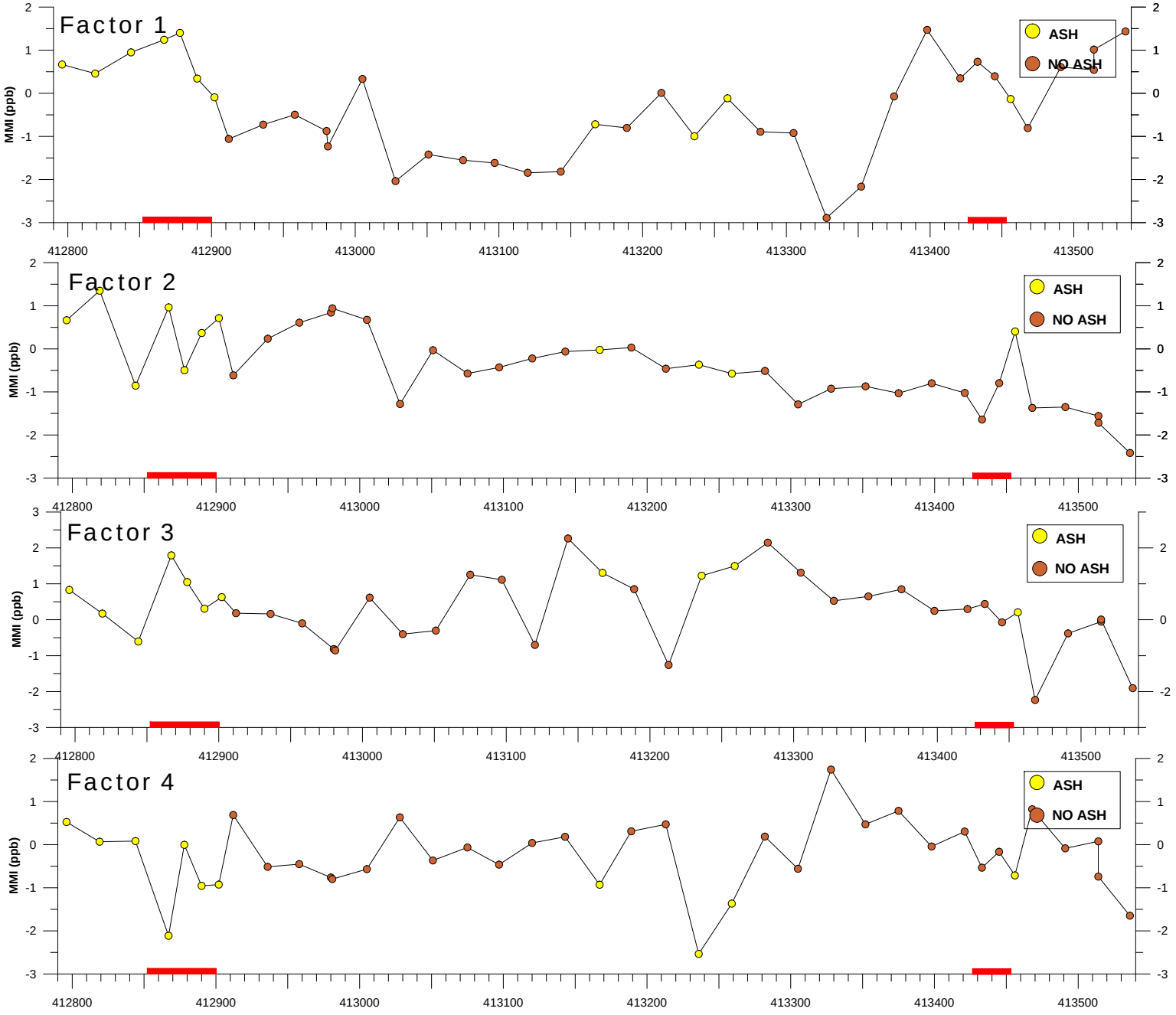

G. N. LUSTIG CONSULTING LTD.- December 27, 2008

Appendix IV
MMI Copper-Gold Profiles

Western Copper MMI Test
Zone 1 - North Profile

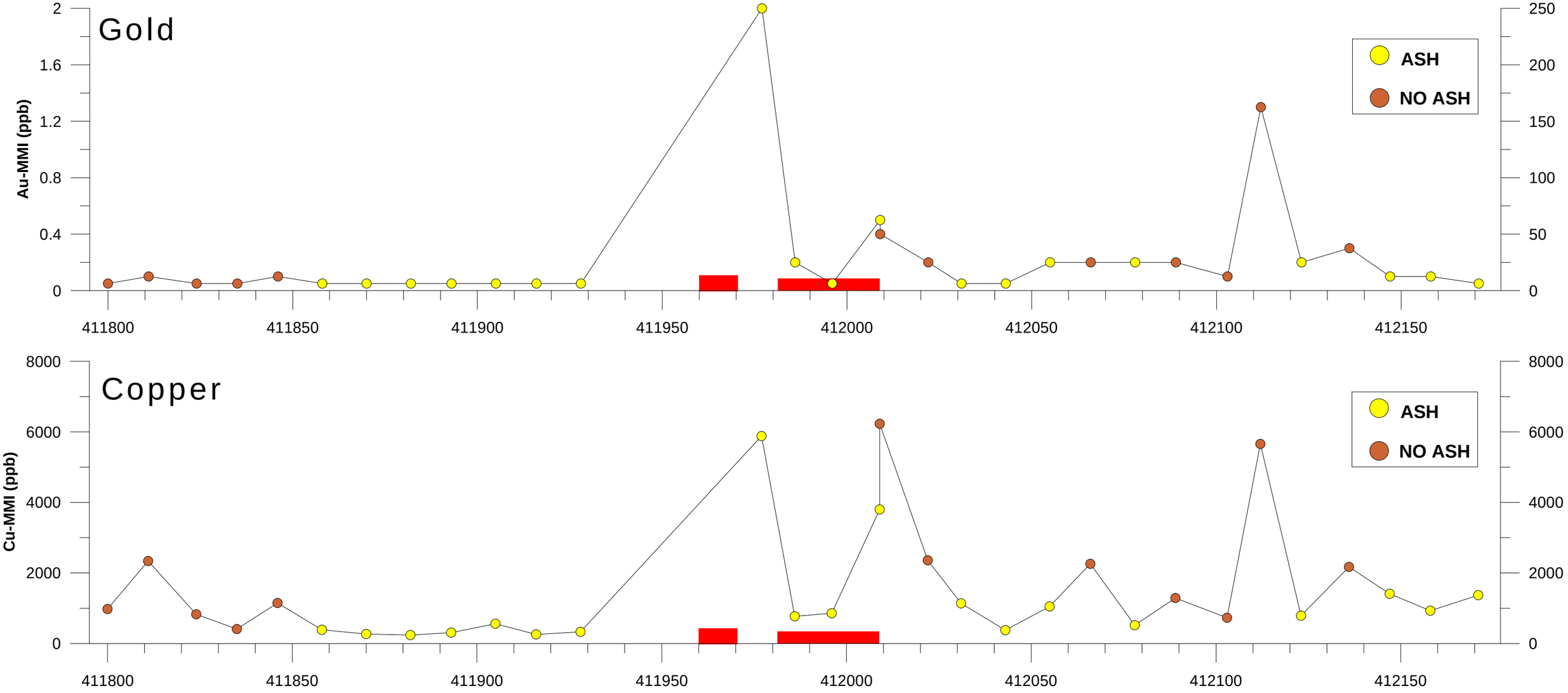

G. N. LUSTIG CONSULTING LTD.- February 4, 2008

Western Copper MMI Test
Line 4400S - 25 m South

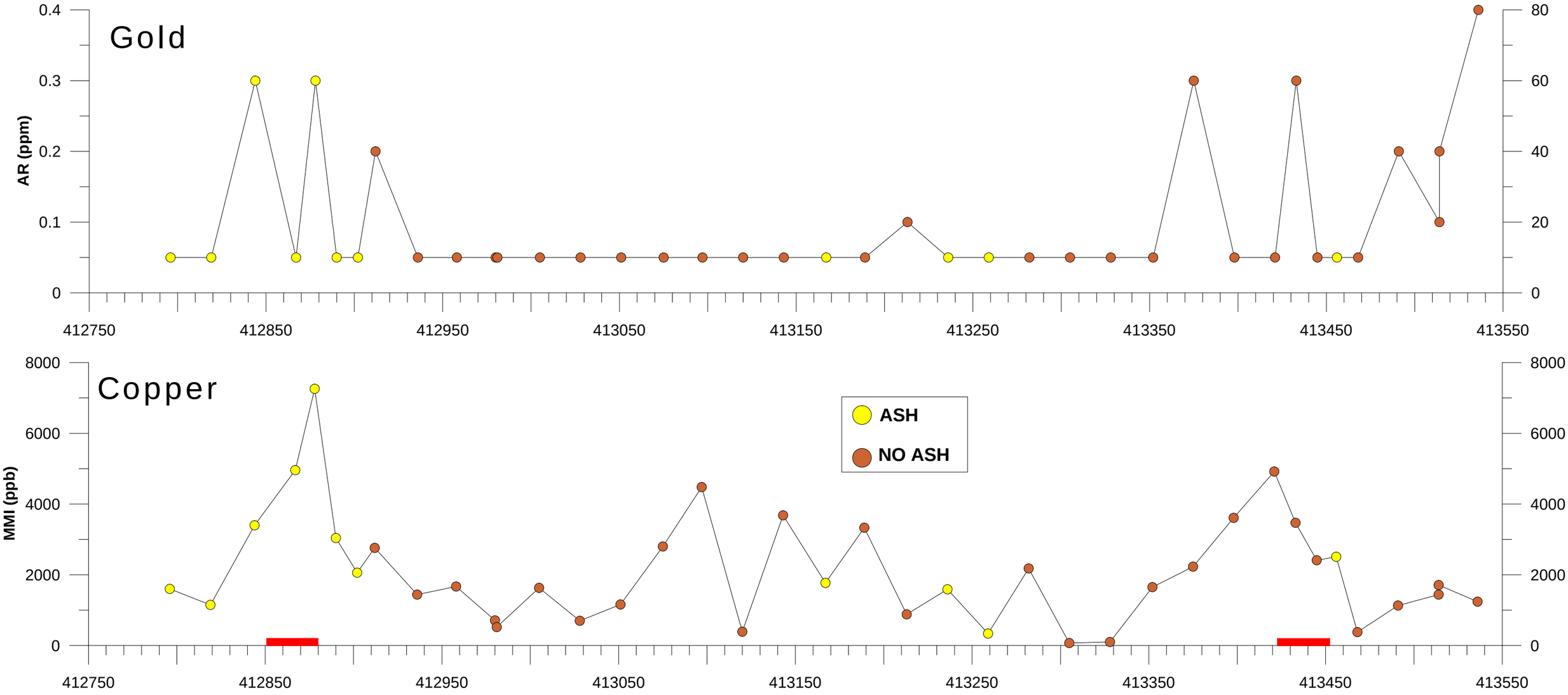

G. N. LUSTIG CONSULTING LTD.- February 3, 2009

Western Copper MMI Test
Line 4400S - 30 m North

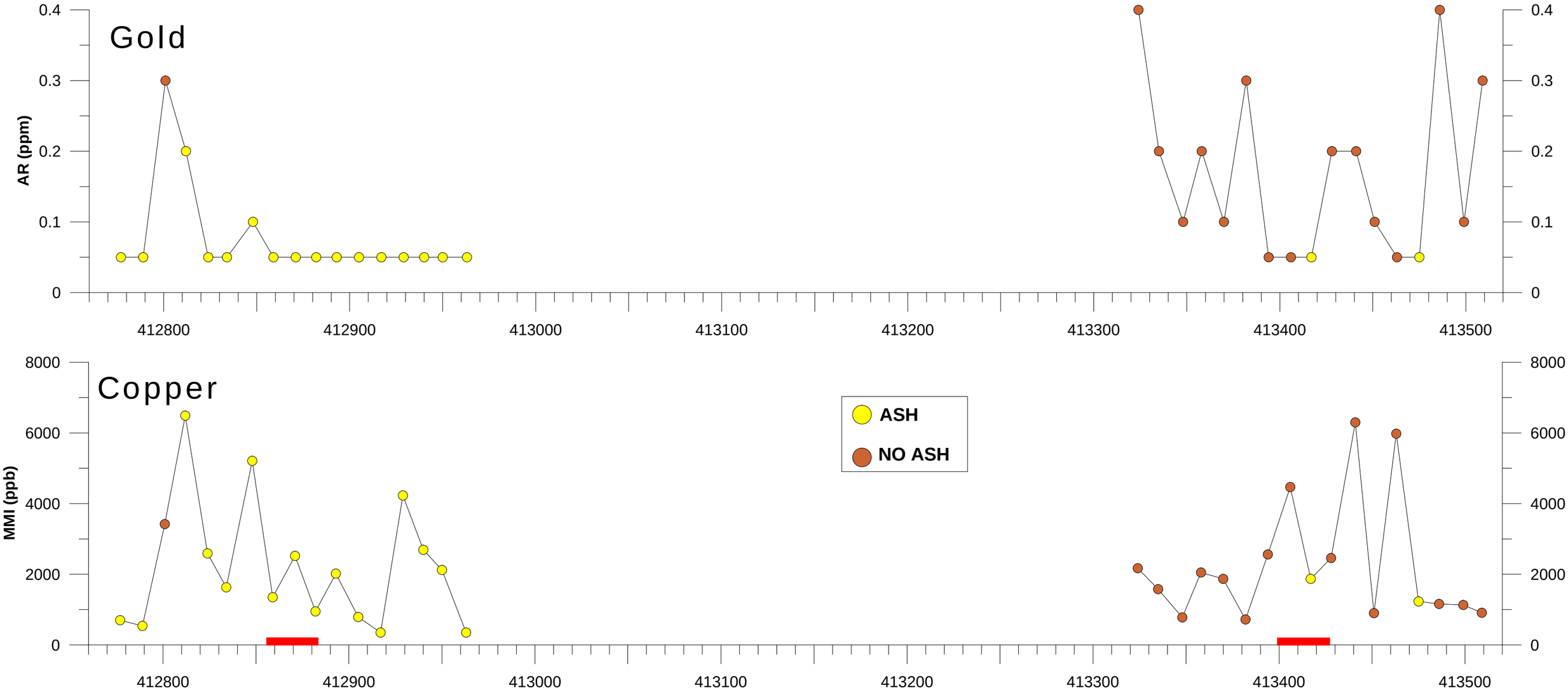

G. N. LUSTIG CONSULTING LTD.- February 3, 2009

Western Copper MMI Test
Zone 1 - South Profile

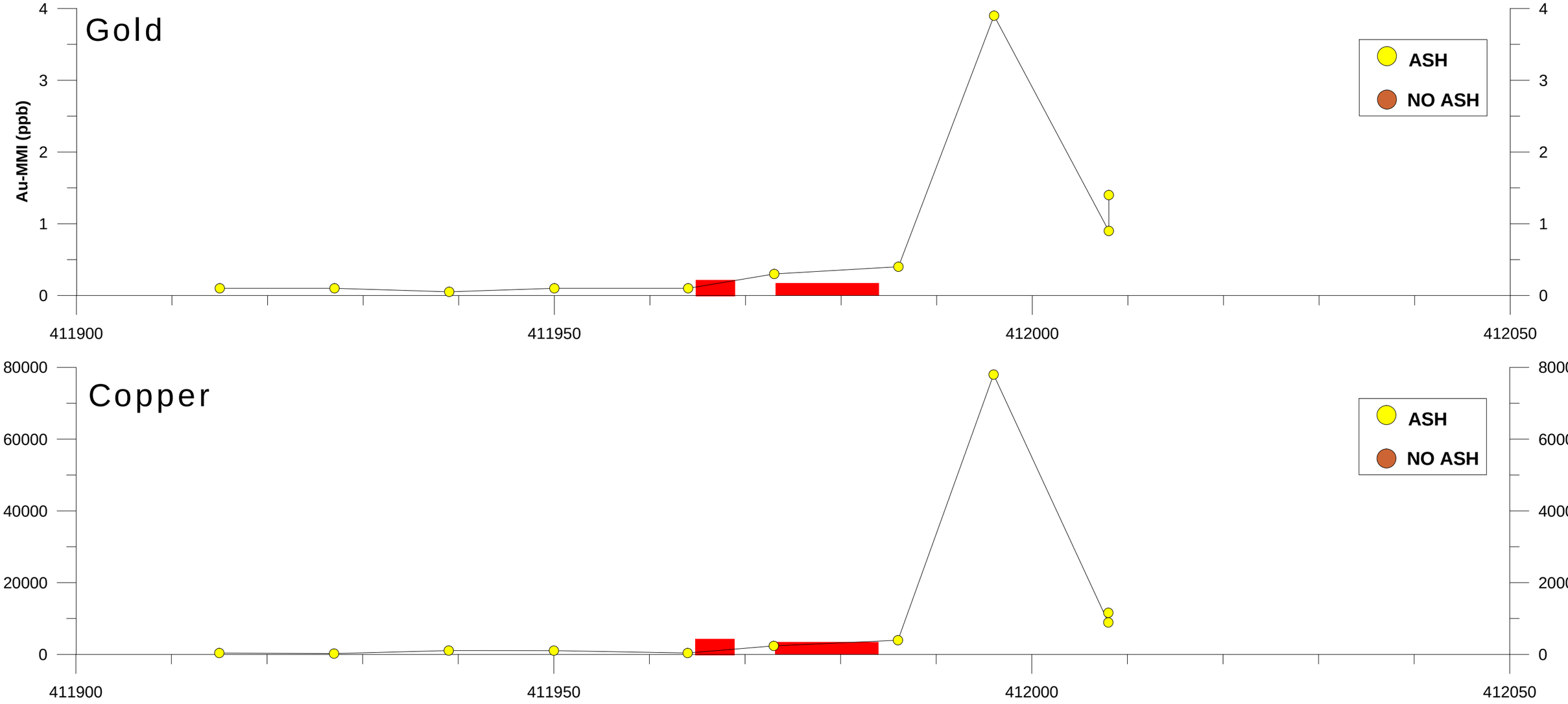

G. N. LUSTIG CONSULTING LTD.- February 4, 2008

Appendix V
MMI-Aqua Regia Profile Plots

Zone 1
North Profile

Western Copper MMI Test
Zone 1 - North Profile
Silver

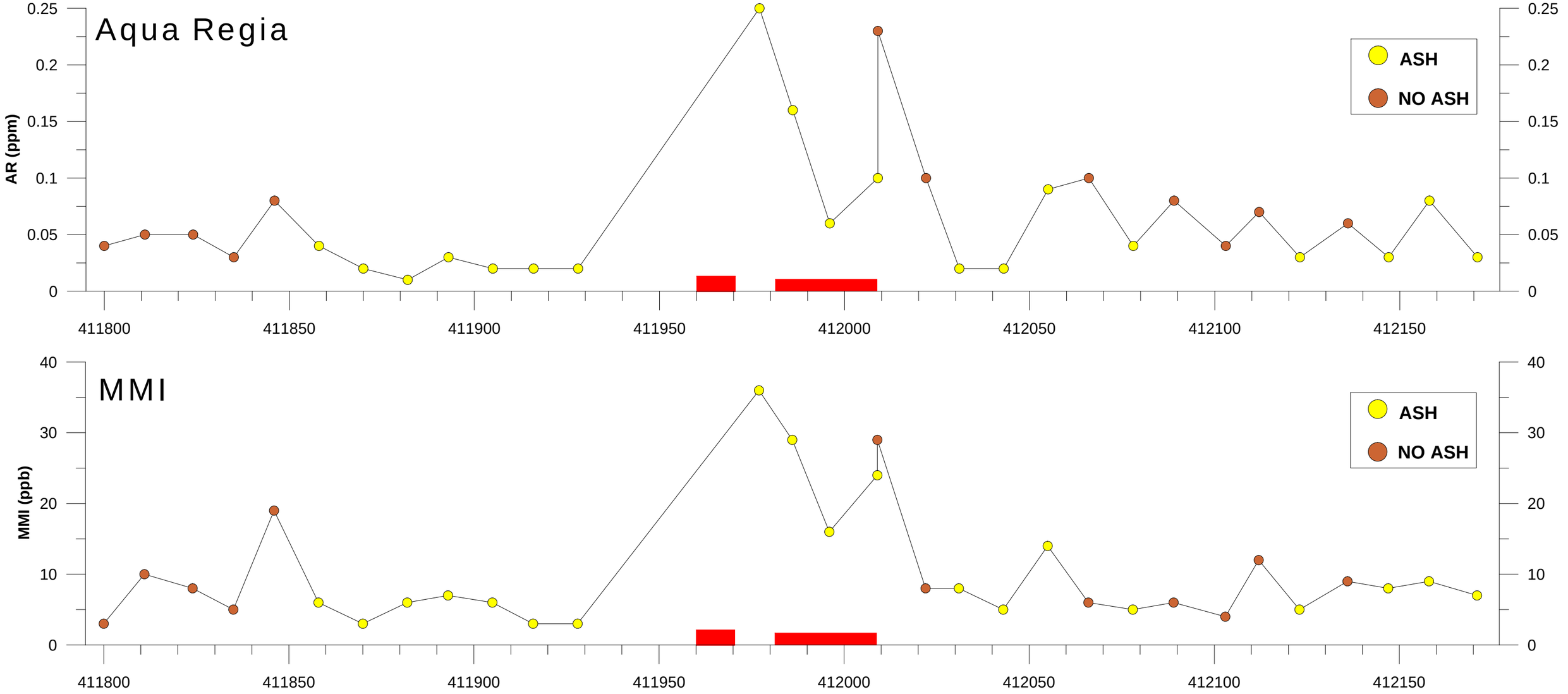

G. N. LUSTIG CONSULTING LTD.- November 13, 2008

Western Copper MMI Test
Zone 1 - North Profile
Aluminum

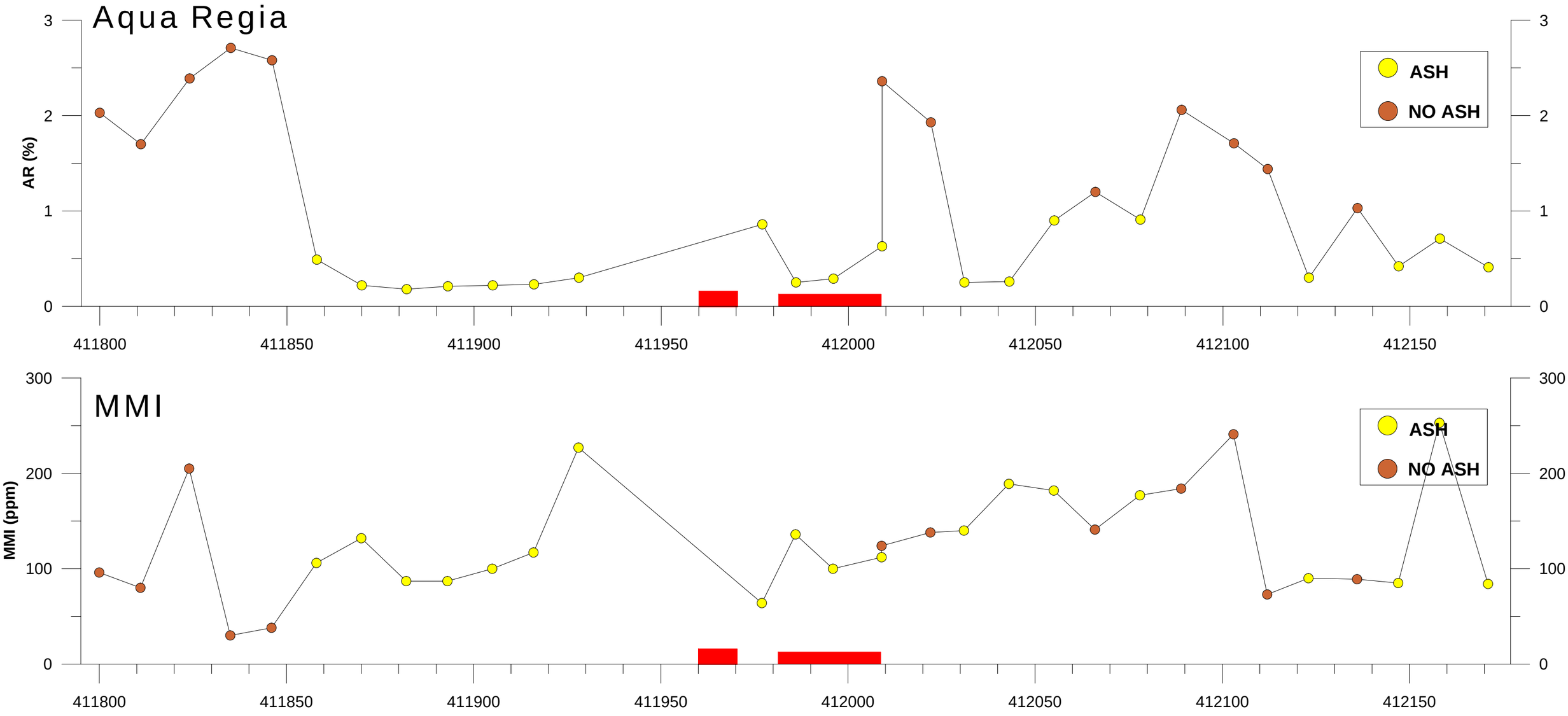

G. N. LUSTIG CONSULTING LTD.- November 13, 2008

Western Copper MMI Test
Zone 1 - North Profile
Arsenic

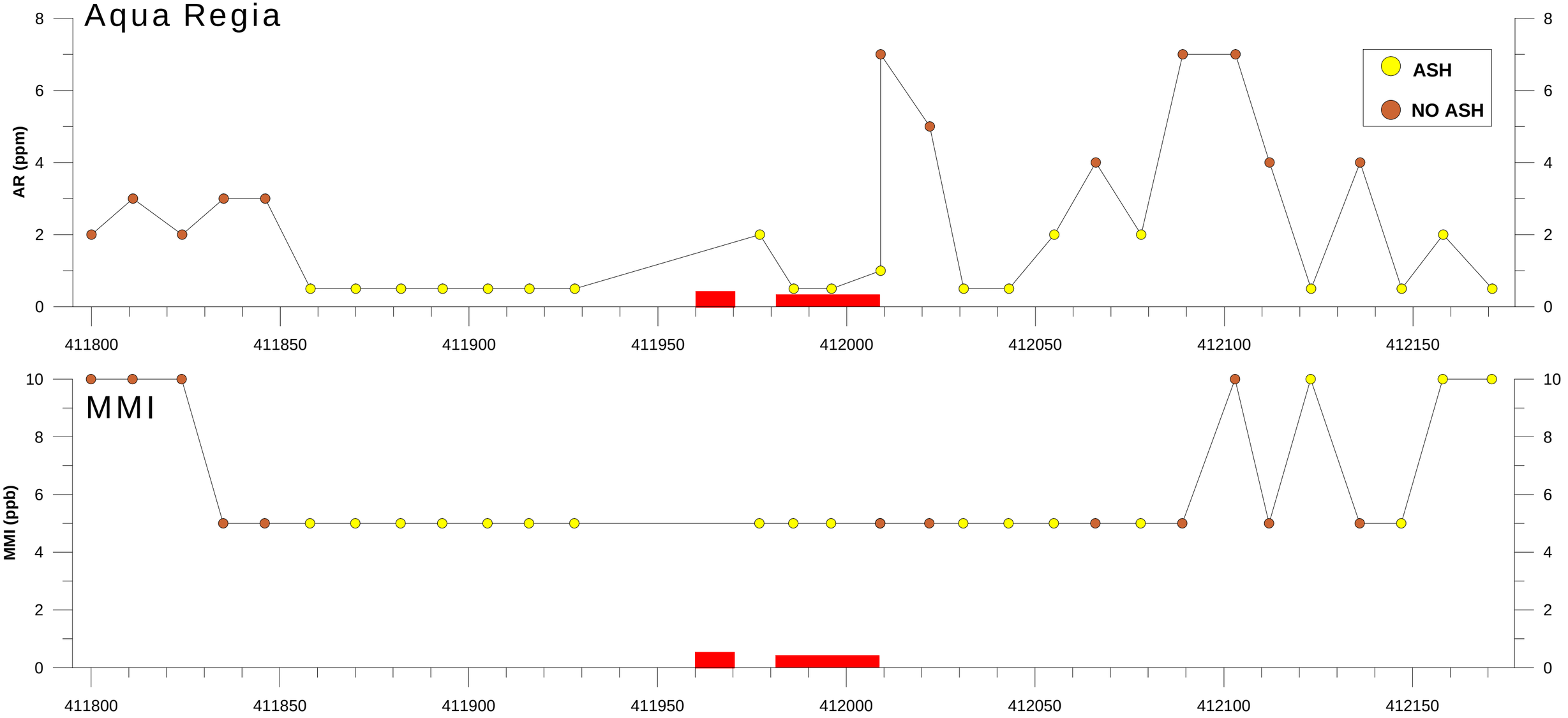

G. N. LUSTIG CONSULTING LTD.- November 13, 2008

Western Copper MMI Test
Zone 1 - North Profile
Barium

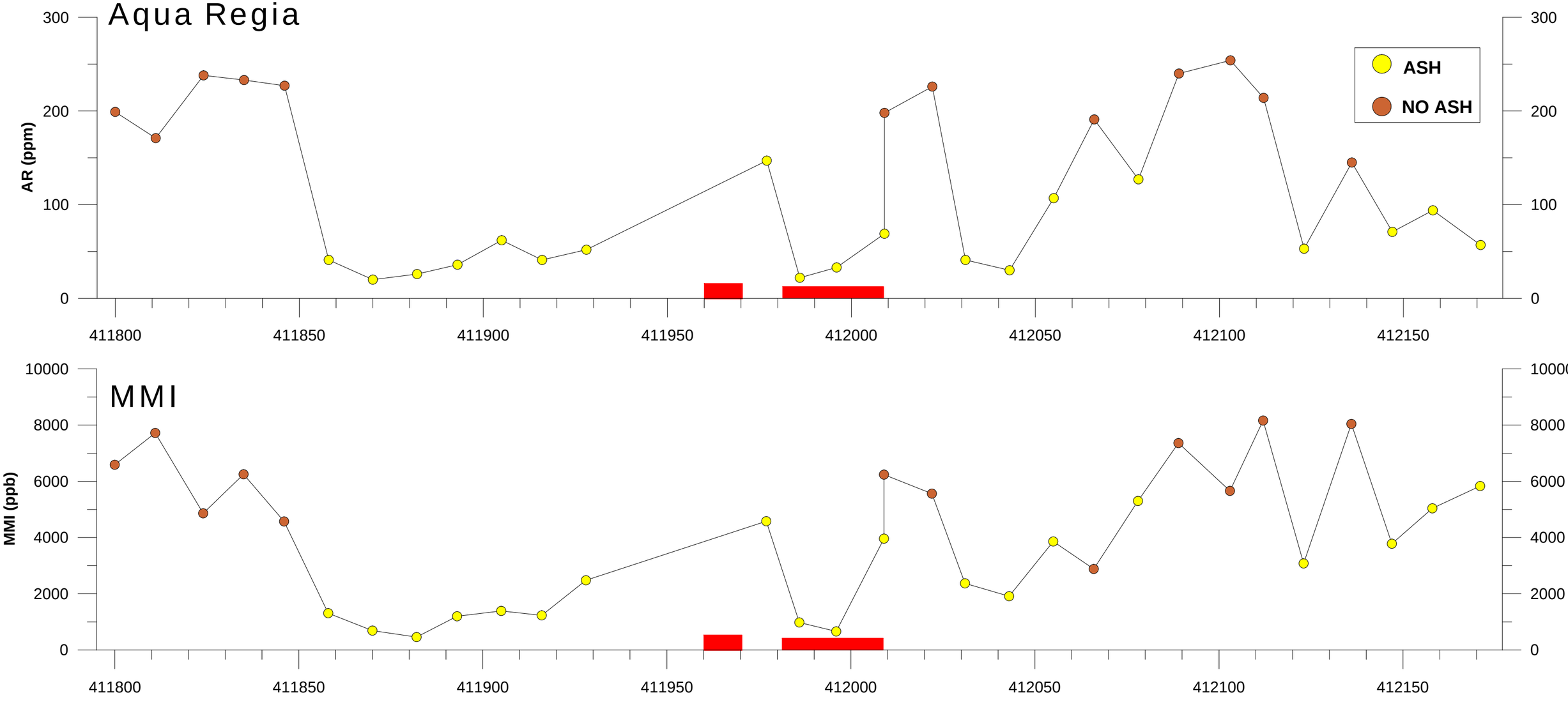

G. N. LUSTIG CONSULTING LTD.- November 13, 2008

Western Copper MMI Test
Zone 1 - North Profile
Bismuth

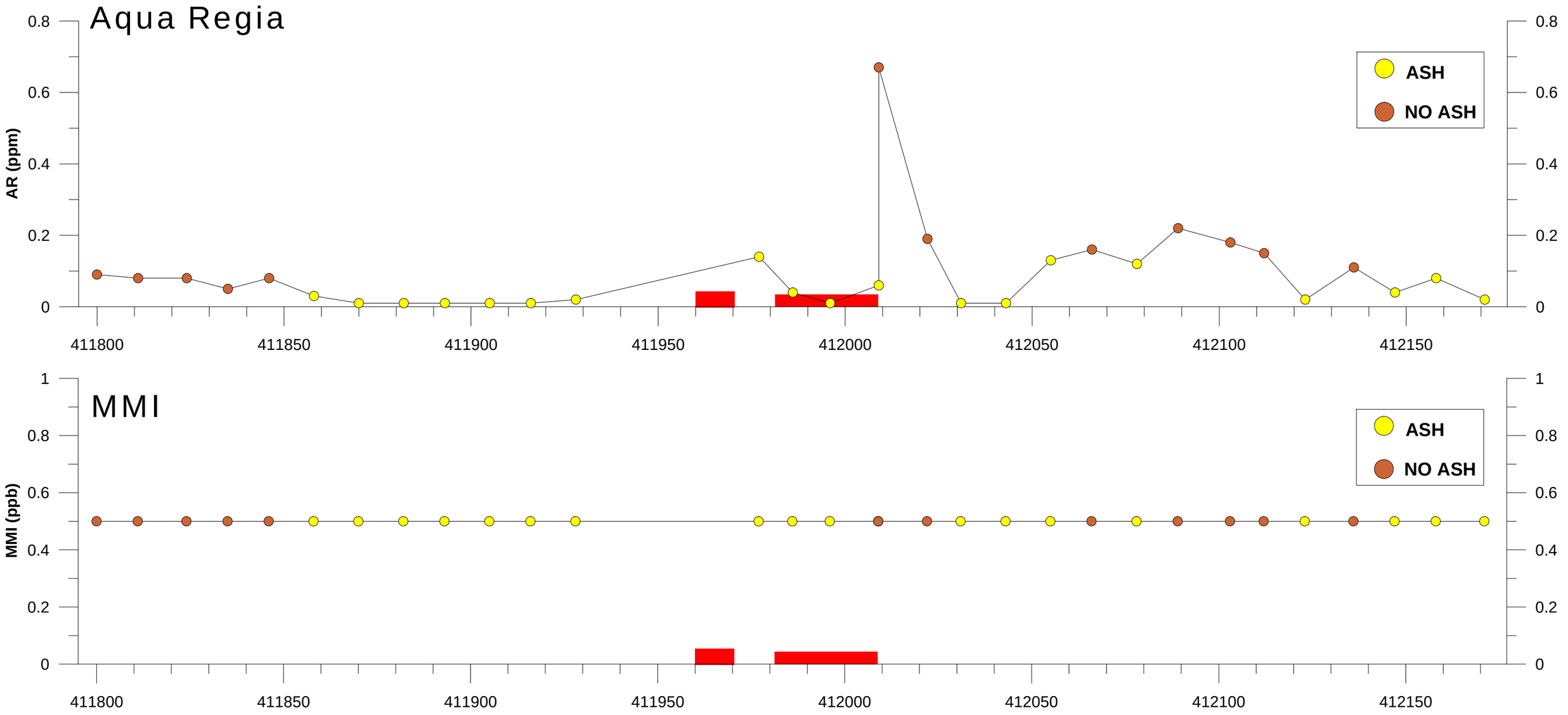

G. N. LUSTIG CONSULTING LTD.- November 13, 2008

Western Copper MMI Test
Zone 1 - North Profile
Calcium

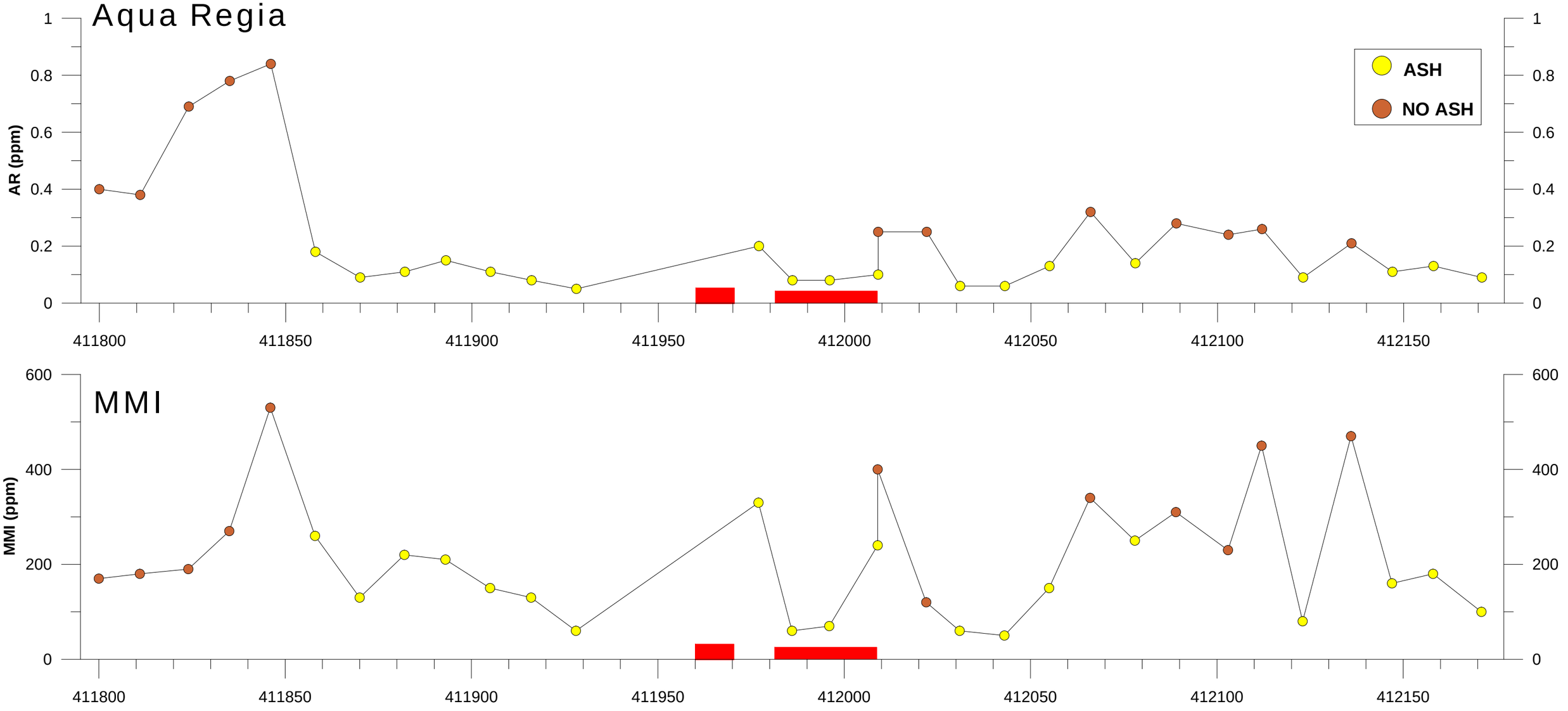

G. N. LUSTIG CONSULTING LTD.- November 13, 2008

Western Copper MMI Test
Zone 1 - North Profile

Cerium

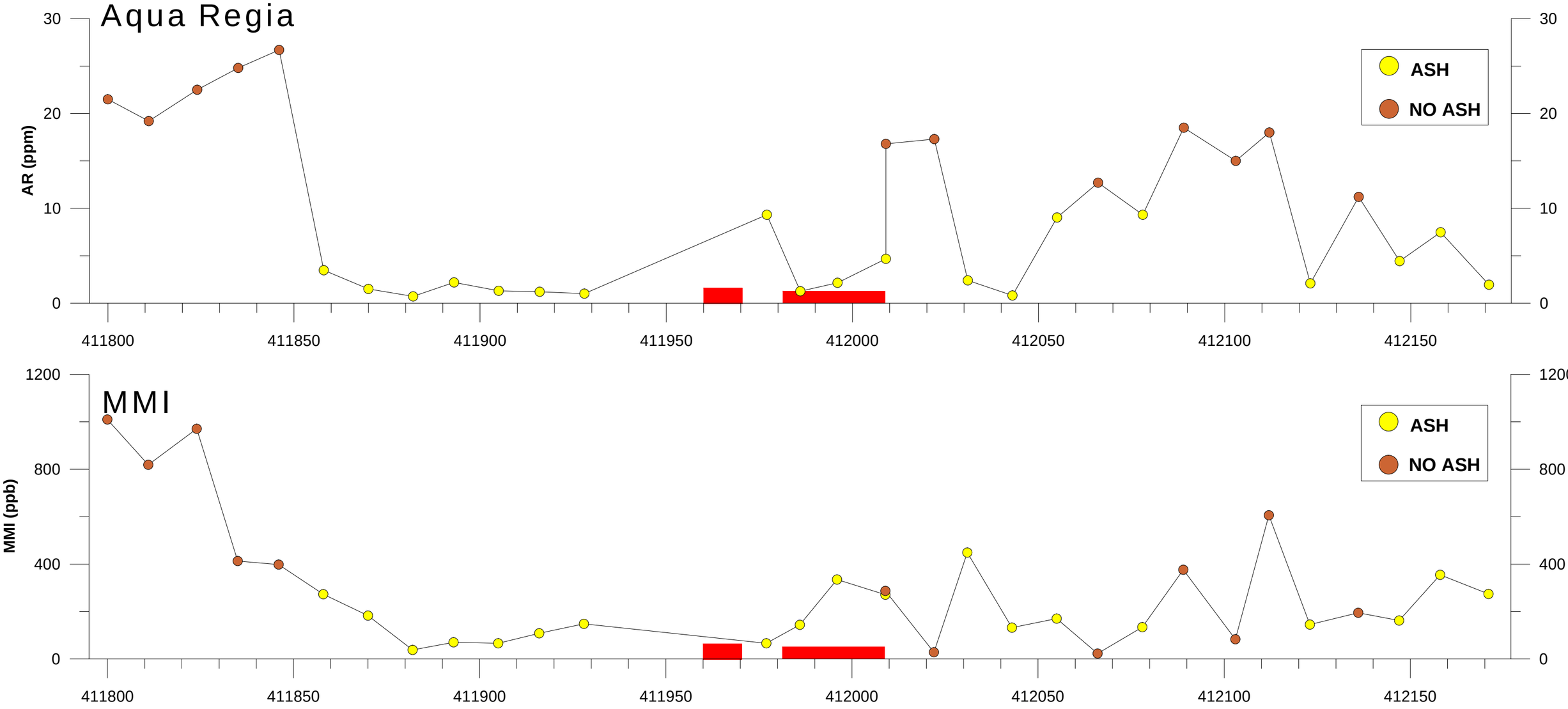

G. N. LUSTIG CONSULTING LTD.- November 13, 2008

Western Copper MMI Test
Zone 1 - North Profile

Cobalt

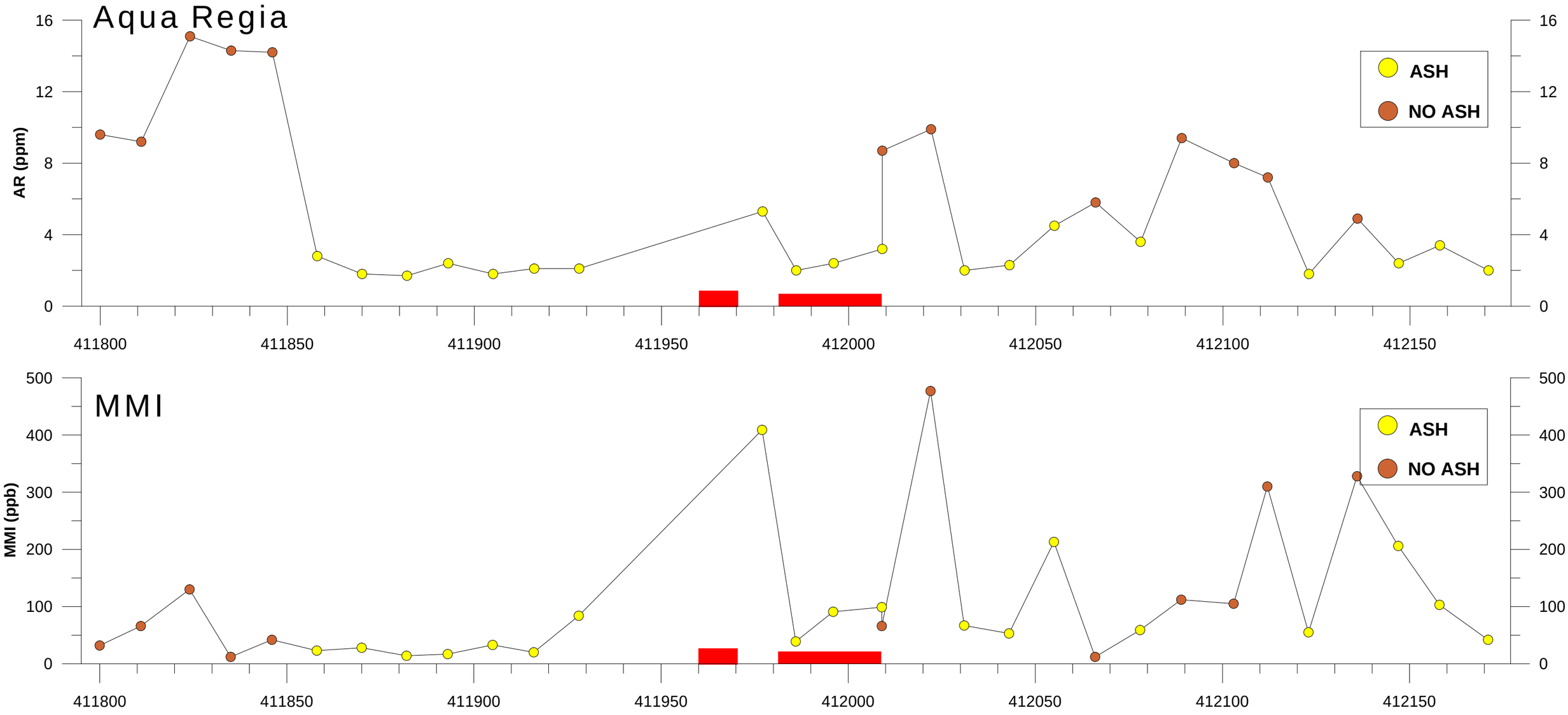

G. N. LUSTIG CONSULTING LTD.- November 13, 2008

Western Copper MMI Test
Zone 1 - North Profile

Chromium

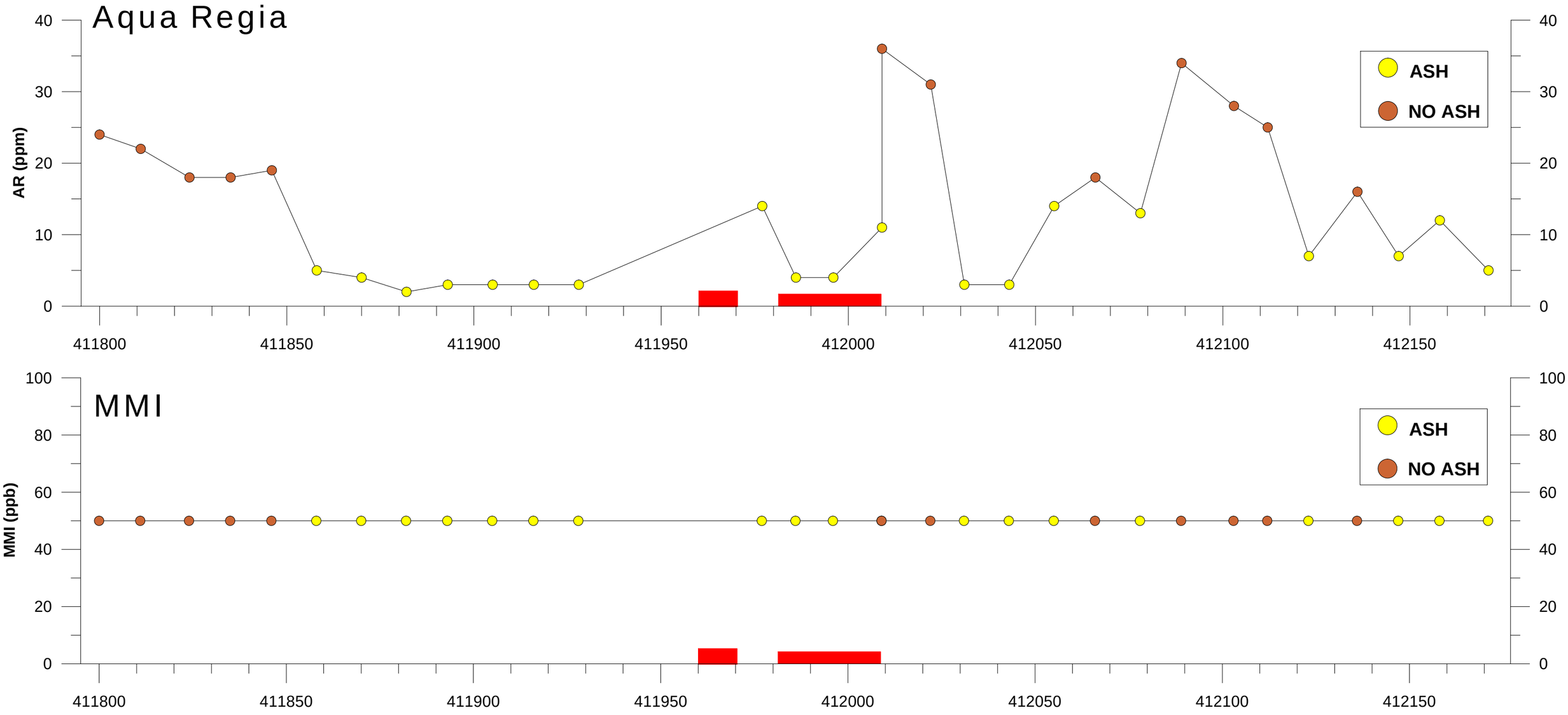

G. N. LUSTIG CONSULTING LTD.- November 13, 2008

Western Copper MMI Test
Zone 1 - North Profile

Copper

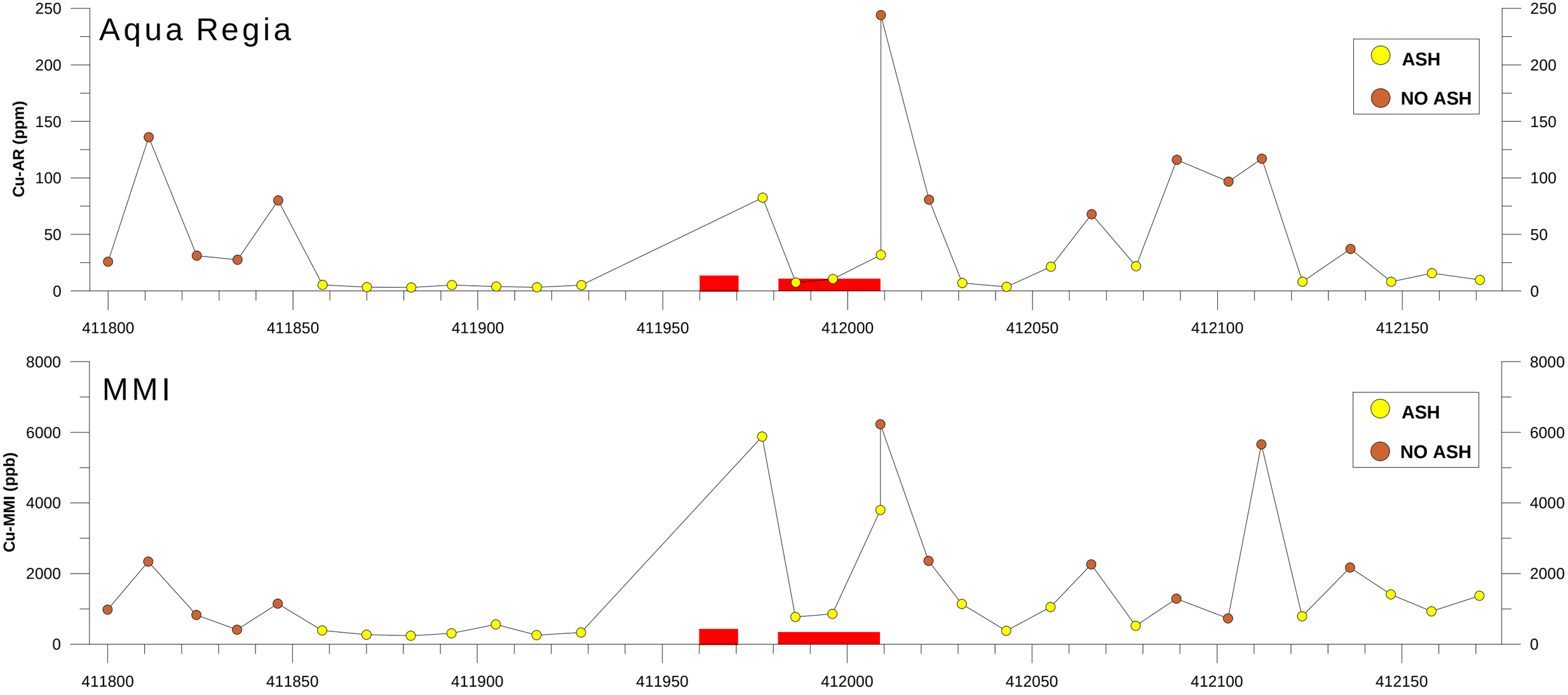

G. N. LUSTIG CONSULTING LTD.- AUGUST 26, 2008

Western Copper MMI Test
Zone 1 - North Profile
Iron

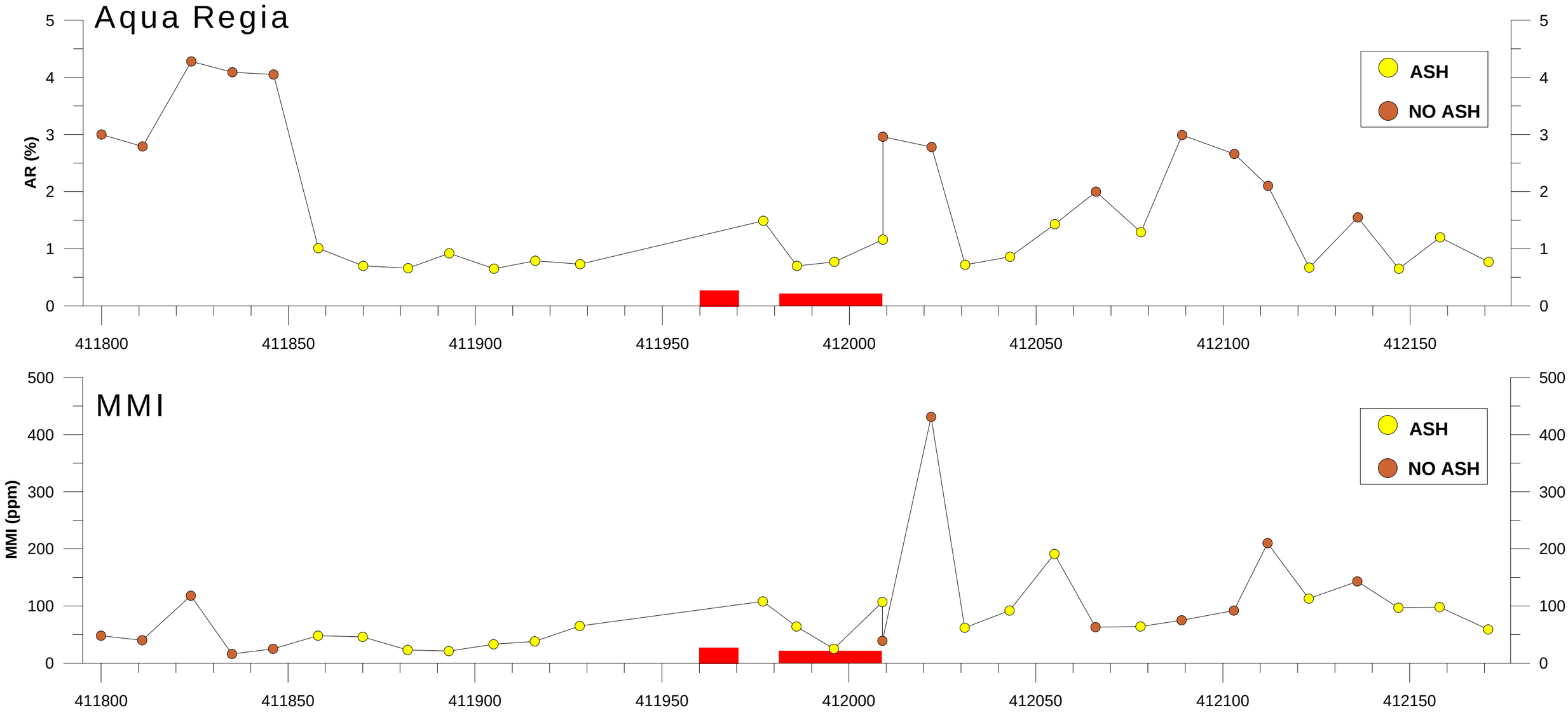

G. N. LUSTIG CONSULTING LTD.- November 13, 2008

Western Copper MMI Test
Zone 1 - North Profile
Lanthanum

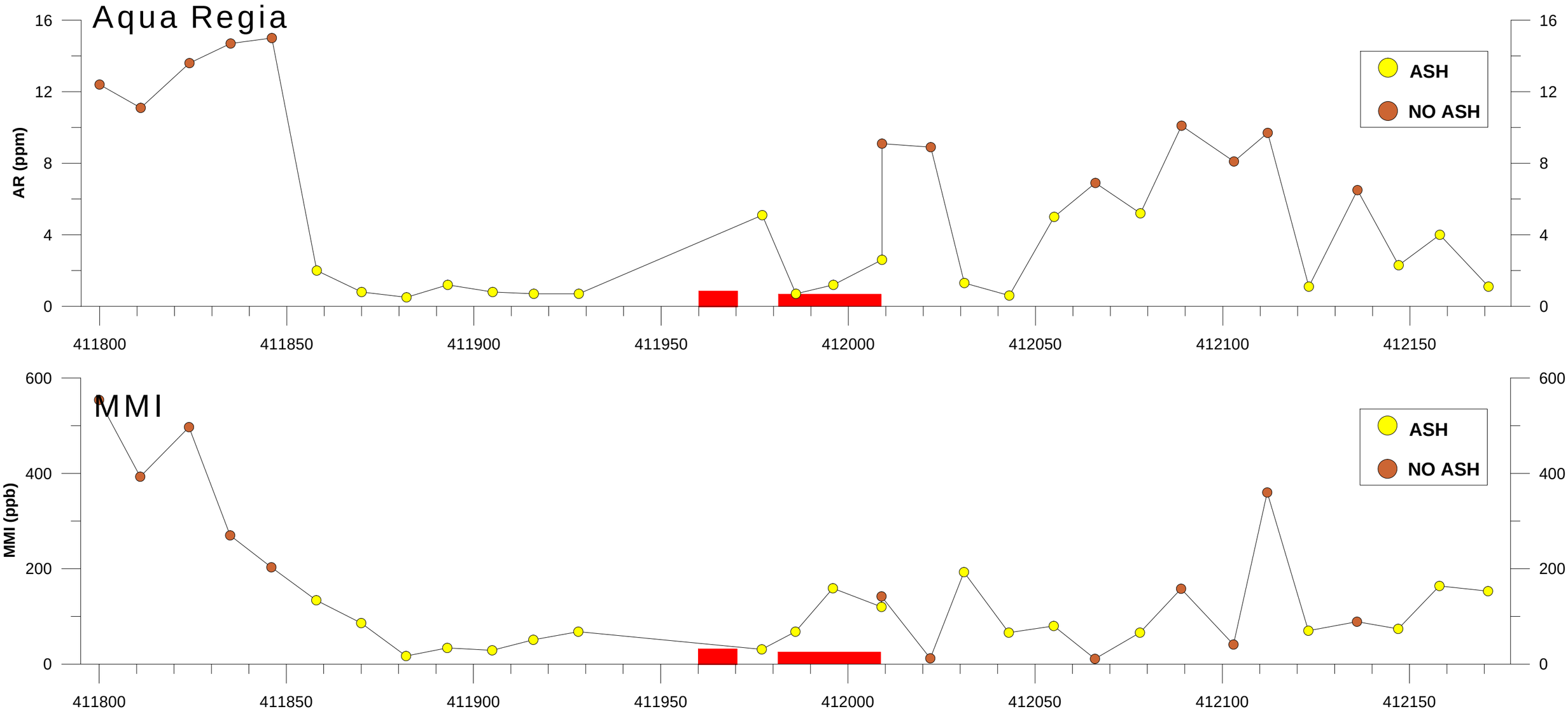

G. N. LUSTIG CONSULTING LTD.- November 13, 2008

Western Copper MMI Test
Zone 1 - North Profile
Lithium

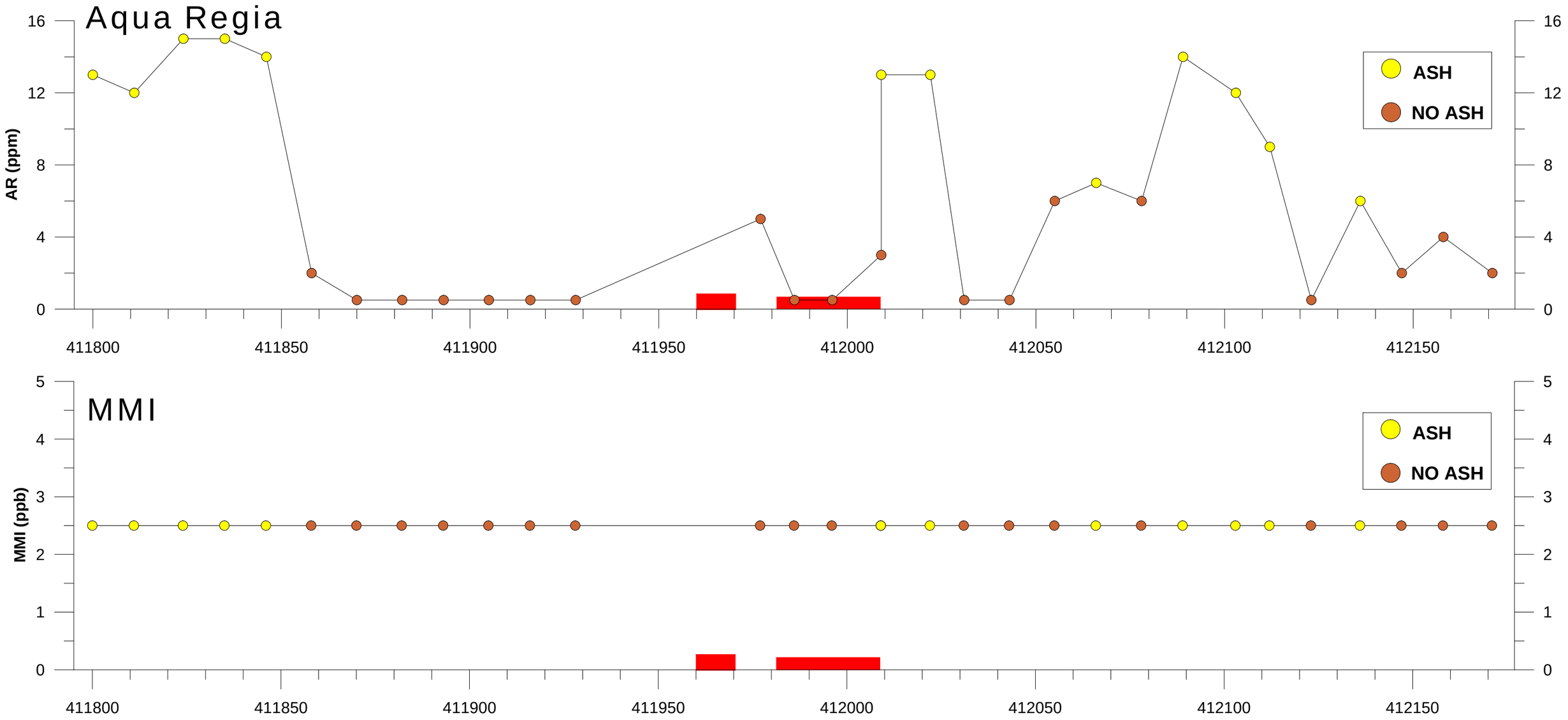

G. N. LUSTIG CONSULTING LTD.- November 13, 2008

Western Copper MMI Test
Zone 1 - North Profile
Magnesuim

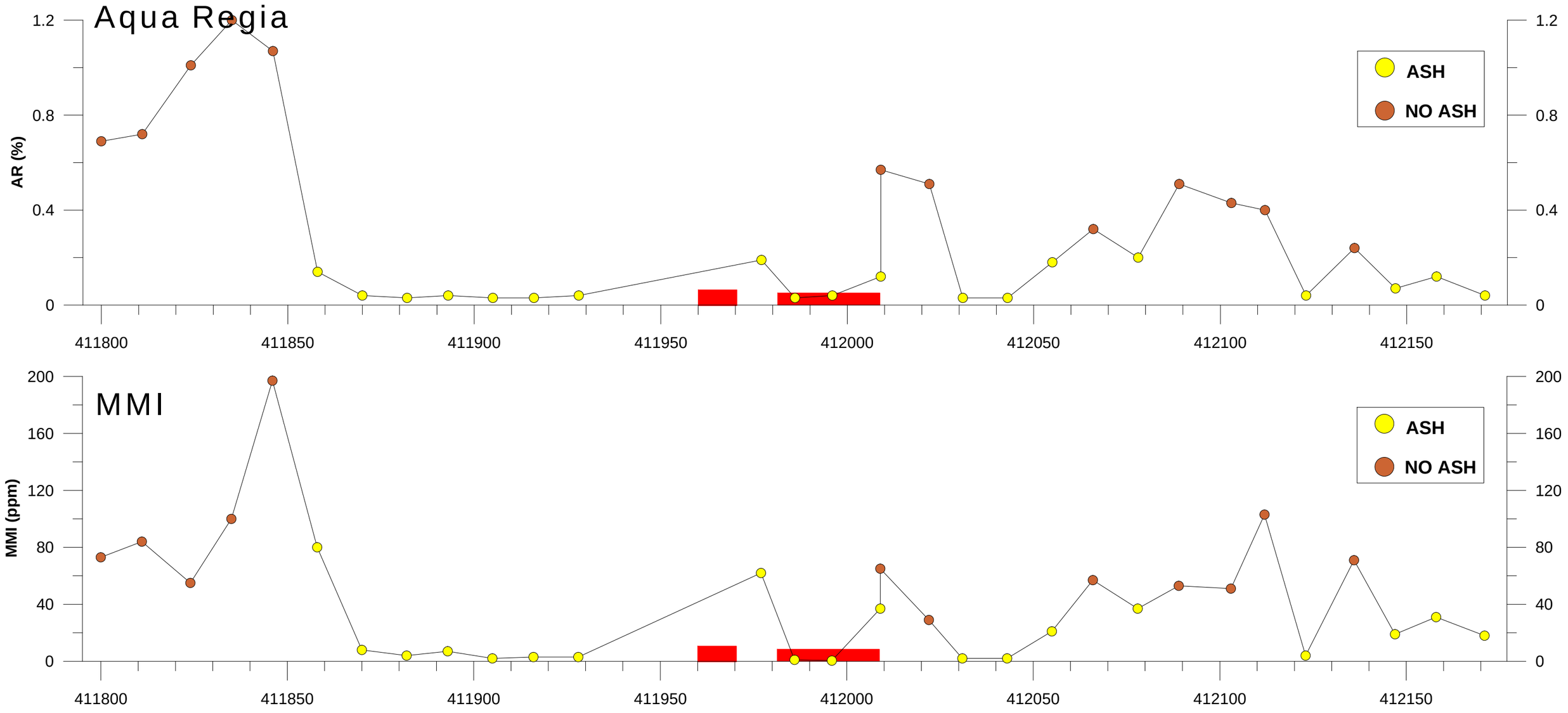

G. N. LUSTIG CONSULTING LTD.- November 17, 2008

Western Copper MMI Test
Zone 1 - North Profile
Molybdenum

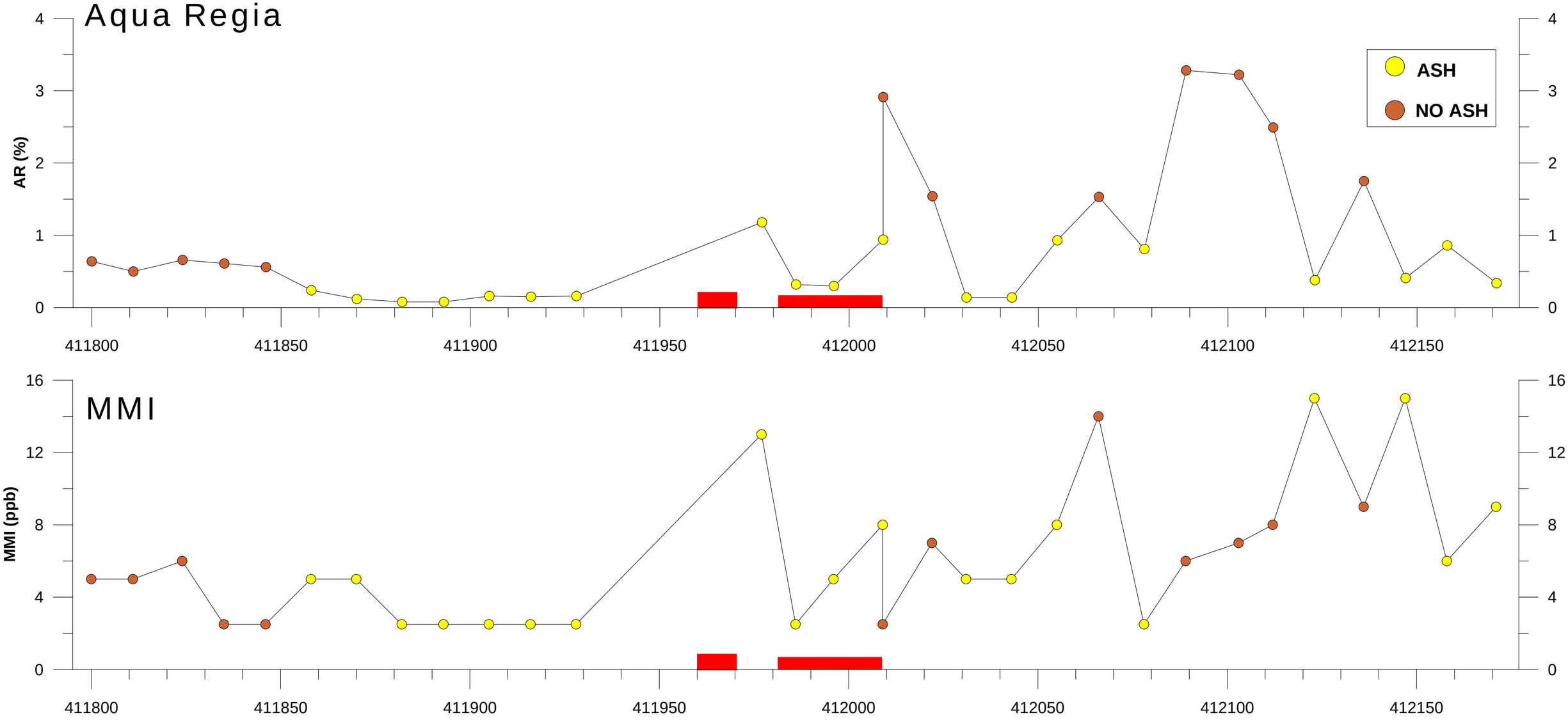

G. N. LUSTIG CONSULTING LTD.- November 17, 2008

Western Copper MMI Test
Zone 1 - North Profile
Niobium

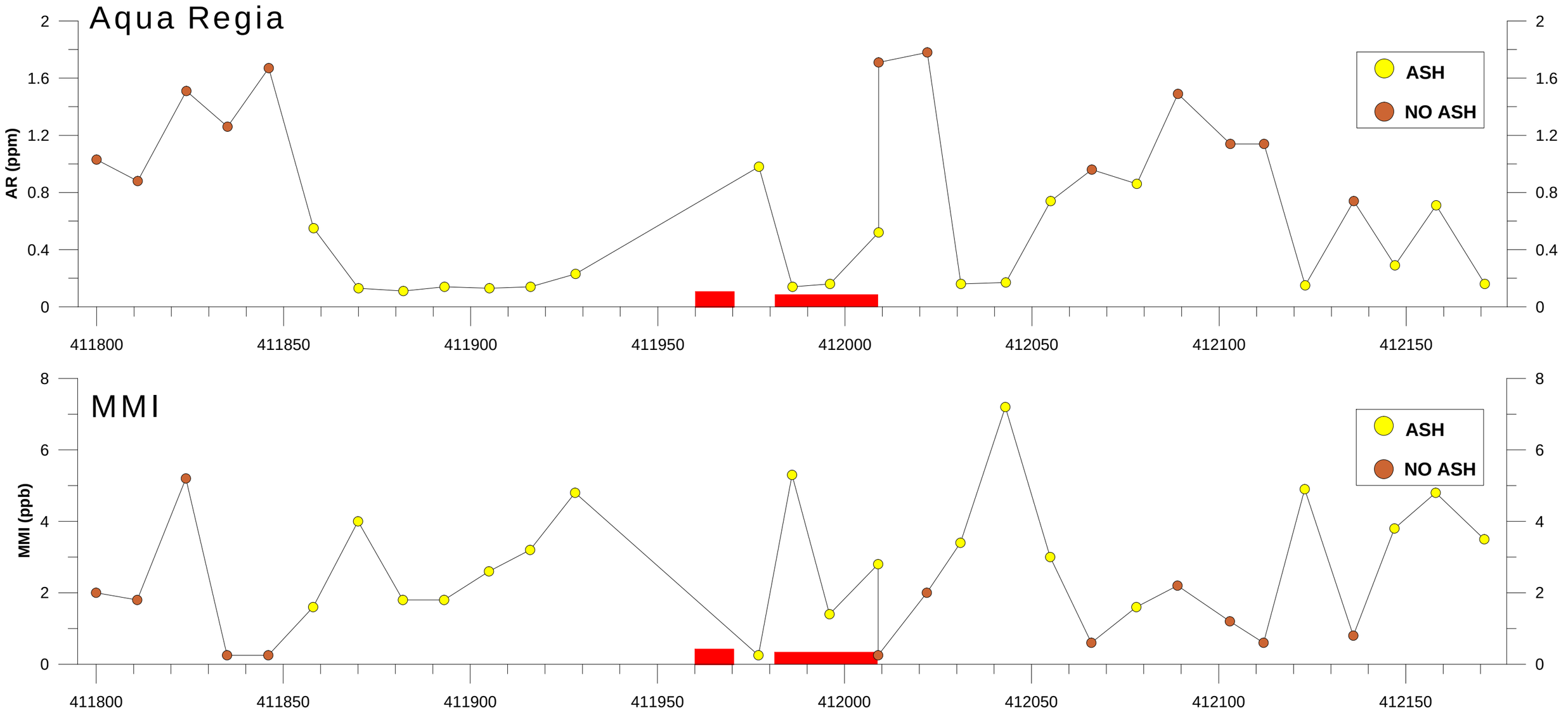

G. N. LUSTIG CONSULTING LTD.- November 17, 2008

Western Copper MMI Test
Zone 1 - North Profile
Nickel

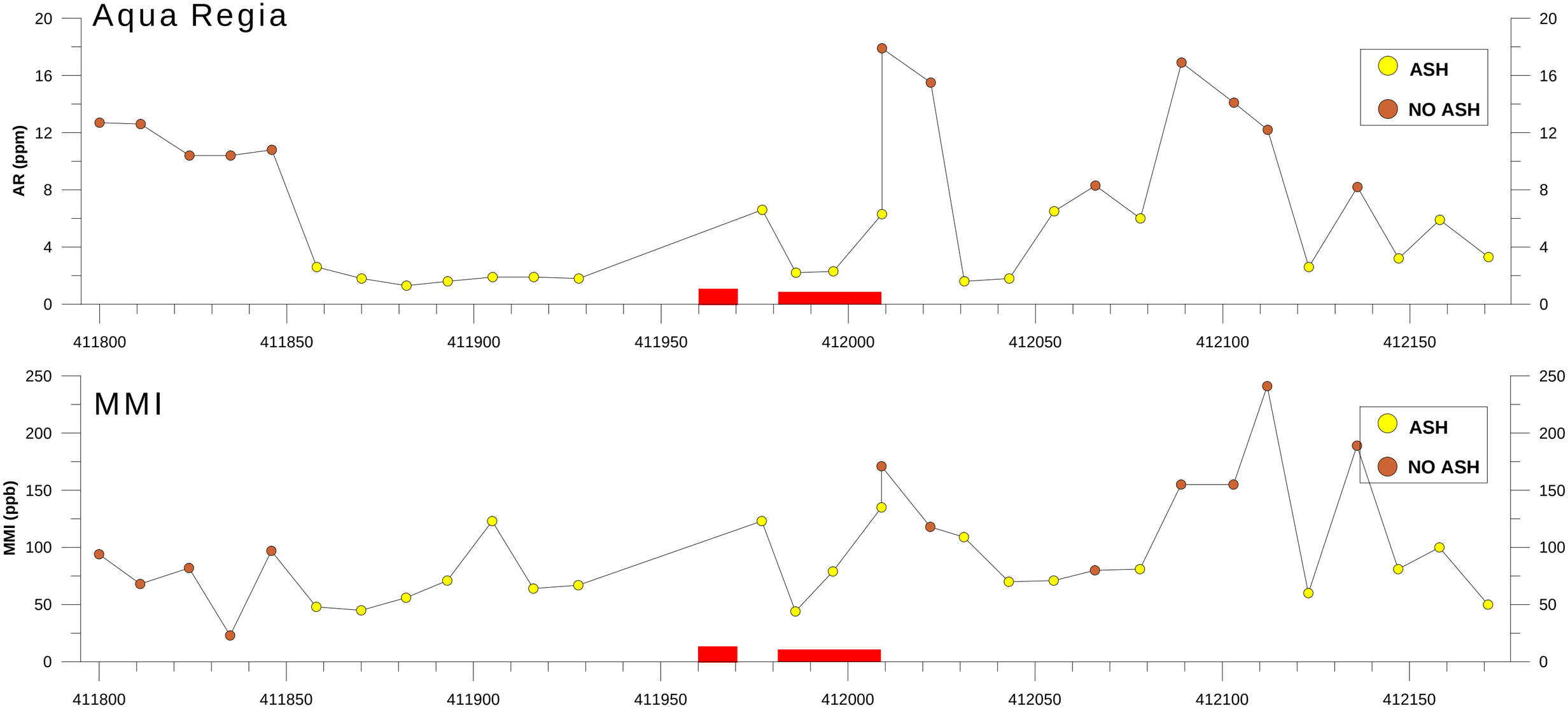

G. N. LUSTIG CONSULTING LTD.- November 17, 2008

Western Copper MMI Test
Zone 1 - North Profile

Lead

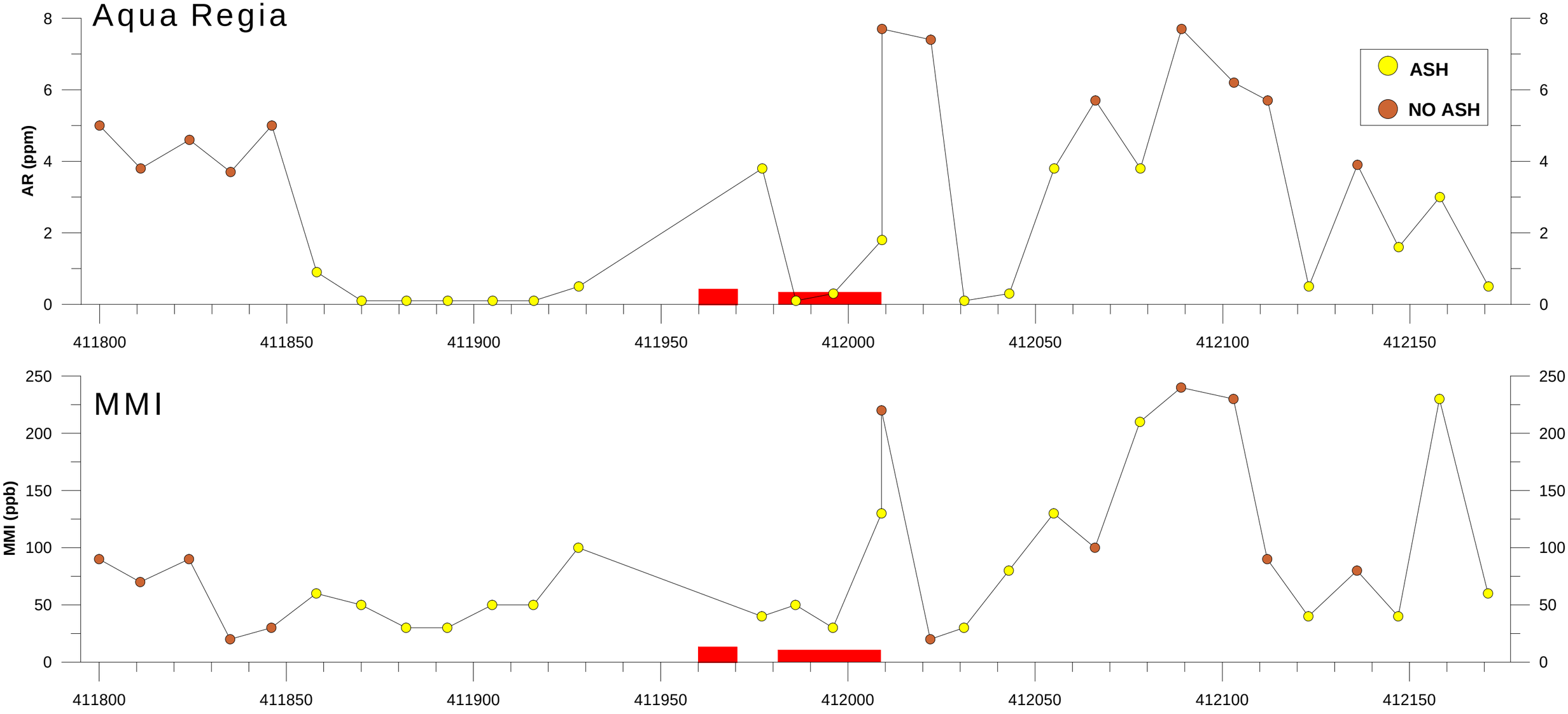

G. N. LUSTIG CONSULTING LTD.- November 17, 2008

Western Copper MMI Test
Zone 1 - North Profile
Rubidium

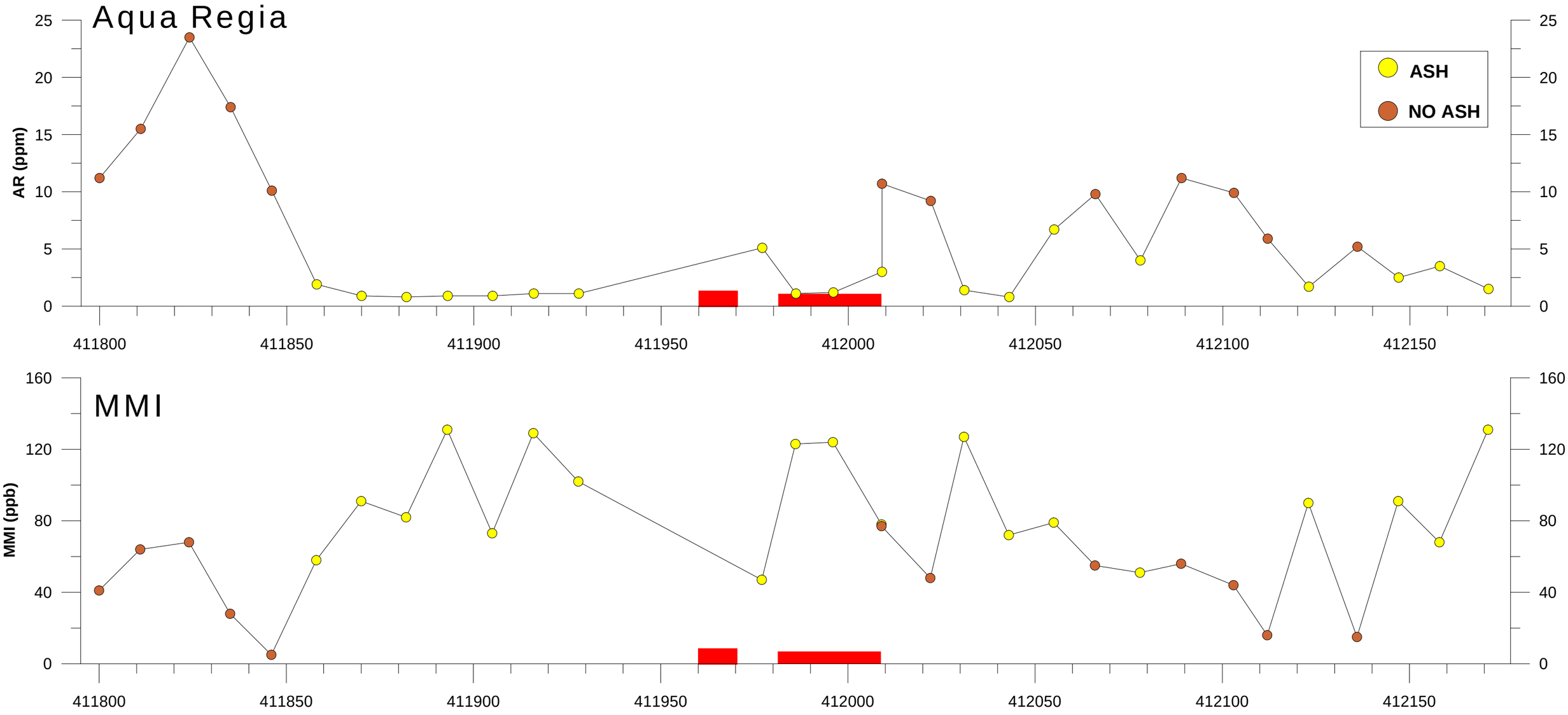

G. N. LUSTIG CONSULTING LTD.- November 17, 2008

Western Copper MMI Test
Zone 1 - North Profile

Scandium

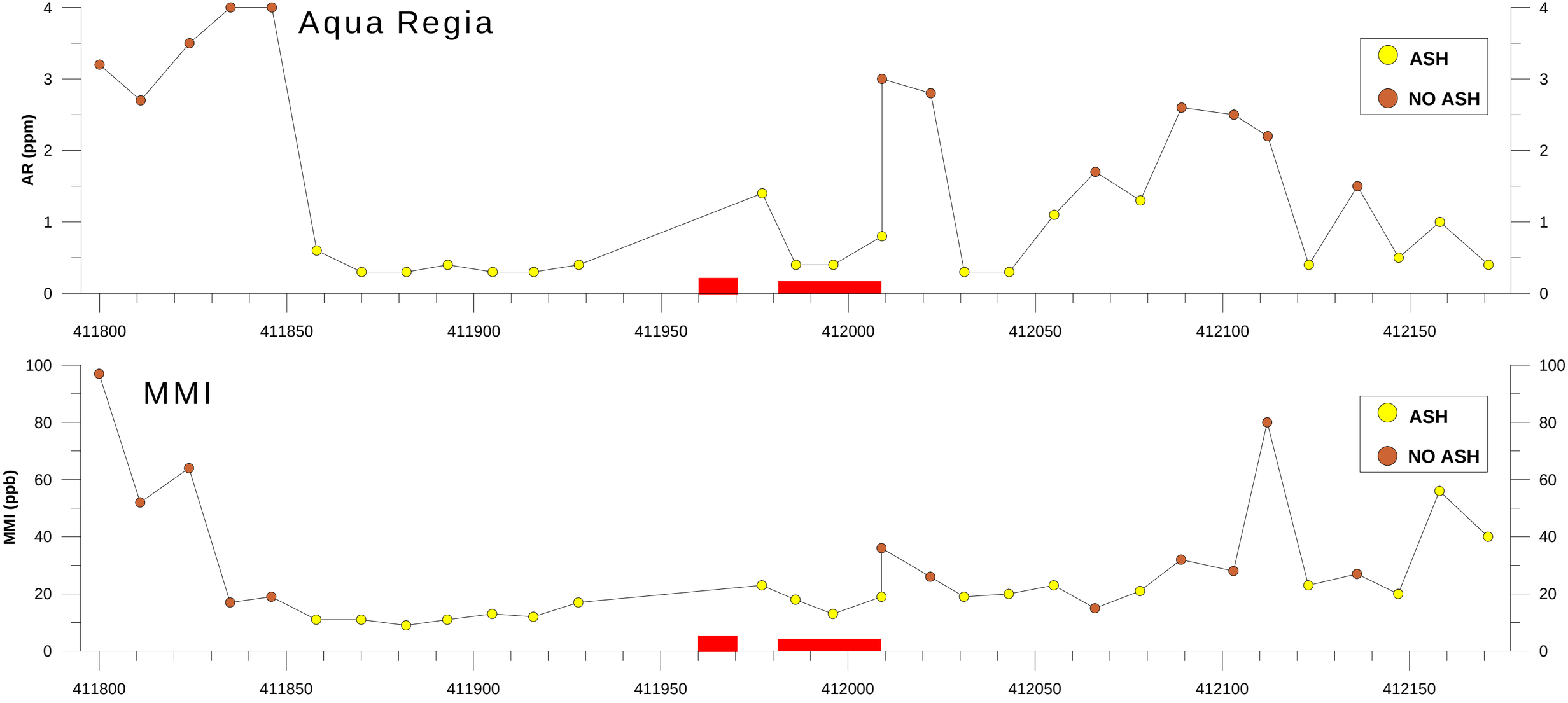

G. N. LUSTIG CONSULTING LTD.- November 17, 2008

Western Copper MMI Test
Zone 1 - North Profile

Tin

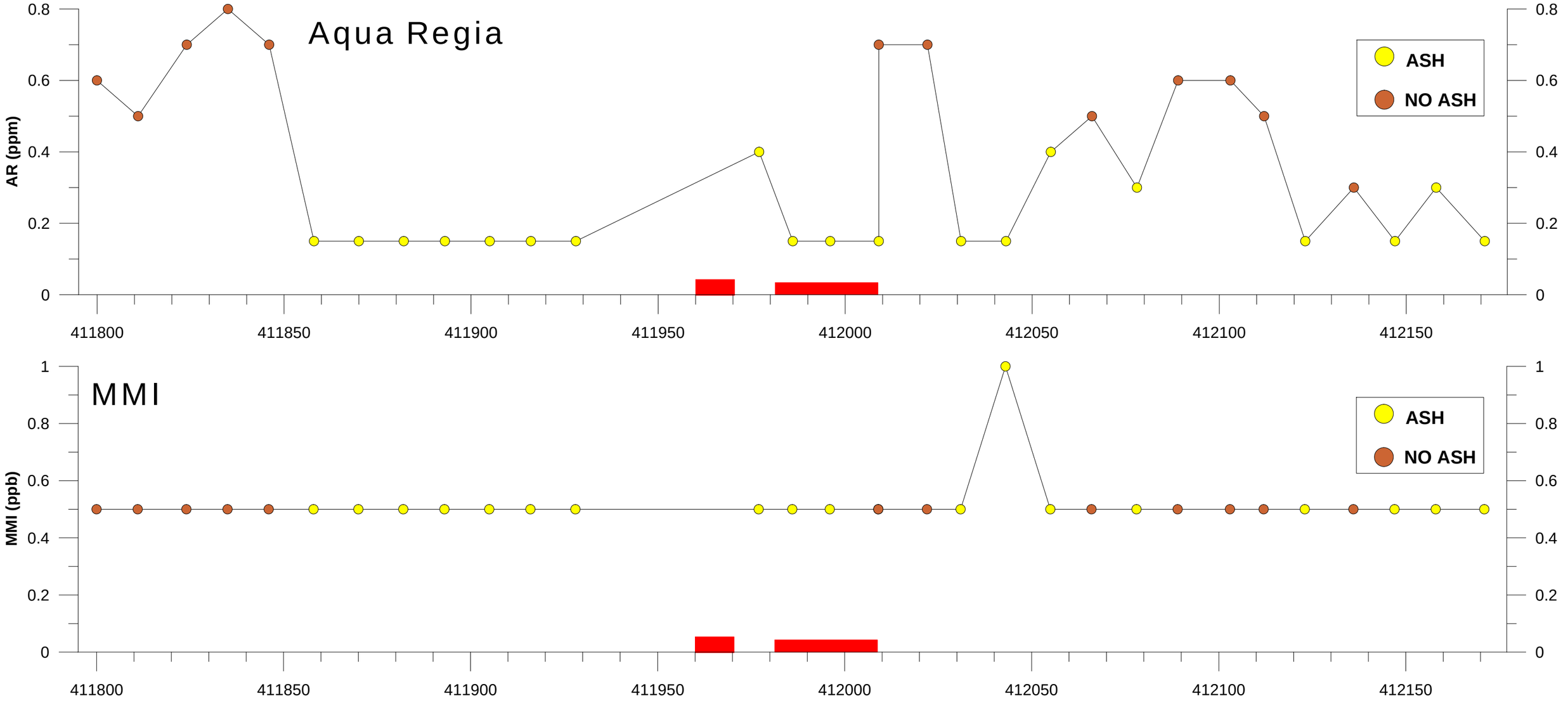

G. N. LUSTIG CONSULTING LTD.- November 17, 2008

Western Copper MMI Test
Zone 1 - North Profile
Strontium

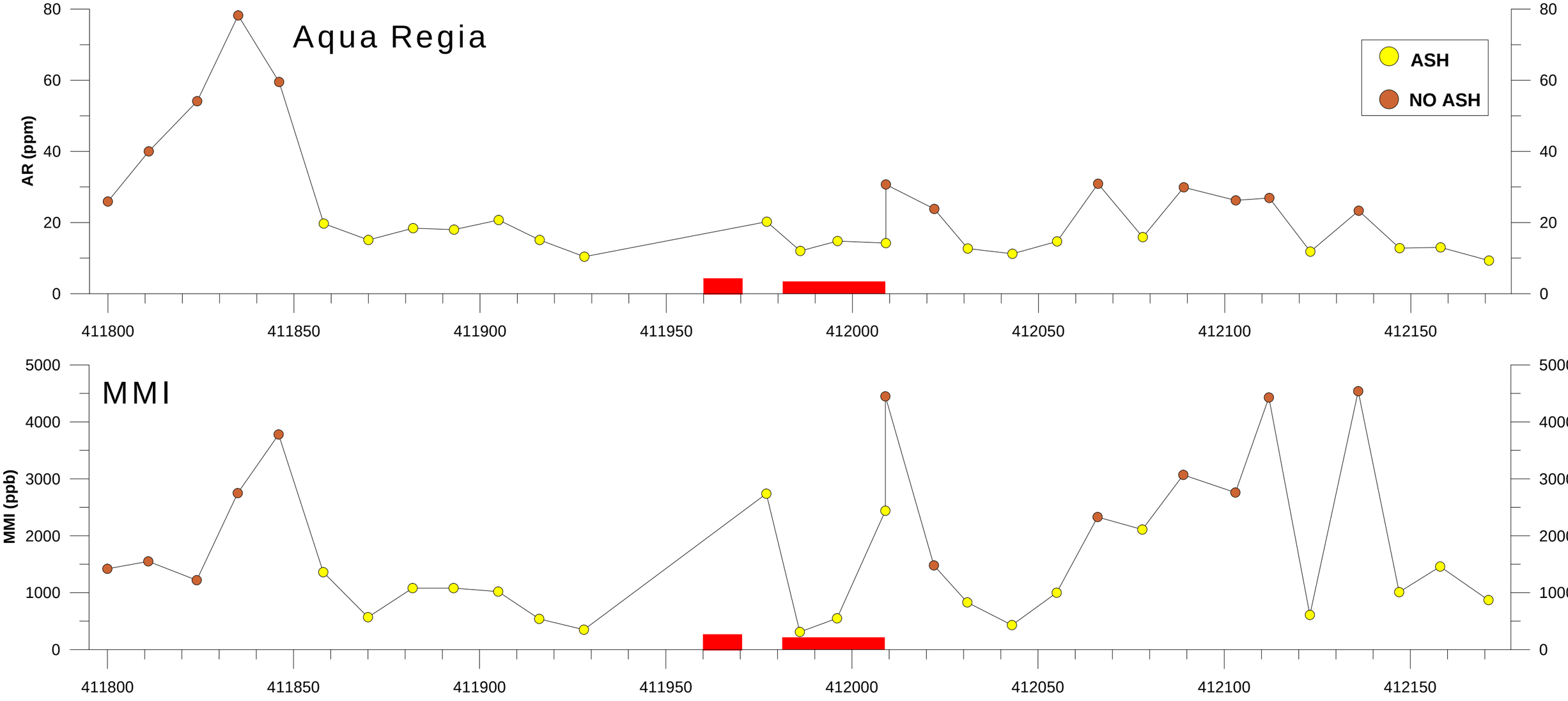

G. N. LUSTIG CONSULTING LTD.- November 17, 2008

Western Copper MMI Test
Zone 1 - North Profile

Tantalum

Aqua Regia

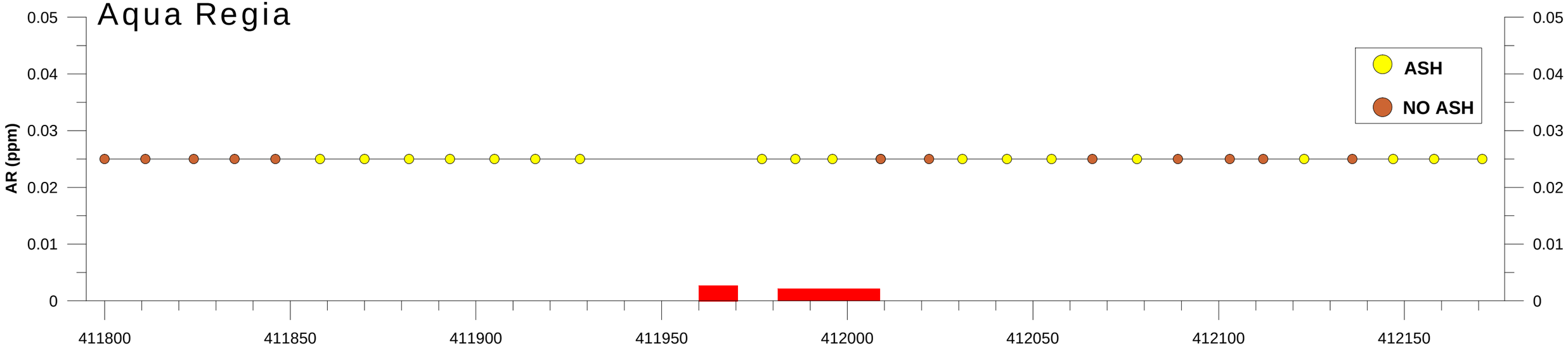

MMI

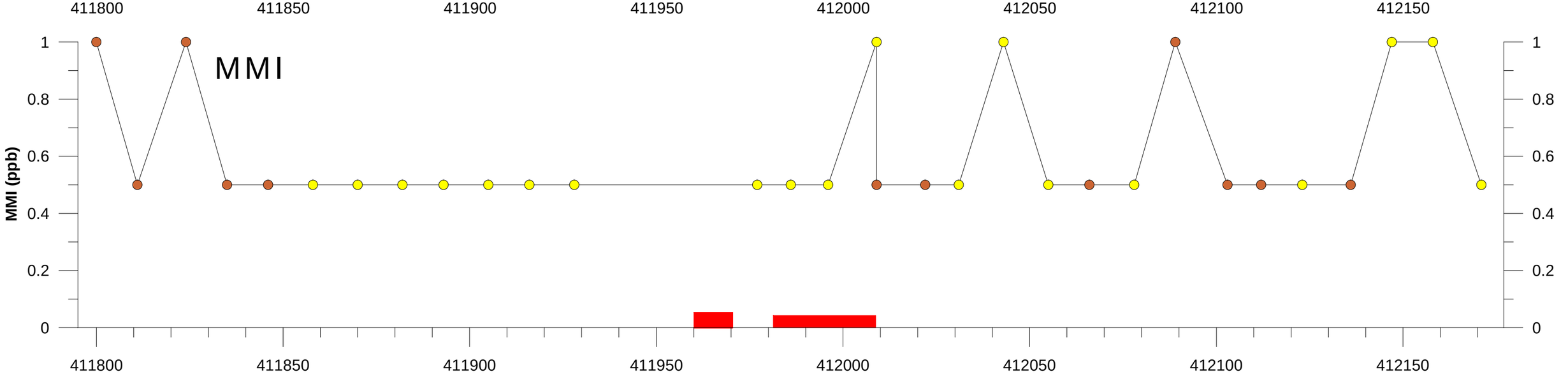

G. N. LUSTIG CONSULTING LTD.- November 17, 2008

Western Copper MMI Test
Zone 1 - North Profile
Terbium

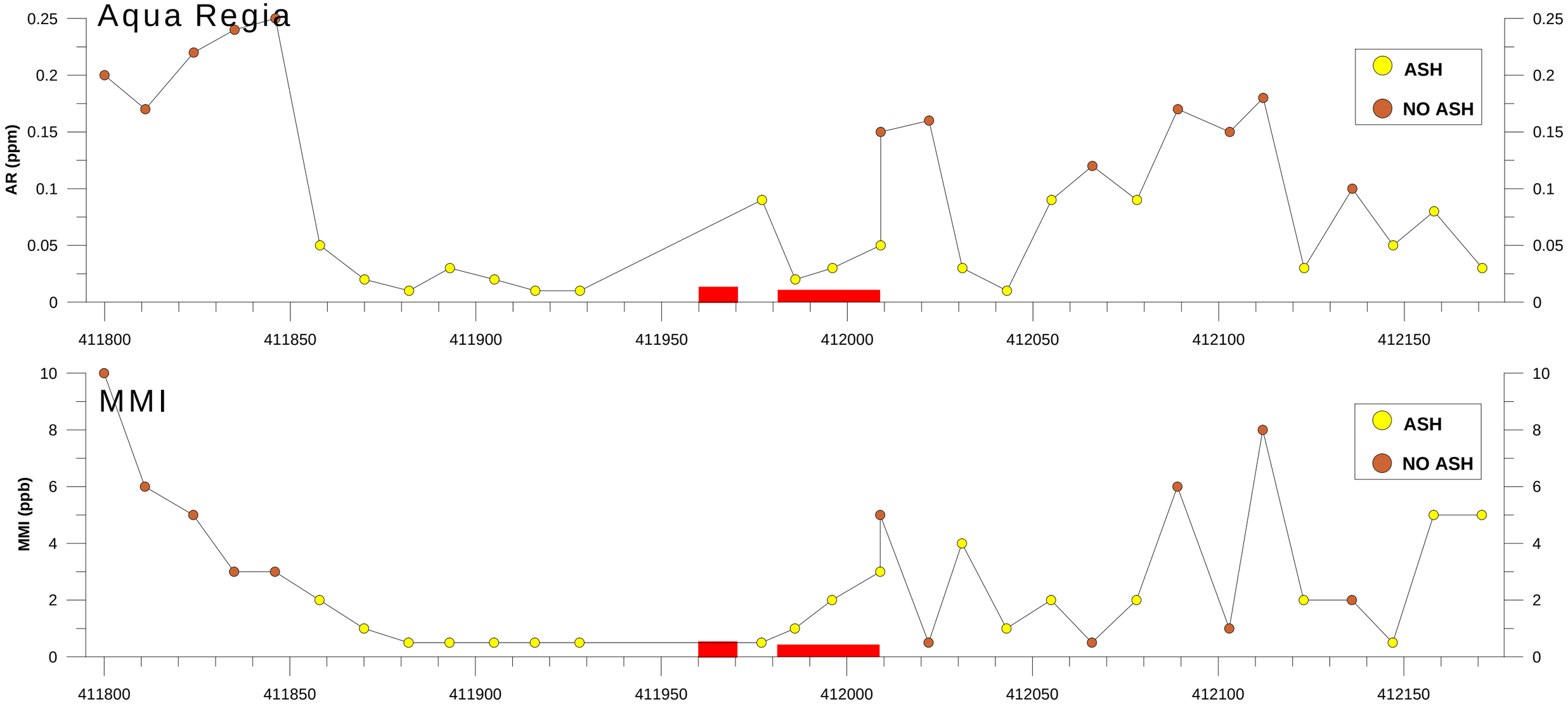

G. N. LUSTIG CONSULTING LTD.- November 17, 2008

Western Copper MMI Test
Zone 1 - North Profile
Tellurium

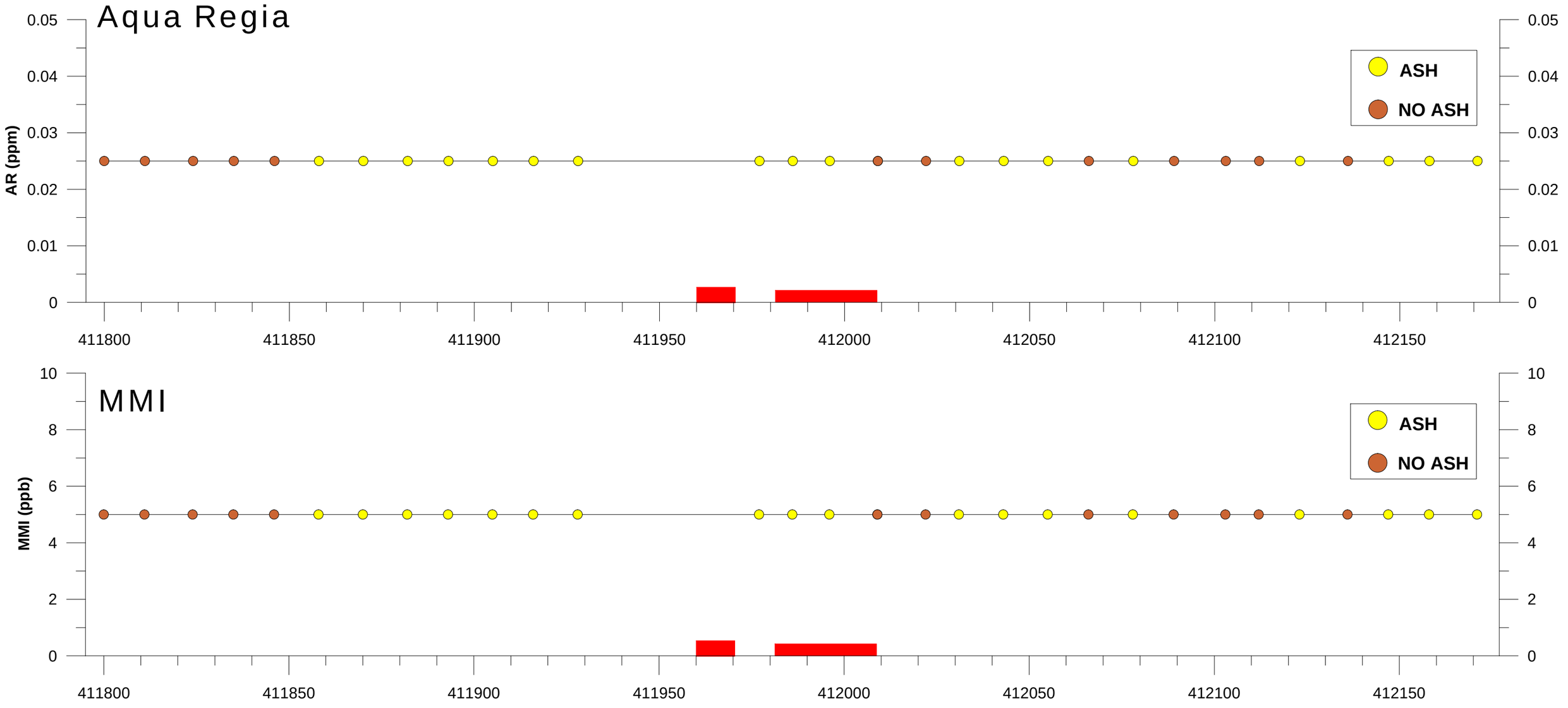

G. N. LUSTIG CONSULTING LTD.- November 17, 2008

Western Copper MMI Test
Zone 1 - North Profile
Thorium

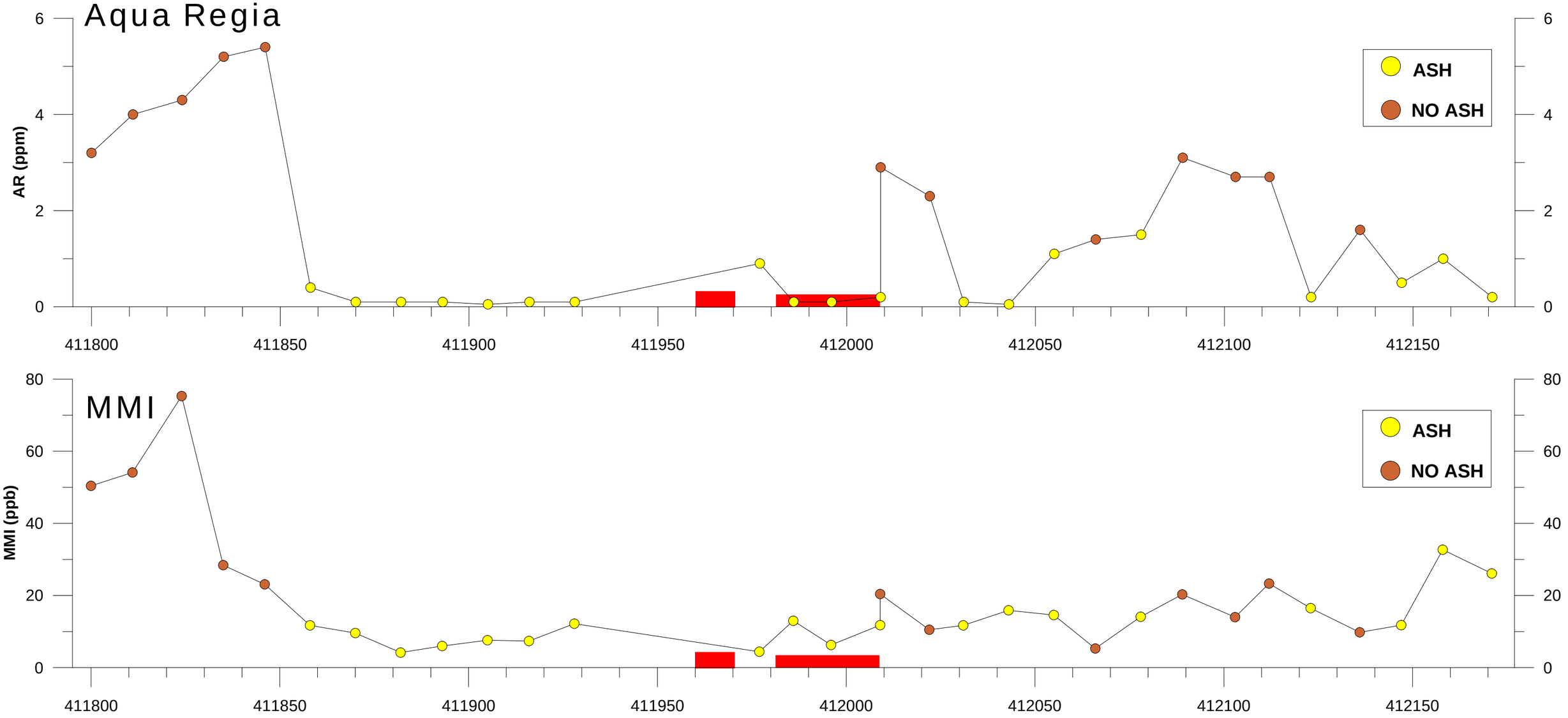

G. N. LUSTIG CONSULTING LTD.- November 17, 2008

Western Copper MMI Test
Zone 1 - North Profile

Titanium

Aqua Regia

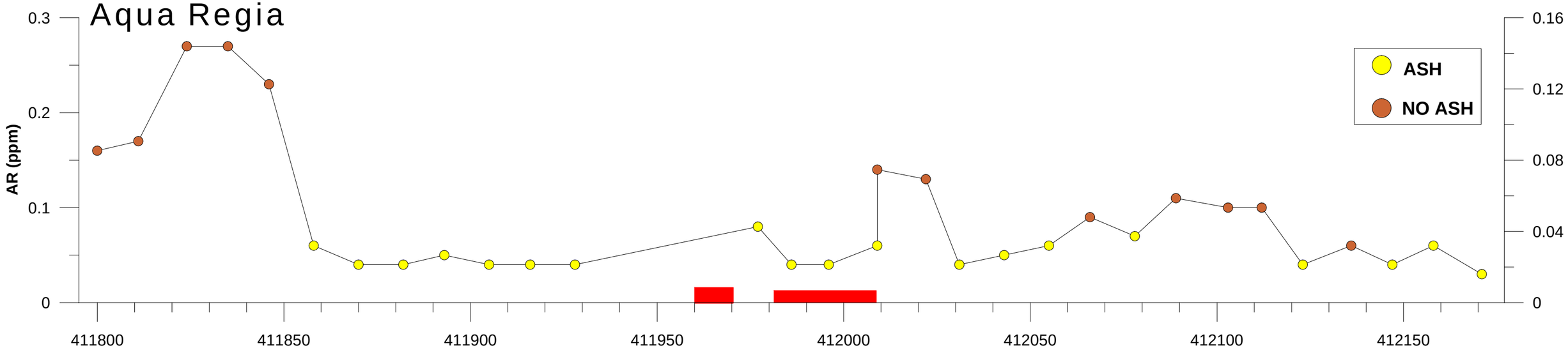

MMI

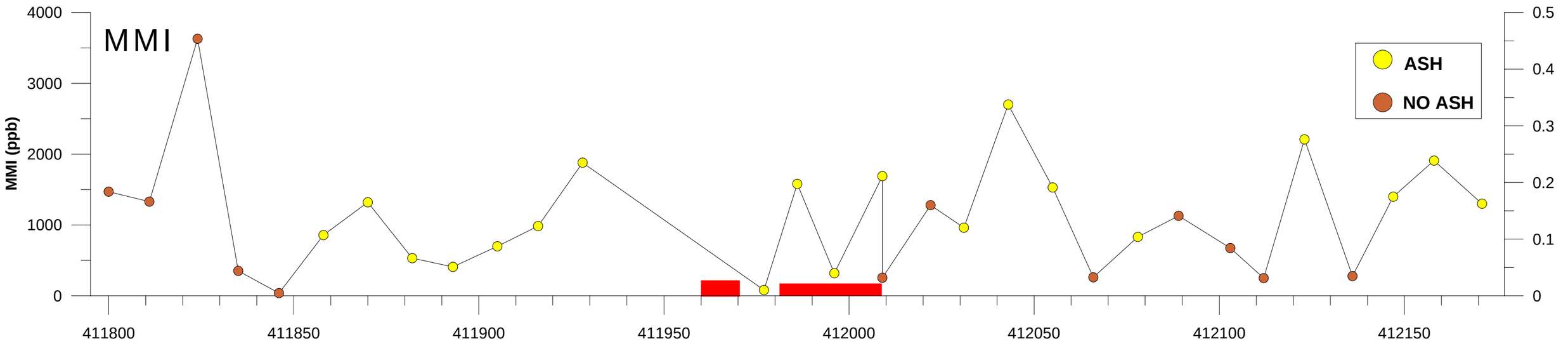

G. N. LUSTIG CONSULTING LTD.- November 17, 2008

Western Copper MMI Test
Zone 1 - North Profile
Thallium

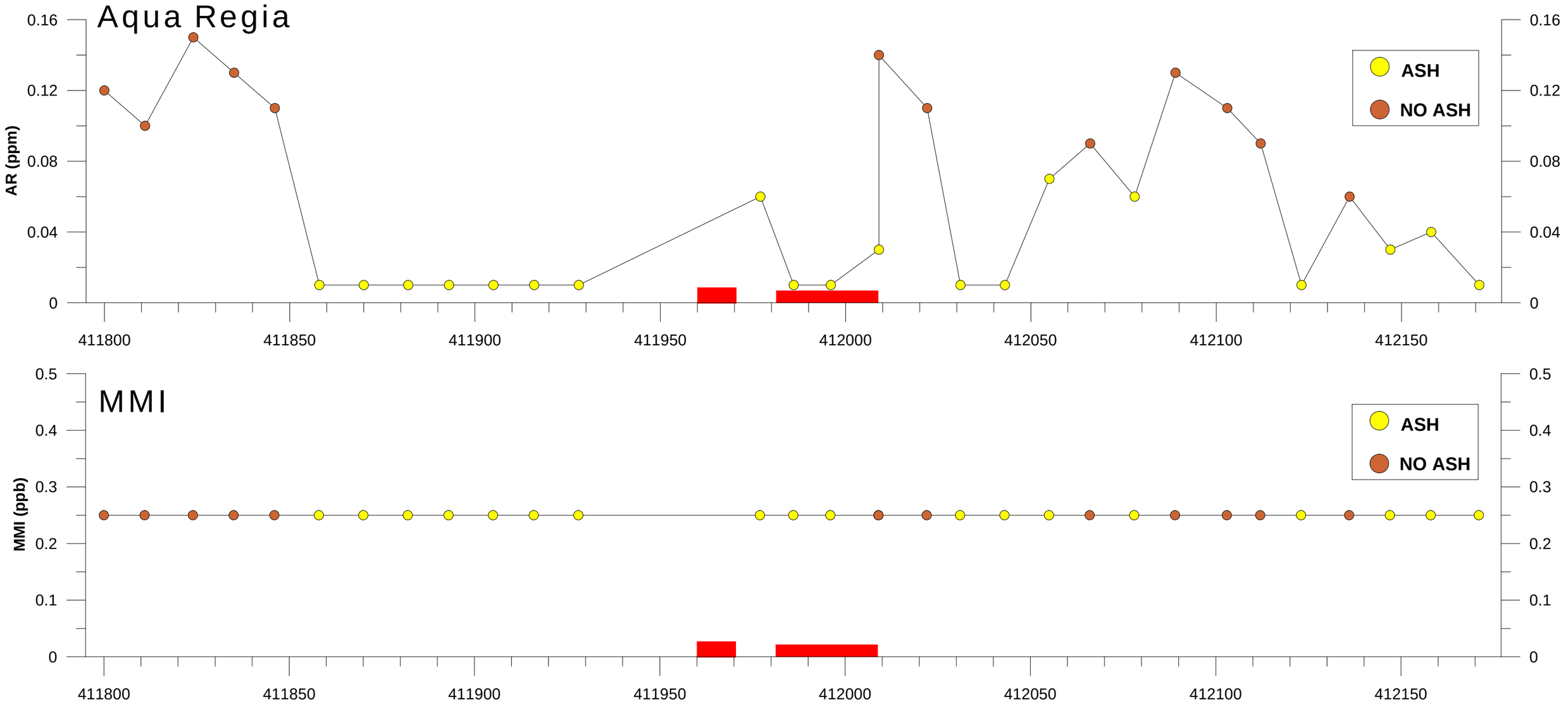

G. N. LUSTIG CONSULTING LTD.- November 17, 2008

Western Copper MMI Test
Zone 1 - North Profile
Uranium

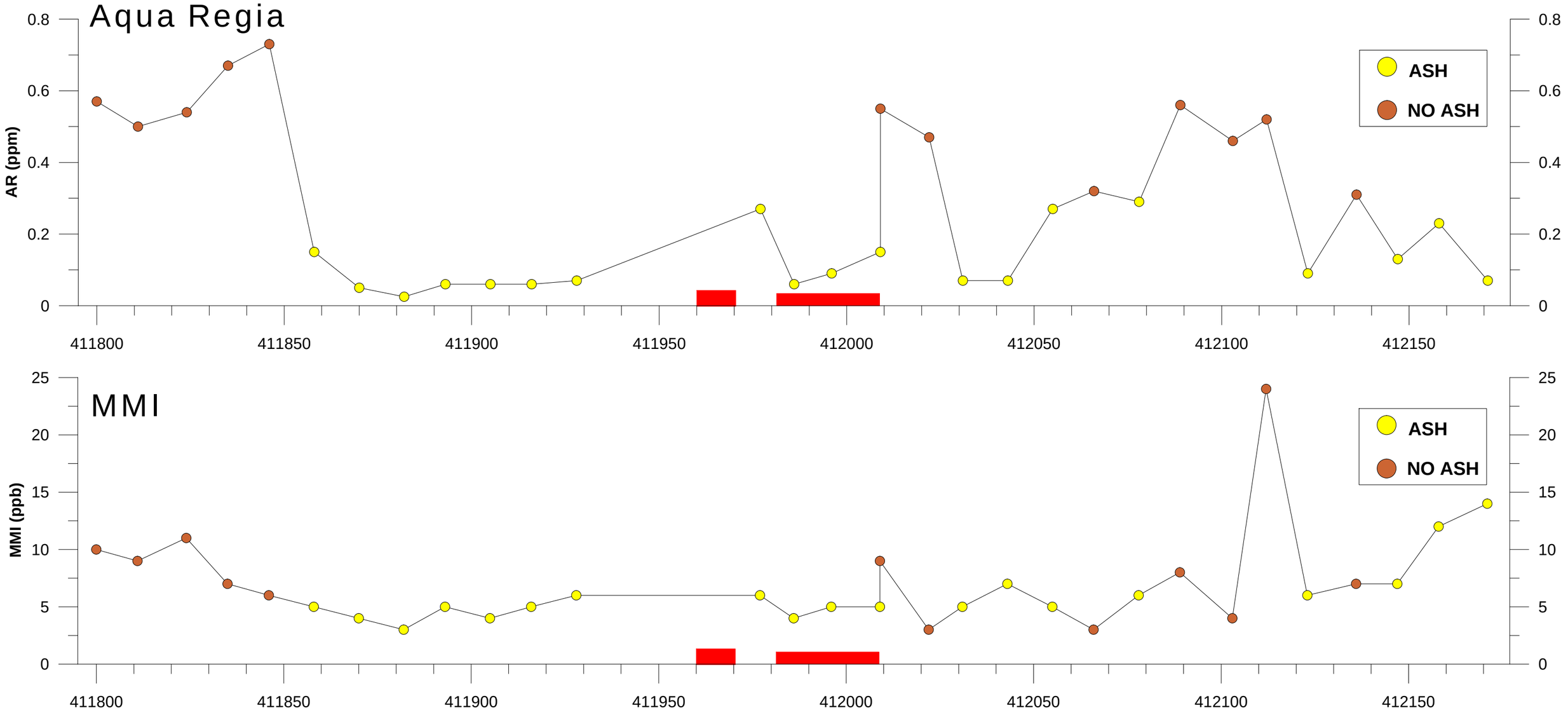

G. N. LUSTIG CONSULTING LTD.- November 17, 2008

Western Copper MMI Test
Zone 1 - North Profile
Tungsten

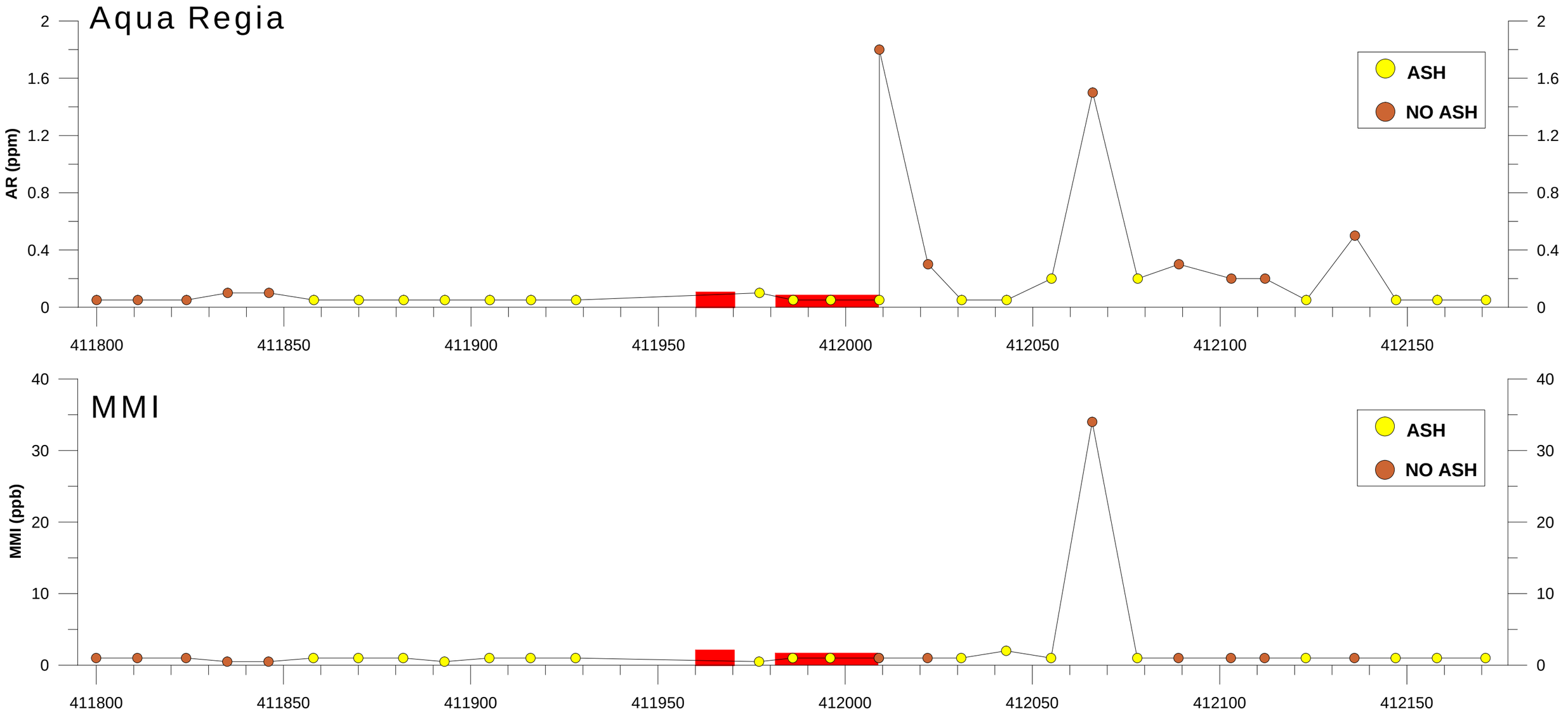

G. N. LUSTIG CONSULTING LTD.- November 17, 2008

Western Copper MMI Test
Zone 1 - North Profile
Ytterbium

Aqua Regia

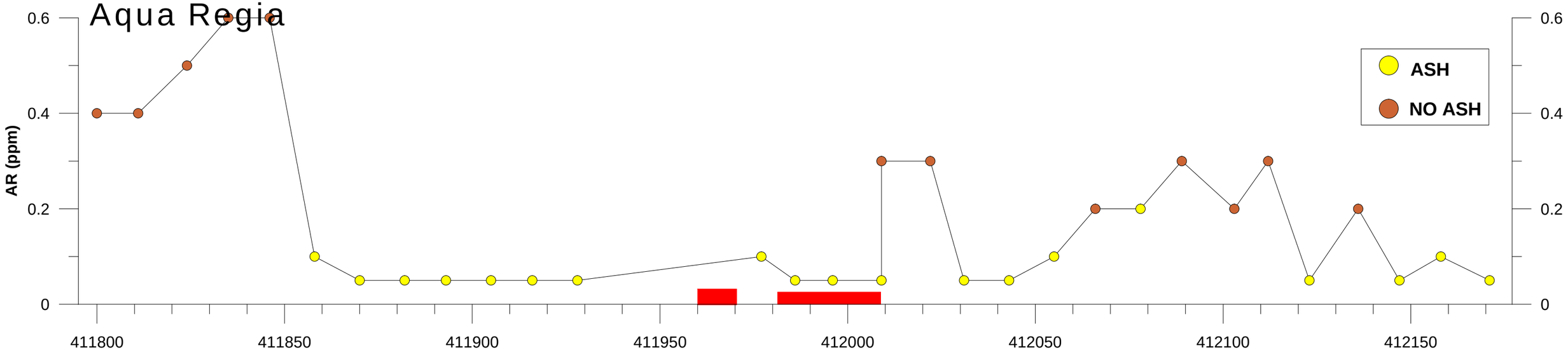

MMI

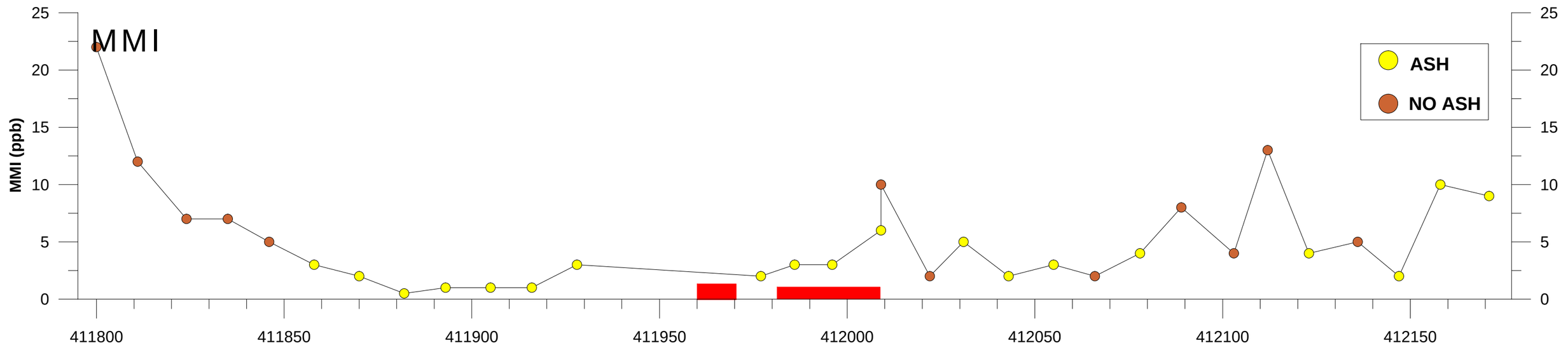

G. N. LUSTIG CONSULTING LTD.- November 17, 2008

Western Copper MMI Test
Zone 1 - North Profile
Yttrium

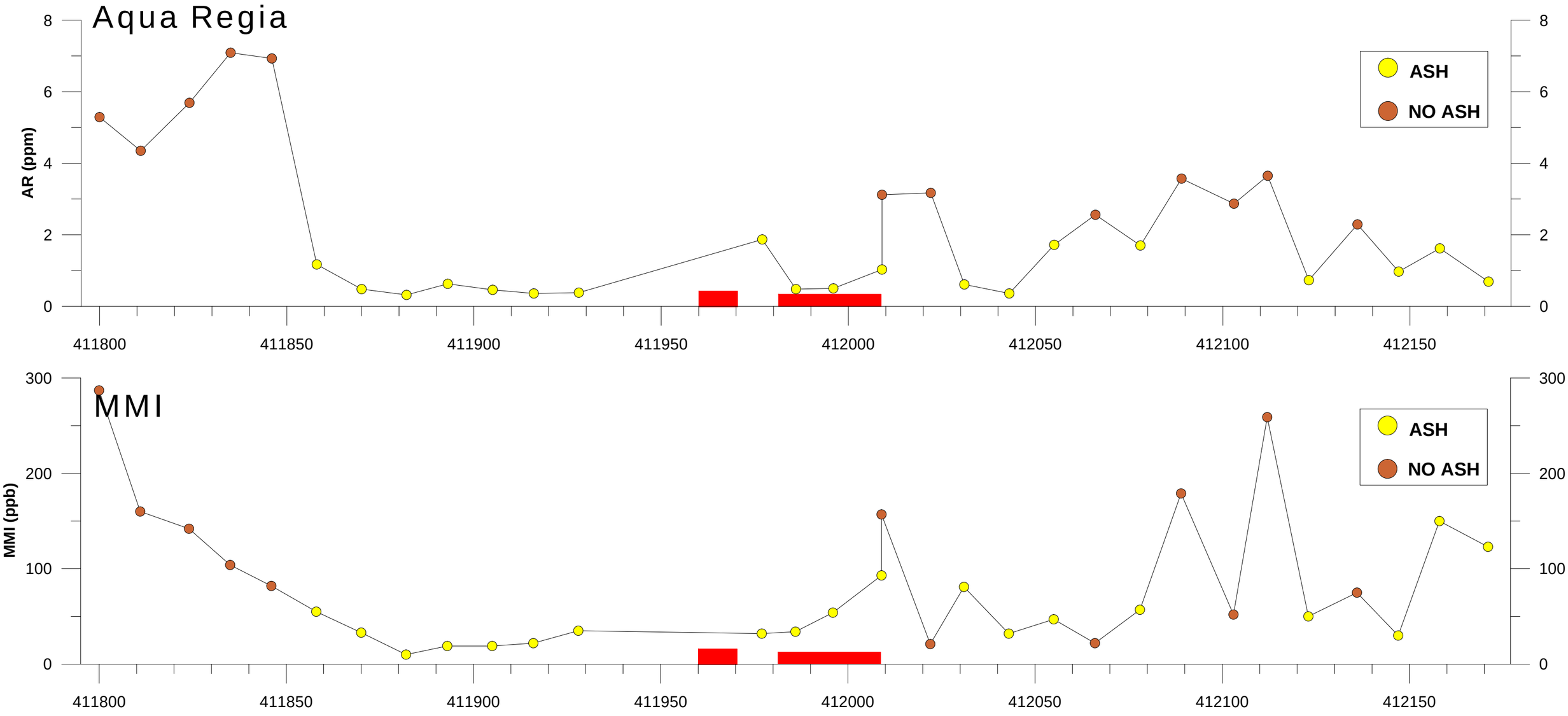

G. N. LUSTIG CONSULTING LTD.- November 17, 2008

Western Copper MMI Test
Zone 1 - North Profile

Zinc

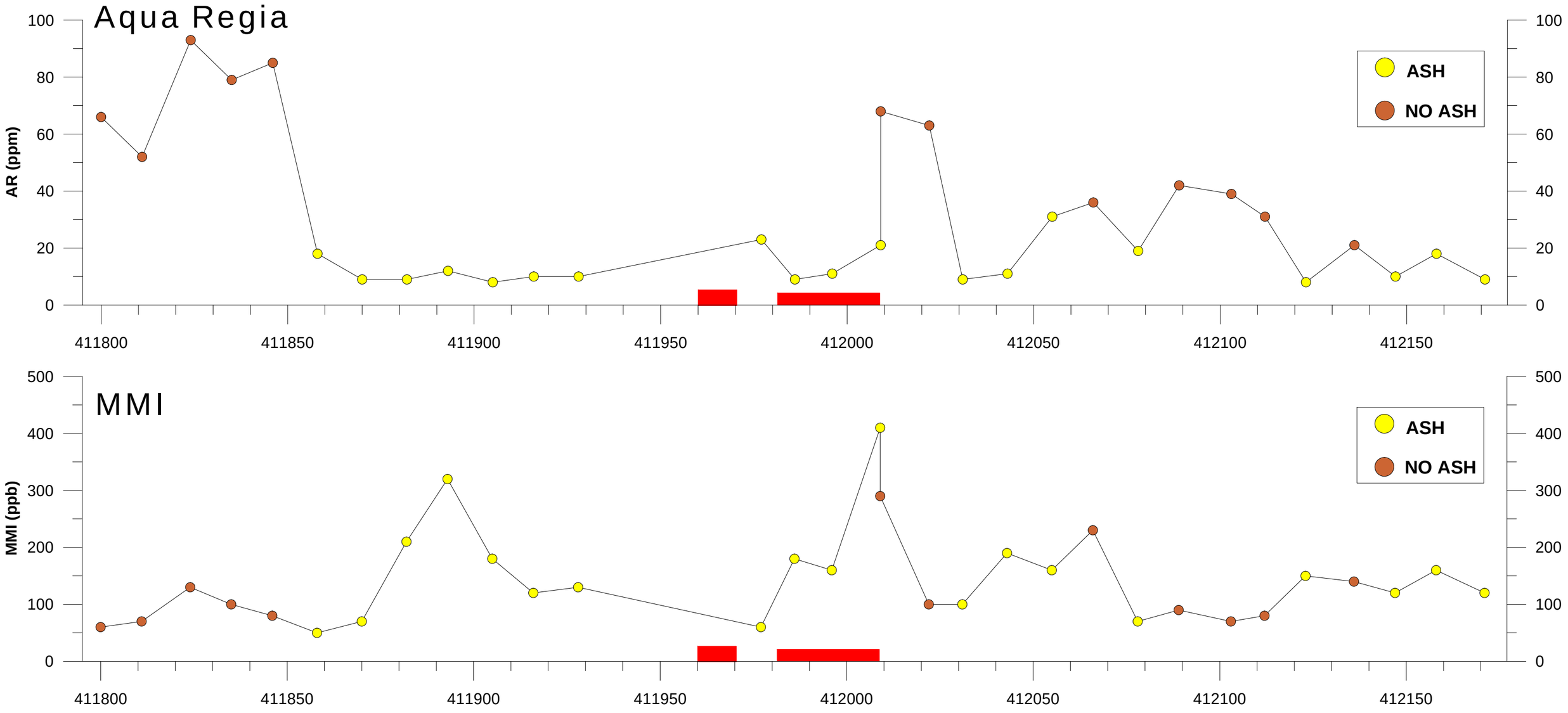

G. N. LUSTIG CONSULTING LTD.- November 17, 2008

Western Copper MMI Test
Zone 1 - North Profile
Zirconium

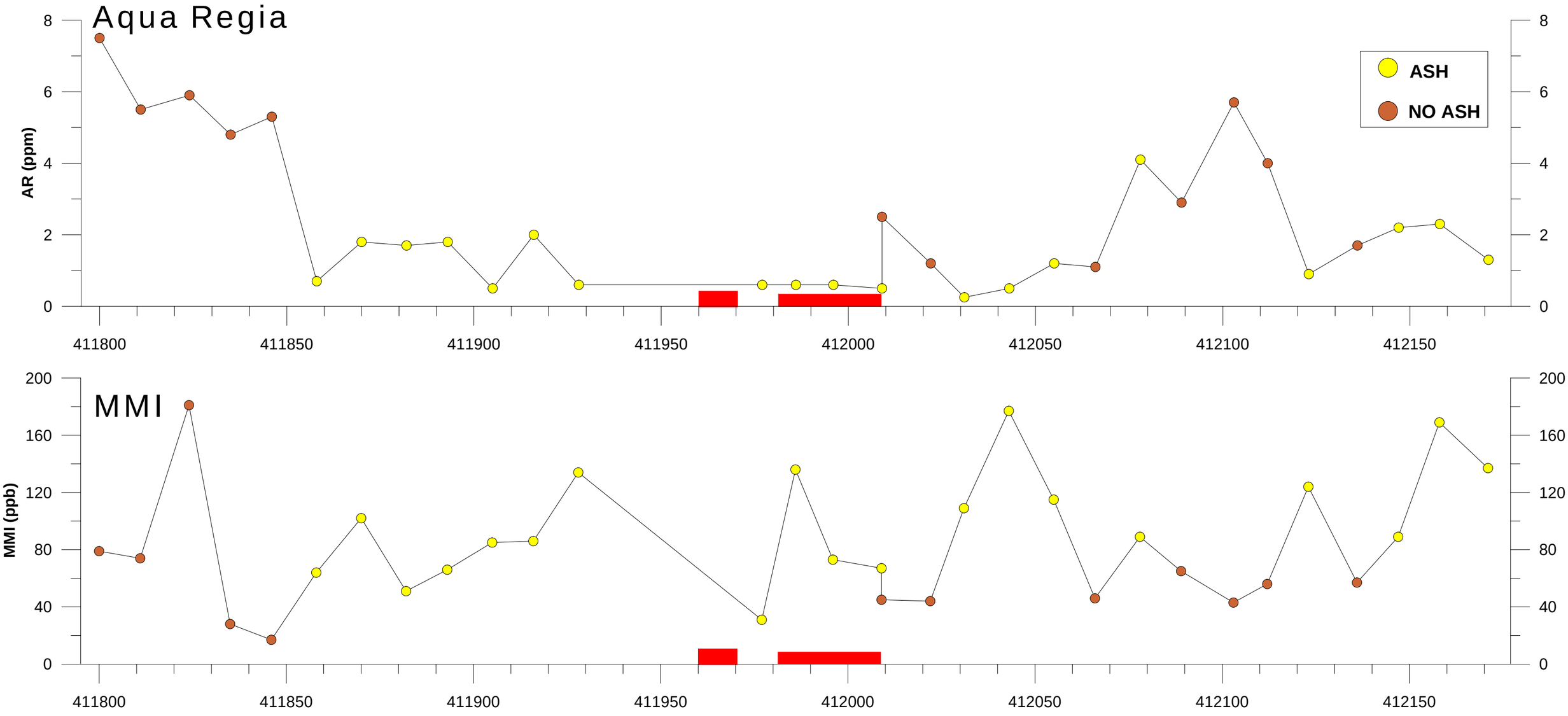

G. N. LUSTIG CONSULTING LTD.- November 17, 2008

Zone 1
South Profile

Western Copper MMI Test
Zone 1 - South Profile
Silver

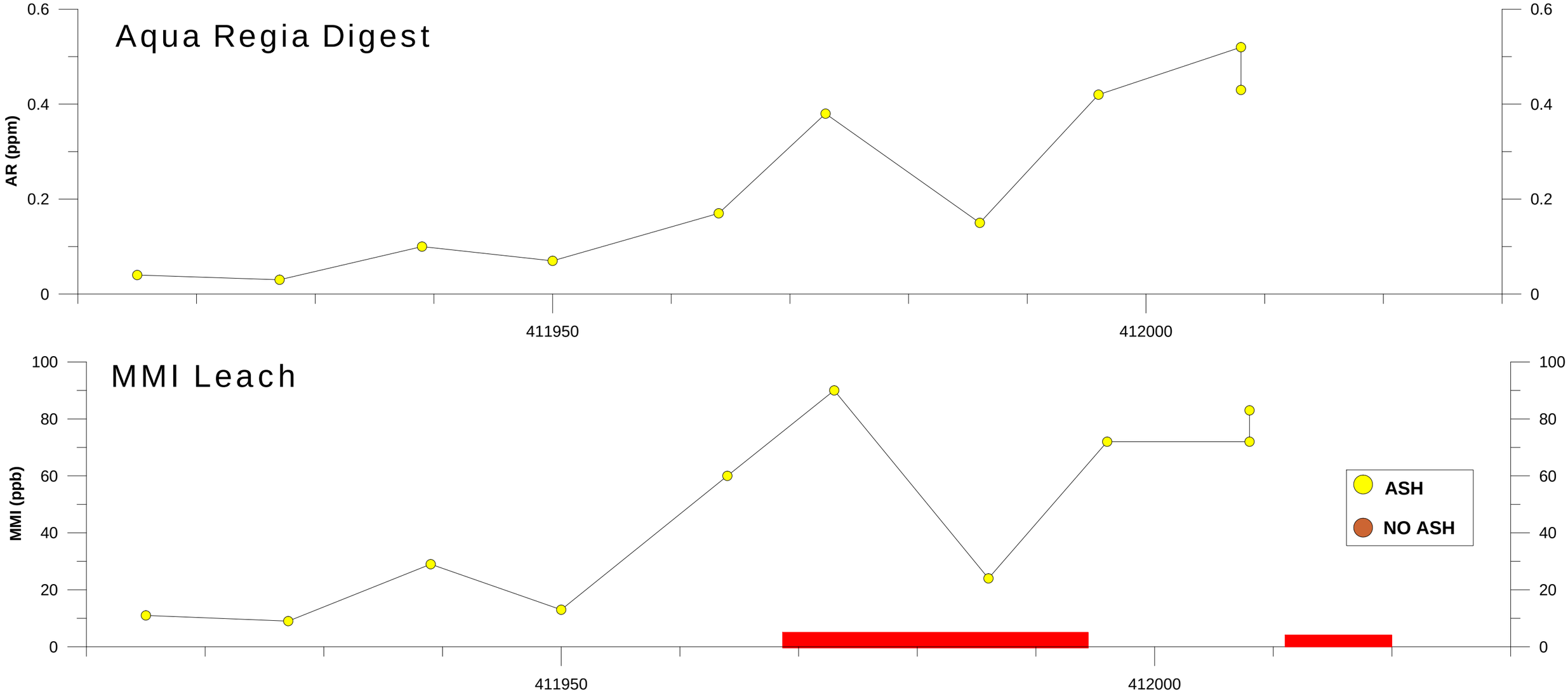

G. N. LUSTIG CONSULTING LTD.- November 20, 2008

Western Copper MMI Test
Zone 1 - South Profile
Aluminum

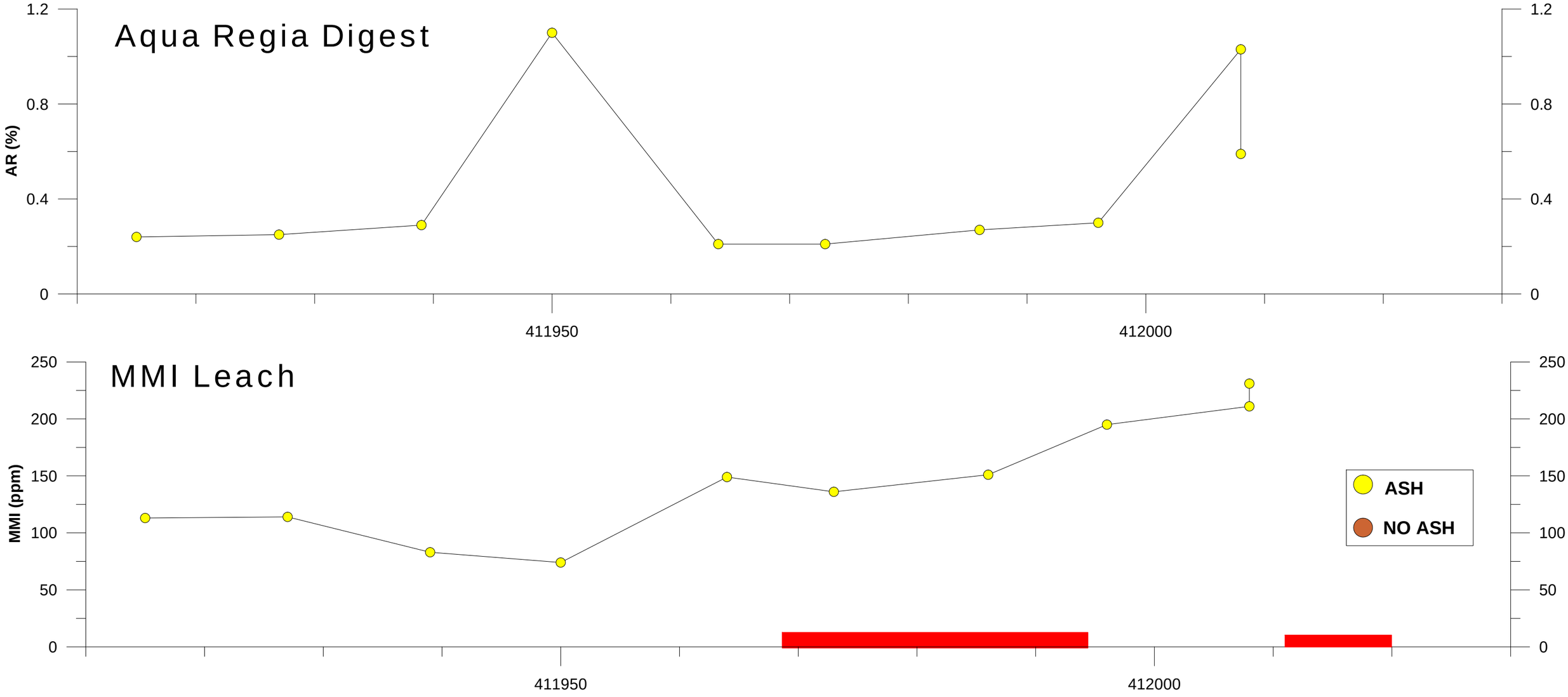

G. N. LUSTIG CONSULTING LTD.- November 20, 2008

Western Copper MMI Test
Zone 1 - South Profile

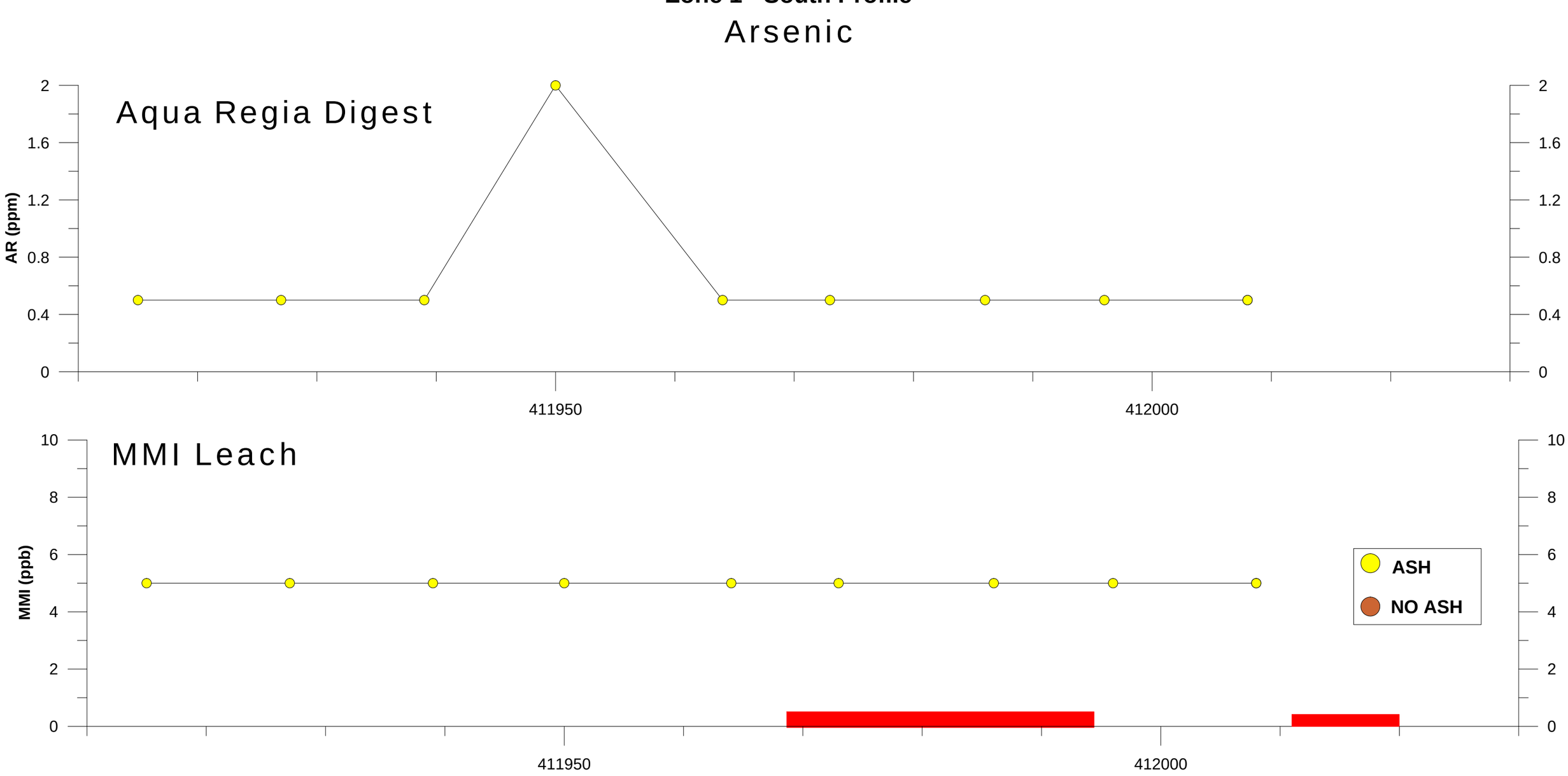

G. N. LUSTIG CONSULTING LTD.- November 20, 2008

Western Copper MMI Test
Zone 1 - South Profile

Barium

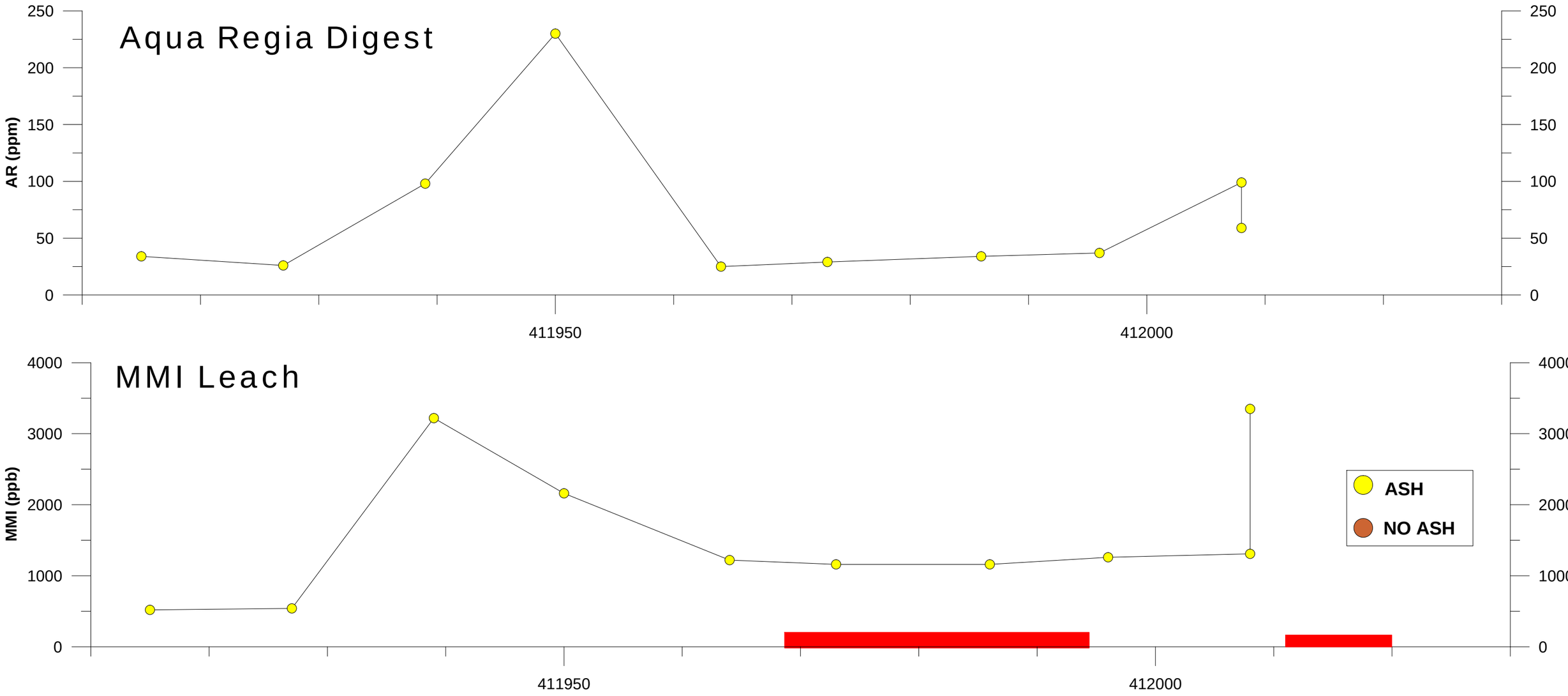

G. N. LUSTIG CONSULTING LTD.- November 20, 2008

Western Copper MMI Test
Zone 1 - South Profile

Bismuth

Aqua Regia Digest

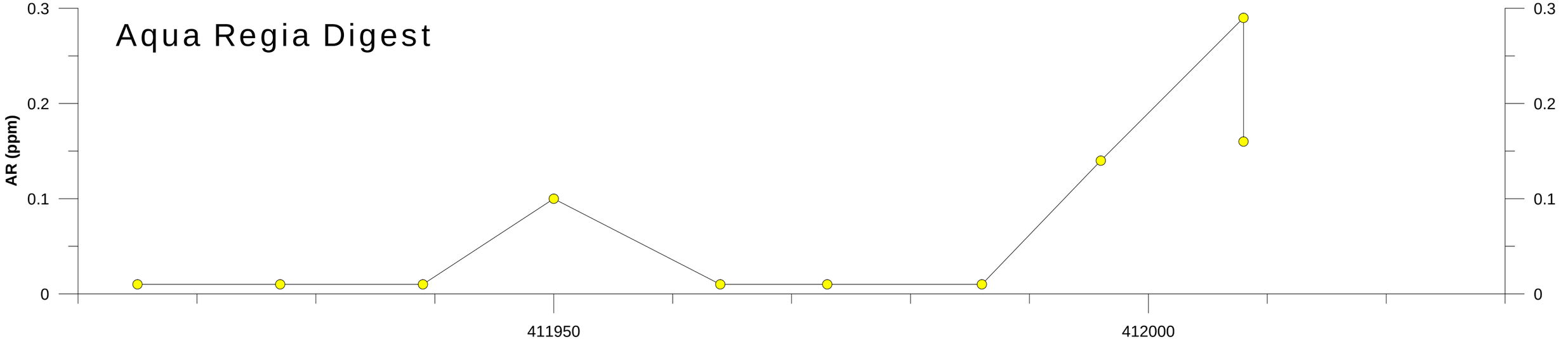

MMI Leach

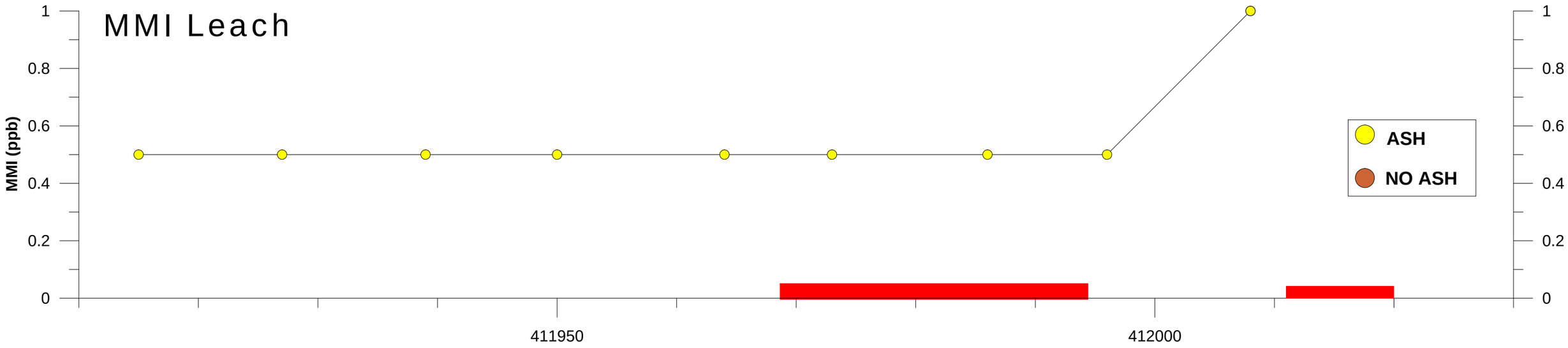

G. N. LUSTIG CONSULTING LTD.- November 20, 2008

Western Copper MMI Test
Zone 1 - South Profile

Calcium

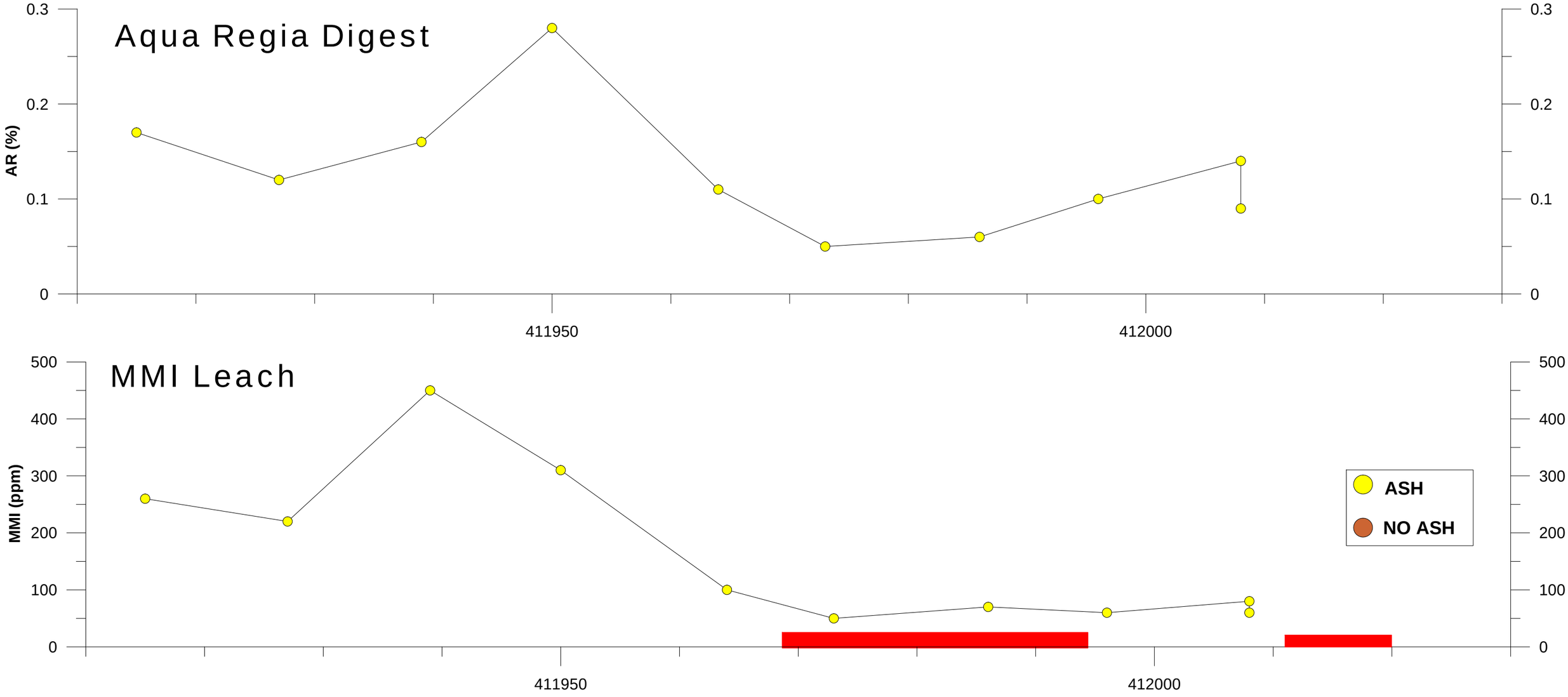

G. N. LUSTIG CONSULTING LTD.- November 20, 2008

Western Copper MMI Test
Zone 1 - South Profile
Cadmium

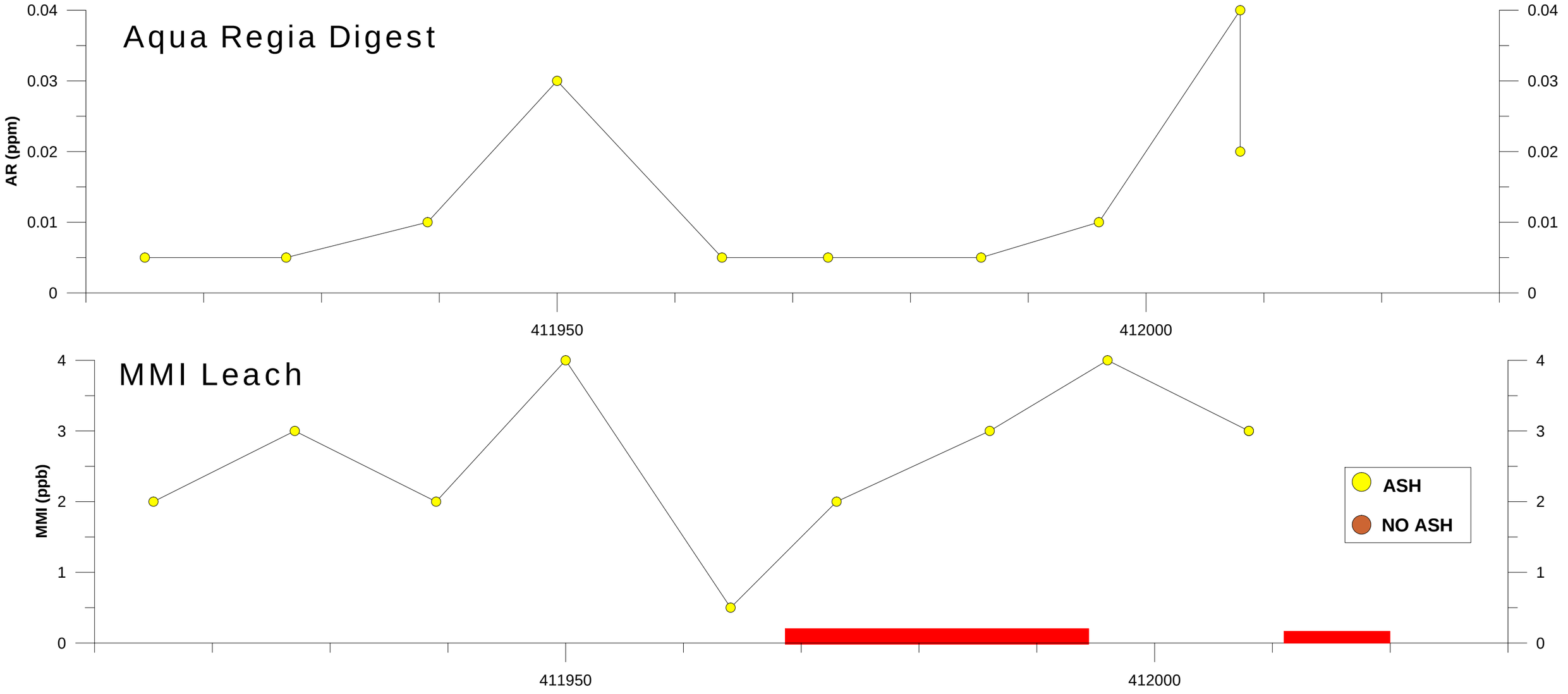

G. N. LUSTIG CONSULTING LTD.- November 20, 2008

Western Copper MMI Test
Zone 1 - South Profile
Cerium

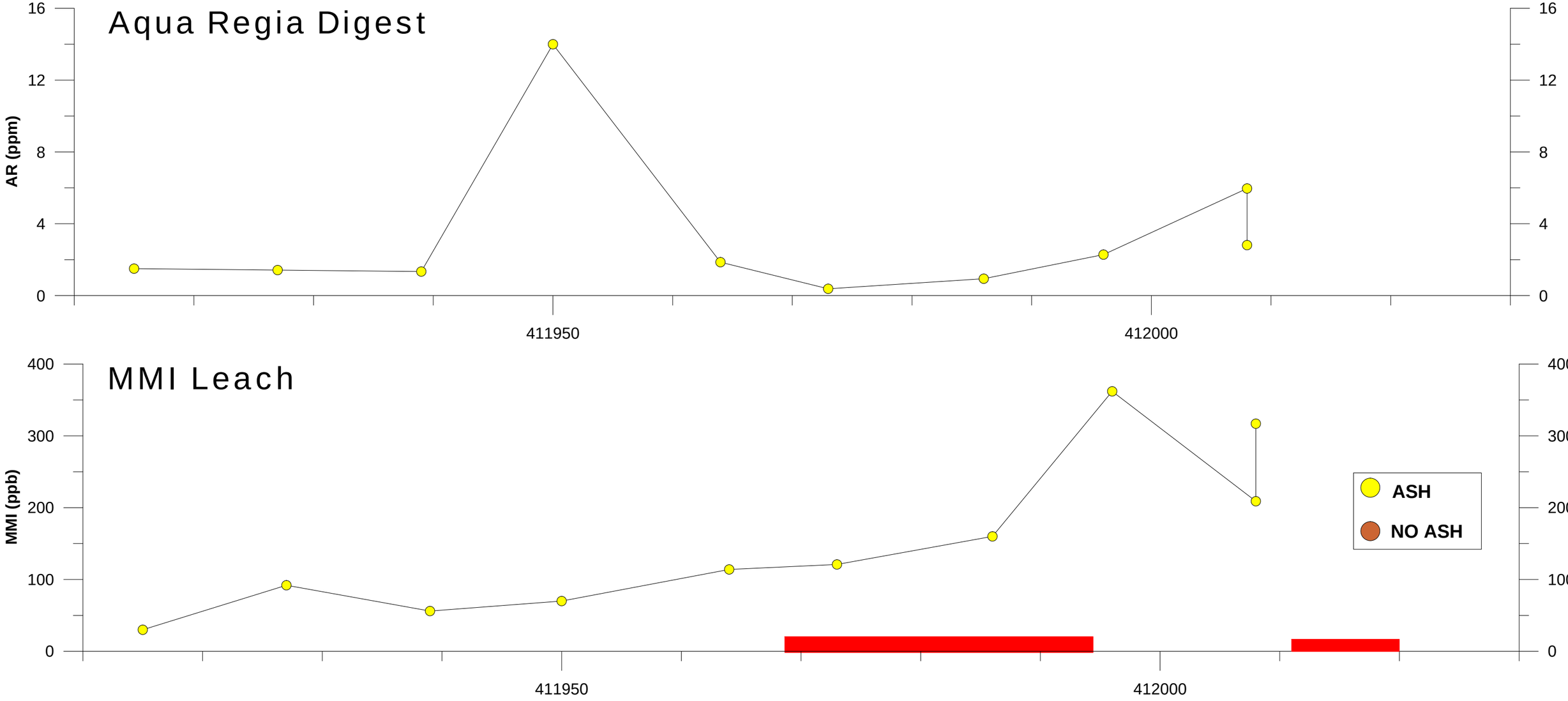

G. N. LUSTIG CONSULTING LTD.- November 20, 2008

Western Copper MMI Test
Zone 1 - South Profile
Cobalt

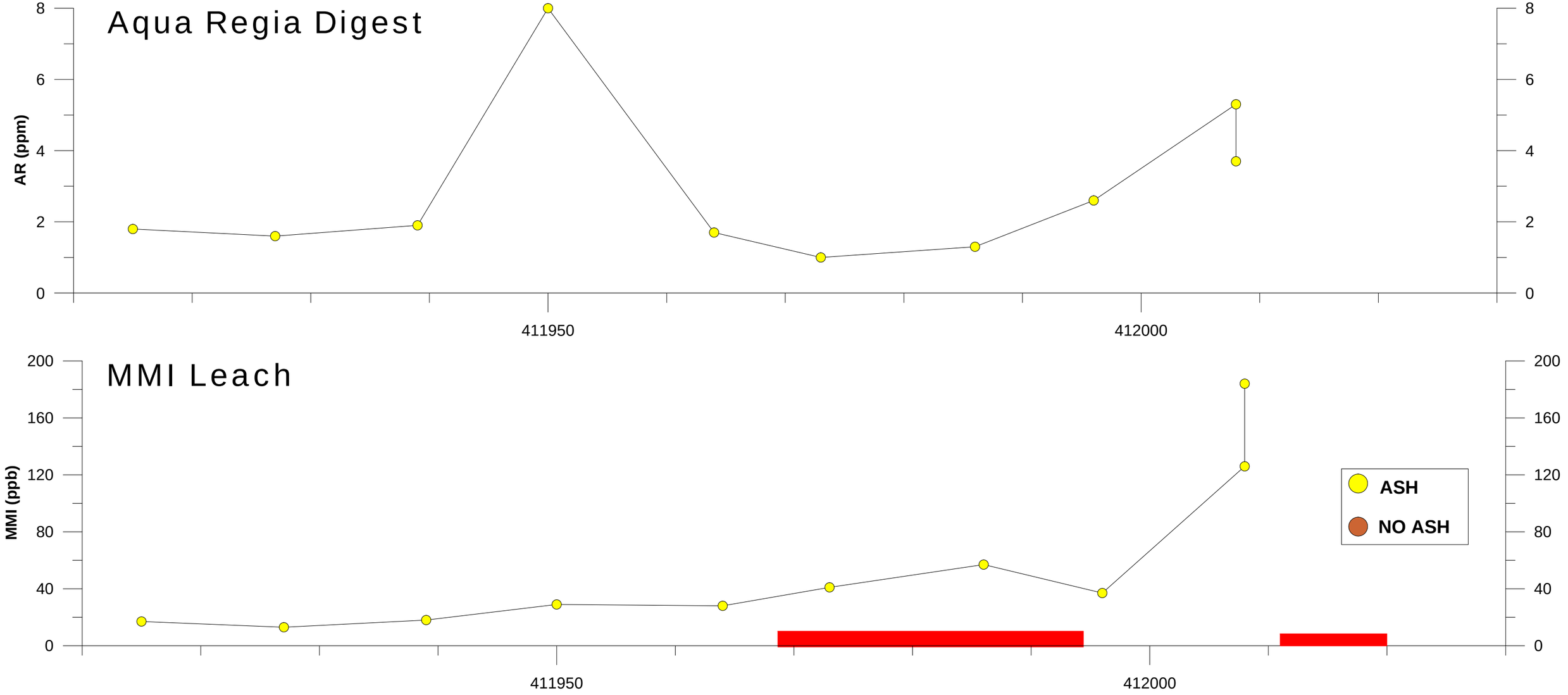

G. N. LUSTIG CONSULTING LTD.- November 20, 2008

Western Copper MMI Test
Zone 1 - South Profile

Chromium

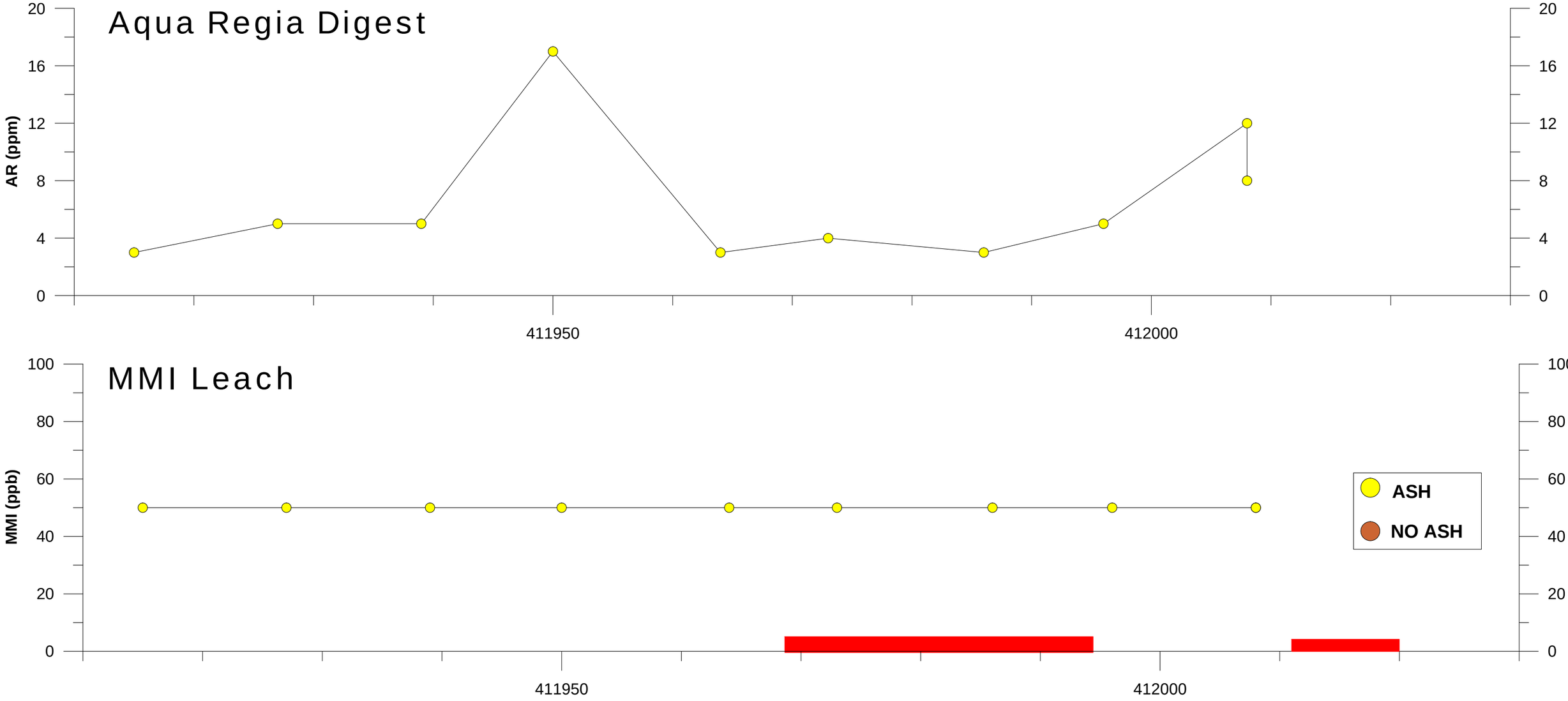

G. N. LUSTIG CONSULTING LTD.- November 20, 2008

Western Copper MMI Test
Zone 1 - South Profile

Copper

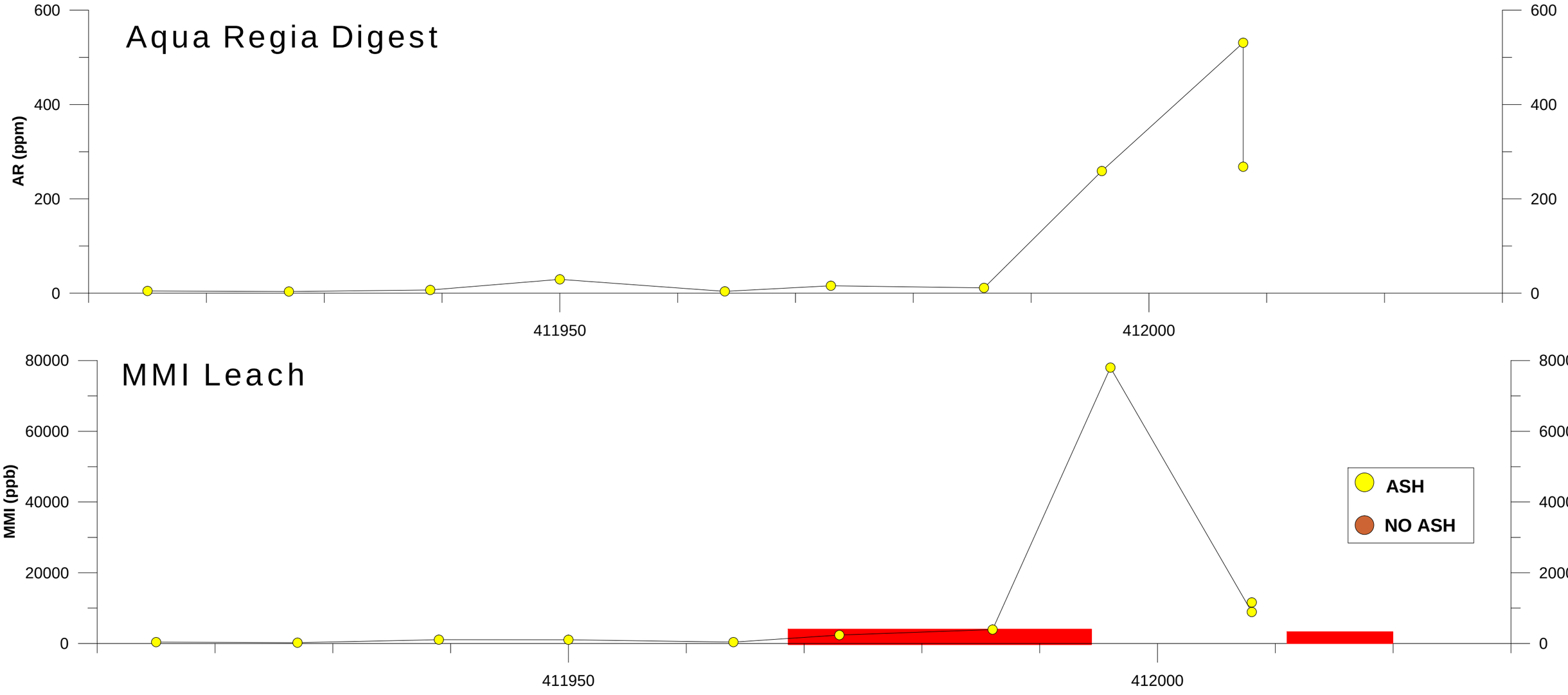

G. N. LUSTIG CONSULTING LTD.- November 20, 2008

Western Copper MMI Test
Zone 1 - South Profile
Iron

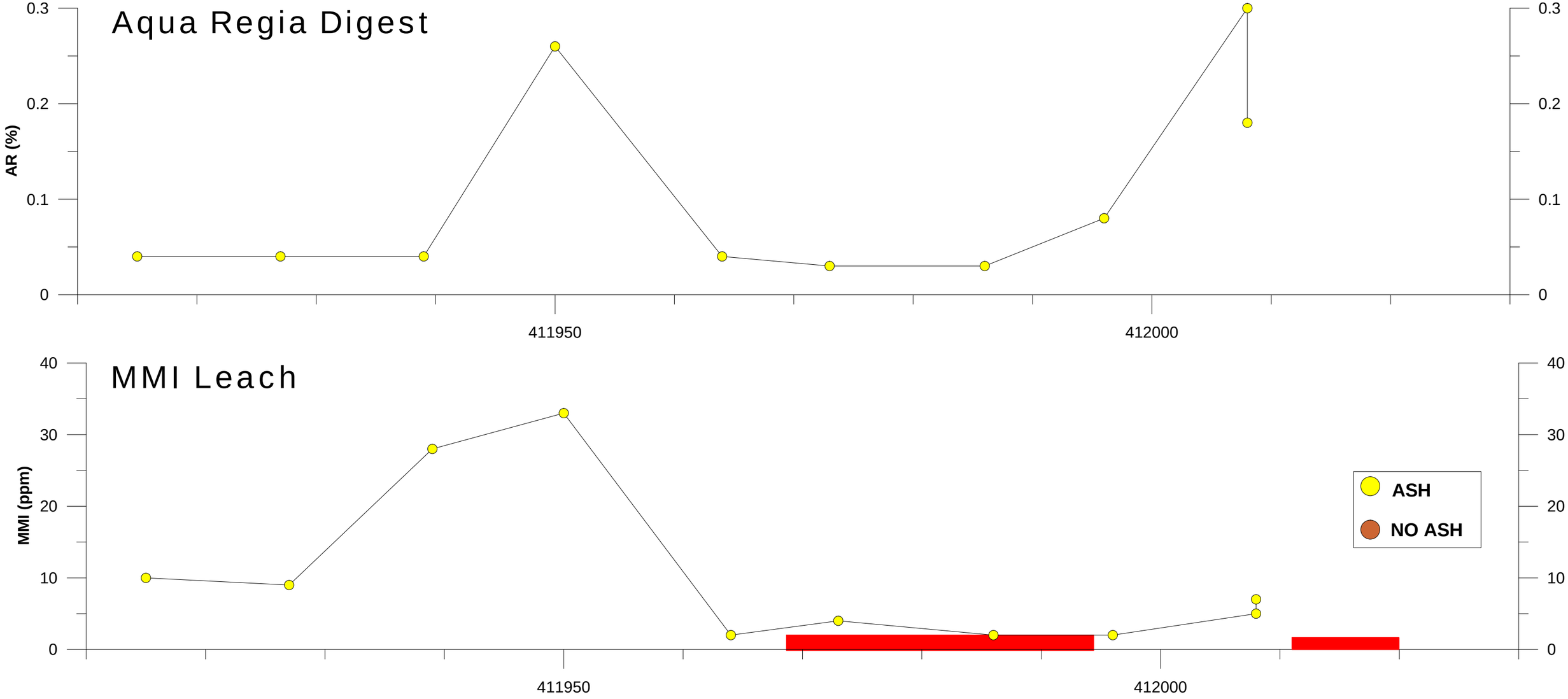

G. N. LUSTIG CONSULTING LTD.- November 20, 2008

Western Copper MMI Test
Zone 1 - South Profile

Lanthanum

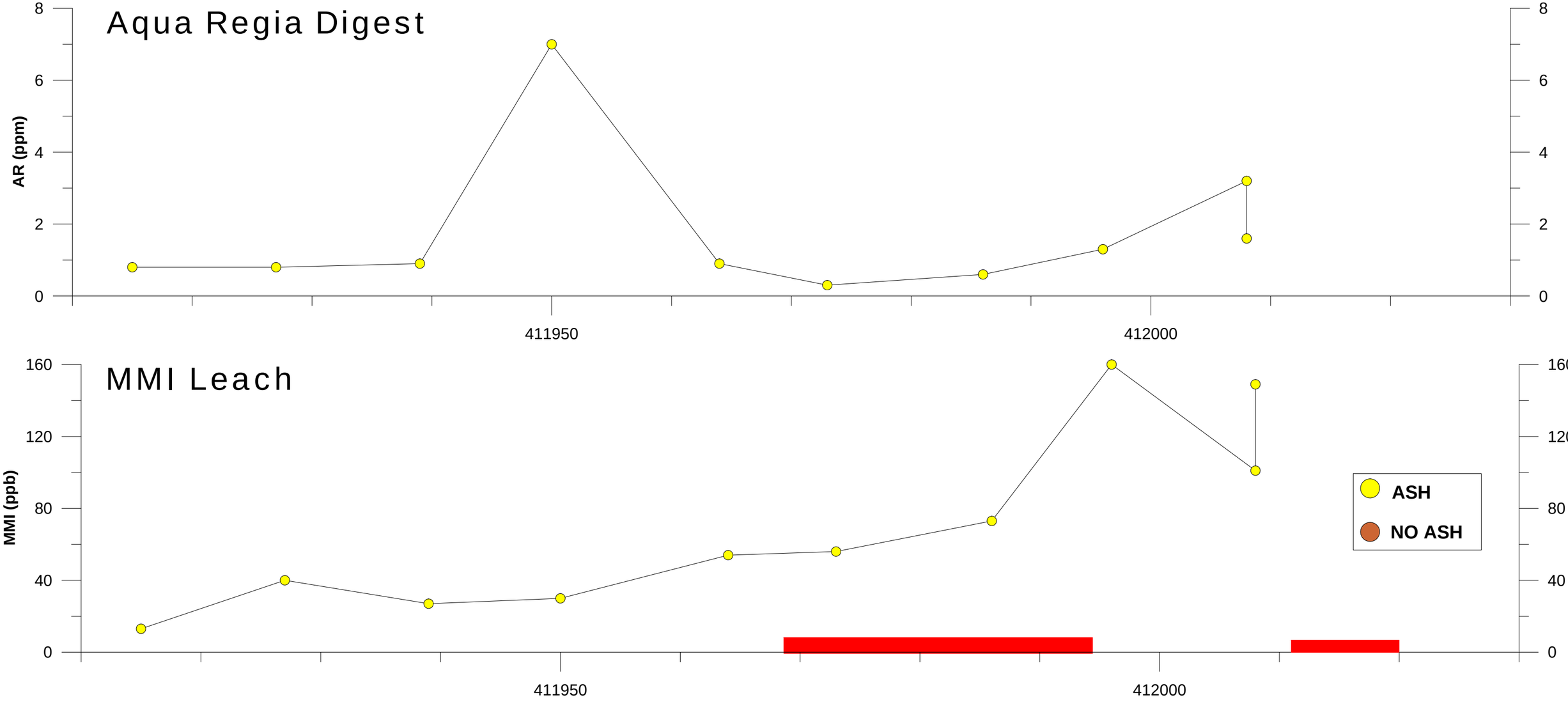

G. N. LUSTIG CONSULTING LTD.- November 20, 2008

Western Copper MMI Test
Zone 1 - South Profile
Lithium

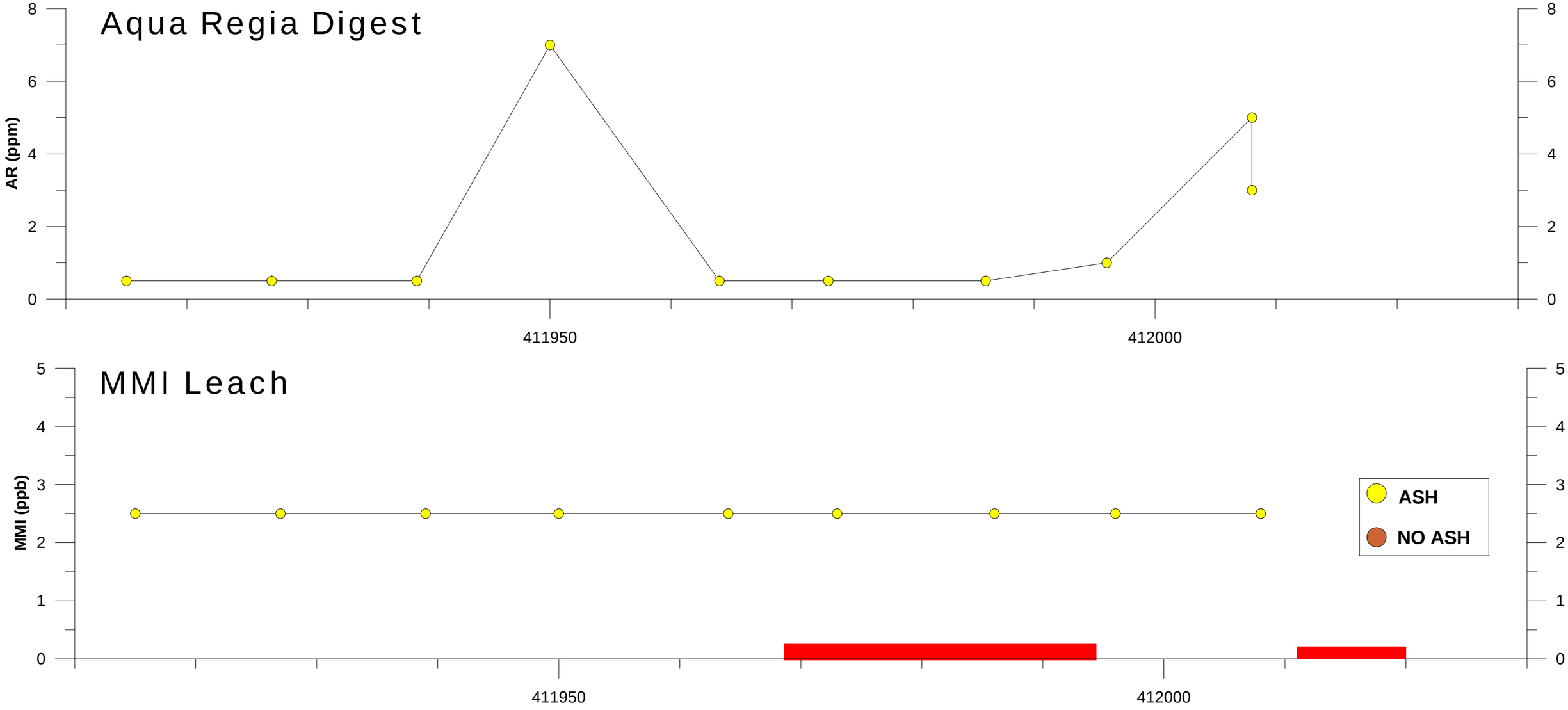

G. N. LUSTIG CONSULTING LTD.- November 20, 2008

Western Copper MMI Test
Zone 1 - South Profile
Magnesium

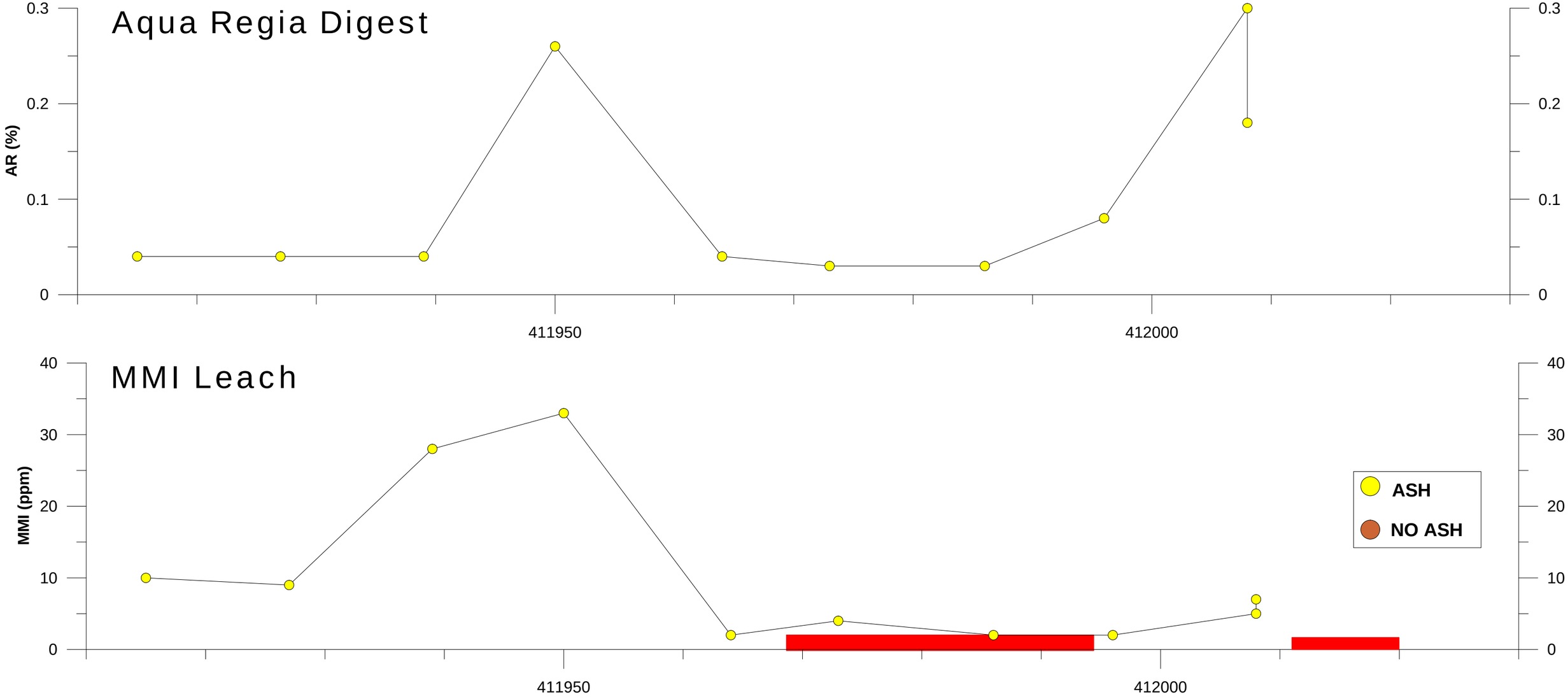

G. N. LUSTIG CONSULTING LTD.- November 20, 2008

Western Copper MMI Test
Zone 1 - South Profile
Molybdenum

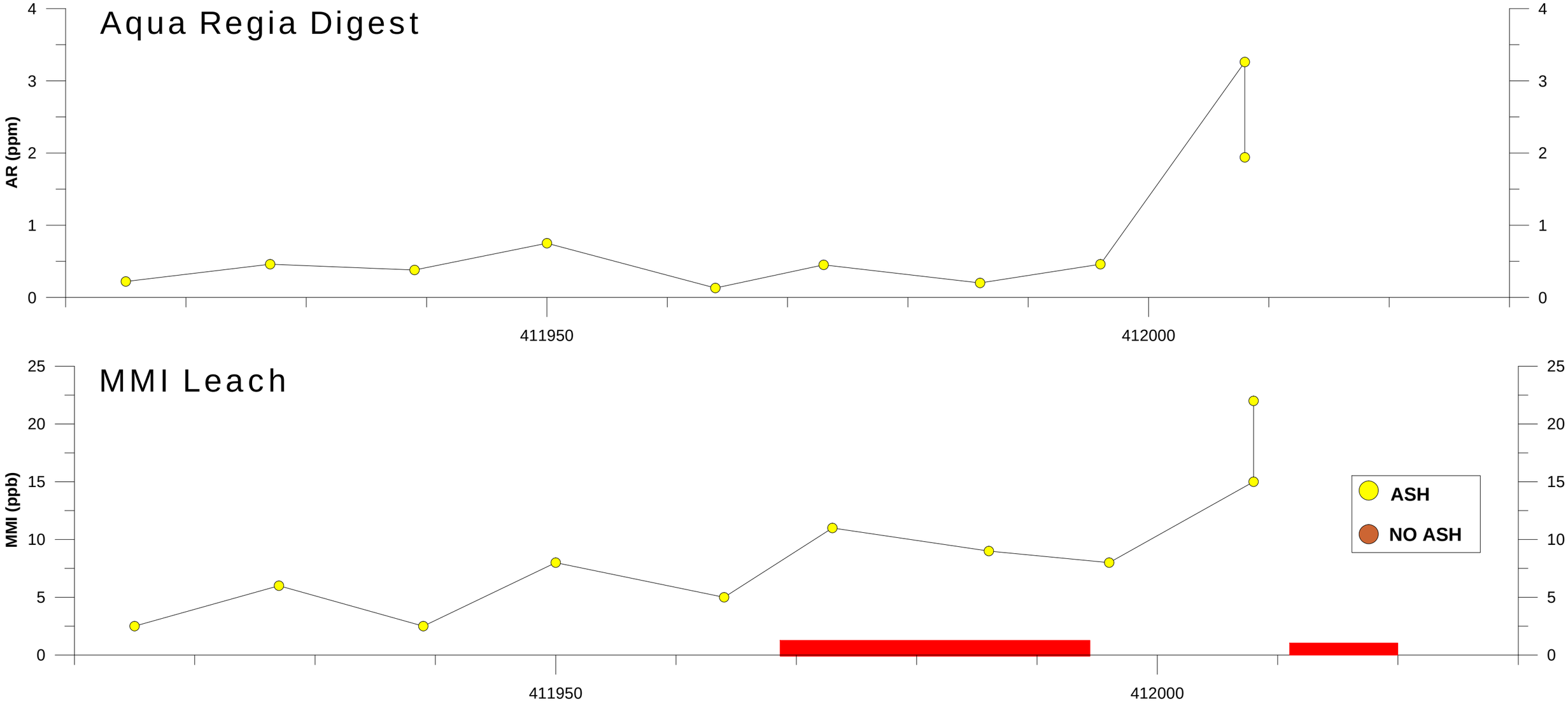

G. N. LUSTIG CONSULTING LTD.- November 20, 2008

Western Copper MMI Test
Zone 1 - South Profile
Niobium

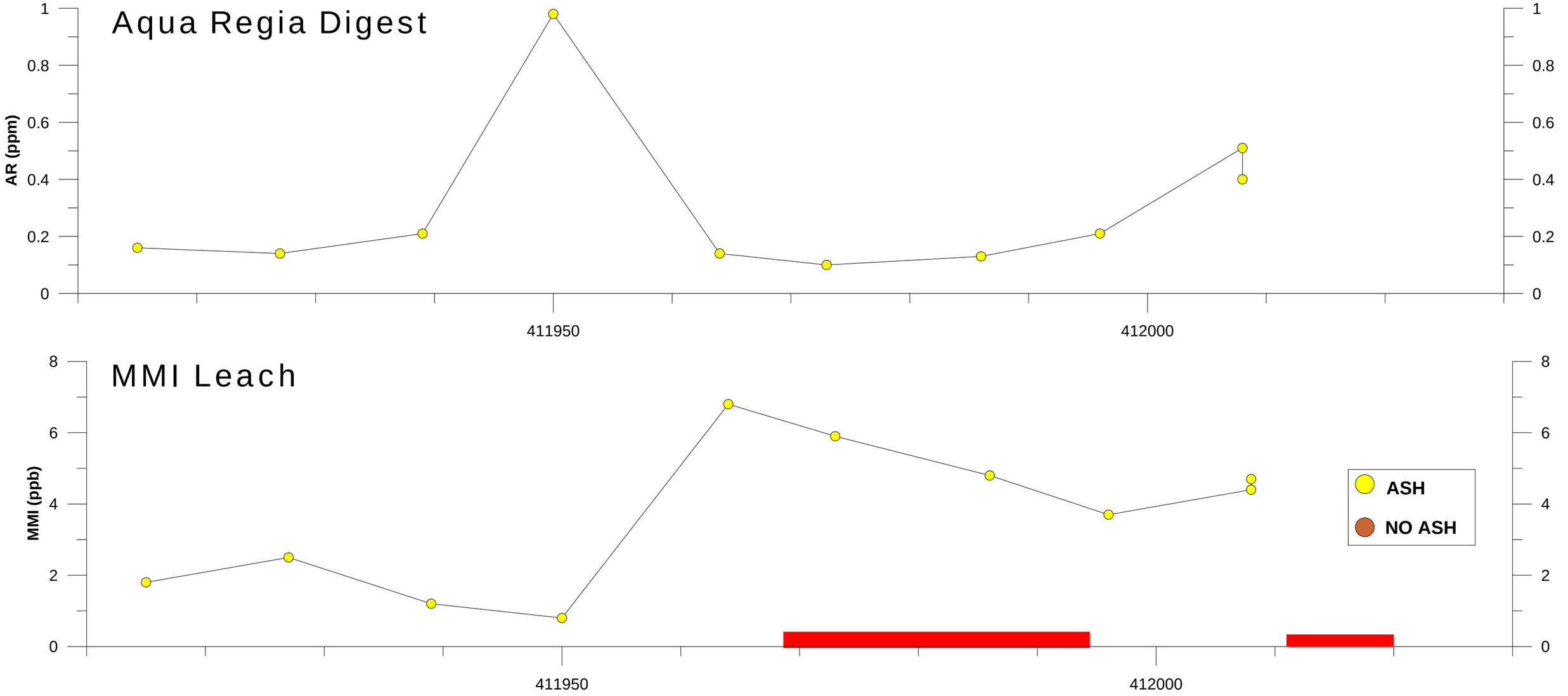

G. N. LUSTIG CONSULTING LTD.- November 20, 2008

Western Copper MMI Test
Zone 1 - South Profile
Nickel

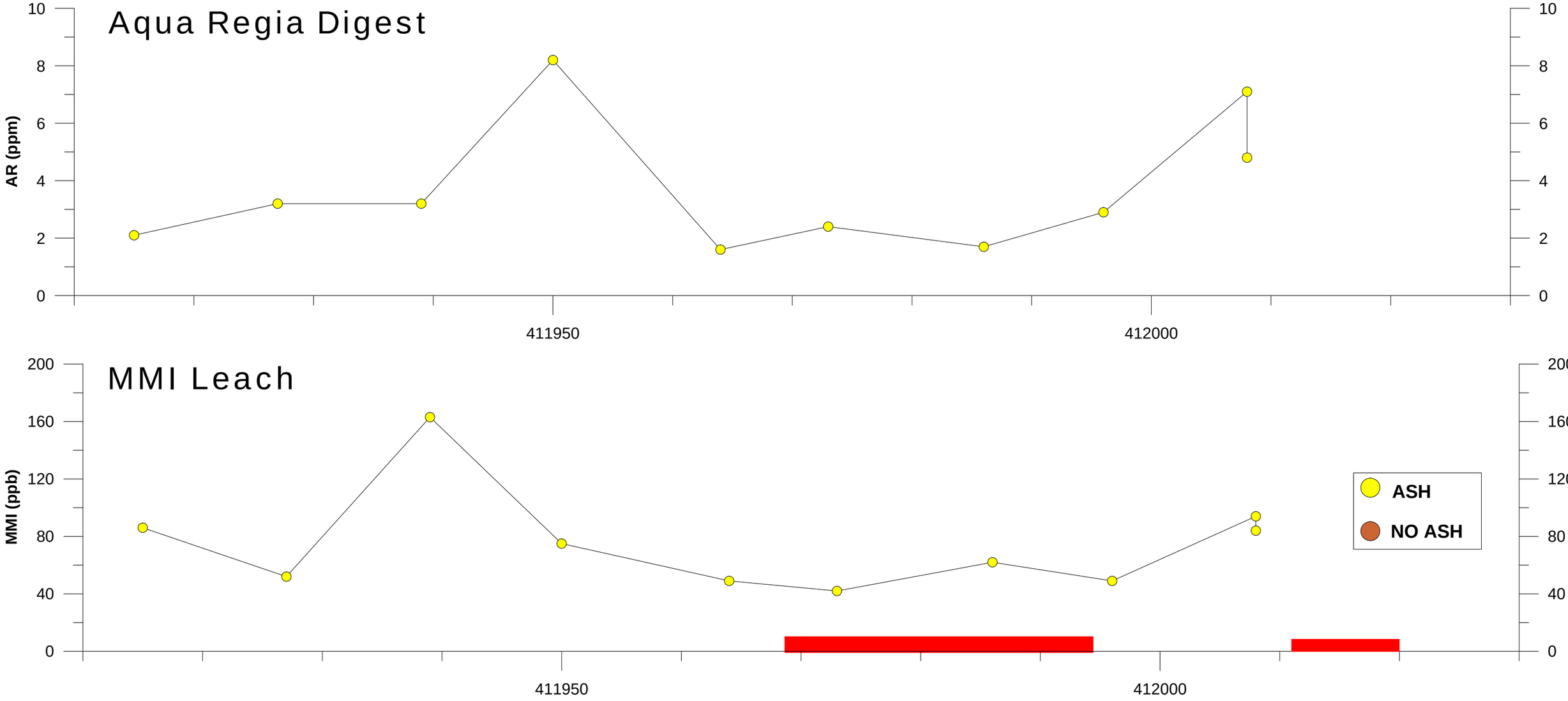

G. N. LUSTIG CONSULTING LTD.- November 20, 2008

Western Copper MMI Test
Zone 1 - South Profile
Lead

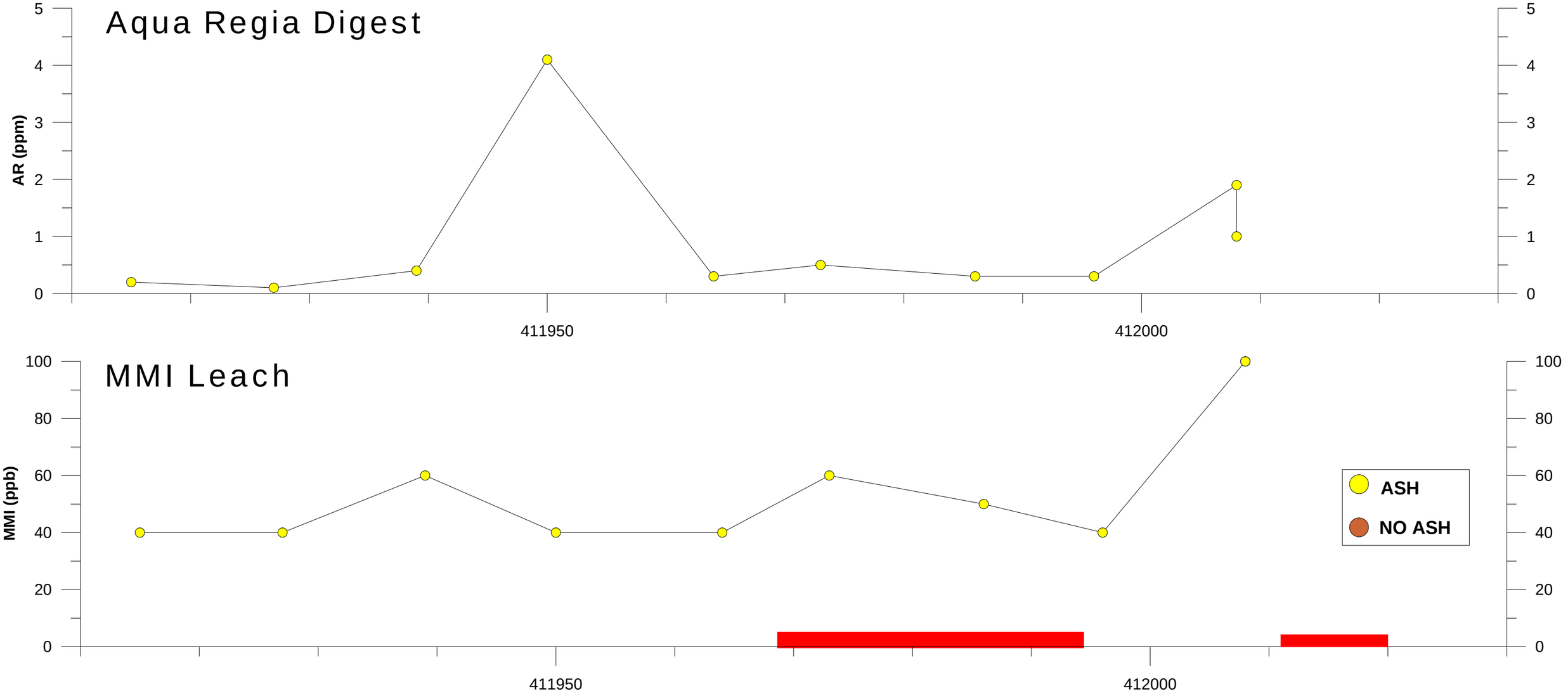

G. N. LUSTIG CONSULTING LTD.- November 20, 2008

Western Copper MMI Test
Zone 1 - South Profile

Rubidium

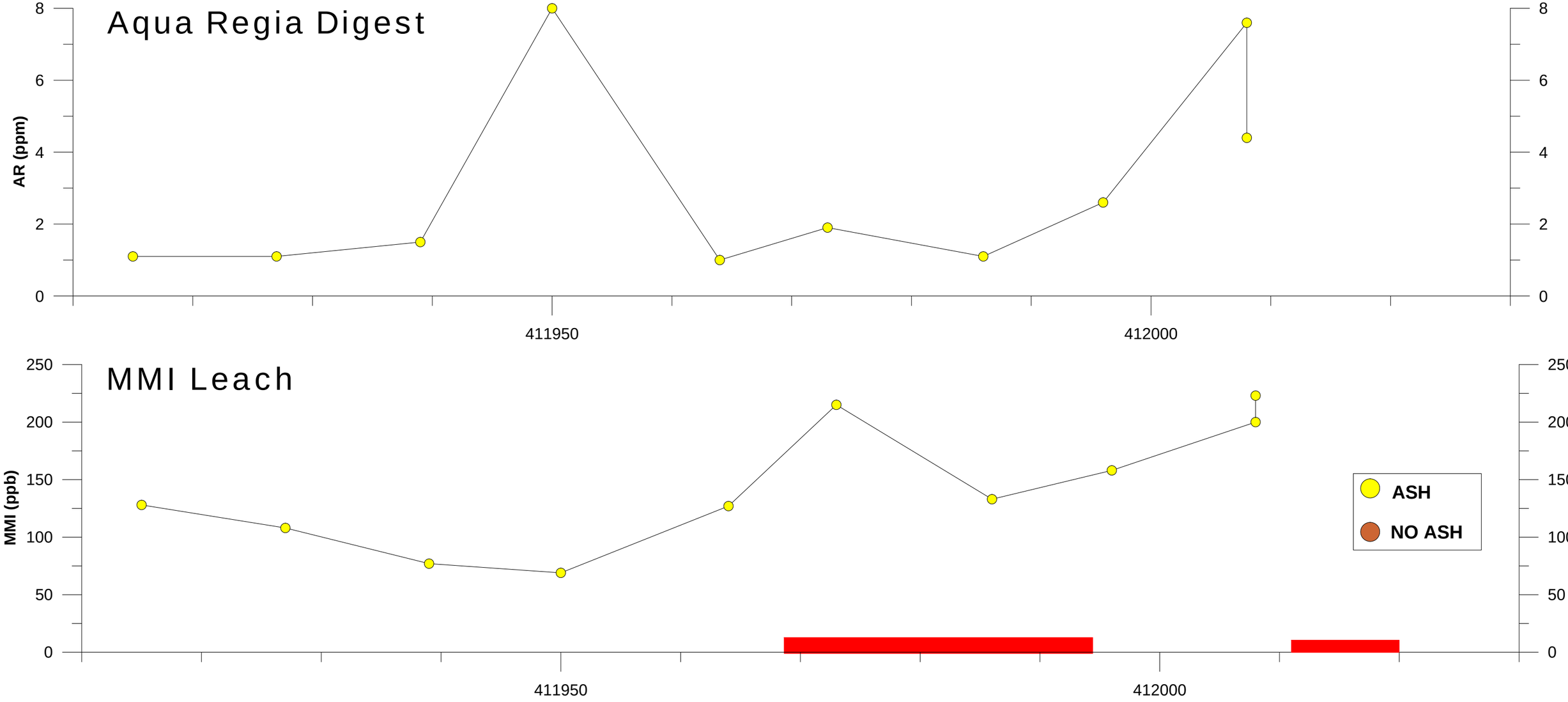

G. N. LUSTIG CONSULTING LTD.- November 20, 2008

Western Copper MMI Test
Zone 1 - South Profile
Antimony

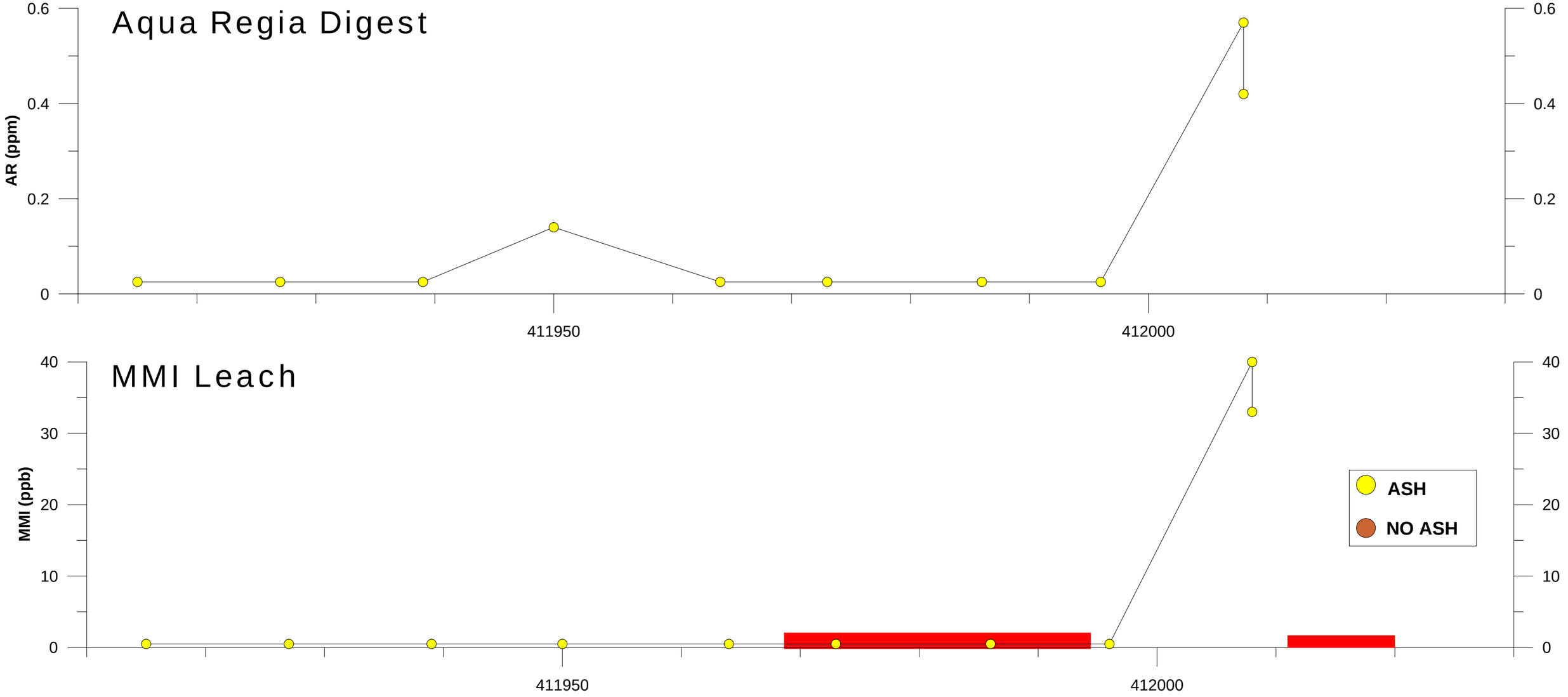

G. N. LUSTIG CONSULTING LTD.- November 20, 2008

Western Copper MMI Test
Zone 1 - South Profile
Scandium

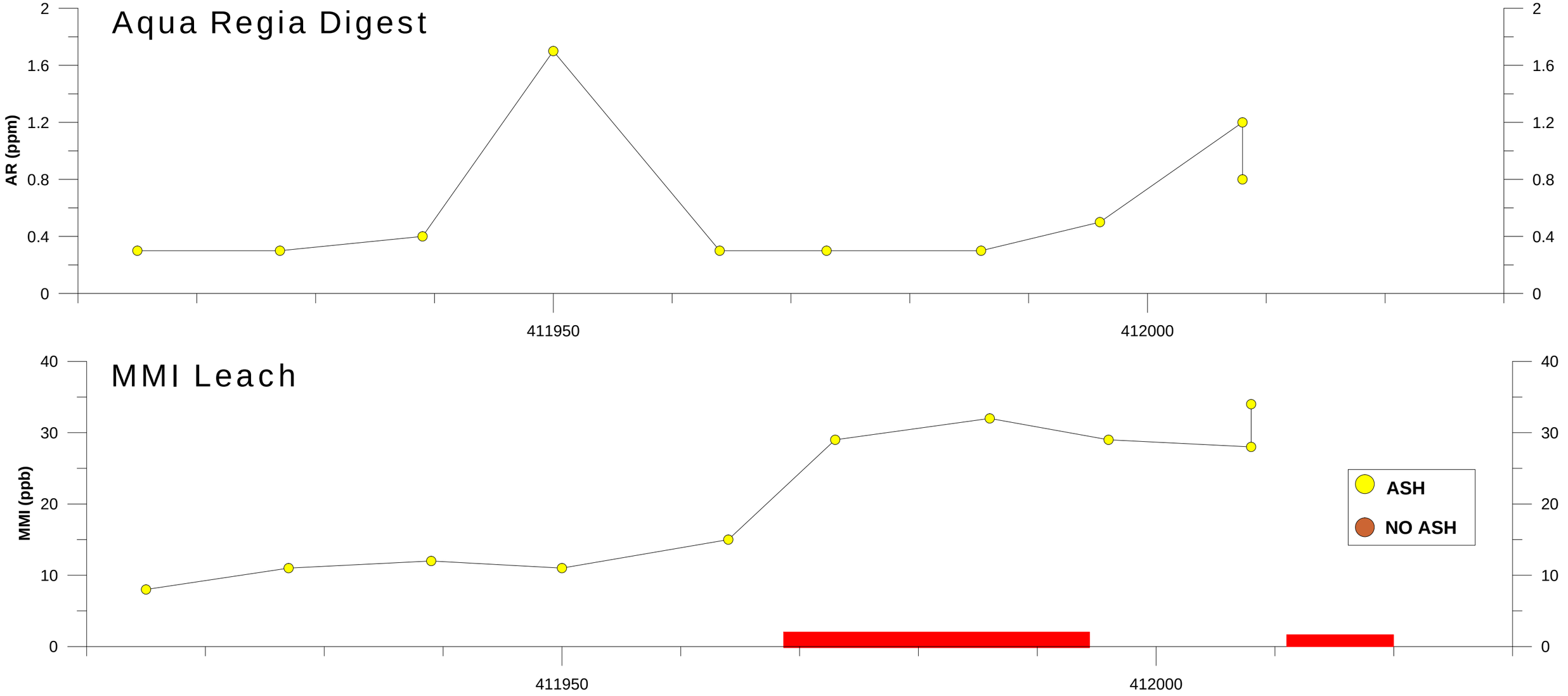

G. N. LUSTIG CONSULTING LTD.- November 20, 2008

Western Copper MMI Test
Zone 1 - South Profile
Tin

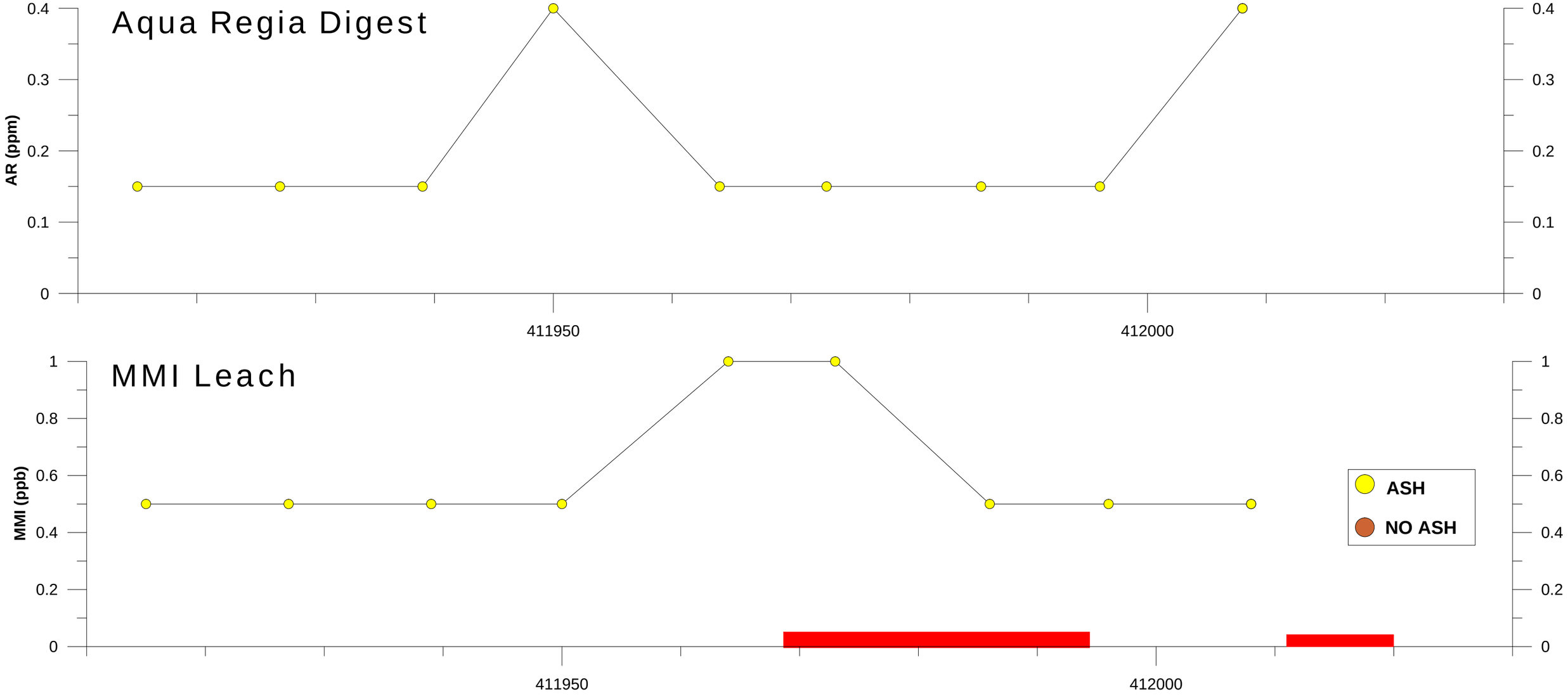

G. N. LUSTIG CONSULTING LTD.- November 20, 2008

Western Copper MMI Test
Zone 1 - South Profile

Strontium

Aqua Regia Digest

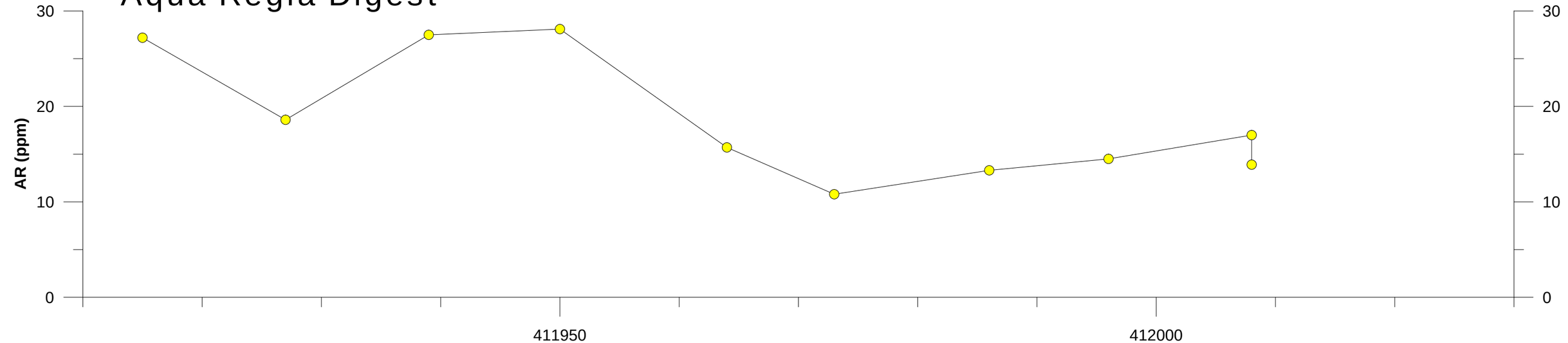

MMI Leach

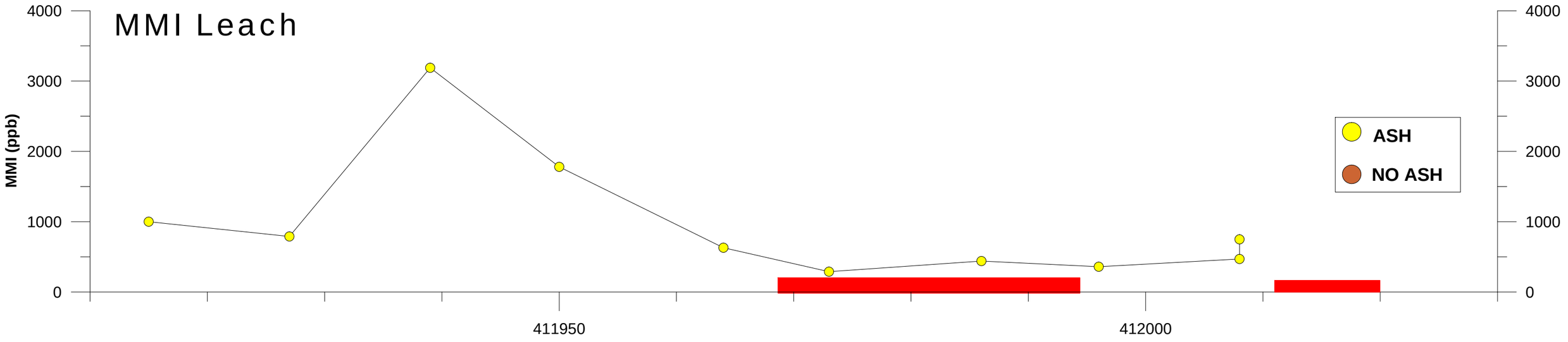

G. N. LUSTIG CONSULTING LTD.- November 20, 2008

Western Copper MMI Test
Zone 1 - South Profile

Tantalum

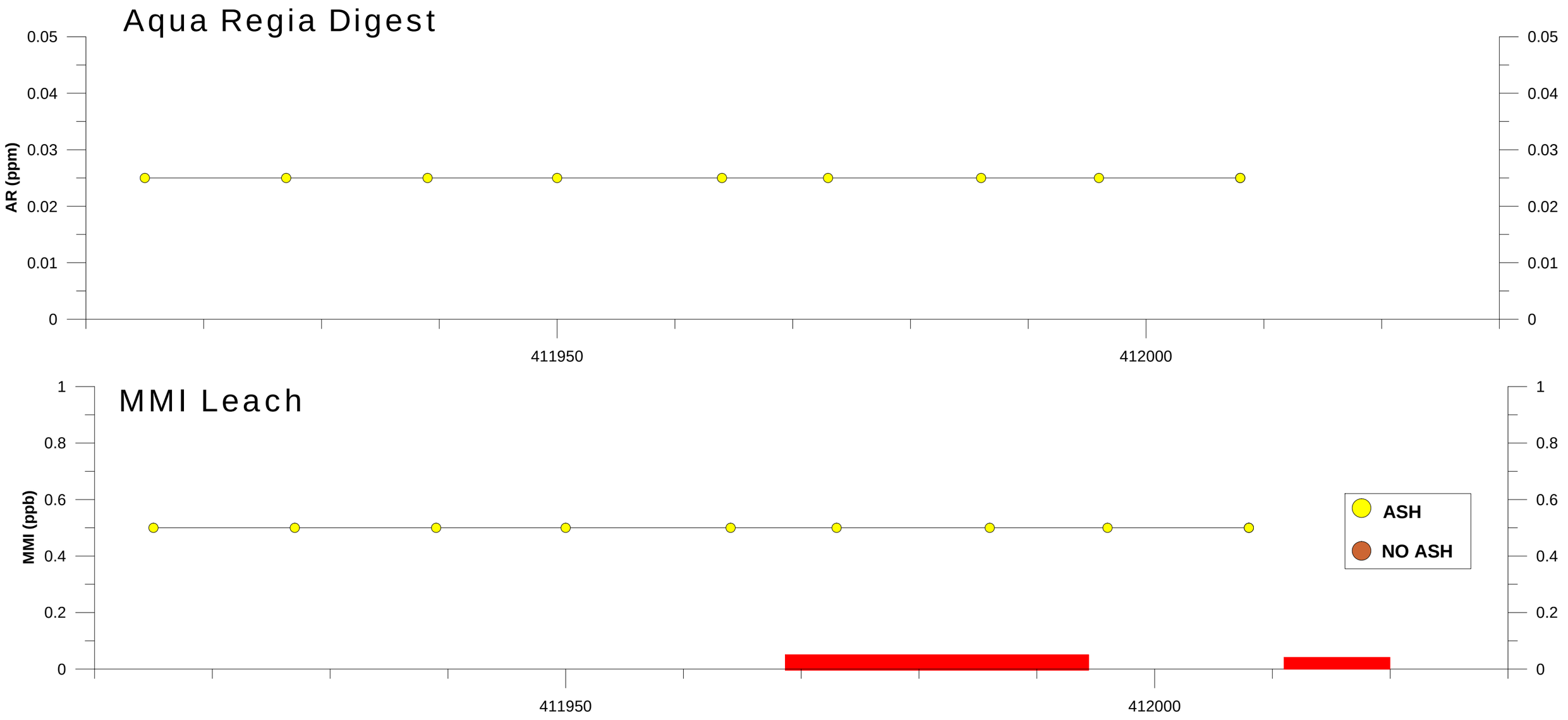

G. N. LUSTIG CONSULTING LTD.- November 20, 2008

Western Copper MMI Test
Zone 1 - South Profile
Terbium

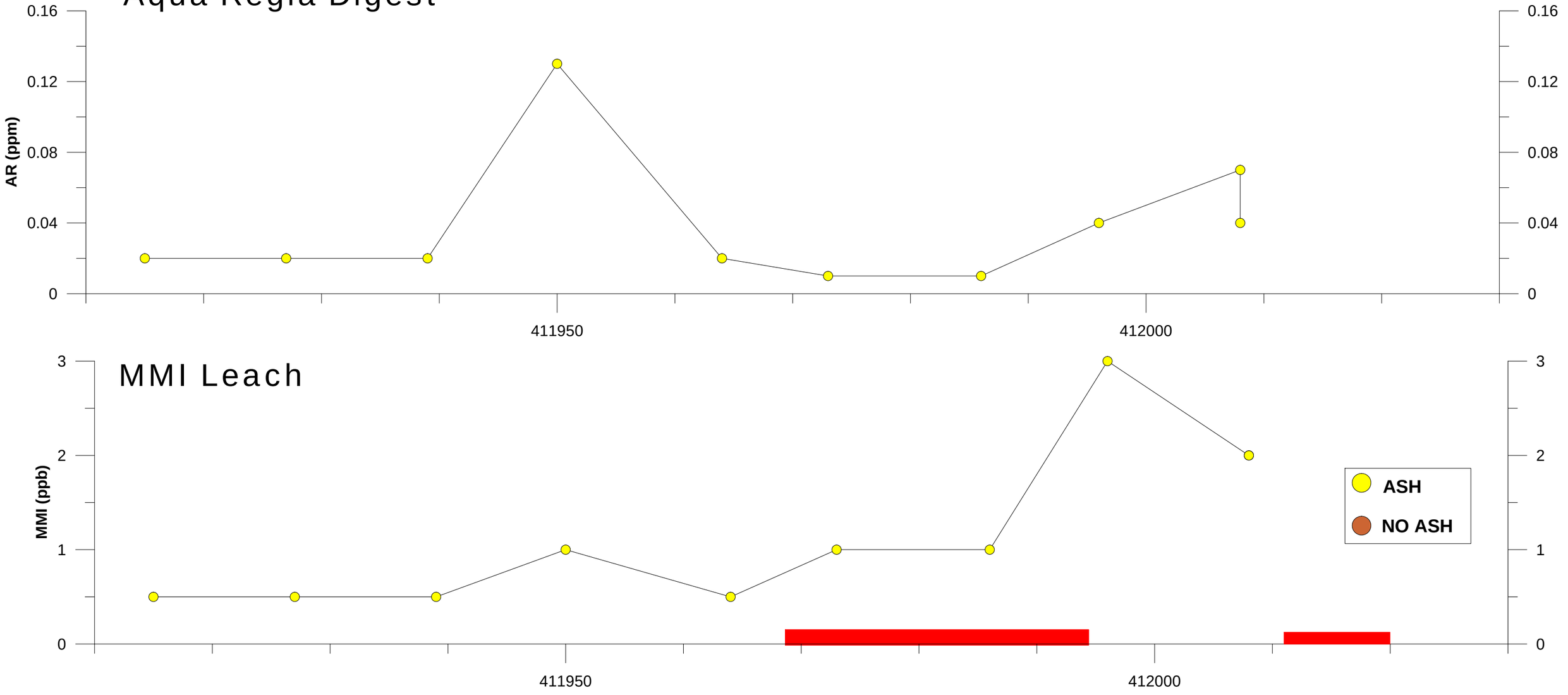

G. N. LUSTIG CONSULTING LTD.- November 20, 2008

Western Copper MMI Test
Zone 1 - South Profile

Thorium

Aqua Regia Digest

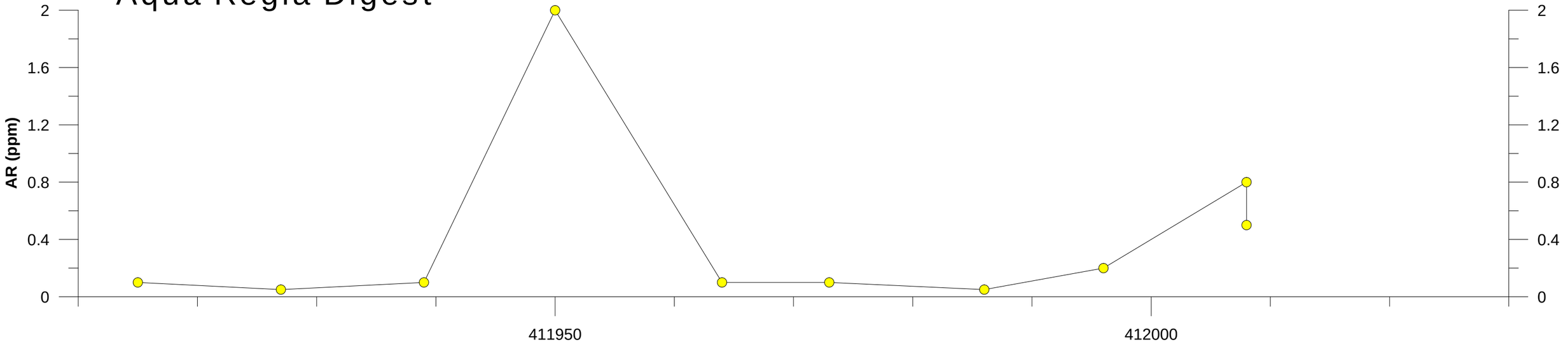

MMI Leach

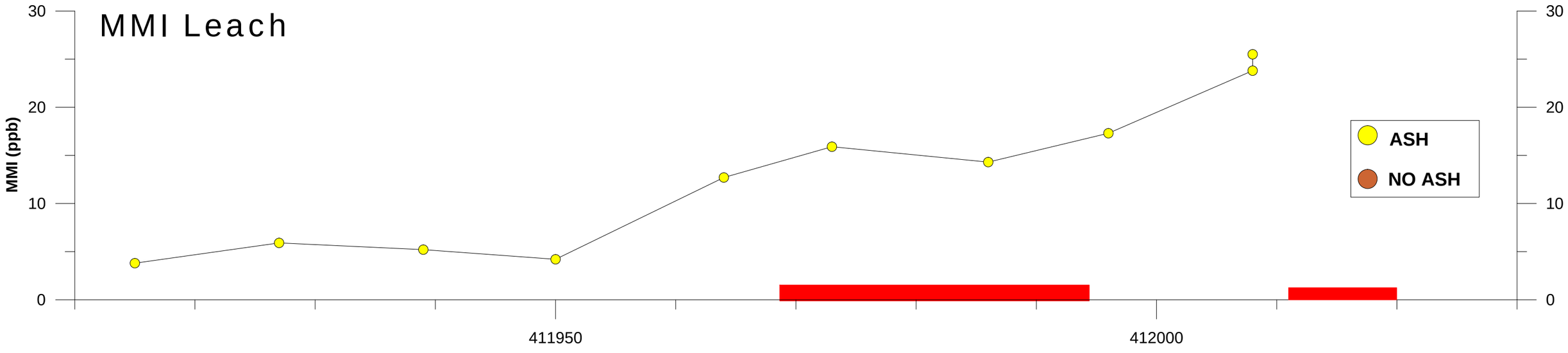

G. N. LUSTIG CONSULTING LTD.- November 20, 2008

Western Copper MMI Test
Zone 1 - South Profile

Titanium

Aqua Regia Digest

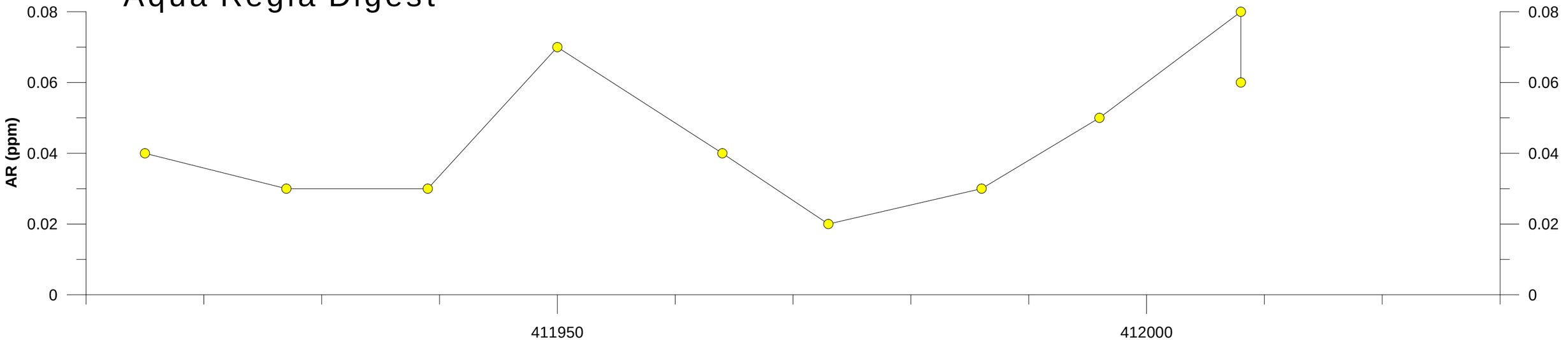

MMI Leach

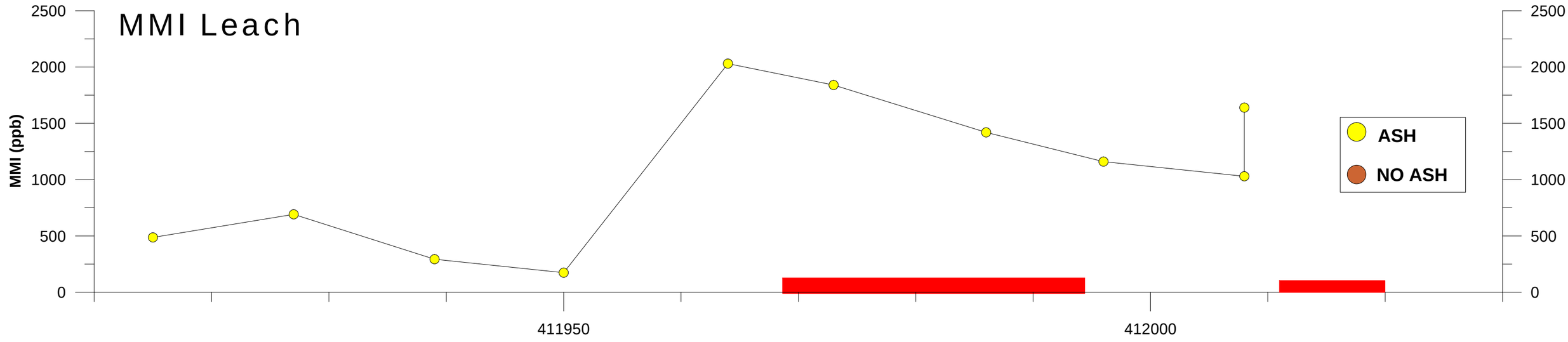

G. N. LUSTIG CONSULTING LTD.- November 20, 2008

Western Copper MMI Test
Zone 1 - South Profile

Thallium

Aqua Regia Digest

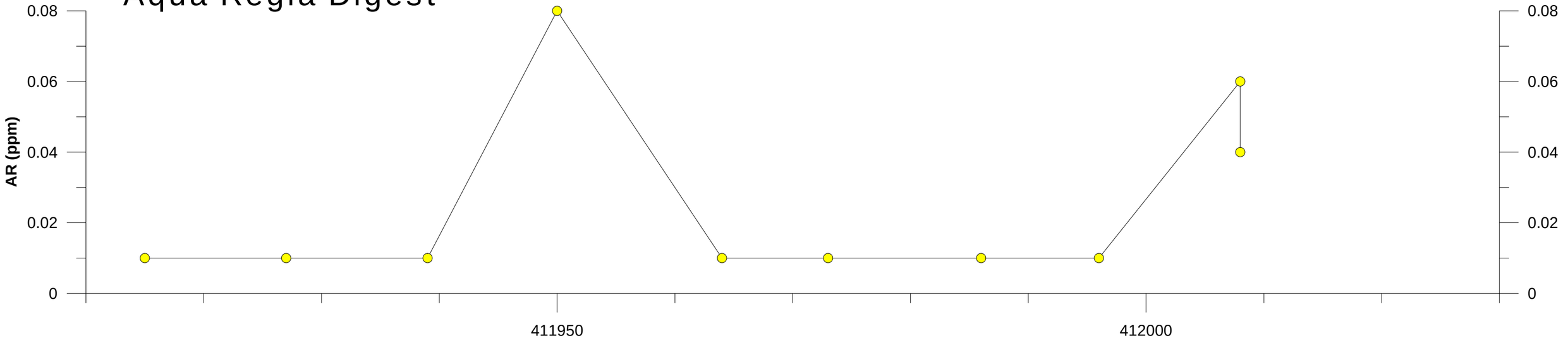

MMI Leach

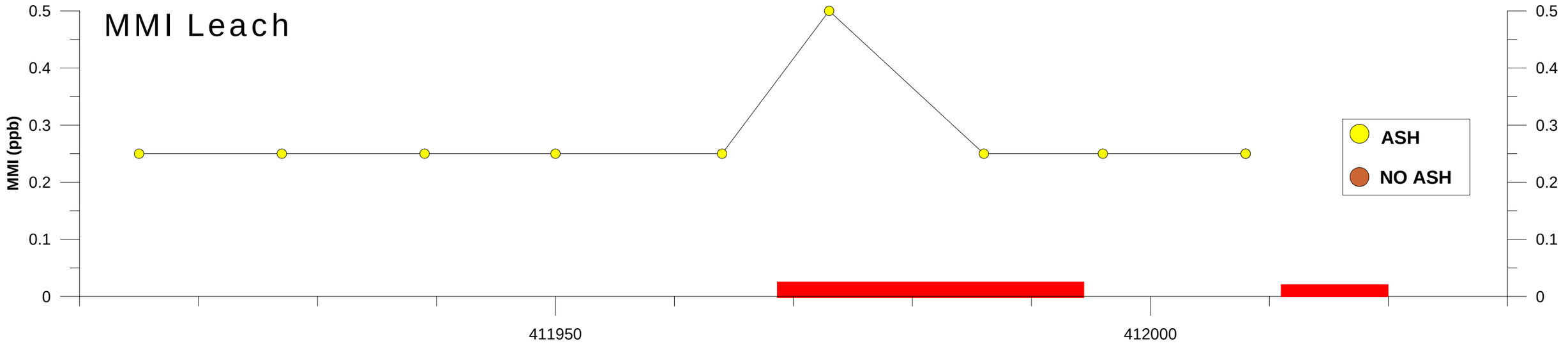

G. N. LUSTIG CONSULTING LTD.- November 20, 2008

Western Copper MMI Test
Zone 1 - South Profile
Uranium

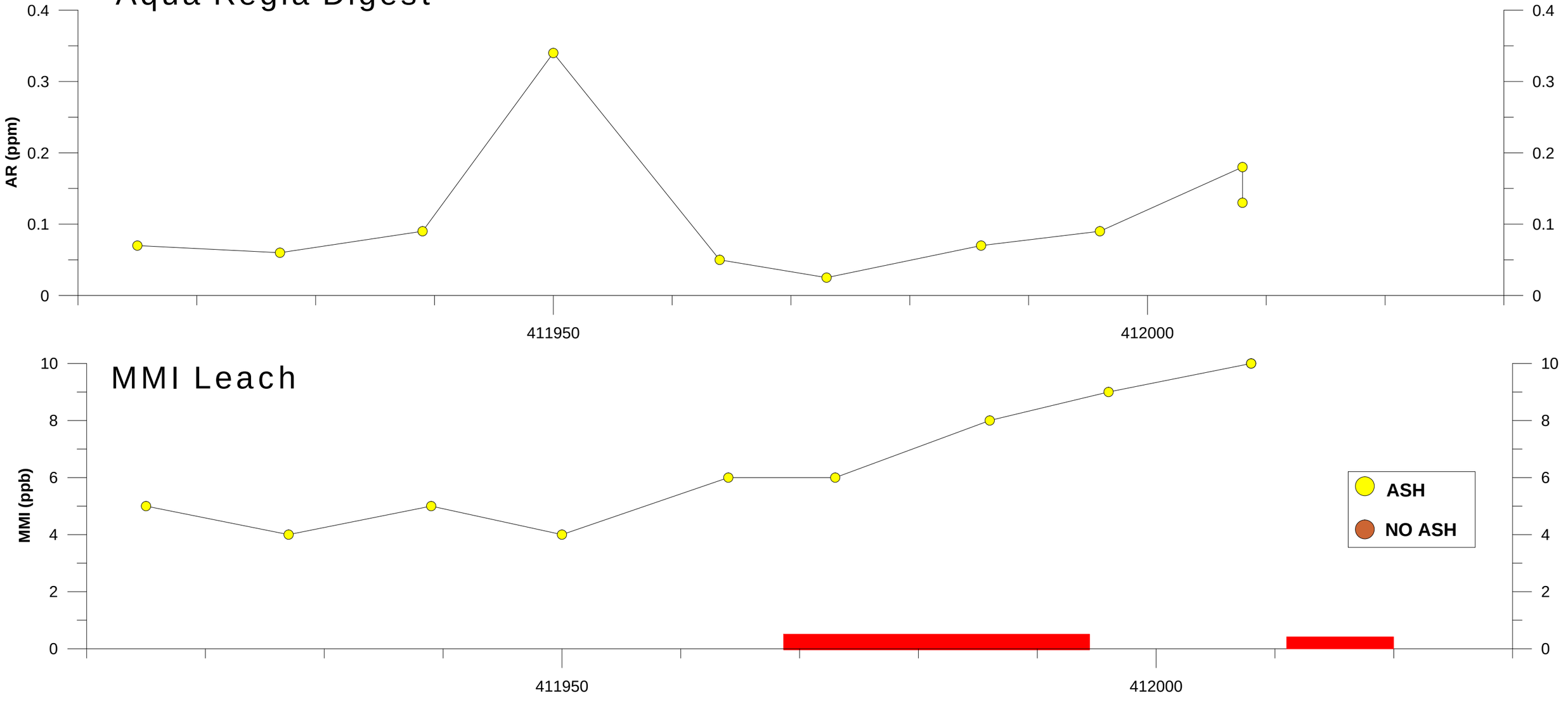

G. N. LUSTIG CONSULTING LTD.- November 20, 2008

Western Copper MMI Test
Zone 1 - South Profile

Tungsten

Aqua Regia Digest

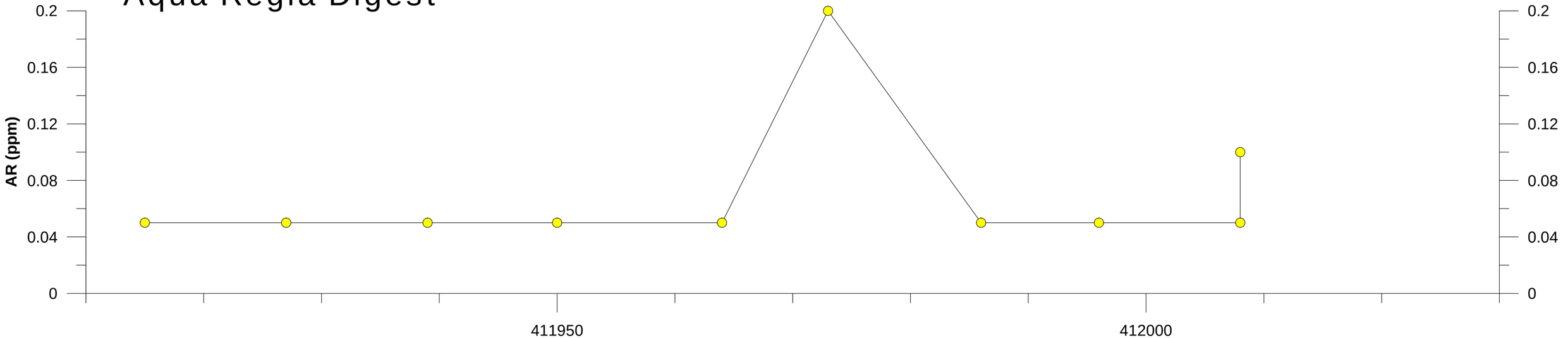

MMI Leach

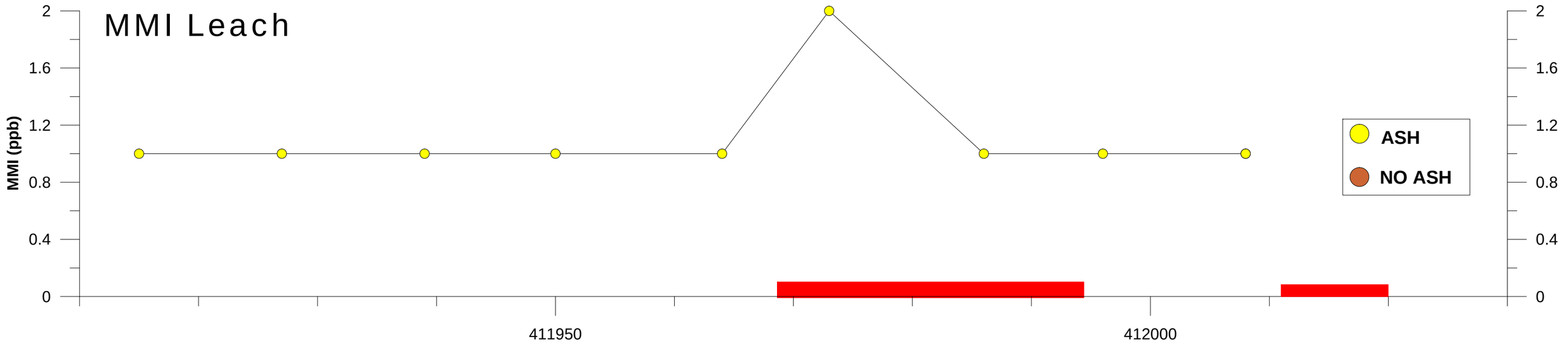

G. N. LUSTIG CONSULTING LTD.- November 20, 2008

Western Copper MMI Test
Zone 1 - South Profile
Ytterbium

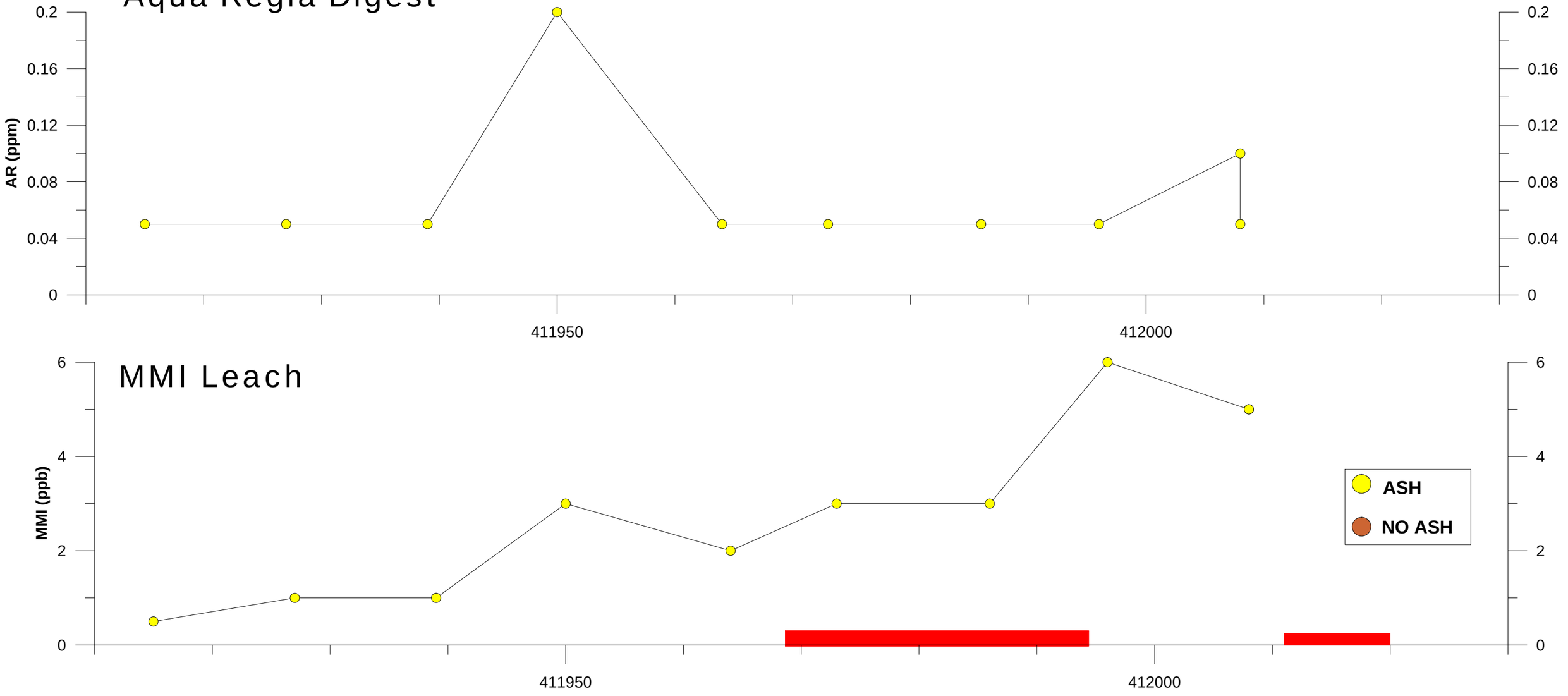

G. N. LUSTIG CONSULTING LTD.- November 20, 2008

Western Copper MMI Test
Zone 1 - South Profile
Yttrium

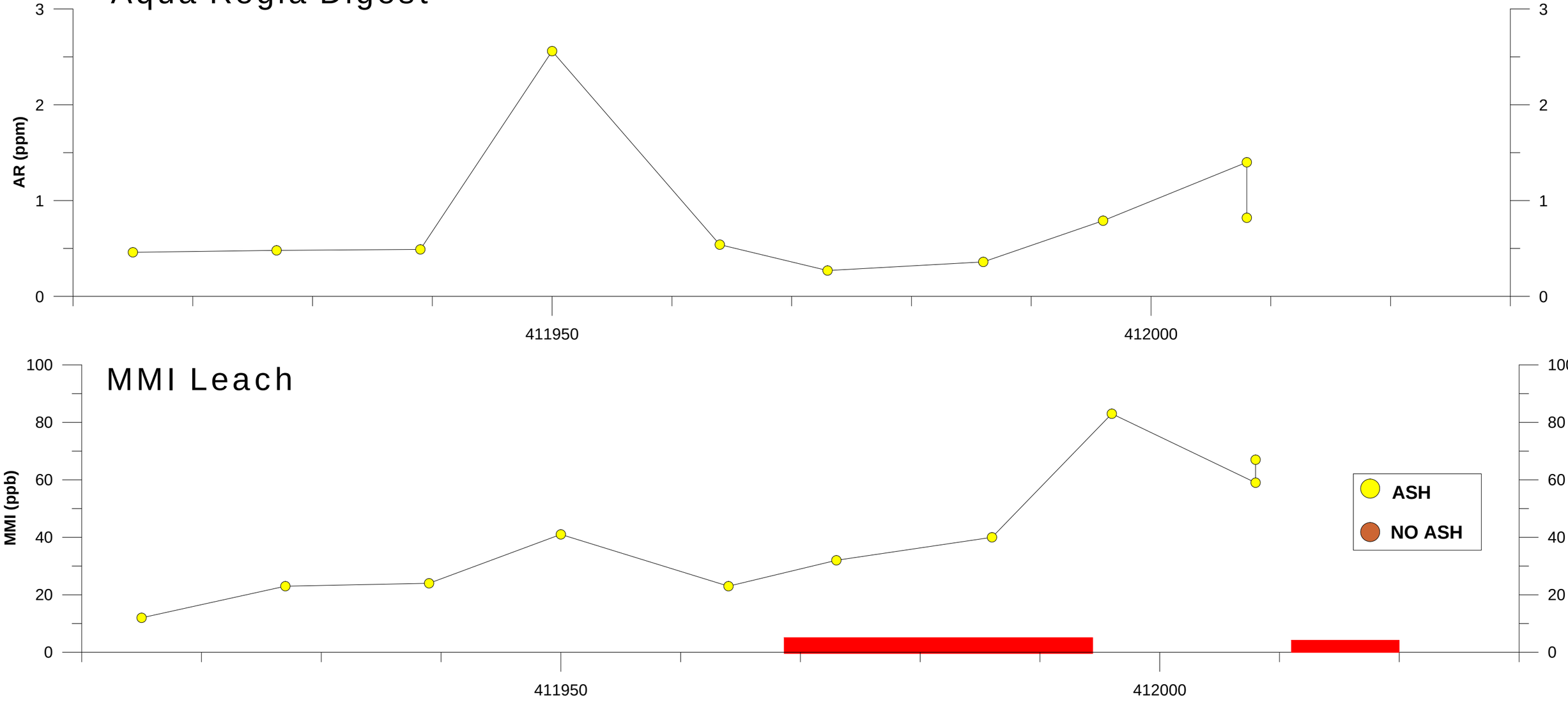

G. N. LUSTIG CONSULTING LTD.- November 20, 2008

Western Copper MMI Test
Zone 1 - South Profile

Zinc

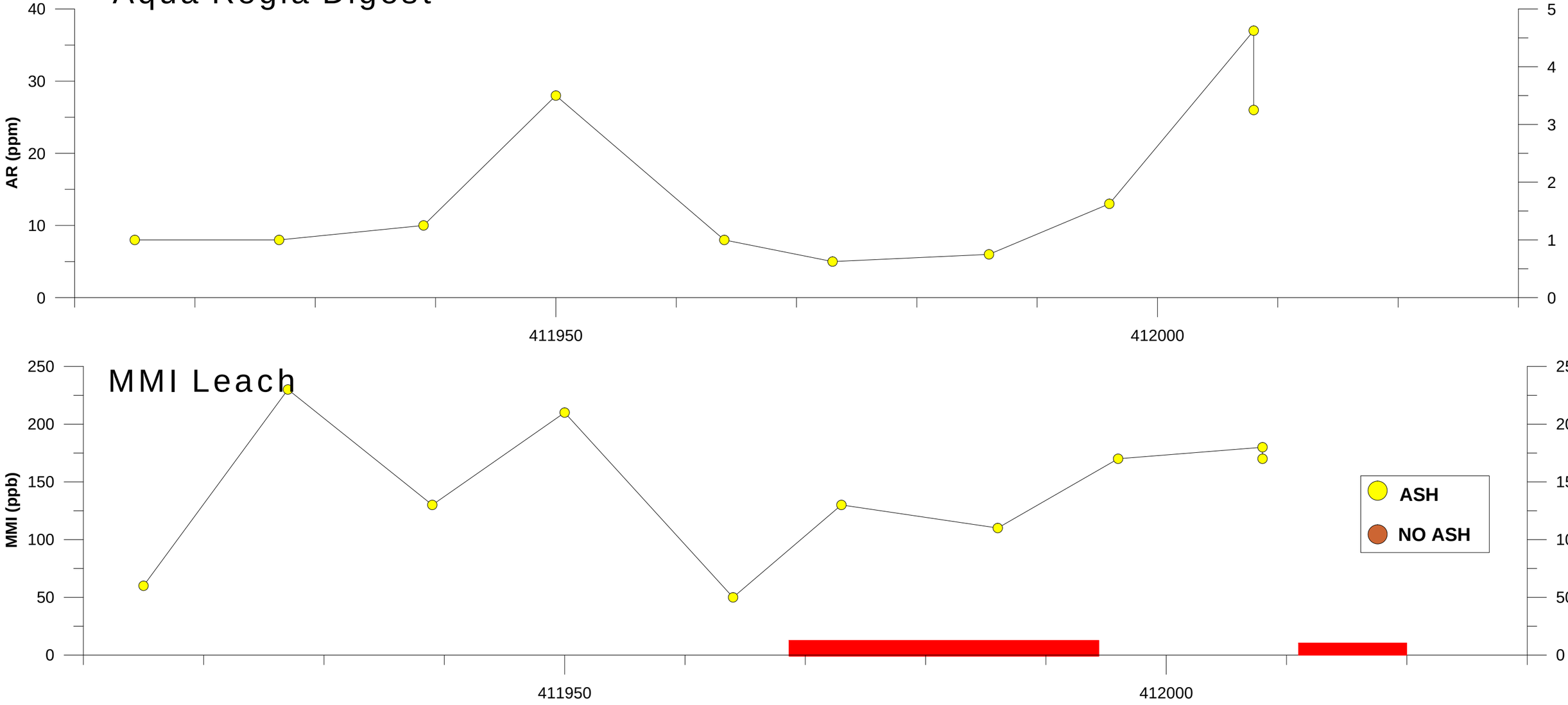

G. N. LUSTIG CONSULTING LTD.- November 20, 2008

Western Copper MMI Test
Zone 1 - South Profile

Zirconium

Aqua Regia Digest

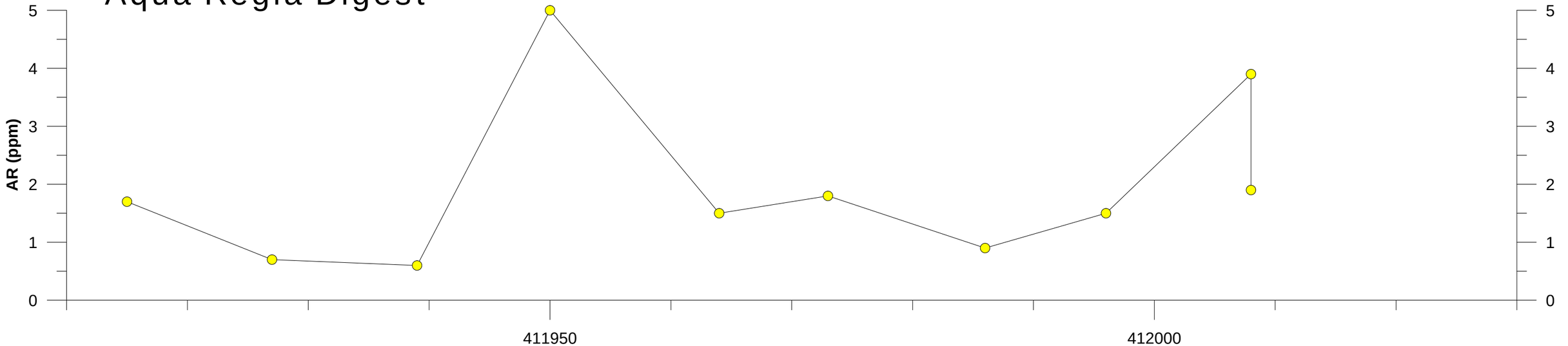

MMI Leach

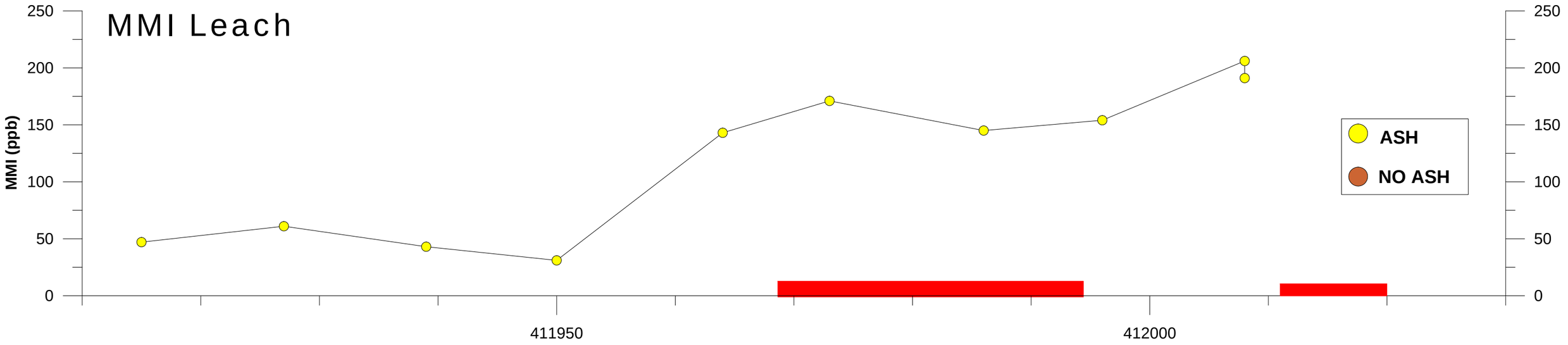

G. N. LUSTIG CONSULTING LTD.- November 20, 2008

Line 4400S
North Profile

Western Copper MMI Test
Line 4400S - 30 m North

Silver

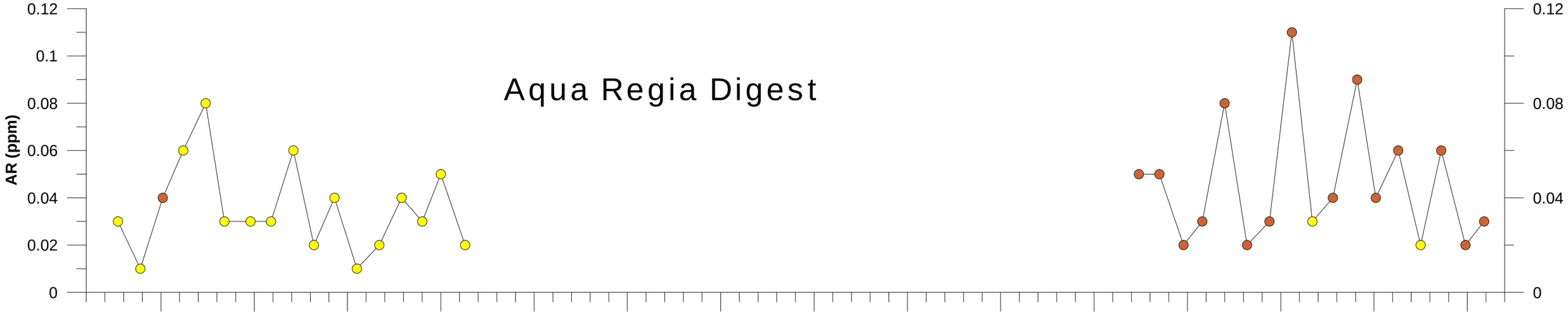

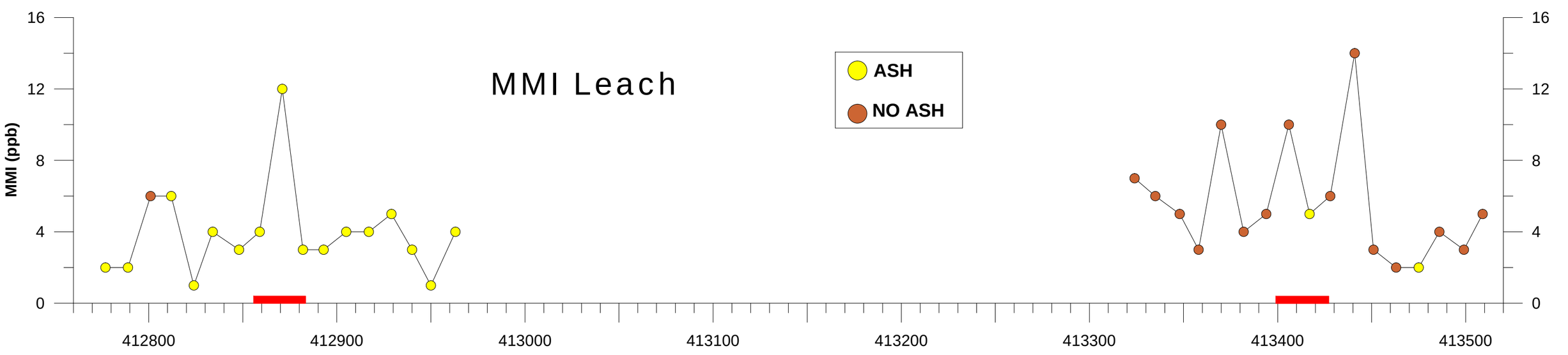

G. N. LUSTIG CONSULTING LTD.- December 11, 2008

Western Copper MMI Test
Line 4400S - 30 m North

Aluminum

Aqua Regia Digest

AR (%)

2
1.6
1.2
0.8
0.4
0
412800
412900
413000
413100
413200
413300
413400
413500

MMI Leach

MMI (ppm)

100
80
60
40
20
0

ASH
NO ASH

412800
412900
413000
413100
413200
413300
413400
413500

G. N. LUSTIG CONSULTING LTD.- December 11, 2008

Western Copper MMI Test
Line 4400S - 30 m North

Arsenic

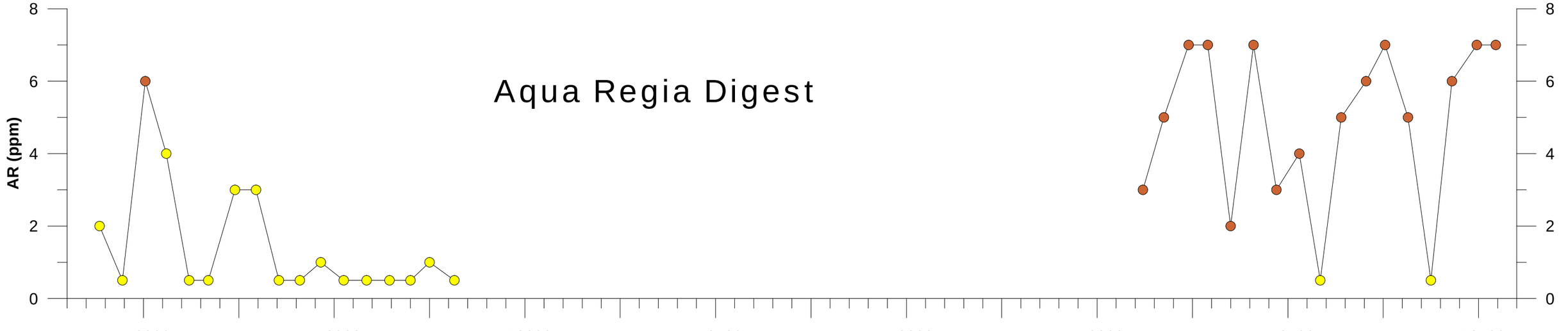

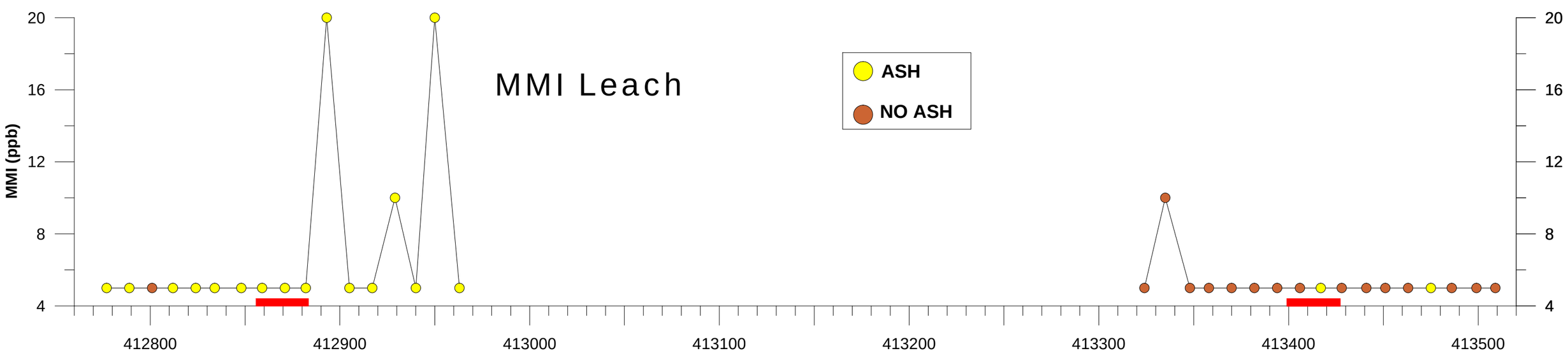

G. N. LUSTIG CONSULTING LTD.- December 11, 2008

Western Copper MMI Test
Line 4400S - 30 m North

Barium

Aqua Regia Digest

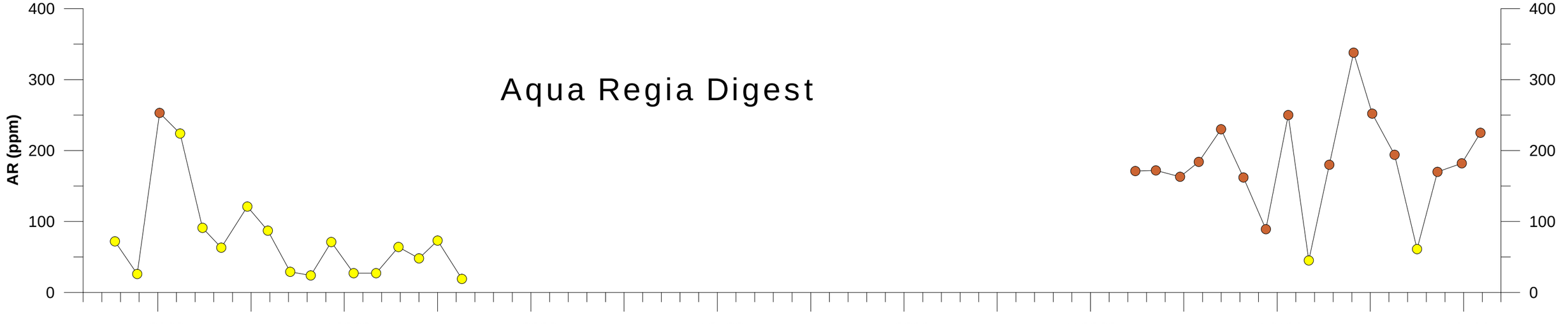

MMI Leach

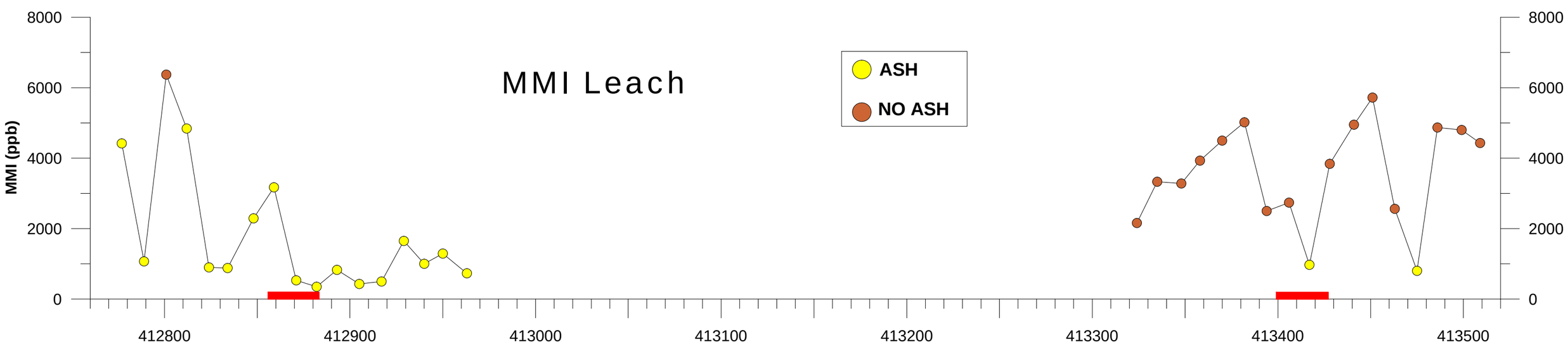

G. N. LUSTIG CONSULTING LTD.- December 11, 2008

Western Copper MMI Test
Line 4400S - 30 m North

Bismuth

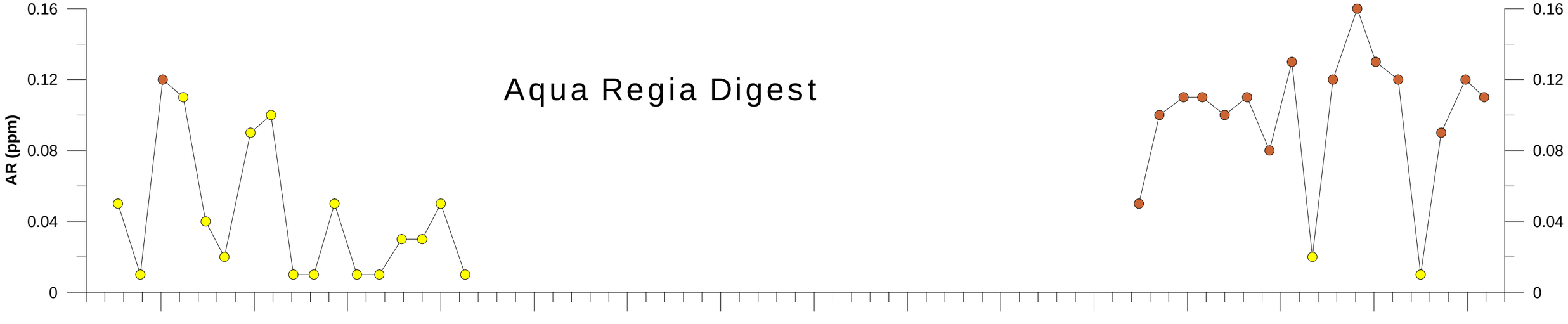

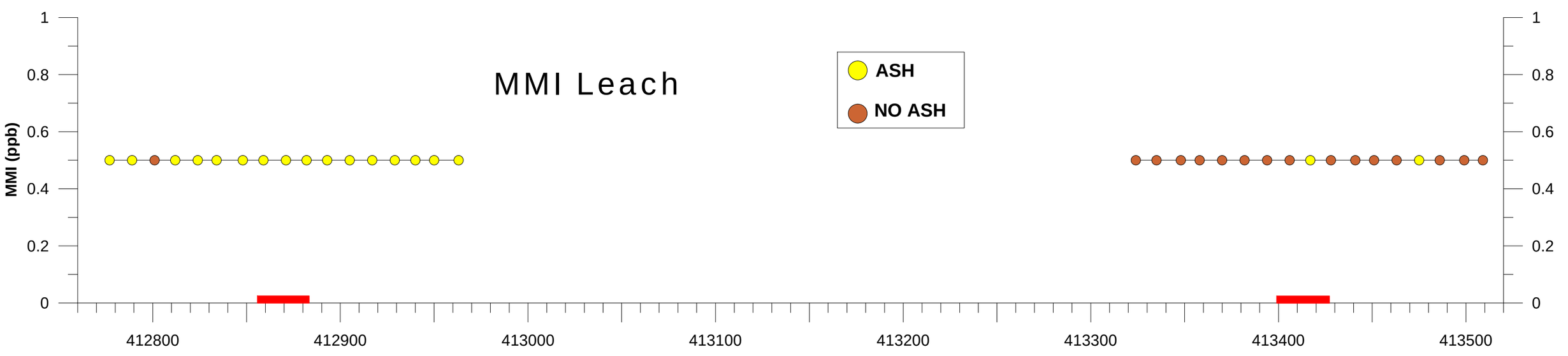

G. N. LUSTIG CONSULTING LTD.- December 11, 2008

Western Copper MMI Test
Line 4400S - 30 m North

Calcium

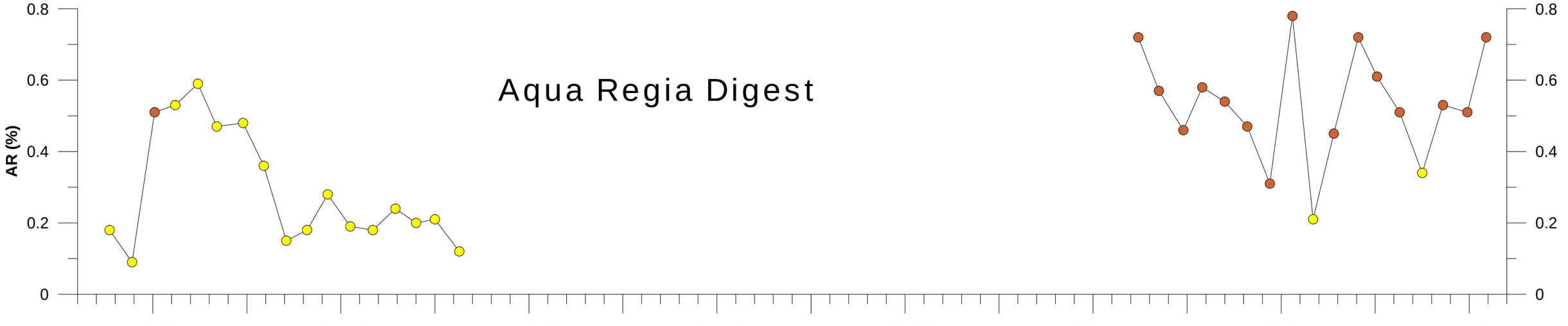

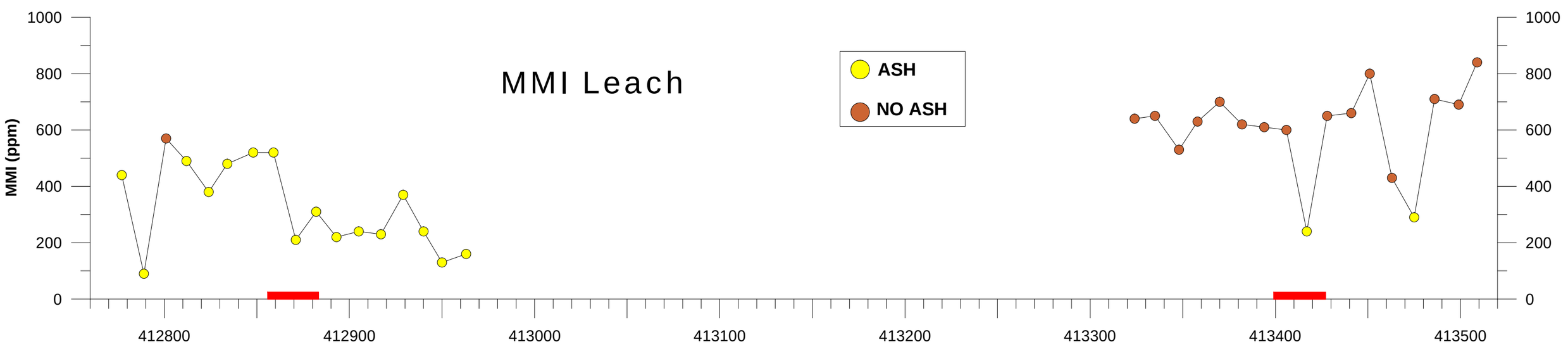

G. N. LUSTIG CONSULTING LTD.- December 11, 2008

Western Copper MMI Test
Line 4400S - 30 m North

Cadmium

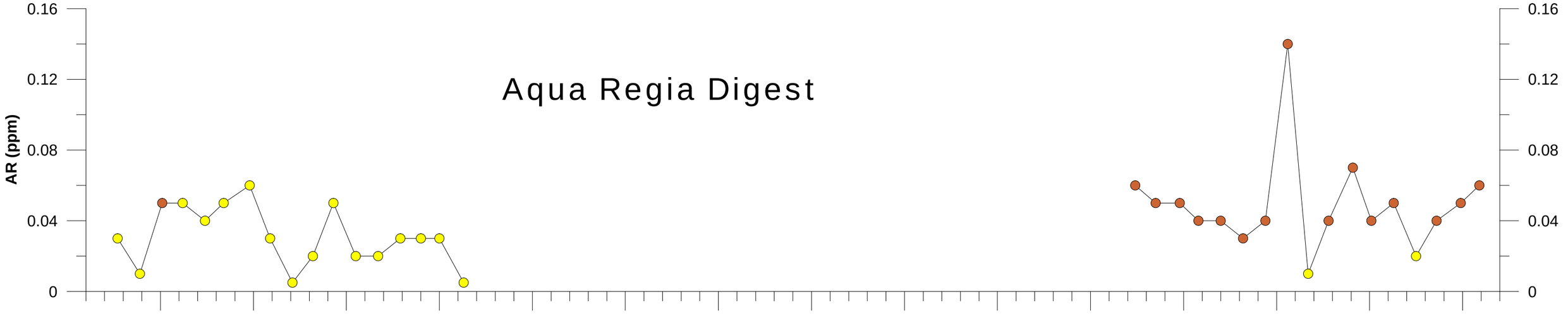

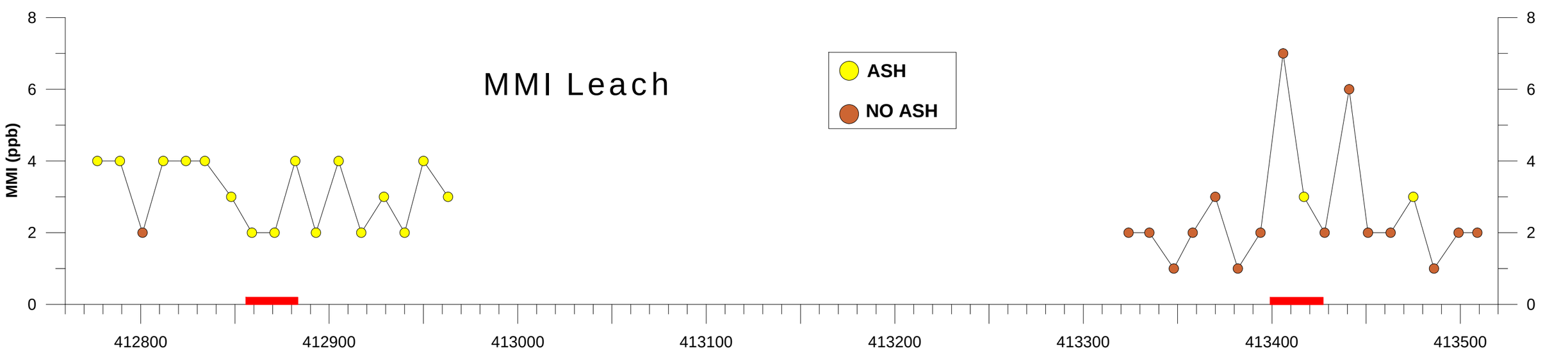

G. N. LUSTIG CONSULTING LTD.- December 11, 2008

Western Copper MMI Test
Line 4400S - 30 m North

Cerium

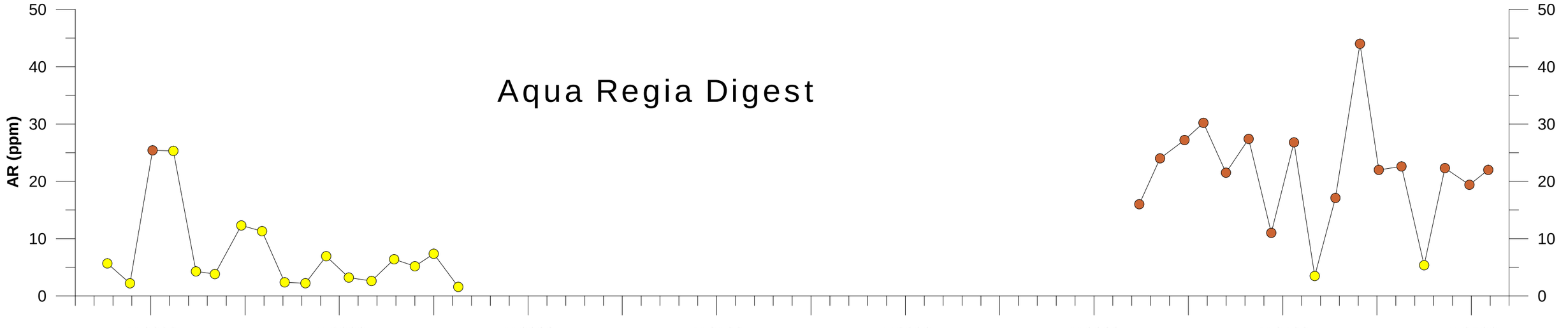

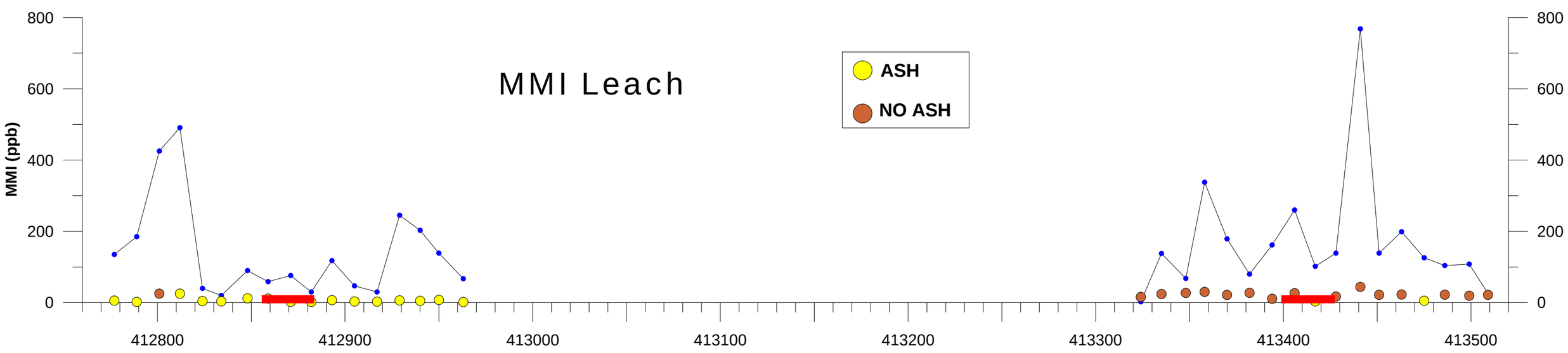

G. N. LUSTIG CONSULTING LTD.- December 11, 2008

Western Copper MMI Test
Line 4400S - 30 m North

Cobalt

Aqua Regia Digest

AR (ppm)

16
12
8
4
0

412800 412900 413000 413100 413200 413300 413400 413500

MMI Leach

MMI (ppb)

800
600
400
200
0

ASH
NO ASH

412800 412900 413000 413100 413200 413300 413400 413500

G. N. LUSTIG CONSULTING LTD.- December 11, 2008

Western Copper MMI Test
Line 4400S - 30 m North

Copper

Aqua Regia Digest

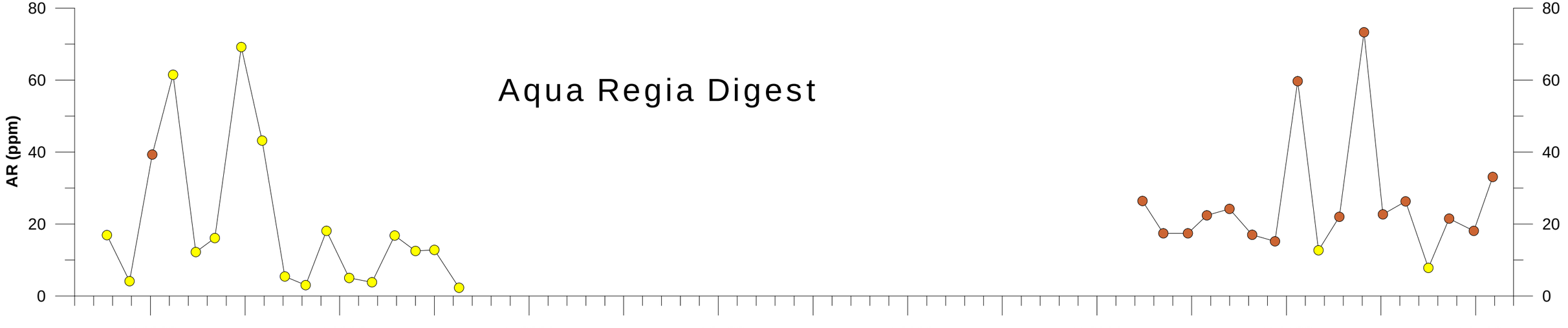

MMI Leach

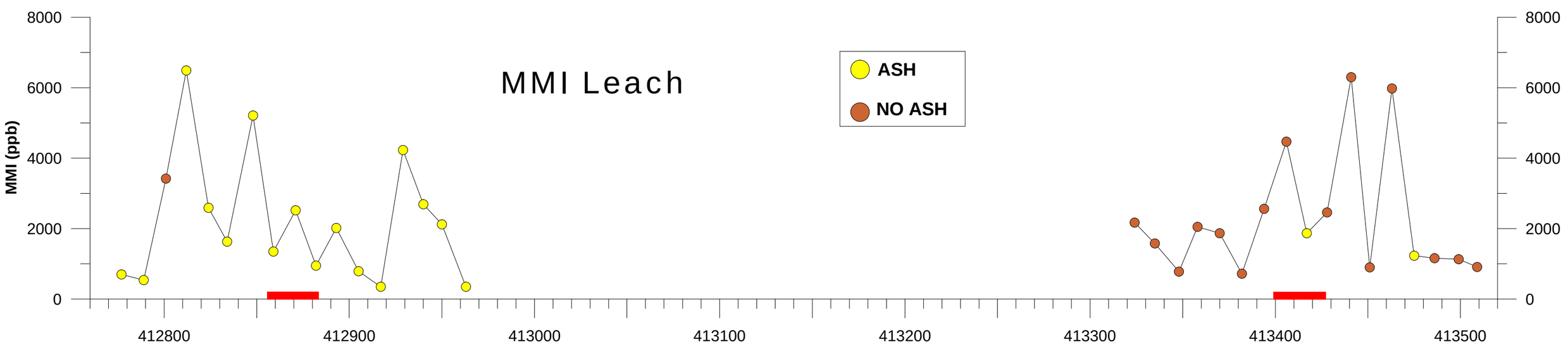

G. N. LUSTIG CONSULTING LTD.- December 11, 2008

Western Copper MMI Test
Line 4400S - 30 m North

Iron

Aqua Regia Digest

AR (%)

3
2.5
2
1.5
1
0.5

412800 412900 413000 413100 413200 413300 413400 413500

MMI Leach

MMI (ppm)

500
400
300
200
100
0

ASH
NO ASH

412800 412900 413000 413100 413200 413300 413400 413500

G. N. LUSTIG CONSULTING LTD.- December 11, 2008

Western Copper MMI Test
Line 4400S - 30 m North

Lanthanum

Aqua Regia Digest

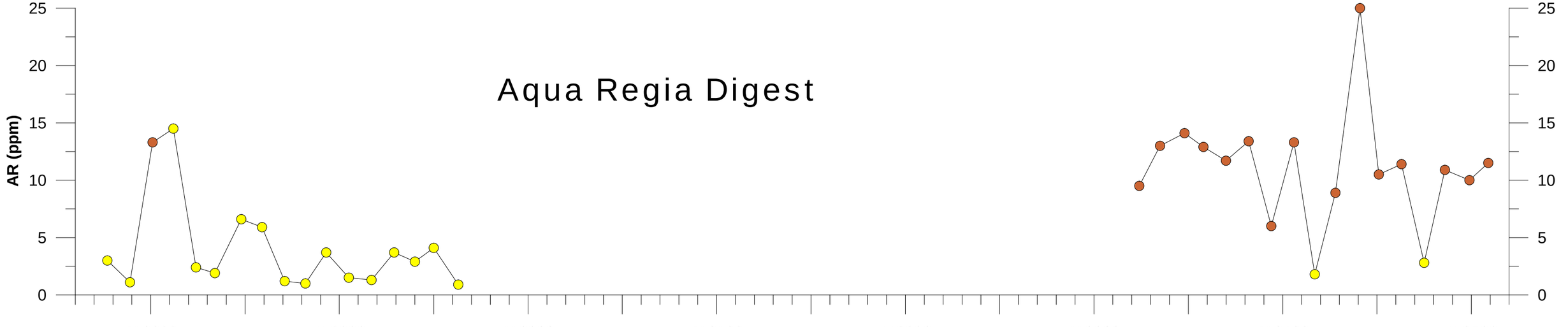

MMI Leach

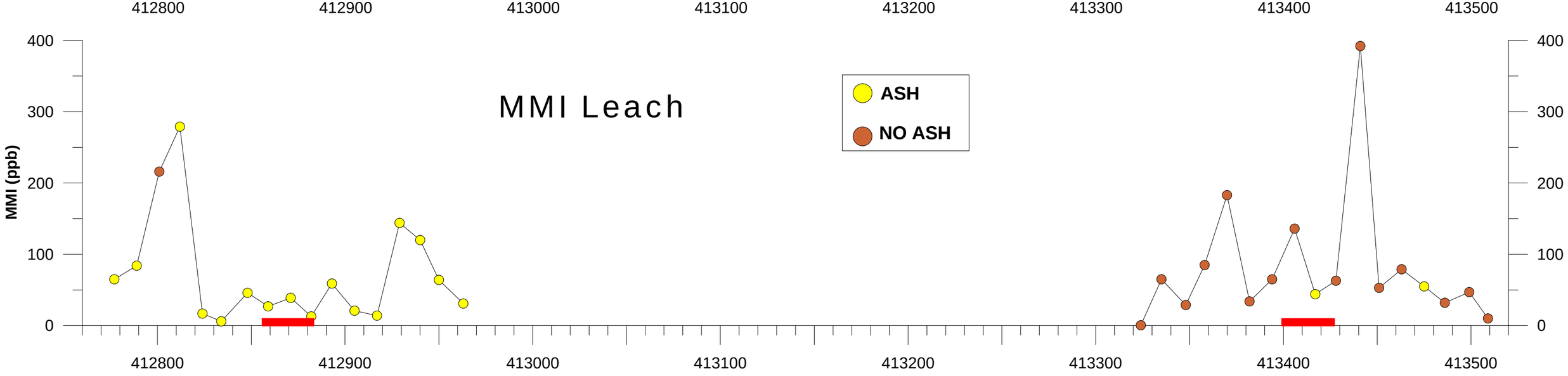

G. N. LUSTIG CONSULTING LTD.- December 11, 2008

Western Copper MMI Test
Line 4400S - 30 m North

Lithium

Aqua Regia Digest

AR (ppm)

12
8
4
0

412800 412900 413000 413100 413200 413300 413400 413500

MMI Leach

MMI (ppb)

8
6
4
2
0

ASH

NO ASH

412800 412900 413000 413100 413200 413300 413400 413500

G. N. LUSTIG CONSULTING LTD.- December 11, 2008

Western Copper MMI Test
Line 4400S - 30 m North

Magnesium

Aqua Regia Digest

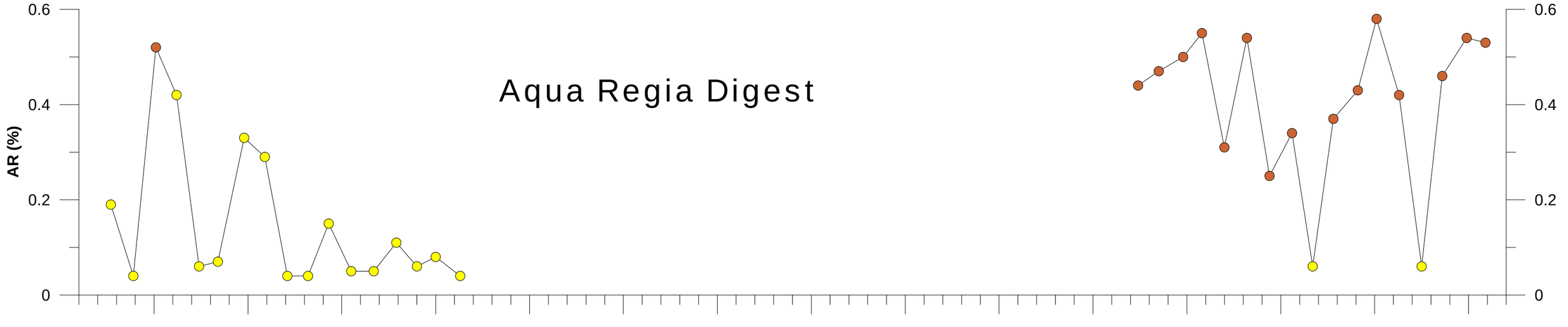

MMI Leach

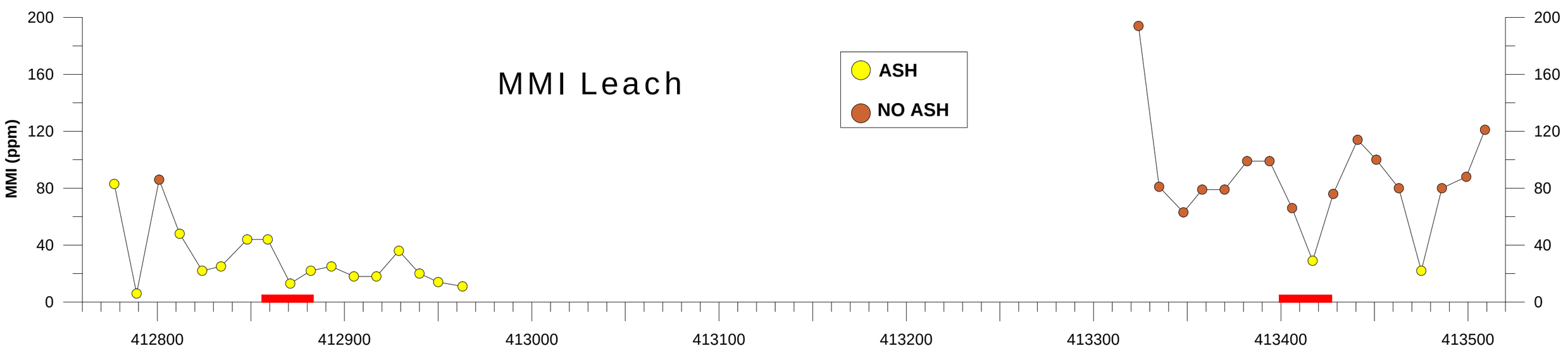

G. N. LUSTIG CONSULTING LTD.- December 11, 2008

Western Copper MMI Test
Line 4400S - 30 m North

Molybdenum

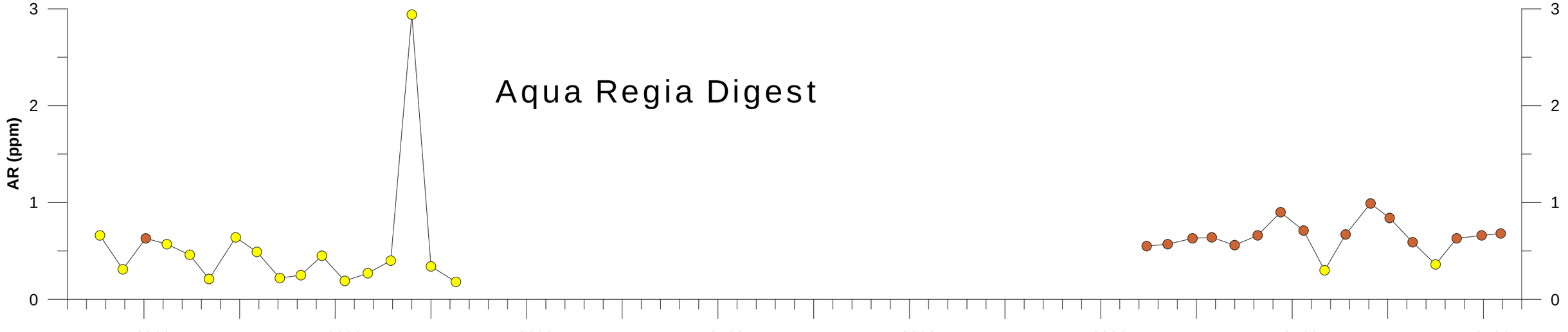

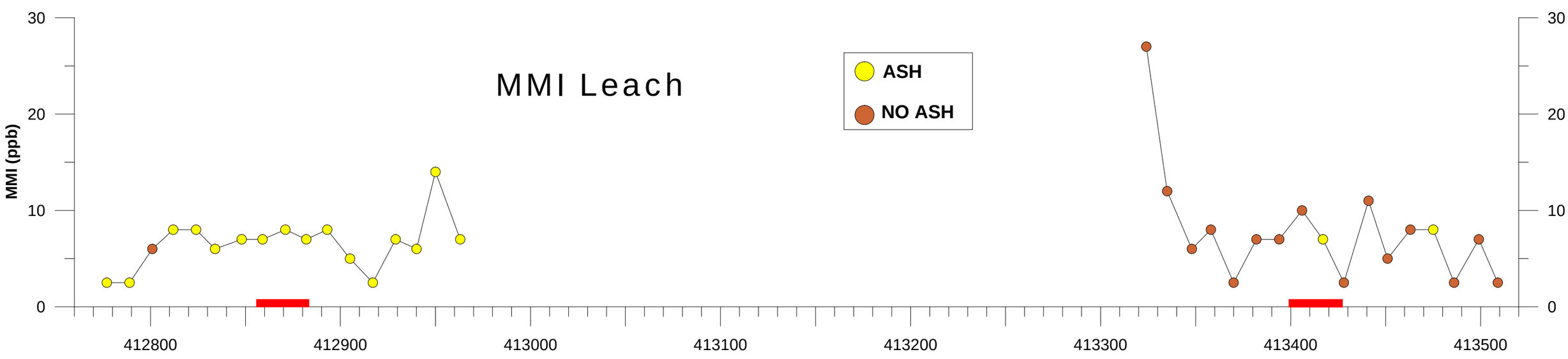

G. N. LUSTIG CONSULTING LTD.- December 11, 2008

Western Copper MMI Test
Line 4400S - 30 m North

Niobium

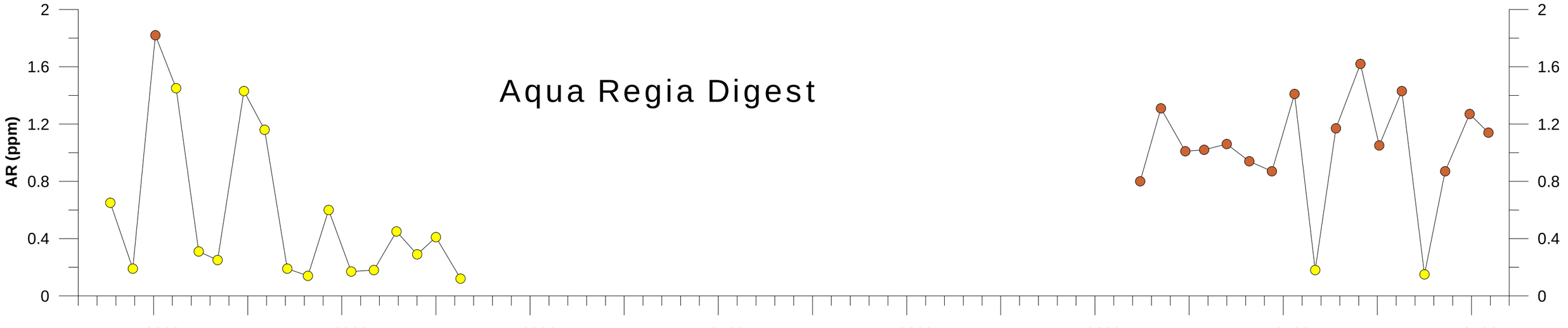

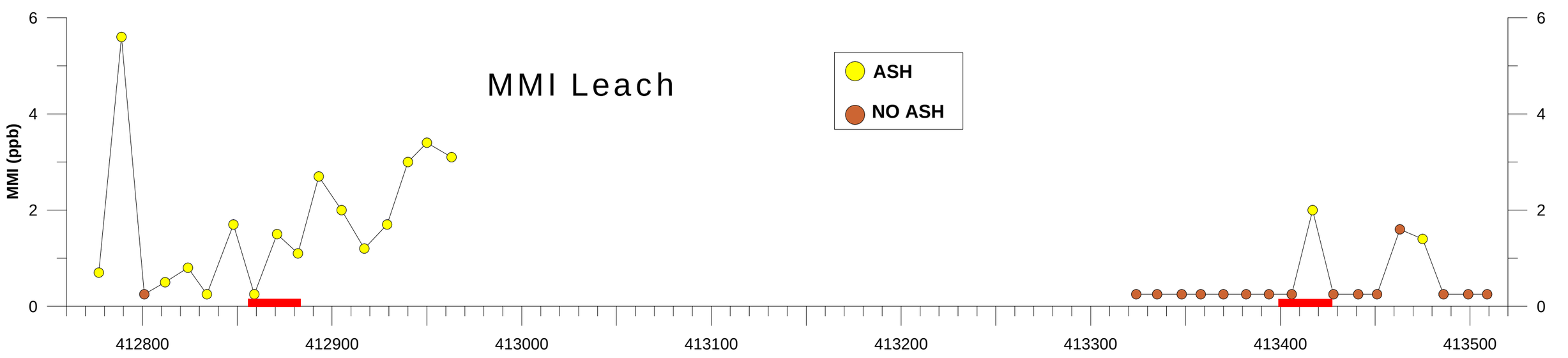

G. N. LUSTIG CONSULTING LTD.- December 11, 2008

Western Copper MMI Test
Line 4400S - 30 m North

Nickel

Aqua Regia Digest



MMI Leach

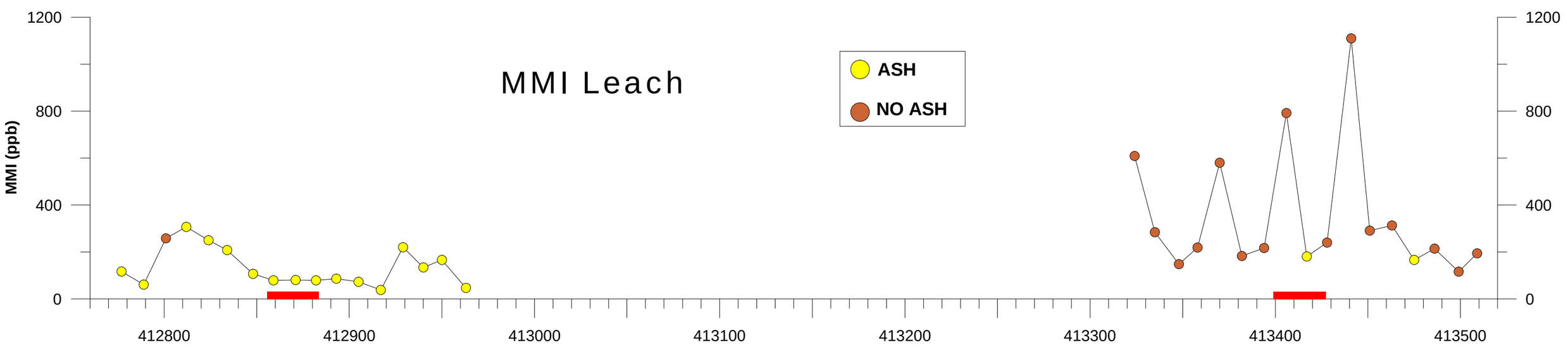

G. N. LUSTIG CONSULTING LTD.- December 11, 2008

Western Copper MMI Test
Line 4400S - 30 m North

Lead

Aqua Regia Digest

AR (ppm)

10
8
6
4
2
0

412800 412900 413000 413100 413200 413300 413400 413500

MMI Leach

MMI (ppb)

80
60
40
20
0

412800 412900 413000 413100 413200 413300 413400 413500

ASH
NO ASH

G. N. LUSTIG CONSULTING LTD.- December 11, 2008

Western Copper MMI Test
Line 4400S - 30 m North

Rubidium

Aqua Regia Digest

AR (ppm)

16
12
8
4
0

412800 412900 413000 413100 413200 413300 413400 413500

MMI Leach

MMI (ppb)

100
80
60
40
20
0

412800 412900 413000 413100 413200 413300 413400 413500

ASH
NO ASH

G. N. LUSTIG CONSULTING LTD.- December 11, 2008

Western Copper MMI Test
Line 4400S - 30 m North

Antimony

Aqua Regia Digest

AR (ppm)

0.4
0.3
0.2
0.1
0

412800 412900 413000 413100 413200 413300 413400 413500

MMI Leach

MMI (ppb)

1
0.8
0.6
0.4
0.2
0

412800 412900 413000 413100 413200 413300 413400 413500

ASH
NO ASH

G. N. LUSTIG CONSULTING LTD.- December 11, 2008

Western Copper MMI Test
Line 4400S - 30 m North

Scandium

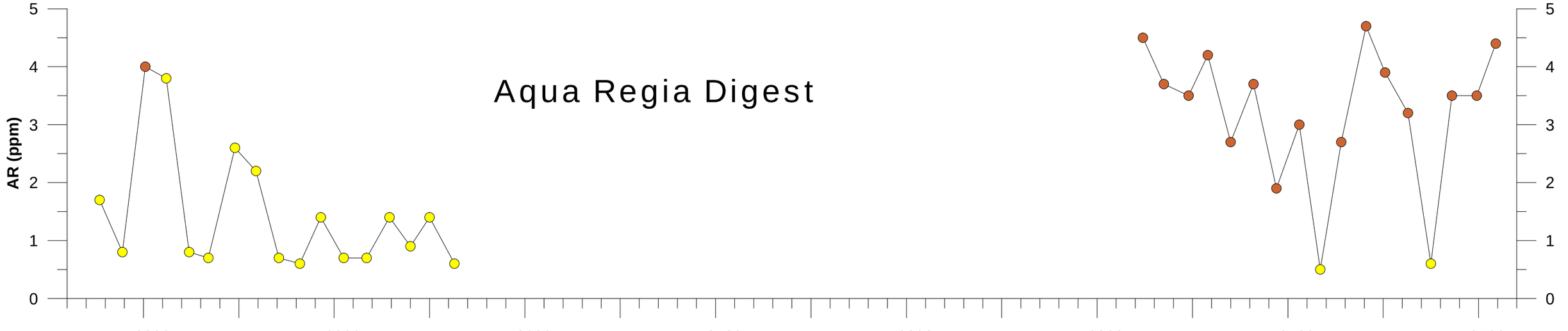

Aqua Regia Digest

MMI Leach

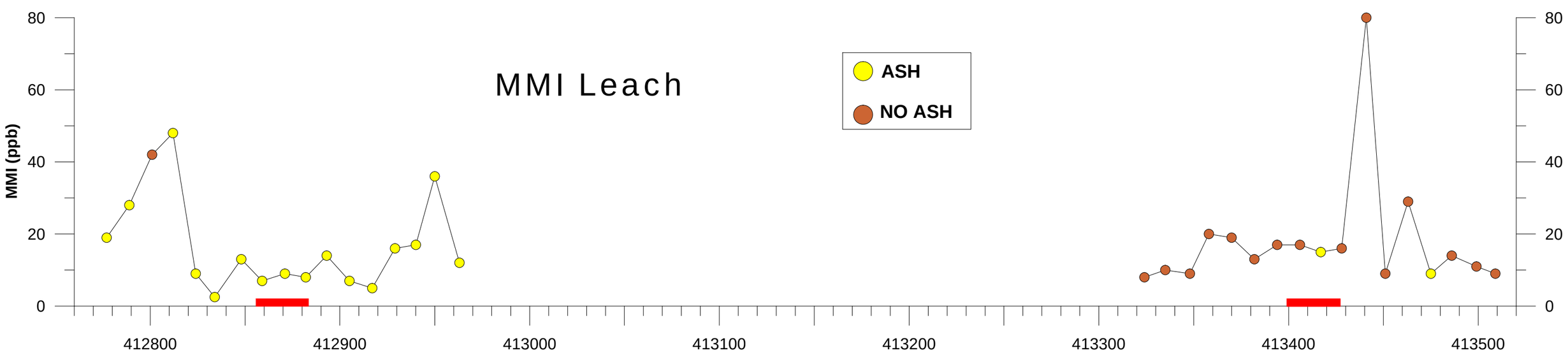

G. N. LUSTIG CONSULTING LTD.- December 11, 2008

Western Copper MMI Test
Line 4400S - 30 m North

Tin

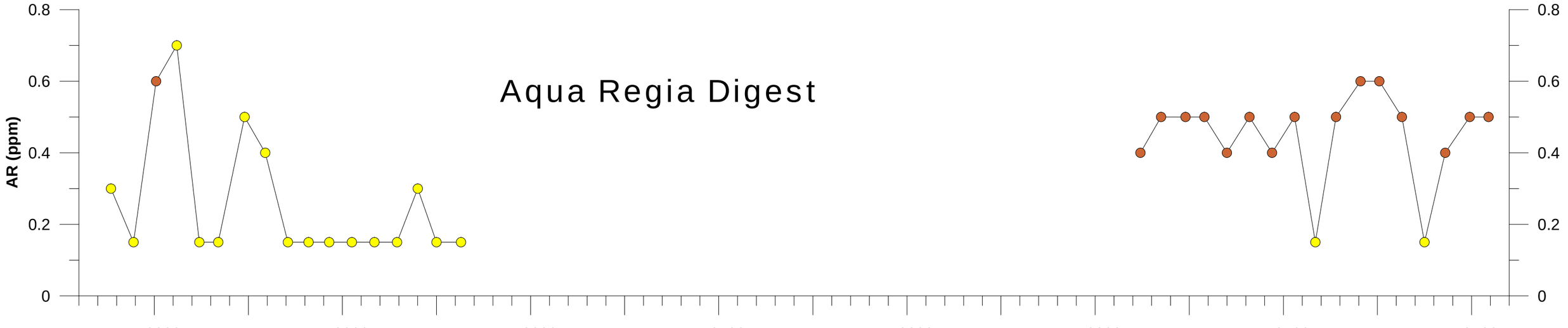

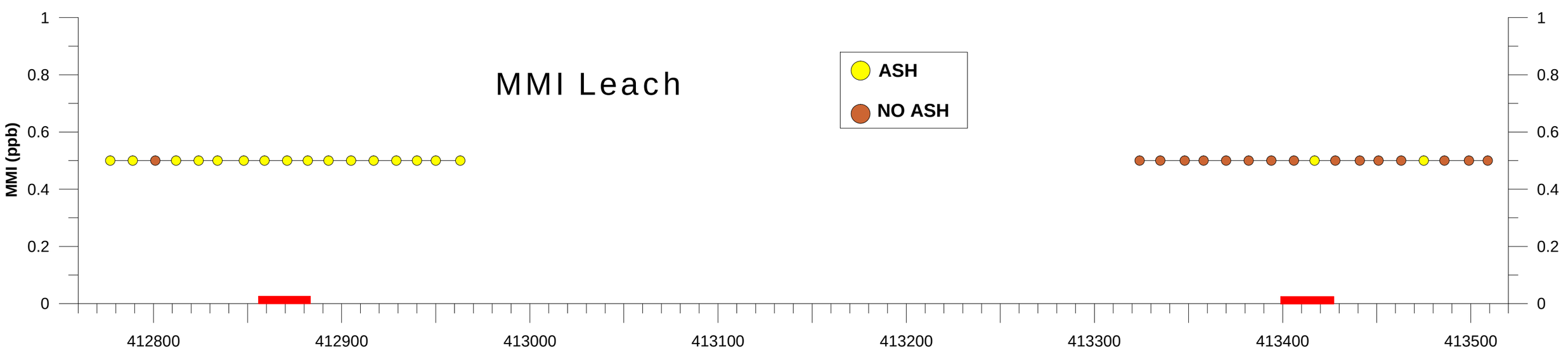

G. N. LUSTIG CONSULTING LTD.- December 11, 2008

Western Copper MMI Test
Line 4400S - 30 m North

Strontium

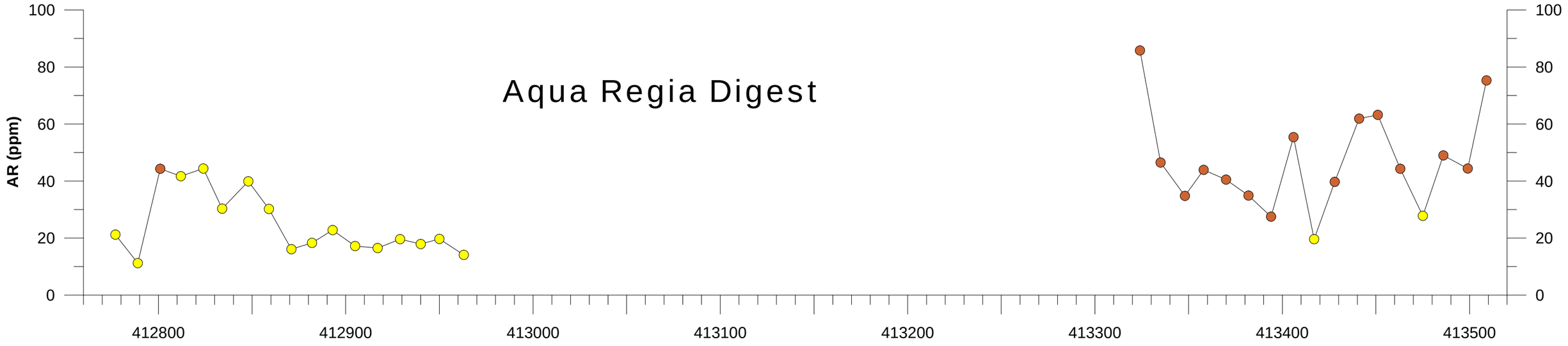

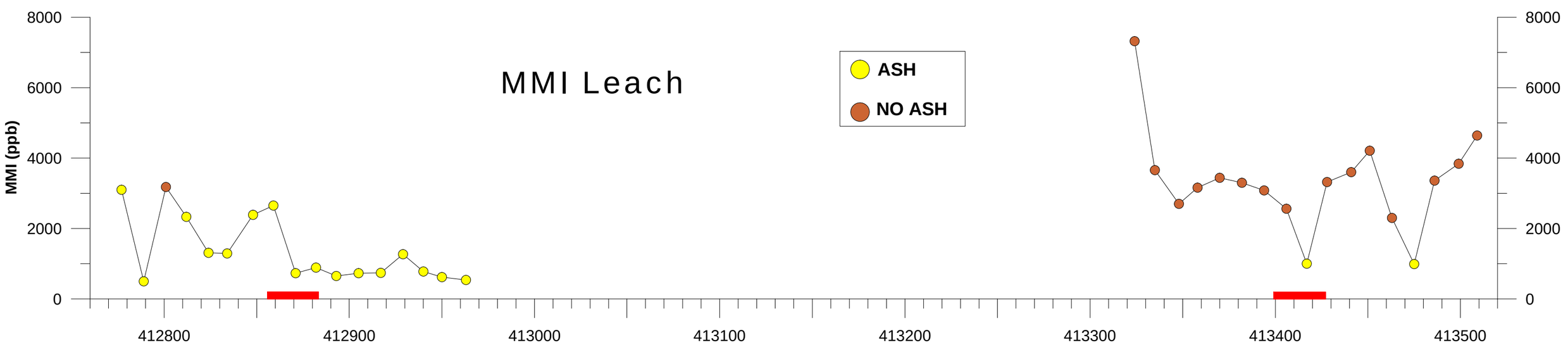

G. N. LUSTIG CONSULTING LTD.- December 11, 2008

Western Copper MMI Test
Line 4400S - 30 m North

Tantalum

Aqua Regia Digest

AR (ppm)

0.05
0.04
0.03
0.02
0.01
0

412800 412900 413000 413100 413200 413300 413400 413500

MMI Leach

MMI (ppb)

1
0.8
0.6
0.4
0.2
0

ASH
NO ASH

412800 412900 413000 413100 413200 413300 413400 413500

G. N. LUSTIG CONSULTING LTD.- December 11, 2008

Western Copper MMI Test
Line 4400S - 30 m North

Terbium

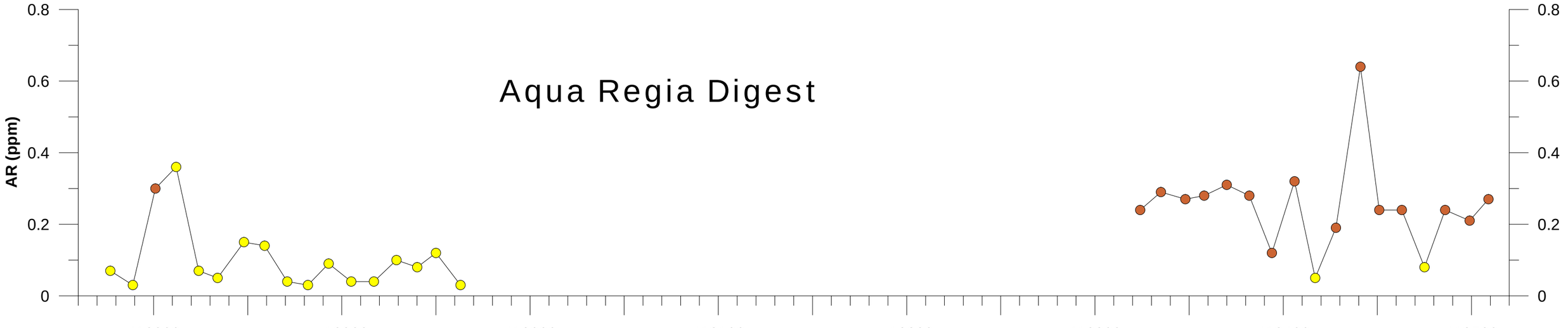

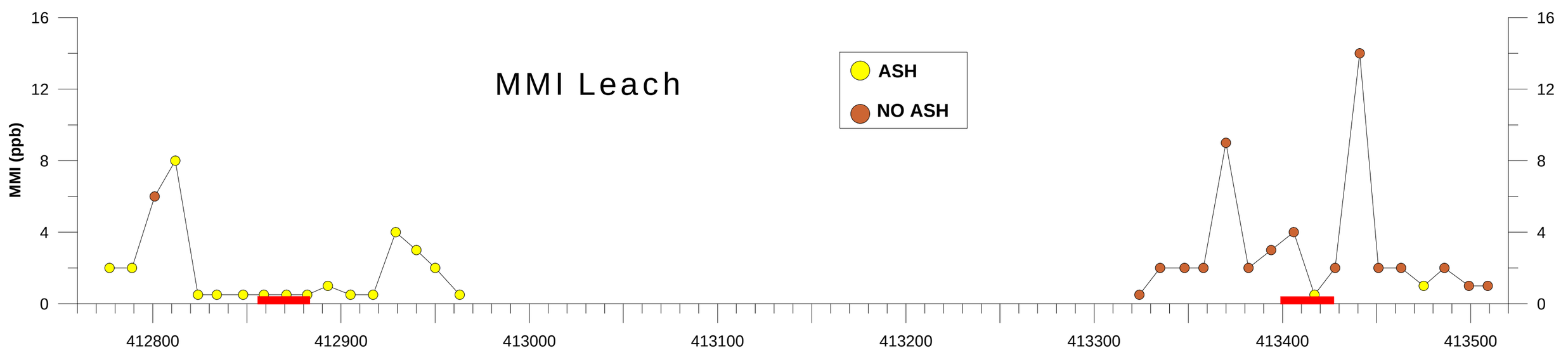

G. N. LUSTIG CONSULTING LTD.- December 11, 2008

Western Copper MMI Test
Line 4400S - 30 m North

Tellurium

Aqua Regia Digest

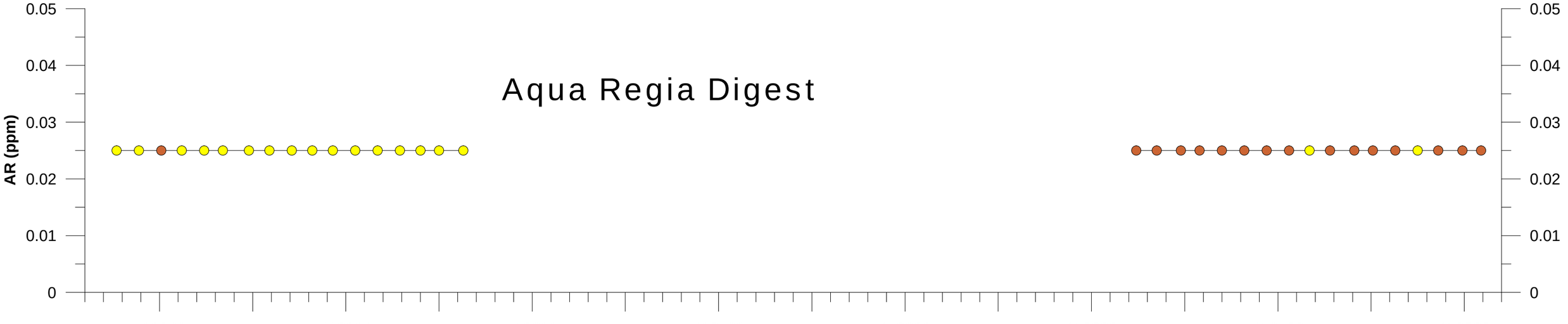

MMI Leach

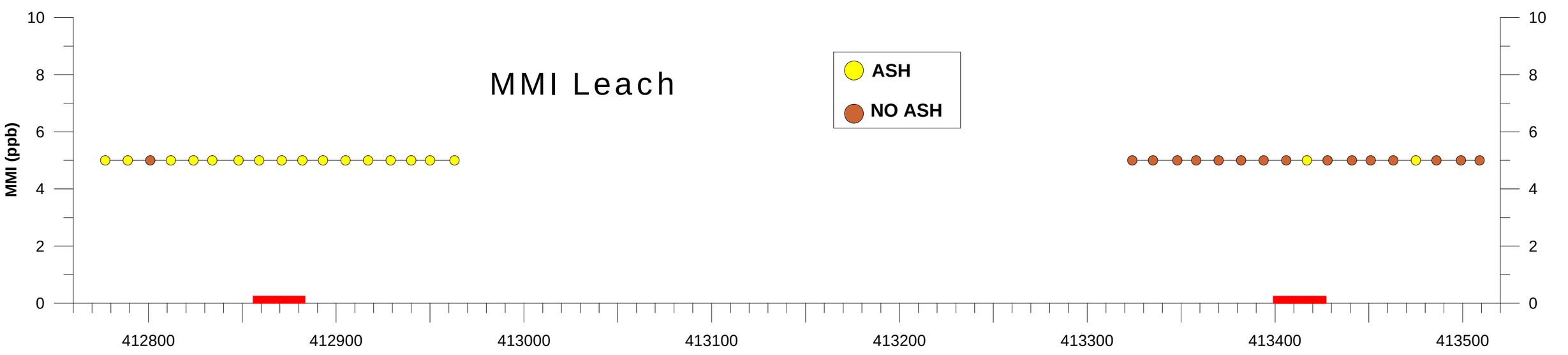

G. N. LUSTIG CONSULTING LTD.- December 11, 2008

Western Copper MMI Test
Line 4400S - 30 m North

Thorium

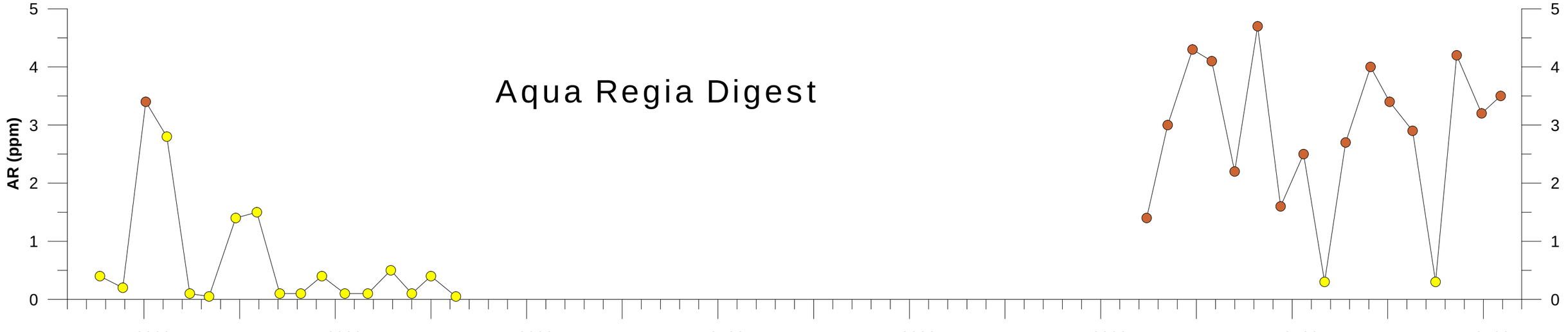

Aqua Regia Digest

MMI Leach

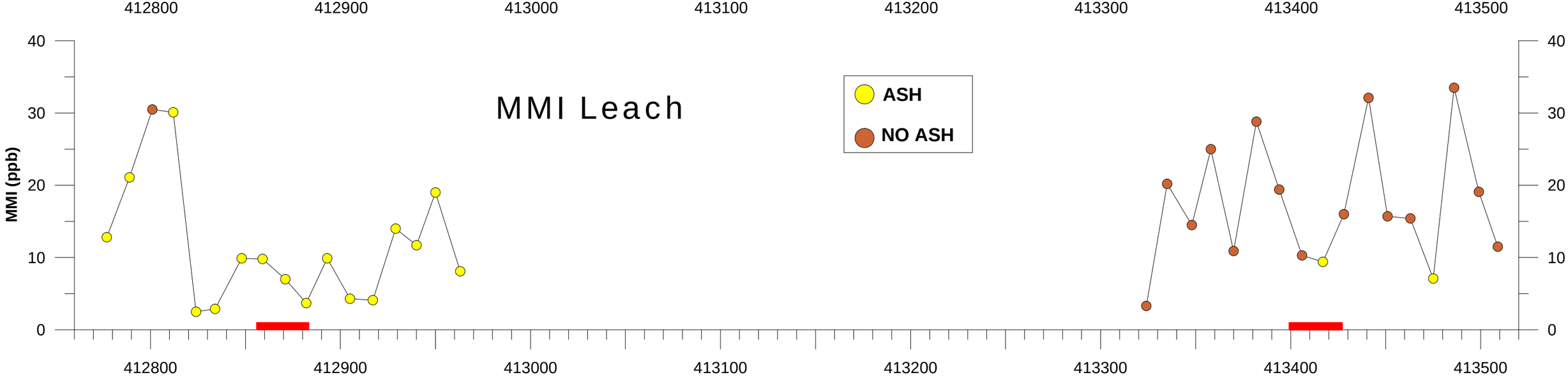

G. N. LUSTIG CONSULTING LTD.- December 11, 2008

Western Copper MMI Test
Line 4400S - 30 m North

Thallium

Aqua Regia Digest

AR (ppm)

0.12
0.08
0.04
0

412800 412900 413000 413100 413200 413300 413400 413500

MMI Leach

MMI (ppb)

0.5
0.4
0.3
0.2
0.1
0

ASH
NO ASH

412800 412900 413000 413100 413200 413300 413400 413500

G. N. LUSTIG CONSULTING LTD.- December 11, 2008

Western Copper MMI Test
Line 4400S - 30 m North

Uranium

Aqua Regia Digest

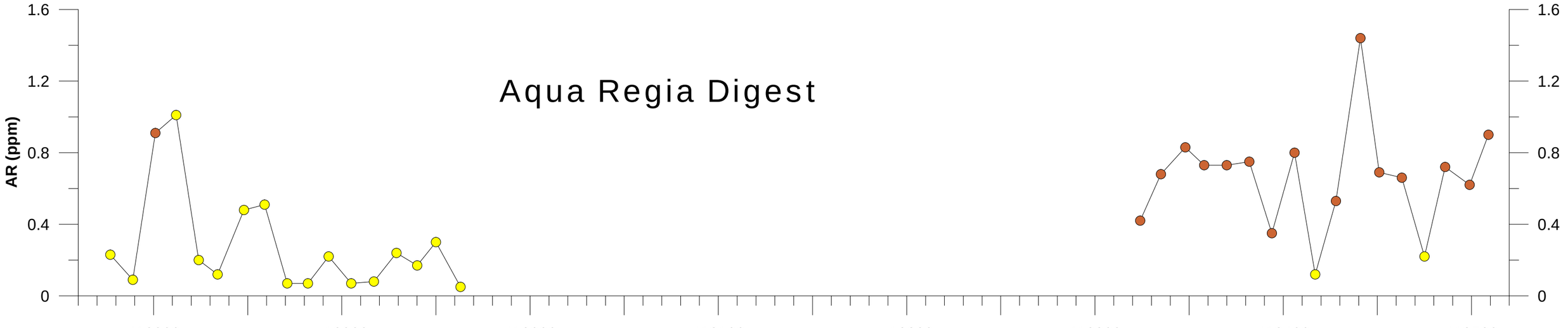

MMI Leach

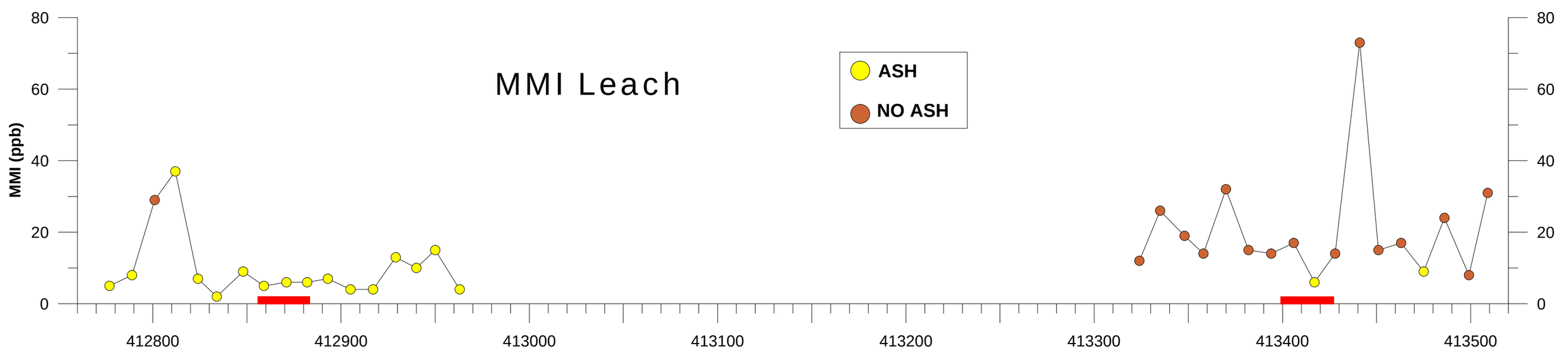

G. N. LUSTIG CONSULTING LTD.- December 11, 2008

Western Copper MMI Test
Line 4400S - 30 m North

Tungsten

Aqua Regia Digest

AR (ppm)

0.3
0.2
0.1
0

412800 412900 413000 413100 413200 413300 413400 413500

MMI Leach

MMI (ppb)

2
1.6
1.2
0.8
0.4
0

412800 412900 413000 413100 413200 413300 413400 413500

ASH
NO ASH

G. N. LUSTIG CONSULTING LTD.- December 11, 2008

Western Copper MMI Test
Line 4400S - 30 m North

Ytterbium

Aqua Regia Digest

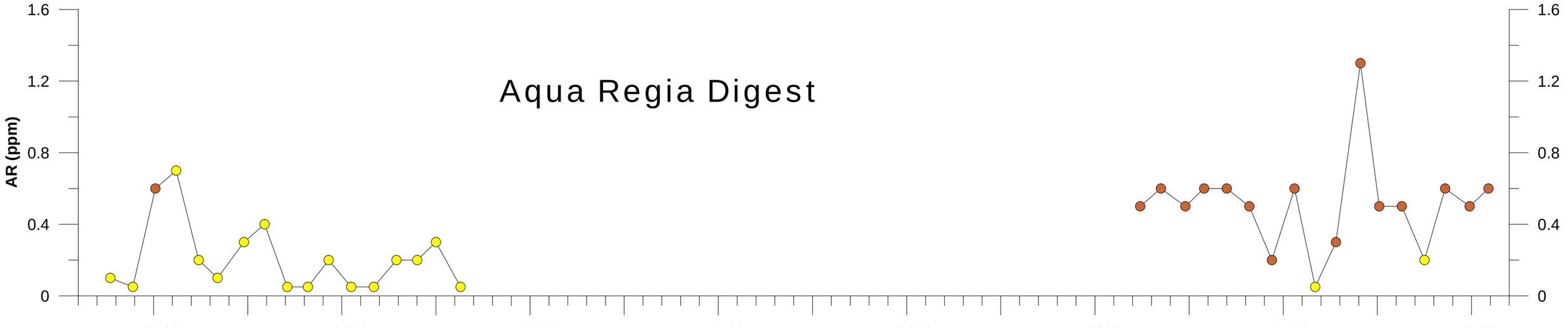

MMI Leach

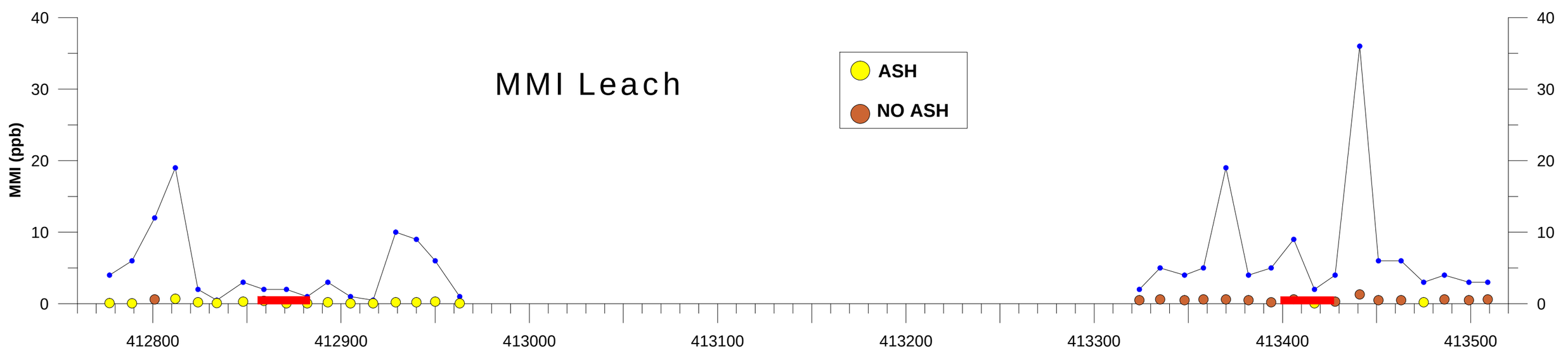

G. N. LUSTIG CONSULTING LTD.- December 11, 2008

Western Copper MMI Test
Line 4400S - 30 m North

Yttrium

Aqua Regia Digest

AR (%)

20
16
12
8
4
0

412800 412900 413000 413100 413200 413300 413400 413500

MMI Leach

MMI (ppb)

600
400
200
0

ASH
NO ASH

412800 412900 413000 413100 413200 413300 413400 413500

G. N. LUSTIG CONSULTING LTD.- December 11, 2008

Western Copper MMI Test
Line 4400S - 30 m North

Zinc

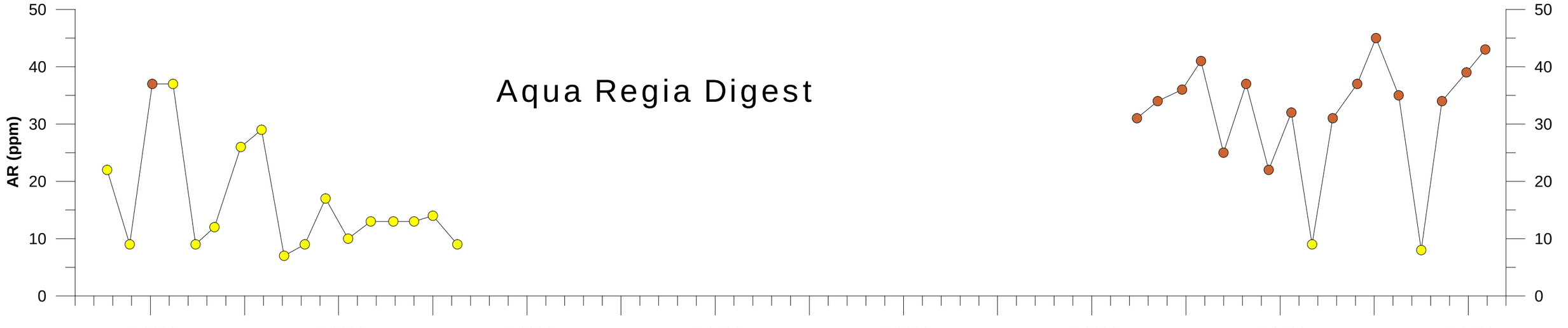

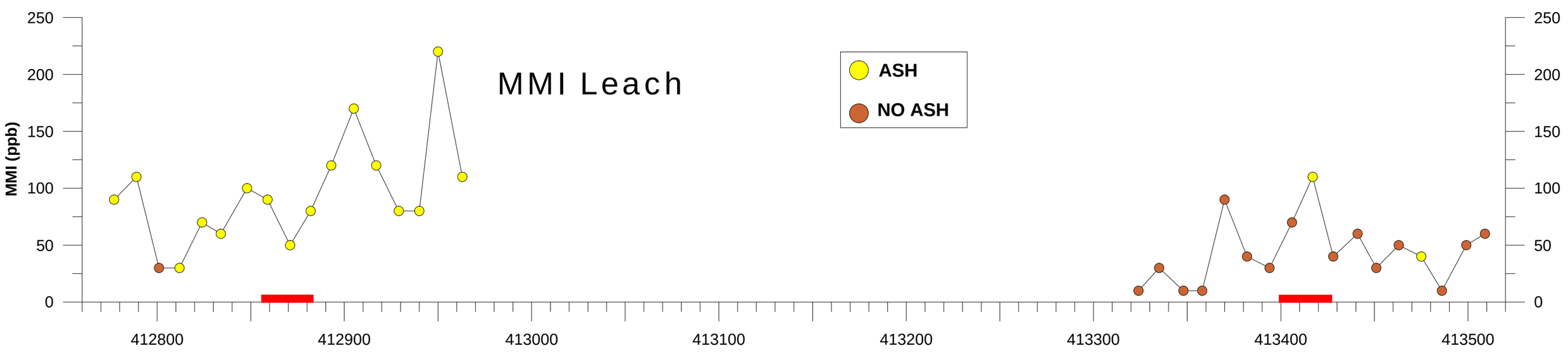

G. N. LUSTIG CONSULTING LTD.- December 11, 2008

Western Copper MMI Test
Line 4400S - 30 m North

Zirconium

Aqua Regia Digest

AR (ppm)

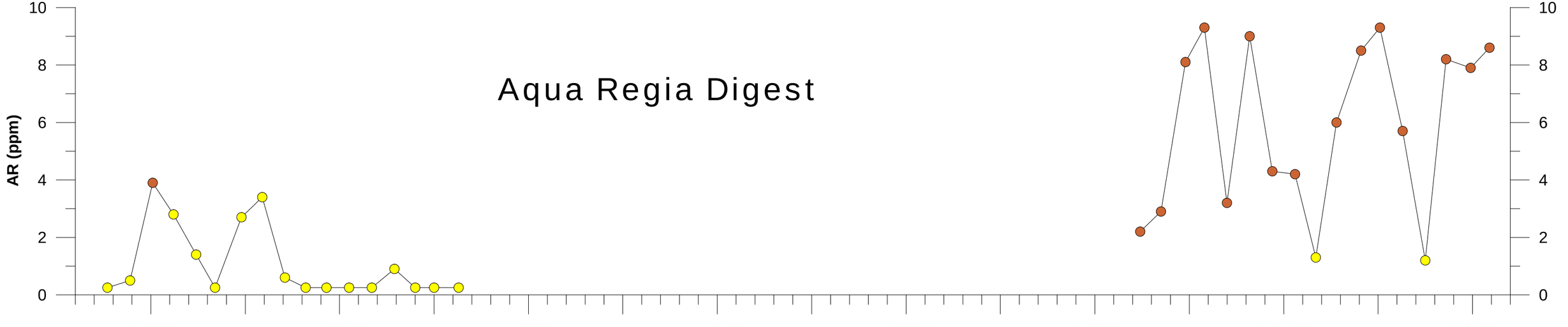

MMI Leach

MMI (ppb)

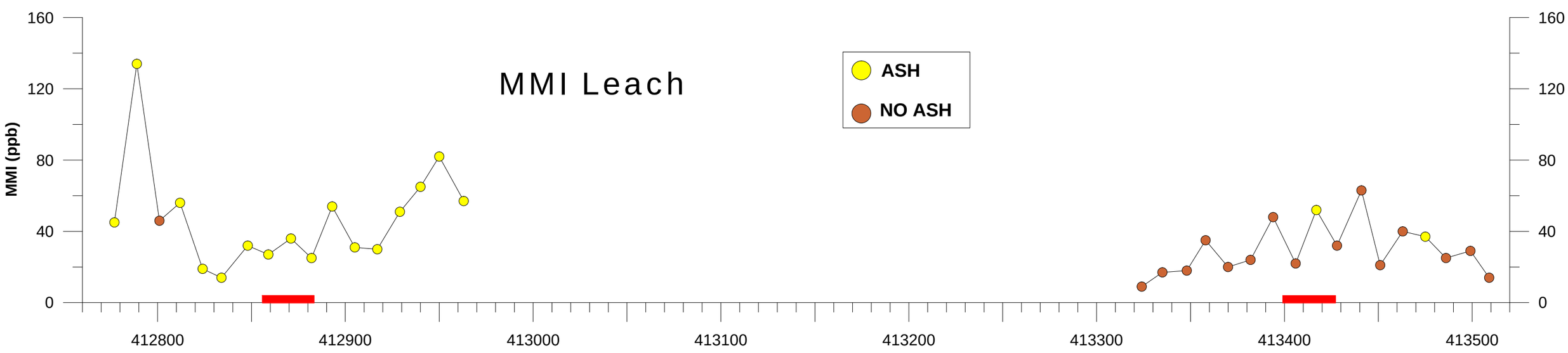

G. N. LUSTIG CONSULTING LTD.- December 11, 2008

Line 4400S
South Profile

Western Copper MMI Test
Line 4400S - 25 m South
SILVER

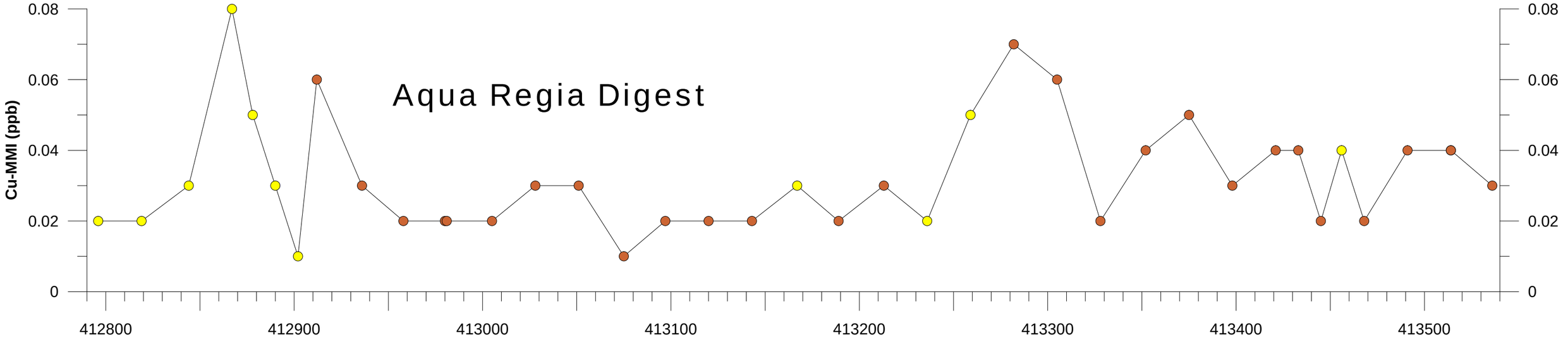

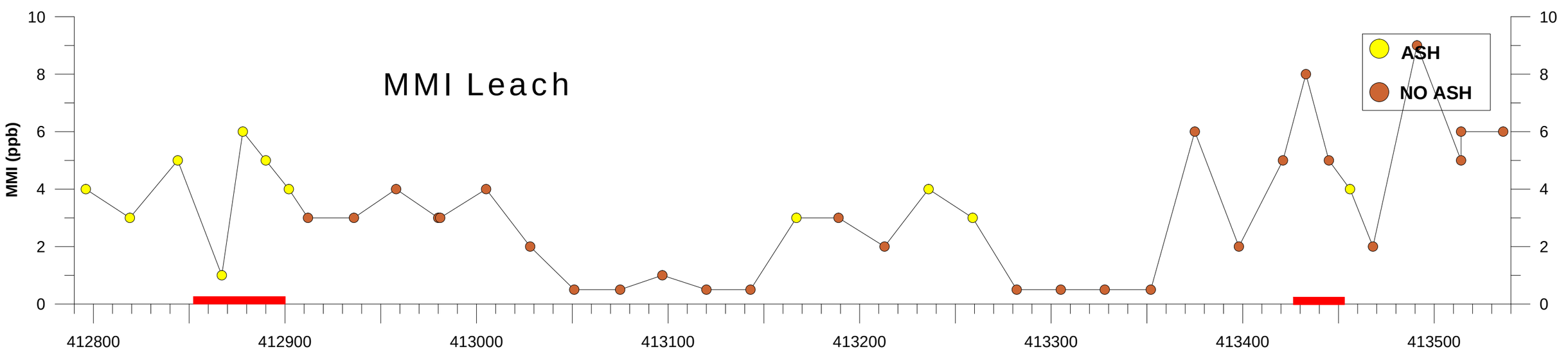

G. N. LUSTIG CONSULTING LTD.- AUGUST 26, 2008

Western Copper MMI Test
Line 4400S - 25 m South

ALUMINUM

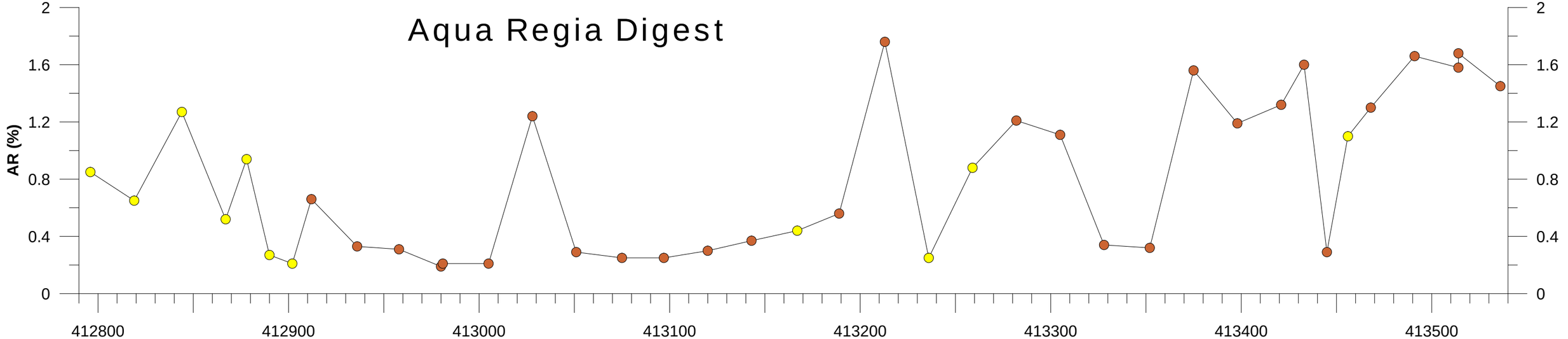

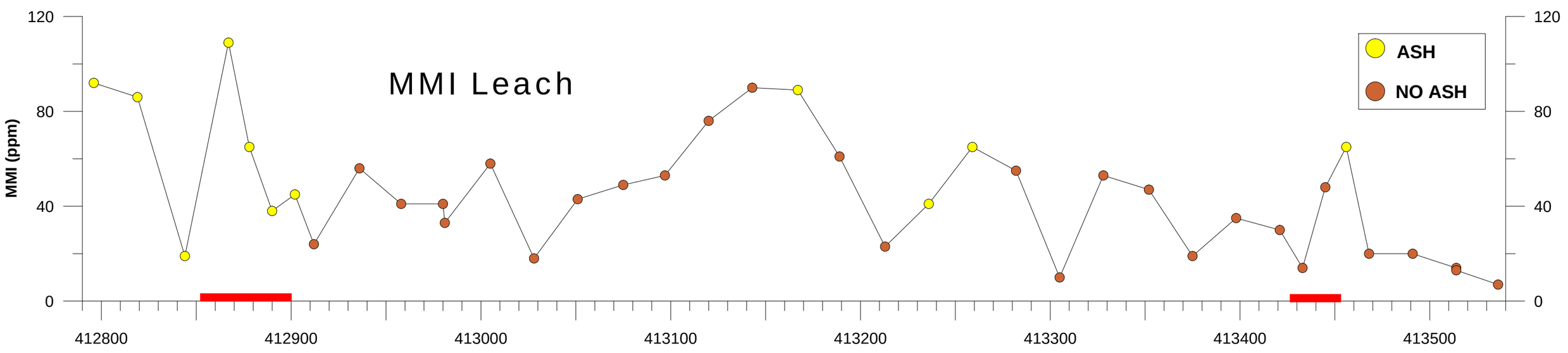

G. N. LUSTIG CONSULTING LTD.- AUGUST 26, 2008

Western Copper MMI Test
Line 4400S - 25 m South

Arsenic

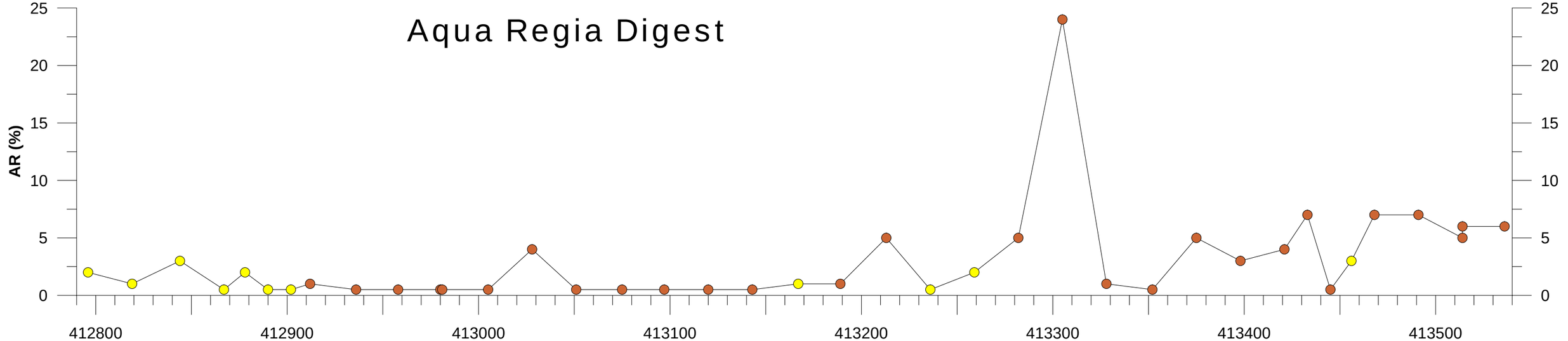

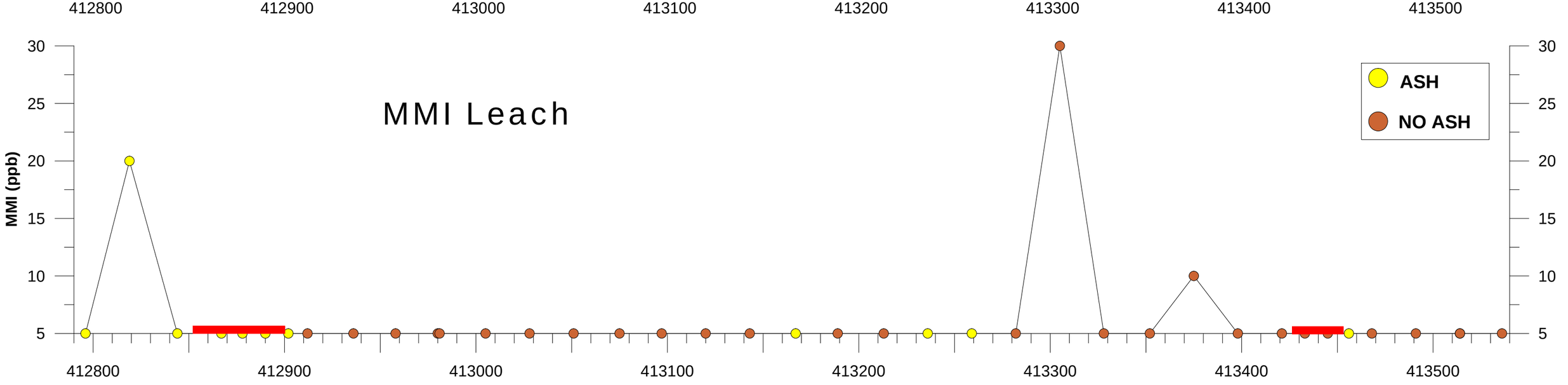

G. N. LUSTIG CONSULTING LTD.- AUGUST 26, 2008

Western Copper MMI Test
Line 4400S - 25 m South

BARIUM

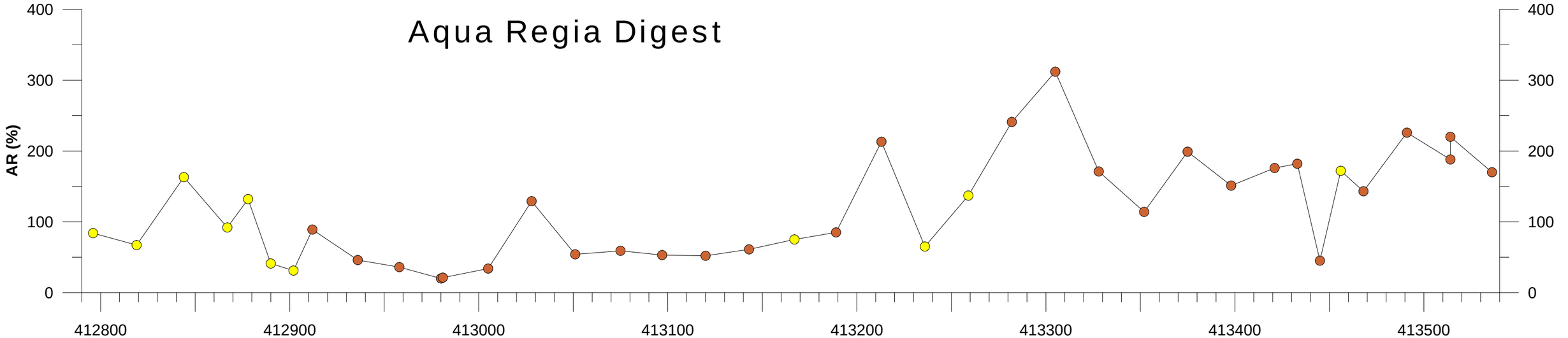

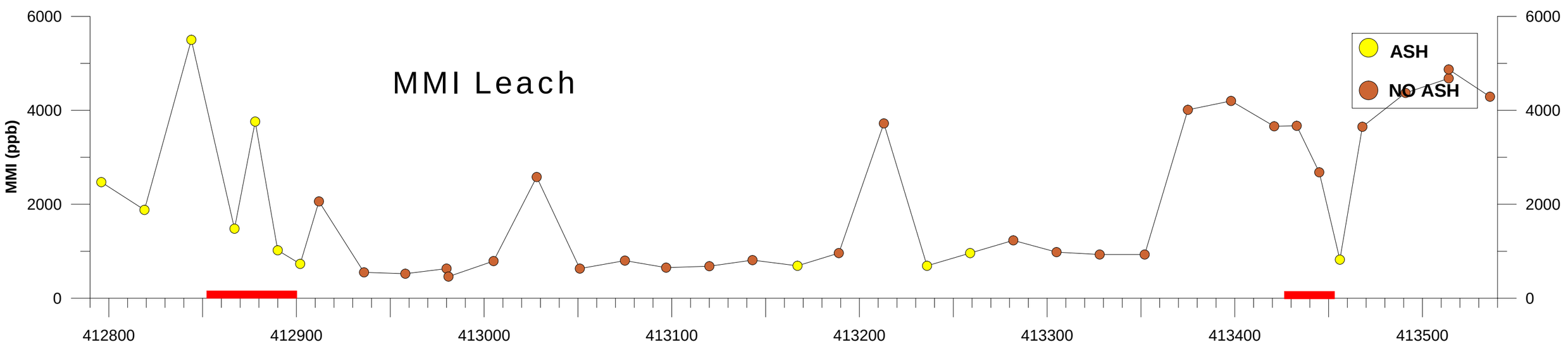

G. N. LUSTIG CONSULTING LTD.- AUGUST 26, 2008

Western Copper MMI Test
Line 4400S - 25 m South

BISMUTH

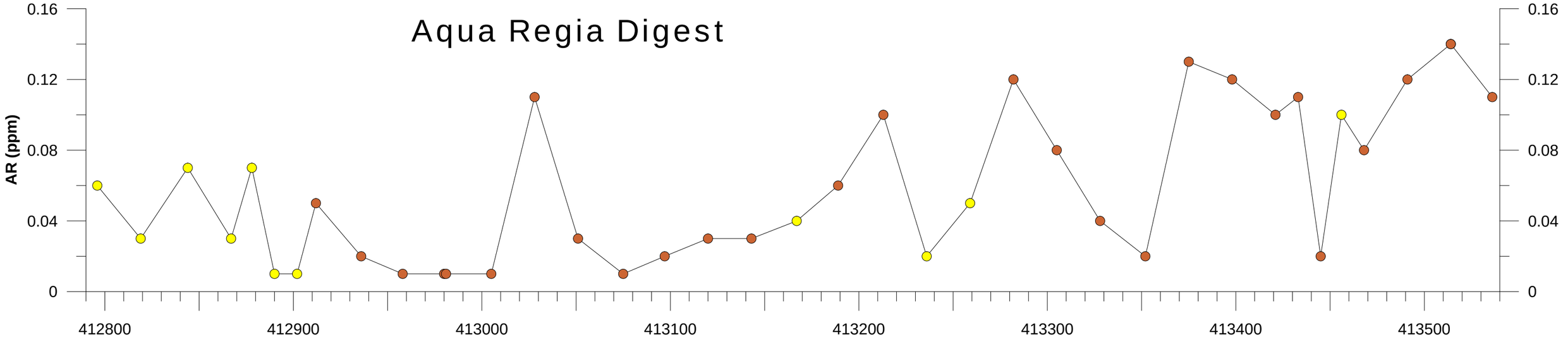

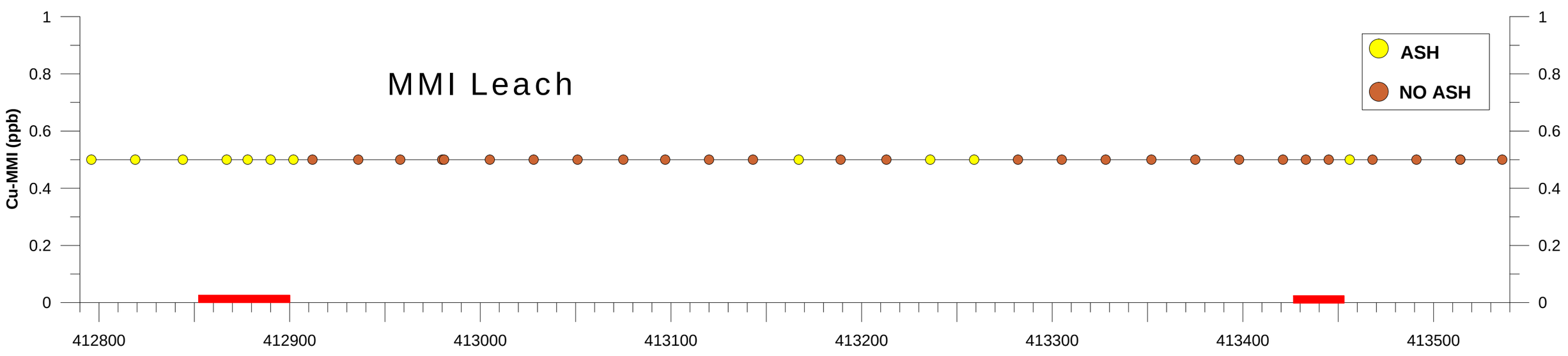

G. N. LUSTIG CONSULTING LTD.- November 18, 2008

Western Copper MMI Test
Line 4400S - 25 m South

Calcium

Aqua Regia Digest

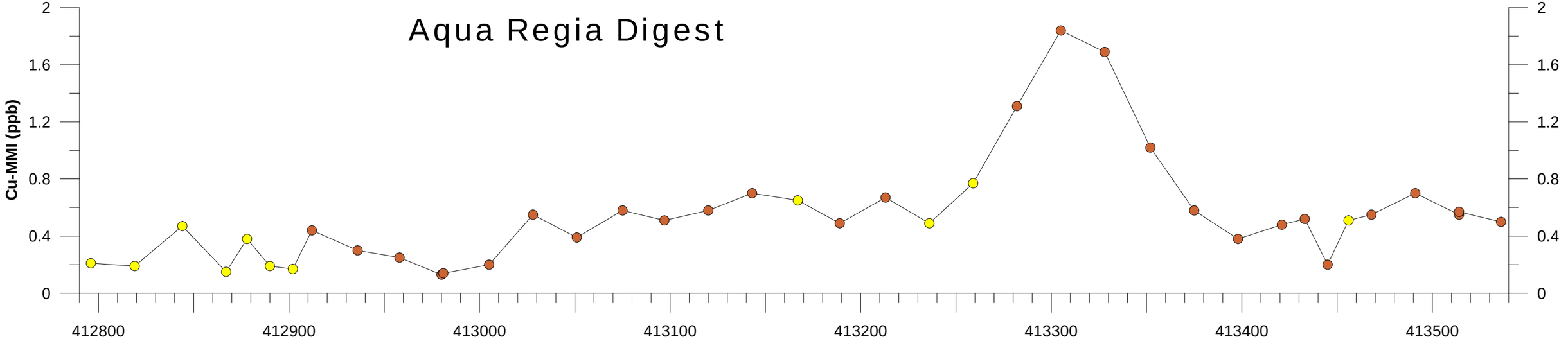

MMI Leach

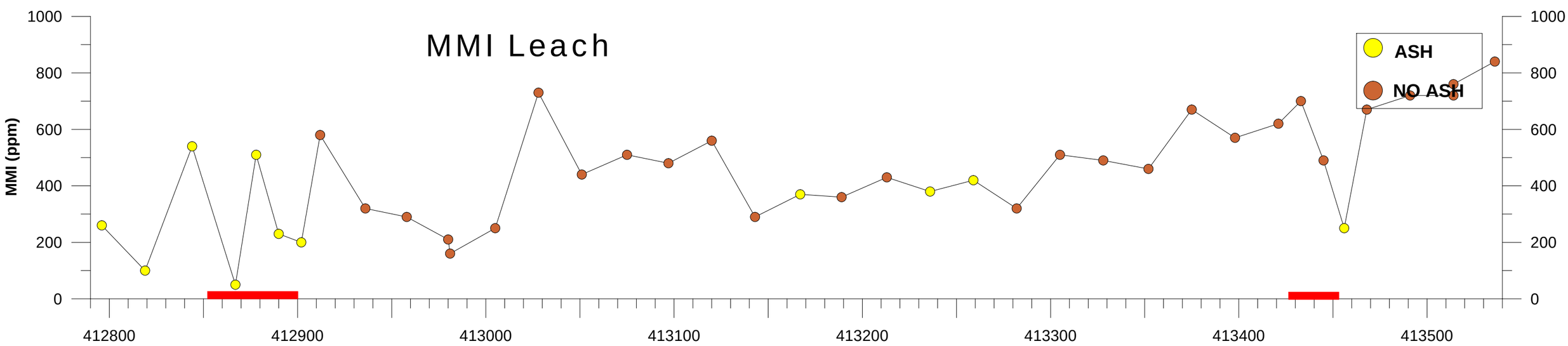

G. N. LUSTIG CONSULTING LTD.- November 18, 2008

Western Copper MMI Test
Line 4400S - 25 m South

Cadmium

Aqua Regia Digest

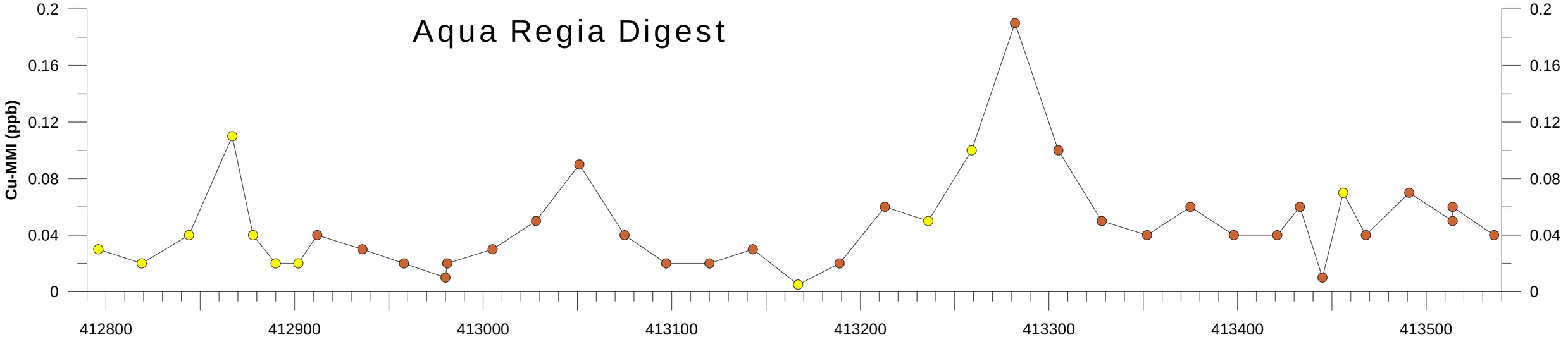

MMI Leach

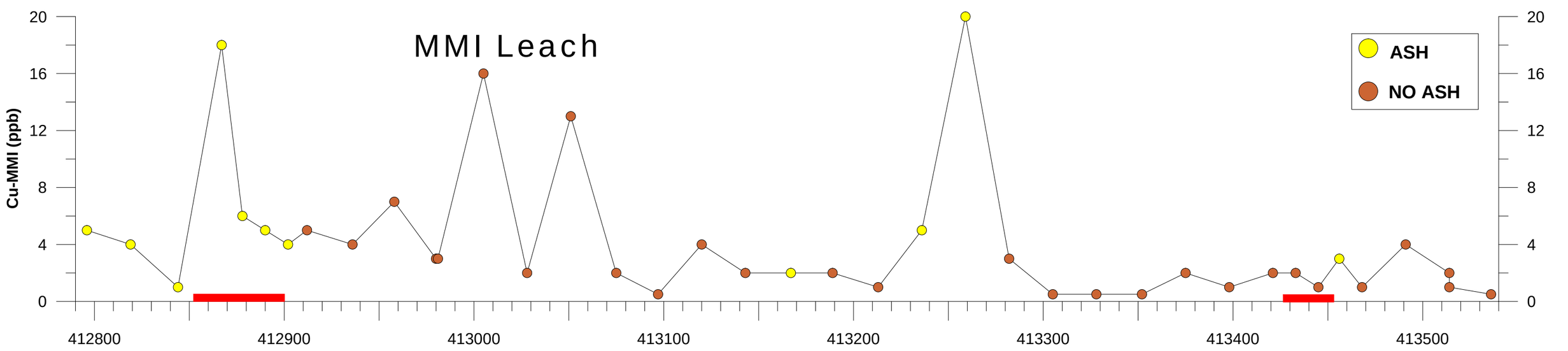

G. N. LUSTIG CONSULTING LTD.- November 18, 2008

Western Copper MMI Test
Line 4400S - 25 m South

Cerium

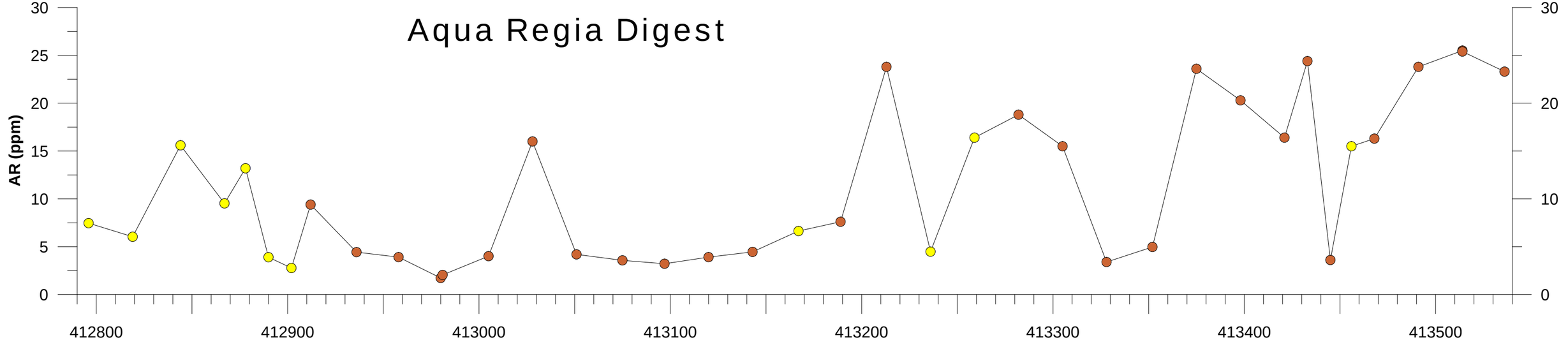

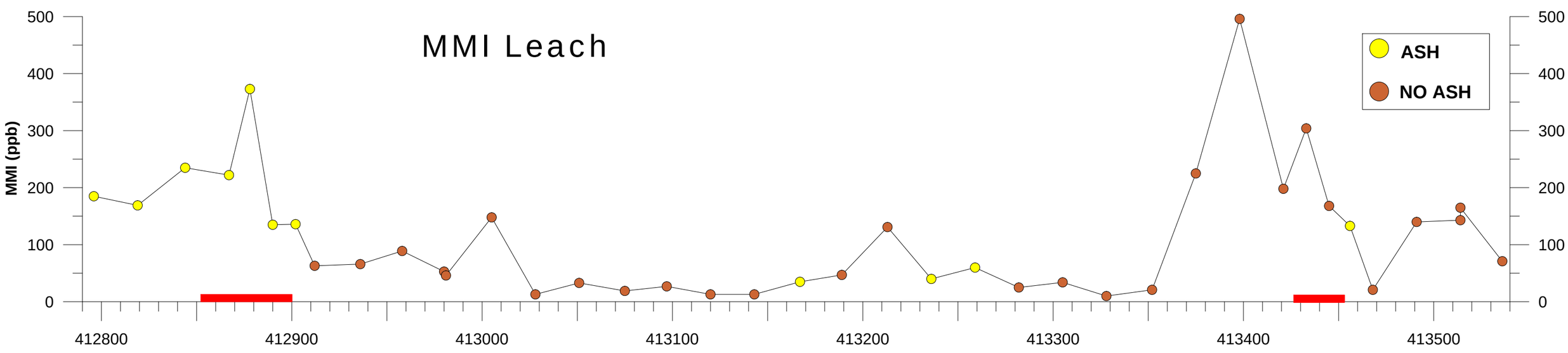

G. N. LUSTIG CONSULTING LTD.- November 18, 2008

Western Copper MMI Test
Line 4400S - 25 m South

Cobalt

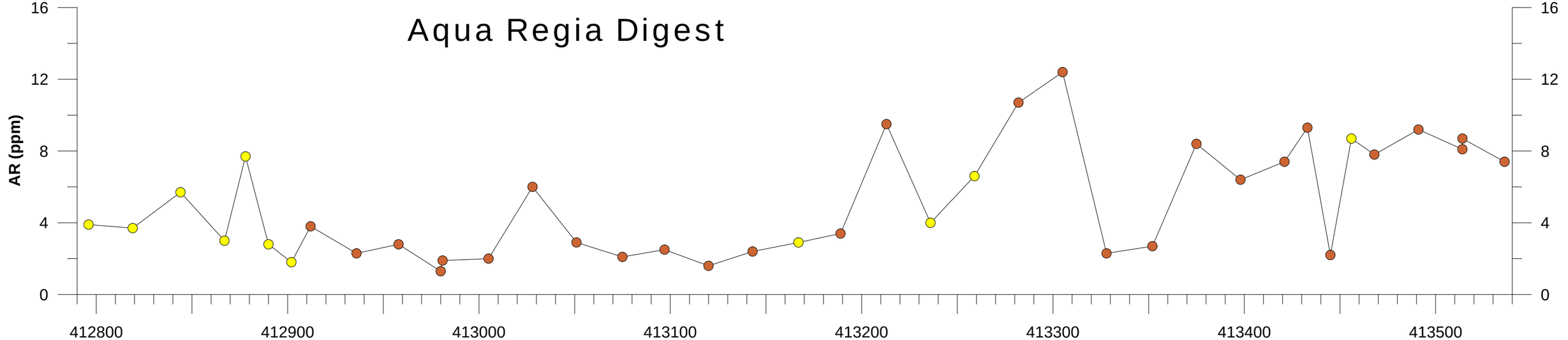

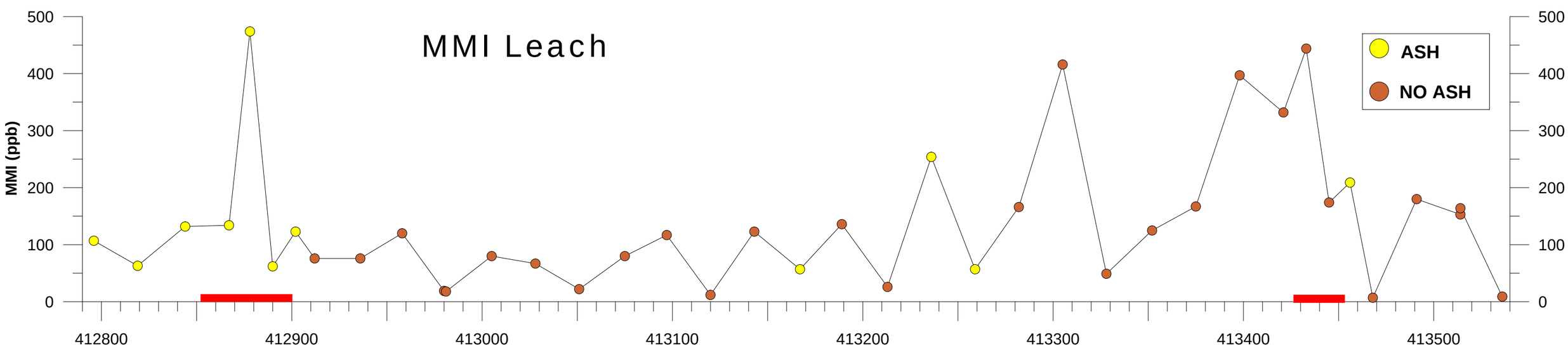

G. N. LUSTIG CONSULTING LTD.- November 18, 2008

Western Copper MMI Test
Line 4400S - 25 m South

COPPER

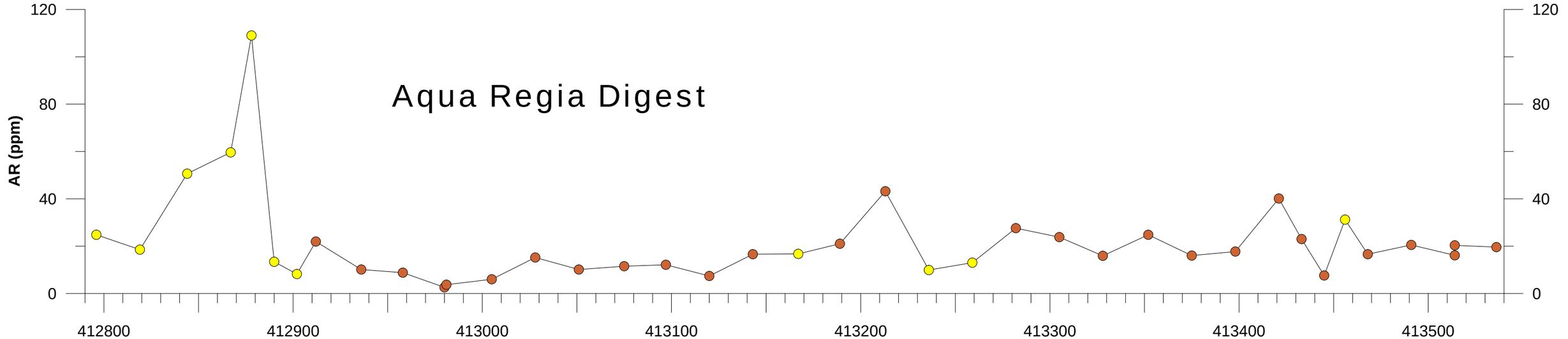

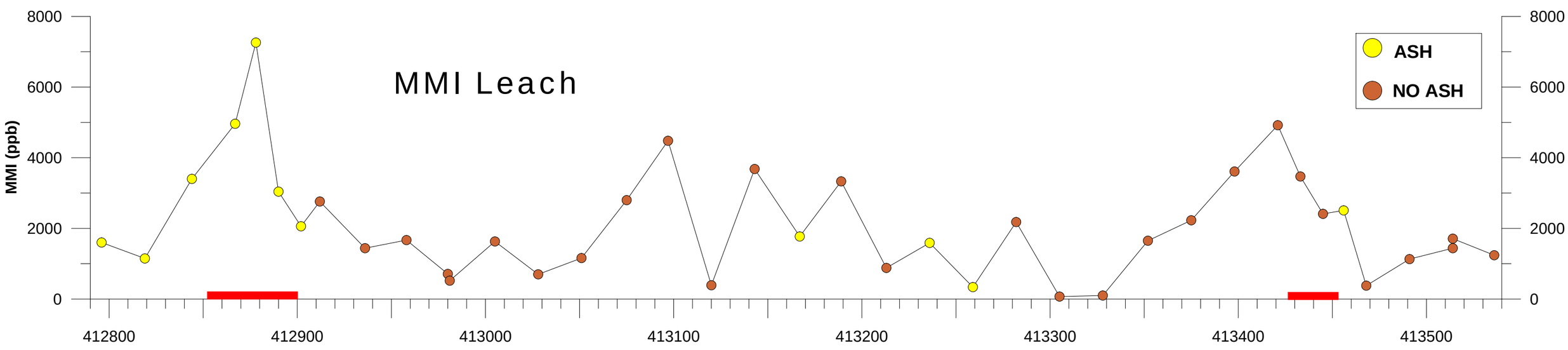

G. N. LUSTIG CONSULTING LTD.- AUGUST 26, 2008

Western Copper MMI Test
Line 4400S - 25 m South

Iron

Aqua Regia Digest

AR (%)

0 1 2 3 4 5

412800 412900 413000 413100 413200 413300 413400 413500

MMI Leach

MMI (ppm)

0 100 200 300 400

ASH

NO ASH

412800 412900 413000 413100 413200 413300 413400 413500

G. N. LUSTIG CONSULTING LTD.- AUGUST 26, 2008

Western Copper MMI Test
Line 4400S - 25 m South

Lanthanum

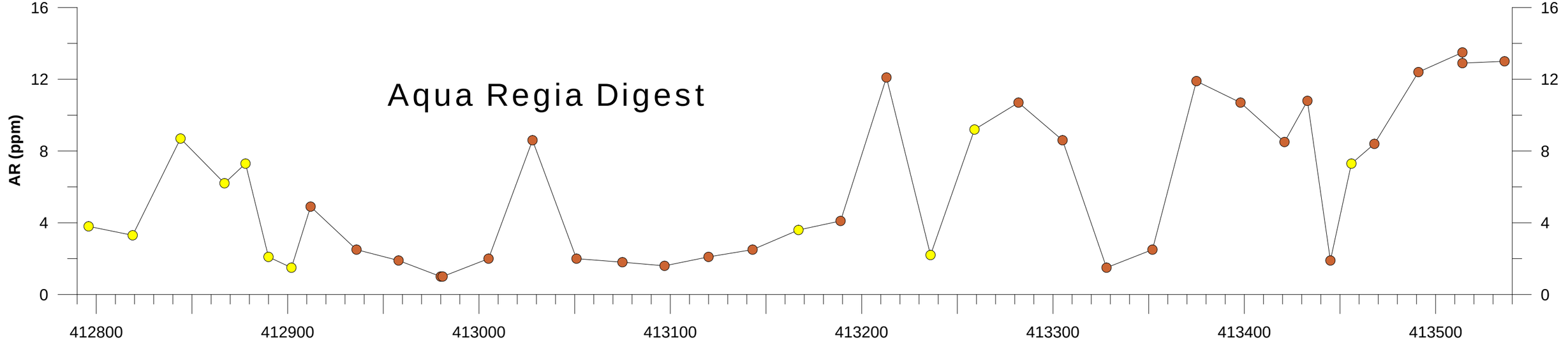

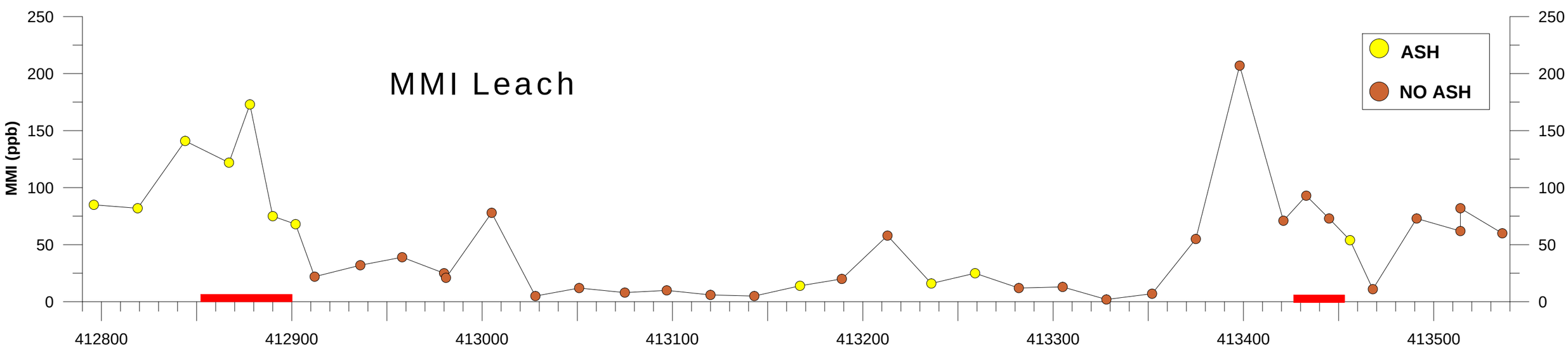

G. N. LUSTIG CONSULTING LTD.- AUGUST 26, 2008

Western Copper MMI Test
Line 4400S - 25 m South

Lithium

Aqua Regia Digest

AR (ppm)

12
8
4
0

412800 412900 413000 413100 413200 413300 413400 413500

MMI Leach

MMI (ppb)

7
6
5
4
3
2

ASH
NO ASH

412800 412900 413000 413100 413200 413300 413400 413500

G. N. LUSTIG CONSULTING LTD.- November 18, 2008

Western Copper MMI Test
Line 4400S - 25 m South

Magnesium

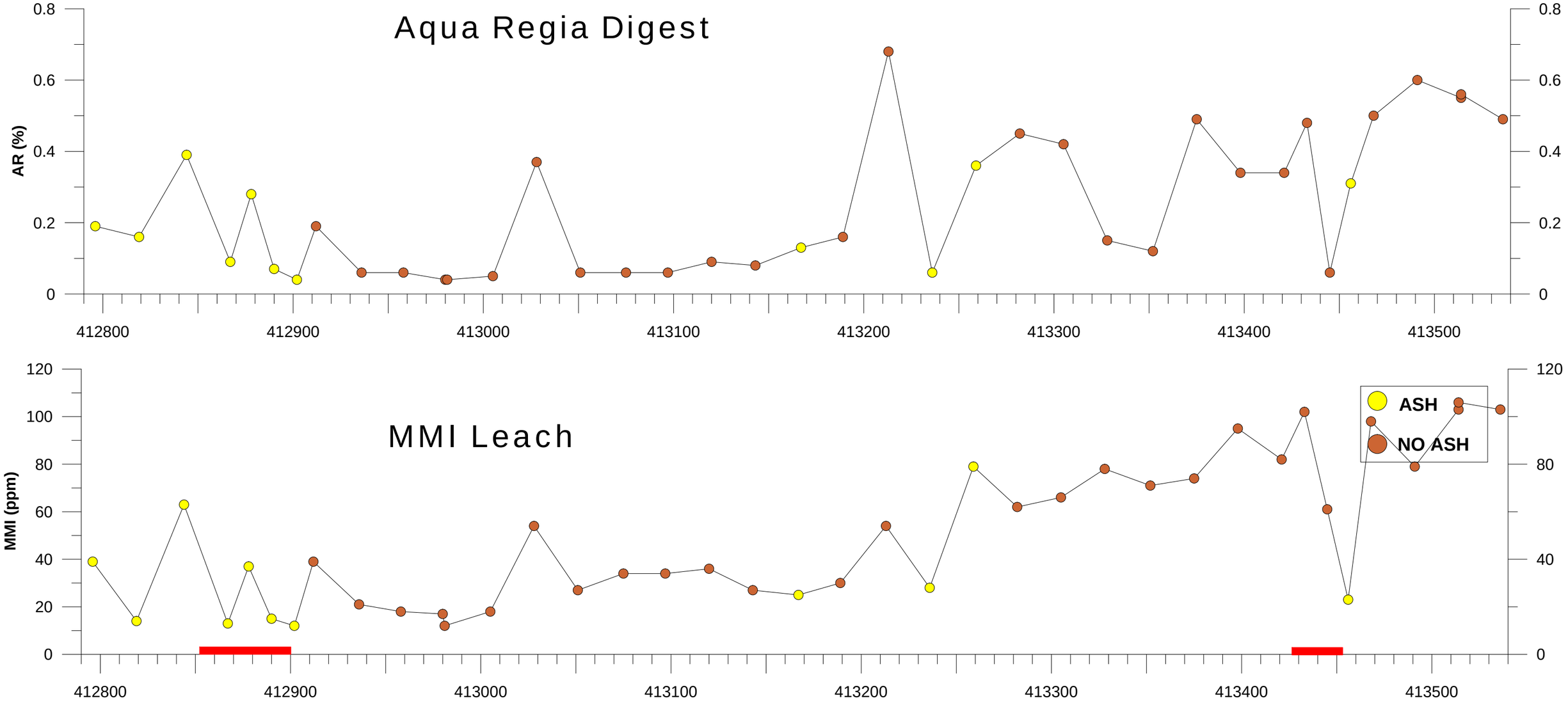

G. N. LUSTIG CONSULTING LTD.- November 18, 2008

Western Copper MMI Test
Line 4400S - 25 m South

Molybdenum

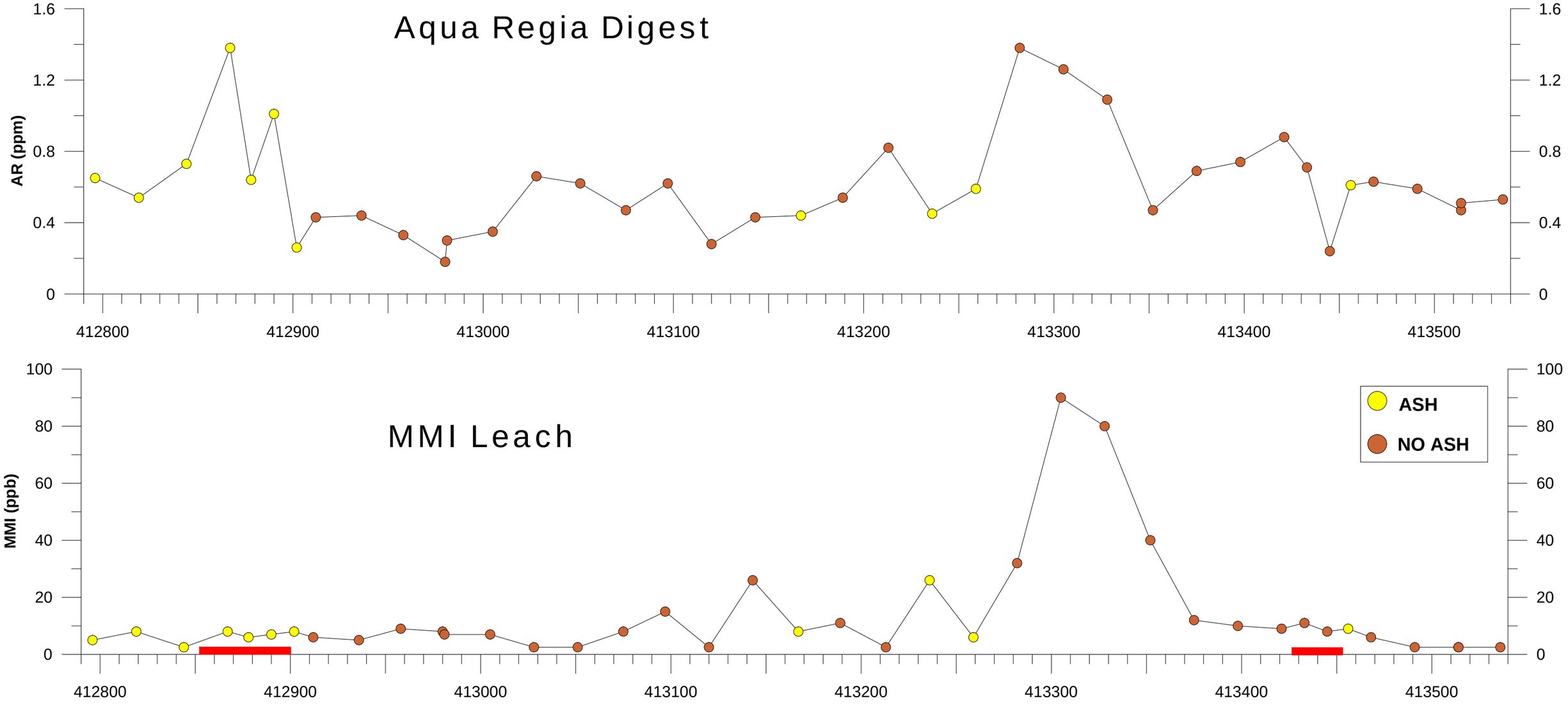

G. N. LUSTIG CONSULTING LTD.- November 18, 2008

Western Copper MMI Test
Line 4400S - 25 m South

Niobium

Aqua Regia Digest

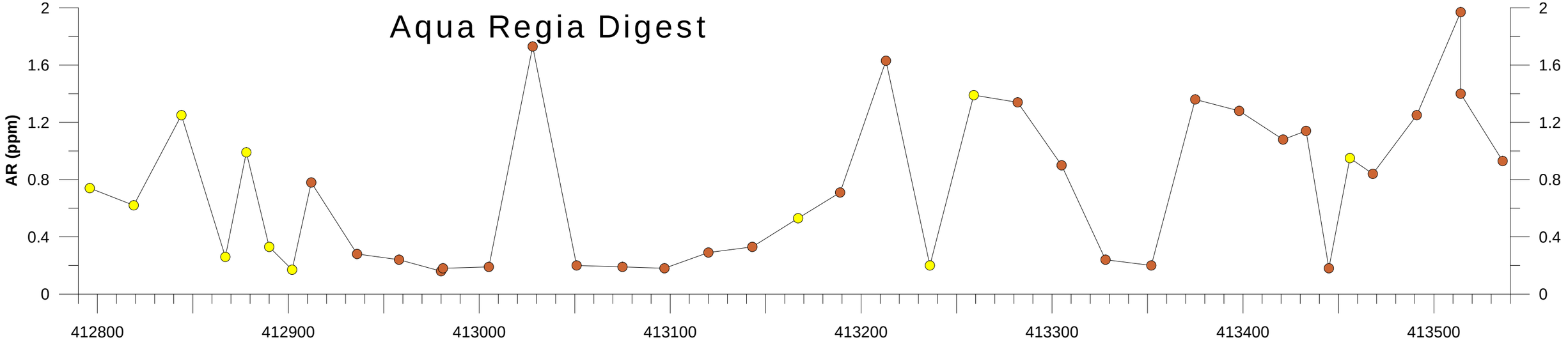

MMI Leach

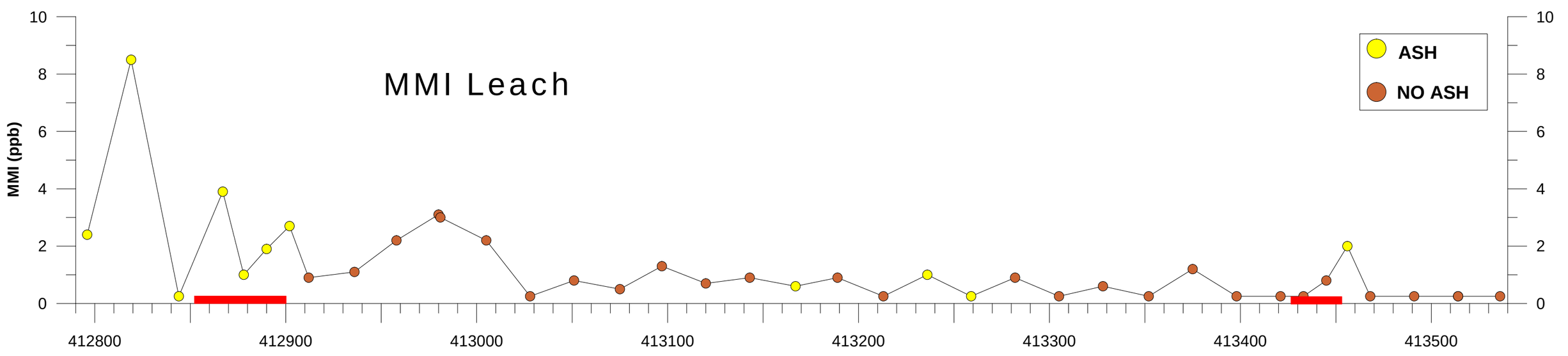

G. N. LUSTIG CONSULTING LTD.- November 18, 2008

Western Copper MMI Test
Line 4400S - 25 m South

Nickel

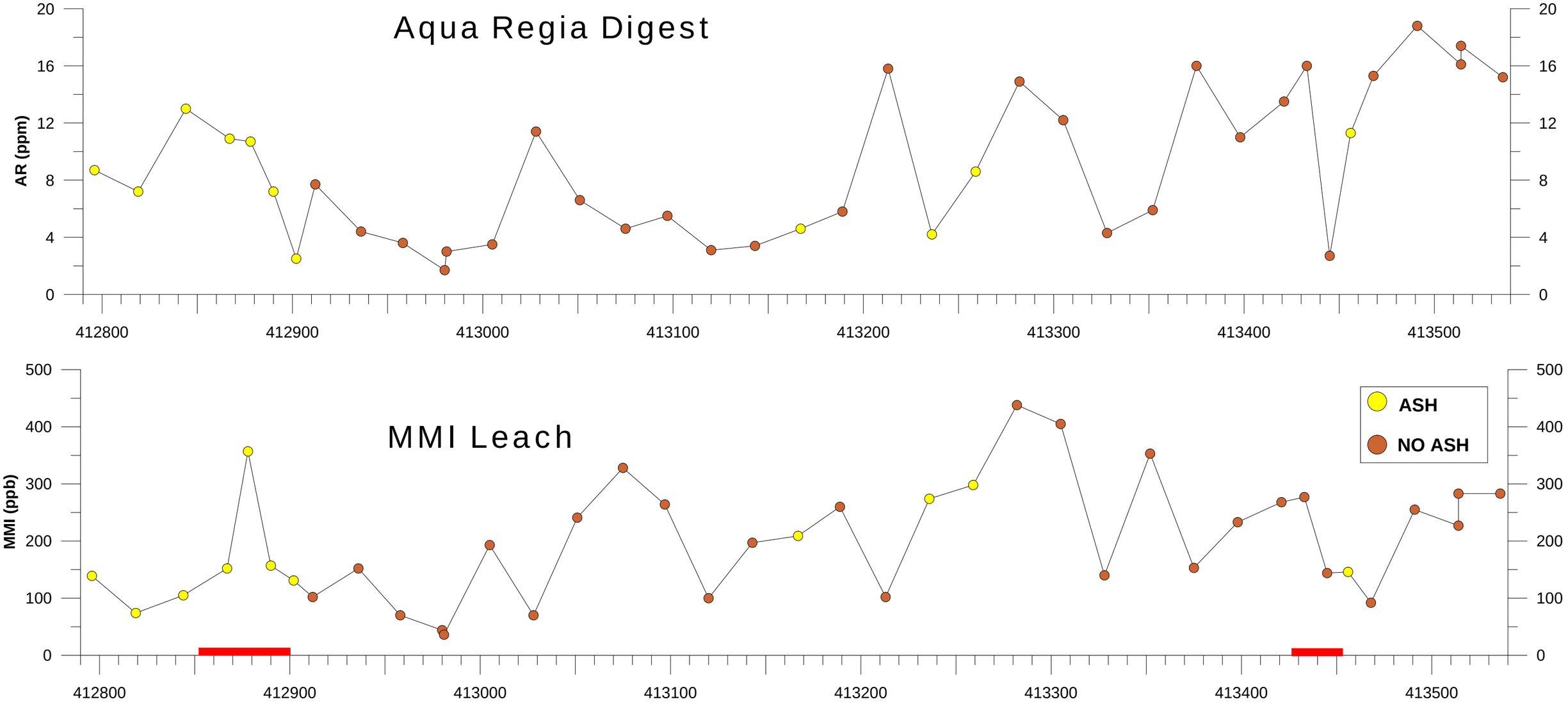

G. N. LUSTIG CONSULTING LTD.- November 18, 2008

Western Copper MMI Test
Line 4400S - 25 m South
Lead

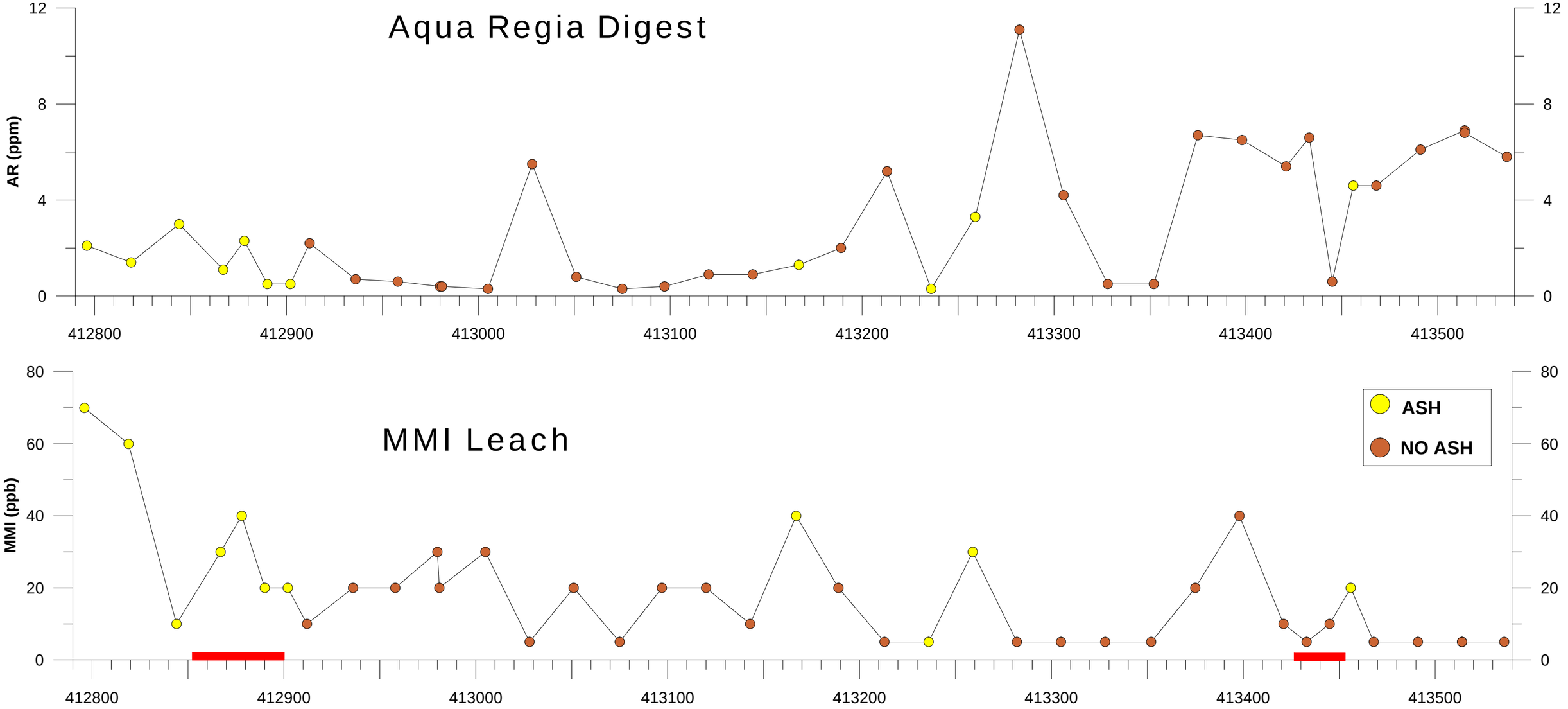

G. N. LUSTIG CONSULTING LTD.- November 18, 2008

Western Copper MMI Test
Line 4400S - 25 m South

Rubidium

Aqua Regia Digest

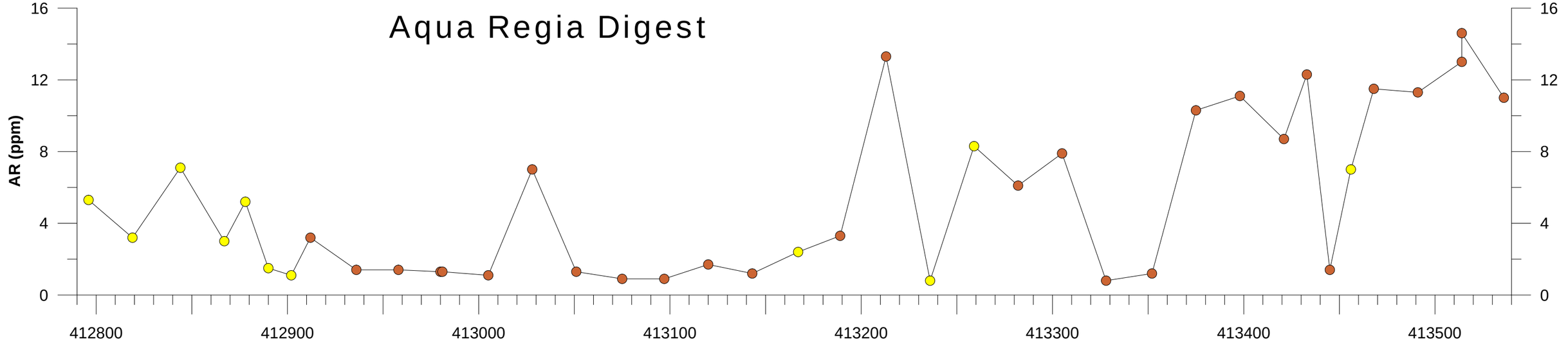

MMI Leach

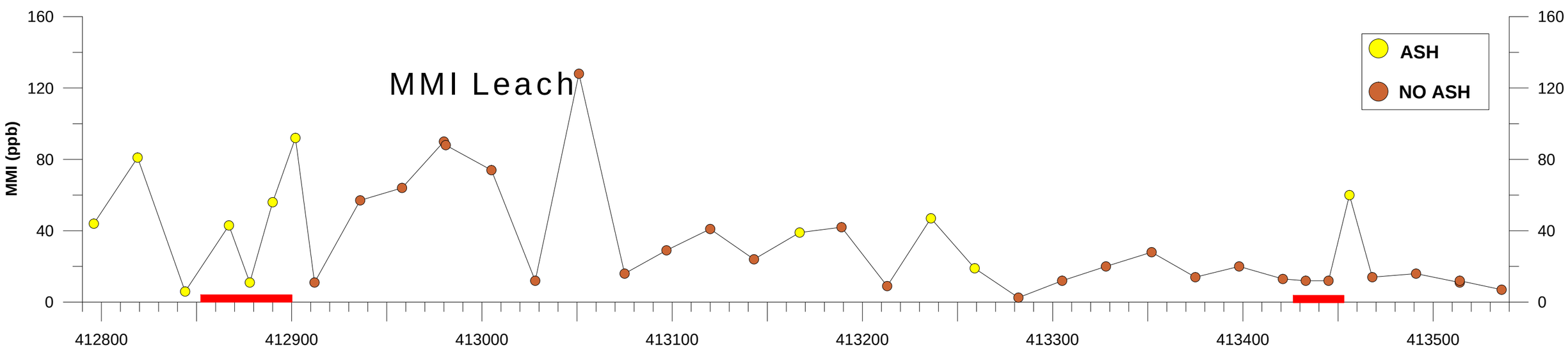

G. N. LUSTIG CONSULTING LTD.- November 18, 2008

Western Copper MMI Test
Line 4400S - 25 m South

Antimony

Aqua Regia Digest

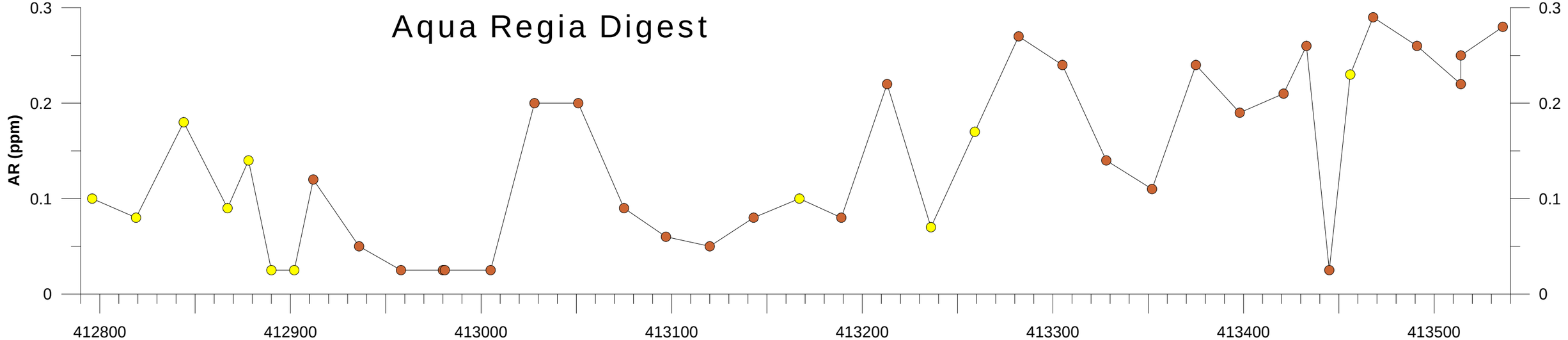

MMI Leach

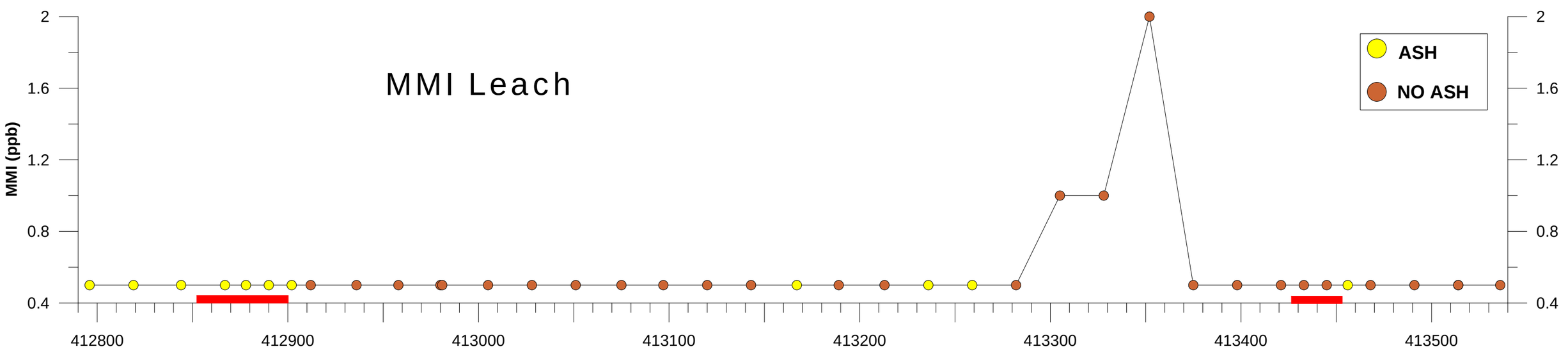

G. N. LUSTIG CONSULTING LTD.- November 18, 2008

Western Copper MMI Test
Line 4400S - 25 m South

Scandium

Aqua Regia Digest

AR (ppm)

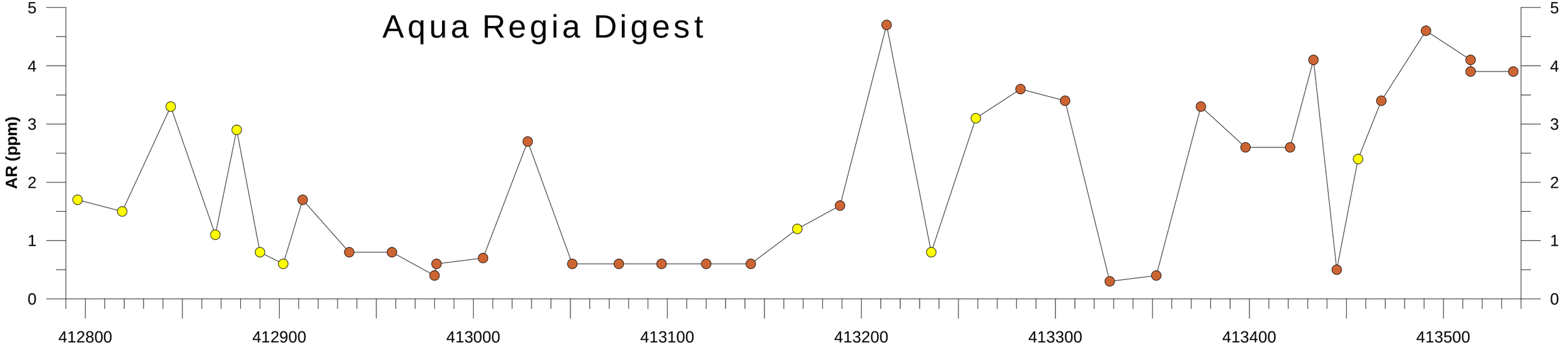

MMI Leach

MMI (ppb)

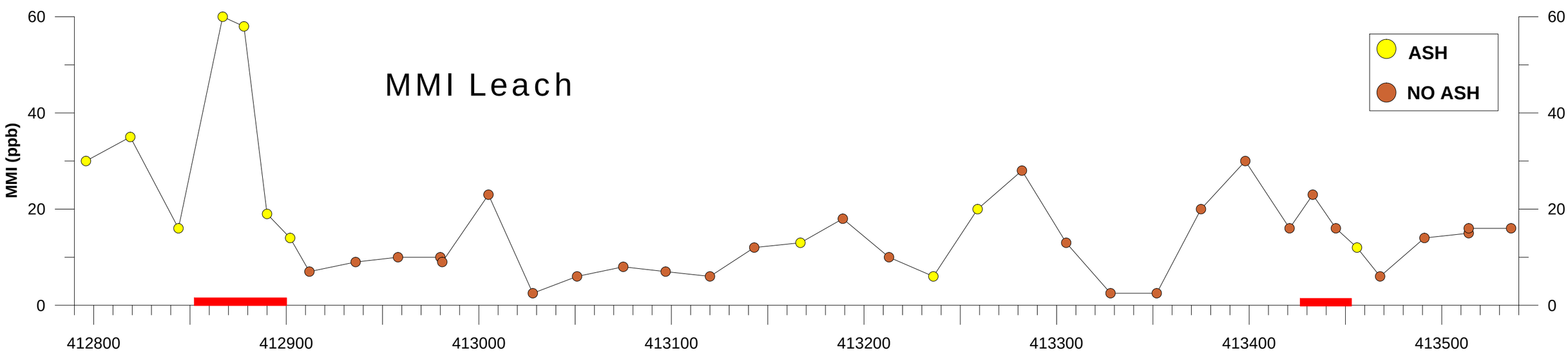

G. N. LUSTIG CONSULTING LTD.- November 18, 2008

Western Copper MMI Test
Line 4400S - 25 m South

Tin

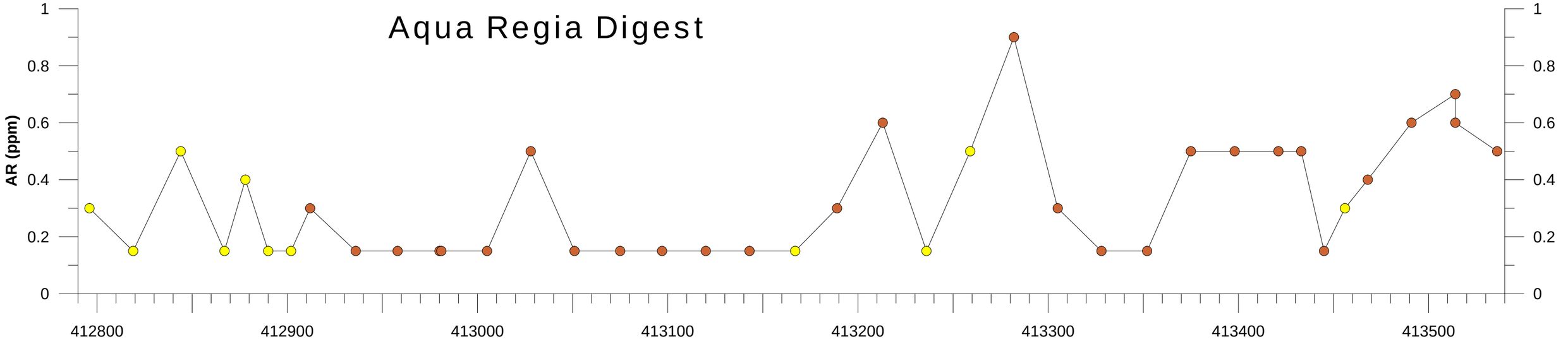

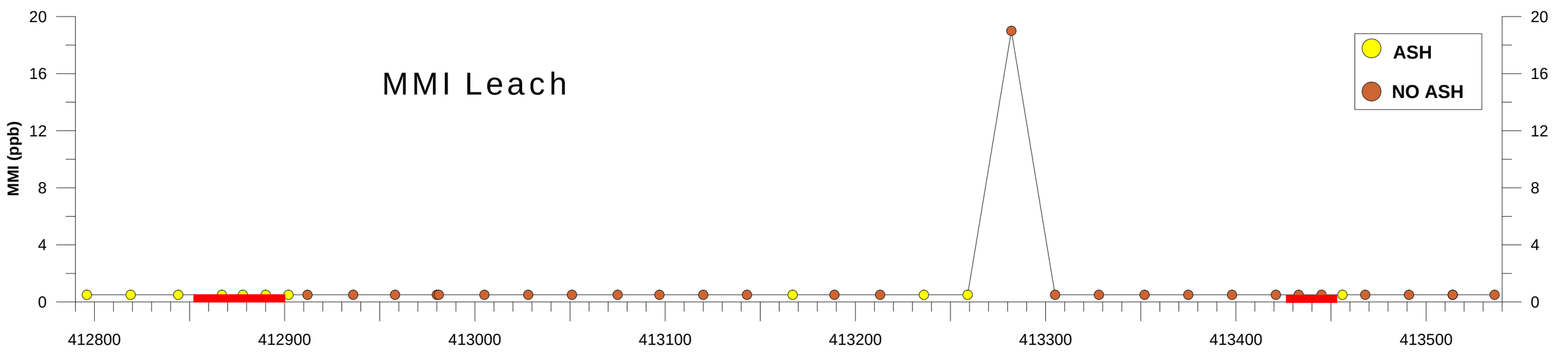

G. N. LUSTIG CONSULTING LTD.- November 18, 2008

Western Copper MMI Test
Line 4400S - 25 m South
Strontium

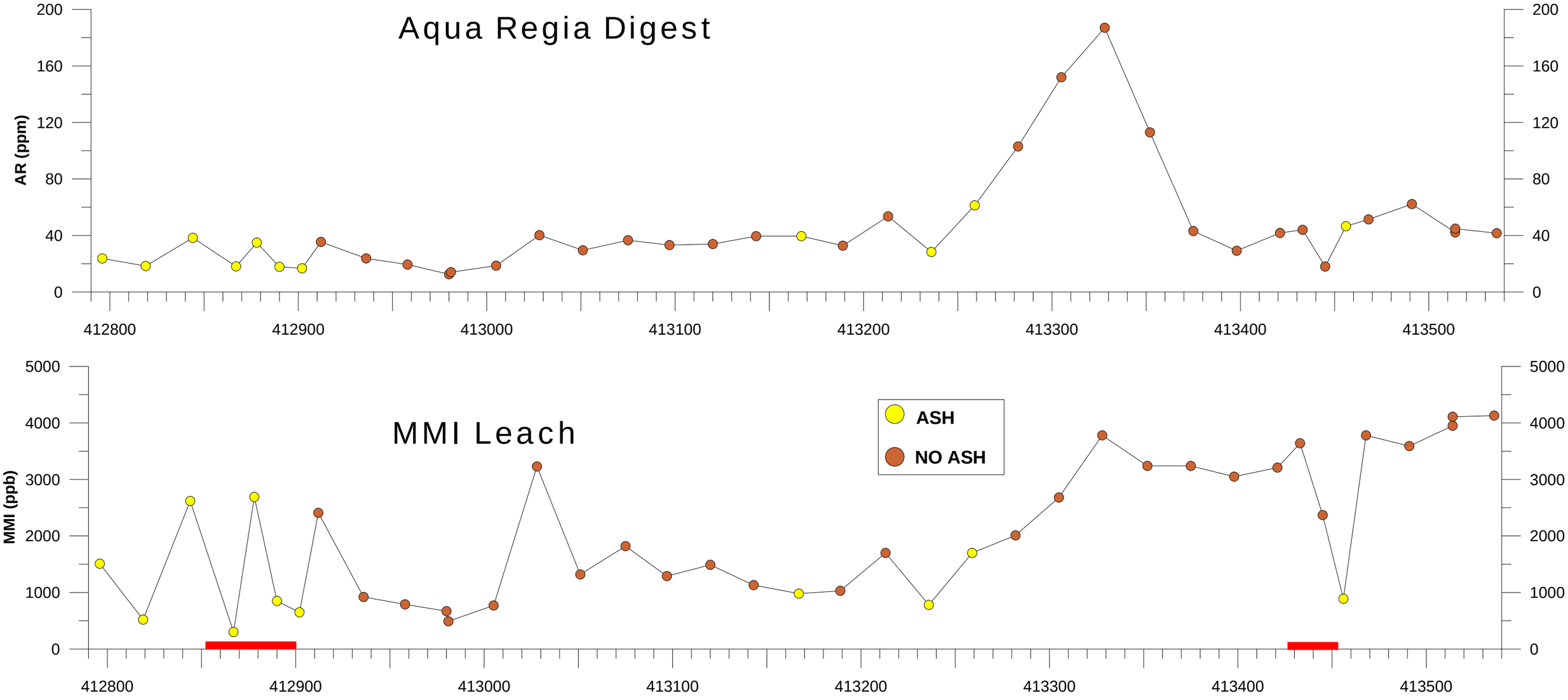

G. N. LUSTIG CONSULTING LTD.- November 18, 2008

Western Copper MMI Test
Line 4400S - 25 m South

Tantalum

Aqua Regia Digest

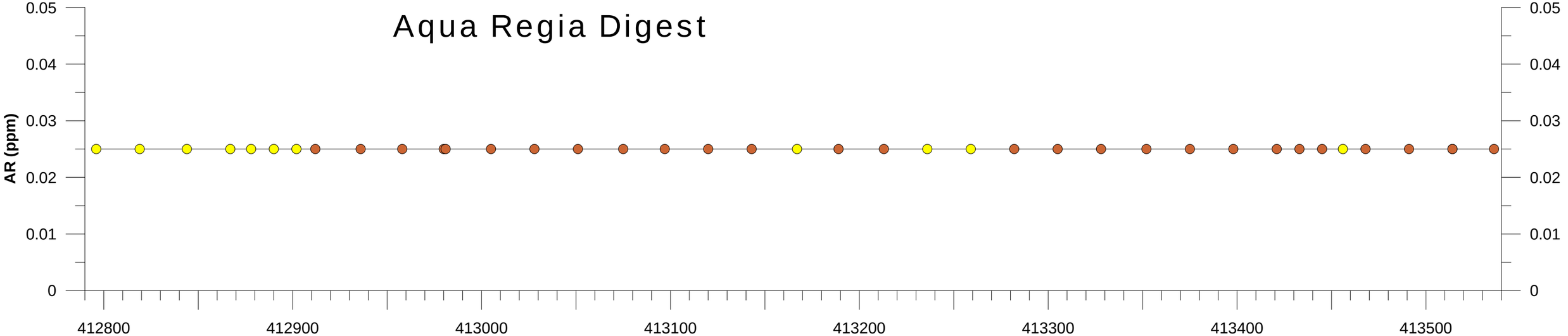

MMI Leach

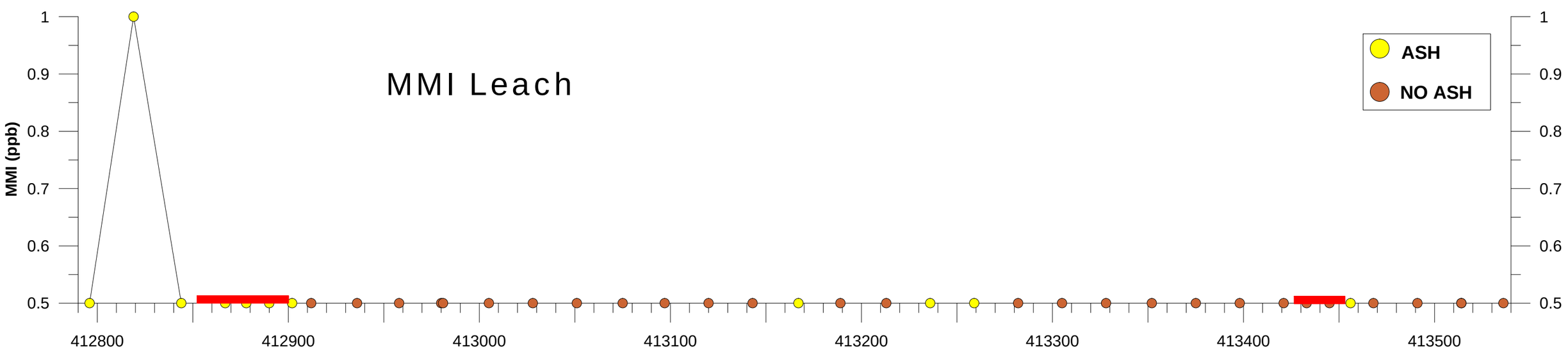

G. N. LUSTIG CONSULTING LTD.- November 18, 2008

Western Copper MMI Test
Line 4400S - 25 m South

Terbium

Aqua Regia Digest

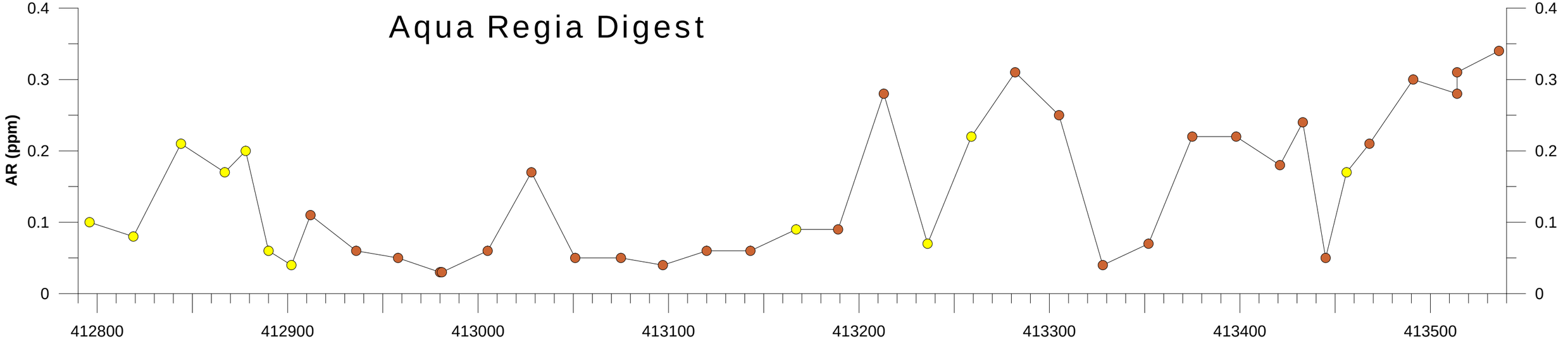

MMI Leach

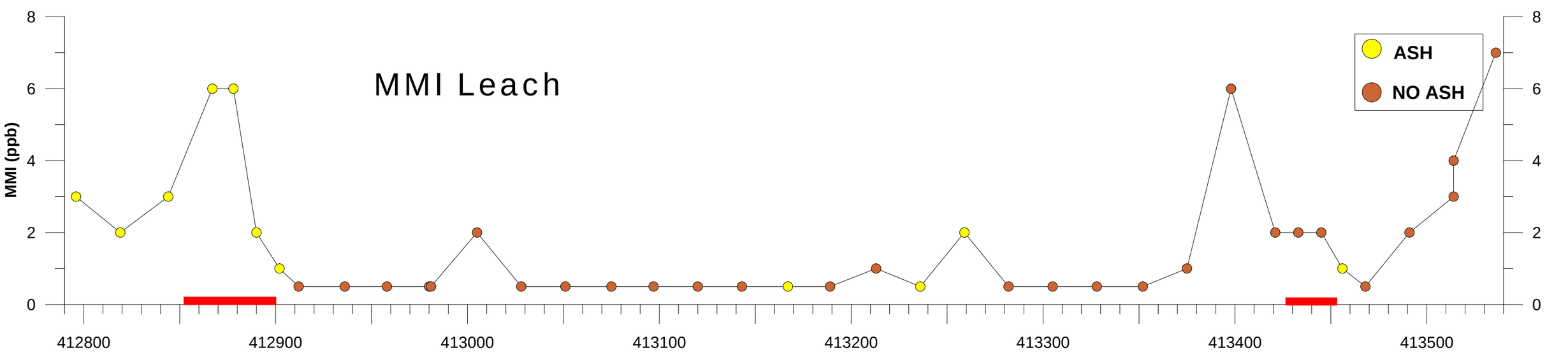

G. N. LUSTIG CONSULTING LTD.- November 18, 2008

Western Copper MMI Test
Line 4400S - 25 m South

Tellurium

Aqua Regia Digest

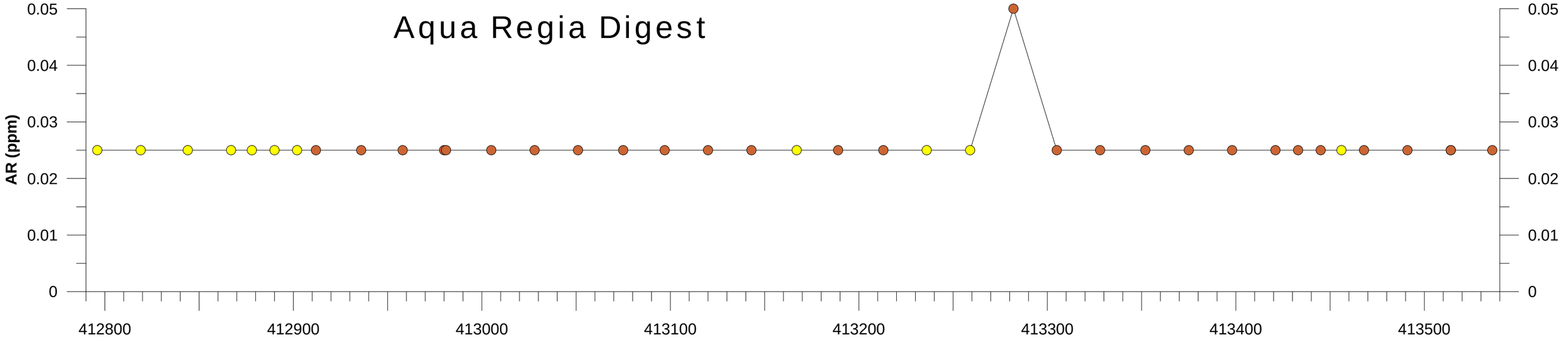

MMI Leach

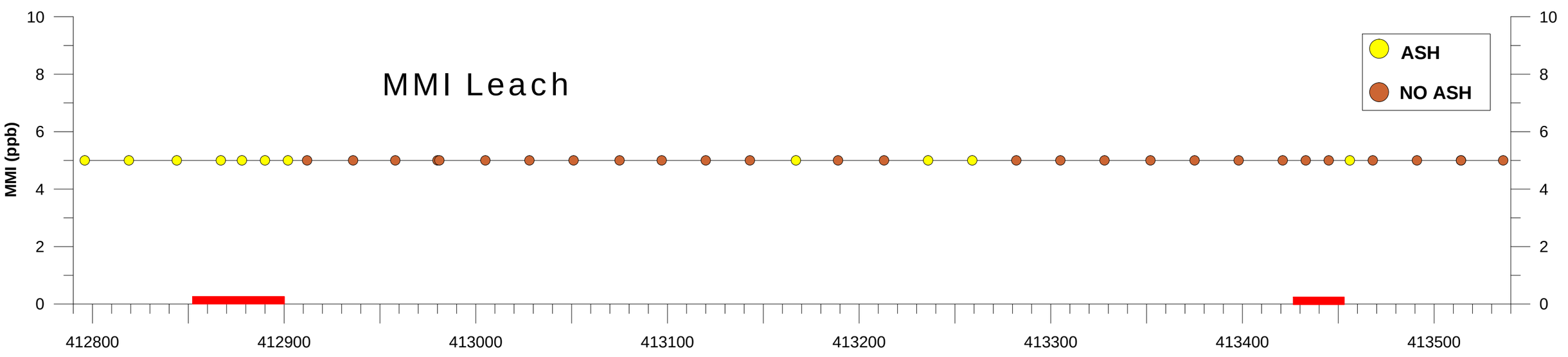

G. N. LUSTIG CONSULTING LTD.- November 18, 2008

Western Copper MMI Test
Line 4400S - 25 m South

Thorium

Aqua Regia Digest

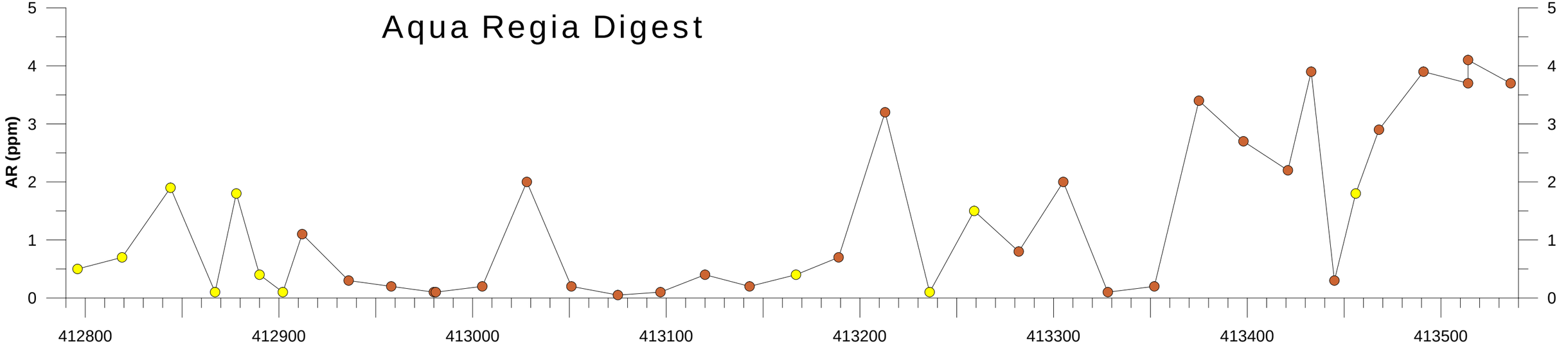

MMI Leach

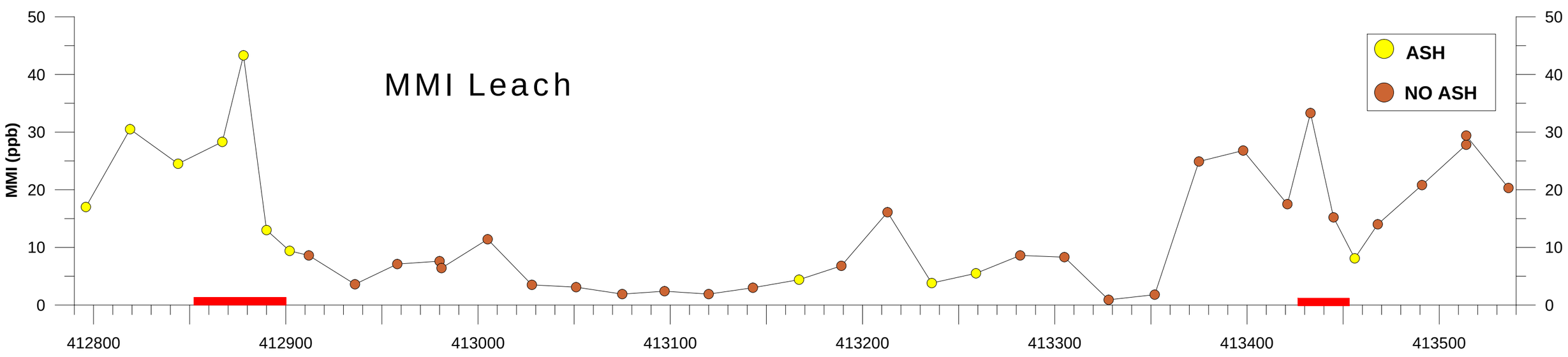

G. N. LUSTIG CONSULTING LTD.- November 18, 2008

Western Copper MMI Test
Line 4400S - 25 m South

Titanium

Aqua Regia Digest

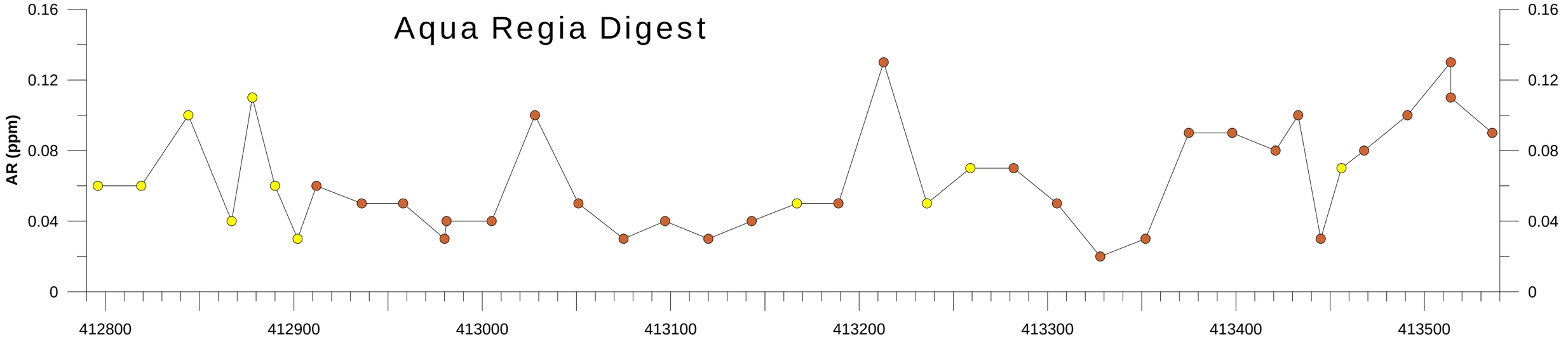

MMI Leach

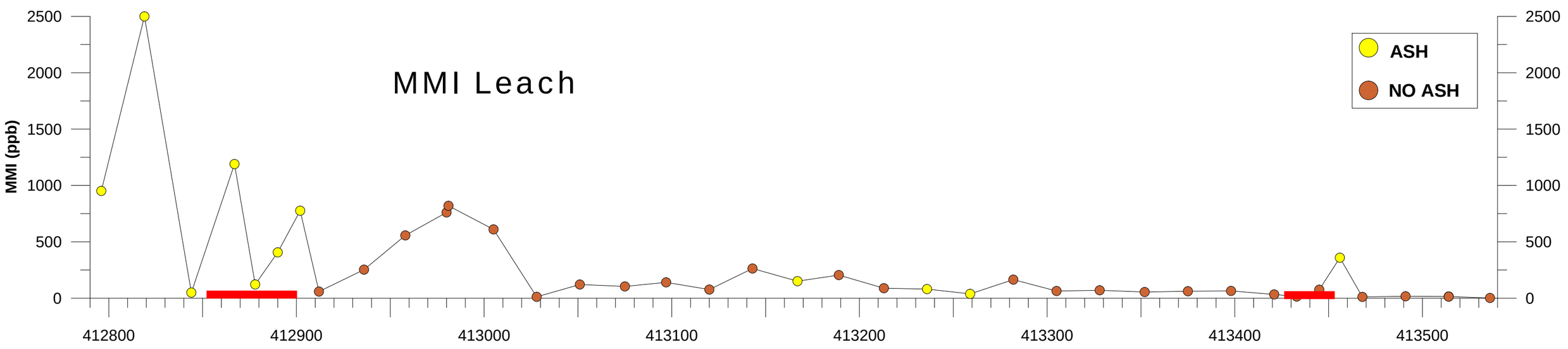

G. N. LUSTIG CONSULTING LTD.- November 18, 2008

Western Copper MMI Test
Line 4400S - 25 m South

Thalium

Aqua Regia Digest

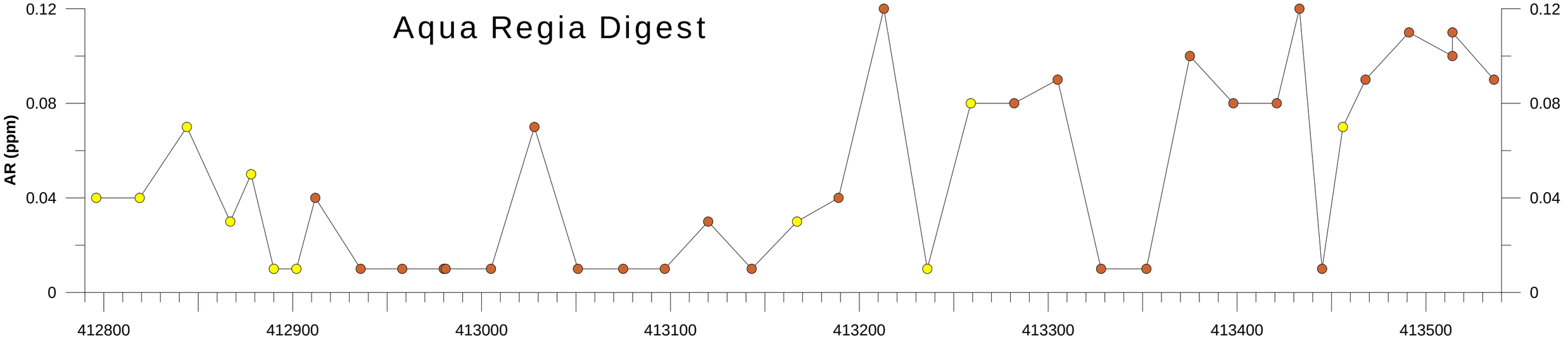

MMI Leach

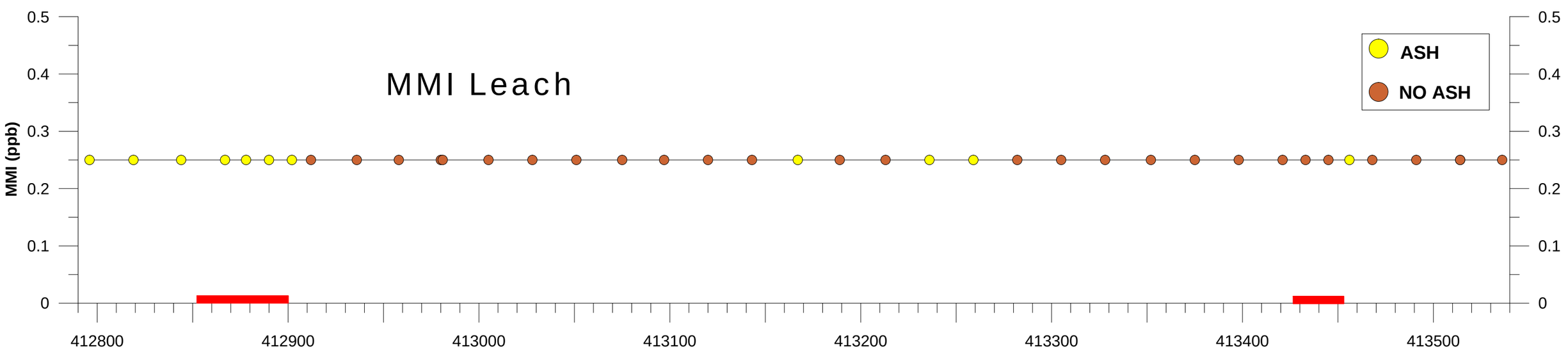

G. N. LUSTIG CONSULTING LTD.- November 18, 2008

Western Copper MMI Test
Line 4400S - 25 m South

Uranium

Aqua Regia Digest

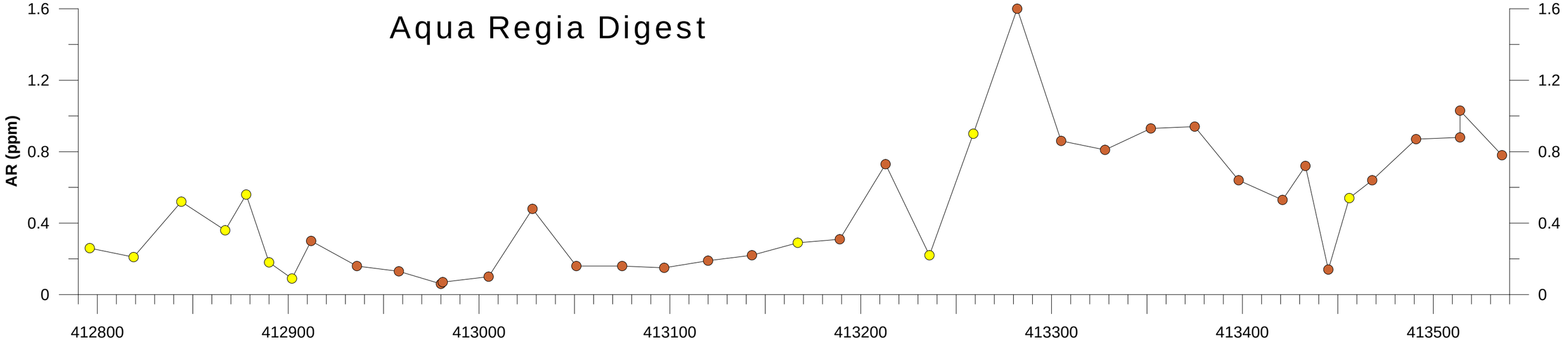

MMI Leach

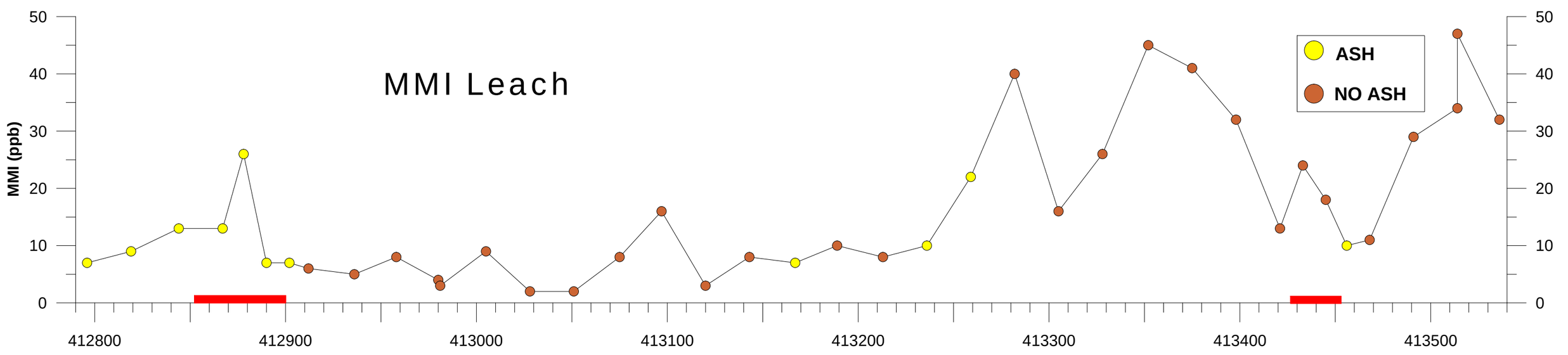

G. N. LUSTIG CONSULTING LTD.- November 18, 2008

Western Copper MMI Test
Line 4400S - 25 m South

Tungsten

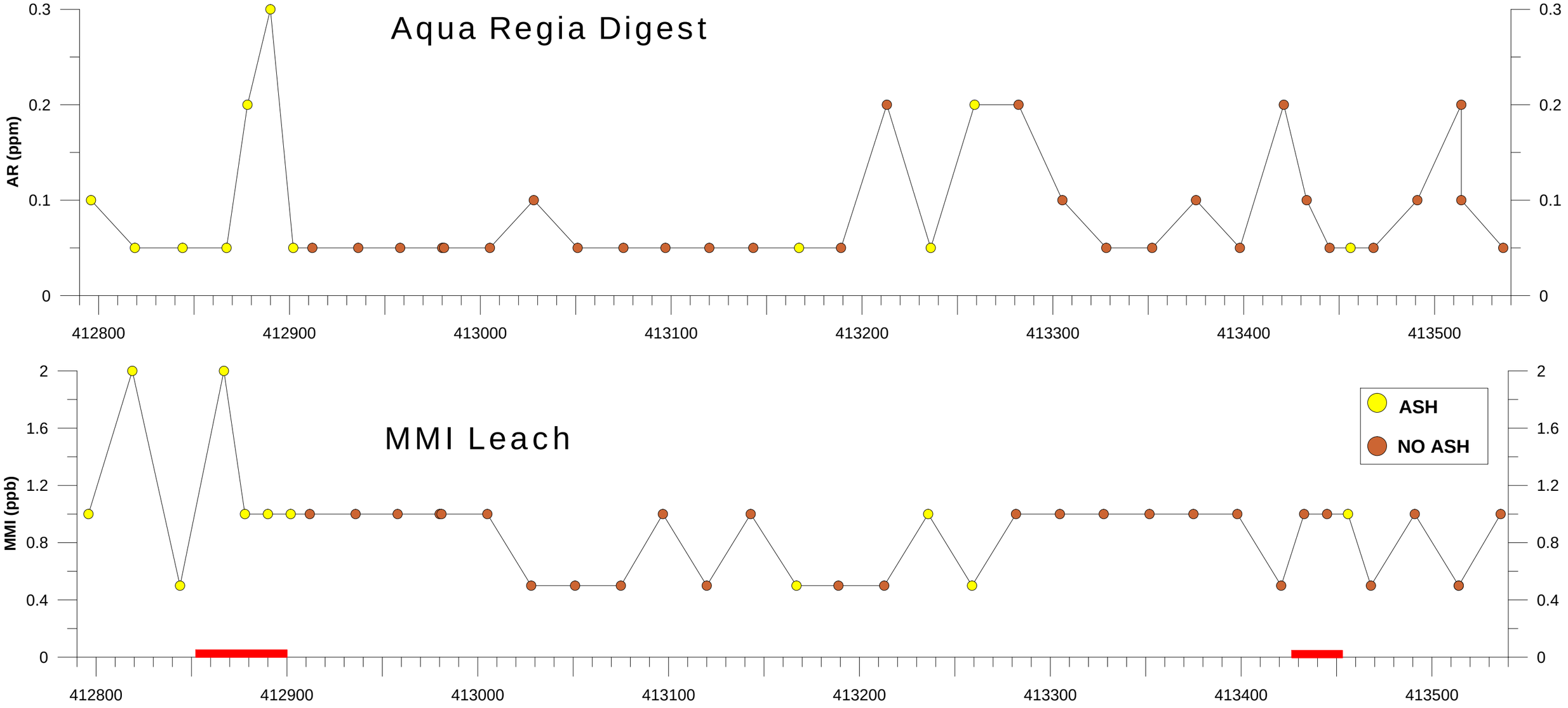

G. N. LUSTIG CONSULTING LTD.- November 18, 2008

Western Copper MMI Test
Line 4400S - 25 m South

Ytterbium

Aqua Regia Digest

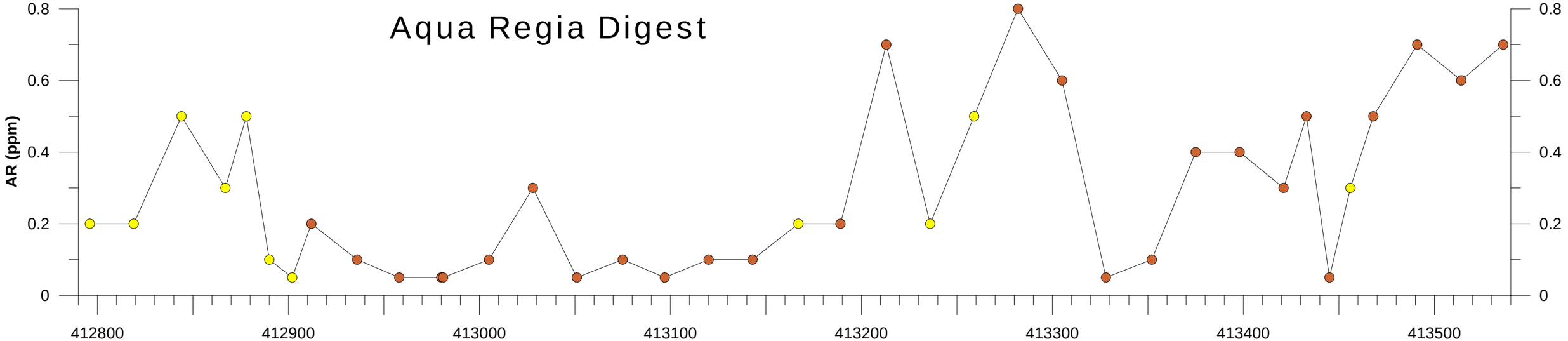

MMI Leach

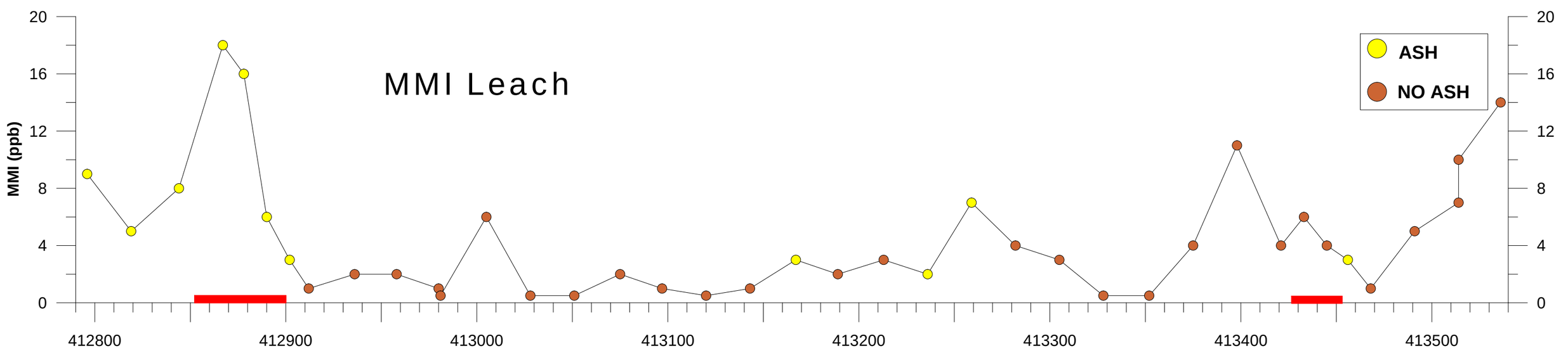

G. N. LUSTIG CONSULTING LTD.- November 18, 2008

Western Copper MMI Test
Line 4400S - 25 m South

Yttrium

Aqua Regia Digest

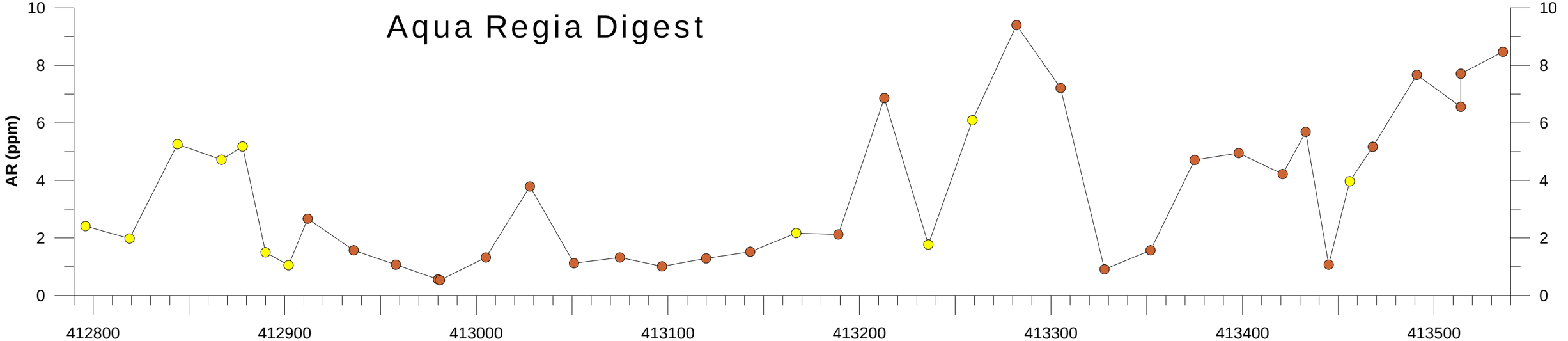

MMI Leach

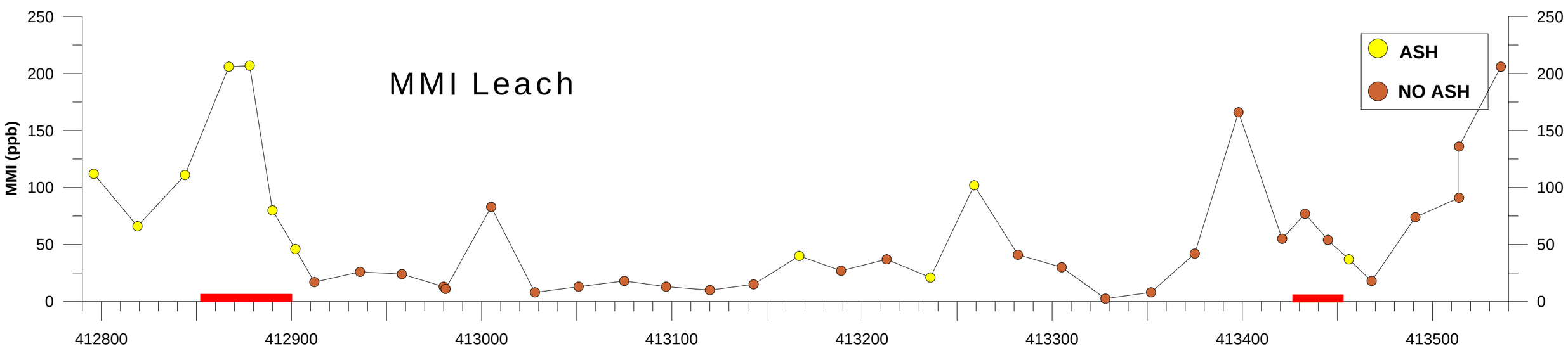

G. N. LUSTIG CONSULTING LTD.- November 18, 2008

Western Copper MMI Test
Line 4400S - 25 m South

Zinc

Aqua Regia Digest

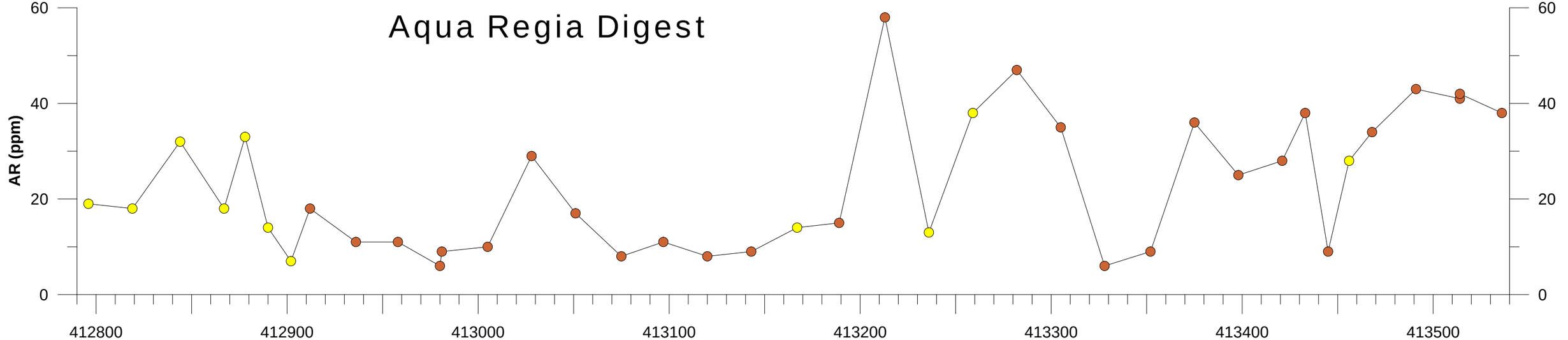

MMI Leach

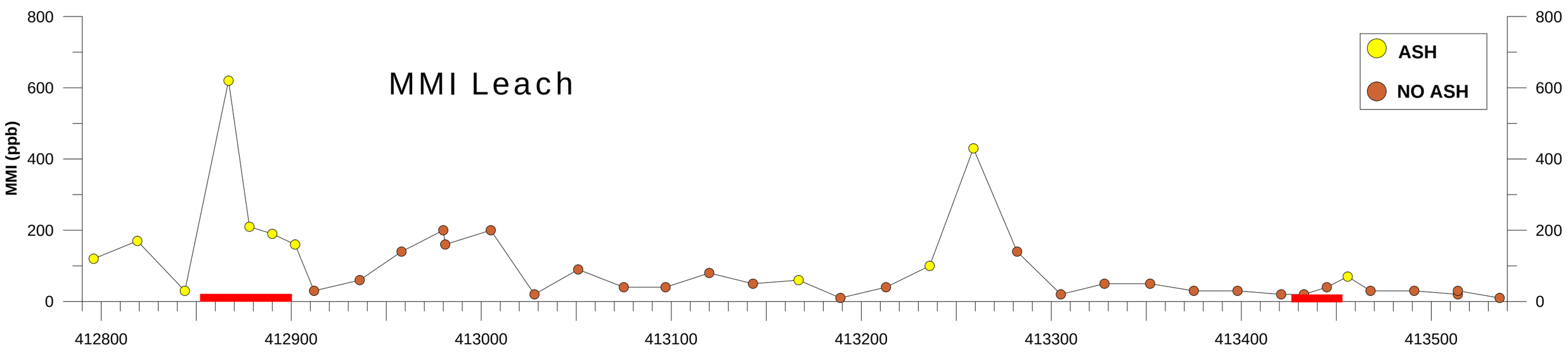

G. N. LUSTIG CONSULTING LTD.- November 18, 2008

Western Copper MMI Test
Line 4400S - 25 m South

Zirconium

Aqua Regia Digest

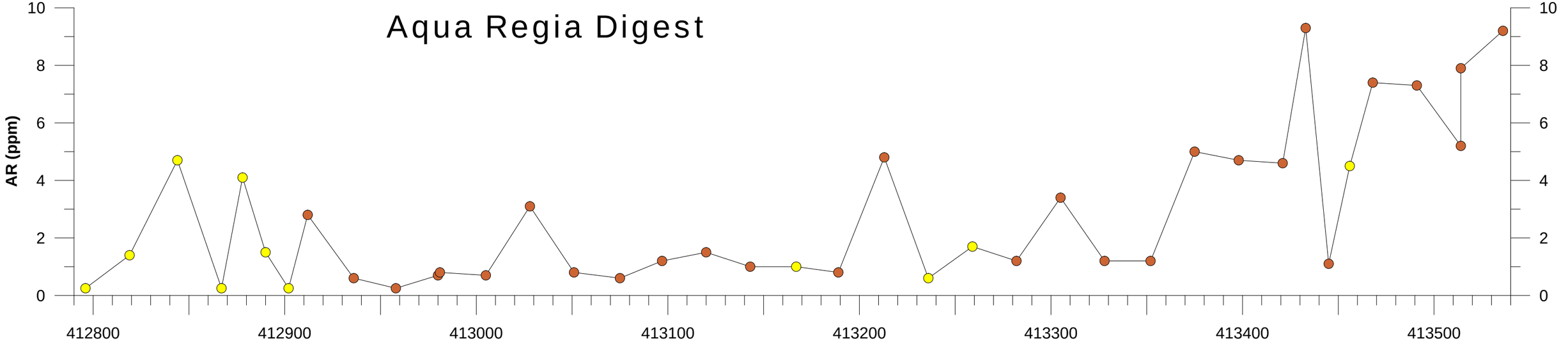

MMI Leach

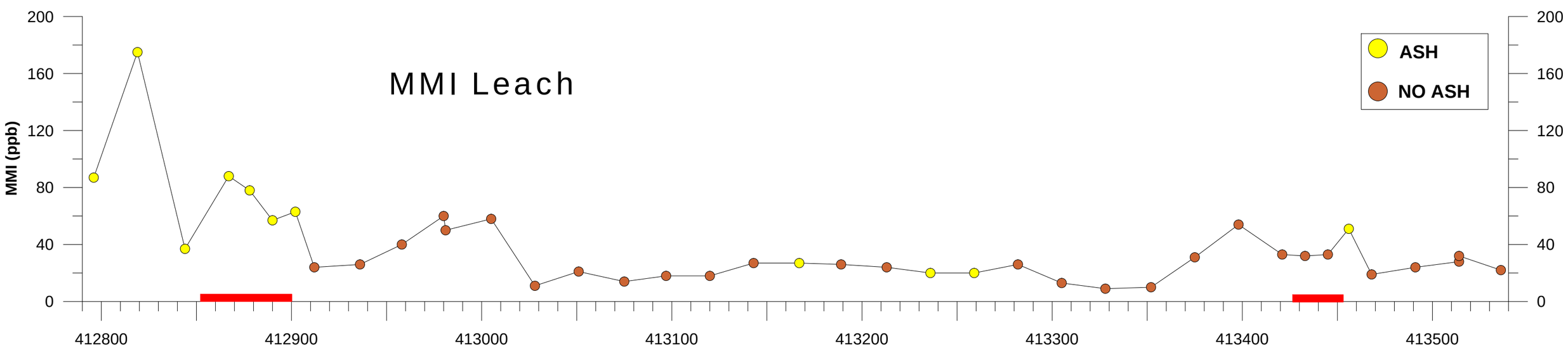

G. N. LUSTIG CONSULTING LTD.- November 18, 2008

Appendix VI
MMI-Aqua Regia Scatter Plots

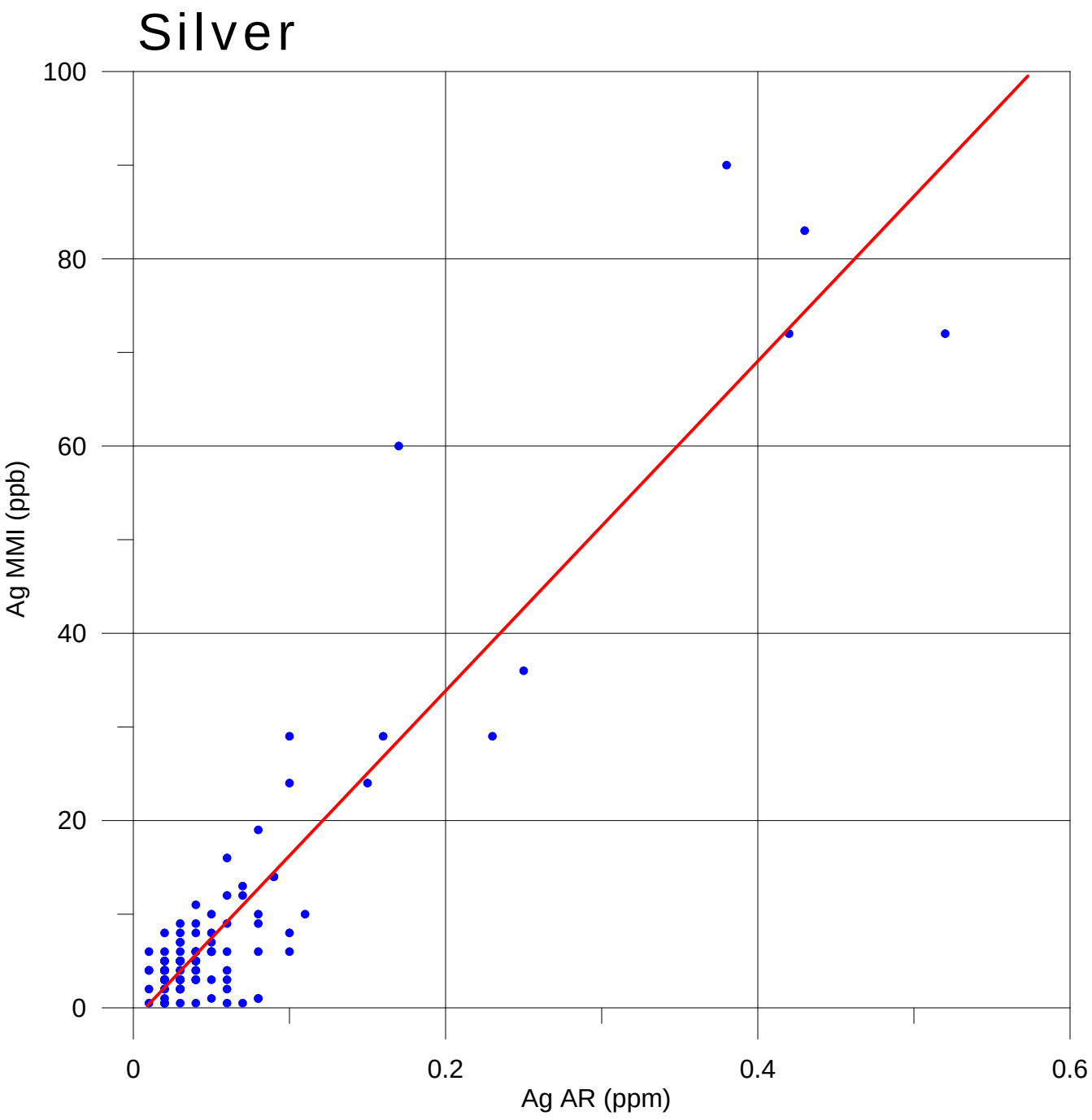
Silver
100
80
60
40
20
0
Ag MMI (ppb)
0
0.2
0.4
0.6
Ag AR (ppm)

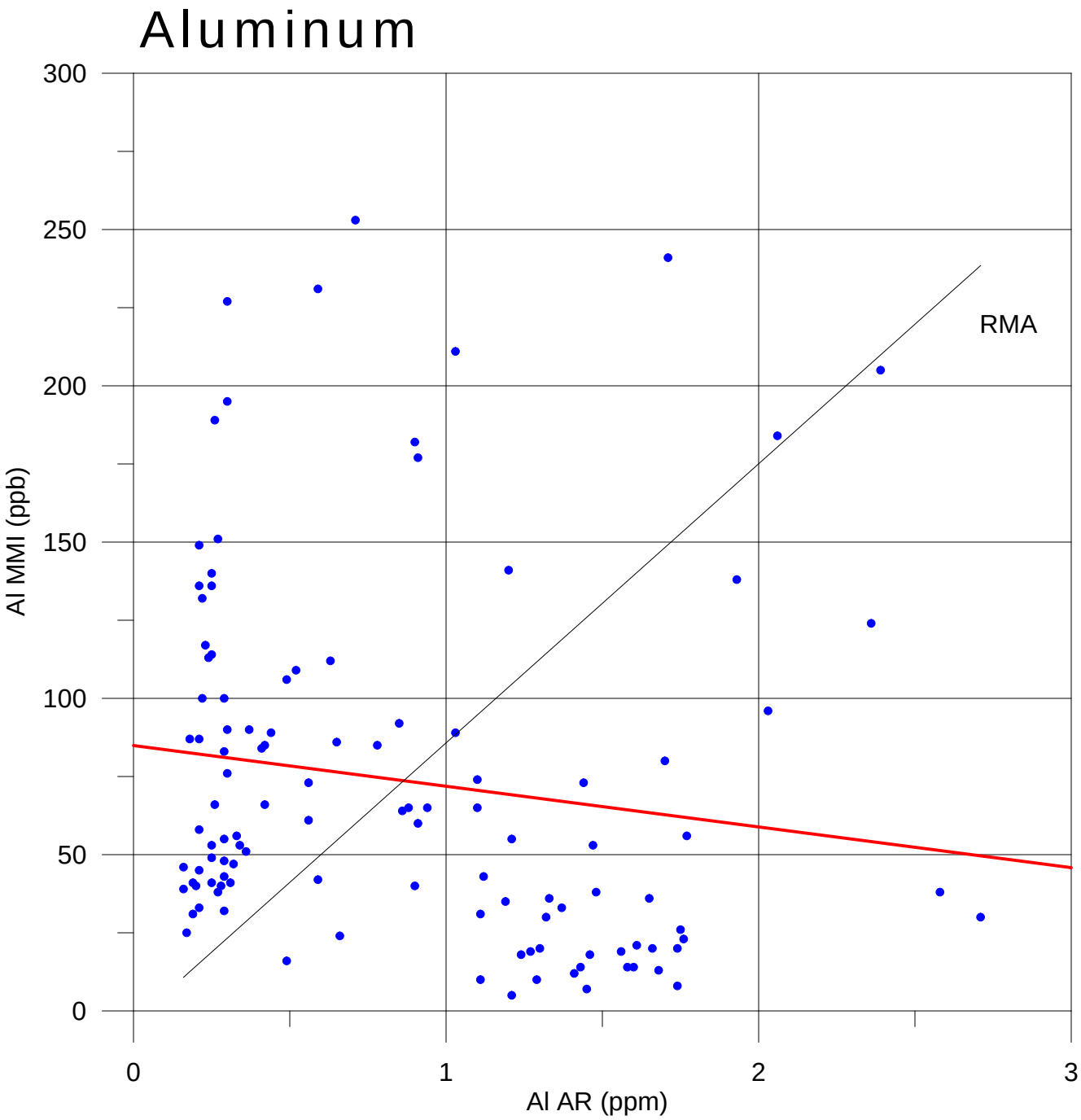
Aluminum
300
250
200
150
100
50
0
Al MMI (ppb)
RMA
0
1
2
3
Al AR (ppm)

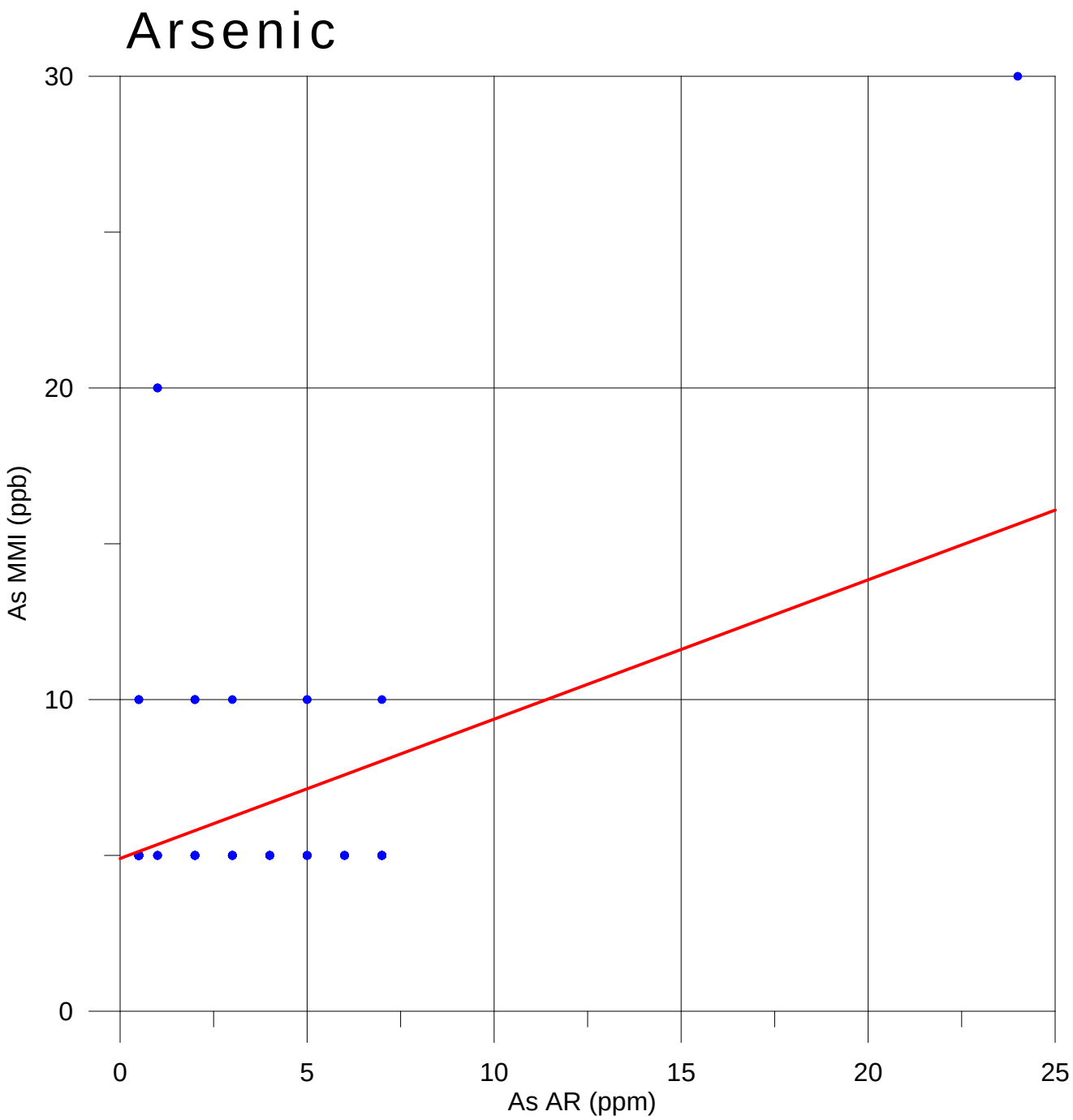
Arsenic
30
20
10
0
As MMI (ppb)
0
5
10
15
20
25
As AR (ppm)

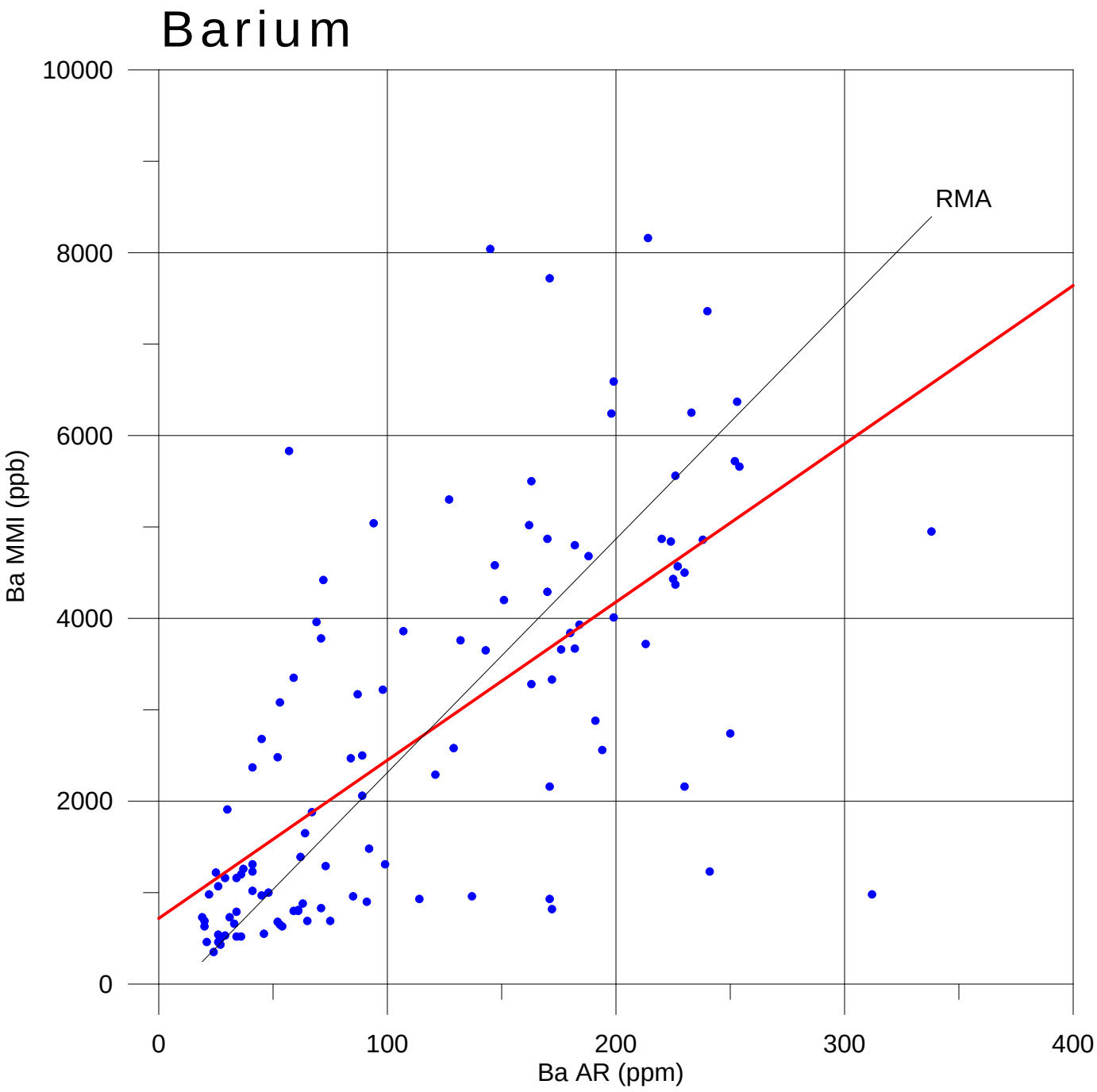
Barium
10000
8000
6000
4000
2000
0
Ba MMI (ppb)
RMA
0
100
200
300
400
Ba AR (ppm)

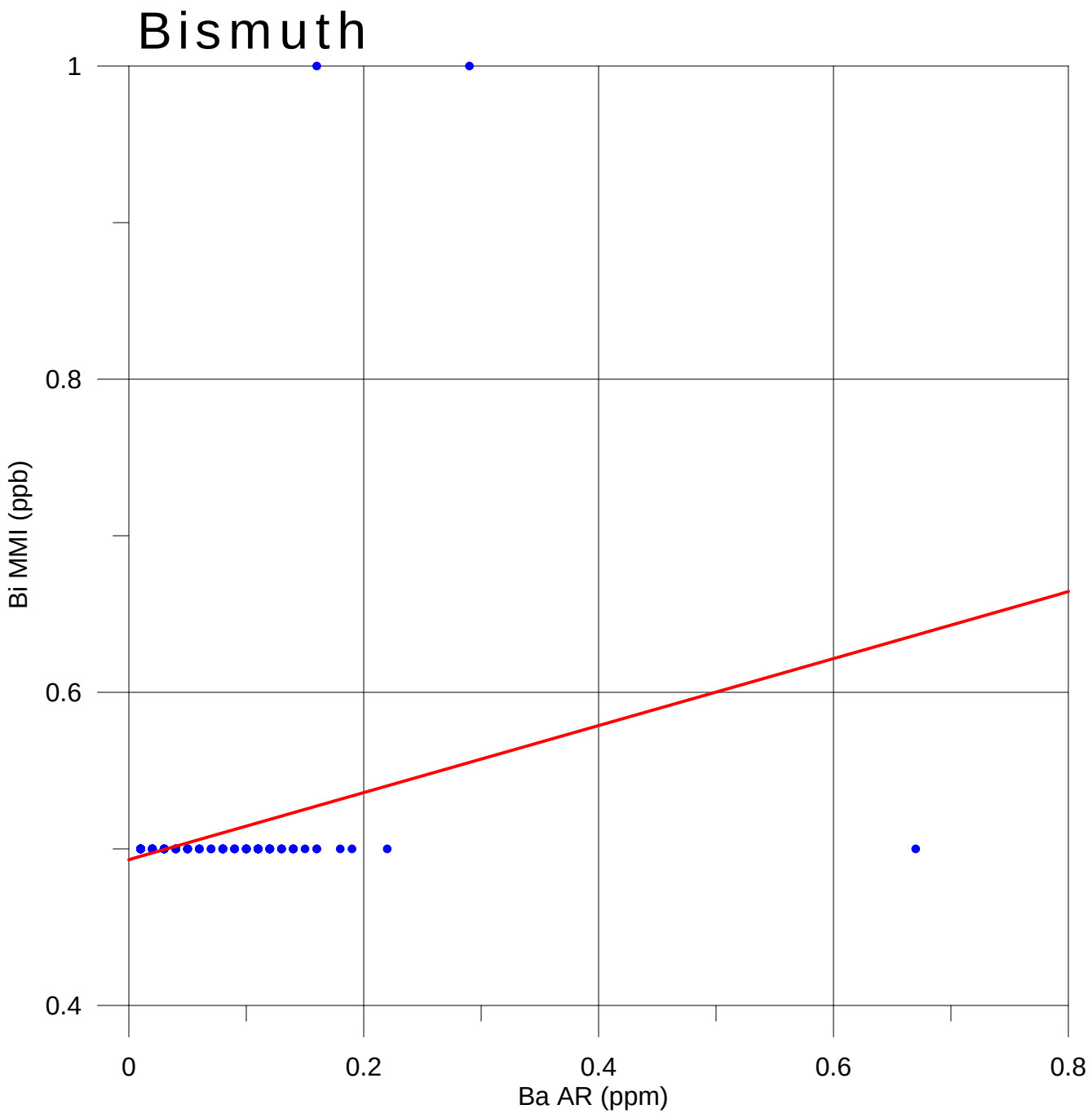
Bismuth
1
0.8
0.6
0.4
Bi MMI (ppb)
0
0.2
0.4
0.6
0.8
Ba AR (ppm)

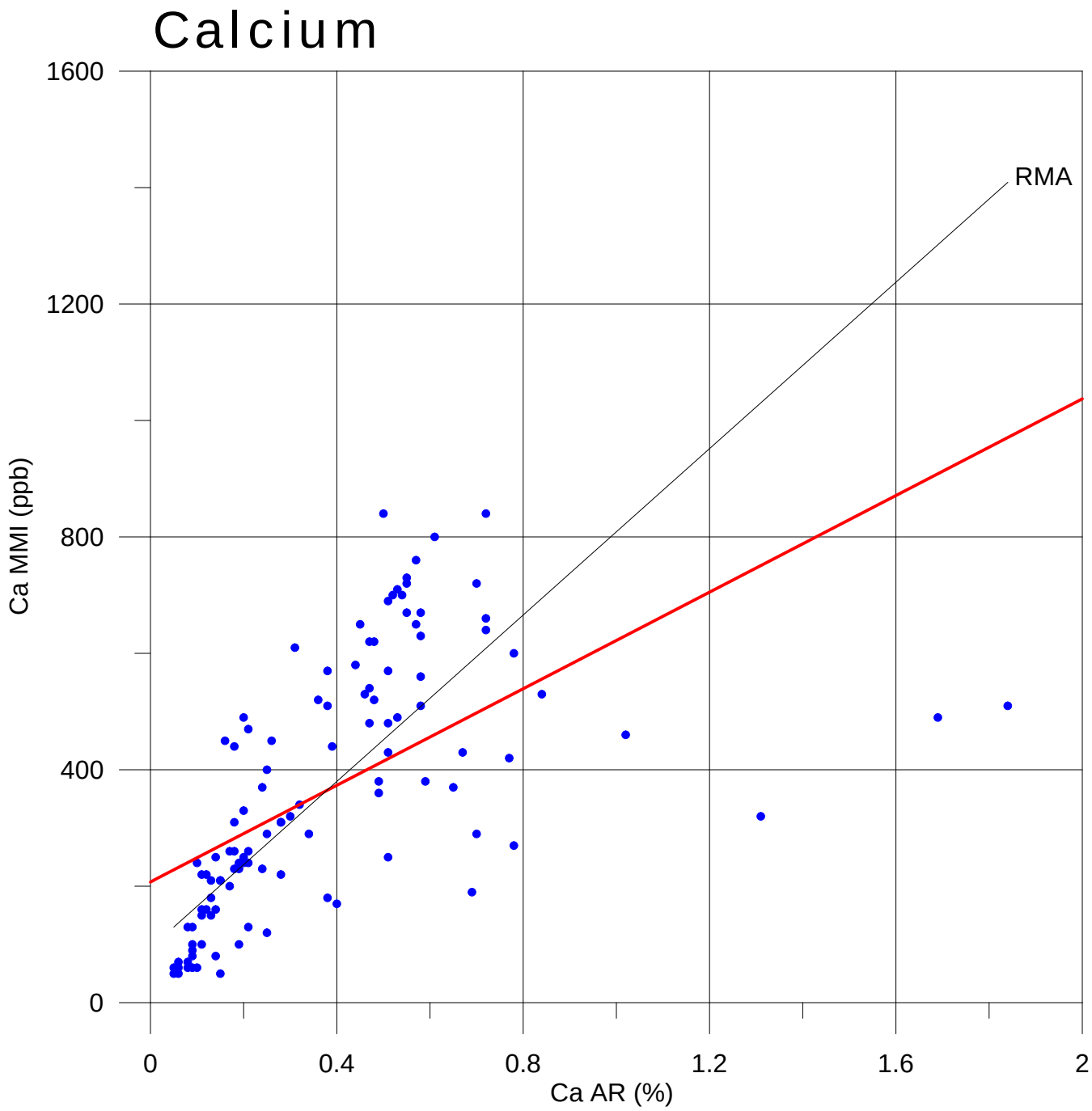
Calcium
1600
1200
800
400
0
Ca MMI (ppb)
RMA
0
0.4
0.8
1.2
1.6
2
Ca AR (%)

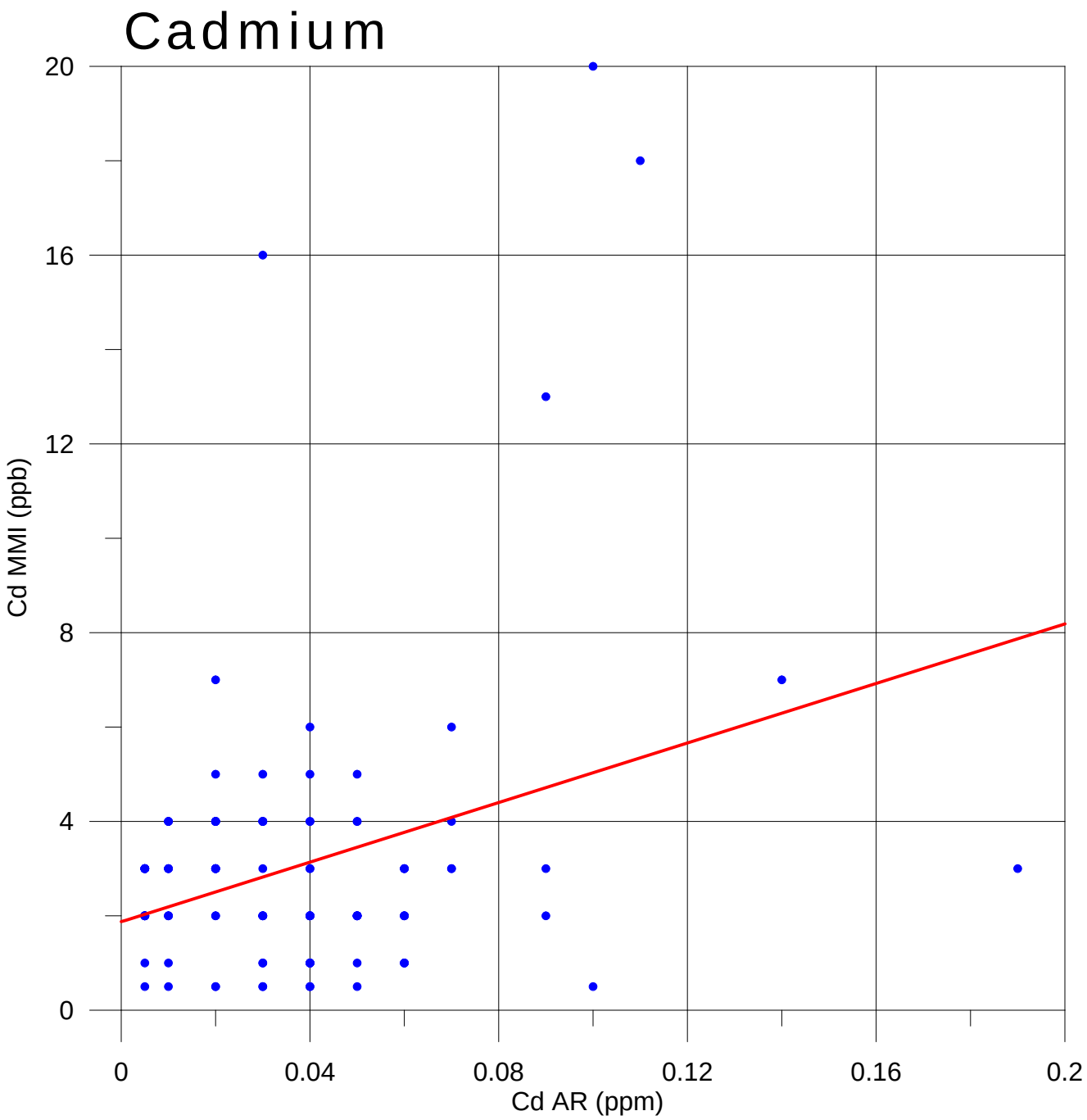
Cadmium
20
16
12
8
4
0
Cd MMI (ppb)
0
0.04
0.08
0.12
0.16
0.2
Cd AR (ppm)

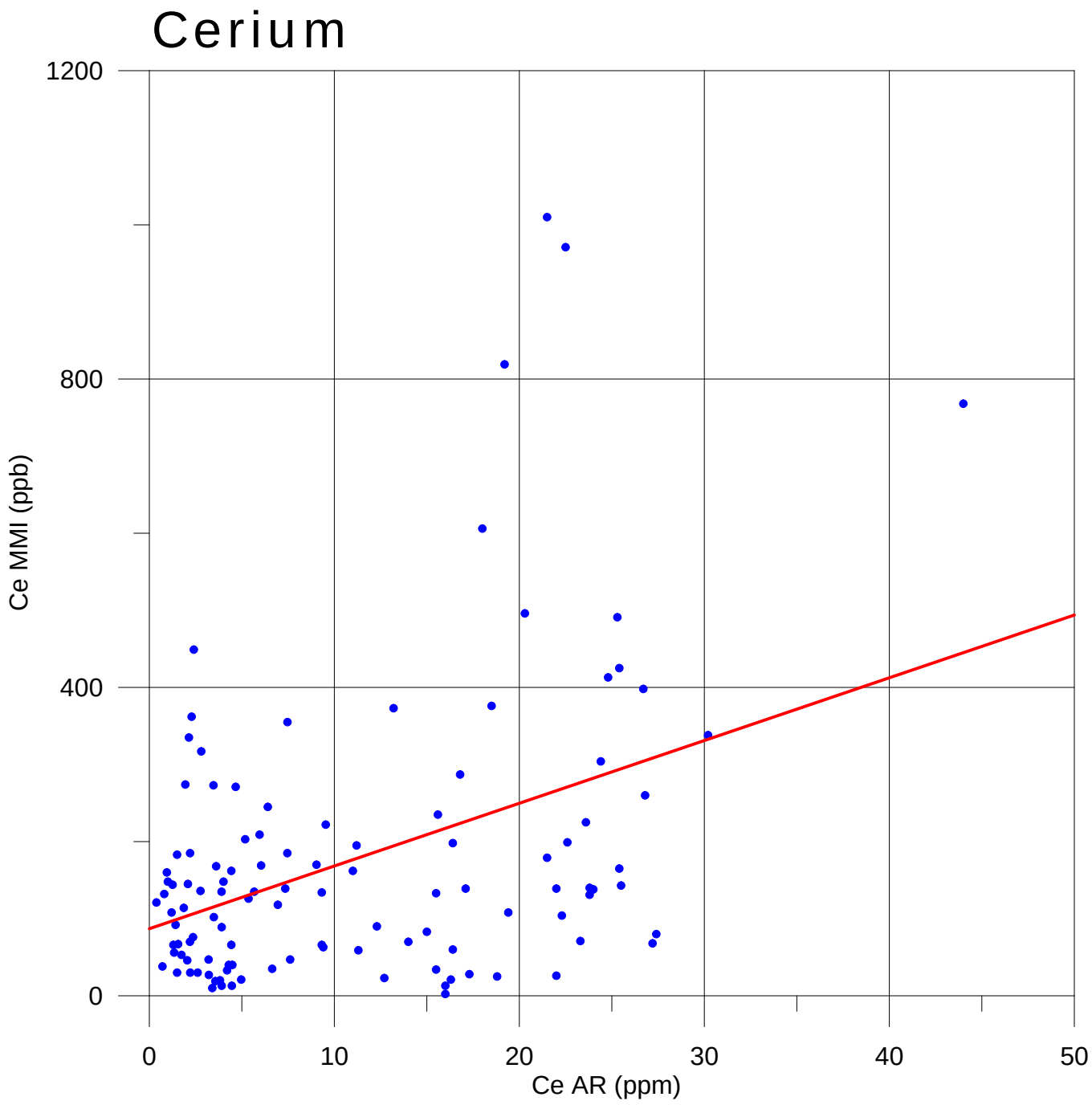
Cerium
1200
800
400
0
Ce MMI (ppb)
0
10
20
30
40
50
Ce AR (ppm)

Cobalt

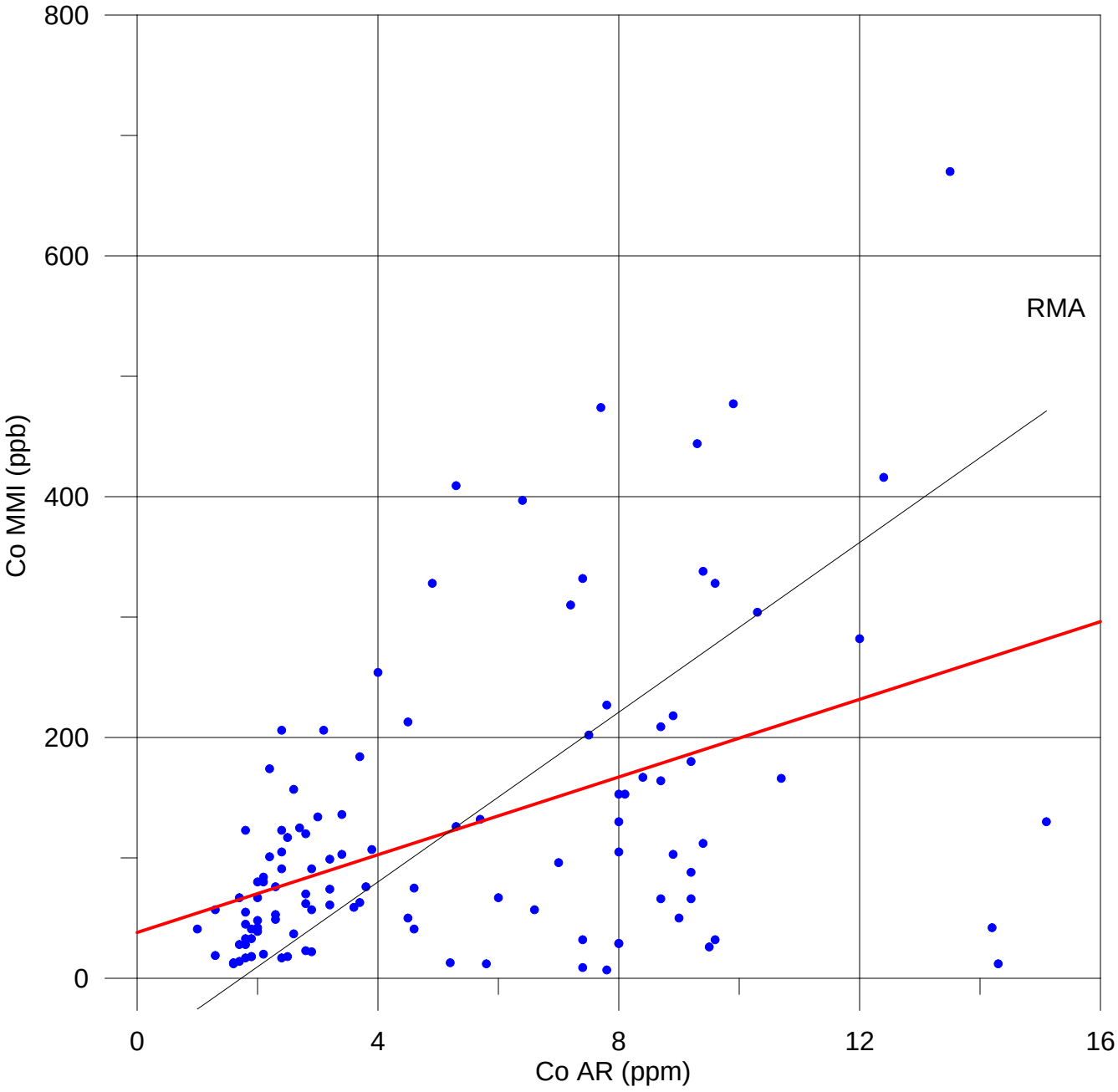

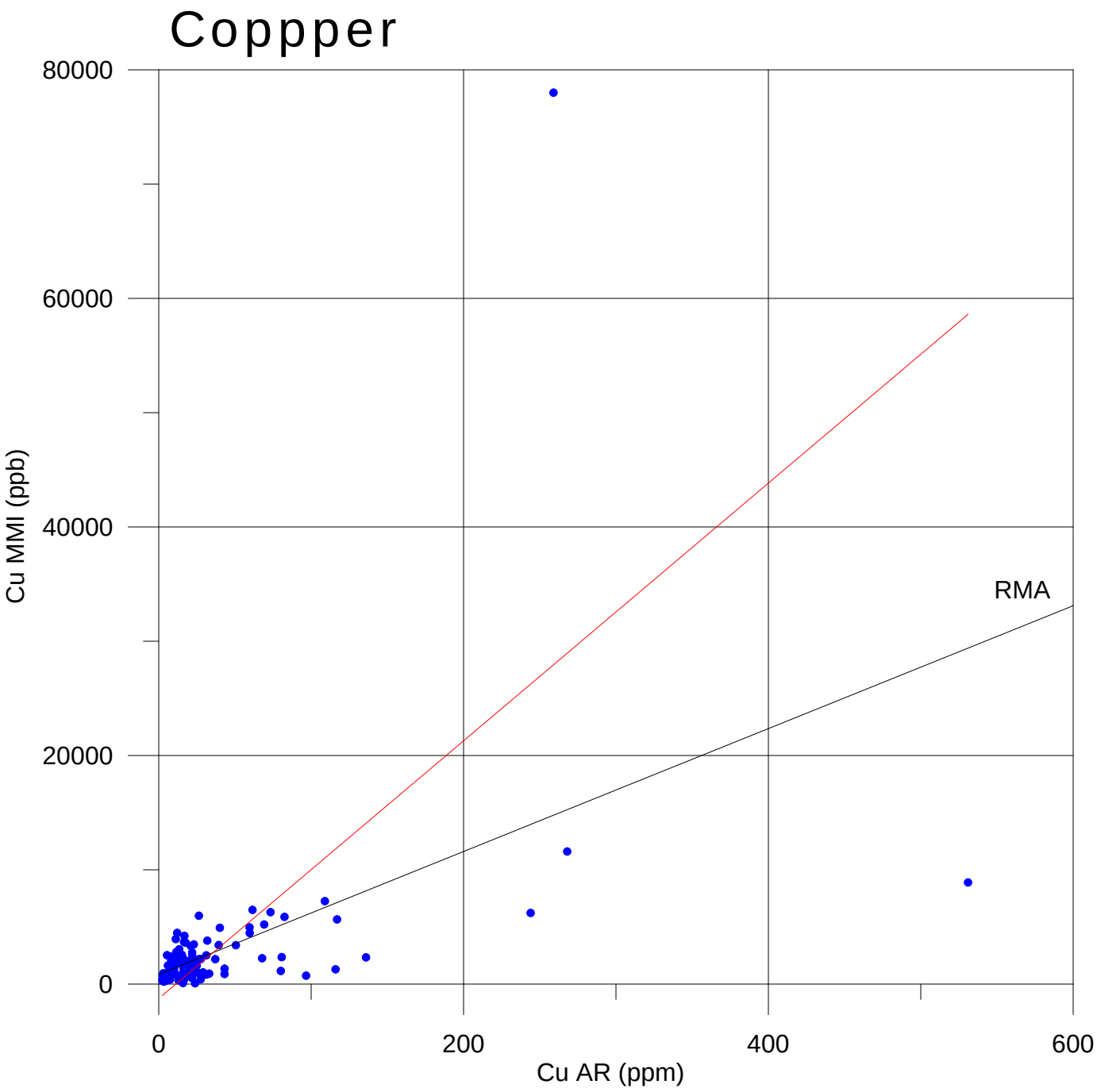
Coppper
80000
60000
40000
20000
0
Cu MMI (ppb)
RMA
0
200
400
600
Cu AR (ppm)

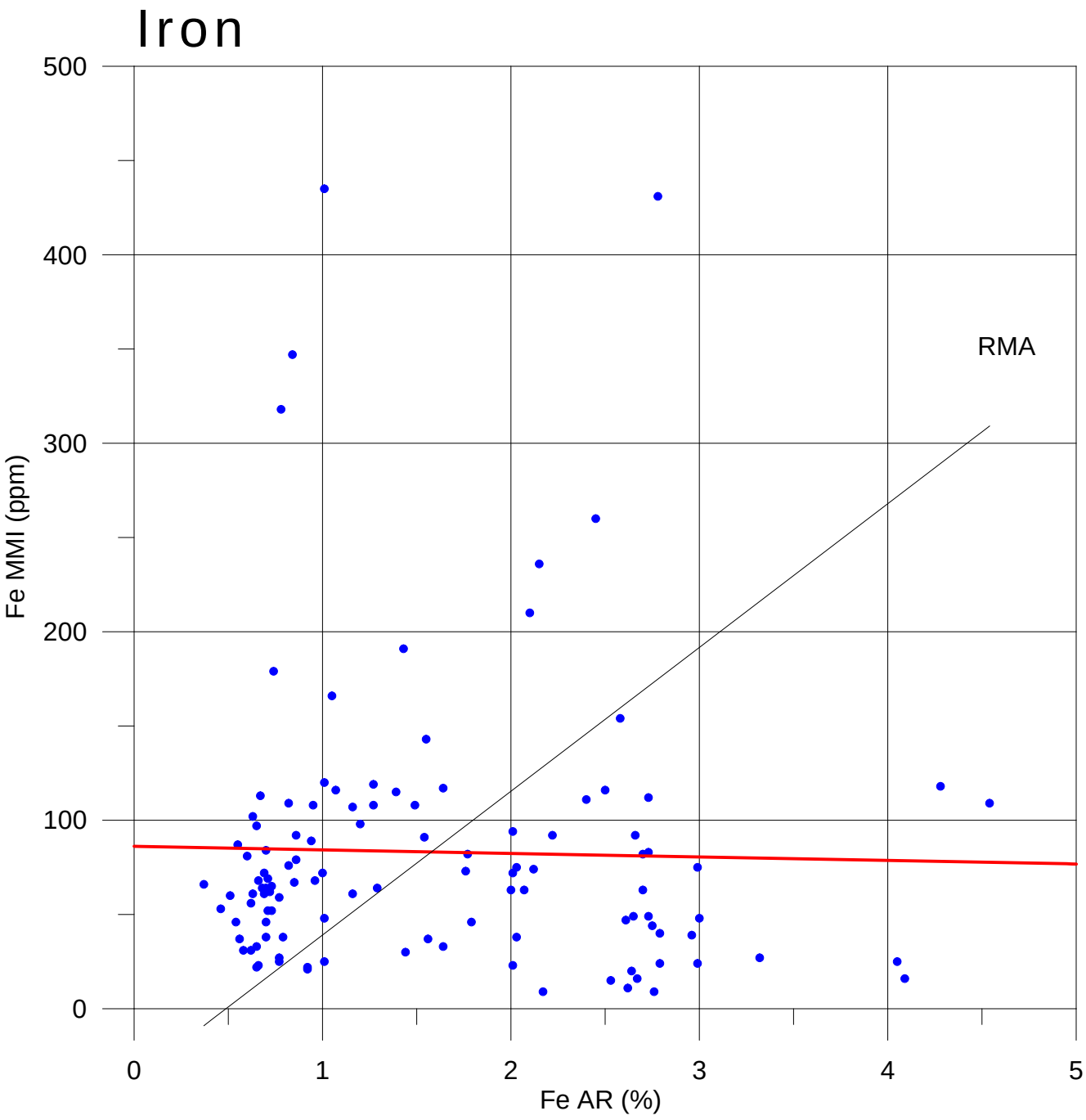
Iron
500
400
300
200
100
0
Fe MMI (ppm)
RMA
0
1
2
3
4
5
Fe AR (%)

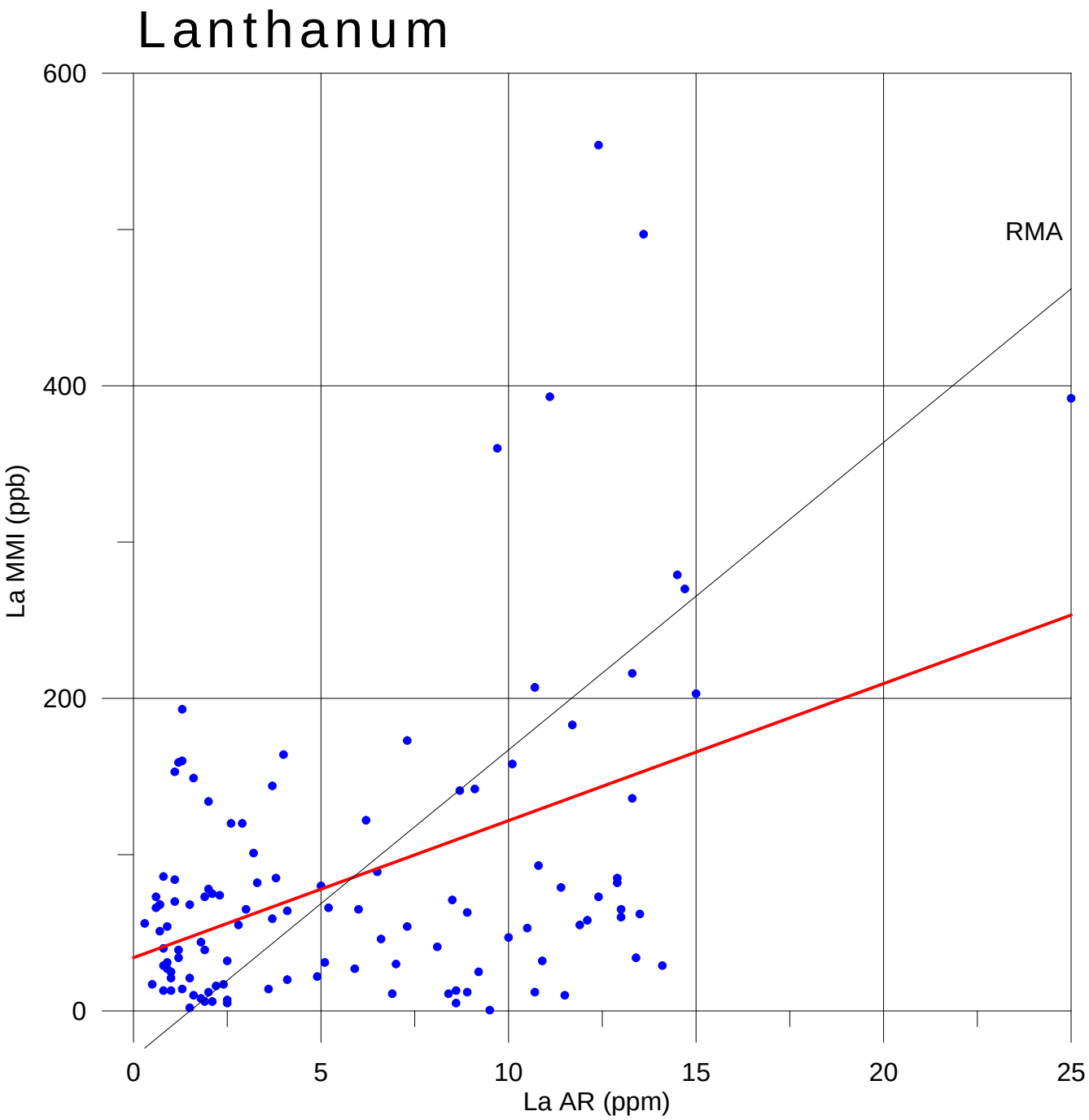
Lanthanum
600
400
200
0
La MMI (ppb)
RMA
0
5
10
15
20
25
La AR (ppm)

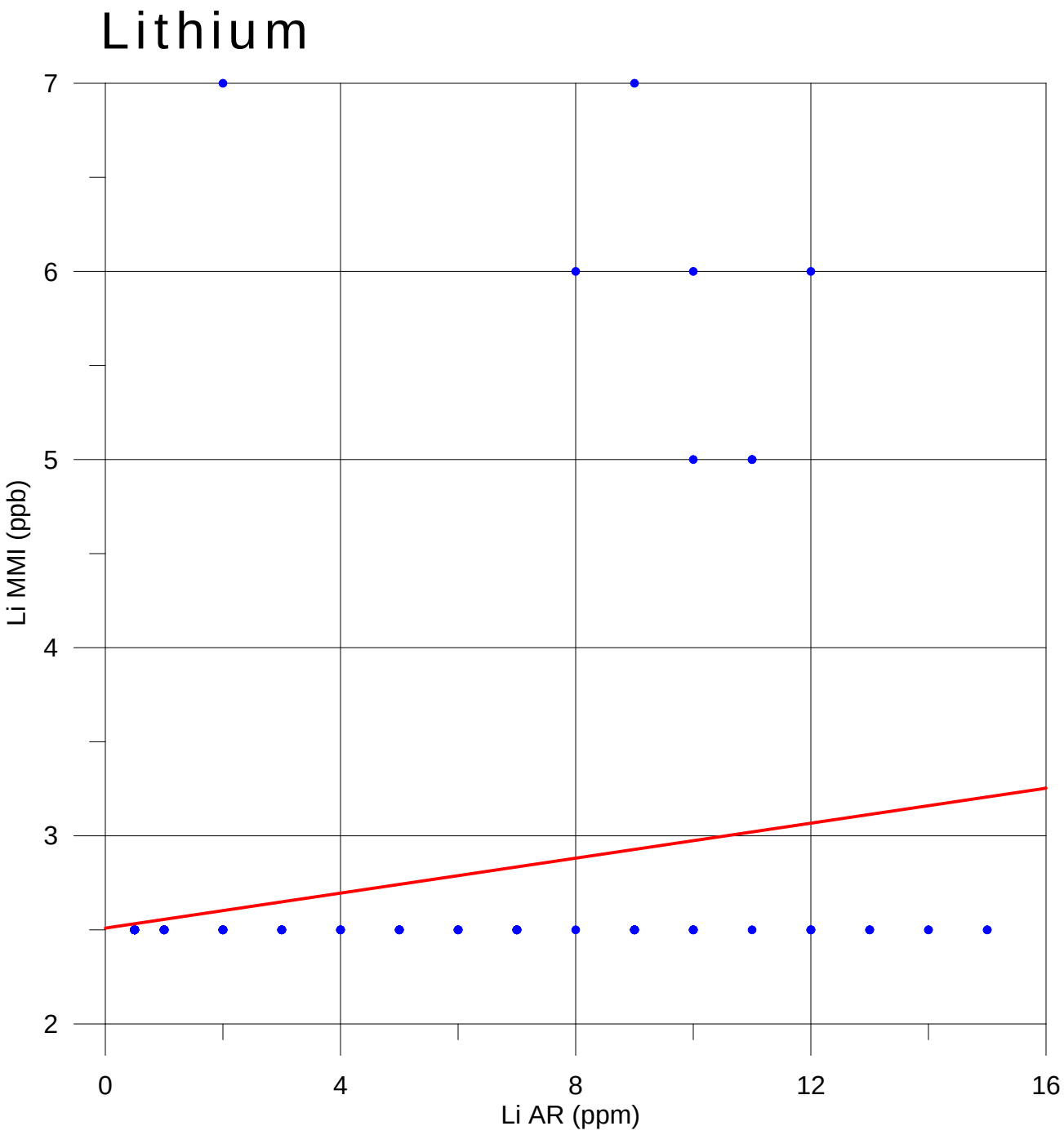
Lithium
Li MMI (ppb)
7
6
5
4
3
2
0
4
8
12
16
Li AR (ppm)

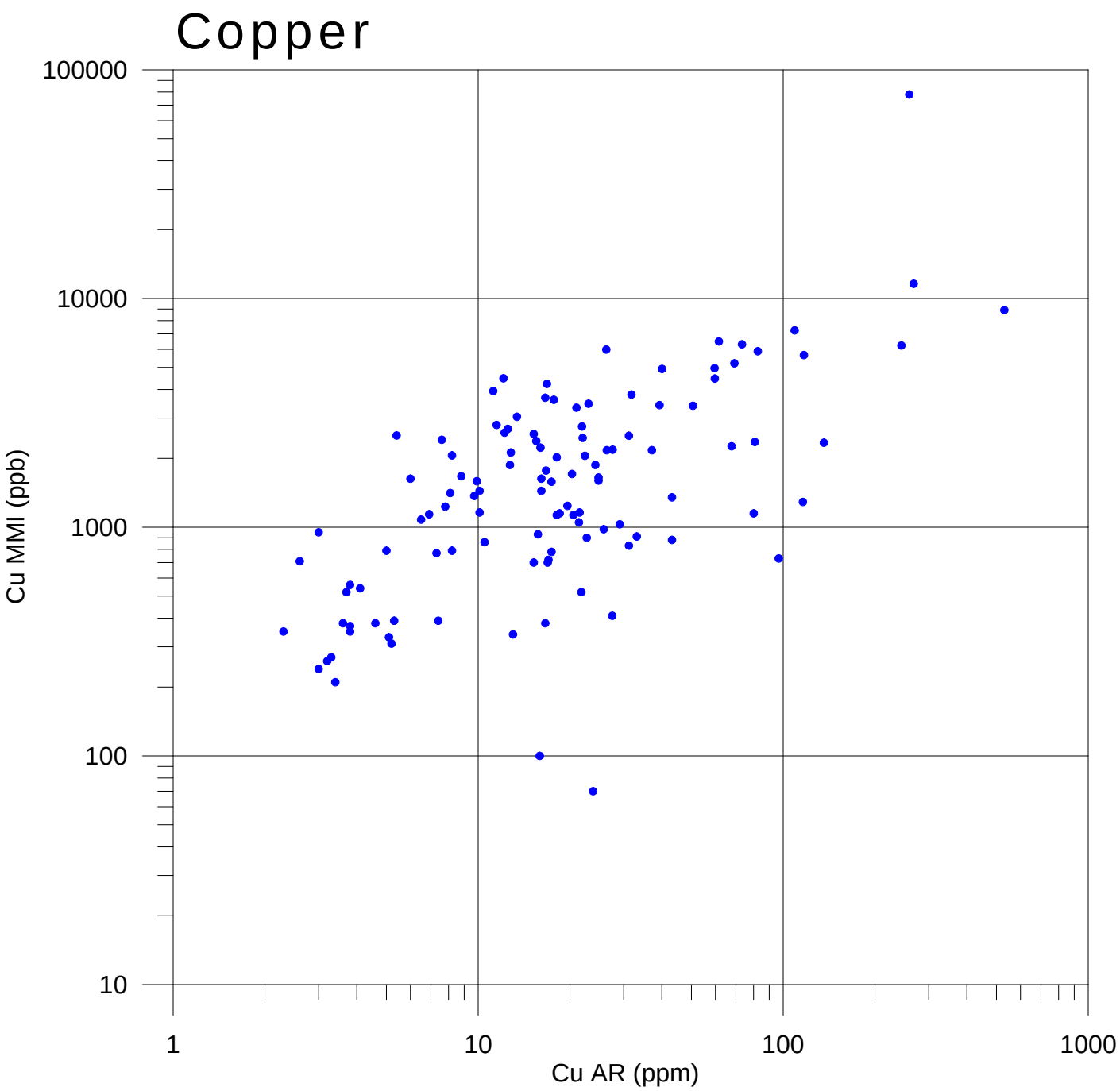
Copper
100000
10000
1000
100
10
Cu MMI (ppb)
1
10
100
1000
Cu AR (ppm)

Strontium

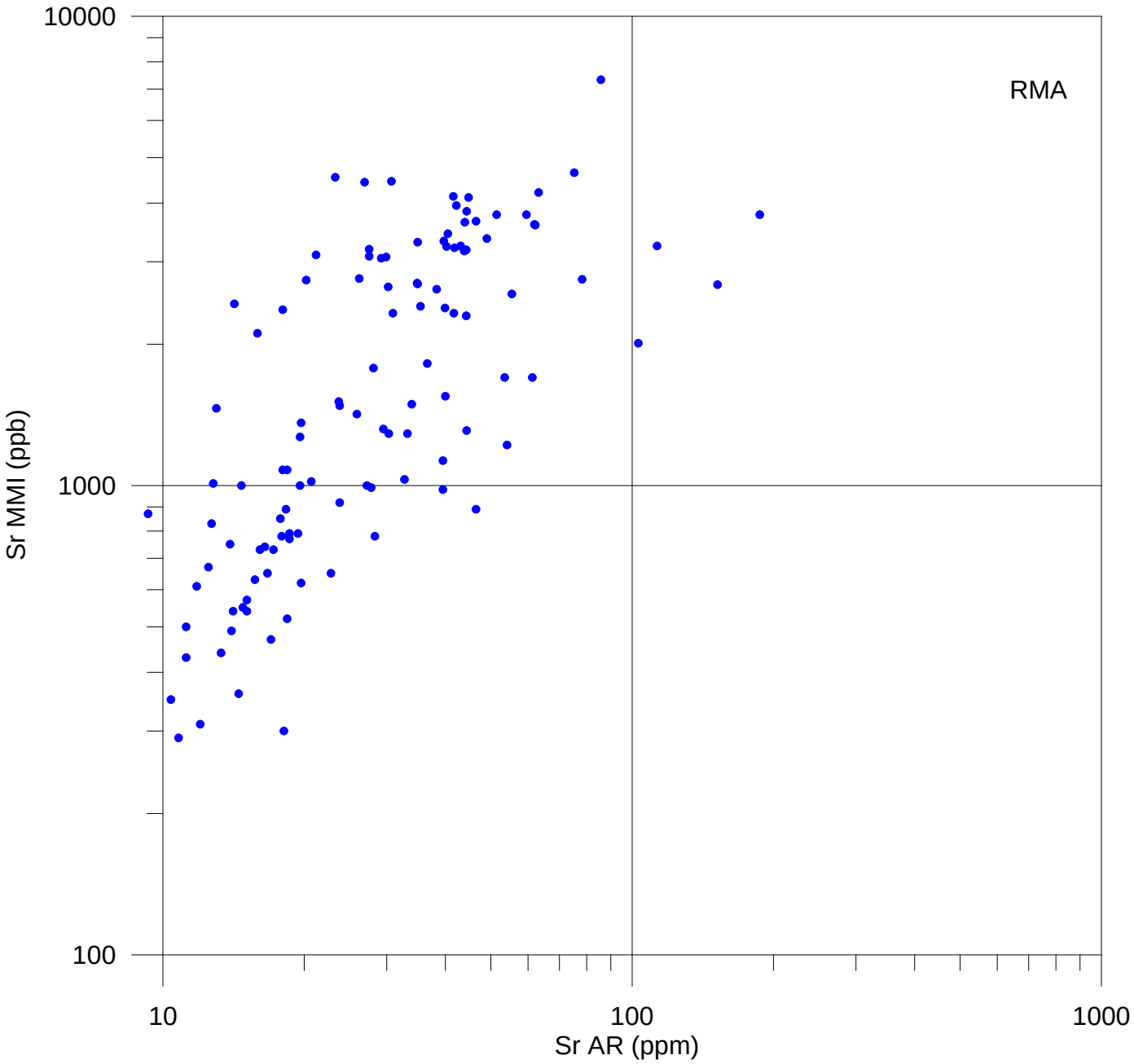

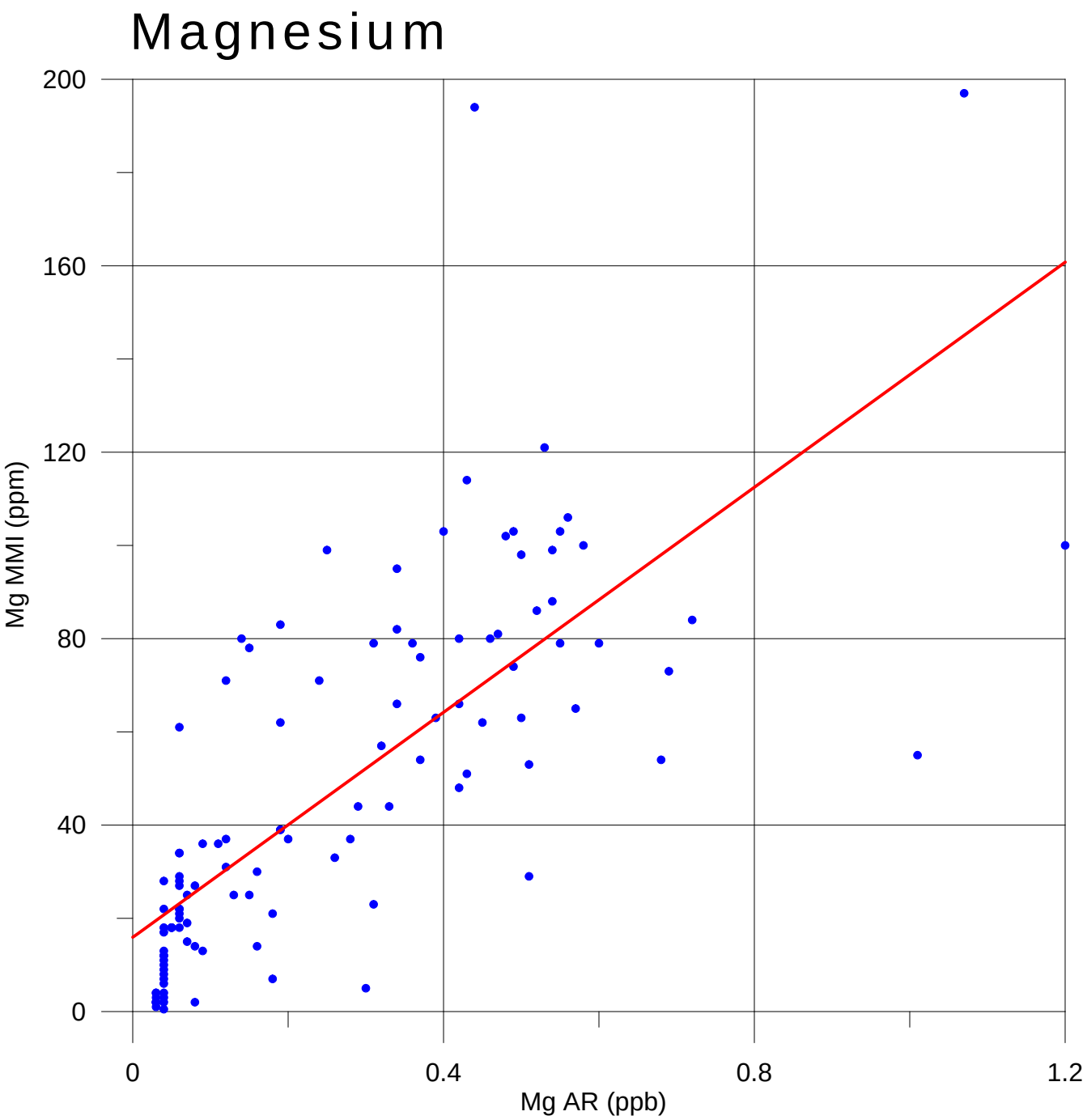
Magnesium
200
160
120
80
40
0
Mg MMI (ppm)
0
0.4
0.8
1.2
Mg AR (ppb)

Molybdenum

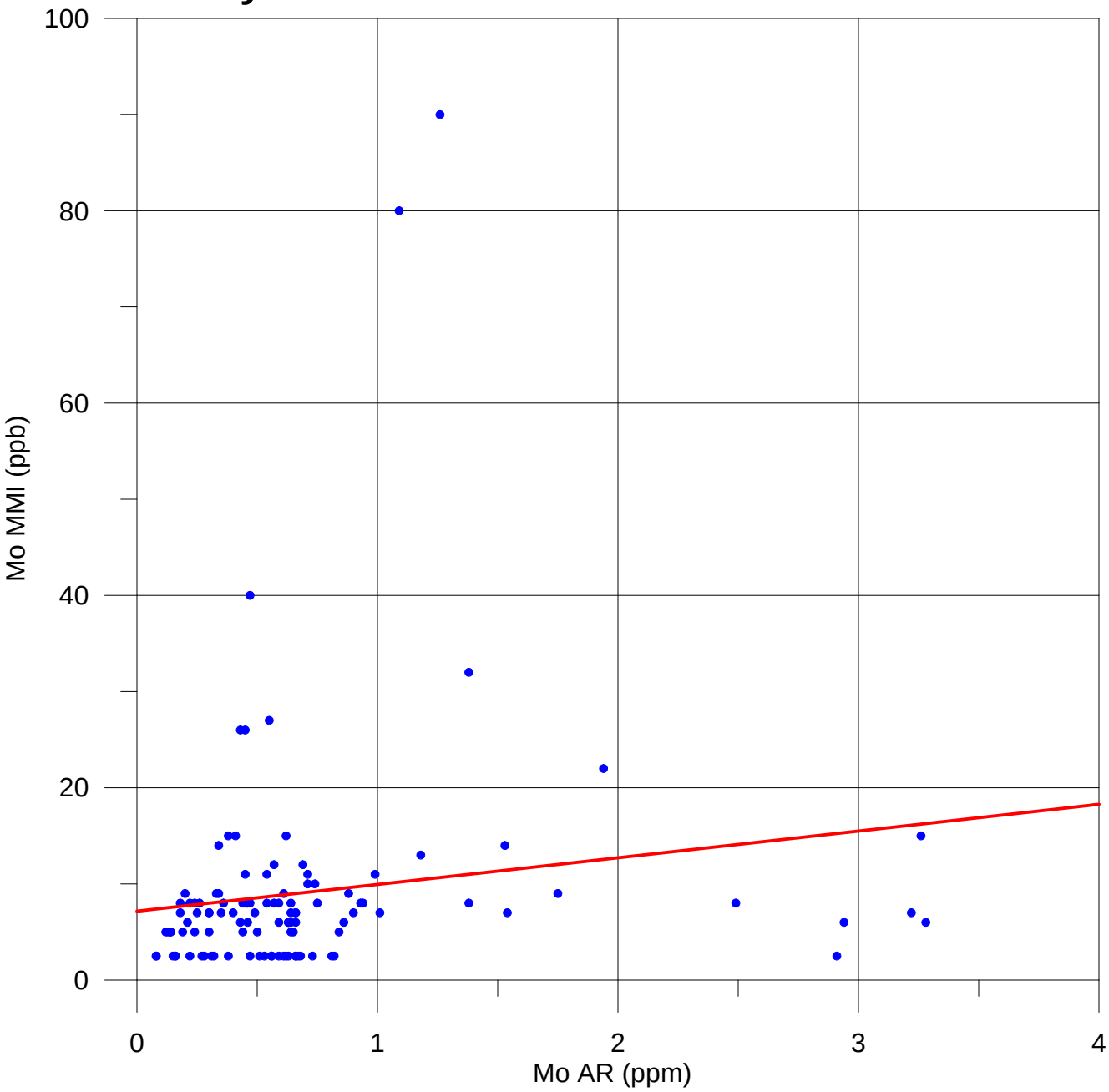

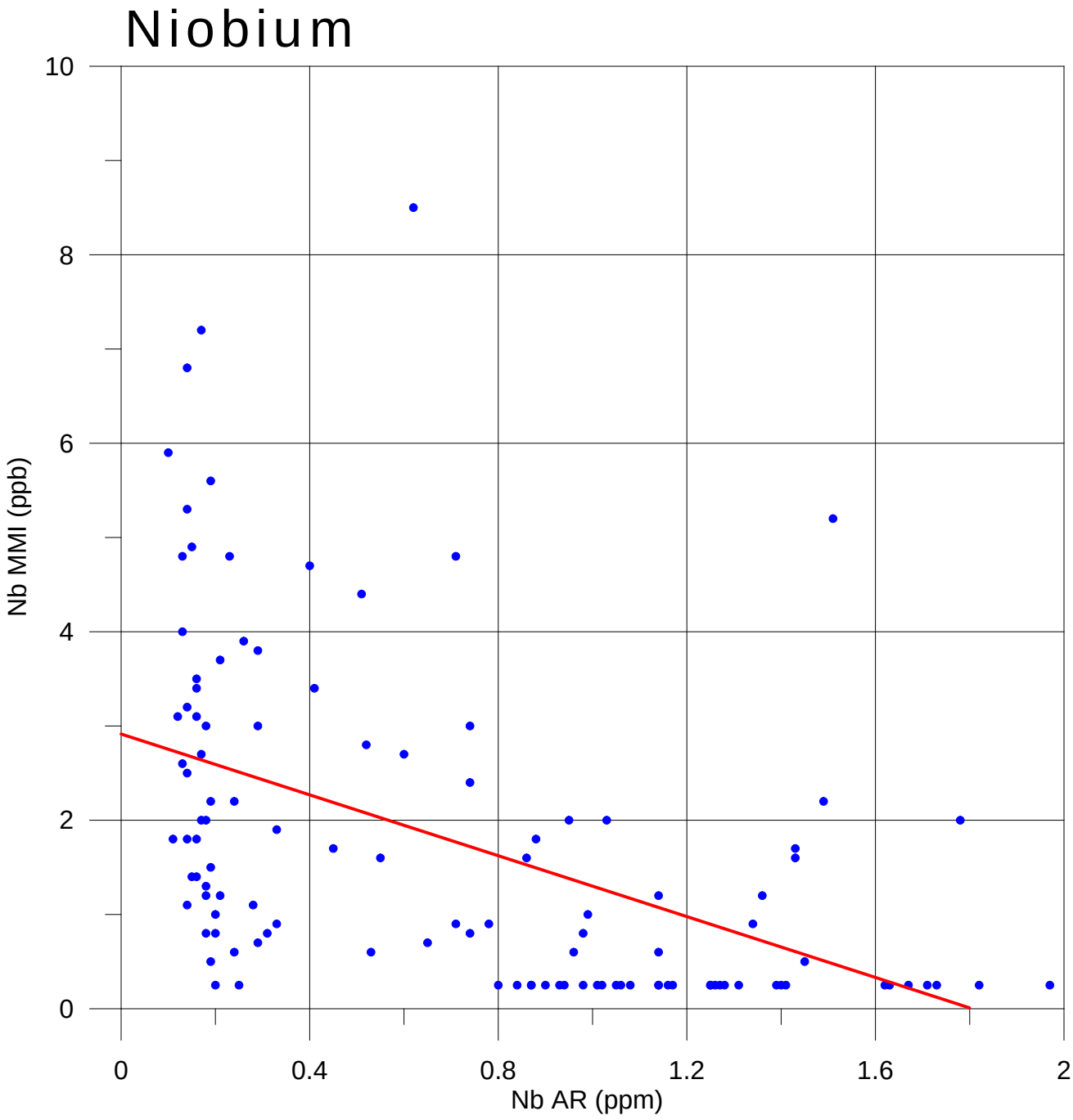
Niobium
10
8
6
4
2
0
Nb MMI (ppb)
0
0.4
0.8
1.2
1.6
2
Nb AR (ppm)

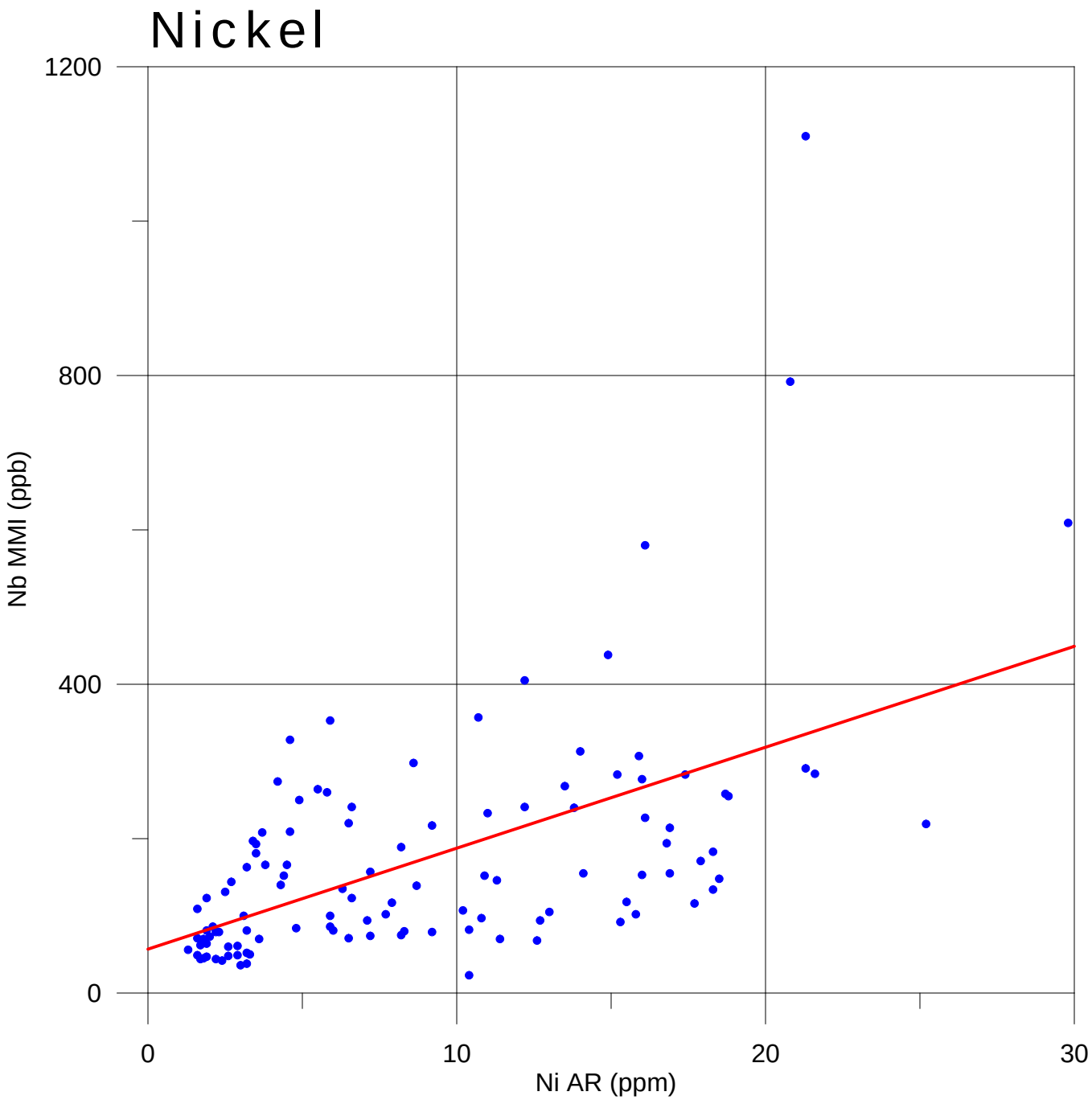
Nickel
1200
800
400
0
Nb MMI (ppb)
0
10
20
30
Ni AR (ppm)

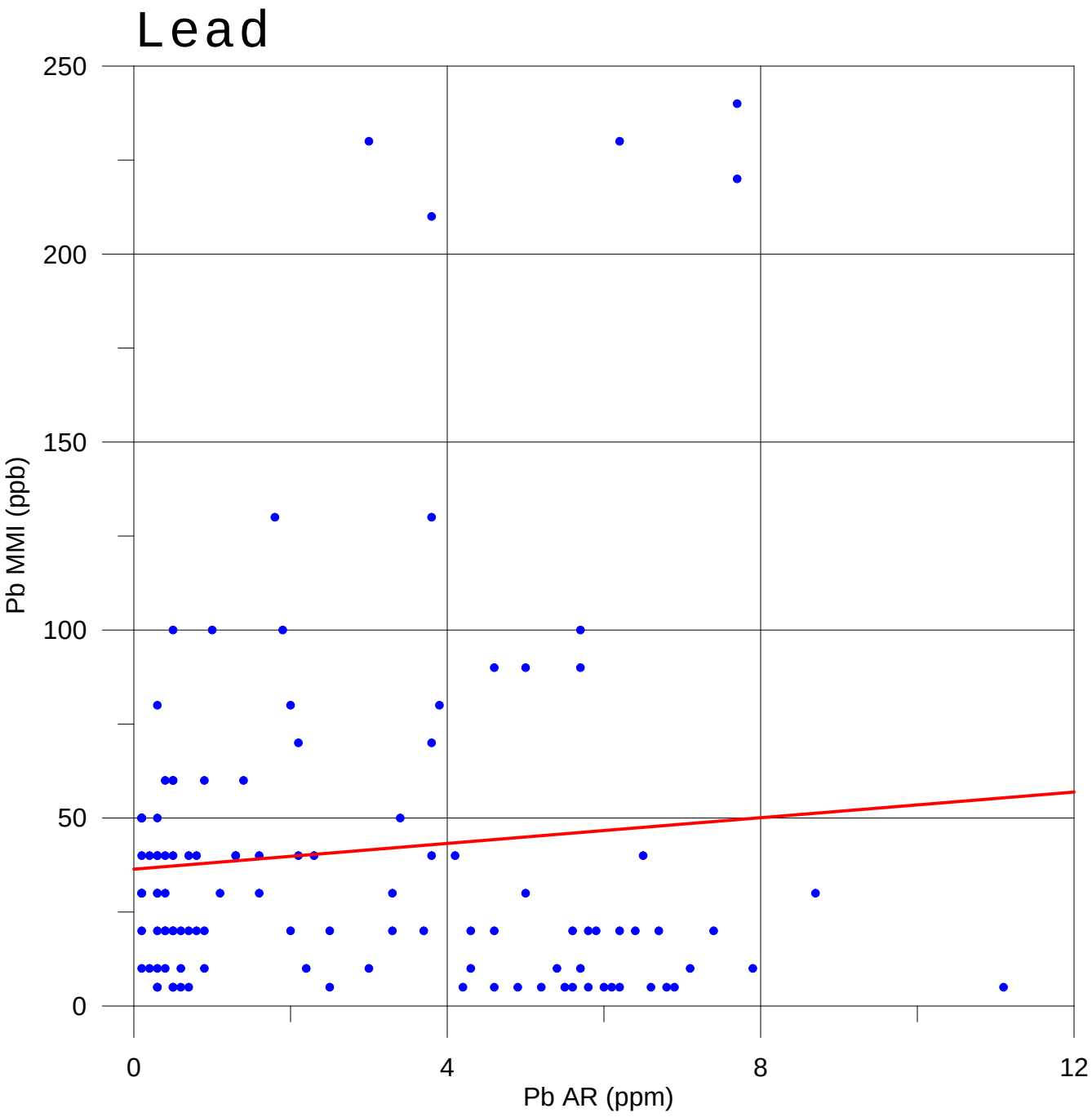
Lead
250
200
150
100
50
0
Pb MMI (ppb)
0
4
8
12
Pb AR (ppm)

Rubidium

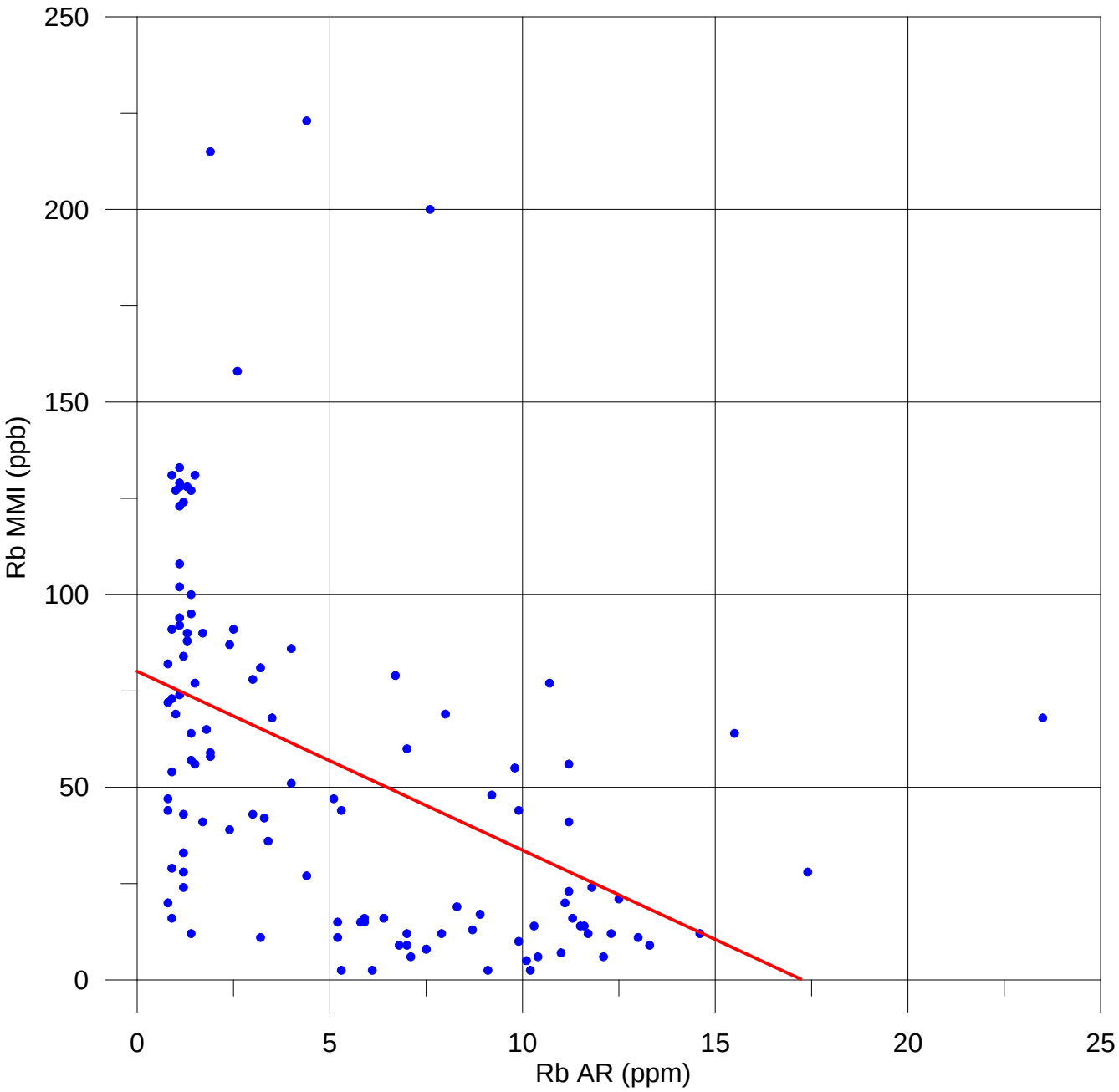

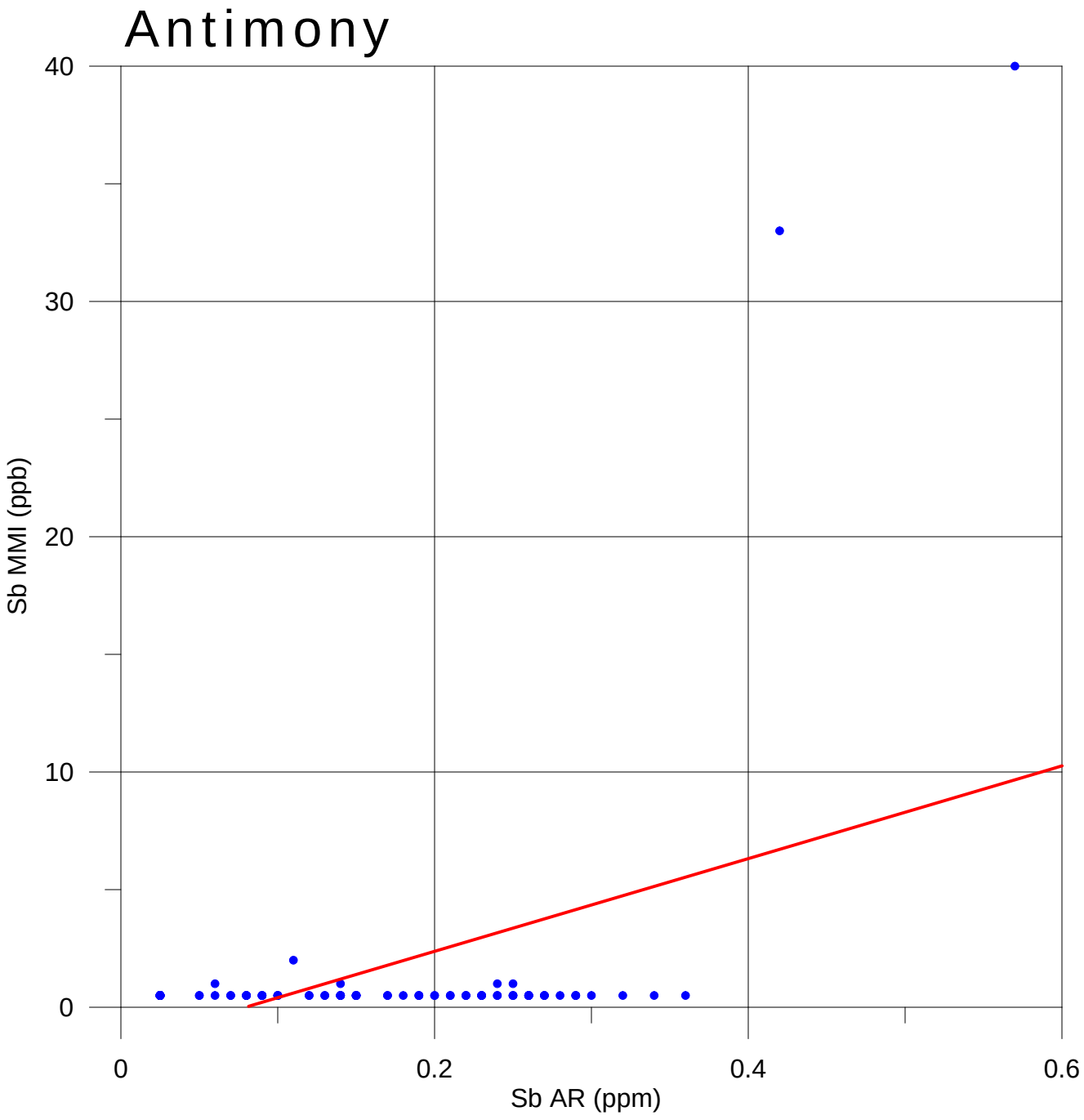
Antimony
40
30
20
10
0
Sb MMI (ppb)
0
0.2
0.4
0.6
Sb AR (ppm)

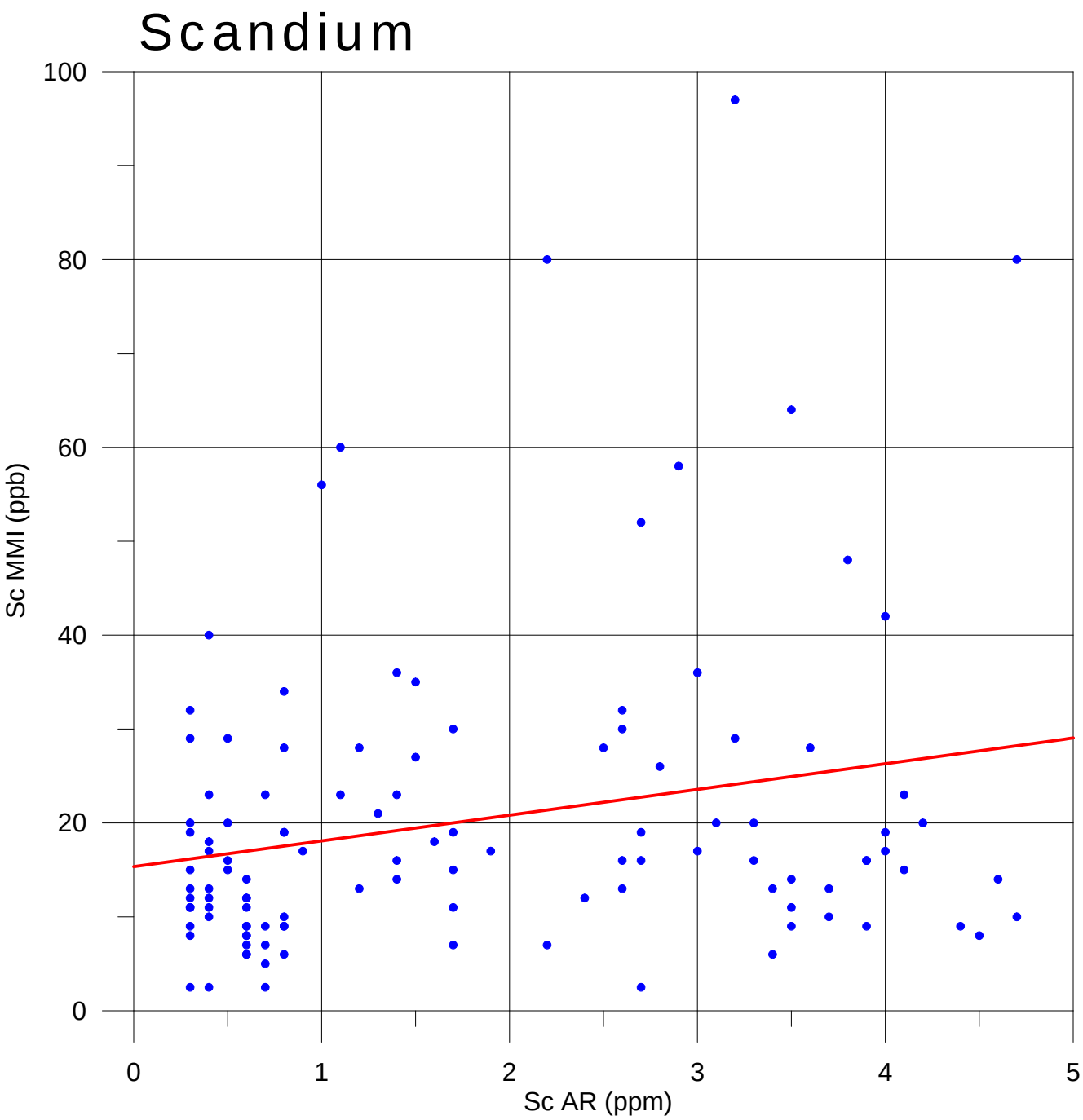
Scandium
100
80
60
40
20
0
Sc MMI (ppb)
0
1
2
3
4
5
Sc AR (ppm)

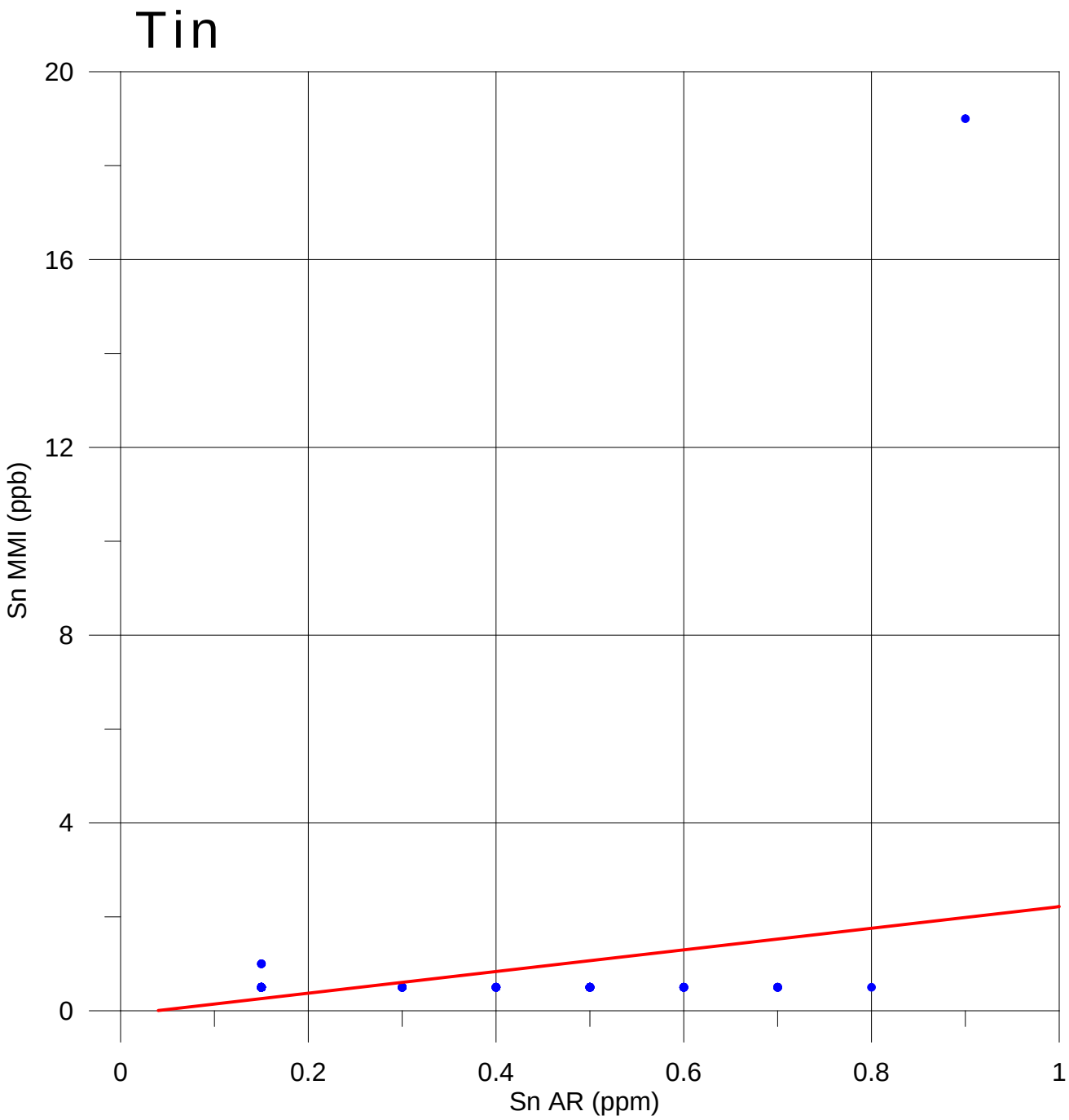
Tin
20
16
12
8
4
0
Sn MMI (ppb)
0
0.2
0.4
0.6
0.8
1
Sn AR (ppm)

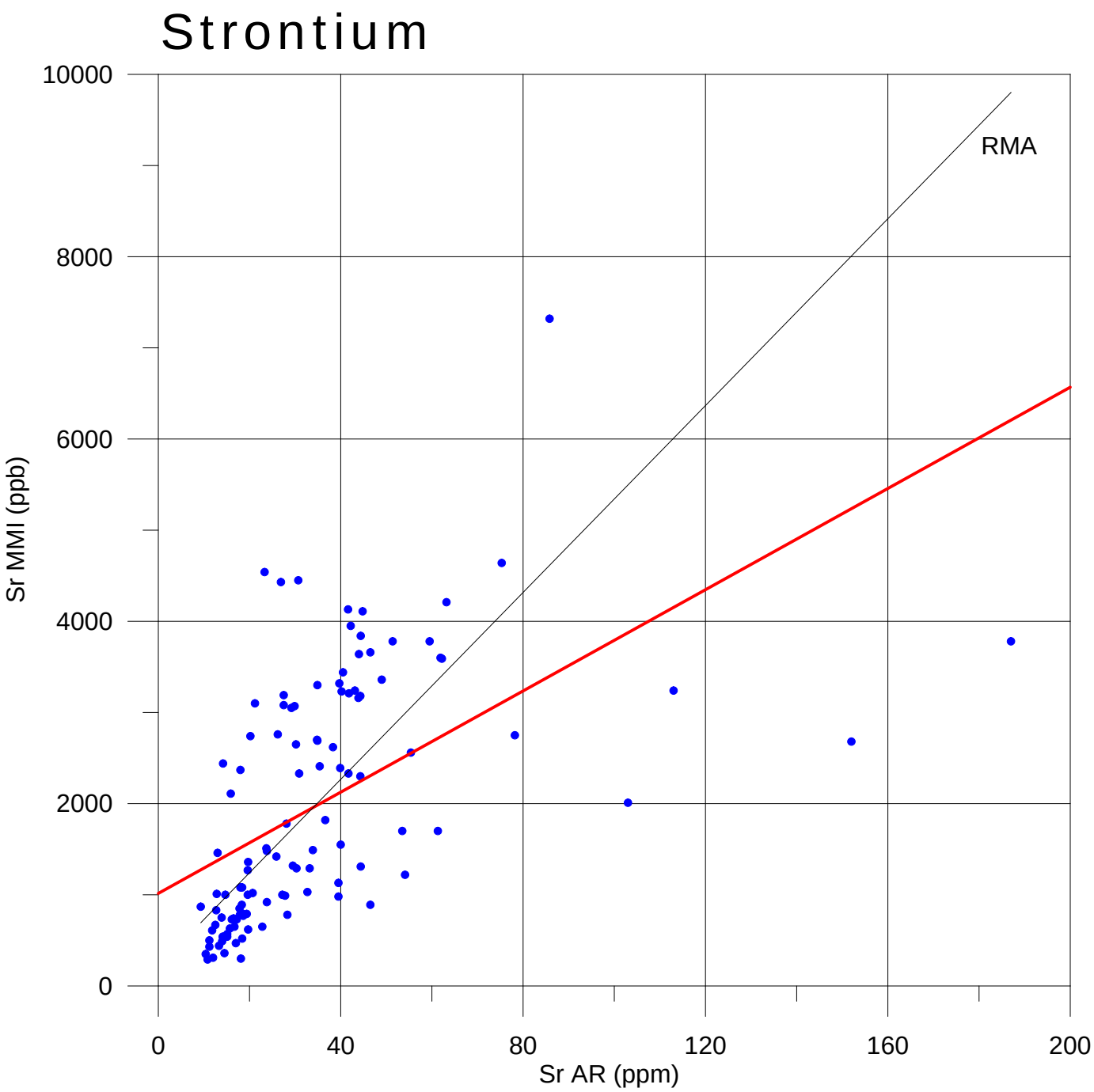
Strontium
10000
8000
6000
4000
2000
0
Sr MMI (ppb)
RMA
0
40
80
120
160
200
Sr AR (ppm)

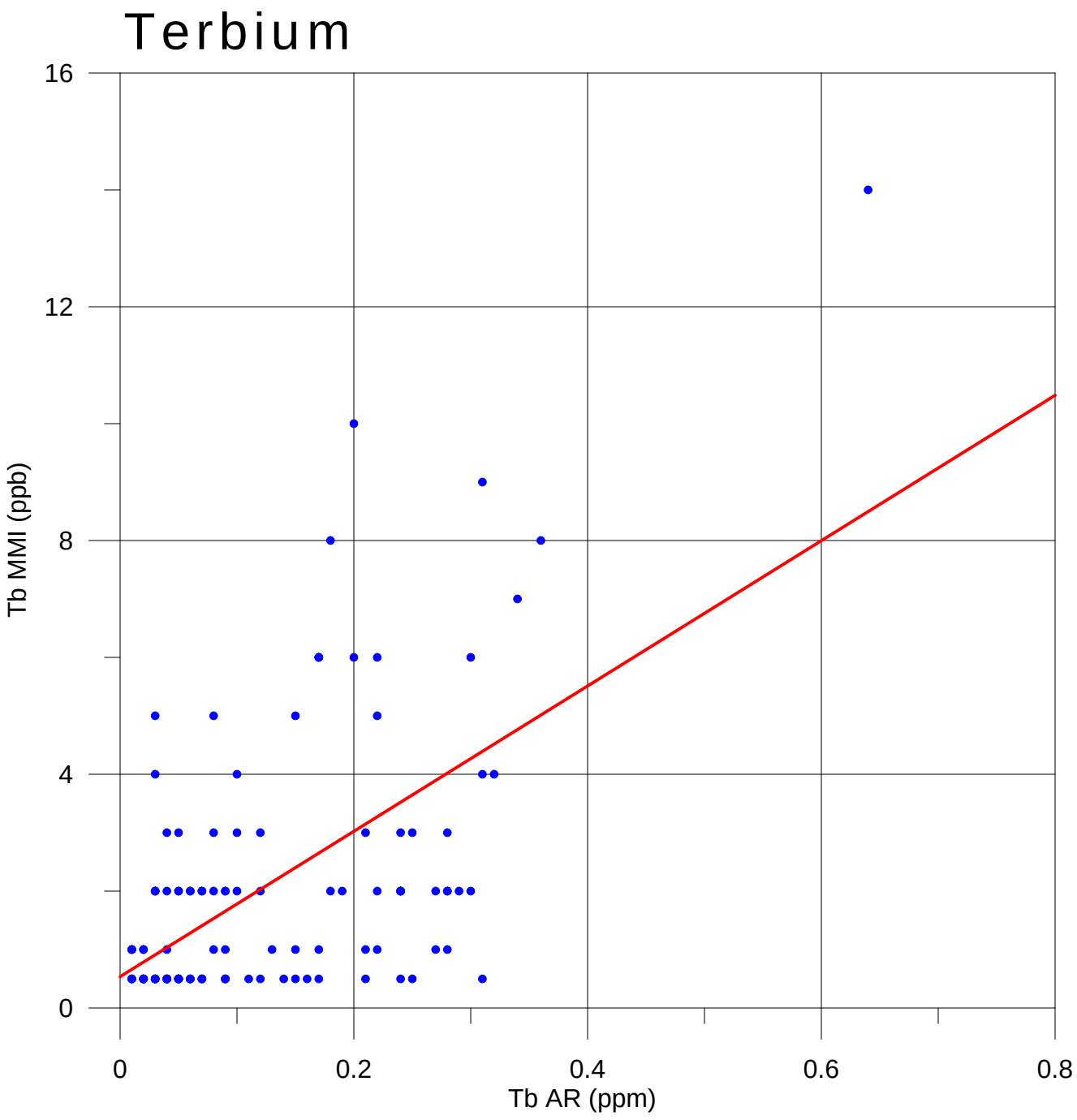
Terbium
16
12
8
4
0
Tb MMI (ppb)
0
0.2
0.4
0.6
0.8
Tb AR (ppm)

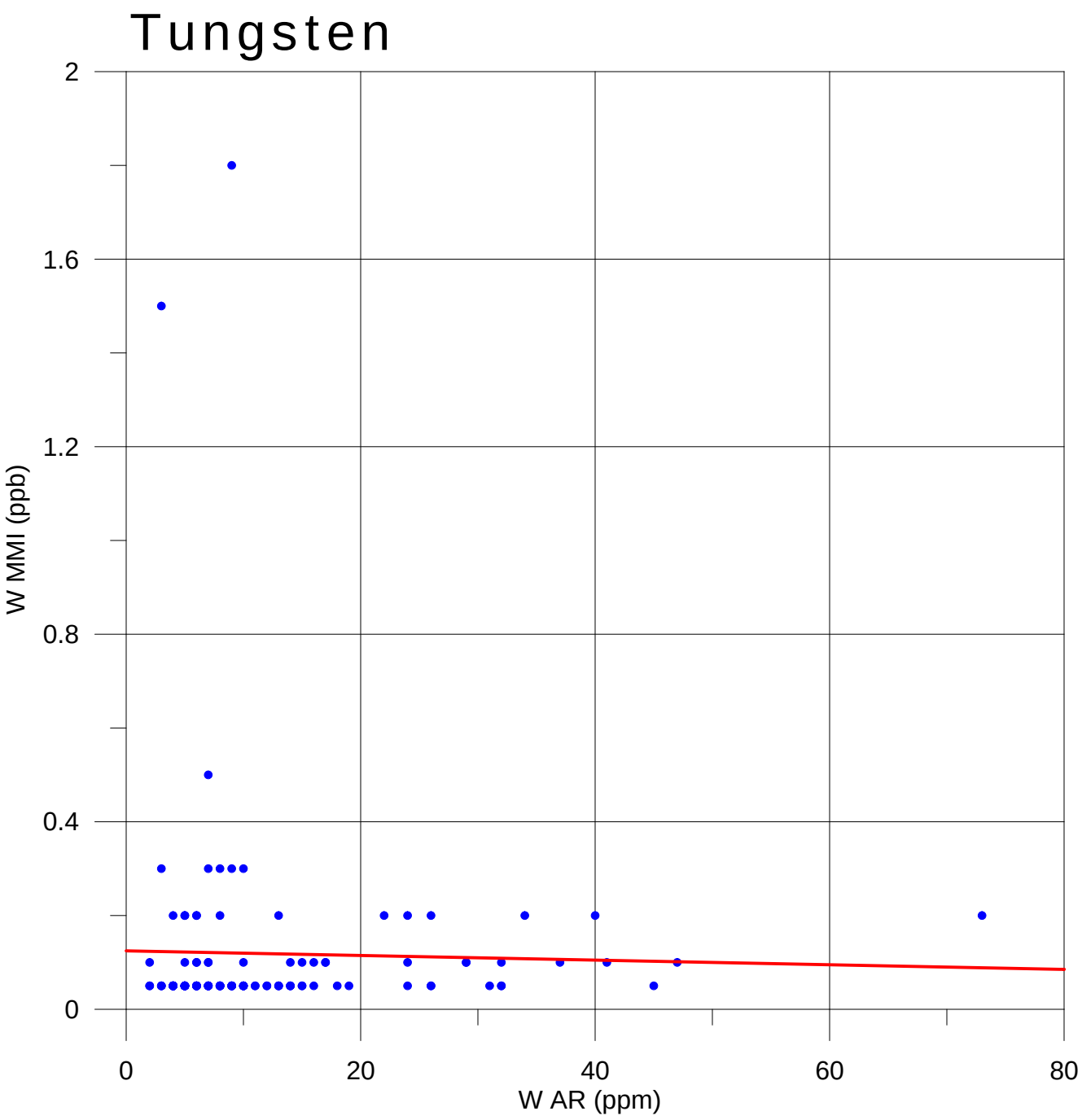
Tungsten
2
1.6
1.2
0.8
0.4
0
W MMI (ppb)
0
20
40
60
80
W AR (ppm)

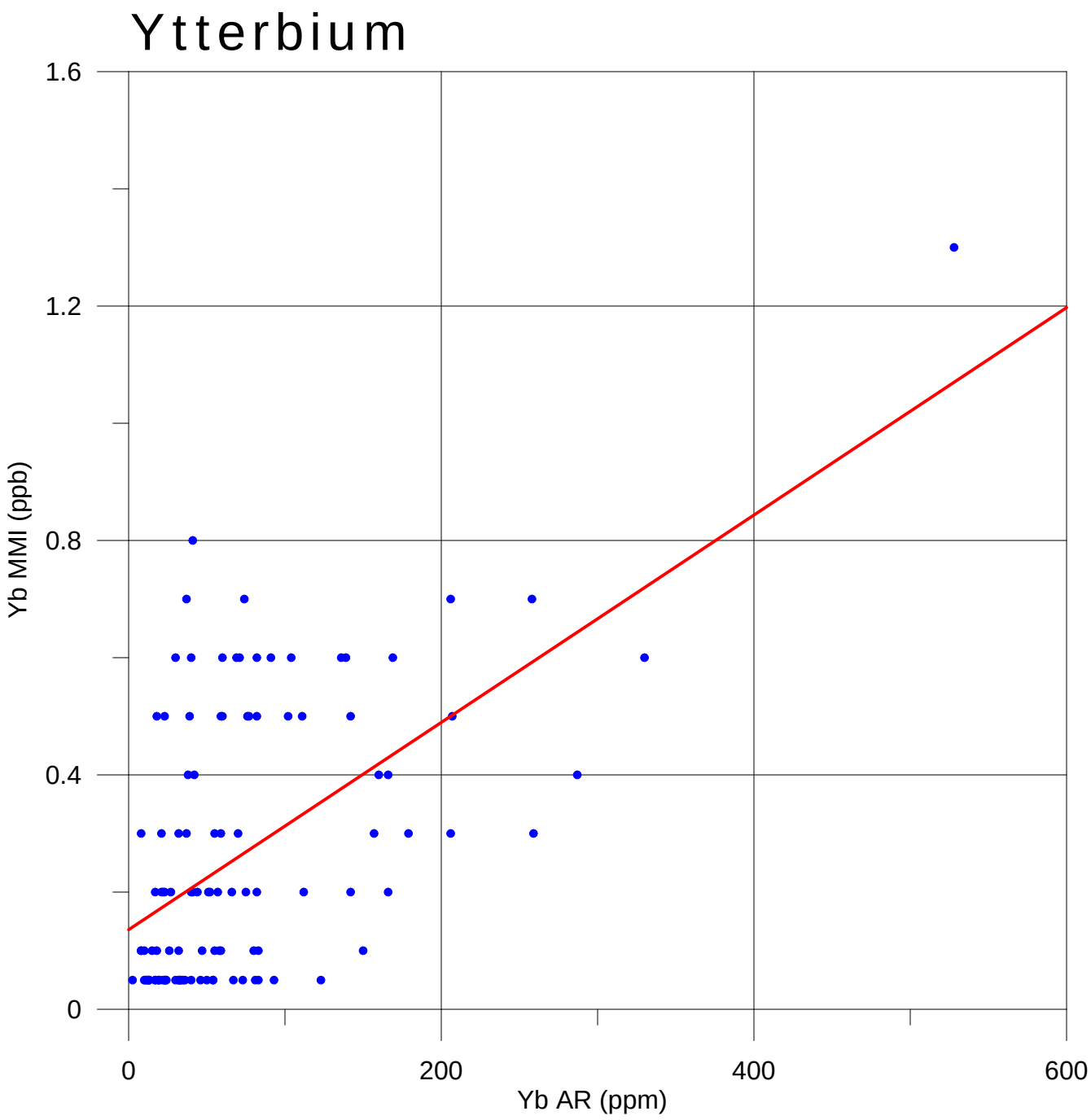
Ytterbium
1.6
1.2
0.8
0.4
0
Yb MMI (ppb)
0
200
400
600
Yb AR (ppm)

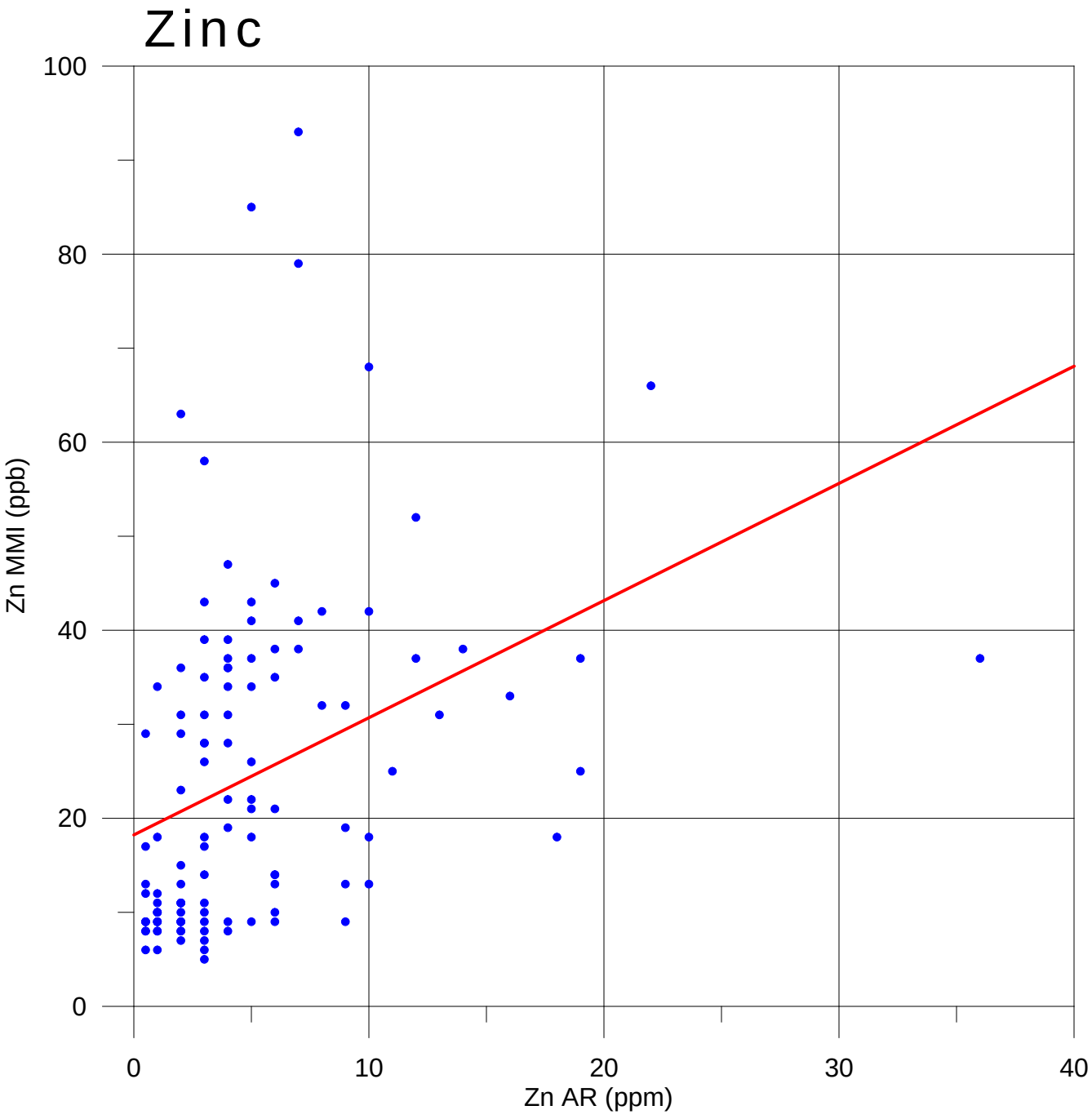
Zinc
100
80
60
40
20
0
Zn MMI (ppb)
0
10
20
30
40
Zn AR (ppm)

Zirconium

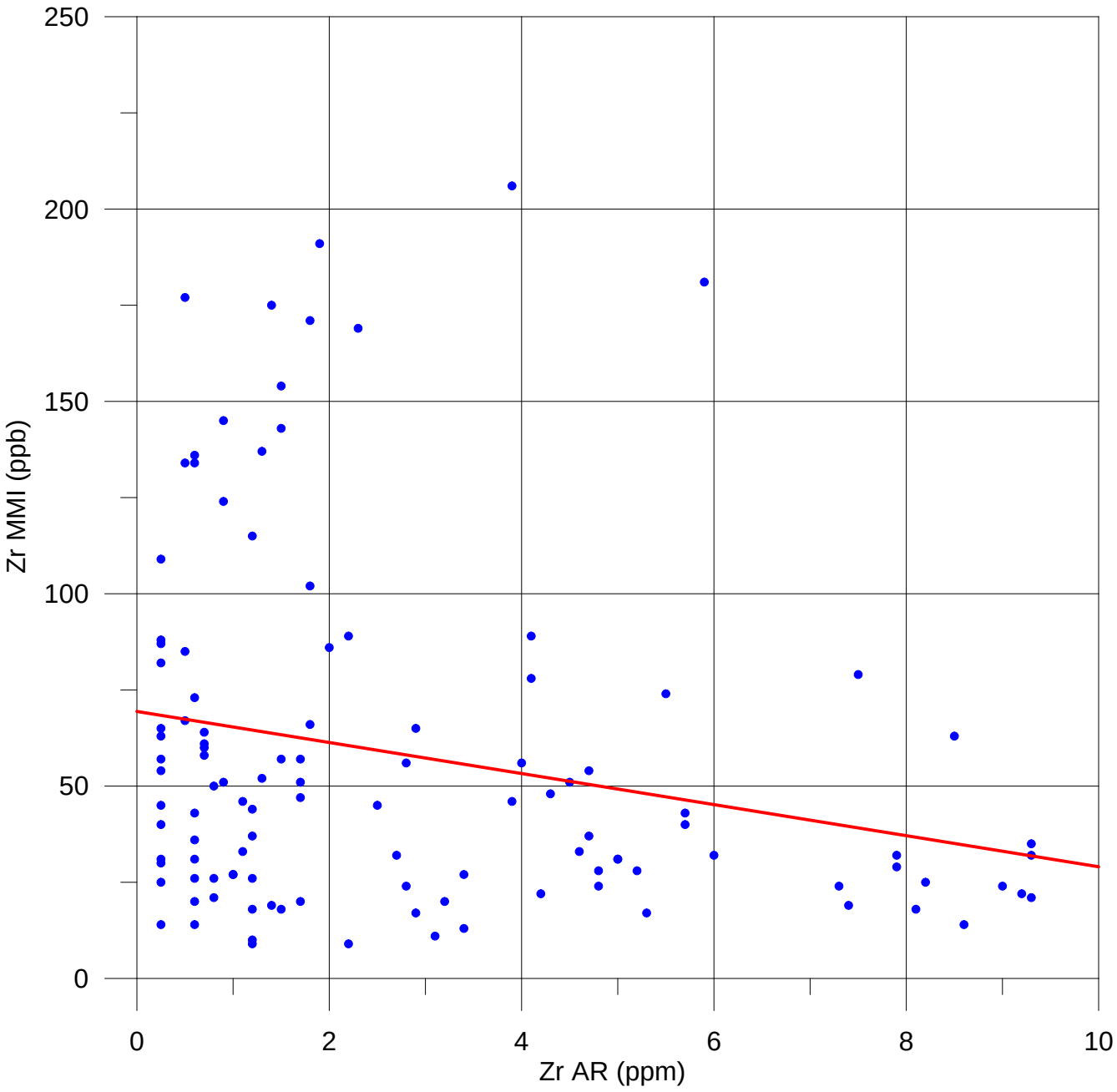

APPENDIX VII:
Infrared Spectroscopy Report
(Fonseca, 2009a)

INFRARED SPECTROSCOPY SURVEY OF DIAMOND DRILL CORE FROM THE CARMACKS COPPER-GOLD PROJECT, YUKON, CANADA

Infrared spectroscopy report prepared for:

BCGold Corp.

Prepared by:

Anna Fonseca, P.Geo.

804, Wood St.
Whitehorse YT Y1A 2G5

January 23, 2008

TABLE OF CONTENTS

Executive Summary……i
Scope and Methodology……1
Dawson Range Geology……1
Infrared Spectroscopy……3
Summary of infrared spectroscopic characteristics of the 2008 drill holes……4
Conclusions and recommendations……7
References……8
Statement of Qualifications……9

LIST OF FIGURES

Figure 1. Regional geology of Dawson Range……2
Figure 2. Hornblende spectral signature……5
Figure 3. Palygorskite spectral signature……5

APPENDIX

Drill hole graphic summaries……10

EXECUTIVE SUMMARY

- Mineralized and geochemically anomalous intervals correspond to intensely foliated metavolcanic rock with extremely low magnetic susceptibility (magnetite destructive alteration) and infrared spectral signature consisting of mafic mineral assemblages.

- Mafic mineral assemblages produce spectral signatures from which it is difficult to derive conclusive mineral species identifications. However, the different mafic spectral signatures may be sufficient to discern mineralized from unmineralized intervals.

- A strong hornblende spectral signature coincident with mineralized metavolcanic rock intervals in drill hole WS08-09 likely represents a mixture of secondary amphiboles (actinolite, uralite) and non-sulphide copper minerals.

- Anomalous multielement geochemistry in metavolcanic rock sections of drill hole WS08-08 lack strong and continuous hornblende alteration signature.

- Chlorite forms a broad envelope including mineralized and anomalous geochemistry metavolcanic intervals in holes WS08-08 and WS08-09B. It is recommended that unmineralized granodiorite intervals with moderate chlorite signature (e.g.: bottom of WS08-11) be investigated using existing geophysical surveys to examine the possibility that chlorite represents halos to nearby metavolcanic intervals.

- Multielement geochemistry of the granodiorite along contacts with mineralized metavolcanic intervals suggest a propylitic alteration mineral assemblage.

- It is recommended to carry out a petrographic survey to characterize: 1) the mineral assemblage constituting hornblende spectral signature in mineralized and in unmineralized intervals; 2) the mineral assemblage constituting palygorskite spectral signature in mineralized and in unmineralized intervals; 3) the mineral assemblage and structural controls of altered granodiorite along contacts with mineralized metavolcanic intervals; and 4) the character of the unaltered granodiorite host, and specifically whether magmatic epidote is present or not.

SCOPE AND METHODOLOGY

This survey of infrared spectra from the 2008 diamond drill program at BC Gold Corp.'s Carmacks Copper Project consists of the interpretation of 2,460 infrared spectra. Small core samples <3 cm wide of drill core were collected in the core shack at 1 m intervals, stored in soil sample kreft bags in which drill hole number and depth in metres was labeled, and the bags were shipped in boxes to BC Gold Corp.'s Vancouver office for analyses. Infrared spectra were collected using Laurentian Goldfields' ASD Terraspec VIS-NIR spectrometer, which has bandwidth from 350 to 2,500 nm, with optical resolution of <9 nm in the higher wavelengths, and 5 nm in the visible wavelengths. At least two spectra were collected from each sample by BC Gold Corp.'s geologist Gary Sidhu. BC Gold Corp. commissioned Anna Fonseca, P.Geo. to perform mineral identification and absorption feature extraction from the infrared spectroscopy dataset, to interpret trends and correlations with logged features and geochemical analyses, and to make recommendations that may assist in future exploration programs.

BC Gold Corp. geologists provided diamond drill hole logs in .xls and .mdb formats, which include detailed information on lithology, veining, sulphide mineralogy and content, alteration, structural, geotechnical, magnetic susceptibility, and geochemical analyses. This information was utilized in conjunction with infrared spectroscopic interpretation information.

DAWSON RANGE GEOLOGY AND MINERALIZATION

Dawson Range refers to the northwest-trending geographical region underlain predominantly by Early Jurassic to late Cretaceous plutons, which extends over 250 km from Carmacks to the Alaska border. The Dawson Range includes three metallogenic districts: 1) Structurally controlled porphyry style Cu-Au deposits associated with Early Jurassic Aishihik Lake plutonic Suite, such as Capstone Resources' Minto Mine (45 million tonnes of 0.7g/t Au and 1% Cu at 0.2% Cu cut-off grade), Western Copper's Carmacks Copper (26 million tones of 0.5 g/t Au and 1% Cu), and the Stu showing; 2) Late Cretaceous Cu-Mo+/-Au porphyry style deposits such as the large Casino (910 million tones of 0.2% Cu and 0.02% Mo) and the smaller Cash (36 million tones of 0.2% Cu and 0.02% Mo) deposits; 3) Low sulphidation epithermal Au-Ag+/-Zn-Pb-Cu deposits associated with subvolcanic intrusions of the Late Cretaceous Mt. Nansen Suite, including the Mt. Nansen deposit (400 thousand tones of 13g/t Au), Laforma (62 thousand tones of 15 g/t Au), Tinta Hill (765 thousand tones of 2.57g/t Au, 183.2 g/t Ag, 6% Zn, 4.71% Pb, 0.35% Cu); and Northern Freegold's Nucleus-Revenue deposits (resources currently being calculated).

Figure 1 shows the most recent interpretation of regional geology in Carmacks Copper belt portion of Dawson Range. BC Gold Corp.'s Carmacks Copper Project's claims surround Western Copper's Carmacks Copper deposit and the Stu prospect in Granite Mountain Batholith, and cover the area to the northwest of the Minto Mine in the co-magmatic Minto Pluton. Biotite-granodiorite and subordinate plutonic lithologies of Granite Mountain Batholith and Minto Pluton intrude the contact between augite-phyric basaltic andesites of Stikinia's Upper Triassic Lewes River Group, and polydeformed Simpson Range Suite equivalent metaplutonic rocks of Yukon Tanana Terrane's Early Mississippian Finlayson Assemblage.

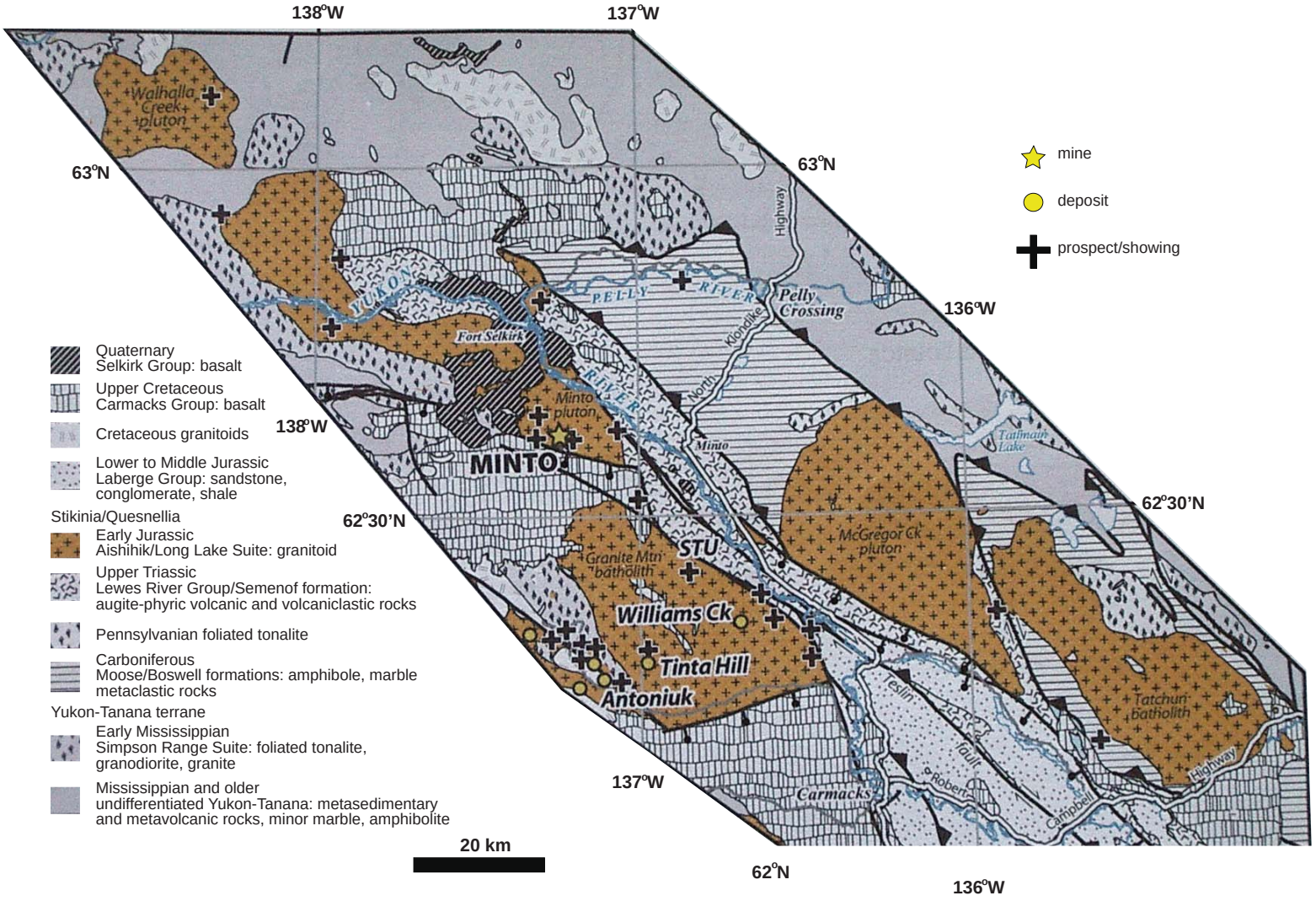

Figure 1. Regional geology of the Carmacks Copper belt, Dawson Range, west-central Yukon (after Hood and others, 2009).

Deep porphyry deposits and resulting alteration assemblages

Porphyry style Cu-Au mineralization of the Dawson Range shares few similarities with British Columbia's belt of shoshonitic rock hosted Cu-Au porphyry style mineralization that includes the large Mount Milligan and Galore Creek deposits. In the Dawson Range and in British Columbia porphyry deposits are associated with Early Jurassic plutonic rocks intruding slightly older augite phyric basaltic andesites of Quesnellia and Stikinia. The British Columbia deposits appear to have formed at typical porphyry depths (<5 km) and fluid to rock ratios, with resulting alteration mineralogy and zoning that are characteristic of porphyry deposits. Deposits of the Dawson Range, on the other hand, formed significantly deeper in the crust. Magmatic epidote, which constitutes an accessory phase in granodioritic rocks of Granite Mountain Batholith and Minto Pluton, and was identified in the Minto and Carmacks Copper deposits indicates minimum emplacement depths of 18 to 20 km (Tafti, 2005). Meteoric fluid circulation is minimal to absent at such depths, and the resulting alteration assemblages reflect low fluid to rock ratios. Potassic zones developed under low fluid to rock ratios is expected to form magnetite-chalcopyrite dominated alteration with restricted pseudomorphic shreddy biotite, and minor to no orthoclase. Sericitic and phyllic zones formed at low fluid to rock ratios are likely to be poorly developed or absent.

Structural and lithological controls

Hypogene Cu-Au porphyry mineralization in the Dawson Range is strongly structurally, and in most cases lithologically controlled. Hypogene mineralization in the Minto Mine is controlled by sub-horizontal zones of gneissically foliated granodiorite to diorite. In Western Copper's Carmacks Copper deposit, mineralized zones consist of subvertical, gneissically foliated augite-phyric volcanic rafts engulfed in barren granodiorite. In both cases, grain boundary reduction associated with and overprinting the gneissic foliation is a critical process controlling the locus of mineralization. Similarly to the Carmacks Copper deposit, Cu-Au mineralization in BC Gold Corp.'s WS claims is bound within mafic volcanic units (Appendix I).

Supergene mineralization

A deep supergene profile is well developed at the Carmacks Copper (<250 m) deposit and at the Stu prospect. The most common supergene minerals include hematite and copper oxides, carbonates, and sulphates such as malachite, chrysocolla, broccantite, and tennorite. Transported supergene minerals fill fractures and fissures. Supergene minerals also replace copper sulphides along mafic domains in the gneissic foliation. Malachite is recorded in the drill log of hole WS08-09B (Appendix I).

INFRARED SPECTROSCOPY

Mineralized intervals in drill hole WS08-09B correlate with infrared spectroscopic signatures of mafic minerals, rather than with white micas or clays. The spectral identification of mafic minerals in a mixture is difficult and often inconclusive. Conclusive mafic mineral mixture identification requires calibration through petrographic and SEM techniques. Spectra interpreted as hornblende and palygorskite likely represent a mixture of these or other minerals, and their interpretation should be viewed as spectral signatures, rather than conclusive mineral identifications. The main spectral characteristics of the most important mafic minerals are discussed below.

Hornblende

"Hornblende" spectral signature correlates closely with the highest gold and copper grade intervals in drill hole WS08-09B. The metavolcanic intervals in drill hole WS08-08 contain hornblende spectral signature only in the narrow intervals with highest anomalous gold and copper grades. This suggests that hornblende can be used to distinguish mineralized from unmineralized metavolcanic intervals that have low magnetic susceptibility values.

It is likely that the spectral signature identified as hornblende represents more typical secondary amphiboles, such as actinolite or uralite, mixed with lesser non-sulphide-Cu minerals. Figure 2 shows the principal spectral characteristics of minerals likely to compose mixtures with hornblende spectral signature.

Palygorskite

Palygorskite is a hydrated Mg-Al hydroxide clay that typically has fibrous habit. Spectrally, palygorskite is characterized by four main absorptions around 2331 nm, 2222 nm, 1922 nm, and 1413 nm. The "Palygorskite" spectral signature should be seen as a possible mix of Mg end member mafic minerals, which may include or be the Mg-Mn-Fe-Ca-dolomite kutnohorite. Figure 3 shows the principal spectral characteristics of minerals likely to compose mixtures with palygorskite spectral signature.

SUMMARY OF INFRARED SPECTROSCOPIC AND OTHER CHACTERISTICS OF THE 2008 DRILL HOLES

WS08-08

Infrared spectroscopic and magnetic susceptibility data was collected for the entire hole at 1 m intervals, whereas geochemical samples were collected over two broad areas straddling volcanic lithologies. Detailed drill core alteration, sulphide/oxide mineralogy, structural, and lithology logs were recorded for the entire hole.

- 108 – 154 m: anomalous Cu-Au associated with very low magnetic susceptibility, hosted in mafic metavolcanic rocks. Carbonate>chlorite>epidote>hematite alteration recorded in the drill log is interpreted as being magnetite destructive. Infrared spectroscopic interpretations show strong chlorite throughout the interval, with associated palygorskite and lesser hornblende in the central part of the interval. Illite, smectite, and kaolinite are strong in the outer parts of the interval, and sparse to absent in the core.
- 191 – 263 m: anomalous Cu-Au associated with very low magnetic susceptibility, hosted in felsic and mafic metavolcanic rocks intercalated with K-spar megacrystic granodiorite, lesser equigranular granodiorite, and rare aplite at the top of the interval. The drill hole alteration log records moderate chlorite>epidote>hematite-carbonate. Spectral mineral interpretations show moderate, discontinuous illite-smectite throughout the interval, with stronger smectite in the top half. Mafic alteration minerals consist of strong discontinuous chlorite throughout the interval, and subordinate hornblende straddling the highest copper and gold grades from 239 m to 250 m.

WS08-09B

Infrared spectroscopic and magnetic susceptibility data was collected for the entire hole at 1 m intervals, whereas geochemical samples were collected continuously from 40.73 to 115 m, over a broad area straddling volcanic lithologies, and sparsely through the rest of the drill hole. Detailed drill core alteration, sulphide/oxide mineralogy, structural, and lithology logs were recorded for the entire hole.

- 35 – 108 m: low magnetic susceptibility coincident with anomalous to high Cu-Au values, hosted in two intervals metavolcanic rocks intercalated with kspar megacrystic-, lesser equigranular granodiorite and minor pegmatite. The alteration log records intense chlorite-kspar-biotite>carbonate-epidote, with the most intense alteration corresponding to the lower metavolcanic/mineralized section. Infrared spectroscopic interpretations shows that illite becomes progressively stronger from the top of the interval downward, and is strongest in the lower mineralized/metavolcanic section. Chlorite occurs

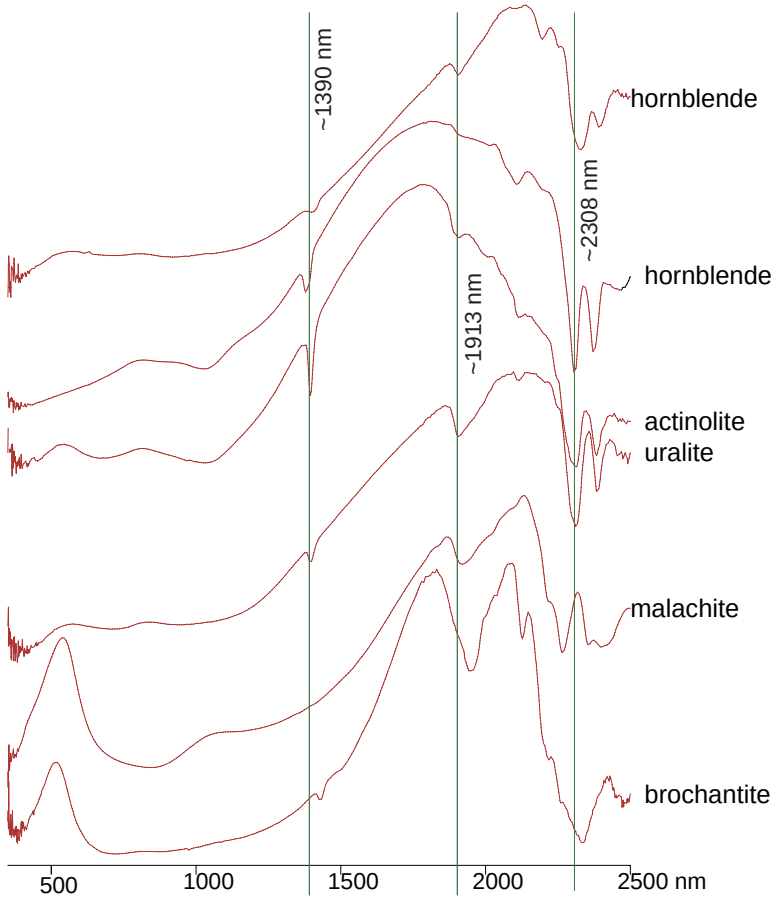

Figure 2. The hornblende spectral signature may consist of a mineral mixture of amphibole (actinolite, uralite, or hornblende), and minor amounts of non-sulphide copper minerals such as the brochantite and malachite.

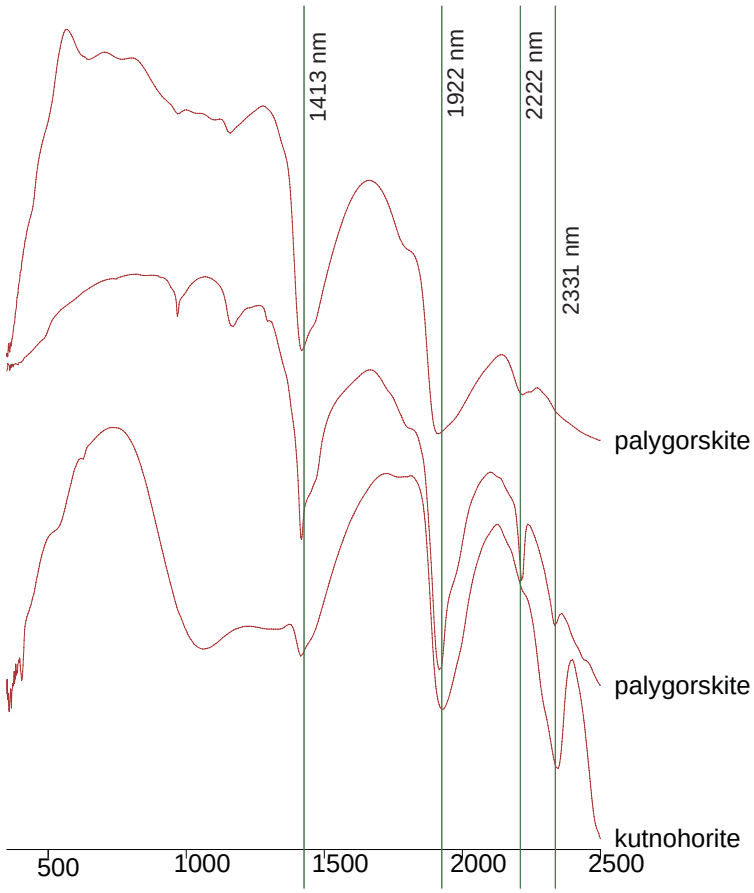

Figure 3. The palygorskite spectral signature may consist of a mineral mixture of Mg-rich mafic minerals, including the carbonate kutnohorite.

discontinuously through both mineralized/metavolcanic sections, and in the immediate footwall and handgingwall of this interval, but is absent in the intervening kspar megacrystic granodiorite. Palygorskite is strongest in the hangingwall and in the intervening kspar megacrystic granodiorite. Palygorskite is also strong in the lower mineralized/metavolcanic section. Hornblende best correlates with copper and gold mineralization.

- 205 – 210 m: low magnetic susceptibility coincident with strong kspar and chlorite reported in drill logs. Gechemical analyses are not available. Infrared spectroscopic interpretations show strong, continuous illite throughout the interval. Palygorskite is strong in the hangingwall, and moderate to weak in the footwall. Chlorite and hornblende are absent.

WS08-10

Infrared spectroscopic and magnetic susceptibility data was collected for the entire hole at 1 m intervals, whereas geochemical samples were collected over three narrow intervals. Detailed drill core alteration, sulphide/oxide mineralogy, structural, and lithology logs were recorded for the entire hole.

- 35 – 47 m: very low magnetic susceptibility along the upper contact of kspar megacrystic granodiorite. The alteration drill log records intense chlorite-sericite, and lesser hematite and kspar. Infrared spectroscopy mineral interpretations do not show a mineral that characterizes this interval.
- 80 – 87 m: moderate to low magnetic susceptibility coincident with weakly anomalous gold and lesser copper, hosted in kspar megacrystic granodiorite. Infrared spectroscopic interpretations show strong illite in the upper part of the interval. Chlorite, palygorskite, and hornblende are absent.
- 145 – 150 m: very low magnetic susceptibility, hosted in kspar megacrystic granodiorite. Spectral interpretations show intense smectite and kaolinite in the interval submitted to geochemical analyses. Chlorite, palygorskite, and hornblende are absent. Low magnetic susceptibility perdures to 161 m, and is coincident with strong kaolinite alteration.

WS08-11

Infrared spectroscopic and magnetic susceptibility data was collected for the entire hole at 1 m intervals, whereas geochemical samples were collected over a single narrow interval. Detailed drill core alteration, sulphide/oxide mineralogy, structural, and lithology logs were recorded for the entire hole.

- 24 – 29 m: high magnetic susceptibility associated with a mafic dike with anomalous Cr and Ni geochemistry. Infrared spectroscopic interpretations show that the dike is smectite altered.
- Throughout the drill hole: Illite is moderate but discontinuous throughout. Chlorite and palygorskite occur discontinuously, whereas hornblende is sparse through the upper half, and nearly absent in the lower half.

WS08-12

Infrared spectroscopic and magnetic susceptibility data was collected for the entire hole at 1 m intervals, whereas geochemical samples were not collected in this hole. Detailed drill core alteration, sulphide/oxide mineralogy, structural, and lithology logs were recorded for the entire hole.

- Throughout the drill hole: Infrared spectroscopic interpretations show that illite, lesser chlorite, and sparse palygorskite occur discontinuously, whereas discontinuous hornblende and epidote are more common in the top 60 m.

CONCLUSIONS AND RECOMMENDATIONS

Spectral signatures of mafic minerals correlate with mineralized and metavolcanic intervals, whereas white micas and kaolinite correlate with altered, barren granodiorite intervals, and smectite correlates with altered mafic dikes. It is difficult to derive conclusive identification of mafic minerals from infrared spectra, and therefore the mafic mineral interpretations presented in this report should be viewed as spectral signatures of mafic+/-phyllosilicate mineral mixtures. In spite of the uncertainty surrounding mafic mineral identification, certain mafic mineral signatures show excellent correlation with mineralized intervals.

The most strongly mineralized intervals in drill hole WS08-09B correlate very well with "hornblende" infrared spectroscopic signature. Hornblende spectral signature is absent or local in unmineralized metavolcanic sections. It is recommended that further spectroscopic analyses of mineralized and unmineralized metavolcanic sections be carried out to verify that the hornblende spectral signature always coincides with mineralization, and if it does, then spectral interpretations can be carried out in the core shack, in order to distinguish mineralized from unmineralized metavolcanic intervals.

Chlorite spectral signature forms broad envelopes around mineralized and geochemically anomalous metavolcanic intervals in drill holes WS08-09B and WS08-08, and occurs discontinuously and sporadically in holes WS08-10, WS08-11, and WS08-12. It is possible that intervals with discernible and nearly continuos chlorite (e.g., bottom of WS08-11) in granodiorite may be indicative of proximity to a metavolcanic interval missed by the drill hole. It is recommended that this possibility be investigated by further infrared spectroscopic surveys in future drill holes, and also using existing geophysical data to infer nearby metavolcanic units.

Mineralized intervals have distinctly low magnetic susceptibility, suggesting that the alteration associated with mineralization is magnetite destructive, rather than the typical magnetite-bearing potassic alteration at the core of porphyry deposits. Based on the data presented in the striplogs, it is plausible that either a late phase of magnetite destructive alteration overprints potassic alteration, or that the mineralized intervals consist of lithology-controlled supergene transported copper. Drill logs record the presence of fracture-fill non-sulphide copper.

It is recommended to conduct a petrographic survey to characterize: lithology and alteration corresponding to hornblende signature in mineralized metavolcanic rocks in drill hole WS08-09B, geochemically anomalous metavolcanic intervals in WS08-08; with and without palygorskite signature; and the interval in WS08-10 with low magnetic susceptibility around 35 to 47 m. If the palygorskite spectral signature is demonstrated through petrographic analyses to consistently constitute or include the carbonate kutnohorite, then carbonate staining with alizarin red will be recommended during drill core logging. Additionally, petrographic samples should be collected from the granodiorite adjacent to mineralized and unmineralized metavolcanic sections, in order to characterize the alteration and structural controls immediately outside of the favourable horizons, and from unaltered granodiorite to characterize its primary mineralogy, and depth of formation (i.e., presence or absence of magmatic epidote).

Multi-element geochemistry shows enrichment in Ca, Fe, Mo, Tl, Te, mafic-associated elements (Mg, Ni, Co), Sn, and sphalerite associated elements (Zn, Se, Cd, V). K, Na, La, and Ce are enriched in the footwall and hangingwall of mineralized zones, suggesting that ore associated mineral alteration assemblage immediately outside ore zones may be propylitic, and possibly overprinting potassic.

REFERENCES

Hood, S., Colpron, M., and Mercer, B., 2009, High-grade hydrothermal copper-gold mineralization in foliated granitoids at the Minto mine, central Yukon. 2008 Yukon Exploration and Geology, in press.

Tafti, R., 2005, Nature, age, and origin of Cu-Au mineralization at the Minto and Williams Creek deposits, Yukon. M.Sc. thesis, University of British Columbia, 213 p.

STATEMENT OF QUALIFICATIONS

I, Anna Fonseca, P. Geo. certify that:

1. I have been involved in geological mapping and mineral exploration in Canada, U.S.A, Russia, and Mexico since 1994.

2. I am a graduate of the University of Alaska Fairbanks with a Degree in Geology (B.Sc., 1993) and I obtained a Masters of Science degree from the University of British Columbia in Mineral Exploration (M.Sc., 1998).

3. I am a member in good standing of the Association of Professional Engineers and Geoscientists of British Columbia.

4. I have previous experience in infrared spectroscopy data interpretation of altered samples from the North and South American Cordillera (Canada, Mexico, and Peru), from the Canadian Shield (Ontario and Northwest Territories), including samples from the Dawson Range.

5. I have previous field experience in the exploration and alteration mapping of porphyry style mineralization.

6. I am the author of all sections of this report on Infrared Spectroscopic Survey of Diamond Drill Core from the Carmacks Copper Project, Yukon, Canada.

7. I did not participate in geological field work in the Carmacks Copper Project of BC Gold Corp.

8. I have no direct or indirect interest in the properties or securities of BC Gold Corp. or affiliated companies, nor do I expect to acquire such interest.

Dated January 25, 2009

_____

Anna Fonseca, P.Geo.

APPENDIX I

DRILL HOLE STRIPLOGS

WS08-08

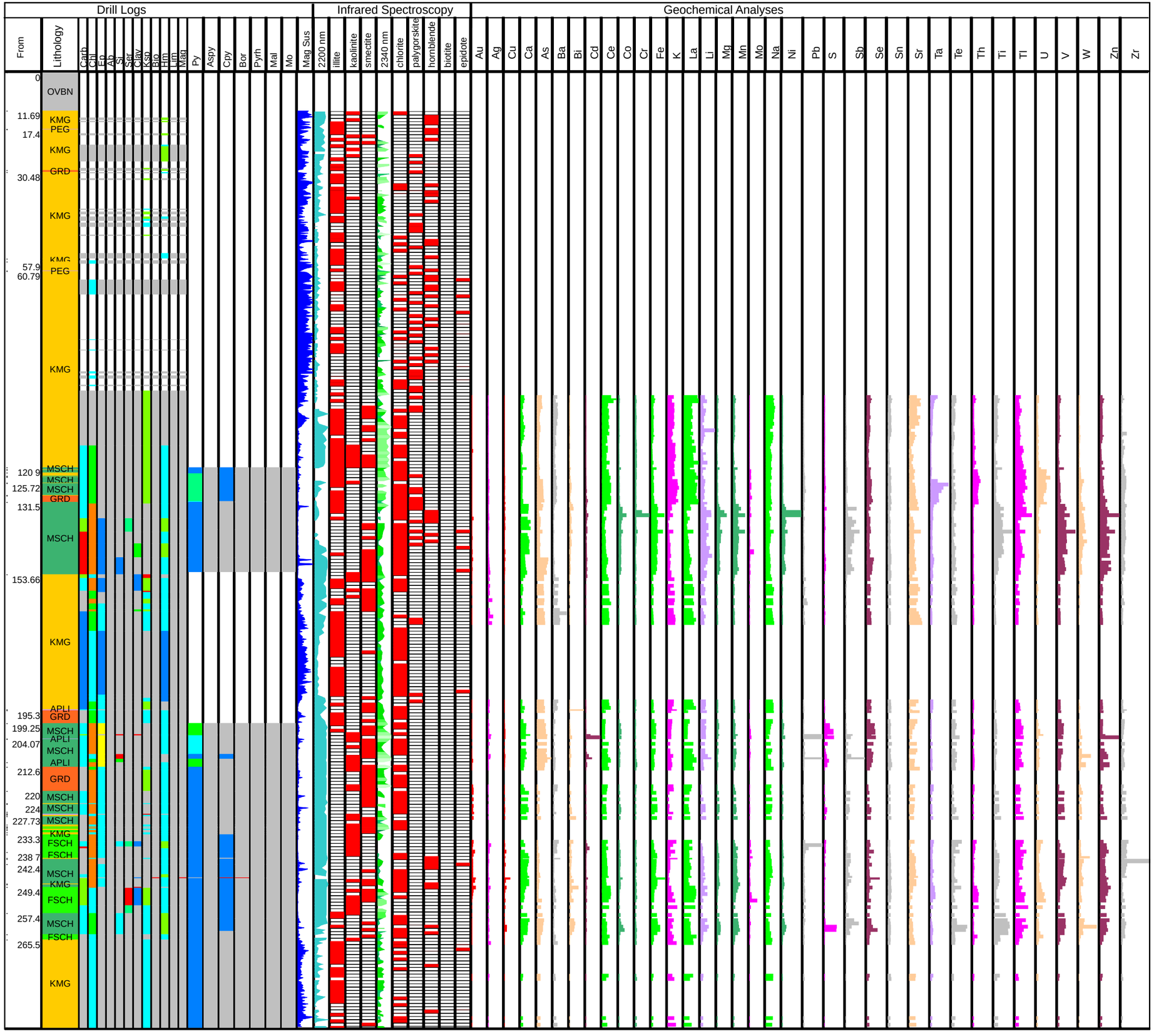
Drill Logs
Infrared Spectroscopy
Geochemical Analyses
From
Lithology
Carb
Chl
Ep
Ab
Sl
Ser
Clay
Ksp
Bio
Hm
Lim
Mag
Py
Aspy
Cpy
Bor
Pyrh
Mal
Mo
Mag Sus
2200 nm
illite
kaolinite
smectite
2340 nm
chlorite
palygorskite
hornblende
biotite
epidote
Au
Ag
Cu
Ca
As
Ba
Bi
Cd
Ce
Co
Cr
Fe
K
La
Li
Mg
Mn
Mo
Na
Ni
Pb
S
Sb
Se
Sn
Sr
Ta
Te
Th
Ti
Tl
U
V
W
Zn
Zr
0
OVBN
11.69
KMG
PEG
17.4
KMG
GRD
30.48
KMG
KMG
57.9
PEG
60.79
KMG
120 9
MSCH
MSCH
125.72
MSCH
GRD
131.5
MSCH
153.66
KMG
APLI
195.3
GRD
199.25
MSCH
APLI
204.07
MSCH
APLI
212.6
GRD
220
MSCH
224
MSCH
227.73
MSCH
KMG
233.3
FSCH
238 7
FSCH
242.4
MSCH
KMG
249.4
FSCH
257.4
MSCH
FSCH
265.5
KMG

WS08-09B

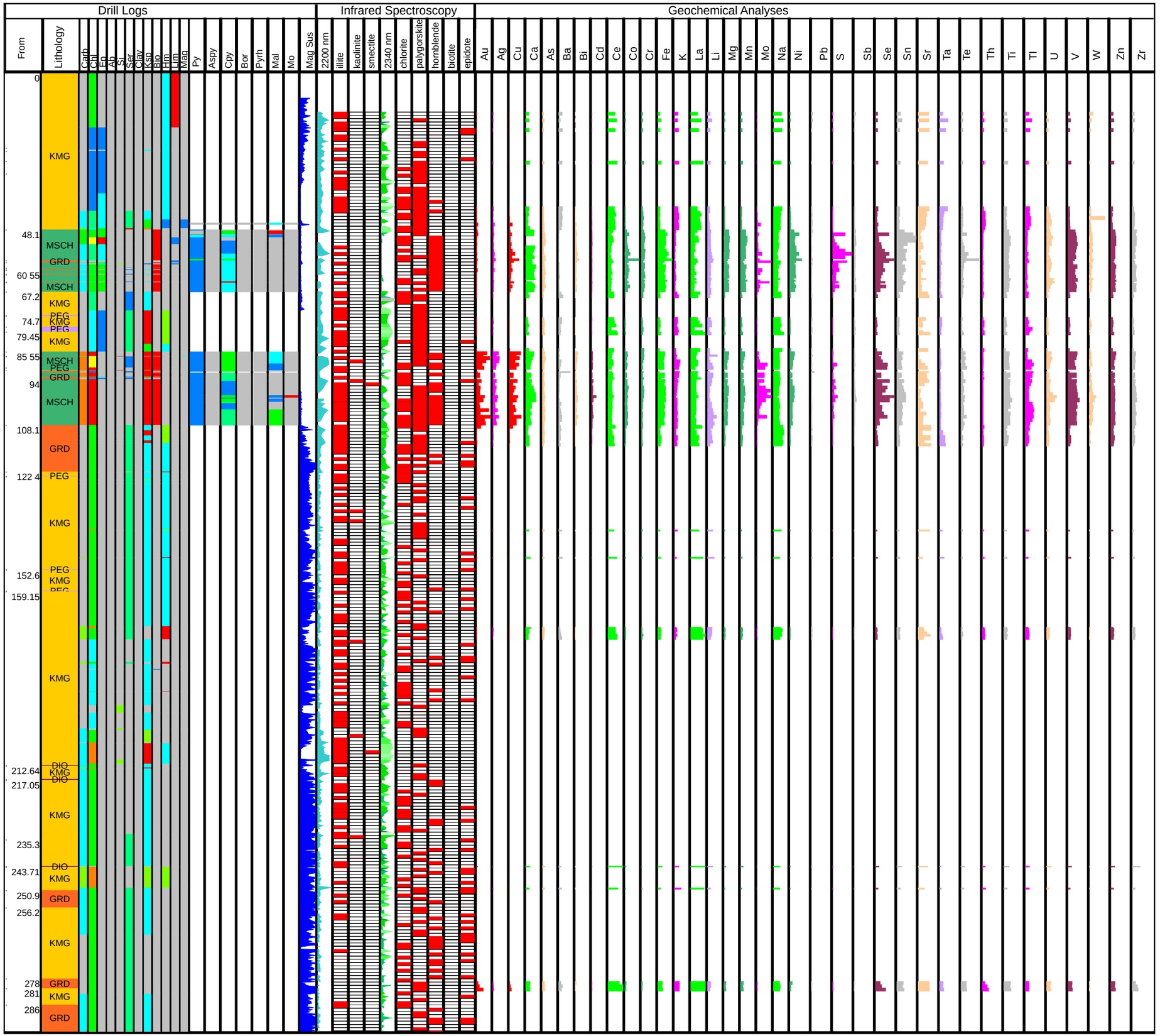
Drill Logs
Infrared Spectroscopy
Geochemical Analyses
From
Lithology
Carb
Chl
Ep
Ab
Sl
Ser
Clay
Ksp
Bio
Hm
Lim
Mag
Py
Aspy
Cpy
Bor
Pyrh
Mal
Mo
Mag Sus
2200 nm
illite
kaolinite
smectite
2340 nm
chlorite
palygorskite
hornblende
biotite
epidote
Au
Ag
Cu
Ca
As
Ba
Bi
Cd
Ce
Co
Cr
Fe
K
La
Li
Mg
Mn
Mo
Na
Ni
Pb
S
Sb
Se
Sn
Sr
Ta
Te
Th
Ti
Tl
U
V
W
Zn
Zr
0
KMG
48.1
MSCH
GRD
60 55
MSCH
67.2
KMG
74.7
PEG
KMG
PEG
79.45
KMG
85 55
MSCH
PEG
GRD
94
MSCH
108.1
GRD
122 4
PEG
KMG
152.6
PEG
KMG
159.15
KMG
212.64
DIO
KMG
217.05
DIO
KMG
235.3
243.71
DIO
KMG
250.9
GRD
256.2
KMG
278
GRD
281
KMG
286
GRD

WS08-10

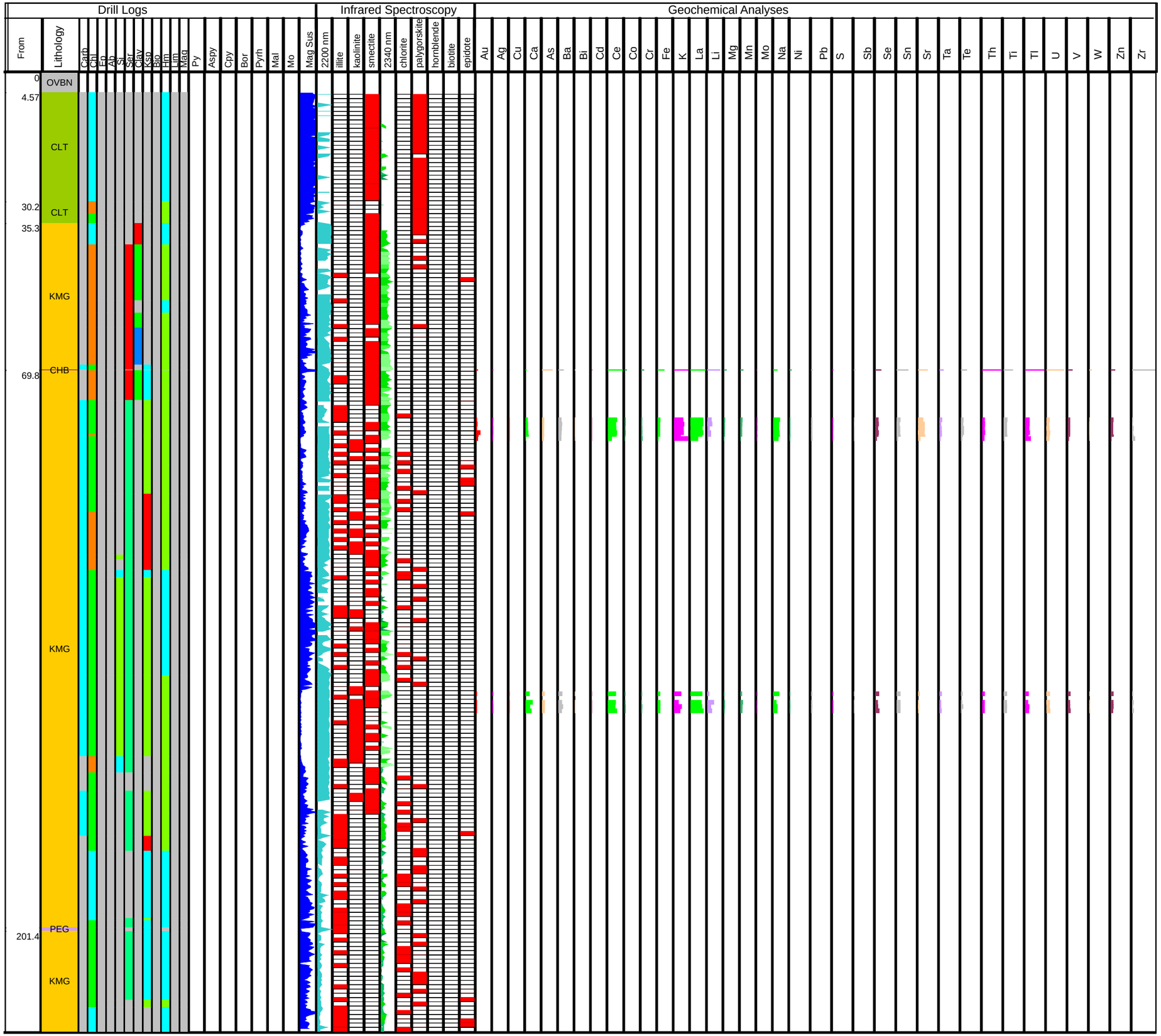
Drill Logs
Infrared Spectroscopy
Geochemical Analyses
From
Lithology
Carb
Chl
Ep
Alt
Ser
Clay
Ksp
Bio
Hm
Lim
Mag
Py
Aspy
Cpy
Bor
Pyrh
Mal
Mo
Mag Sus
2200 nm
illite
kaolinite
smectite
2340 nm
chlorite
palygorskite
hornblende
biotite
epidote
Au
Ag
Cu
Ca
As
Ba
Bi
Cd
Ce
Co
Cr
Fe
K
La
Li
Mg
Mn
Mo
Na
Ni
Pb
S
Sb
Se
Sn
Sr
Ta
Te
Th
Ti
Tl
U
V
W
Zn
Zr
0
4.57
30.2
35.3
69.8
201.4
OVBN
CLT
CLT
KMG
CHB
KMG
PEG
KMG

WS08-11

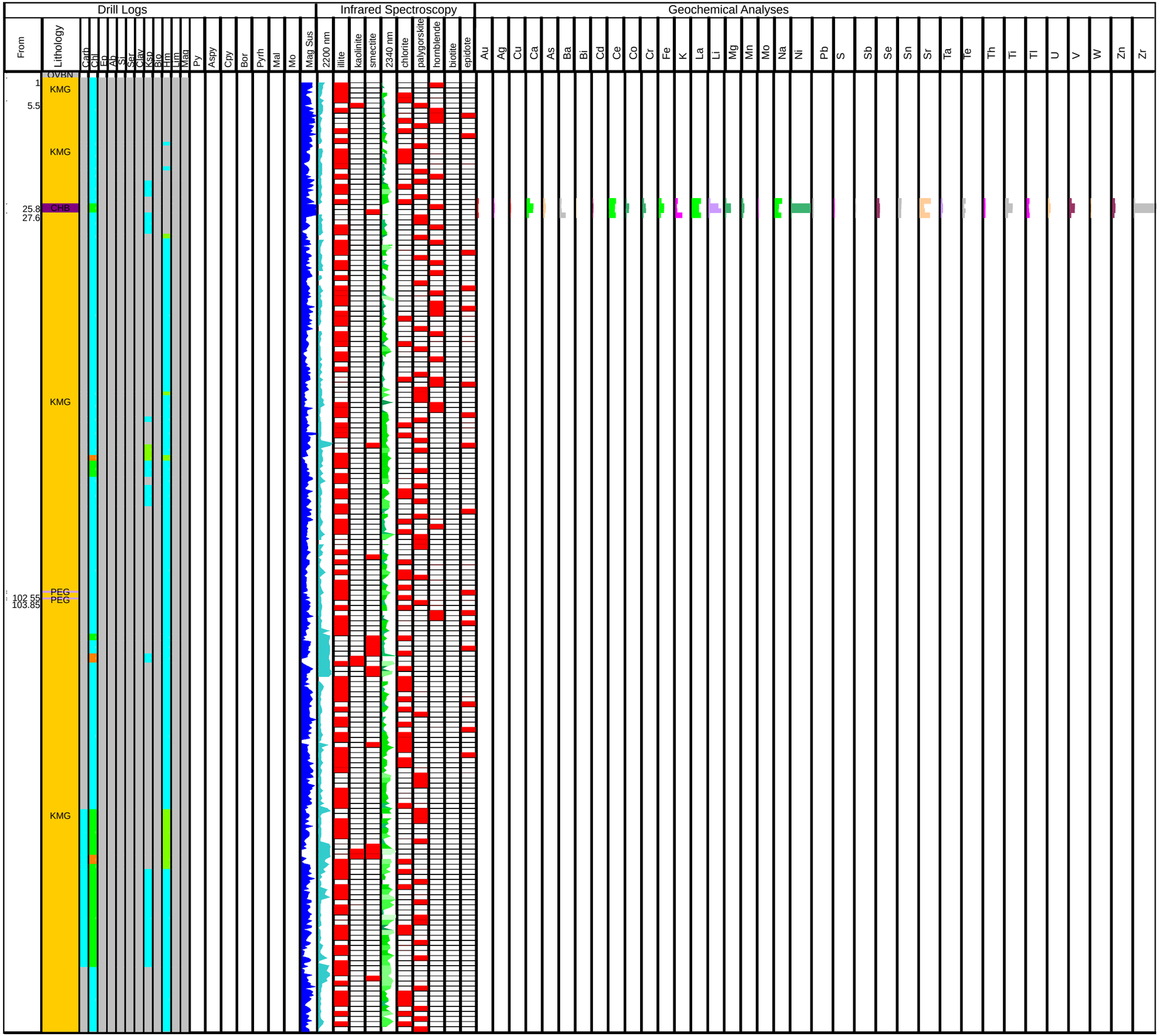

Drill Logs
Infrared Spectroscopy
Geochemical Analyses
From
Lithology
Carb
Chl
Ep
Ab
Si
Ser
Clay
Ksp
Bio
Hm
Lim
Mag
Py
Aspy
Cpy
Bor
Pyrh
Mal
Mo
Mag Sus
2200 nm
illite
kaolinite
smectite
2340 nm
chlorite
palygorskite
hornblende
biotite
epidote
Au
Ag
Cu
Ca
As
Ba
Bi
Cd
Ce
Co
Cr
Fe
K
La
Li
Mg
Mn
Mo
Na
Ni
Pb
S
Sb
Se
Sn
Sr
Ta
Te
Th
Ti
Tl
U
V
W
Zn
Zr
OVBN
1
KMG
5.5
KMG
25.8
CHB
27.6
KMG
PEG
102.55
PEG
103.85
KMG

WS08-12

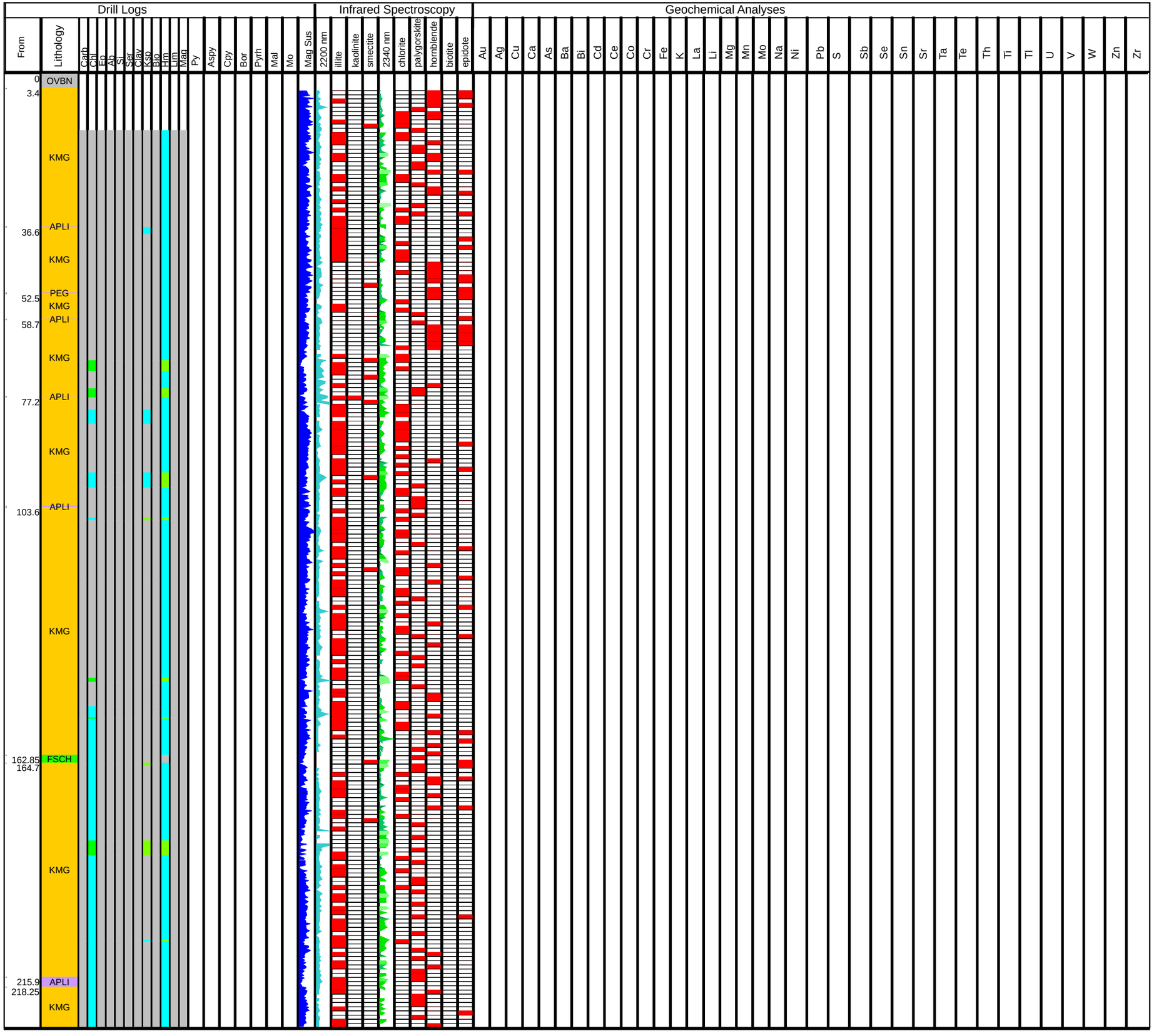
Drill Logs
Infrared Spectroscopy
Geochemical Analyses
From
Lithology
Carb
Chl
Ep
Ab
Sl
Ser
Clay
Ksp
Bio
Hm
Lim
Mag
Py
Aspy
Cpy
Bor
Pyrh
Mal
Mo
Mag Sus
2200 nm
illite
kaolinite
smectite
2340 nm
chlorite
palygorskite
hornblende
biotite
epidote
Au
Ag
Cu
Ca
As
Ba
Bi
Cd
Ce
Co
Cr
Fe
K
La
Li
Mg
Mn
Mo
Na
Ni
Pb
S
Sb
Se
Sn
Sr
Ta
Te
Th
Ti
Tl
U
V
W
Zn
Zr
0
OVBN
3.4
KMG
36.6
APLI
KMG
52.5
PEG
KMG
58.7
APLI
KMG
77.2
APLI
KMG
103.6
APLI
KMG
162.85
FSCH
164.7
KMG
215.9
APLI
218.25
KMG

APPENDIX VIII:
Petrographic Report
(Fonseca, 2009b)

SUMMARY REPORT ON THE

PETROGRAPHIC SURVEY OF DRILL CORE SAMPLES

FROM THE CARMACKS COPPER PROJECT,

YUKON TERRITORY

Petrographic report prepared

for

BCGold Corp.

1400-624 Howe St.
Vancouver, B.C. Canada

Prepared by:

Anna Fonseca, P.Geo.

804, Wood St.
Whitehorse YT Y1A 2G5
Canada

April 9, 2009

INTRODUCTION, SCOPE AND METHODOLOGY

A suite of 3 polished sections and 9 standard uncovered thin sections from BCGold Corp.'s 2008 diamond drilling program in the Carmacks Copper area, Yukon is described in this report. The samples were prepared into petrographic sections by Vancouver GeoTech Labs. Thin section billots were not available.

Infrared spectra were collected using Laurentian Goldfields' ASD Terraspec spectrometer and are described in a separate report. Multi-element geochemical analyses of the drill holes were made available to assist in this survey

Petrographic observations were done using a Leitz Ortholux II Pol-BK microscope. Digital photographs were taken using a Canon PowerShot S51S connected directly to a laptop. A minimum of six digital photographs were taken for each sample to illustrate the prinicpal features and mineralogy. The first photograph was always taken at the lowest magnification in order to display the characteristic texture and mineralogy of the sample. Modal abundances were done as visual estimates, and reflect the total volume of each mineral in the thin section (including veins and fine-grained groundmass). Observations were input into an Access database that contains a combination of memo and lookup fields for descriptions of hand specimen, lithology, structure, texture, primary and alteration minerals and opaques.

An absolute intensity was assigned for each secondary mineral on a scale of 1 (weak) to 4 (very strong). An alteration index (AI) was assigned for each secondary mineral in order to take into account the influence of primary mineralogy on the alteration intensity recorded. For instance, a mafic rock with abundant secondary epidote may be assigned an absolute epidote intensity of 4, whereas epidote alteration index may be 2 or 3. Furthermore, a sample with abundant chlorite that formed as a devitrification product of volcanic glass may be assigned an absolute chlorite intensity of 4, whereas the chlorite alteration index would be 0. Mineral alteration indexes were summed to produce a rock alteration index. In most cases a rock alteration index of 10 or higher is indicative of significant alteration. A rock alteration index of 8 or higher should be considered indicative of significant alteration.

Figures 1 and 2 are striplogs of drill holes WS-08-08 and WS-08-09B, from which the thin sections were prepared.

LITHOLOGIC CLASSIFICATION

Visual estimates of modal mineralogy were used for rock classification. Additional comments on uncertainties or possible protoliths were recorded and are presented beneath the Lithology field in the individual thin section reports. The modal mineralogy fields describe the entire current rock composition (i.e., it includes secondary metamorphic and hydrothermal alteration minerals). Where pseudomorphism is recognized, the rock name was given based on the inferred original rock composition.

Classification of igneous rocks were based on IUGS (International Union of the Geological Sciences) standard classification system developed by the Subcommission on the Systematics of Igneous Rocks in 1973 for igneous rocks with colour index smaller than 90.

Plutonic Lithologies

Granite and quartz-monzonite were identified in the sample suite. Plutonic rocks are equigranular, medium- to coarse-grained and unfoliated. Hornblende and biotite are the main mafic minerals, forming up to 22% of the rock. Sphene is present as an accessory. Sample CC08-06 presents a centimeter-scale mafic, strongly foliated band within undeformed granite.

"Volcanic" Lithologies

Quartz latite is the dominant "volcanic" lithology. Mafic minerals consist of hornblende, biotite, and minor sphene, forming up to 40% of the rock. "Volcanic" rocks are fine-grained and strongly foliated. It is possible that the mafic minerals are a product of metamorphism rather than primary.

DEFORMATION AND METAMORPHISM

Mafic "volcanic" lithologies are strongly deformed, displaying one to two well developed foliations defined by the alignment of mafic grains forming melanocratic domains. Strongly foliated domains in plutonic rocks (sample CC08-06) form bands that control the locus of intense alteration and sulphide mineralization.

ALTERATION AND MINERALIZATION

Veins

Albite+/-epidote veinlets are common in samples containing propylitic alteration. Calcite veinlets cut sample CC08-01. Fe-oxyhydroxides form fissure fill in sample CC08-11.

Sulphides

Pyrite and trace chalcopyrite occur along foliated domains and as fine-grained disseminations. Sulphides replace mafic grains in melanocratic foliation domains. Hematite and Fe-oxyhydroxides partly replace pyrite grains.

Hydrothermal Alteration

Sample CC08-01 has pervasive texture destructive carbonate-chlorite-clay-white mica alteration. Most of the remaining samples display a characteristic propylitic assemblage consisting of epidote+/-chlorite-opaques replacing mafic grains, albite partly replacing feldspars. Varying intensities of illite+/-kaolinite partly replace feldspars throughout the sample suite. The intensity of illite+/-kaolinite alteration is proportional to the intensity of propylitic alteration.
Sample CC08-09 contains a dense ferromagnesian phyllosilicate (palygorskite?) partly replacing hornblende. This may be the mineral producing the "palygorskite" spectral signature.

INTERPRETATIONS AND RECOMMENDATIONS

Interpretations

The principal control over alteration and sulphide deposition appears to be deformation zones or bands that coincide with mafic lithologies. Sample CC08-06 presents a centimeter-scale deformation band within undeformed granite. This deformation band has high mafic content and well developed foliation that is similar to the mafic quartz-latite samples. This suggests that "volcanic" units may constitute mafic segregations within the intrusive body that control the locus of deformation, thereby producing secondary permeability that allows hydrothermal fluid migration and sulphide deposition. Note that this interpretation is based strictly on petrographic observations of sample CC08-06, and should be challenged by more robust field or drill core logging observations and interpretations.

Recommendations

It is recommended that BCGoldcorp geologists perform a statistical analysis of drill hole logging data to test a direct correlation between deformation intensity, mafic content and mineralization.

REFERENCES

Streckeisen, A. L., 1974. Classification and Nomenclature of Plutonic Rocks. Recommendations of the IUGS Subcommission on the Systematics of Igneous Rocks. Geologische Rundschau. Internationale Zeitschrift für Geologie. Stuttgart. Vol.63, p.773-785.

Streckeisen, A. L., 1978. IUGS Subcommission on the Systematics of Igneous Rocks. Classification and Nomenclature of Volcanic Rocks, Lamprophyres, Carbonatites and Melilite Rocks. Recommendations and Suggestions. Neues Jahrbuch für Mineralogie, Abhandlungen, Vol. 141, 1-14.

STATEMENT OF QUALIFICATIONS

I, Anna Fonseca, P. Geo. certify that:

1. I have been involved in geological mapping and mineral exploration in British Columbia, Yukon, Alaska, Russia, and Mexico since 1994.

2. I am a graduate of the University of Alaska Fairbanks with a Degree in Geology (B.Sc., 1993) and I obtained a Masters of Science degree from the University of British Columbia in Mineral Exploration (M.Sc., 1998).

3. I am a member in good standing of the Association of Professional Engineers and Geoscientists of British Columbia.

4. I have previous experience in petrographic descriptions of strongly altered samples from porphyry deposits and prospects in British Columbia, Yukon, Mexico and the South American Cordillera.

5. I have previous field experience in the exploration and alteration mapping porphyry style mineralization.

6. I am the author of all sections of this report on Summary Report on Petrographic Survey of Drill Core Samples From the Carmacks Copper Project, Yukon.

7. I did not participate in geological fieldwork in the Carmacks Copper project of BCGold Corp, or in adjacent areas.

8. I have no direct or indirect interest in the properties or securities of BCGold Corp. or affiliated companies, nor do I expect to acquire such interest.

Dated April 9, 2009

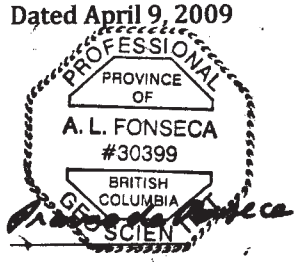

Anna Fonseca, P.Geo.

CC08-01 *Lithology:* ? *Alteration Assemblage:* intermediate argillic, carbonate *AI:* 20

Pervasive texture-destructive carbonate-chlorite-clay+/-illite alteration obliterates most primary textures and minerals.

DDH WS-08-08

Depth (m): 209.7

Mode Mineralogy

%		Source
35	*Quartz*	volcanic
	Plagioclase	
	Kspar	
12	*White Mica*	hydrothermal1
15	*Clay*	hydrothermal1
20	*Carbonate*	hydrothermal1
	Biotite	
	Epidote	
15	*Chlorite*	hydrothermal1
3	*Opaques*	hydrothermal1
	Fe-oxyhydroxi	
	Cu-silicates	
	Cu-carbonates	
0		
0		
0		
0		

Texture 1

Texture 2

Grain Size medium grained (>0.25<2mm)

Structure penetrative foliation

Strength: well developed

Modal Mineralogy Comments

Quartz is the only primary mineral, forming interfingering grains that define two well developed foliation. Felspars originally formed up to 40% of the rock, but are completely converted to carbonate-clay-illite. Mafics (likely pyroxenes) are completely converted to chlorite-carbonate+/-clay.

Veins

	Mineral 1	*Mineral 2*	*Mineral 3*	*Envelope*
Vein 1	Calcite			
Vein 2				
Vein 3				

carbonate+/-clay veinlets <3 mm wide

Opaque Mineralogy

%	Opaque	How
	Hema	
0	*Mag*	
0	*Py*	
	Po	
0	*Cpy*	
	Moly	
	Asp	
	Sph	
	Gn	

Secondary Mineralogy

	Mineral Intensity	How	How 2	AI
White Mica	very strong	pervasive		5
Carb.	very strong	pervasive		5
Clay	very strong	pseudomorph	pervasive	5
Epidote				
Chlorite	very strong	pervasive	pseudomorph	5
Albite				
Biotite				
Kspar				
Quartz				
Fe-oxihydrox				
Cu-Silicate				
Cu-Carbonate				

Alteration Comments

Very strong pervasive, texture destructive to locally pseudomorphic carbonate-chlorite completely replaces mafic grains. Very strong pervasive, texture destructive illite-carbonate-clay completely replaces feldspars. Interpretation: The clay-chlorite may represent a retrograde overprint over potassic alteration.

CC08-01

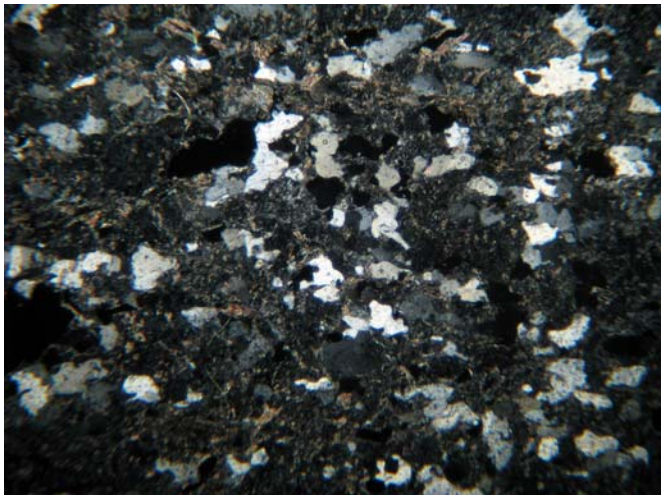

CC08-01_001 FOV (mm): 6 Crossed polars

Two well developed foliations defined by mineral alignment: lower left to upper right and upper left to lower right.

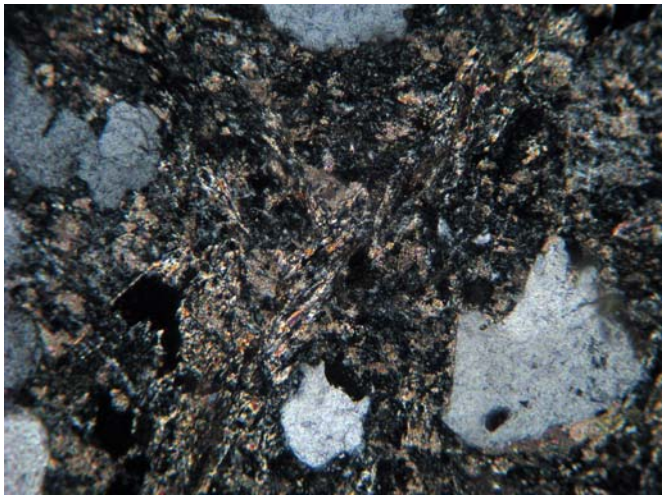

CC08-01_002 FOV (mm): 1.7 Crossed polars

Intense carbonate, white mica and chlorite completely replace primary mafic grains.

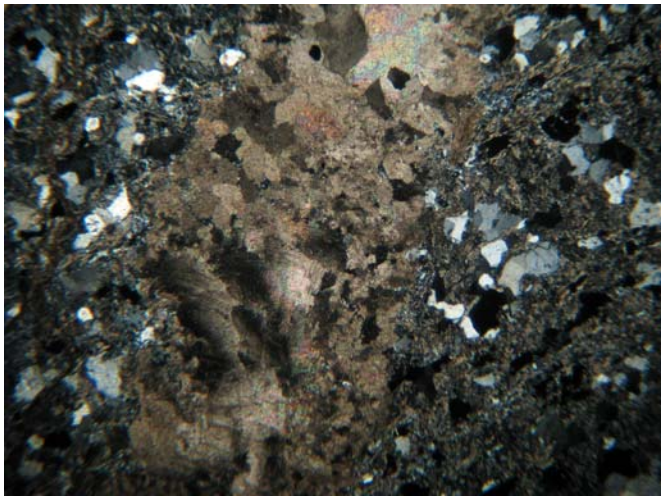

CC08-01_003 FOV (mm): 6 Crossed polars

Carbonate veinlet with local feathery calcite texture.



CC08-01_004 FOV (mm): 1.7 Crossed polars

Carbonate-chlorite-clay and lesser opaques completely replace primary mafic grains.

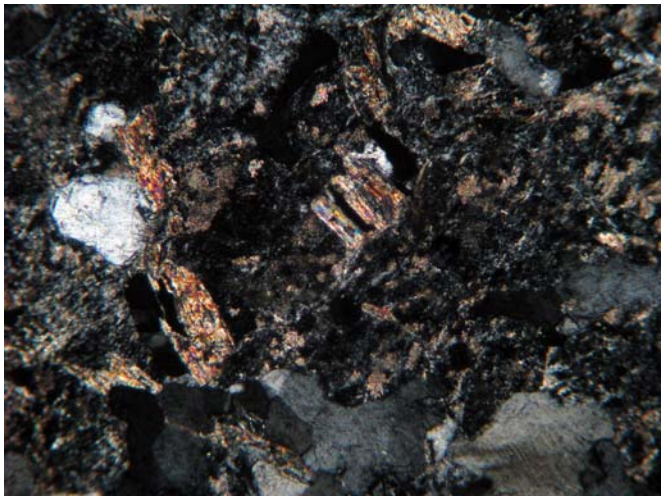

CC08-01_005 FOV (mm): 1.7 Crossed polars

Locally white mica (illite) forms pseudomorphic replacements after prismatic grains.

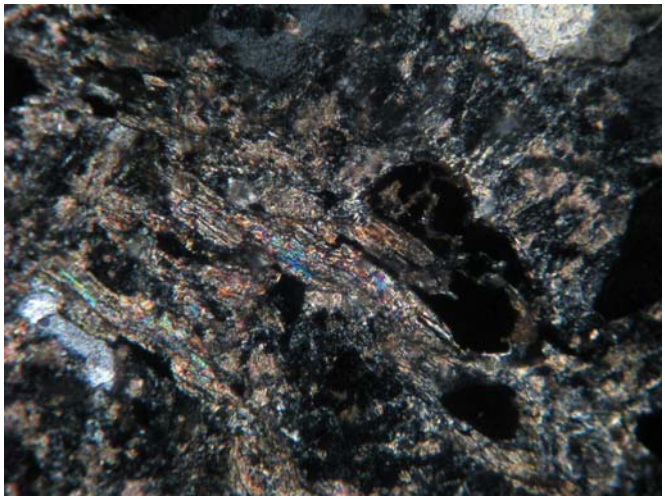

CC08-01_006 FOV (mm): 1.7 Crossed polars

Mafic grains are completely replaced by chlorite-carbonate-clay.

CC08-02 *Lithology:* Quartz latite *Alteration Assemblage:* *AI:* 0

DDH WS-08-08

Depth (m): 262.7

Mode Mineralogy

%		Source
8	*Quartz*	volcanic
15	*Plagioclase*	volcanic
12	*Kspar*	volcanic
	White Mica	
	Clay	
1	*Carbonate*	hydrothermal1
12	*Biotite*	volcanic/metamorp
1	*Epidote*	volcanic
0	*Chlorite*	hydrothermal1
5	*Opaques*	metamorphic?
	Fe-oxyhydroxi	
	Cu-silicates	
	Cu-carbonates	
1	*Sphene*	volcanic
45	*Hornblende*	volcanic
0		
0		

Texture 1 polygonal texture *Structure* penetrative foliation

Texture 2 *Strength:* very strongly developed

Grain Size medium grained (>0.25<2mm)

Modal Mineralogy Comments

Subhedral to euhedral stubby hornblende prismatic and pinacoidal sections <1.5 mm have well developed amphibole cleavages and form the dominant mineral phase in this sample. Biotite forms elongate subhedral laths <0.8 mm, associated with hornblende. Quartz and felspars have foam (polygonal) texture and form small grains <0.3 mm defining subordinate leucocratic domains in the foliation.

Veins

	Mineral 1	Mineral 2	Mineral 3	Envelope
Vein 1				
Vein 2				
Vein 3				

Opaque Mineralogy

%	Opaque	How
	Hema	
	Mag	
5	*Py*	subhedral
	Po	
0	*Cpy*	disseminated
	Moly	
	Asp	
	Sph	
	Gn	

<5% subhedral pyrite replacing mafic grains that define the foliation and as sparse disseminations. Trace very fine-grained disseminated chalcopyrite. Trace hematite disseminated.

Secondary Mineralogy

	Mineral Intensity	How	How 2	AI
White Mica				
Carb.	very weak	fracture filled		0
Clay				
Epidote				
Chlorite	very weak	fracture filled		0
Albite				
Biotite				
Kspar				
Quartz				
Fe-oxihydrox				
Cu-Silicate				
Cu-Carbonate				

Alteration Comments

Unaltered amphibole grade metamorphic rock. Trace chlorite-carbonate heals fractures in feldspars adjacent to opaques.

CC08-02



CC08-02_001 FOV (mm): 6 Plane polarized light

Metamorphic biotite, hornblende, feldspars and quartz define the foliation.

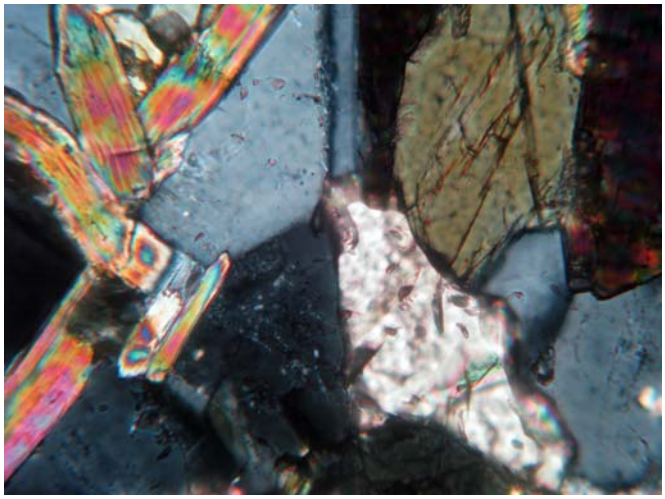

CC08-02_002 FOV (mm): 0.4 Crossed polars

Subhedral sphene (lower left, pink-beige birrefringence).

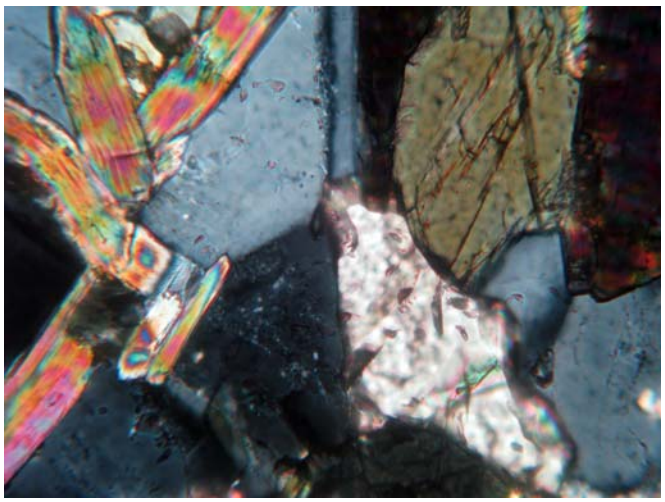

CC08-02_003 FOV (mm): 0.4 Crossed polars

Foam texture in quartzofeldspathic grains.

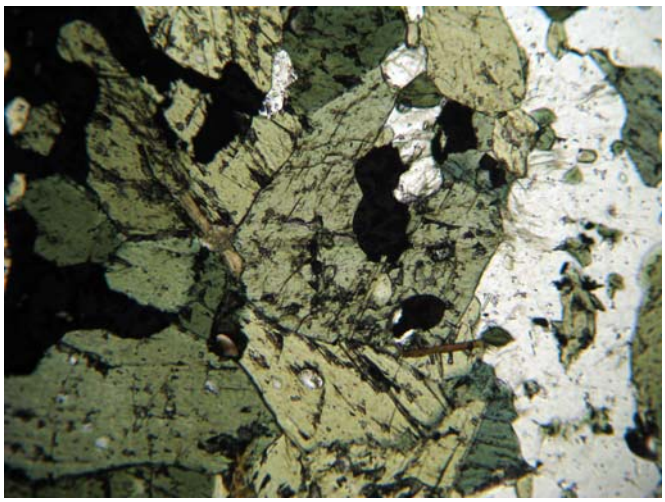

CC08-02_004 FOV (mm): 1.7 Plane polarized light

Opaques (black extinct) intergrown with hornblende.



CC08-02_005 FOV (mm): 0.4 Crossed polars

Euhedral epidote grains adjacent to opaques.

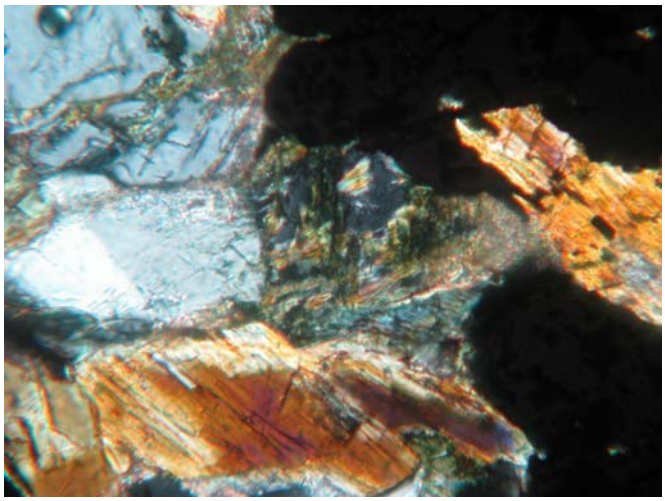

CC08-02_006 FOV (mm): 0.4 Crossed polars

Weak fine-grained chlorite-carbonate partly healing fractures in feldspars.

CC08-02

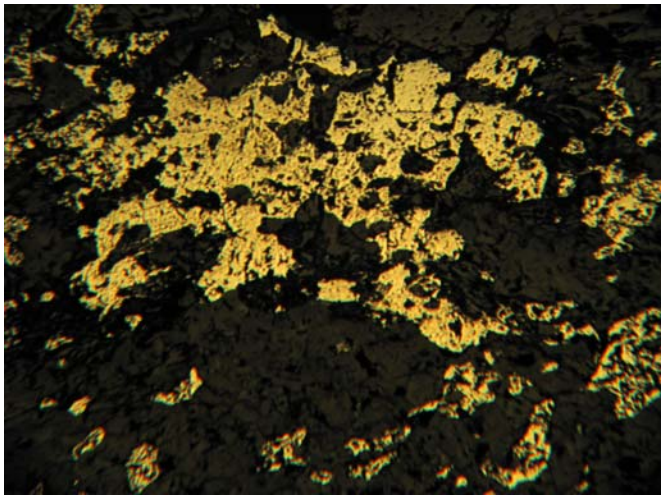

CC08-02_007 FOV (mm): 4 Reflected light.

Subhedral to anhedral pyrite aligned along the dominant foliation.

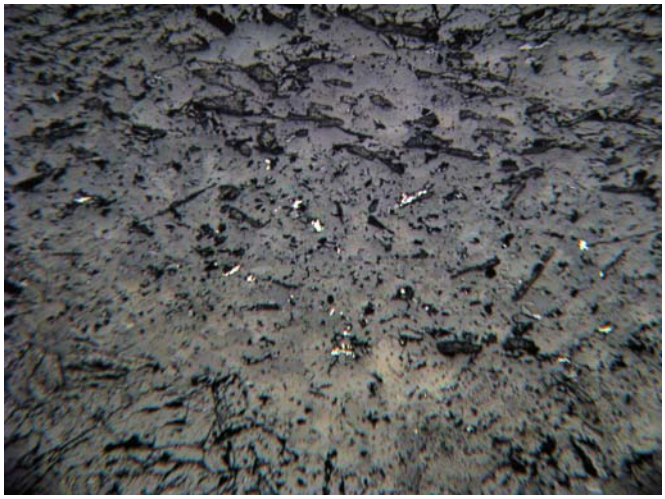

CC08-02_008 FOV (mm): 4 Reflected light.

Very fine-grained disseminated pyrite and trace chalcopyrite along the dominant foliation.

CC08-03 ***Lithology:*** Quartz monzonite ***Alteration Assemblage:*** propylitic(?) ***AI:*** 11

hornblende-quartz-monzonite

DDH WS-08-09B

Depth (m): 84.8

Mode Mineralogy

%		Source
8	*Quartz*	plutonic
40	*Plagioclase*	plutonic
30	*Kspar*	plutonic
2	*White Mica*	hydrothermal1
6	*Clay*	hydrothermal1
	Carbonate	
	Biotite	
3	*Epidote*	hydrothermal+pluto
7	*Chlorite*	hydrothermal1
1	*Opaques*	hydrothermal1
	Fe-oxyhydroxi	
	Cu-silicates	
	Cu-carbonates	
3	*Hornblende*	plutonic
0		
0		
0		

Texture 1 equigranular ***Structure***

Texture 2 ***Strength:***

Grain Size coarse grained (>2<16 mm)

Modal Mineralogy Comments

Medium-grained plutonic rock with subhedral plagioclase and kspar grains <4 mm, subordinate anhedral quartz grains <0.3 mm, subhedral to anhedral hornblende prisms < 3 mm, and euhedral to subhedral epidote.

Veins

	Mineral 1	*Mineral 2*	*Mineral 3*	*Envelope*
Vein 1	albite?			
Vein 2				
Vein 3				

discontinuous albite veinlets

Opaque Mineralogy

%	Opaque	How
	Hema	
0	*Mag*	
0	*Py*	
	Po	
0	*Cpy*	
	Moly	
	Asp	
	Sph	
	Gn	

Secondary Mineralogy

	Mineral Intensity	How	How 2	AI
White Mica	very weak	domainal		1
Carb.				
Clay	moderate	pseudomorph		3
Epidote	moderate	pseudomorph		2
Chlorite	very strong	pseudomorph		4
Albite	very weak	fracture filled		1
Biotite				
Kspar				
Quartz				
Fe-oxihydrox				
Cu-Silicate				
Cu-Carbonate				

Alteration Comments

Very strong pseudomorphic chlorite replacing hornblende along cleavage planes or completely replacing hornblende. Moderate clay (kaolinite) and very weak illite partly replacing feldspars. Moderate epidote partly replacing hornblende

CC08-03

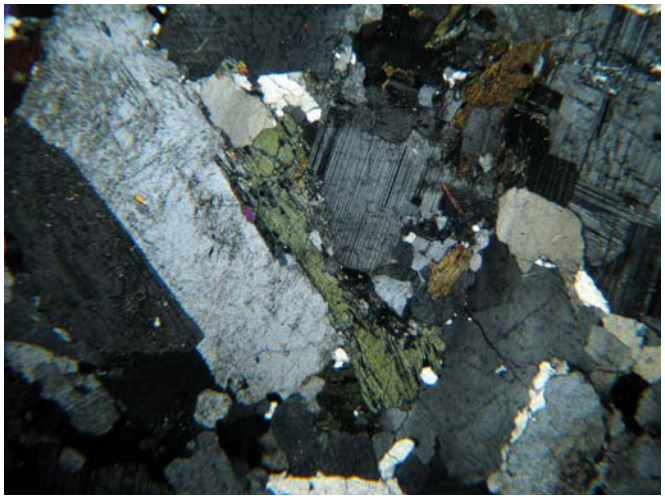

CC08-03_001 FOV (mm): 6 Crossed polars

Medium- to coarse grained seriate textured rock with sparse anhedral to subhedral hronblende, abundant feldspars, lesser quartz and minor epidote.

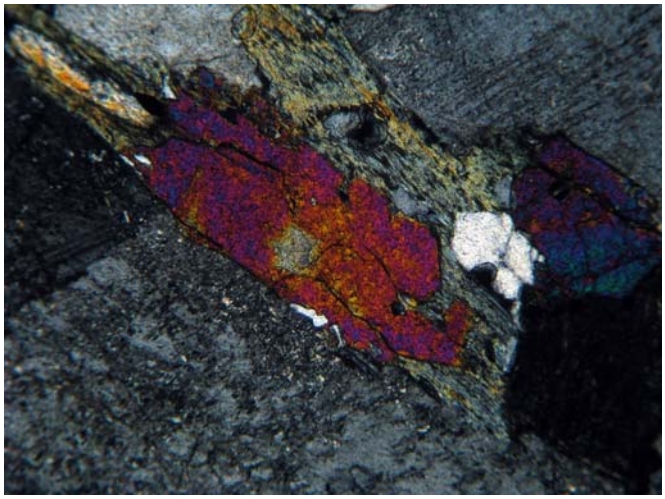

CC08-03_002 FOV (mm): 1.7 Crossed polars

Subhedral epidote and chlorite replacing primary mafic grains, and fine-grained kaolinite+/-illite partly replace feldspars.

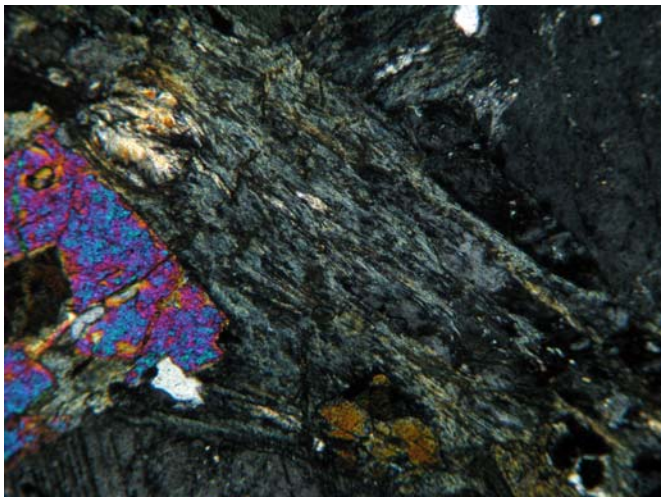

CC08-03_003 FOV (mm): 1.7 Crossed polars

Dark blue-green chlorite, epidote (bright birrefringence) and white mica (or palygosrkite - yellow-white birrefringence) completely replace mafic grains.

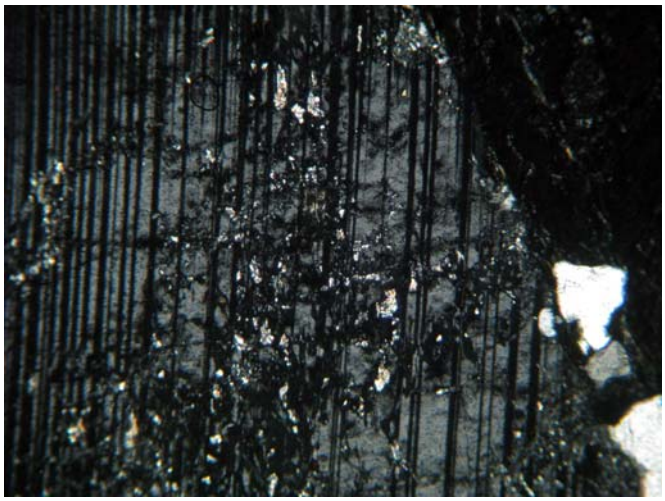

CC08-03_004 FOV (mm): 1.7 Crossed polars

Fine-grained kaolinite partly replaces plagioclase.

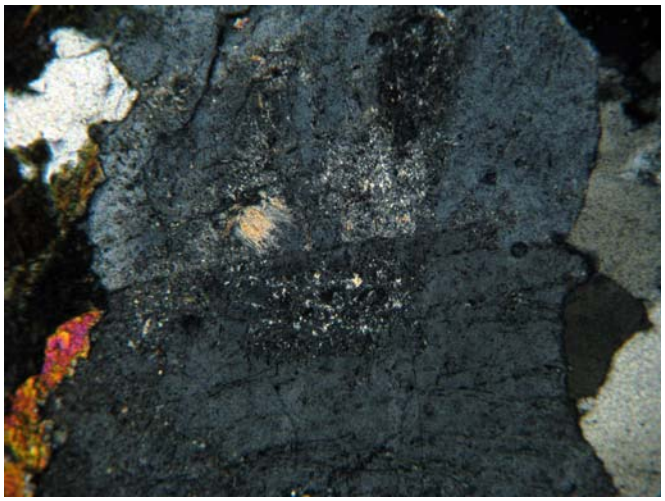

CC08-03_005 FOV (mm): 1.4 Crossed polars

Weak illite and kaolinite replacing potassic feldspar.

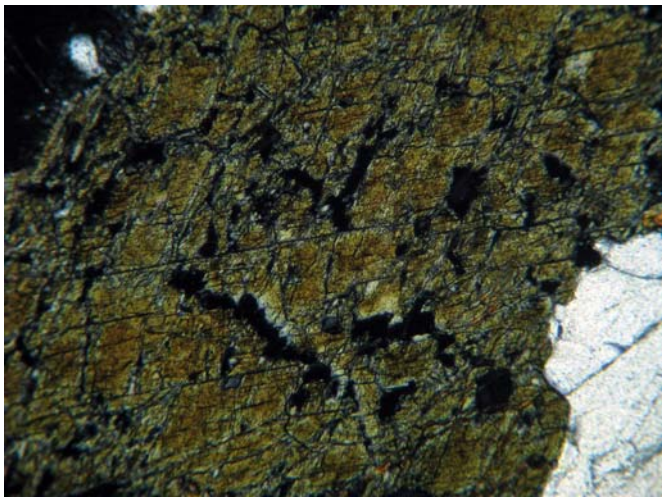

CC08-03_006 FOV (mm): 1.7 Crossed polars

Relic hornblende moderately replaced by chlorite along fractures.

CC08-04 *Lithology:* Quartz latite *Alteration Assemblage:* intermediate argillic *AI:* 6

Amphibolite grade metamorphic rock with actinolite as the dominant mineral phase. Protolith is likely mafic volcanic or mafic plutonic rock.

DDH WS-08-09B

Depth (m): 85.5

Mode Mineralogy

%		Source
3	*Quartz*	volcanic
7	*Plagioclase*	volcanic
18	*Kspar*	volcanic
3	*White Mica*	hydrothermal1
5	*Clay*	hydrothermal1
	Carbonate	
	Biotite	
1	*Epidote*	hydrothermal1
	Chlorite	
1	*Opaques*	hydrothermal1
1	*Fe-oxyhydroxi*	hydrothermal1
	Cu-silicates	
	Cu-carbonates	
58	*Hornblende*	volcanic?
1	*Sphene*	volcanic
1	*Zircon*	volcanic
1	*apatite*	volcanic

Texture 1

Texture 2

Grain Size medium grained (>0.25<2mm)

Structure penetrative foliation

Strength: well developed

Modal Mineralogy Comments

Green amphibole (hornblende; possibly actinolite - extinction angle <20 degrees) is the dominant mineral phase, forming euhedral to subhedral prismatic grains <1mm. Feldspars (kspar>plagioclase) form anhedral grains <0.6 mm. Quartz forms sparse, very small (<0.2 mm) anhedral grains. Zircon, apatite, and sphene form sparse subhedral grains.

Veins

	Mineral 1	*Mineral 2*	*Mineral 3*	*Envelope*
Vein 1	Albite			
Vein 2				
Vein 3				

albite veinlets with Fe-oxyhydroxides and minor zoisite (epidote) along contacts.

Opaque Mineralogy

%	Opaque	How
	Hema	
0	*Mag*	
1	*Py*	disseminated
	Po	
0	*Cpy*	
	Moly	
	Asp	
	Sph	
	Gn	

<1% anhedral pyrite associated with Fe-oxyhydroxides (hematite) and locally replacing the core of hornblende grains.

Secondary Mineralogy

	Mineral Intensity	How	How 2	AI
White Mica	moderate	pseudomorph		3
Carb.				
Clay	moderate	pseudomorph		3
Epidote				
Chlorite				
Albite				
Biotite				
Kspar				
Quartz				
Fe-oxihydrox				
Cu-Silicate				
Cu-Carbonate				

Alteration Comments

Moderate kaolinite-illite partly replacing feldspars and producing a dusty aspect.

CC08-04

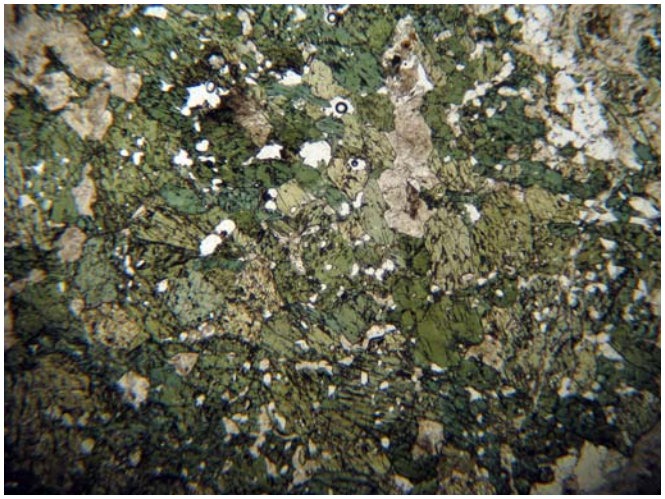

CC08-04_001 FOV (mm): 6 Plane polarized light

Green metamorphic hornblende/actinolite is the dominant constituent of this rock. Note the cloudy aspect of feldspars.

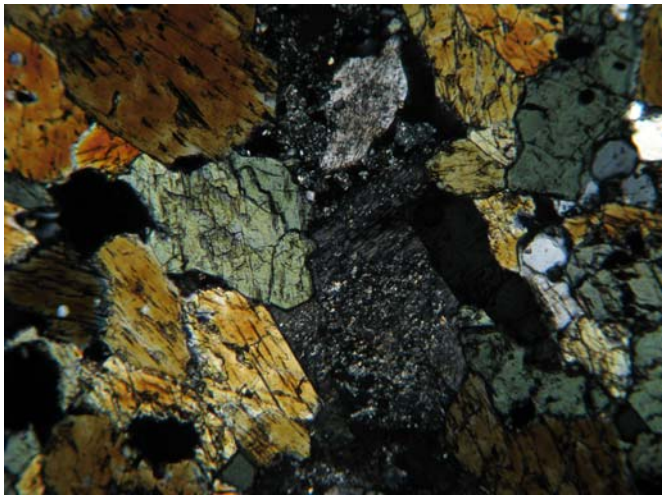

CC08-04_002 FOV (mm): 1.7 Crossed polars

Feldspars (grey, centre) are strongly to moderately affected by illite-kaolinite alteration.

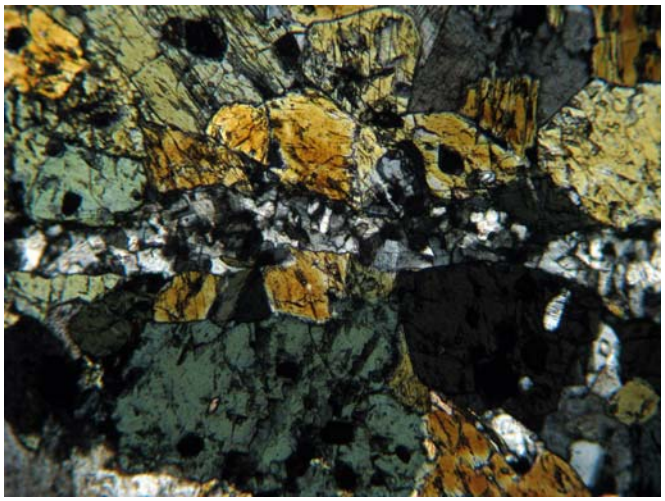

CC08-04_003 FOV (mm): 1.7 Crossed polars

Albite veinlet.

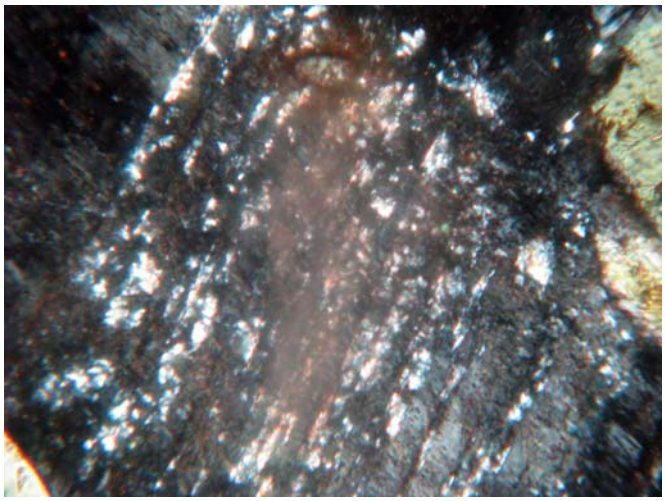

CC08-04_004 FOV (mm): 0.4 Crossed polars

Illite-clay altered plagioclase.

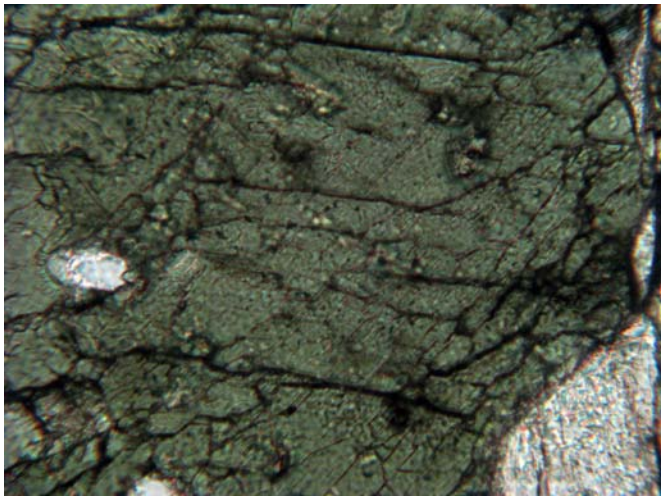

CC08-04_005 FOV (mm): 0.4 Plane polarized light

Typical amphibole cleavages in hornblende/actinolite.

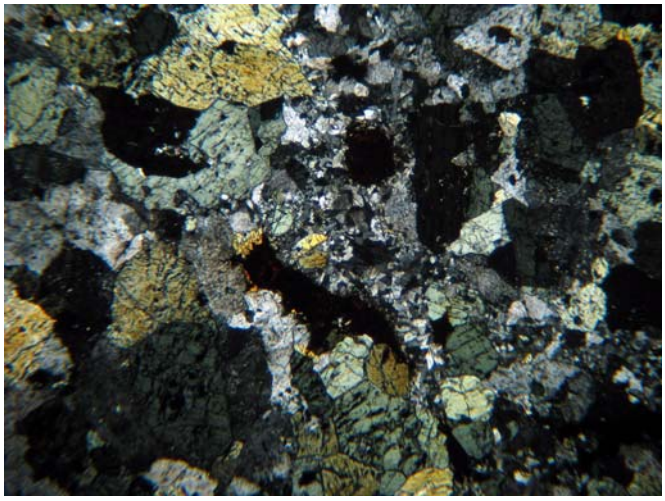

CC08-04_006 FOV (mm): 6 Crossed polars

Fe-oxyhydroxide in and along contacts of an albite veinlet.

CC08-04

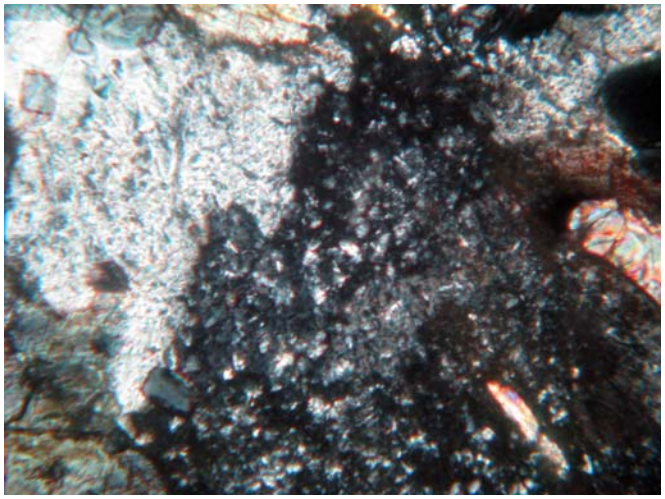

CC08-04_007 FOV (mm): 0.4 Crossed polars

Fine-grained kaolinite partly replacing kspar.

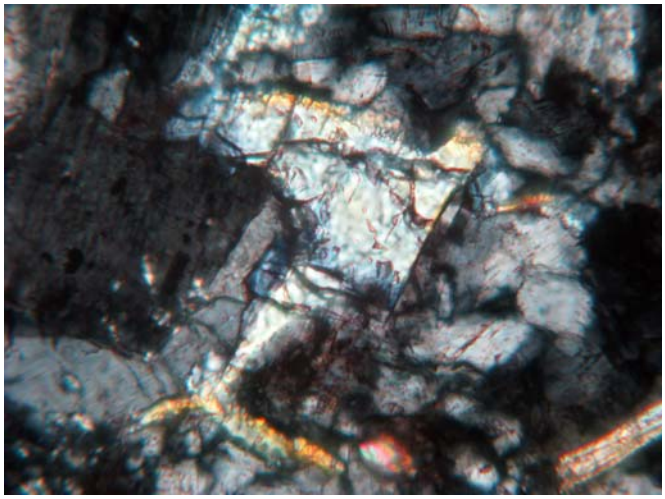

CC08-04_008 FOV (mm): 0.4 Crossed polars

Zoisite (blue and yellow birrefringence) along contacts of an albite veinlet.

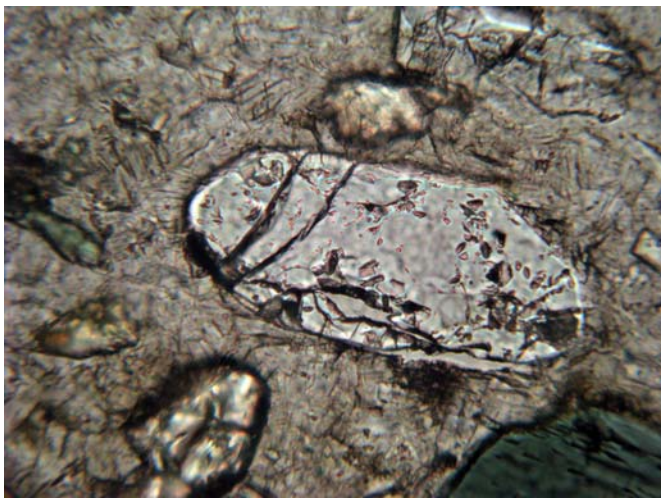

CC08-04_009 FOV (mm): 0.4 Plane polarized light

Clear rounded prismatic apatite with fluid inclusions (pinkish).

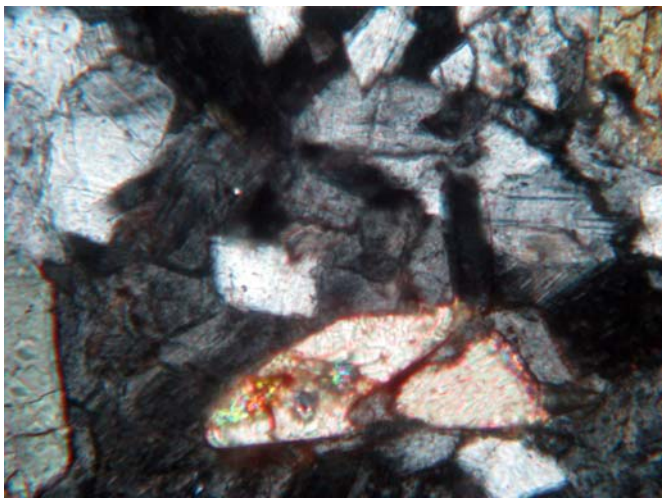

CC08-04_010 FOV (mm): 0.4 Crossed polars

Subhedral to euhedral sphene.

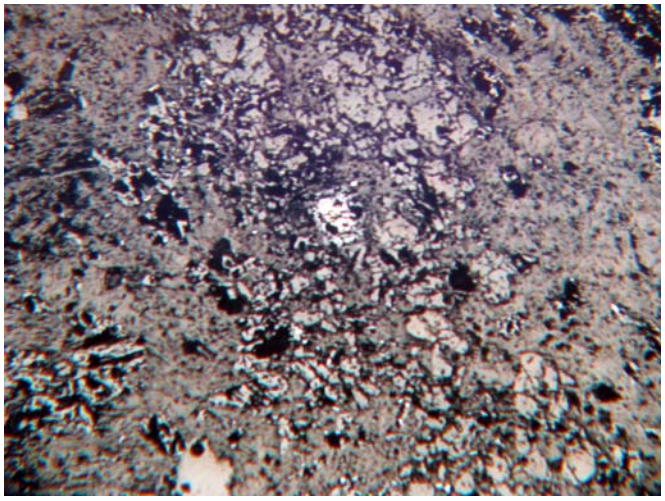

CC08-04_011 FOV (mm): 4 Reflected light.

Pyrite grain replacing the core of a hornblende crystal.

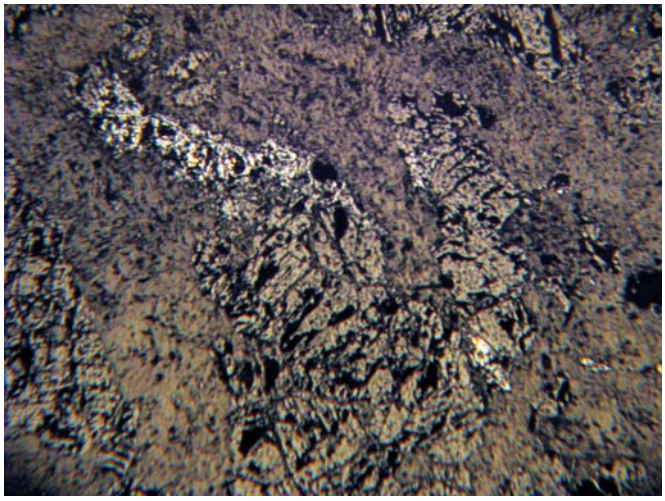

CC08-04_012 FOV (mm): 4 Reflected light.

Pyrite surrounded by grey reflectance Fe-oxyhydroxide.

CC08-05 *Lithology:* Quartz latite *Alteration Assemblage:* intermediate argillic *AI:* 13

Amphibolite grade metamorphic rock with actinolite as the dominant mineral phase. Protolith is likely mafic volcanic or mafic plutonic rock.

DDH WS-08-09B

Depth (m): 90

Mode Mineralogy

%		Source
3	*Quartz*	volcanic
10	*Plagioclase*	volcanic
18	*Kspar*	volcanic
3	*White Mica*	hydrothermal1
7	*Clay*	hydrothermal1
	Carbonate	
	Biotite	
2	*Epidote*	hydrothermal1
	Chlorite	
1	*Opaques*	hydrothermal1
3	*Fe-oxyhydroxi*	weathering
	Cu-silicates	
	Cu-carbonates	
7	*Augite*	volcanic
45	*Hornblende*	volcanic
1	*Sphene*	volcanic
0		

Texture 1 poikilitic *Structure* penetrative foliation

Texture 2 *Strength:* well developed

Grain Size medium grained (>0.25<2mm)

Modal Mineralogy Comments

Hornblende is the dominant mineral, forming subhedral to anhedral prismatic grains <4 mm with common poikilitic texture (quartz and feldsar inclusions). Augite forms sparse anhedral to subhedral prismatic grains. Kspar and lesser plagioclase are anhedral and strongly replaced by kaolinite+/-illite and Fe-oxyhydroxides. Quartz forms anhedral grains <0.2 mm.

Veins

	Mineral 1	Mineral 2	Mineral 3	Envelope
Vein 1				
Vein 2				
Vein 3				

Opaque Mineralogy

%	Opaque	How
	Hema	
0	*Mag*	
1	*Py*	disseminated
	Po	
0	*Cpy*	
	Moly	
	Asp	
	Sph	
	Gn	

<1% disseminated pyrite is strongly replaced by Fe-oxyhydroxides.

Secondary Mineralogy

Mineral	Intensity	How	How 2	AI
White Mica	weak	pseudomorph		2
Carb.				
Clay	strong	pseudomorph		4
Epidote	moderate	disseminated		3
Chlorite				
Albite				
Biotite				
Kspar				
Quartz				
Fe-oxihydrox	strong			4
Cu-Silicate				
Cu-Carbonate				

Alteration Comments

Moderate disseminated epidote associated with opaques and open-space fill Fe-oxyhydroxides. Strong kaolinite and lesser white mica partly replace feldspars, producing a grungy aspect.

CC08-05

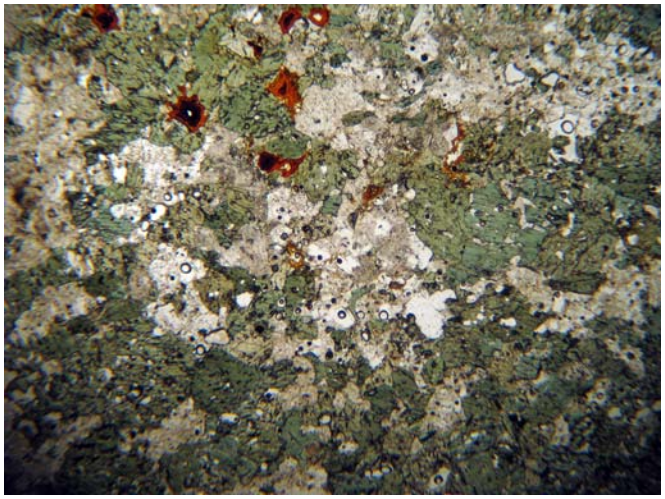

CC08-05_001 FOV (mm): 6 Plane polarized light

Green hornblende/actinolite is the dominant mafic mineral in this rock. Sparse, late Fe-oxyhydroxides occur throughout the sample.

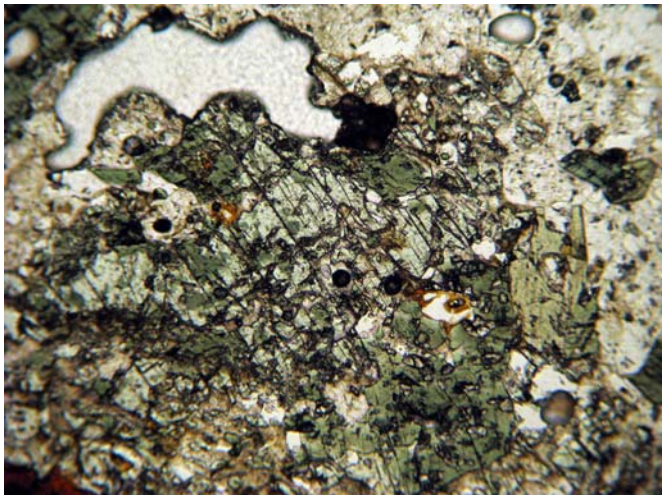

CC08-05_002 FOV (mm): 1.7 Plane polarized light

Green hornblende/actinolite forms replacement spots on clear augite.

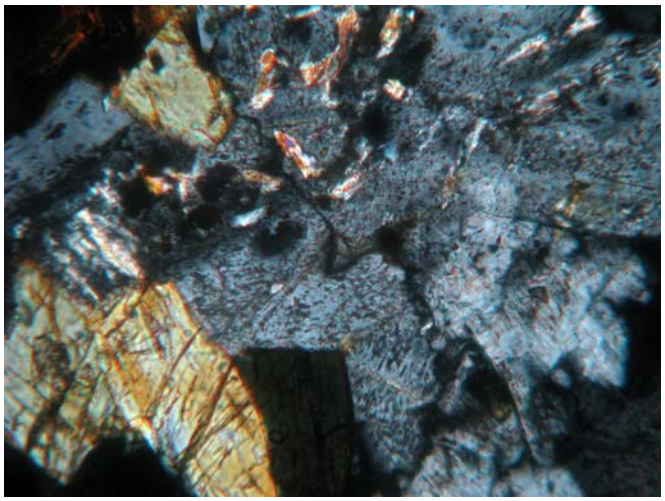

CC08-05_003 FOV (mm): 0.4 Crossed polars

Fine-grained illite and Fe-oxyhydroxides partly replace feldspars.

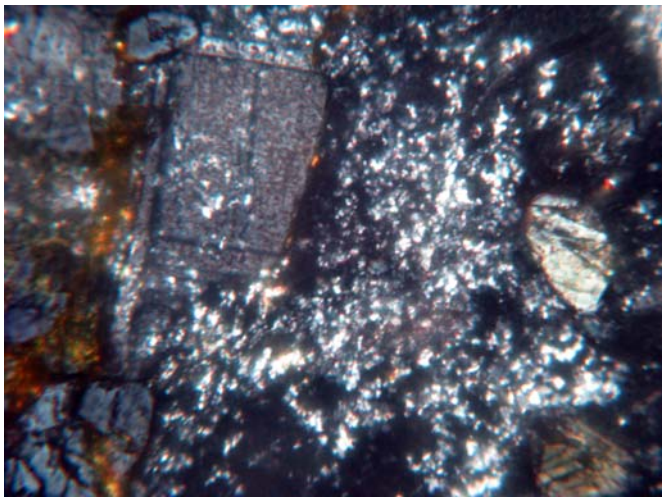

CC08-05_004 FOV (mm): 0.4 Crossed polars

Fine-grained kaolinite and lesser illite partly replace feldspars. Orange-brown Fe-oxyhydroxides fill fractures.

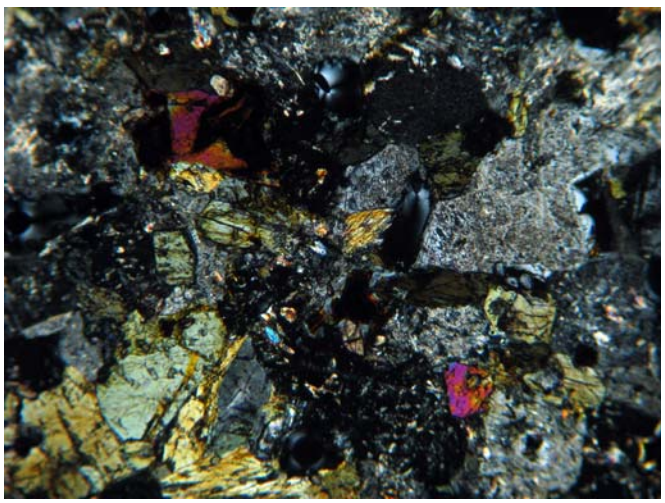

CC08-05_005 FOV (mm): 0.4 Crossed polars

Epidote (high birrefringence colours occurs in sites that are associated with open-space filling Fe-oxyhydroxides.

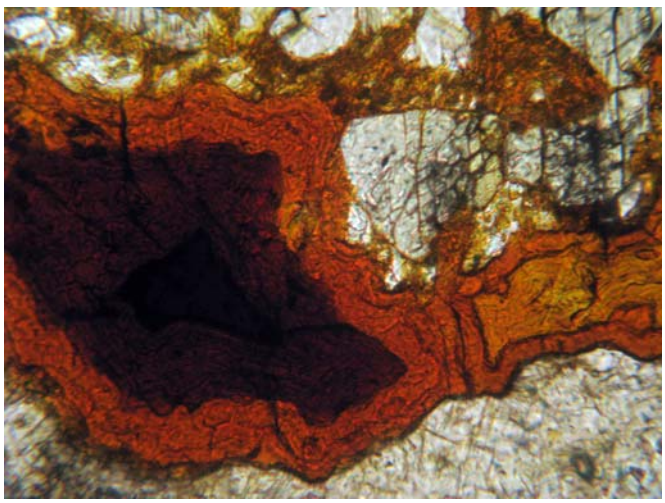

CC08-05_006 FOV (mm): 0.4 Plane polarized light

Open space fill crustiform texture of Fe-oxyhydroxides surrounding an opaque grain.

CC08-05

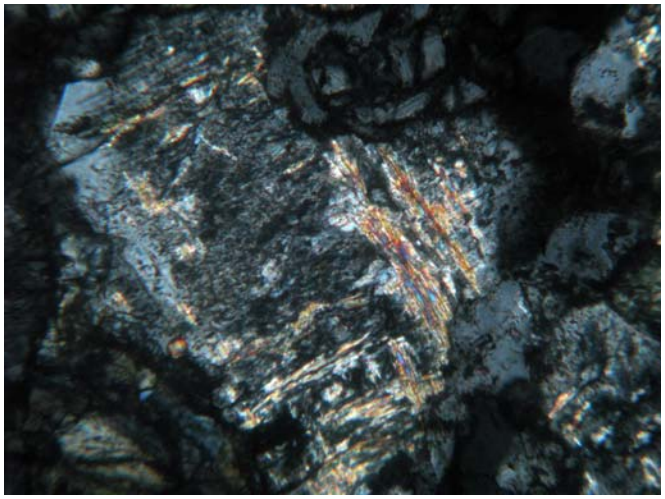

CC08-05_007 FOV (mm): 0.4 Crossed polars

Fine-grained white mica (illite) and kaolinite partly replacing a kspar grain.

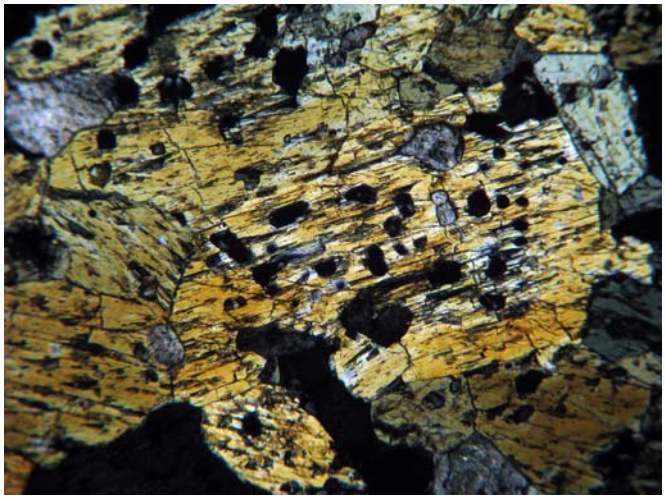

CC08-05_008 FOV (mm): 0.4 Crossed polars

Poikilitic texture in hornblende/actinolite.

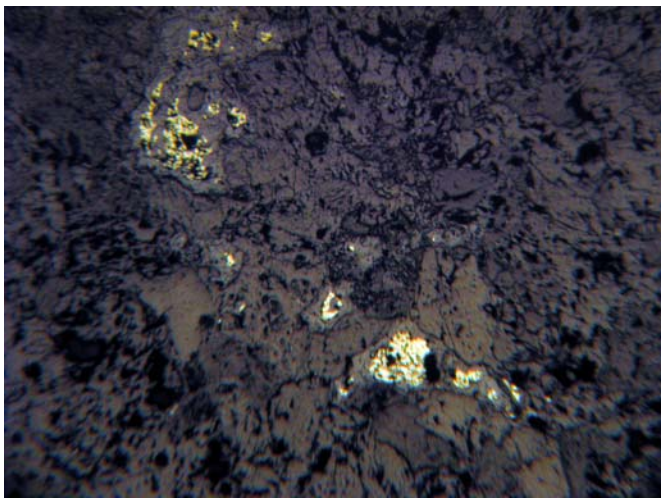

CC08-05_009 FOV (mm): 4 Reflected light.

Pyrite is partly replaced by Fe-oxyhydroxides.

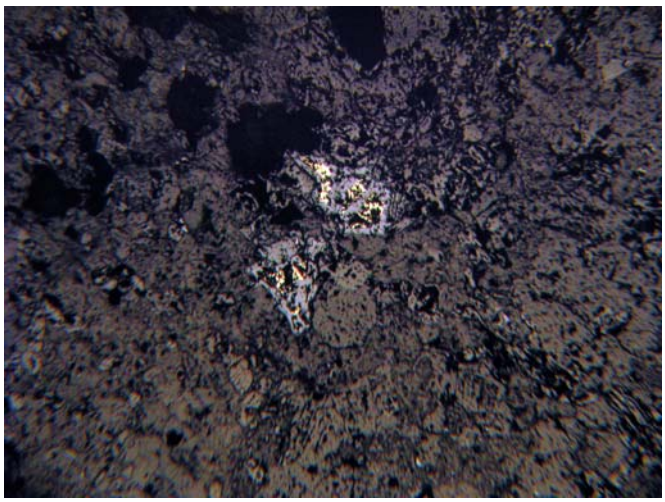

CC08-05_010 FOV (mm): 4 Reflected light.

Pyrite is strongly replaced by Fe-oxyhydroxides.

CC08-06 *Lithology:* granite and schist *Alteration Assemblage:* intermediate argillic *AI:* 16

The thin section contains domains of undeformed granite and of foliated mafic metaplutonic or metavolcanic rock.

DDH WS-08-09B

Depth (m): 91.3

Mode Mineralogy

%		Source
25	*Quartz*	plutonic
12	*Plagioclase*	plutonic
26	*Kspar*	plutonic
2	*White Mica*	hydrothermal1
7	*Clay*	hydrothermal1
1	*Carbonate*	hydrothermal1
15	*Biotite*	plutonic
2	*Epidote*	hydrothermal1+plut
0	*Chlorite*	hydrothermal1
1	*Opaques*	hydrothermal1
1	*Fe-oxyhydroxi*	weathering
	Cu-silicates	
	Cu-carbonates	
8	*Hornblende*	plutonic(?)
0		
0		
0		

Texture 1 equigranular

Texture 2

Grain Size coarse grained (>2<16 mm)

Structure penetrative foliation

Strength: well developed

Modal Mineralogy Comments

The sample contains domains of unfoliated, medium- to coarse-grained quartzofeldspathic plutonic rock and of strongly foliated mafic, medium- to fine-grained schistose rock. The plutonic texture domain consists of anhedral kspar>quartz>plagioclase>>biotite>epidote, with kspar grains up to 7 mm and local biotite < 9 mm long. Quartz commonly forms exsolutions after feldspars. The foliated domain contains similar amounts of anhedral and poikilitic hornblende and subhedral to euhedral biotite laths, with significantly finer-grained (<0.25 mm) quartz and feldspar grains than in the plutonic domain. All epidote in the foliated domain appears to be secondary.

Veins

	Mineral 1	Mineral 2	Mineral 3	Envelope
Vein 1				
Vein 2				
Vein 3				

Opaque Mineralogy

%	Opaque	How
	Hema	
0	*Mag*	
0	*Py*	
	Po	
0	*Cpy*	
	Moly	
	Asp	
	Sph	
	Gn	

Secondary Mineralogy

	Mineral Intensity	How	How 2	AI
White Mica	weak	domainal	pseudomorph	2
Carb.	weak	domainal	vein hosted	3
Clay	moderate	pseudomorph		4
Epidote	moderate	domainal		4
Chlorite	very weak	domainal		1
Albite				
Biotite				
Kspar				
Quartz				
Fe-oxihydrox	very weak	domainal		2
Cu-Silicate				
Cu-Carbonate				

Alteration Comments

The alteration appears to be most strongly associated with the interface between foliated mafic domain and unfoliated granitic domain. Carbonate, chlorite and epidote form very weak to moderate (respectively) domainal replacement after mafic grains along the foliated-unfoliated interface. Kaolinite and lesser illite partly replace feldspars throughout the thin section, are stronger along the interface and in the foliated domain. Sparse Fe-oxyhydroxide occurs along the interface.

CC08-06

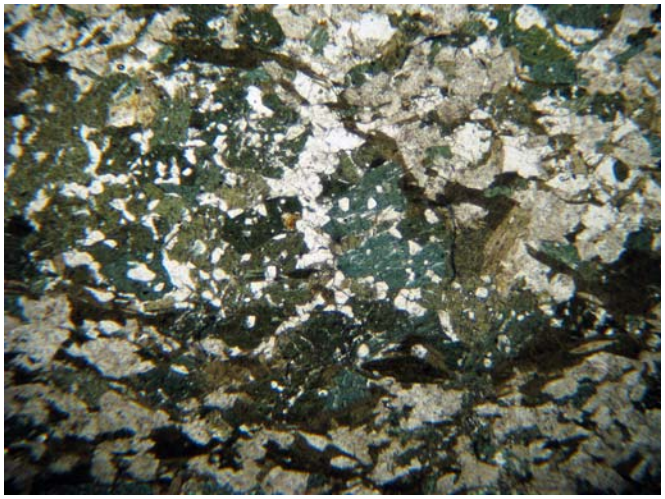

CC08-06_001 FOV (mm): 6 Plane polarized light

Brown biotite and green hornblende are the dominant mafic metamorphic minerals.

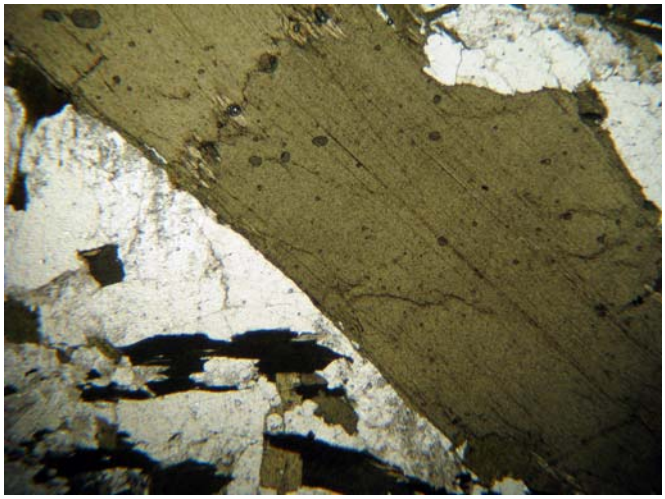

CC08-06_002 FOV (mm): 6 Plane polarized light

Biotite grains reach 8 mm length.

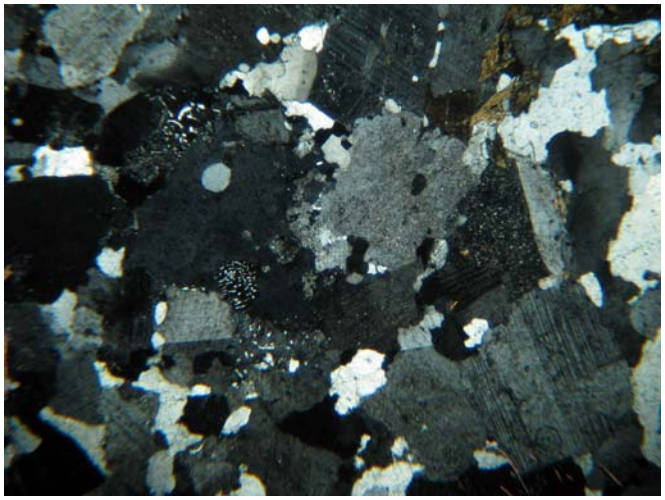

CC08-06_003 FOV (mm): 6 Crossed polars

Medium-grained equigranular texture with local exsolution (myrmekitic) texture.

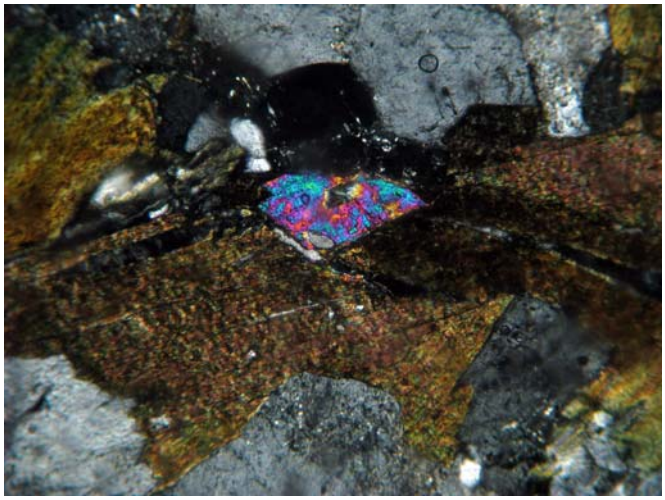

CC08-06_004 FOV (mm): 1.7 Crossed polars

Euhedral epidote associated with biotite.

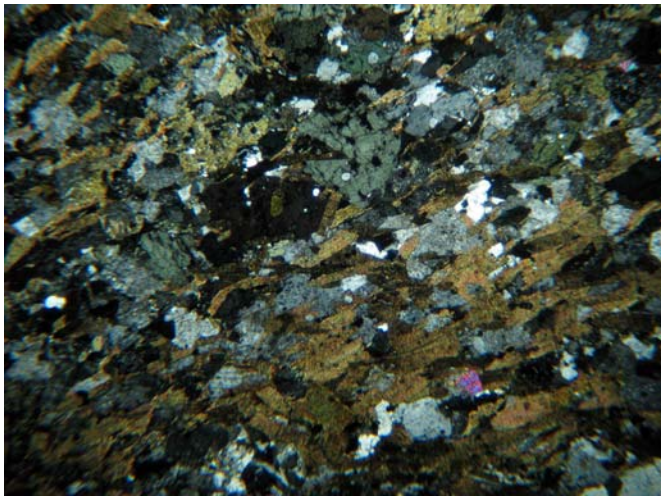

CC08-06_005 FOV (mm): 6 Crossed polars

Biotite defines a foliation in segments of the thin section.

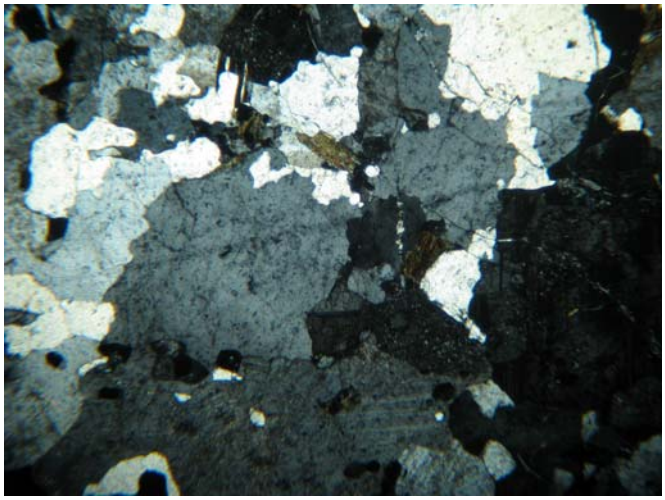

CC08-06_006 FOV (mm): 6 Crossed polars

Other segments of the thin section display a well preserved medium-grained plutonic texture with no evidence of a tectonic foliation.

CC08-06



CC08-06_007 FOV (mm): 1.7 Crossed polars

Plagioclase is moderately replaced by kaolinite and lesser illite, and cut by a discontinuous carbonate veinlet.

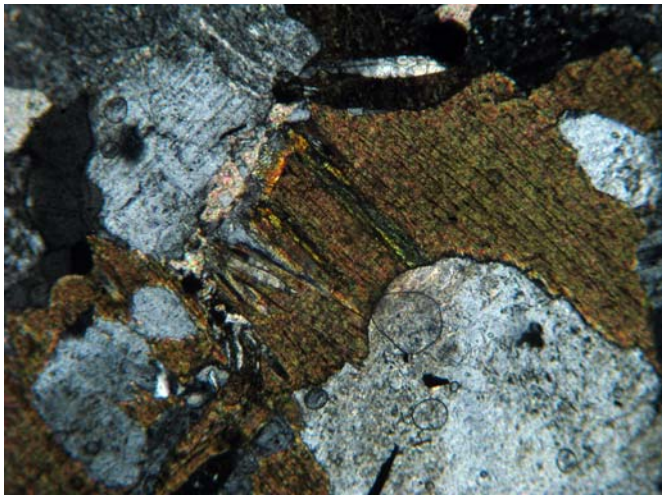

CC08-06_008 FOV (mm): 1.7 Crossed polars

Minor chlorite locally replacing biotite along cleavage planes, associated with discontinuous carbonate veinlets.

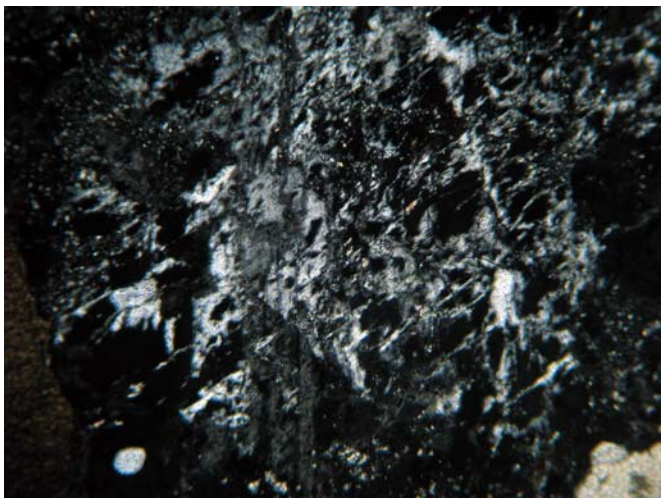

CC08-06_009 FOV (mm): 1.7 Crossed polars

Exsolution texture in plagioclase. The feldspar sections of this grain is moderately replaced by kaolinite-illite.

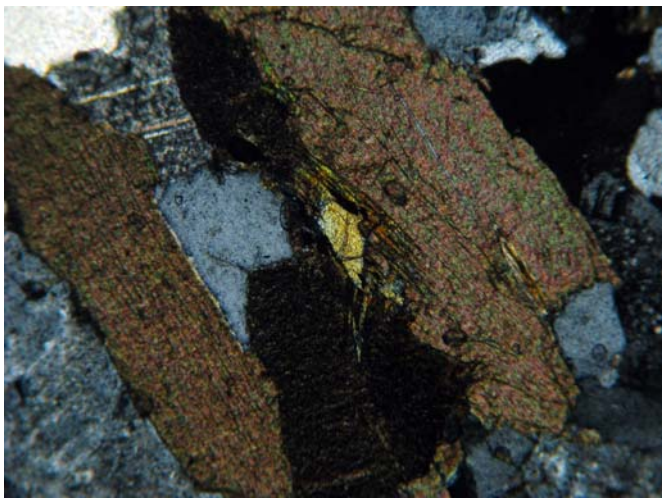

CC08-06_010 FOV (mm): 1.7 Crossed polars

Epidote partly replaces biotite.

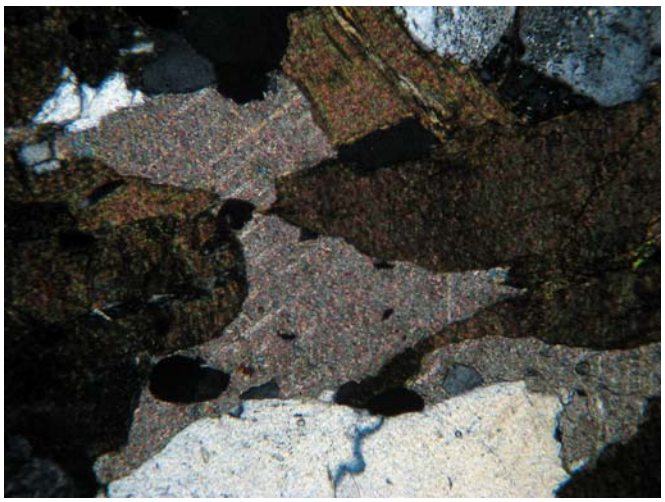

CC08-06_011 FOV (mm): 1.7 Crossed polars

Carbonate (beige birrefringence) replaces mafics predominantly along the interface between foliated and unfoliated rock.

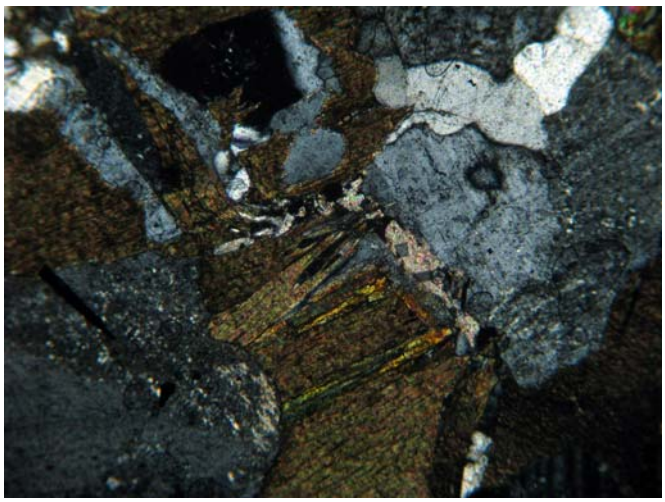

CC08-06_012 FOV (mm): 1.7 Crossed polars

Carbonate and epidote partly replace biotite, and illite-kaolinite partly replace feldspars along the interface between foliated and unfoliated rocks.

CC08-07 *Lithology:* quartz-latite *Alteration Assemblage:* propylitic *AI:* 18

DDH WS-08-09B

Depth (m): 93.4

Mode Mineralogy

%		Source
3	*Quartz*	volcanic
15	*Plagioclase*	volcanic
25	*Kspar*	volcanic
10	*White Mica*	hydrothermal1
3	*Clay*	hydrothermal1
	Carbonate	
3	*Biotite*	volcanic
5	*Epidote*	hydrothermal1
5	*Chlorite*	hydrothermal1
1	*Opaques*	hydrothermal1
1	*Fe-oxyhydroxi*	weathering
	Cu-silicates	
	Cu-carbonates	
25	*Hornblende*	volcanic
1	*Sphene*	volcanic
5	*Albite*	hydrothermal1
0		

Texture 1 poikilitic *Structure*

Texture 2 *Strength:*

Grain Size medium grained (>0.25<2mm)

Modal Mineralogy Comments

Hornblende forms subhedral grains <1 mm with common poikilitic texture. Felspars form subhedral grains < 0.5 mm, and quartz forms small anhedral grains <0.25 mm. Sphene is sparse and subhedral. Biotite originally formed up to 8 % of the rock, but is now nearly completely replaced by chlorite.

Veins

	Mineral 1	*Mineral 2*	*Mineral 3*	*Envelope*
Vein 1	Albite			
Vein 2				
Vein 3				

albite veinlets with local Fe-oxyhydroxides

Opaque Mineralogy

%	Opaque	How
	Hema	
0	*Mag*	
0	*Py*	
	Po	
0	*Cpy*	
	Moly	
	Asp	
	Sph	
	Gn	

Secondary Mineralogy

	Mineral Intensity	How	How 2	AI
White Mica	very strong	pseudomorph		5
Carb.				
Clay	weak	pseudomorph		1
Epidote	very strong	disseminated		4
Chlorite	very strong	pseudomorph		4
Albite	very strong	vein hosted	pseudomorph	4
Biotite				
Kspar				
Quartz				
Fe-oxihydrox	weak	vein hosted		1
Cu-Silicate				
Cu-Carbonate				

Alteration Comments

White mica and lesser clay form strong partial replacement after feldspars. Chlorite forms very strong near complete pseudomorphic replacement after biotite. Epidote and lesser opaques form disseminations locally replacing hornblende. Albite forms local clear (unaffected by white mica) replacements after primary feldspars and discontinuous veinlets.

CC08-07

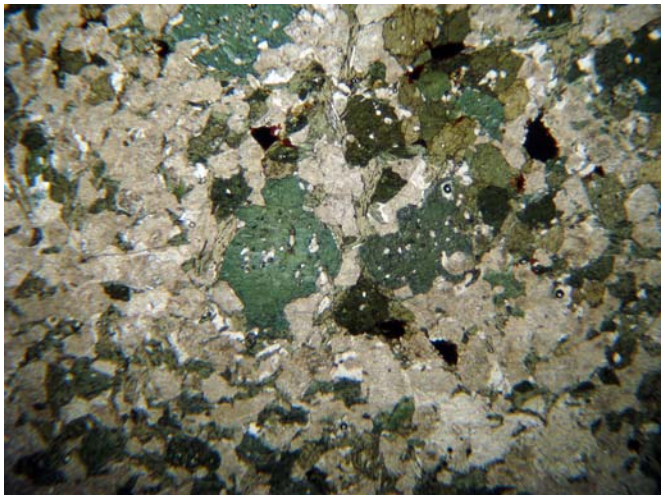

CC08-07_001 FOV (mm): 6 Plane polarized light

Green hornblende is the dominant mafic mineral in this sample.

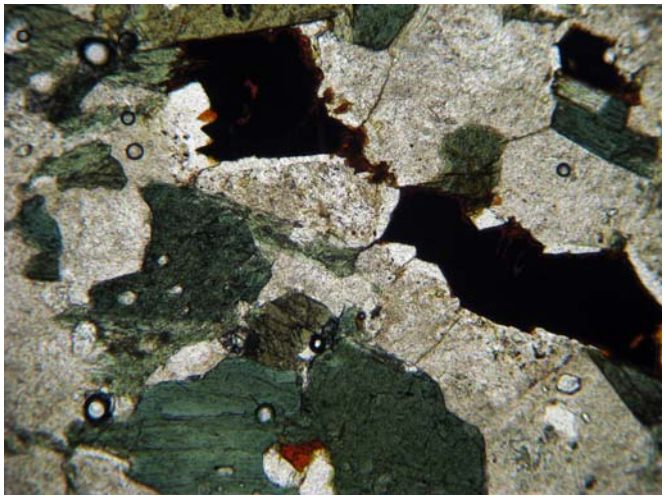

CC08-07_002 FOV (mm): 1.7 Crossed polars

Clear quartz is associated with Fe-oxyhydroxides (likely replacing sulphides).

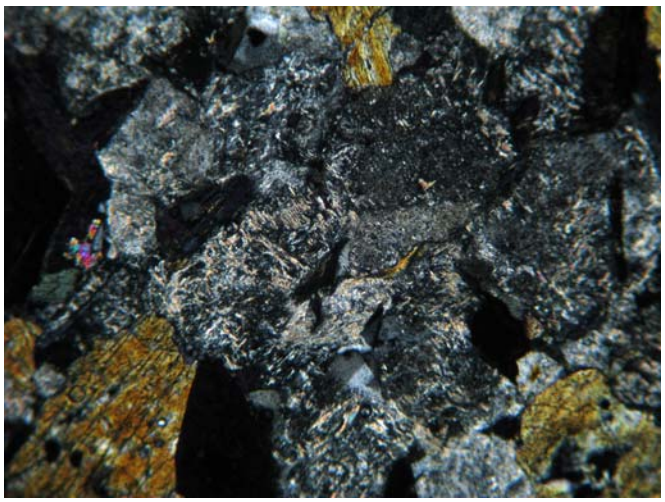

CC08-07_003 FOV (mm): 1.7 Crossed polars

Strong fine-grained white mica (illite) replacing feldspars.

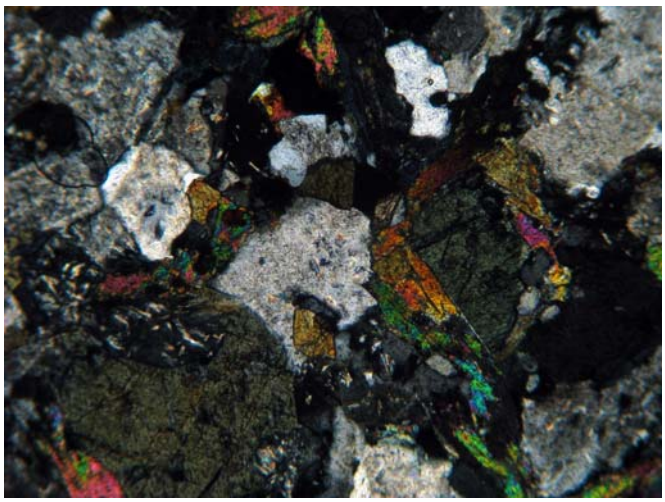

CC08-07_004 FOV (mm): 1.7 Crossed polars

Epidote is widespread and replaces hornblende.

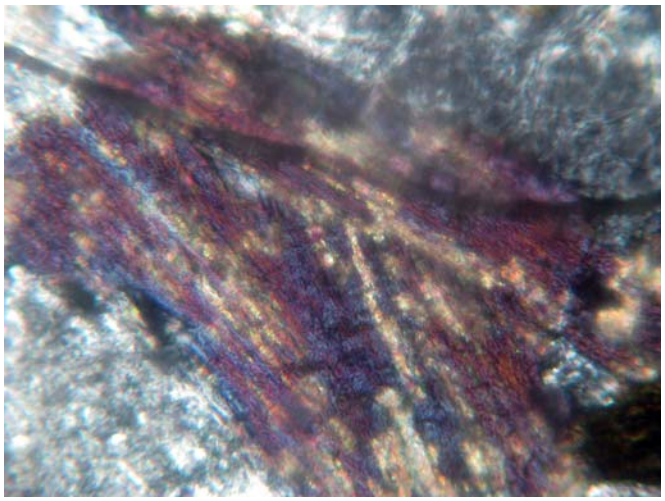

CC08-07_005 FOV (mm): 0.4 Crossed polars

Sparse biotite grains are nearly completely replaced by chlorite.

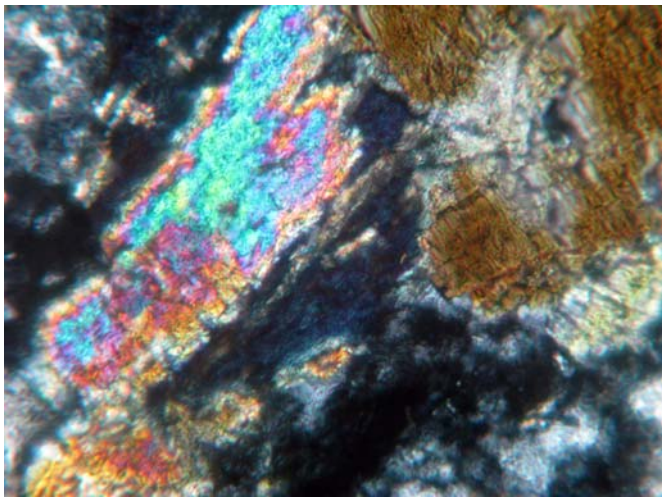

CC08-07_006 FOV (mm): 0.4 Crossed polars

Chlorite (dark blue-grey birrefringence) is associated secondary with epidote.

CC08-07

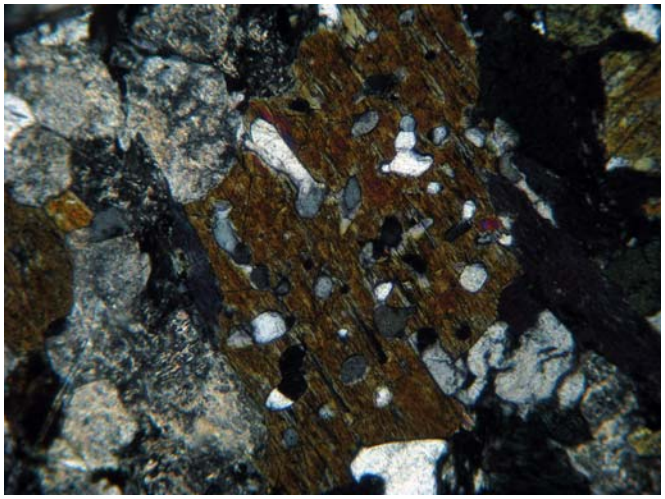

CC08-07_007 FOV (mm): 1.7 Crossed polars

Poikilitic texture in hornblende, and strong white mica with lesser kaolinite partly replacing feldspars.

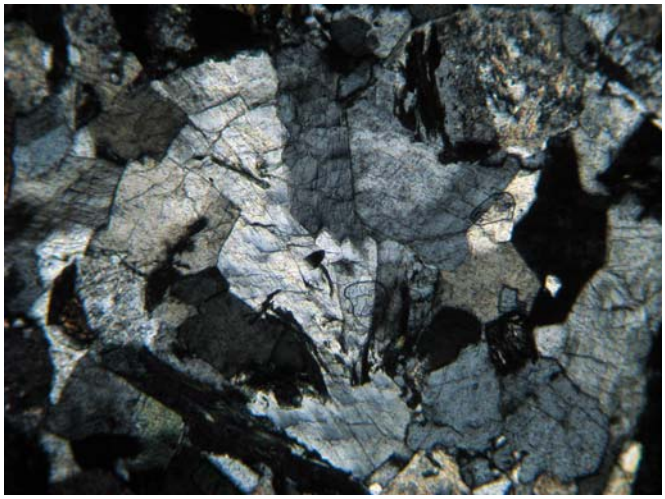

CC08-07_008 FOV (mm): 1.7 Crossed polars

Clear (unaltered) albite replacing primary feldspars.

CC08-08 *Lithology:* Granite *Alteration Assemblage:* propylitic, sericitic *AI:* 11

DDH WS-08-09B

Depth (m): 93.9

Mode Mineralogy

%		Source
15	*Quartz*	plutonic
35	*Plagioclase*	plutonic
28	*Kspar*	plutonic
5	*White Mica*	hydrothermal1
3	*Clay*	hydrothermal1
	Carbonate	
10	*Biotite*	plutonic
3	*Epidote*	hydrothermal1
	Chlorite	
	Opaques	
	Fe-oxyhydroxi	
	Cu-silicates	
	Cu-carbonates	
1	*Albite*	vein
1	*Sphene*	plutonic
0		
0		

Texture 1 equigranular *Structure* deformed band

Texture 2 *Strength:* very strongly developed

Grain Size coarse grained (>2<16 mm)

Modal Mineralogy Comments

Quartz forms anhedral, irregular interfingering grains <4 mm wide. Feldspars form irregular anhedral grains that are variably replaced by white mica-kaolinite. Biotite forms subhedral laths <2 mm. Sphene forms rare euhedral to subhedral grains.

Veins

	Mineral 1	*Mineral 2*	*Mineral 3*	*Envelope*
Vein 1	Albite			
Vein 2				
Vein 3				

albite veinlets

Opaque Mineralogy

%	Opaque	How
	Hema	
0	*Mag*	
0	*Py*	
	Po	
0	*Cpy*	
	Moly	
	Asp	
	Sph	
	Gn	

Secondary Mineralogy

	Mineral Intensity	How	How 2	AI
White Mica	moderate	pseudomorph	domainal	5
Carb.				
Clay	weak	pseudomorph		2
Epidote	moderate	pseudomorph		4
Chlorite				
Albite	weak	vein hosted		1
Biotite				
Kspar				
Quartz				
Fe-oxihydrox				
Cu-Silicate				
Cu-Carbonate				

Alteration Comments

White mica (illite) forms strong to moderate partial replacement after kspar. Illite locally partly replaces biotite along cleavage planes. Illite-kaolinite form moderate partial replacement after plagioclase. Epidote forms moderate disseminations replacing biotite. Albite forms sparse veinlets.

CC08-08

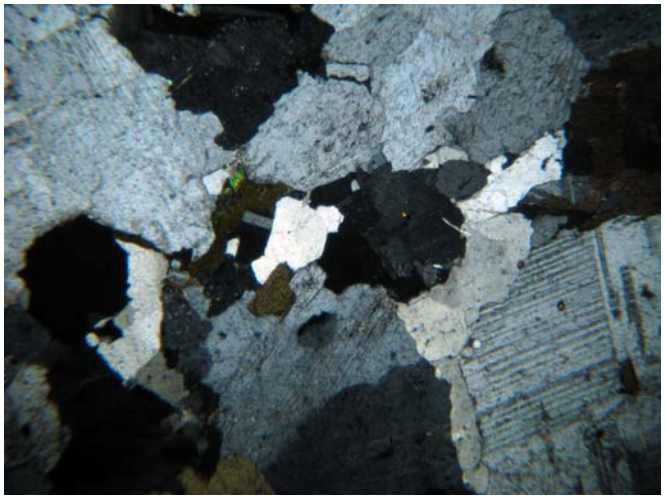

CC08-08_001 FOV (mm): 6 Crossed polars

Coarse-grained equigranular plutonic texture.

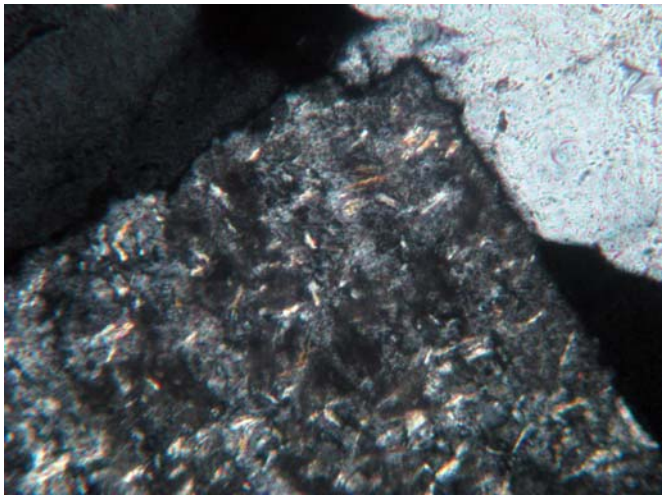

CC08-08_002 FOV (mm): 0.4 Crossed polars

Fine-grained white mica (illite) partly replaces feldspars.

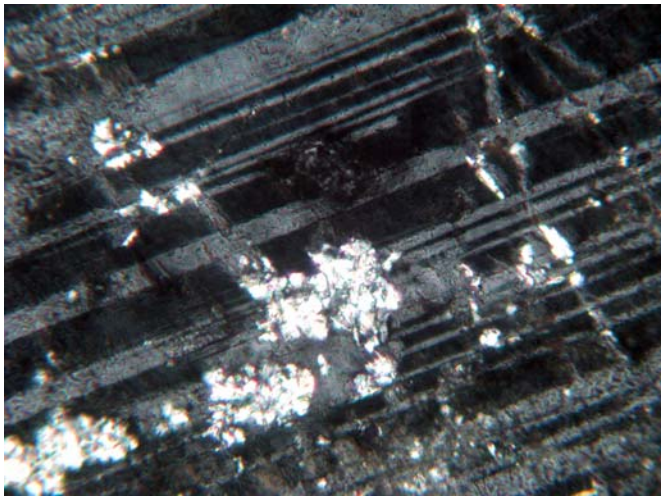

CC08-08_003 FOV (mm): 0.4 Crossed polars

Fine-grained kaolinite partly replacing plagioclase.

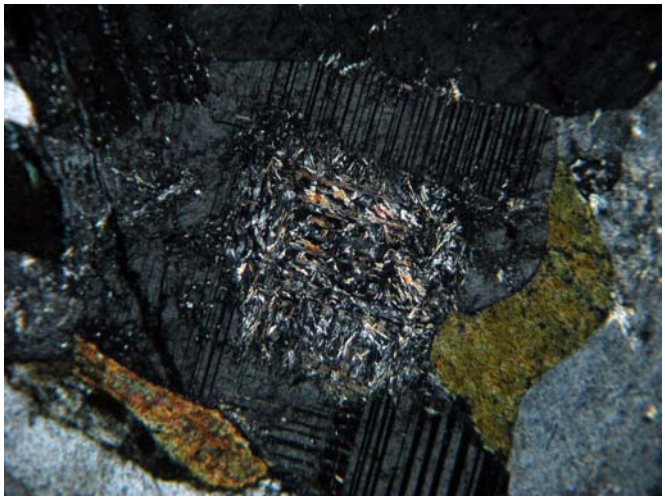

CC08-08_004 FOV (mm): 1.7 Crossed polars

White mica (illite) selectively replaces the kspar core and does not greatly affect the plagioclase rim of a zoned feldspar grain.

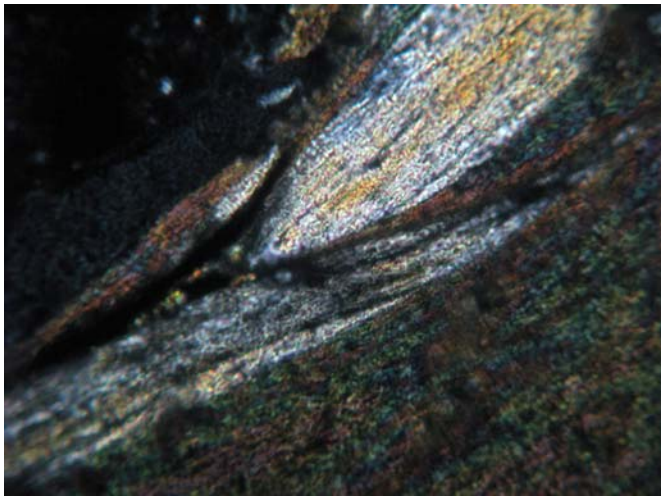

CC08-08_005 FOV (mm): 0.4 Crossed polars

White mica (illite) partly replaces biotite along cleavage planes.

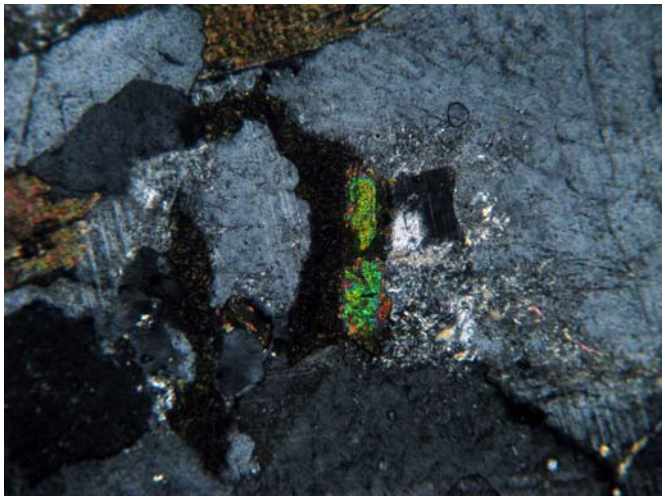

CC08-08_006 FOV (mm): 1.7 Crossed polars

Epidote partly repalces a biotite grain, and white mica (illite)-kaolinite strongly replaces feldspars.

CC08-09 *Lithology:* quartz latite *Alteration Assemblage:* propylitic *AI:* 18

DDH WS-08-09B

Depth (m): 104.3

Mode Mineralogy

%		Source
3	*Quartz*	volcanic
18	*Plagioclase*	volcanic
22	*Kspar*	volcanic
7	*White Mica*	hydrothermal1
5	*Clay*	hydrothermal1
	Carbonate	
3	*Biotite*	volcanic
1	*Epidote*	hydrothermal1
7	*Chlorite*	hydrothermal1
1	*Opaques*	hydrothermal1
1	*Fe-oxyhydroxi*	weathering
	Cu-silicates	
	Cu-carbonates	
40	*Hornblende*	volcanic
1	*Albite*	hydrothermal1
1	*Sphene*	hydrothermal1
0		

Texture 1 poikilitic *Structure* mineral alignment

Texture 2 *Strength:* moderately developed

Grain Size medium grained (>0.25<2mm)

Modal Mineralogy Comments

Green hornblende forms subhedral to anhedral grains < 1 mm with common poikilitic texture. Biotite originally formed up to 8% of the rock, but is completely replaced by chlorite-epidote and an uncertain phyllosilicate (palygorskite?). Quartz forms sparse, fine (<0.25 mm) anhedral grains. Feldspars form subhedral grains < 0.5 mm that are strongly affected by white mica-clay alteration. Sphene forms sparse euhedral to subhedral grains <0.1 mm.

Veins

	Mineral 1	*Mineral 2*	*Mineral 3*	*Envelope*
Vein 1	Albite			
Vein 2				
Vein 3				

albite veinlets with local Fe-oxyhydroxide staining

Opaque Mineralogy

%	Opaque	How
	Hema	
0	*Mag*	
0	*Py*	
	Po	
0	*Cpy*	
	Moly	
	Asp	
	Sph	
	Gn	

Secondary Mineralogy

	Mineral Intensity	How	How 2	AI
White Mica	strong	pseudomorph		4
Carb.				
Clay	strong	pseudomorph		4
Epidote	moderate	disseminated	pseudomorph	3
Chlorite	strong	pseudomorph		4
Albite	very weak	vein hosted		2
Biotite				
Kspar				
Quartz				
Fe-oxihydrox	very weak	vein hosted		1
Cu-Silicate				
Cu-Carbonate				

Alteration Comments

Strong white mica (illite) and lesser kaolinite partly replace feldspars. Moderate disseminated epidote. Strong pseudomorphic chlorite+/-epidote nearly completely replacing all biotite. Weak discontinuous albite veinlets with local Fe-oxyhydroxide staining. Local uncertain phyllosilicate (palygorskite?) replacing biotite.

CC08-09

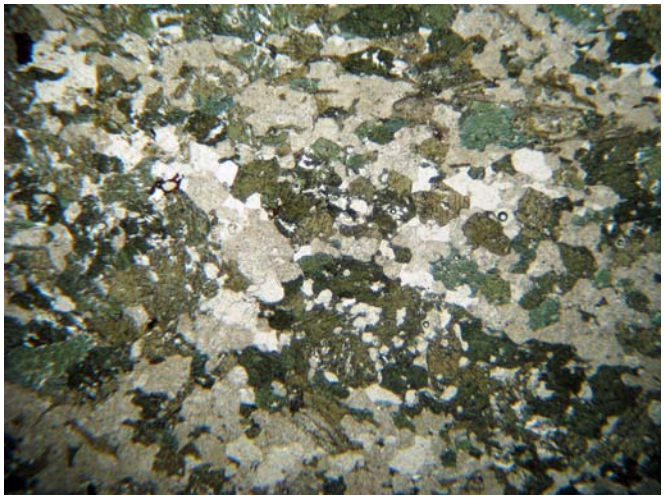

CC08-09_001 FOV (mm): 6 Plane polarized light

Green hornblende and lesser brownish biotite define two foliations in this sample.

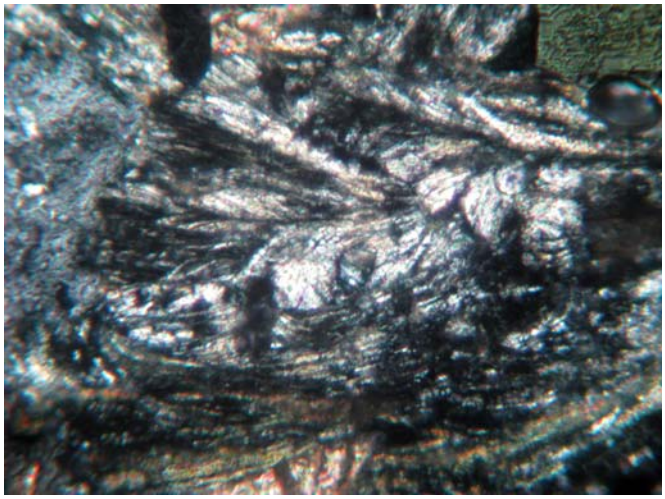

CC08-09_002 FOV (mm): 0.4 Crossed polars

Strong pseudomorphic phyllosilicate (palygorskite?) replacing mafic grains.



CC08-09_003 FOV (mm): 0.4 Crossed polars

Chlorite (blue-grey birrefringence) strongly replacing biotite.

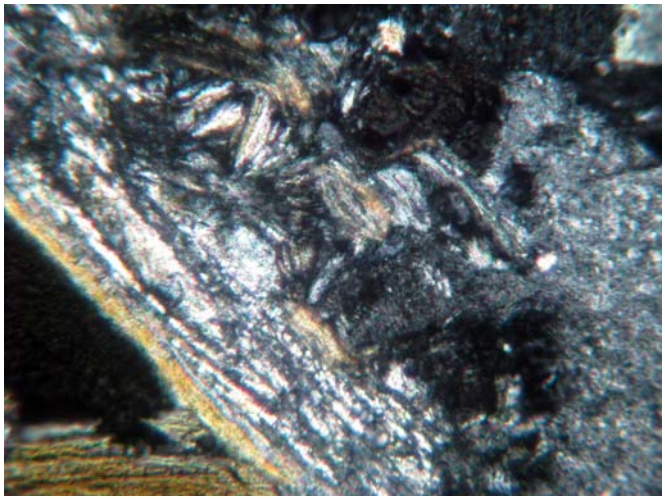

CC08-09_004 FOV (mm): 0.4 Crossed polars

Pseudomorphic fibrous phyllosilicate (palygorskite?) nearly completely replacing hornblende grains.

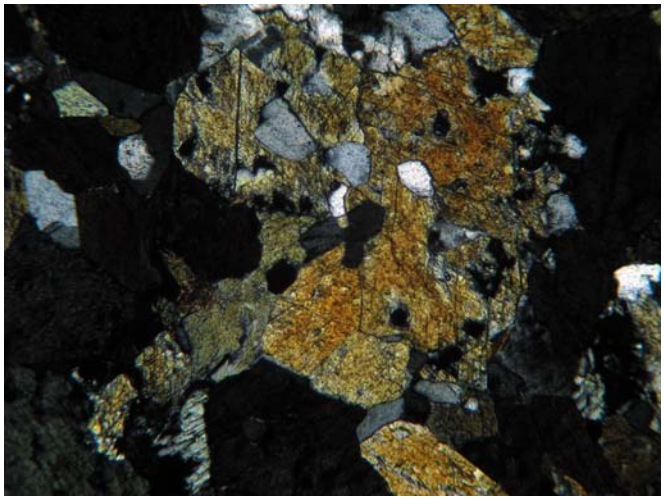

CC08-09_005 FOV (mm): 1.7 Crossed polars

Poikilitic texture in hornblende.

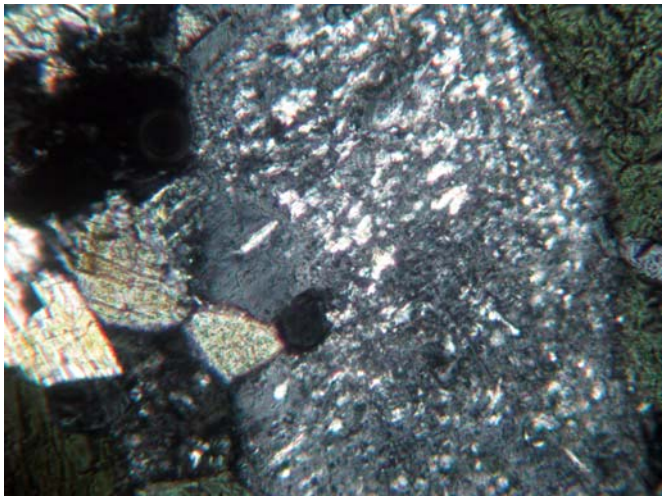

CC08-09_006 FOV (mm): 0.4 Crossed polars

Strong illite-kaolinite partly replacing a kspar grain.

CC08-09

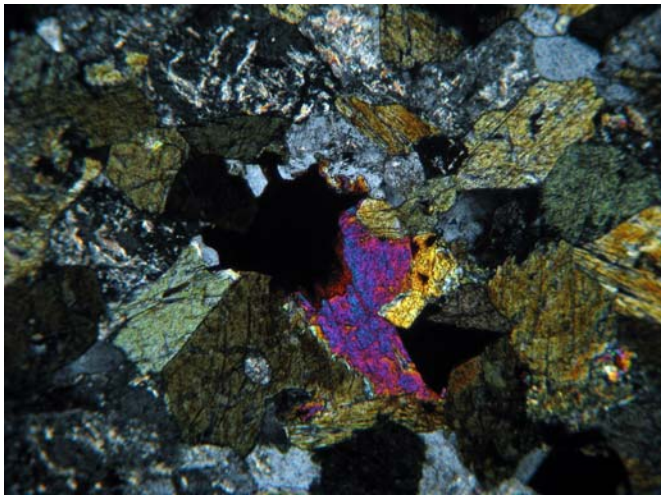

CC08-09_007 FOV (mm): 1.7 Crossed polars

Epidote, Fe-oxyhydroxides and intense illite replacing feldspars in association with opaques.

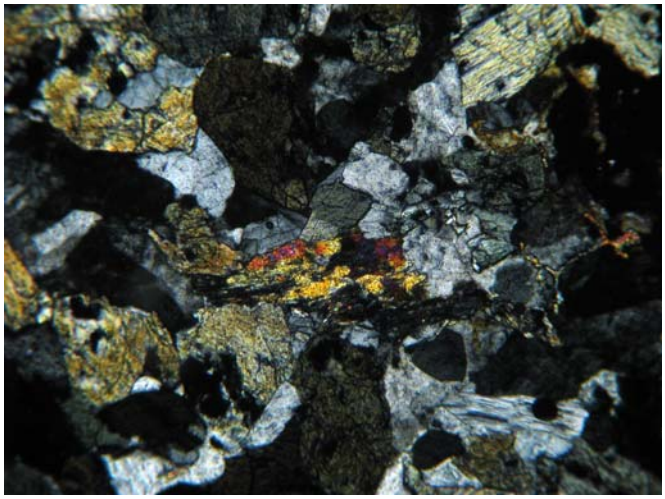

CC08-09_008 FOV (mm): 1.7 Crossed polars

Epidote and chlorite replacing biotite (centre).



CC08-09_009 FOV (mm): 1.7 Crossed polars

Chlorite-epidote nearly completely replace a biotite grain.

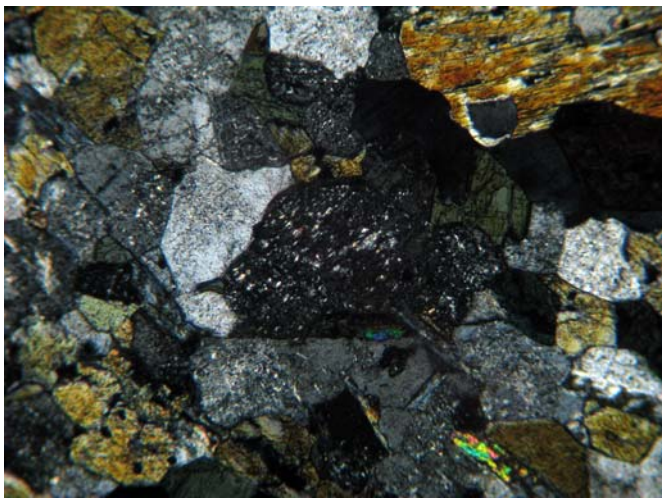

CC08-09_010 FOV (mm): 1.7 Crossed polars

Kaolinite and white mica partly replacing feldspars, and epidote-chlorite nearly completely replacing biotite.

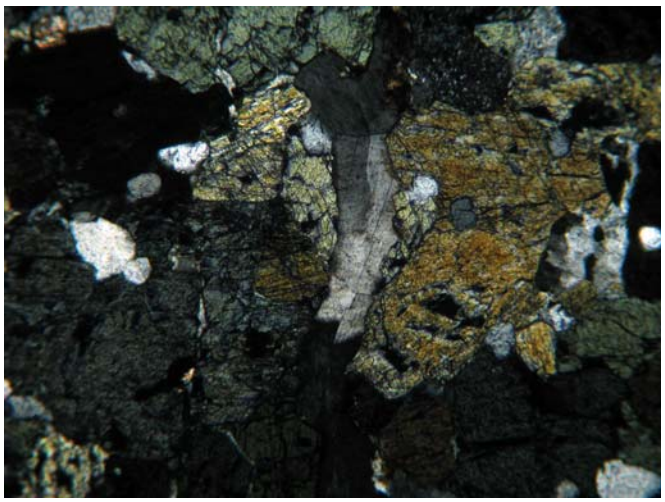

CC08-09_011 FOV (mm): 1.7 Crossed polars

Discontinuous albite veinlet (subvertical).

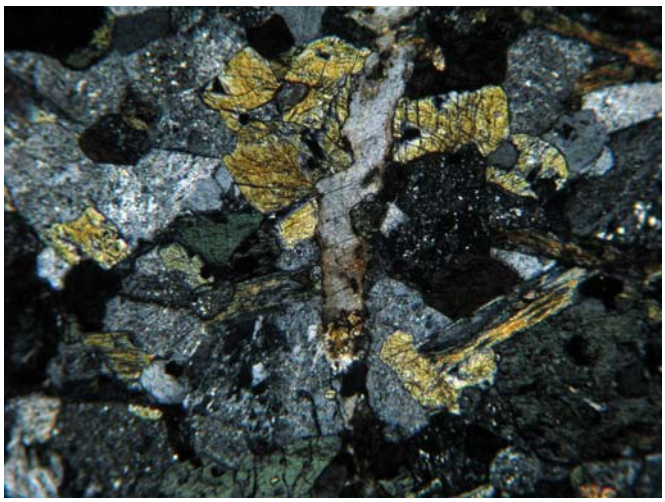

CC08-09_012 FOV (mm): 1.7 Crossed polars

Fe-oxyhydroxide staining in albite veinlet.

CC08-10 *Lithology:* quartz latite *Alteration Assemblage:* propylitic *AI:* 21

DDH WS-08-09B

Depth (m): 105.9

Mode Mineralogy

%		Source
3	*Quartz*	volcanic+hydrother
15	*Plagioclase*	volcanic
18	*Kspar*	volcanic
7	*White Mica*	hydrothermal1
5	*Clay*	hydrothermal1
	Carbonate	
2	*Biotite*	volcanic
2	*Epidote*	hydrothermal1
8	*Chlorite*	volcanic
1	*Opaques*	hydrothermal1
2	*Fe-oxyhydroxi*	weathering
	Cu-silicates	
	Cu-carbonates	
35	*Hornblende*	volcanic
1	*Albite*	hydrothermal1
1	*Sphene*	hydrothermal1
0		

Texture 1 poikilitic *Structure* mineral alignment

Texture 2 *Strength:* well developed

Grain Size medium grained (>0.25<2mm)

Modal Mineralogy Comments

Green hornblende forms subhedral to anhedral grains < 1 mm with common poikilitic texture. Biotite originally formed up to 8% of the rock, but is nearly completely replaced by chlorite-epidote. Quartz forms sparse, fine (<0.25 mm) anhedral grains, and also occurs as a secondary phase associated with epidote. Feldspars form subhedral grains < 0.5 mm that are strongly affected by white mica-clay alteration. Sphene forms sparse euhedral to subhedral grains <0.1 mm.

Veins

	Mineral 1	Mineral 2	Mineral 3	Envelope
Vein 1				
Vein 2				
Vein 3				

Opaque Mineralogy

%	Opaque	How
	Hema	
0	*Mag*	
0	*Py*	
	Po	
0	*Cpy*	
	Moly	
	Asp	
	Sph	
	Gn	

Secondary Mineralogy

	Mineral Intensity	How	How 2	AI
White Mica	strong	pseudomorph		4
Carb.				
Clay	strong	pseudomorph		4
Epidote	moderate	pseudomorph		3
Chlorite	very strong	pseudomorph		4
Albite	moderate	vein associated		2
Biotite				
Kspar				
Quartz	very weak	vein associated		2
Fe-oxihydrox	moderate	laminated		2
Cu-Silicate				
Cu-Carbonate				

Alteration Comments

Strong white mica (illite) and lesser kaolinite partly replace feldspars. Strong pseudomorphic chlorite+/-epidote nearly completely replacing all biotite. Disseminated clear albite associated with Fe-oxyhydroxide and rare quartz along the dominant foliation.

CC08-10

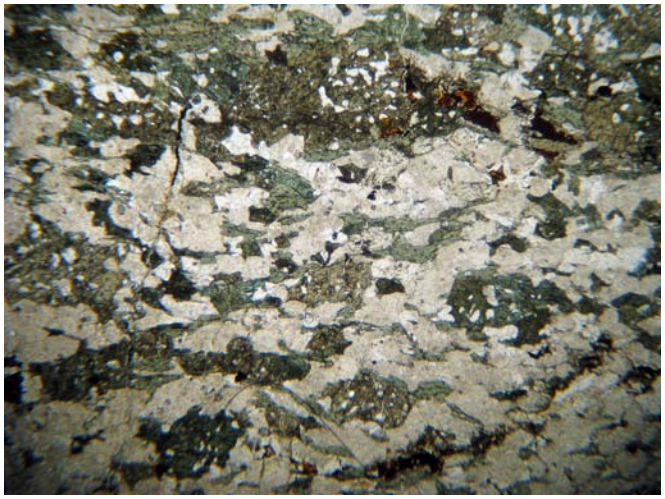

CC08-10_001 FOV (mm): 6 Plane polarized light

Green hornblende is the dominant mineral defining the foliation.

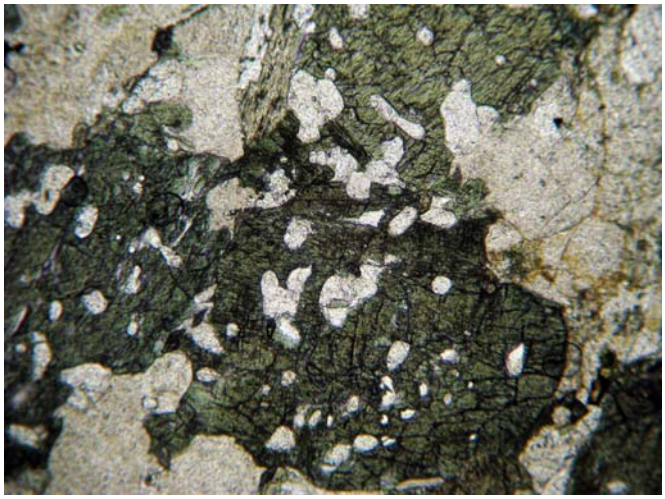

CC08-10_002 FOV (mm): 1.7 Plane polarized light

Poikilitic texture in hornblende.

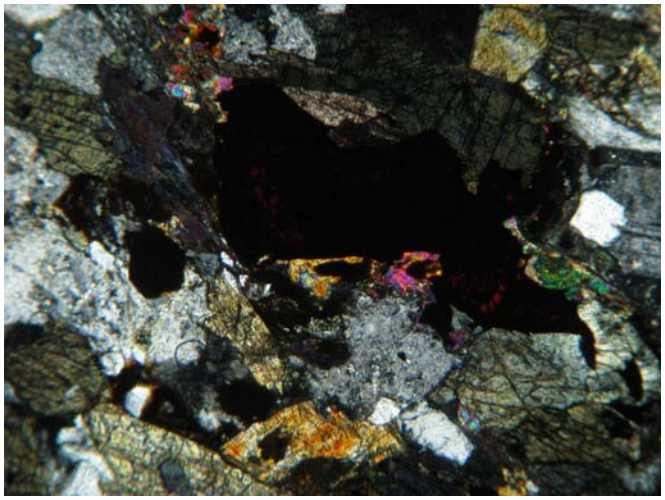

CC08-10_003 FOV (mm): 1.7 Crossed polars

Dark brown Fe-oxyhydroxides, chlorite (dark blue-grey birrefringence, left of centre), and epidote (high birrefringence colours) replacing mafic grains.

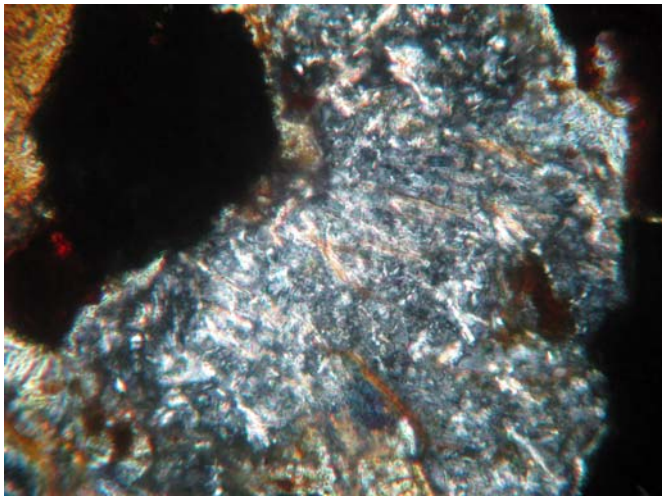

CC08-10_004 FOV (mm): 0.4 Crossed polars

Intense white mica (illite)-kaolinite partly replacing a feldspar grain adjacent to Fe-oxyhydroxides.



CC08-10_005 FOV (mm): 6 Plane polarized light

Fe-oxyhydroxides and clear (secondary) quartz along the foliation.

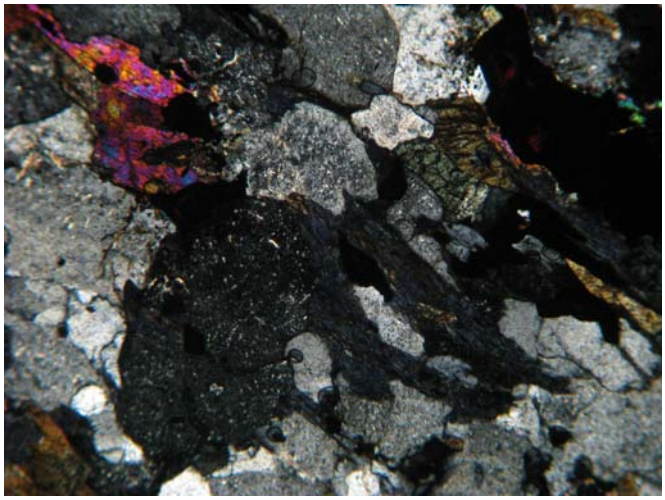

CC08-10_006 FOV (mm): 1.7 Crossed polars

Biotite is nearly completely replaced by pseudomorphic chlorite and epidote.

CC08-10

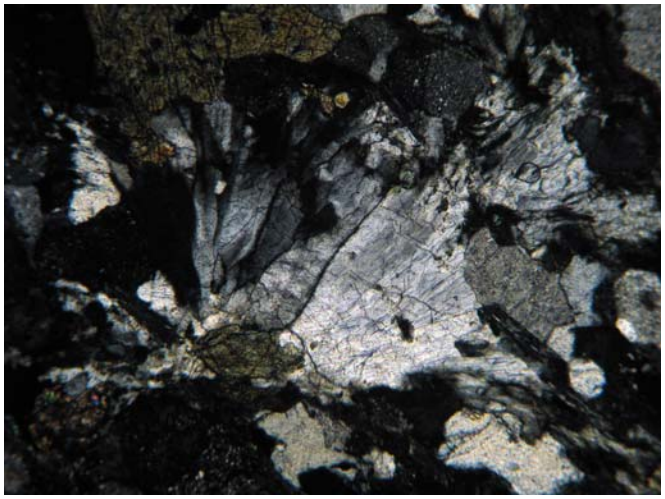

CC08-10_007 FOV (mm): 1.7 Crossed polars

Hydrothermal albite.

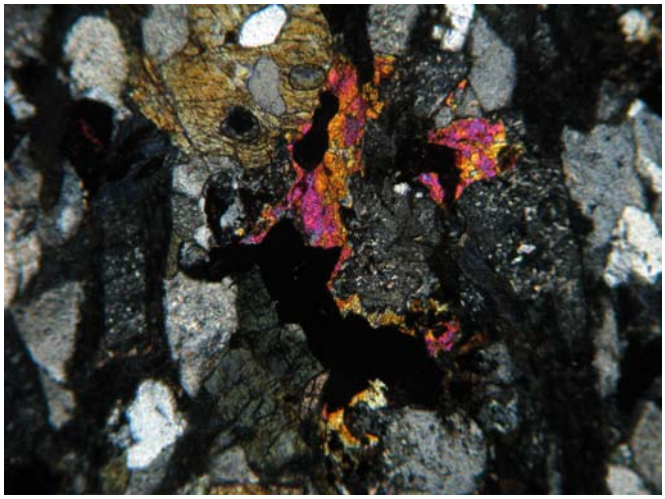

CC08-10_008 FOV (mm): 1.7 Crossed polars

Epidote and Fe-oxyhydroxides replacing primary mafic grains.

CC08-11 *Lithology:* quartz latite *Alteration Assemblage:* propylitic *AI:* 9

DDH WS-08-09B

Depth (m): 106.2

Mode Mineralogy

%		Source
18	*Quartz*	volcanic
10	*Plagioclase*	volcanic
20	*Kspar*	volcanic
5	*White Mica*	hydrothermal1
2	*Clay*	hydrothermal1
	Carbonate	
10	*Biotite*	volcanic
1	*Epidote*	hydrothermal1
1	*Chlorite*	hydrothermal1
	Opaques	
1	*Fe-oxyhydroxi*	weathering
	Cu-silicates	
	Cu-carbonates	
30	*Hornblende*	volcanic
2	*Sphene*	volcanic
0		
0		

Texture 1 polygonal (foam) *Structure* penetrative foliation

Texture 2 *Strength:* well developed

Grain Size medium grained (>0.25<2mm)

Modal Mineralogy Comments

Quartz and feldspars form small (<0.2 mm) polygonal grains suggesting annealing. Green hornblende forms subhedral to anhedral grains < 0.8 mm. Brown biotite forms euhedral to subhedral laths <0.8 mm long. Biotite and hornblende define the foliation. Sphene form minute subhedral to euhedral grains.

Veins

	Mineral 1	*Mineral 2*	*Mineral 3*	*Envelope*
Vein 1	Fe-oxyhydroxides			
Vein 2				
Vein 3				

Fe-oxyhydroxides fill fissures

Opaque Mineralogy

%	Opaque	How
	Hema	
0	*Mag*	
0	*Py*	
	Po	
0	*Cpy*	
	Moly	
	Asp	
	Sph	
	Gn	

Secondary Mineralogy

	Mineral Intensity	How	How 2	AI
White Mica	moderate	pseudomorph		3
Carb.				
Clay	weak	pseudomorph		3
Epidote	weak	pseudomorph		1
Chlorite	weak	pseudomorph		1
Albite				
Biotite				
Kspar				
Quartz				
Fe-oxihydrox	weak	fracture filled	disseminated	1
Cu-Silicate				
Cu-Carbonate				

Alteration Comments

White mica (illite) and lesser clay (kaolinite) partly replace feldspars, particularly along melanococratic foliation domains. Epidote and lesser chlorite form sparse pseudomorphic replacement after biotite. Fe-oxyhydroxides occur filling fissures and sparsely along melanocratic foliation domains.

CC08-11



CC08-11_001 FOV (mm): 6 Plane polarized light

A tectonic foliation is well defined by the alignment of biotite and hornblende.

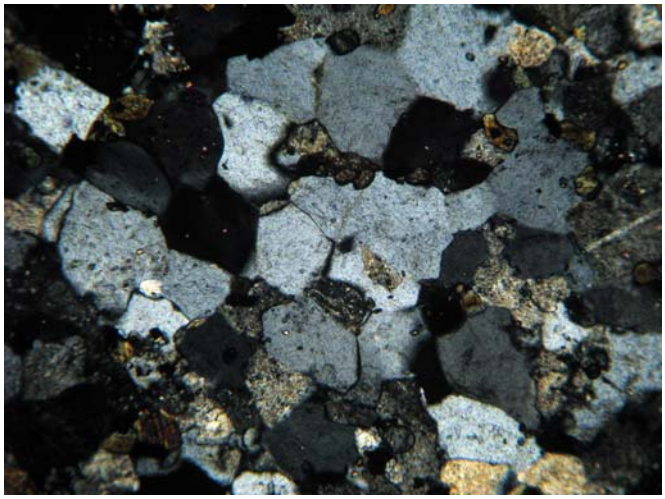

CC08-11_002 FOV (mm): 1.7 Crossed polars

Well developed polygonal texture in quartz and feldspars.

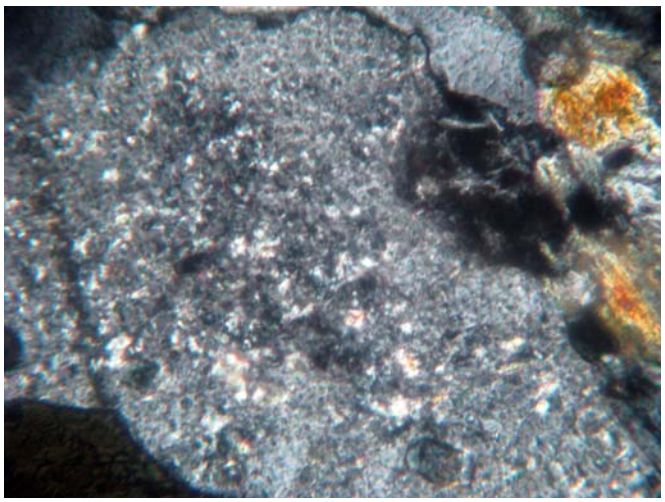

CC08-11_003 FOV (mm): 0.4 Crossed polars

Moderate illite after kspars.

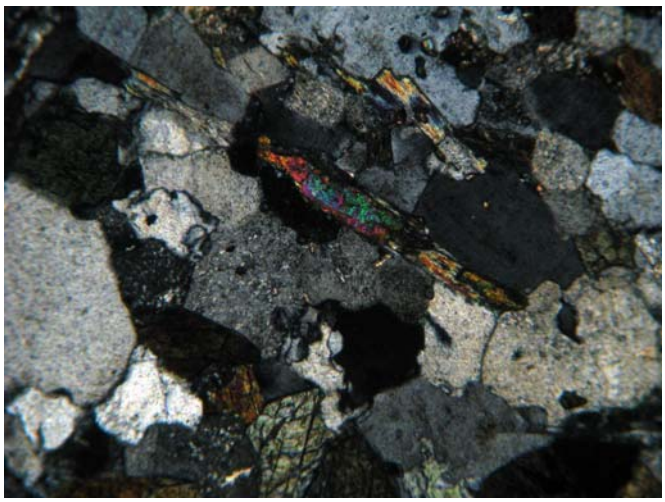

CC08-11_004 FOV (mm): 1.7 Crossed polars

Pseudomorphic epidote after biotite.



CC08-11_005 FOV (mm): 1.7 Plane polarized light

Fracture-fill Fe-oxyhydroxides.

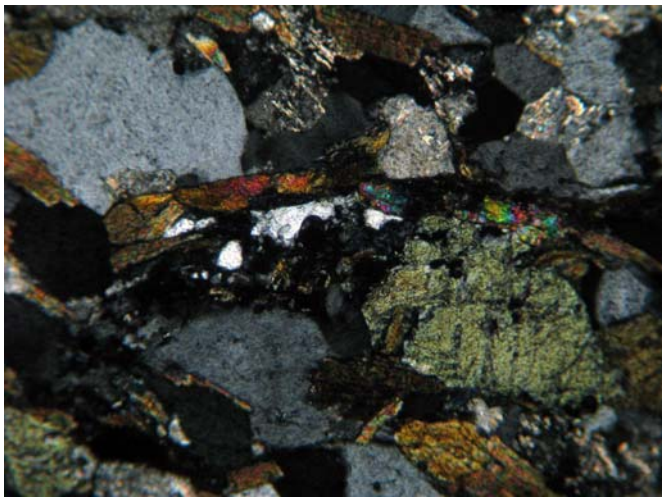

CC08-11_006 FOV (mm): 1.7 Crossed polars

Epidote (high birrefringence colours) and minor chlorite (dark blue-grey birrefringence) form pseudomorphic replacement after biotite. Kspars are partly replaced by illite.

CC08-12 *Lithology:* Quartz monzonite *Alteration Assemblage:* propylitic *AI:* 16

DDH WS-08-09B

Depth (m): 109.3

Mode Mineralogy

%		Source
7	*Quartz*	plutonic
25	*Plagioclase*	plutonic
35	*Kspar*	plutonic
7	*White Mica*	hydrothermal1
7	*Clay*	hydrothermal1
	Carbonate	
	Biotite	
8	*Epidote*	hydrothermal1
7	*Chlorite*	hydrothermal1
1	*Opaques*	hydrothermal1
	Fe-oxyhydroxi	
	Cu-silicates	
	Cu-carbonates	
2	*Hornblende*	plutonic
1	*Biotite*	plutonic
0		
0		

Texture 1 equigranular *Structure*

Texture 2 *Strength:*

Grain Size coarse grained (>2<16 mm)

Modal Mineralogy Comments

Kspar and lesser plagiolase form subhedral prismatic grains <4 mm wide. Quartz forms small (<0.3 mm) anhedral grains interstitial to feldspars. Primary hornblende and biotite formed up to 18 % of the rock, but are now nearly completely converted to secondary epidote-chlorite+/-opaques.

Veins

	Mineral 1	*Mineral 2*	*Mineral 3*	*Envelope*
Vein 1	Albite			
Vein 2				
Vein 3				
albite-epidote				

Opaque Mineralogy

%	Opaque	How
	Hema	
0	*Mag*	
0	*Py*	
	Po	
0	*Cpy*	
	Moly	
	Asp	
	Sph	
	Gn	

Secondary Mineralogy

	Mineral Intensity	How	How 2	AI
White Mica	moderate	pseudomorph		3
Carb.				
Clay	moderate	pseudomorph		3
Epidote	very strong	pseudomorph	vein hosted	4
Chlorite	very strong	pseudomorph		4
Albite	weak	vein hosted		2
Biotite				
Kspar				
Quartz				
Fe-oxihydrox				
Cu-Silicate				
Cu-Carbonate				

Alteration Comments

Moderate to strong white mica (illite) and kaolinite partly replacing feldspars. Very strong pseudomorphic epidote and lesser chlorite nearly completely replace primary mafic grains. Albite+/-epidote form veinlets.

CC08-12

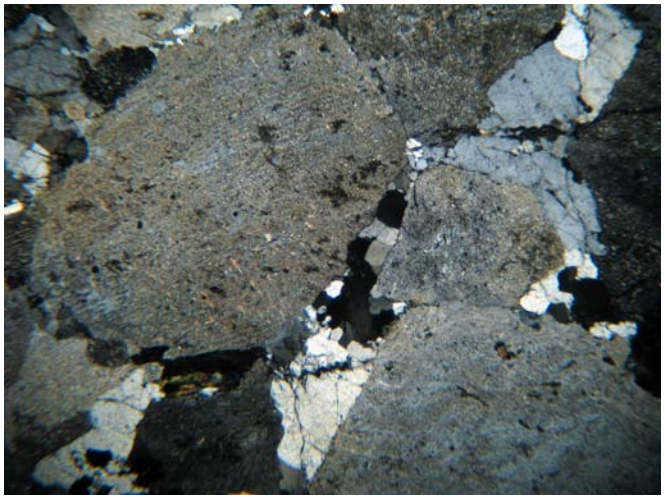

CC08-12_001 FOV (mm): 6 Crossed polars

Coarse-grained equigranular plutonic texture showing evidence of grain boundary migration.

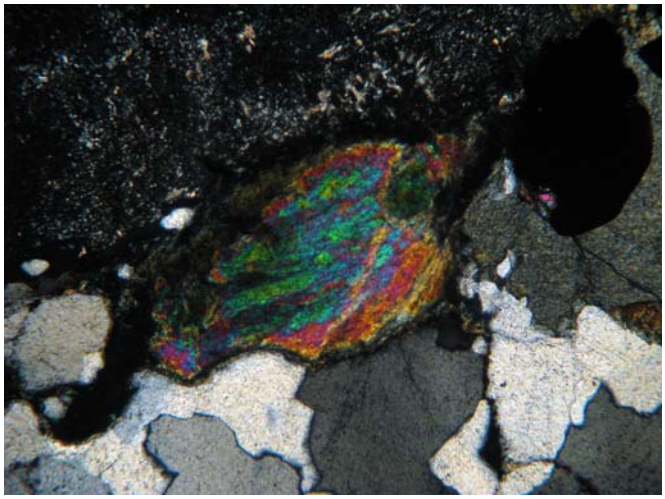

CC08-12_002 FOV (mm): 1.7 Crossed polars

Epidote (high birrefringence colours), chlorite (dark blue-grey birrefringence) and opaques replace primary mafics, whereas feldspars are moderately to strongly replaced by illite-kaolinite.

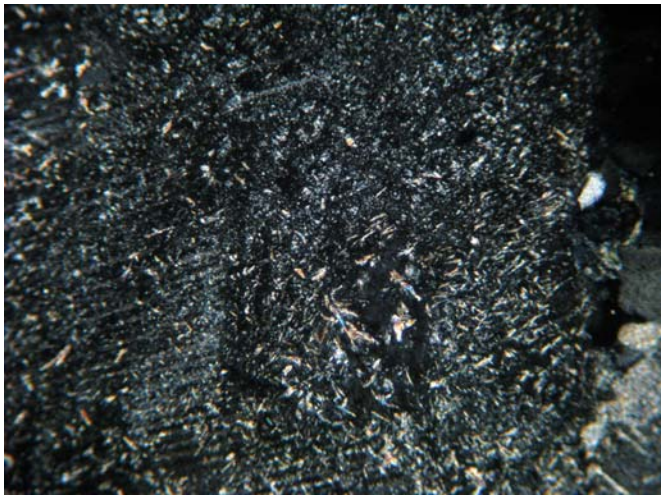

CC08-12_003 FOV (mm): 1.7 Crossed polars

Intense illite-kaolinite partly replacing a plagioclase grain.

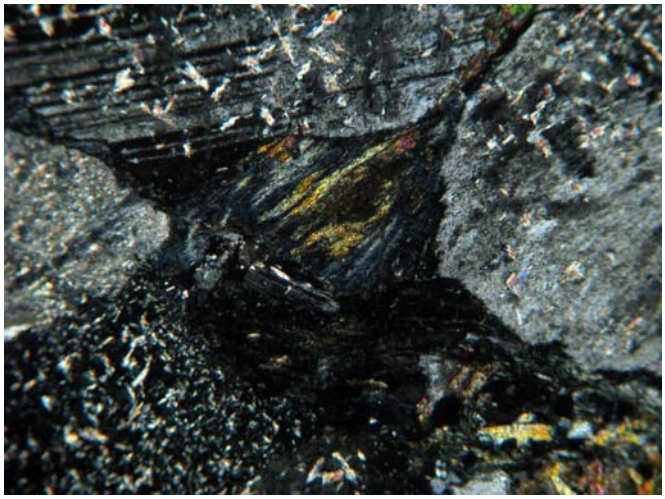

CC08-12_004 FOV (mm): 1.7 Crossed polars

Chlorite and epidote replace mafic grains. Strong illite and lesser kaolinite after feldspars.

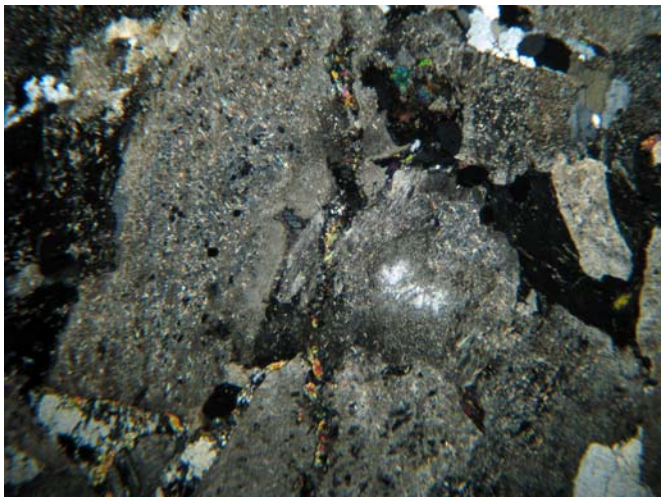

CC08-12_005 FOV (mm): 6 Crossed polars

Discontinuous epidote veinlet (subvertical)

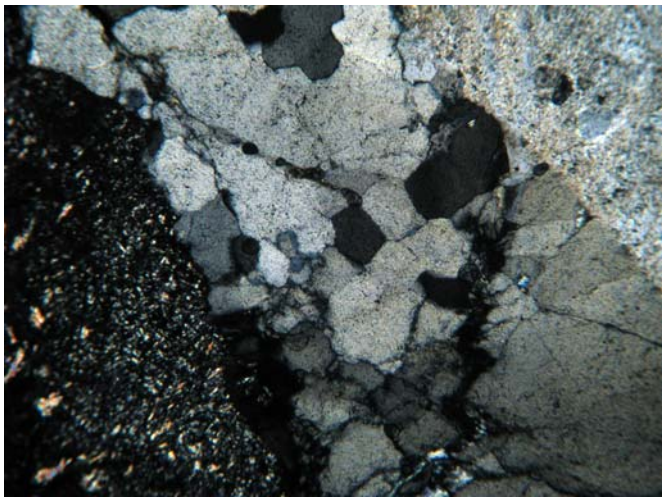

CC08-12_006 FOV (mm): 1.7 Crossed polars

Recrystallized (polygonal texture) quartz filling interstitial spaces between strongly illite-kaolinite altered feldspars.

CC08-12



CC08-12_007 FOV (mm): 1.7 Crossed polars

Albite veinlet (subvertical.

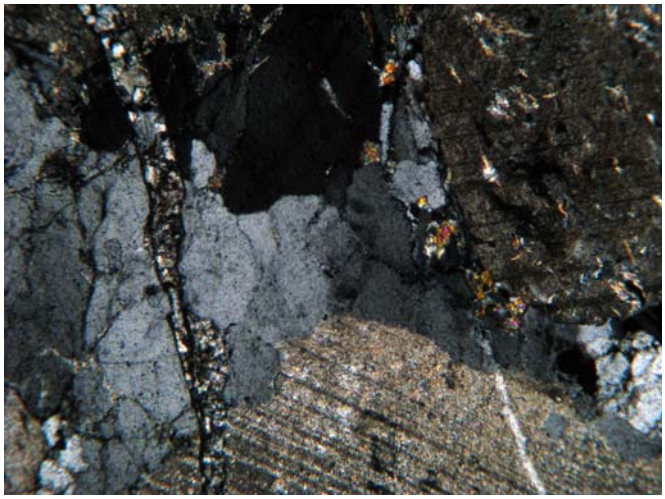

CC08-12_008 FOV (mm): 1.7 Crossed polars

Albite veinlet with minor epidote.

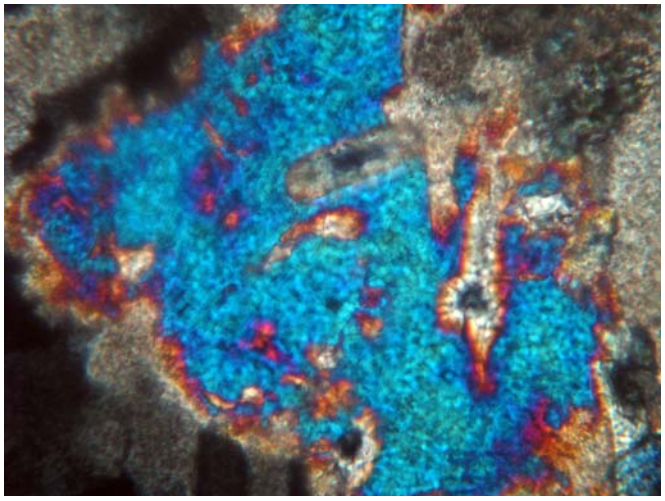

CC08-12_009 FOV (mm): 0.4 Crossed polars

Trace late anhydrite filling interstitial spaces.

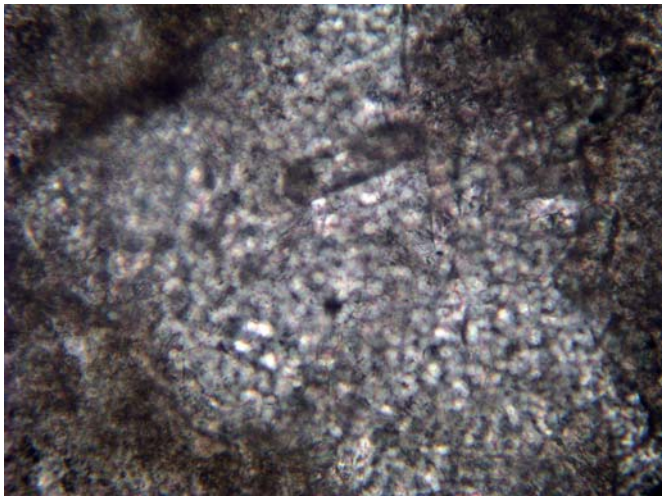

CC08-12_010 FOV (mm): 0.4 Plane polarized light

Same, under plane polarized light. Note that the anhydrite has lower relief than feldspar prisms.

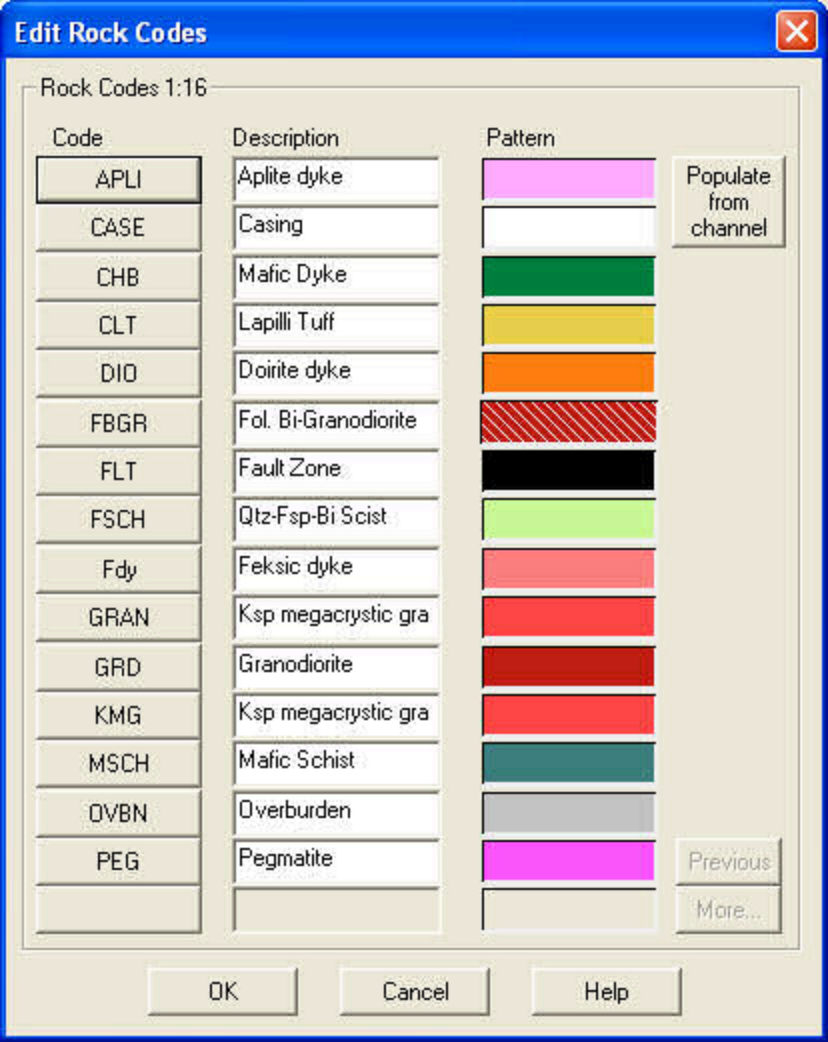
Edit Rock Codes
Rock Codes 1:16
Code
Description
Pattern
APLI
Aplite dyke
CASE
Casing
CHB
Mafic Dyke
CLT
Lapilli Tuff
DIO
Doirite dyke
FBGR
Fol. Bi-Granodiorite
FLT
Fault Zone
FSCH
Qtz-Fsp-Bi Scist
Fdy
Feksic dyke
GRAN
Ksp megacrystic gra
GRD
Granodiorite
KMG
Ksp megacrystic gra
MSCH
Mafic Schist
OVBN
Overburden
PEG
Pegmatite
Populate from channel
Previous
More...
OK
Cancel
Help

BCGold Corp. - Carmacks Project

Hole Name :ICE-07-01		Hole Length :181.36		
Collar X :417505.00	Collar Y :6905999.00	Collar Z :770.00	Azm :130	Dip :-80

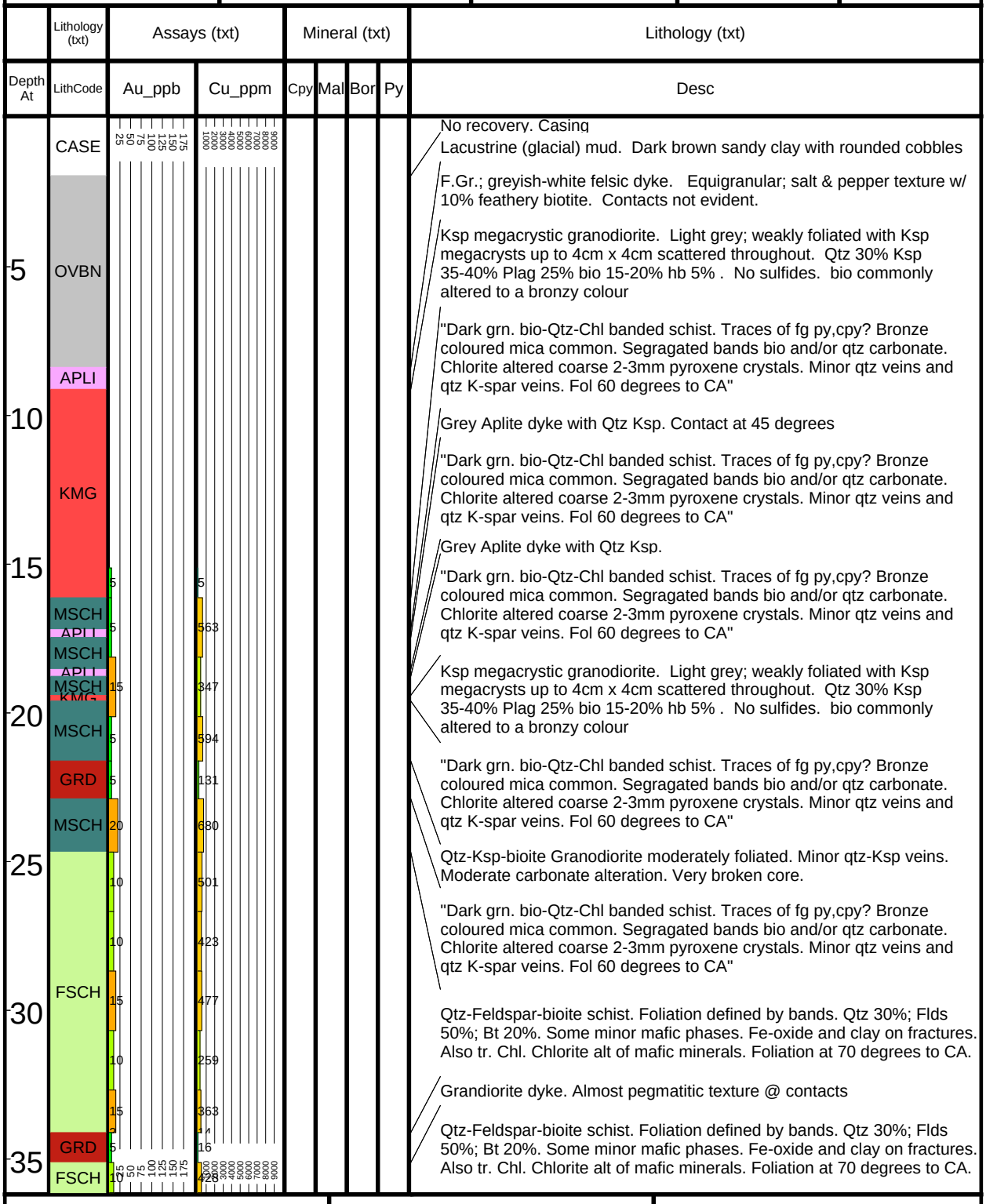

Scale 1:200	Date: May 03, 2009	Hole Page 1 of 6

BCGold Corp. - Carmacks Project

Hole Name :ICE-07-01		Hole Length :181.36		
Collar X :417505.00	Collar Y :6905999.00	Collar Z :770.00	Azm :130	Dip :-80

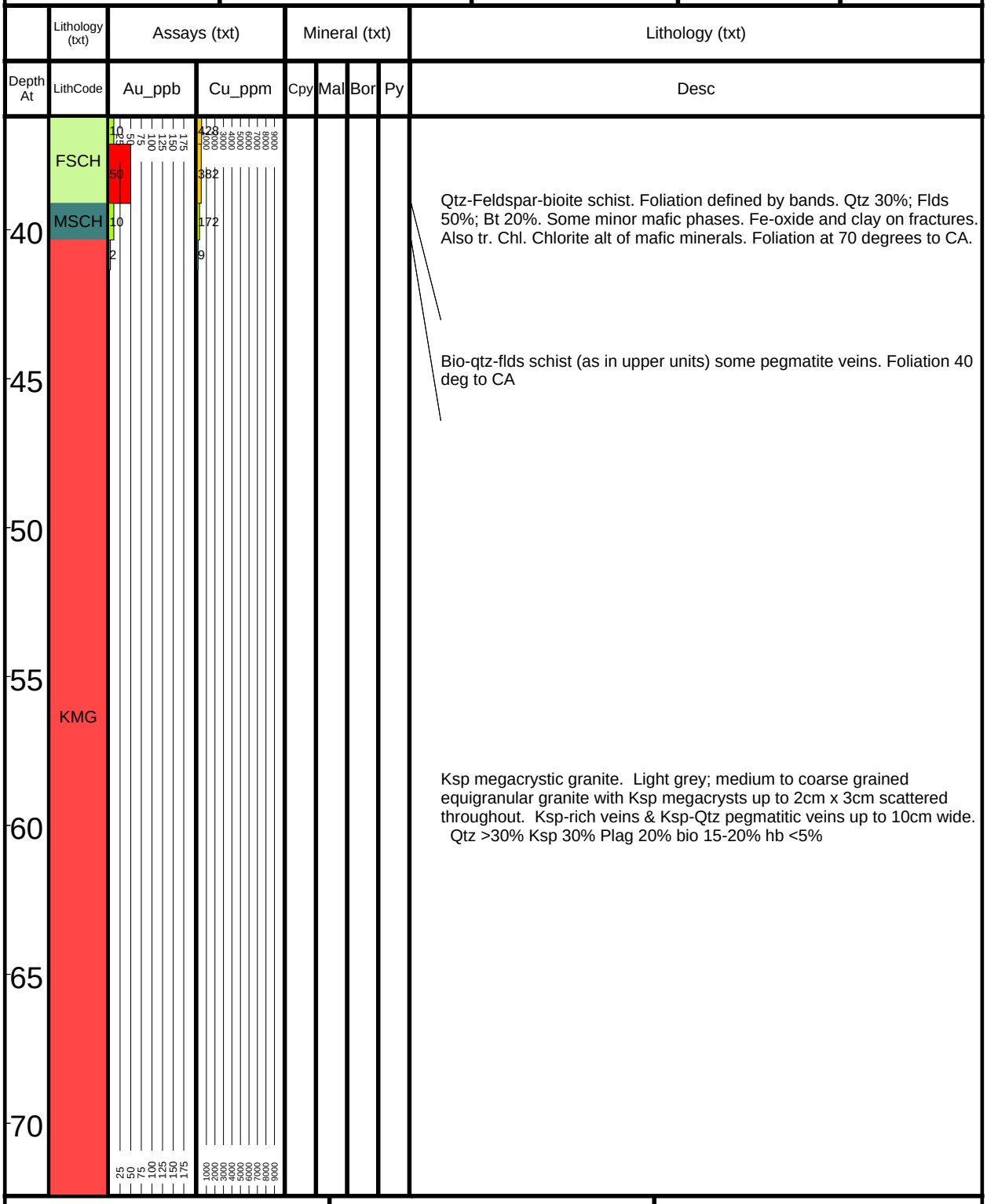

Scale 1:200	Date: May 03, 2009	Hole Page 2 of 6

BCGold Corp. - Carmacks Project

Hole Name :ICE-07-01	Hole Length :181.36			
Collar X :417505.00	Collar Y :6905999.00	Collar Z :770.00	Azm :130	Dip :-80

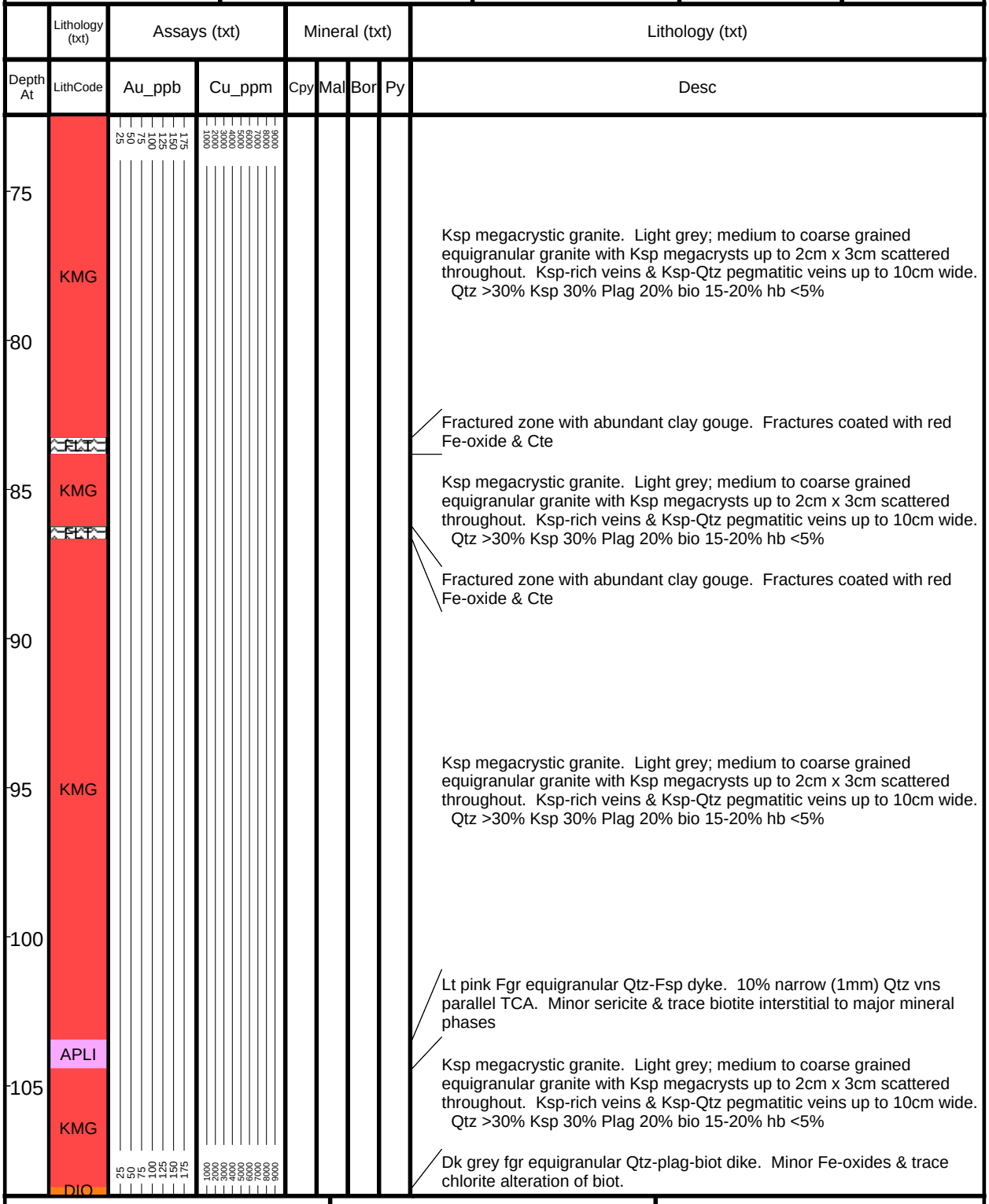

BCGold Corp. - Carmacks Project

Hole Name :ICE-07-01	Hole Length :181.36			
Collar X :417505.00	Collar Y :6905999.00	Collar Z :770.00	Azm :130	Dip :-80

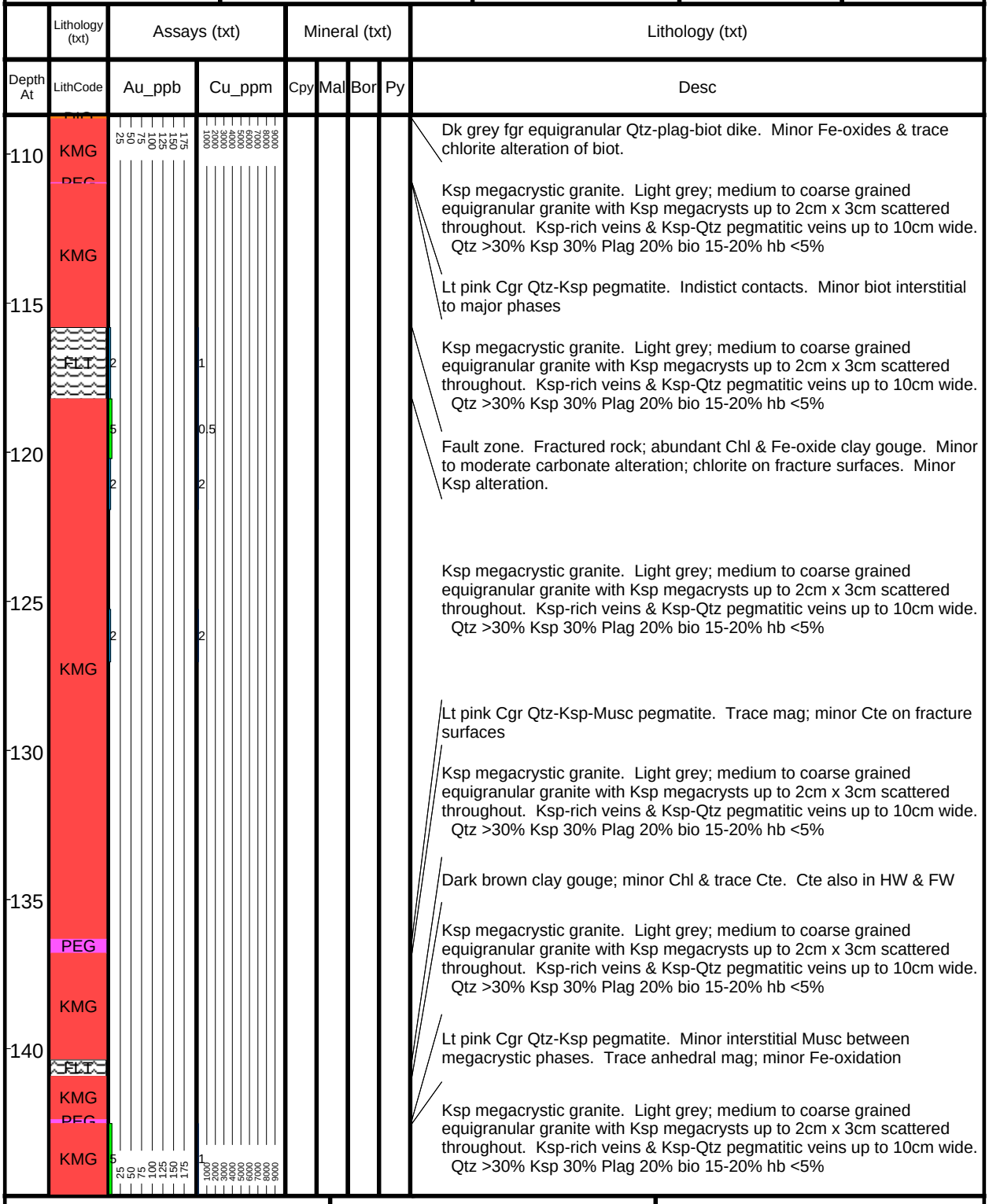

Scale 1:200	Date: May 03, 2009	Hole Page 4 of 6

BCGold Corp. - Carmacks Project

Hole Name :ICE-07-01	Hole Length :181.36			
Collar X :417505.00	Collar Y :6905999.00	Collar Z :770.00	Azm :130	Dip :-80

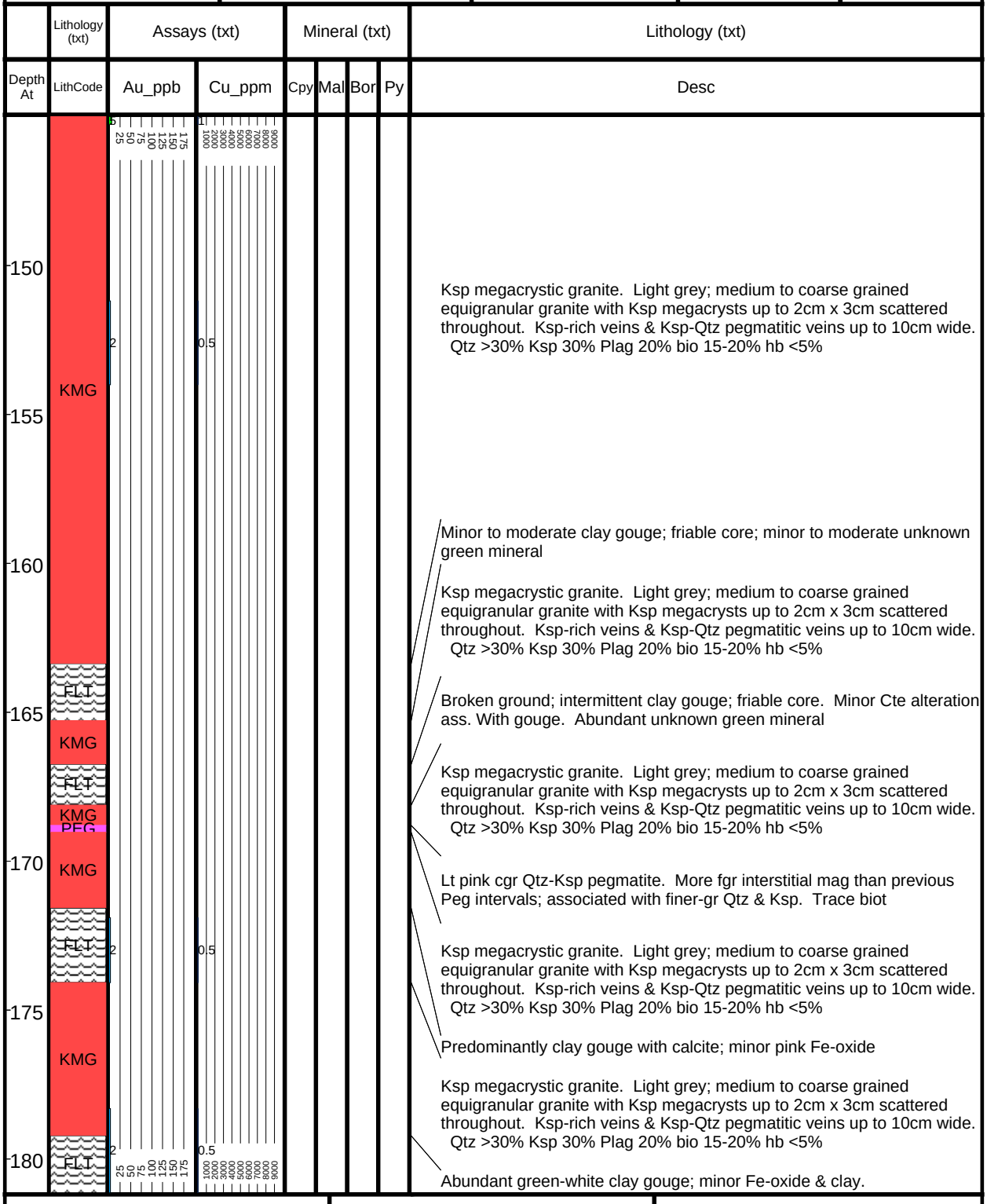

BCGold Corp. - Carmacks Project

Hole Name :ICE-07-01		Hole Length :181.36		
Collar X :417505.00	Collar Y :6905999.00	Collar Z :770.00	Azm :130	Dip :-80

	Lithology (txt)	Assays (txt)		Mineral (txt)				Lithology (txt)
Depth At	LithCode	Au_ppb	Cu_ppm	Cpy	Mal	Bor	Py	Desc
		25 50 75 100 125 150 175	1000 2000 3000 4000 5000 6000 7000 8000 9000					Abundant green-white clay gouge; minor Fe-oxide & clay.
185								
190								
195								
200								
205								
210								
215								

Scale 1:200	Date: May 03, 2009	Hole Page 6 of 6

BCGold Corp. - Carmacks Project

Hole Name :ICE-07-02		Hole Length :267.61		
Collar X :417892.00	Collar Y :6905887.00	Collar Z :825.00	Azm :210	Dip :-65

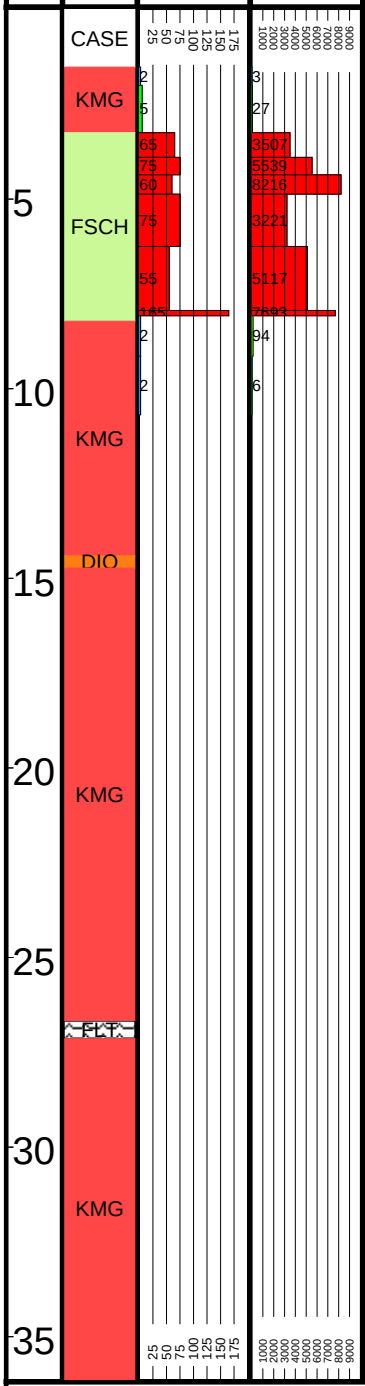

Lithology (txt)
Desc
No recovery. Casing
Lt grey brown; Ksp-megacrystic; friable; Cgr Qtz-Plag-Ksp-bio granite. Equigranular except for minor Ksp megacrysts up to 10mm x 20mm
Lt grey Mgr equigranular felsic schist. Foliated version of Ksp megacrystic granite; above. Weakly oxidized. Weakly oxidized. Minor Cgr pegmatite (contains possible crysophase)
Lt pink ; Ksp-megacrystic; Cgr Qtz-Pag-bio granite. Minor mag. Rare Chl replacing bio; increasing with depth. Minor vuggy patches with increased modal bio. Rock becomes harder with depth. Rare oxidized fault/broken zones. Minor Fgr. Felsic dykes
Grey Fgr massive Qtz-Plag-bio diorite dyke. Disseminated anhedral mag
Lt pink ; Ksp-megacrystic; Cgr Qtz-Pag-bio granite. Minor mag. Rare Chl replacing bio; increasing with depth. Minor vuggy patches with increased modal bio. Rock becomes harder with depth. Rare oxidized fault/broken zones. Minor Fgr. Felsic dykes
Broken ground; Fe-oxide staining on broken surfaces; minor Fe-clay gouge
Lt pink ; Ksp-megacrystic; Cgr Qtz-Pag-bio granite. Minor mag. Rare Chl replacing bio; increasing with depth. Minor vuggy patches with increased modal bio. Rock becomes harder with depth. Rare oxidized fault/broken zones. Minor Fgr. Felsic dykes

BCGold Corp. - Carmacks Project

Hole Name :ICE-07-02		Hole Length :267.61		
Collar X :417892.00	Collar Y :6905887.00	Collar Z :825.00	Azm :210	Dip :-65

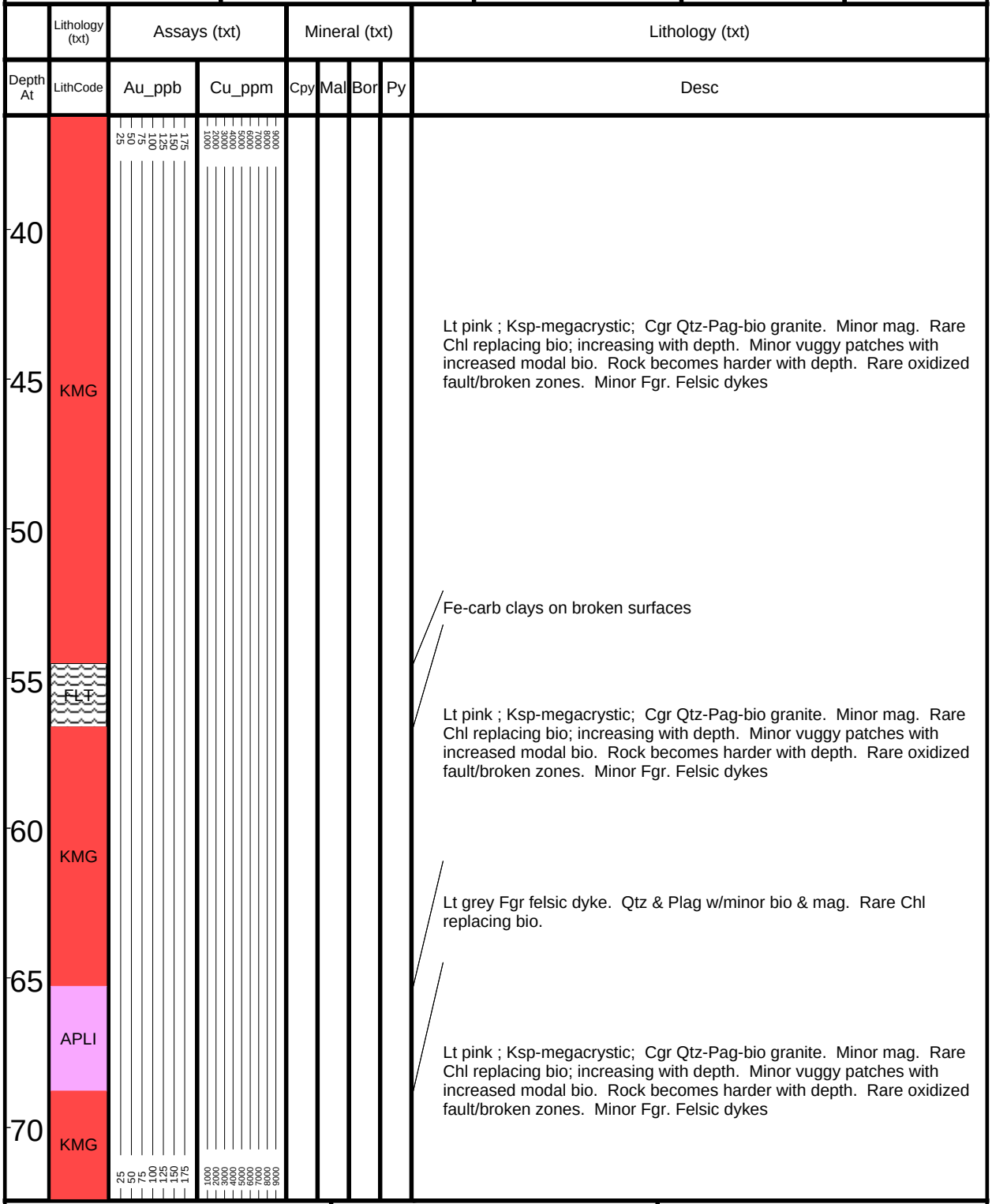

Lithology (txt)

Desc

Lt pink ; Ksp-megacrystic; Cgr Qtz-Pag-bio granite. Minor mag. Rare Chl replacing bio; increasing with depth. Minor vuggy patches with increased modal bio. Rock becomes harder with depth. Rare oxidized fault/broken zones. Minor Fgr. Felsic dykes

Fe-carb clays on broken surfaces

Lt pink ; Ksp-megacrystic; Cgr Qtz-Pag-bio granite. Minor mag. Rare Chl replacing bio; increasing with depth. Minor vuggy patches with increased modal bio. Rock becomes harder with depth. Rare oxidized fault/broken zones. Minor Fgr. Felsic dykes

Lt grey Fgr felsic dyke. Qtz & Plag w/minor bio & mag. Rare Chl replacing bio.

Lt pink ; Ksp-megacrystic; Cgr Qtz-Pag-bio granite. Minor mag. Rare Chl replacing bio; increasing with depth. Minor vuggy patches with increased modal bio. Rock becomes harder with depth. Rare oxidized fault/broken zones. Minor Fgr. Felsic dykes

BCGold Corp. - Carmacks Project

Hole Name :ICE-07-02		Hole Length :267.61		
Collar X :417892.00	Collar Y :6905887.00	Collar Z :825.00	Azm :210	Dip :-65

	Lithology (txt)	Assays (txt)		Mineral (txt)				Lithology (txt)
Depth At	LithCode	Au_ppb	Cu_ppm	Cpy	Mal	Bor	Py	Desc
75	KMG							Lt pink ; Ksp-megacrystic; Cgr Qtz-Pag-bio granite. Minor mag. Rare Chl replacing bio; increasing with depth. Minor vuggy patches with increased modal bio. Rock becomes harder with depth. Rare oxidized fault/broken zones. Minor Fgr. Felsic dykes
80	APLI							Lt grey Fgr felsic dyke. Qtz & Plag w/minor bio & mag. Rare Chl replacing bio.
85								
90	KMG							Lt pink ; Ksp-megacrystic; Cgr Qtz-Pag-bio granite. Minor mag. Rare Chl replacing bio; increasing with depth. Minor vuggy patches with increased modal bio. Rock becomes harder with depth. Rare oxidized fault/broken zones. Minor Fgr. Felsic dykes
95								
100	PEG							Lt pink VCGr Qtz-plag-Ksp Pegmatitie. Cgr bio laths interstitial to felsic minerals. mag replacing bio. Trace Fgr euhedral Chl. Trace Cte in vugs
105	KMG							Lt pink ; Ksp-megacrystic; Cgr Qtz-Pag-bio granite. Minor mag. Rare Chl replacing bio; increasing with depth. Minor vuggy patches with increased modal bio. Rock becomes harder with depth. Rare oxidized fault/broken zones. Minor Fgr. Felsic dykes

Scale 1:200	Date: May 03, 2009	Hole Page 3 of 8

BCGold Corp. - Carmacks Project

Hole Name :ICE-07-02		Hole Length :267.61		
Collar X :417892.00	Collar Y :6905887.00	Collar Z :825.00	Azm :210	Dip :-65

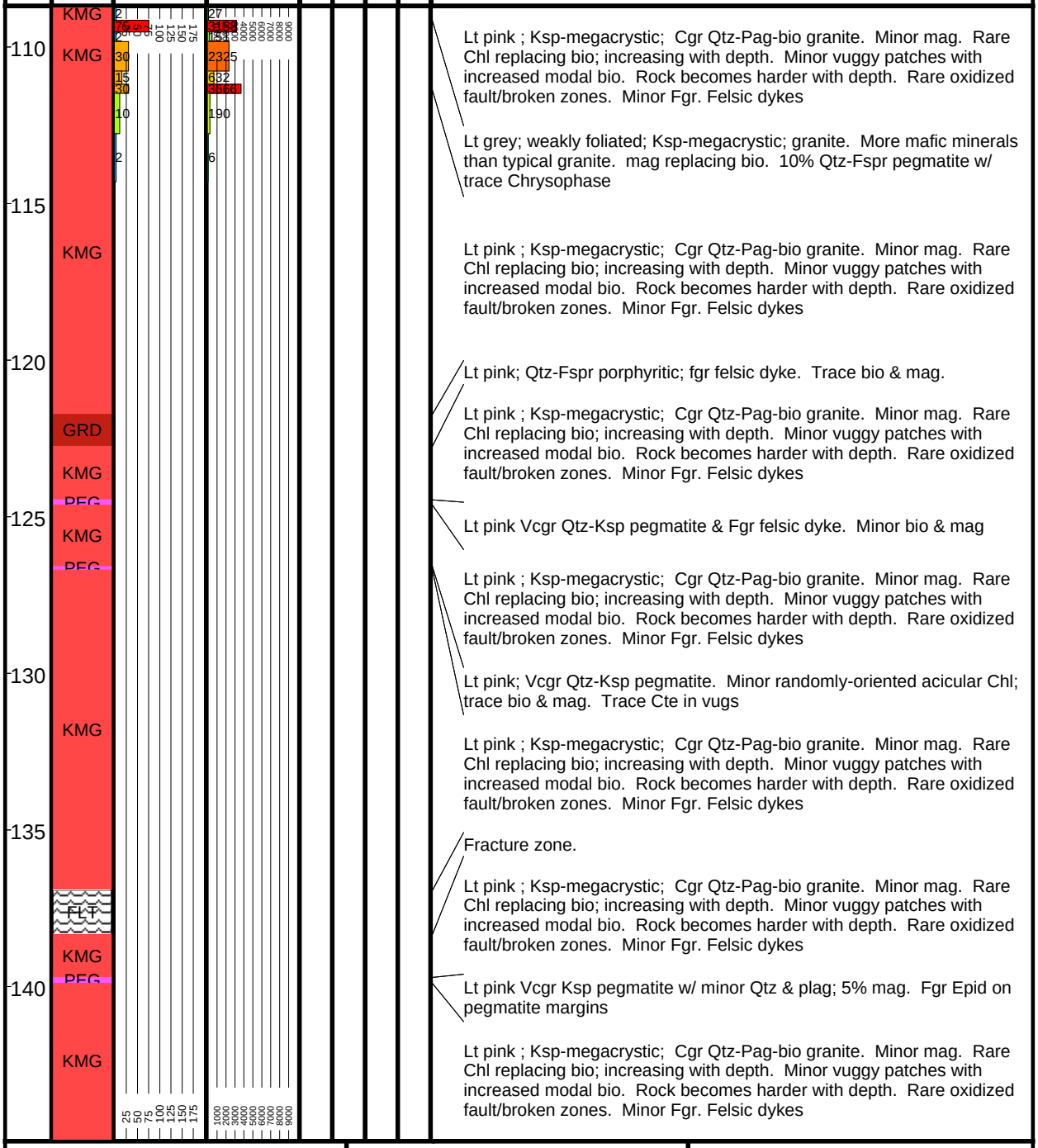

Scale 1:200	Date: May 03, 2009	Hole Page 4 of 8

BCGold Corp. - Carmacks Project

Hole Name :ICE-07-02		Hole Length :267.61		
Collar X :417892.00	Collar Y :6905887.00	Collar Z :825.00	Azm :210	Dip :-65

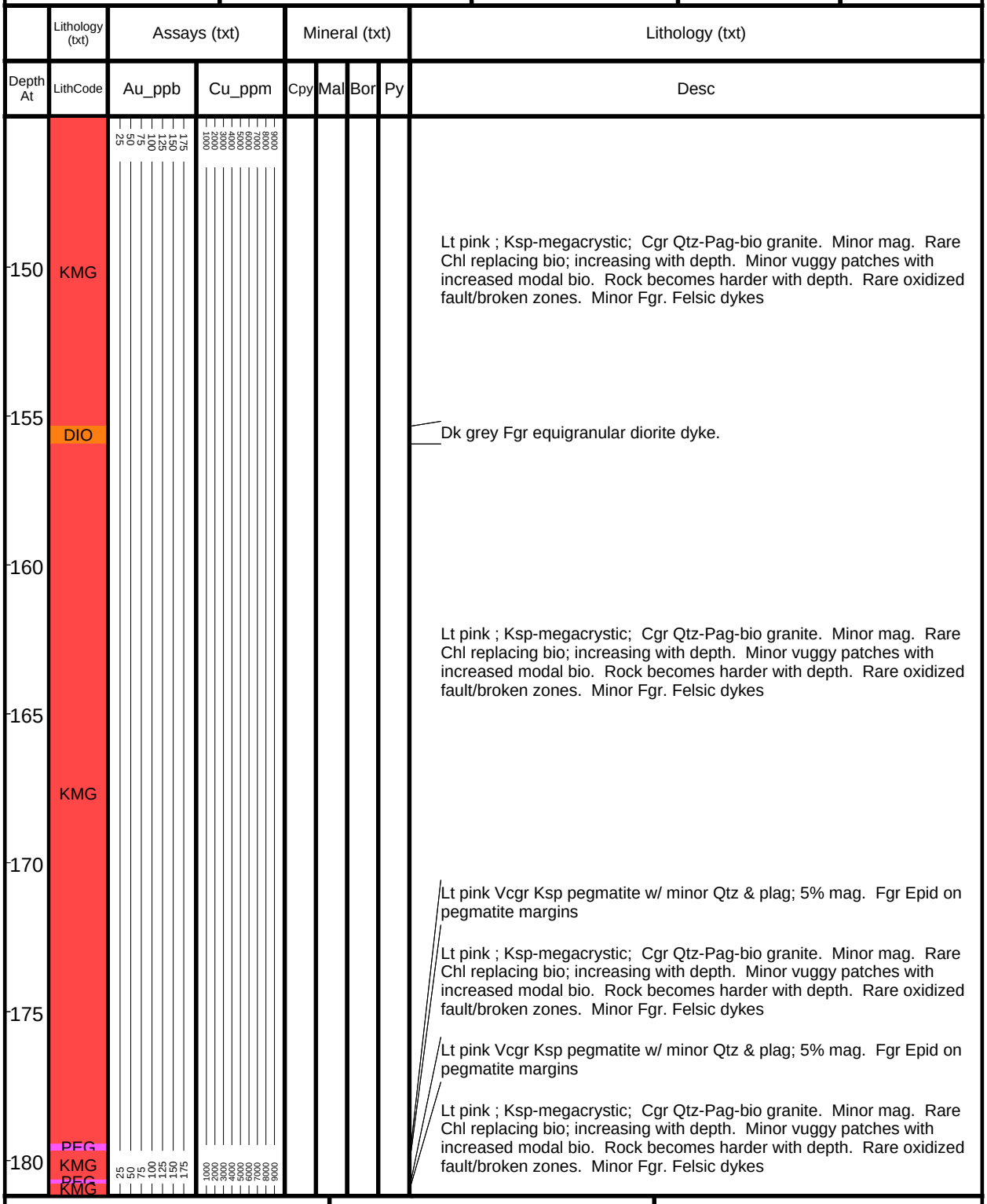

BCGold Corp. - Carmacks Project

Hole Name :ICE-07-02	Hole Length :267.61			
Collar X :417892.00	Collar Y :6905887.00	Collar Z :825.00	Azm :210	Dip :-65

Depth At	Lithology (txt) LithCode	Assays (txt) Au_ppb	Assays (txt) Cu_ppm	Mineral (txt) Cpy	Mal	Bor	Py	Lithology (txt) Desc
185	KMG	25 50 75 100 125 150 175	1000 2000 3000 4000 5000 6000 7000 8000 9000					Lt pink ; Ksp-megacrystic; Cgr Qtz-Pag-bio granite. Minor mag. Rare Chl replacing bio; increasing with depth. Minor vuggy patches with increased modal bio. Rock becomes harder with depth. Rare oxidized fault/broken zones. Minor Fgr. Felsic dykes
	PEG							Lt pink Vcgr Ksp pegmatite w/ minor Qtz & plag; 5% mag. Fgr Epid on pegmatite margins
190	KMG							Lt pink ; Ksp-megacrystic; Cgr Qtz-Pag-bio granite. Minor mag. Rare Chl replacing bio; increasing with depth. Minor vuggy patches with increased modal bio. Rock becomes harder with depth. Rare oxidized fault/broken zones. Minor Fgr. Felsic dykes
195	GRD							Lt pink; Fgr Plag-porphyritic felsic dyke. Minor vuggy patches
200	KMG							Lt pink ; Ksp-megacrystic; Cgr Qtz-Pag-bio granite. Minor mag. Rare Chl replacing bio; increasing with depth. Minor vuggy patches with increased modal bio. Rock becomes harder with depth. Rare oxidized fault/broken zones. Minor Fgr. Felsic dykes
	PEG							Lt pink ; Qtz; Ksp pegmatite w/ minor interstitial euhedral bio; mag & Ank.
205	KMG							Lt pink ; Ksp-megacrystic; Cgr Qtz-Pag-bio granite. Minor mag. Rare Chl replacing bio; increasing with depth. Minor vuggy patches with increased modal bio. Rock becomes harder with depth. Rare oxidized fault/broken zones. Minor Fgr. Felsic dykes
	GRD							Fgr Plag-porphyritic felsic dyke.
210	KMG							Lt pink ; Ksp-megacrystic; Cgr Qtz-Pag-bio granite. Minor mag. Rare Chl replacing bio; increasing with depth. Minor vuggy patches with increased modal bio. Rock becomes harder with depth. Rare oxidized fault/broken zones. Minor Fgr. Felsic dykes
	GRAN							Dk grey Plag-porphyritic Fgr felsic dyke. Fgr chilled margins
215	KMG	25 50 75 100 125 150 175	1000 2000 3000 4000 5000 6000 7000 8000 9000					Lt pink ; Ksp-megacrystic; Cgr Qtz-Pag-bio granite. Minor mag. Rare Chl replacing bio; increasing with depth. Minor vuggy patches with increased modal bio. Rock becomes harder with depth. Rare oxidized fault/broken zones. Minor Fgr. Felsic dykes

BCGold Corp. - Carmacks Project

Hole Name :ICE-07-02		Hole Length :267.61		
Collar X :417892.00	Collar Y :6905887.00	Collar Z :825.00	Azm :210	Dip :-65

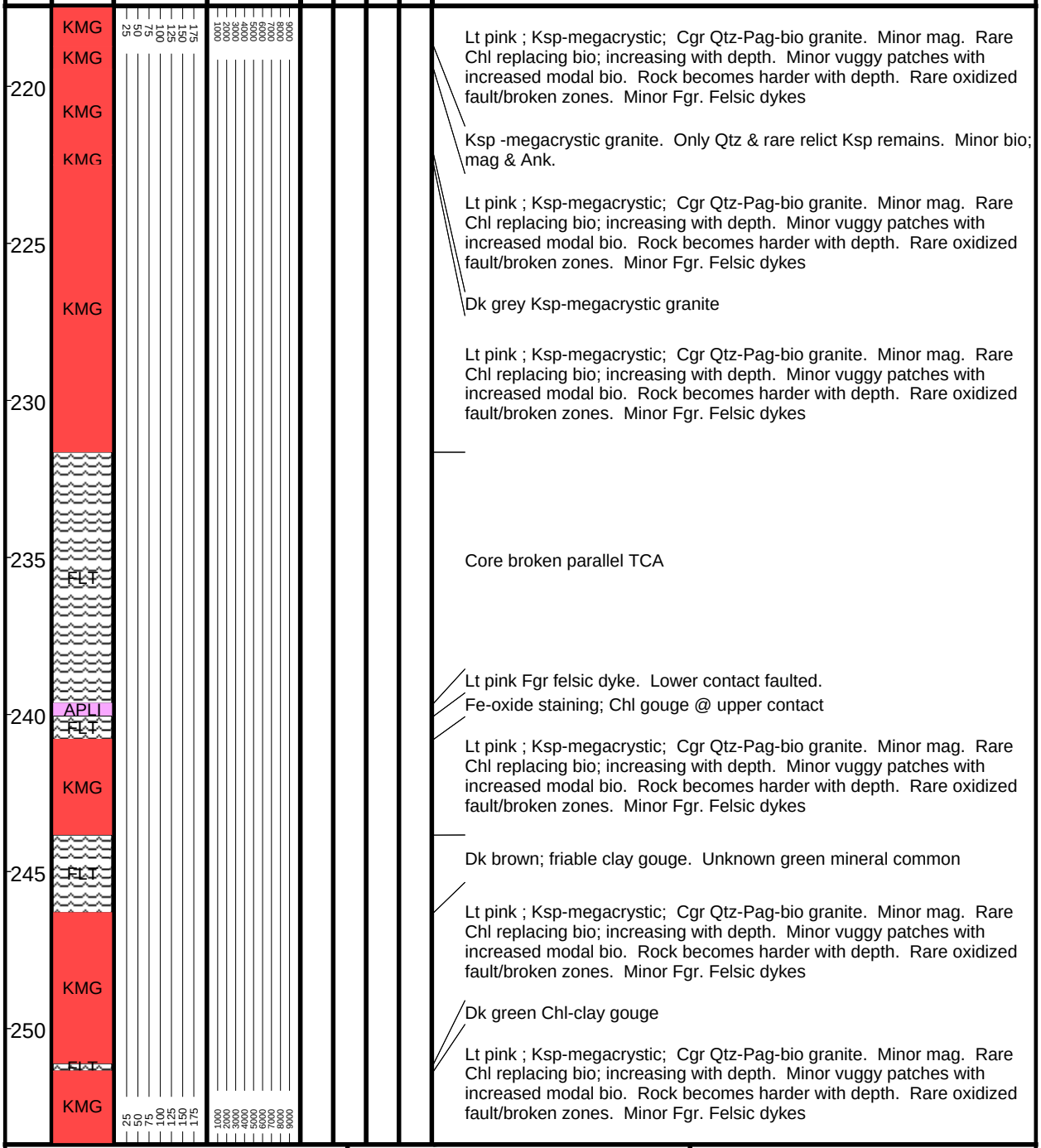

BCGold Corp. - Carmacks Project

Hole Name :ICE-07-02		Hole Length :267.61		
Collar X :417892.00	Collar Y :6905887.00	Collar Z :825.00	Azm :210	Dip :-65

	Lithology (txt)	Assays (txt)		Mineral (txt)				Lithology (txt)
Depth At	LithCode	Au_ppb	Cu_ppm	Cpy	Mal	Bor	Py	Desc
255								
260	KMG							Lt pink ; Ksp-megacrystic; Cgr Qtz-Pag-bio granite. Minor mag. Rare Chl replacing bio; increasing with depth. Minor vuggy patches with increased modal bio. Rock becomes harder with depth. Rare oxidized fault/broken zones. Minor Fgr. Felsic dykes
265	GRD	2 2 2	1 2 2					Dk grey Qtz-plag porphyritic Fgr felsic dyke.
270								
275								
280								
285								

Au_ppb scale: 25 50 75 100 125 150 175

Cu_ppm scale: 1000 2000 3000 4000 5000 6000 7000 8000 9000

Scale 1:200	Date: May 03, 2009	Hole Page 8 of 8

BCGold Corp. - Carmacks Project

Hole Name :ICE-07-03		Hole Length :192.55		
Collar X :417787.00	Collar Y :6905849.00	Collar Z :826.00	Azm :230	Dip :-70

Depth At	Lithology (txt) / LithCode	Assays (txt) Au_ppb	Assays (txt) Cu_ppm	Mineral (txt) Cpy	Mal	Bor	Py	Lithology (txt) Desc
0	CASE							No recovery. Casing
5	KMG							Orange-brown Ksp-megacrystic granite. Cgr; equigranular Qtz; Plag; minor bio. Ksp crystals up to 30mm x 20mm. Strongly weathered; 30% broken/gouge.
10	FLT							Broken; friable KMG. Fractures parallel TCA
15	KMG	2	0.5					Orange-brown Ksp-megacrystic granite. Pervasibely weathered. Fractures parallel TCA
20	FLT	2	4					Orange-brown clay gouge. Primary mineralogy & texture destroyed
25	KMG	2	0.5					Ksp-megacrystic granite. Cgr; equigranular Qtz; Plag; minor bio. Ksp crystals up to 30mm x 20mm.
30	KMG	2	0.5					Ksp-megacrystic granite. Cgr; equigranular Qtz; Plag; minor bio. Ksp crystals up to 30mm x 20mm.
35								

BCGold Corp. - Carmacks Project

Hole Name :ICE-07-03		Hole Length :192.55		
Collar X :417787.00	Collar Y :6905849.00	Collar Z :826.00	Azm :230	Dip :-70

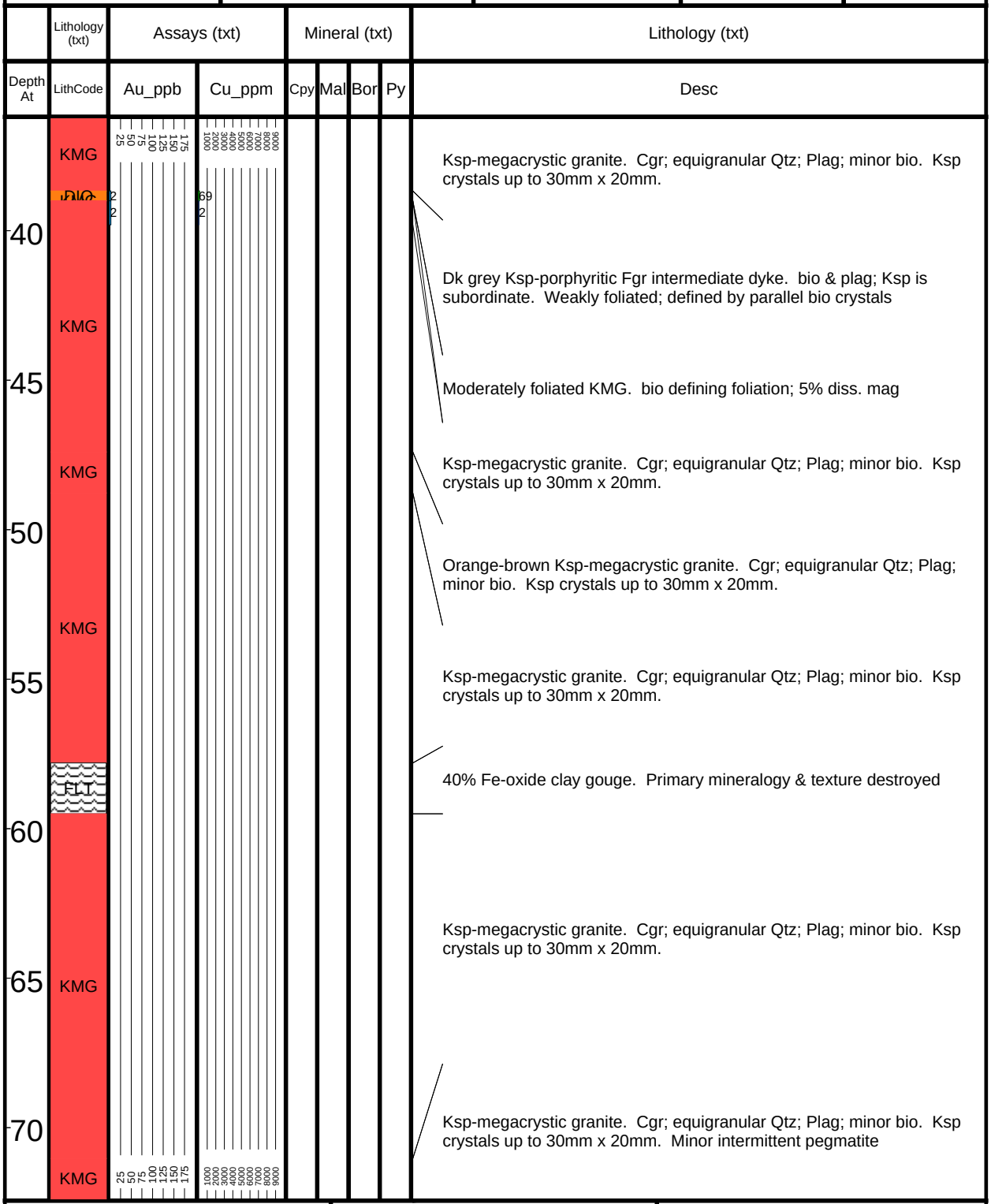

Scale 1:200	Date: May 03, 2009	Hole Page 2 of 6

BCGold Corp. - Carmacks Project

Hole Name :ICE-07-03	Hole Length :192.55			
Collar X :417787.00	Collar Y :6905849.00	Collar Z :826.00	Azm :230	Dip :-70

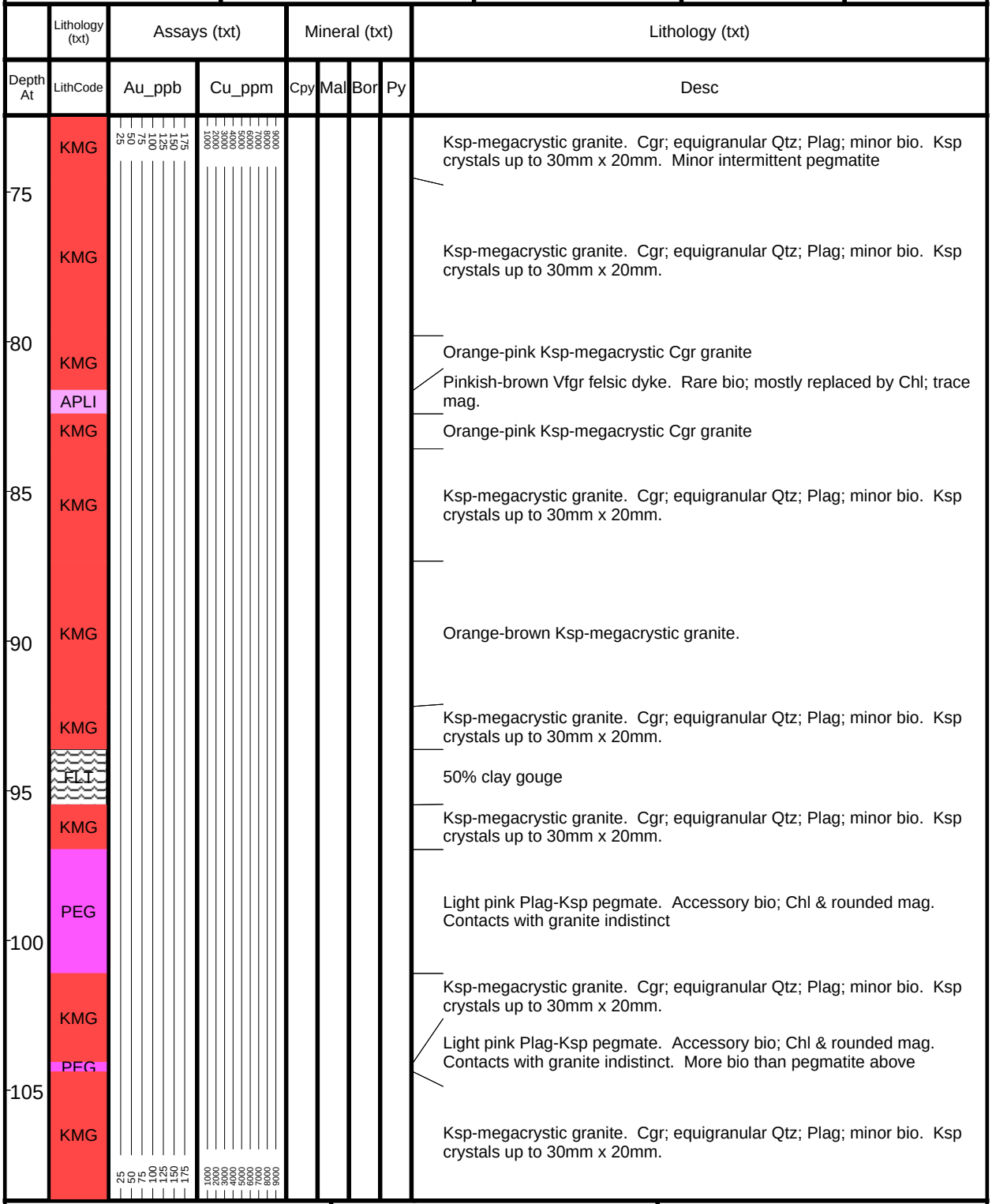

BCGold Corp. - Carmacks Project

Hole Name :ICE-07-03	Hole Length :192.55			
Collar X :417787.00	Collar Y :6905849.00	Collar Z :826.00	Azm :230	Dip :-70

Depth At	Lithology (txt) LithCode	Assays (txt) Au_ppb	Assays (txt) Cu_ppm	Mineral (txt) Cpy	Mal	Bor	Py	Lithology (txt) Desc
110	KMG							Ksp-megacrystic granite. Cgr; equigranular Qtz; Plag; minor bio. Ksp crystals up to 30mm x 20mm.
	Fdy							Lt grey Qtz-plag-sericite porphyritic Fgr felsic dyke. Accessory bio & mag
115	KMG							Ksp-megacrystic granite. Cgr; equigranular Qtz; Plag; minor bio. Ksp crystals up to 30mm x 20mm.
120								
125	PEG							Pink Qtz-plag-Ksp pegmatite. Accessory bio & mag.
	KMG							Ksp-megacrystic granite. Cgr; equigranular Qtz; Plag; minor bio. Ksp crystals up to 30mm x 20mm.
130	FLT							Minor gouge
	KMG							Ksp-megacrystic granite. Cgr; equigranular Qtz; Plag; minor bio. Ksp crystals up to 30mm x 20mm.
	KMG	2	1					Ksp-megacrystic granite
	APLI							Lt pink aphanitic felsic dyke
135	KMG	2	0.5					Ksp-megacrystic granite
		2	0.5					
	KMG							Ksp-megacrystic granite. Cgr; equigranular Qtz; Plag; minor bio. Ksp crystals up to 30mm x 20mm.
	DIO							Dk grey Fgr Qtz-plag diorite intemediate dyke
140	FLT							Faulted KMG. 10% clay gouge
	KMG							Ksp-megacrystic granite. Cgr; equigranular Qtz; Plag; minor bio. Ksp crystals up to 30mm x 20mm.
	FLT							Faulted KMG. 10% clay gouge
	KMG							Ksp-megacrystic granite. Cgr; equigranular Qtz; Plag; minor bio. Ksp crystals up to 30mm x 20mm.

BCGold Corp. - Carmacks Project

Hole Name :ICE-07-03	Hole Length :192.55			
Collar X :417787.00	Collar Y :6905849.00	Collar Z :826.00	Azm :230	Dip :-70

Depth At	LithCode	Au_ppb	Cu_ppm	Cpy	Mal	Bor	Py	Desc
	Lithology (txt)	Assays (txt)		Mineral (txt)				Lithology (txt)
150	KMG							Ksp-megacrystic granite. Cgr; equigranular Qtz; Plag; minor bio. Ksp crystals up to 30mm x 20mm.
	FLT							Faulted KMG
	KMG							Ksp-megacrystic granite. Cgr; equigranular Qtz; Plag; minor bio. Ksp crystals up to 30mm x 20mm.
	APLI							Lt pink aphanitic felsic dyke. Rare Fgr bio laths & mag
	KMG							Ksp-megacrystic granite. Cgr; equigranular Qtz; Plag; minor bio. Ksp crystals up to 30mm x 20mm.
	FLT							Faulted KMG. Minor clay gouge. Unknown green mineral
155	KMG							Ksp-megacrystic granite. Cgr; equigranular Qtz; Plag; minor bio. Ksp crystals up to 30mm x 20mm.
	FLT							Faulted KMG. 20% clay gouge
160	CHB							Dk green aphanitic mafic dyke. Strongly magnetic. 20% brecciated
	KMG							Ksp-megacrystic granite. Cgr; equigranular Qtz; Plag; minor bio. Ksp crystals up to 30mm x 20mm.
165	FLT							Faulted KMG. Minor gouge
	KMG							Ksp-megacrystic granite. Cgr; equigranular Qtz; Plag; minor bio. Ksp crystals up to 30mm x 20mm.
170	FLT							Faulted KMG. Minor gouge
175	KMG							Ksp-megacrystic granite. Cgr; equigranular Qtz; Plag; minor bio. Ksp crystals up to 30mm x 20mm.
180								

BCGold Corp. - Carmacks Project

Hole Name :ICE-07-03		Hole Length :192.55		
Collar X :417787.00	Collar Y :6905849.00	Collar Z :826.00	Azm :230	Dip :-70

	Lithology (txt)	Assays (txt)		Mineral (txt)				Lithology (txt)
Depth At	LithCode	Au_ppb	Cu_ppm	Cpy	Mal	Bor	Py	Desc
185	KMG GRD	25 50 75 100 125 150 175	1000 2000 3000 4000 5000 6000 7000 8000 9000					Ksp-megacrystic granite. Cgr; equigranular Qtz; Plag; minor bio. Ksp crystals up to 30mm x 20mm. Fgr Qtz-Plag seriate porphyritic texture accessory bio; minor mag.
190	KMG	2 2 2	1 2 2					Ksp-megacrystic granite. Cgr; equigranular Qtz; Plag; minor bio. Ksp crystals up to 30mm x 20mm.
195								
200								
205								
210								
215		25 50 75 100 125 150 175	1000 2000 3000 4000 5000 6000 7000 8000 9000					

Scale 1:200	Date: May 03, 2009	Hole Page 6 of 6

BCGold Corp. - Carmacks Project

Hole Name :ICE-07-04		Hole Length :217.93		
Collar X :417893.00	Collar Y :6905887.00	Collar Z :825.00	Azm :240	Dip :-75

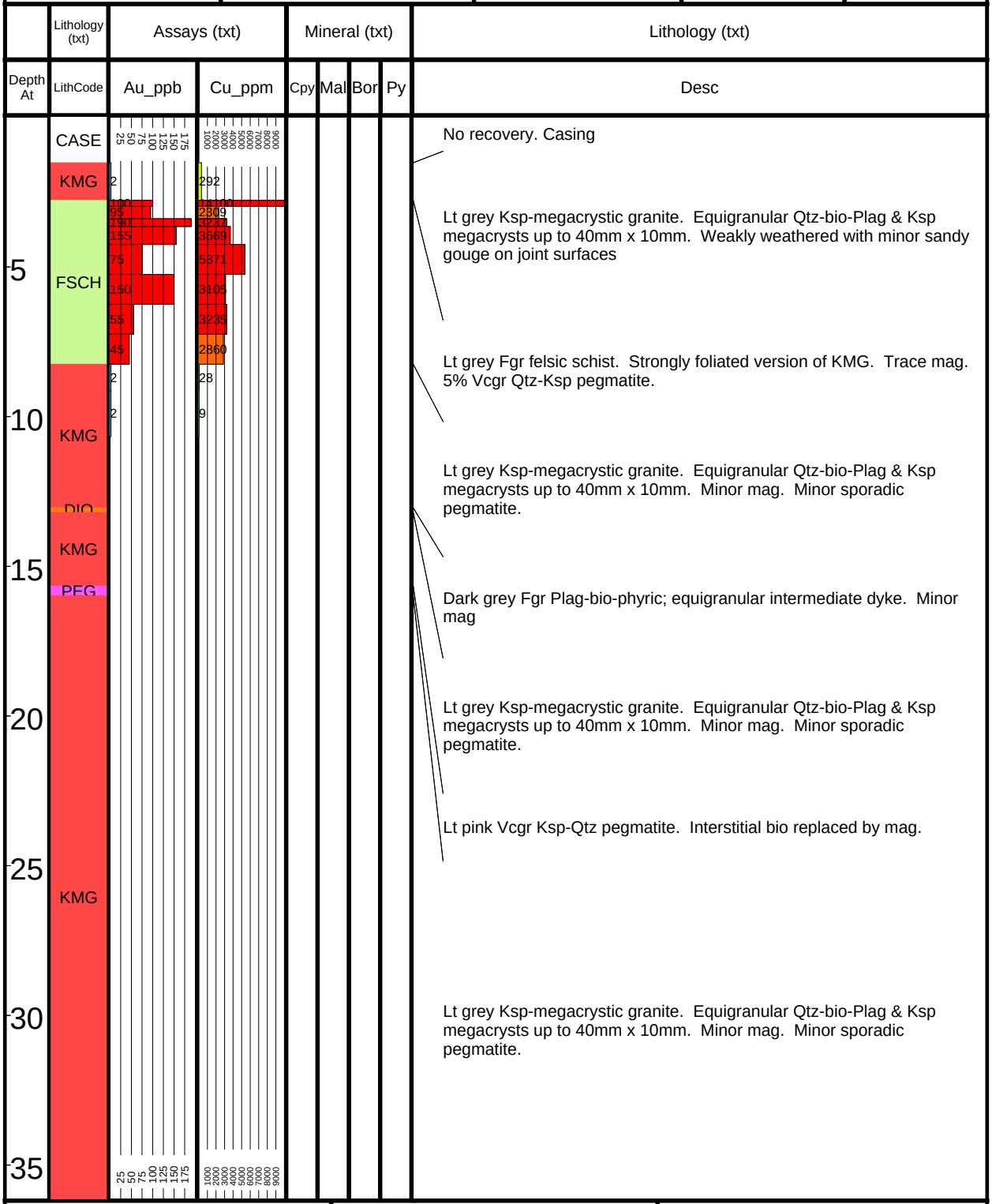

Scale 1:200	Date: May 03, 2009	Hole Page 1 of 7

BCGold Corp. - Carmacks Project

Hole Name :ICE-07-04		Hole Length :217.93		
Collar X :417893.00	Collar Y :6905887.00	Collar Z :825.00	Azm :240	Dip :-75

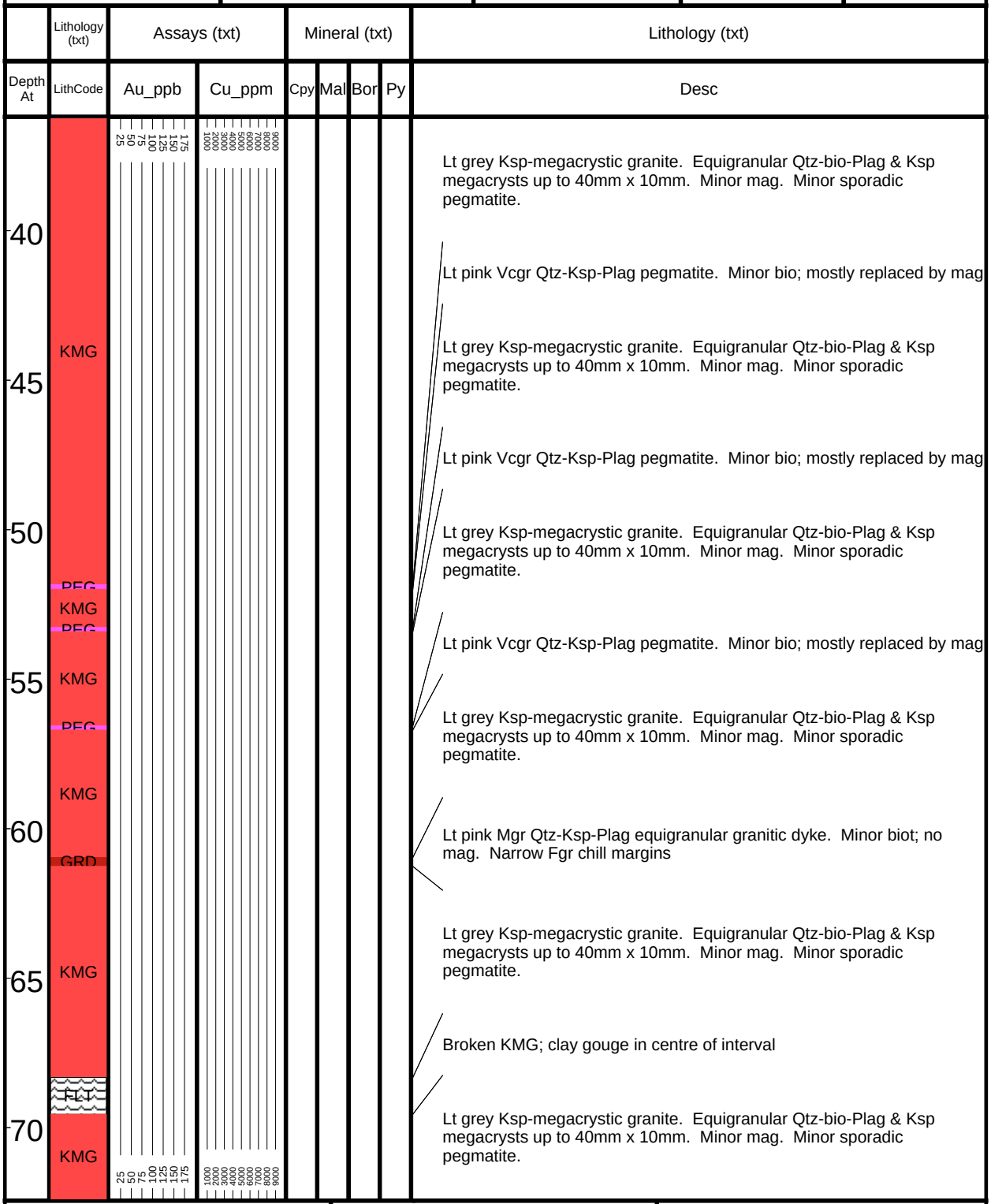

Scale 1:200	Date: May 03, 2009	Hole Page 2 of 7

BCGold Corp. - Carmacks Project

Hole Name :ICE-07-04		Hole Length :217.93		
Collar X :417893.00	Collar Y :6905887.00	Collar Z :825.00	Azm :240	Dip :-75

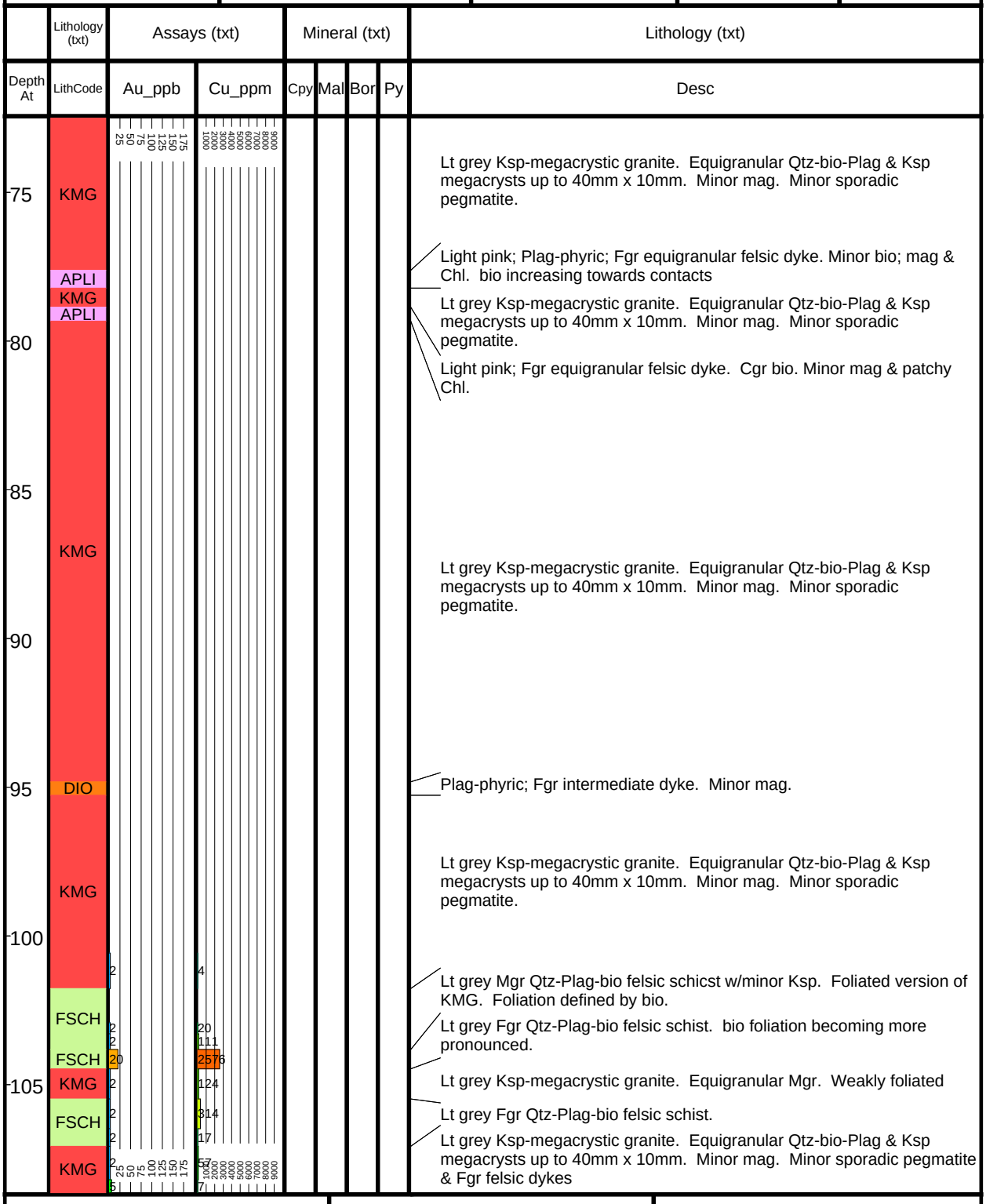

Scale 1:200	Date: May 03, 2009	Hole Page 3 of 7

BCGold Corp. - Carmacks Project

Hole Name :ICE-07-04		Hole Length :217.93		
Collar X :417893.00	Collar Y :6905887.00	Collar Z :825.00	Azm :240	Dip :-75

Depth At	Lithology (txt) LithCode	Assays (txt) Au_ppb	Assays (txt) Cu_ppm	Mineral (txt) Cpy	Mal	Bor	Py	Lithology (txt) Desc
110	KMG	5, 25, 50, 75, 100, 125, 150, 175	100, 200, 300, 400, 500, 600, 700, 800, 900					Lt grey Ksp-megacrystic granite. Equigranular Qtz-bio-Plag & Ksp megacrysts up to 40mm x 10mm. Minor mag. Minor sporadic pegmatite & Fgr felsic dykes
115	KMG							
120	KMG							
125	KMG							Orange-pink Ksp-megacrystic granite. Cgr equigranular Qtz-bio-Plag. Minor mag & Chl.
130	KMG							
135	KMG							Lt grey Ksp-megacrystic granite. Equigranular Qtz-bio-Plag & Ksp megacrysts up to 40mm x 10mm. Minor mag. Minor sporadic pegmatite & Fgr felsic dykes
140	KMG	25, 50, 75, 100, 125, 150, 175	1000, 2000, 3000, 4000, 5000, 6000, 7000, 8000, 9000					

BCGold Corp. - Carmacks Project

Hole Name :ICE-07-04	Hole Length :217.93			
Collar X :417893.00	Collar Y :6905887.00	Collar Z :825.00	Azm :240	Dip :-75

Depth At	Lithology (txt) LithCode	Assays (txt) Au_ppb	Assays (txt) Cu_ppm	Mineral (txt) Cpy	Mal	Bor	Py	Lithology (txt) Desc
150	KMG	25 50 75 100 125 150 175	1000 2000 3000 4000 5000 6000 7000 8000 9000					Lt grey Ksp-megacrystic granite. Equigranular Qtz-bio-Plag & Ksp megacrysts up to 40mm x 10mm. Minor mag. Minor sporadic pegmatite & Fgr felsic dykes
	FLT							Broken KMG; minor clay gouge; minor diss mag.
155	KMG							Lt grey Ksp-megacrystic granite. Equigranular Qtz-bio-Plag & Ksp megacrysts up to 40mm x 10mm. Minor mag. Minor sporadic pegmatite & Fgr felsic dykes
	DIO							Dk grey Plag-phyric Fgr intermediate dyke. Abundant coarser bio.
160	KMG							Dk grey Ksp-megacrystic granite. Minor narrow fauling with clay gouge
	KMG							Lt grey Ksp-megacrystic granite. Equigranular Qtz-bio-Plag & Ksp megacrysts up to 40mm x 10mm. Minor mag. Minor sporadic pegmatite & Fgr felsic dykes
	KMG							Pinkish-grey Ksp-megacrystic granite.
165	KMG							Lt grey Ksp-megacrystic granite. Equigranular Qtz-bio-Plag & Ksp megacrysts up to 40mm x 10mm. Minor mag. Minor sporadic pegmatite & Fgr felsic dykes
170	FLT							Broken KMG. Fractures parallel TCA. Fractures filled with waxy green gouge.
	KMG							Lt grey Ksp-megacrystic granite. Equigranular Qtz-bio-Plag & Ksp megacrysts up to 40mm x 10mm. Minor mag. Minor sporadic pegmatite & Fgr felsic dykes
175	APLI							Lt pink Fgr felsic dyke. Moderatley foliation; defined by bio.
	KMG							Lt grey Ksp-megacrystic granite. Equigranular Qtz-bio-Plag & Ksp megacrysts up to 40mm x 10mm. Minor mag. Minor sporadic pegmatite & Fgr felsic dykes
180		25 50 75 100 125 150 175	1000 2000 3000 4000 5000 6000 7000 8000 9000					

BCGold Corp. - Carmacks Project

Hole Name :ICE-07-04		Hole Length :217.93		
Collar X :417893.00	Collar Y :6905887.00	Collar Z :825.00	Azm :240	Dip :-75

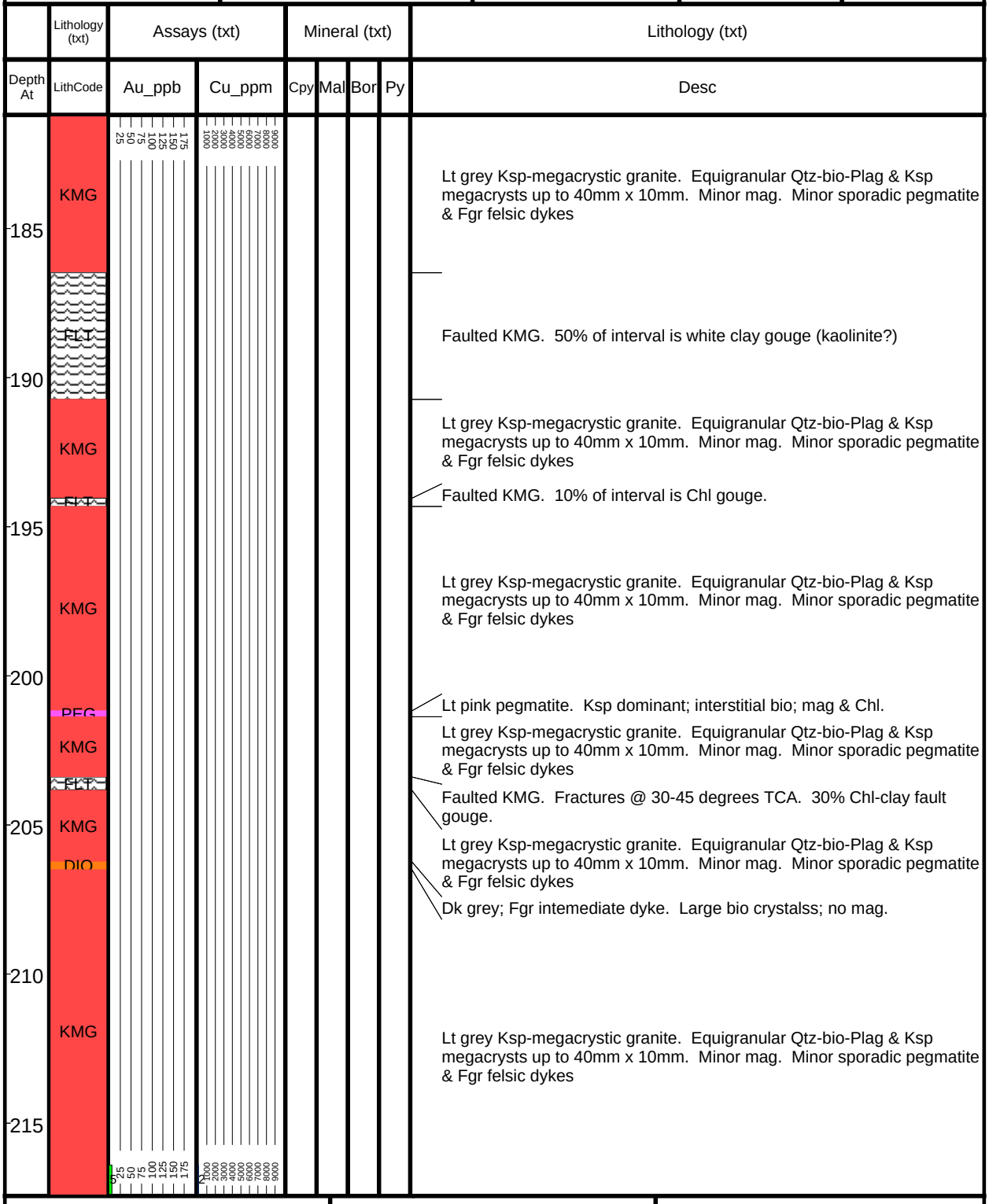

Scale 1:200	Date: May 03, 2009	Hole Page 6 of 7

BCGold Corp. - Carmacks Project

Hole Name :ICE-07-04		Hole Length :217.93		
Collar X :417893.00	Collar Y :6905887.00	Collar Z :825.00	Azm :240	Dip :-75

	Lithology (txt)	Assays (txt)		Mineral (txt)				Lithology (txt)
Depth At	LithCode	Au_ppb	Cu_ppm	Cpy	Mal	Bor	Py	Desc
220	KMG	5	2					Lt grey Ksp-megacrystic granite. Equigranular Qtz-bio-Plag & Ksp megacrysts up to 40mm x 10mm. Minor mag. Minor sporadic pegmatite & Fgr felsic dykes
225								
230								
235								
240								
245								
250								

Scale 1:200	Date: May 03, 2009	Hole Page 7 of 7

BCGold Corp. - Carmacks Project

Hole Name :WS-07-05		Hole Length :217.93		
Collar X :414753.00	Collar Y :6910415.00	Collar Z :857.00	Azm :230	Dip :-50

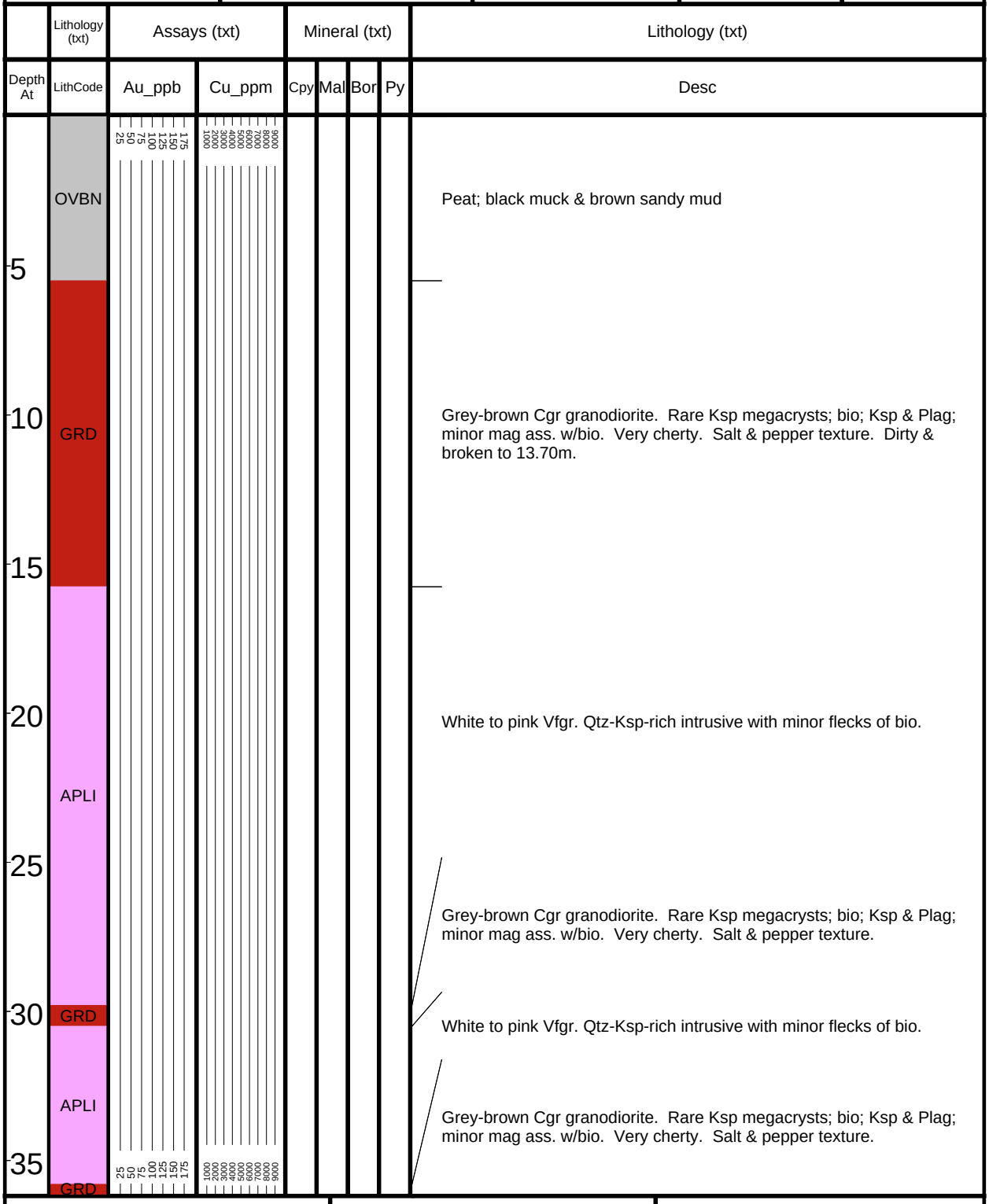

Scale 1:200	Date: May 03, 2009	Hole Page 1 of 7

BCGold Corp. - Carmacks Project

Hole Name :WS-07-05		Hole Length :217.93		
Collar X :414753.00	Collar Y :6910415.00	Collar Z :857.00	Azm :230	Dip :-50

Depth At	Lithology (txt) / LithCode	Assays (txt) Au_ppb	Assays (txt) Cu_ppm	Mineral (txt) Cpy	Mal	Bor	Py	Lithology (txt) Desc
40	GRD	25 50 75 100 125 150 175	100 200 3000 4000 5000 6000 7000 8000 9000					Grey-brown Cgr granodiorite. Rare Ksp megacrysts; bio; Ksp & Plag; minor mag ass. w/bio. Very cherty. Salt & pepper texture.
	APLI							White to pink Vfgr. Qtz-Ksp-rich intrusive with minor flecks of bio.
45	APLI							Very broken core & rubble
	APLI							White to pink Vfgr. Qtz-Ksp-rich intrusive with minor flecks of bio.
50	APLI							Very broken core & rubble
	APLI							White to pink Vfgr. Qtz-Ksp-rich intrusive with minor flecks of bio.
55	APLI							
	MSCH							grn Vfgr; well-foliated Qtz-Chl-bio mafic schist. Foliation @ 45-60 degrees TCA.
60	MSCH							
	GRD							Grey to pinkish-grey Mgr to Cgr bio granodiorite.
65	GRD							
	GRD							
70	GRD							

Scale 1:200	Date: May 03, 2009	Hole Page 2 of 7

BCGold Corp. - Carmacks Project

Hole Name :WS-07-05		Hole Length :217.93		
Collar X :414753.00	Collar Y :6910415.00	Collar Z :857.00	Azm :230	Dip :-50

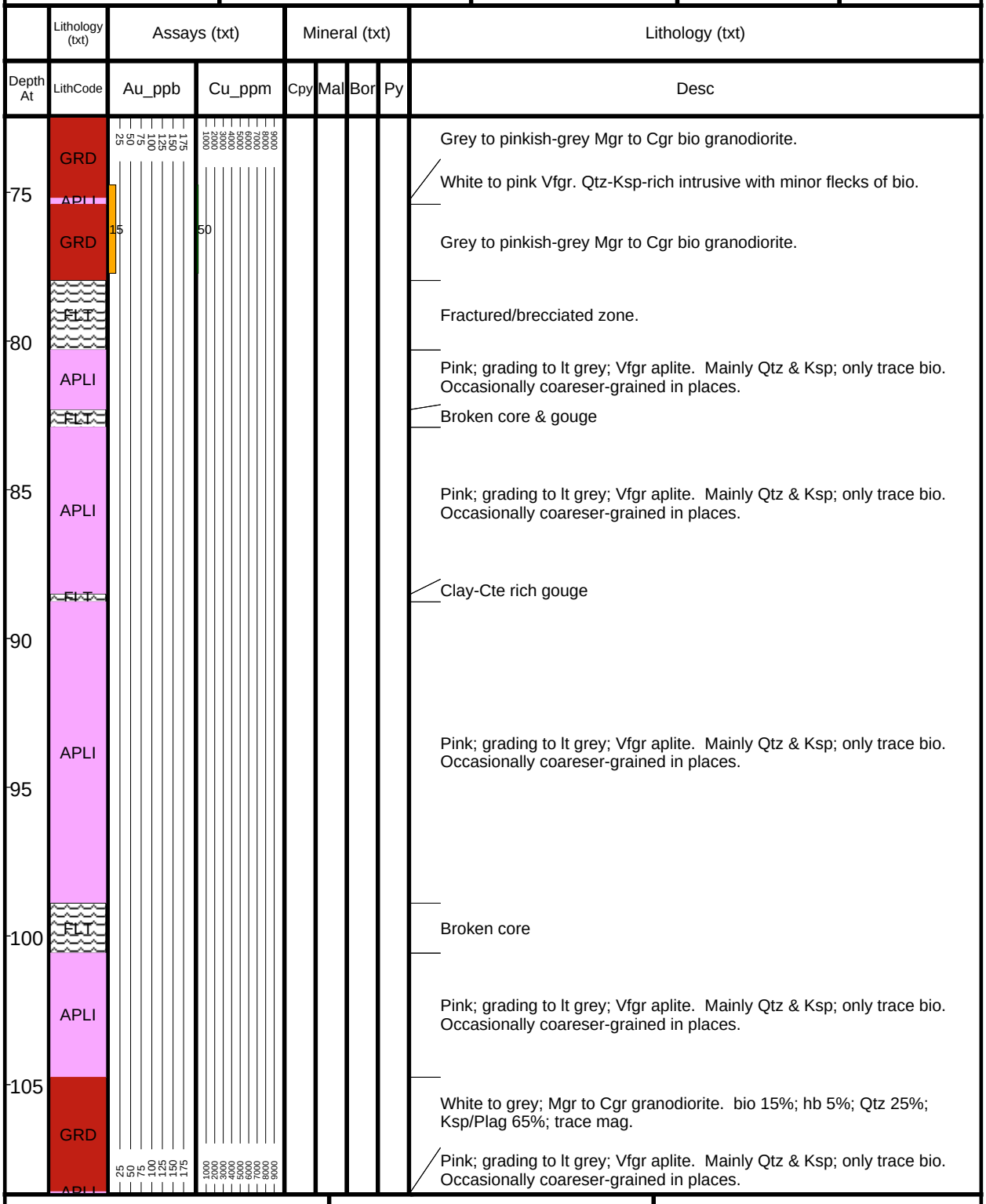

Scale 1:200	Date: May 03, 2009	Hole Page 3 of 7

BCGold Corp. - Carmacks Project

Hole Name :WS-07-05	Hole Length :217.93			
Collar X :414753.00	Collar Y :6910415.00	Collar Z :857.00	Azm :230	Dip :-50

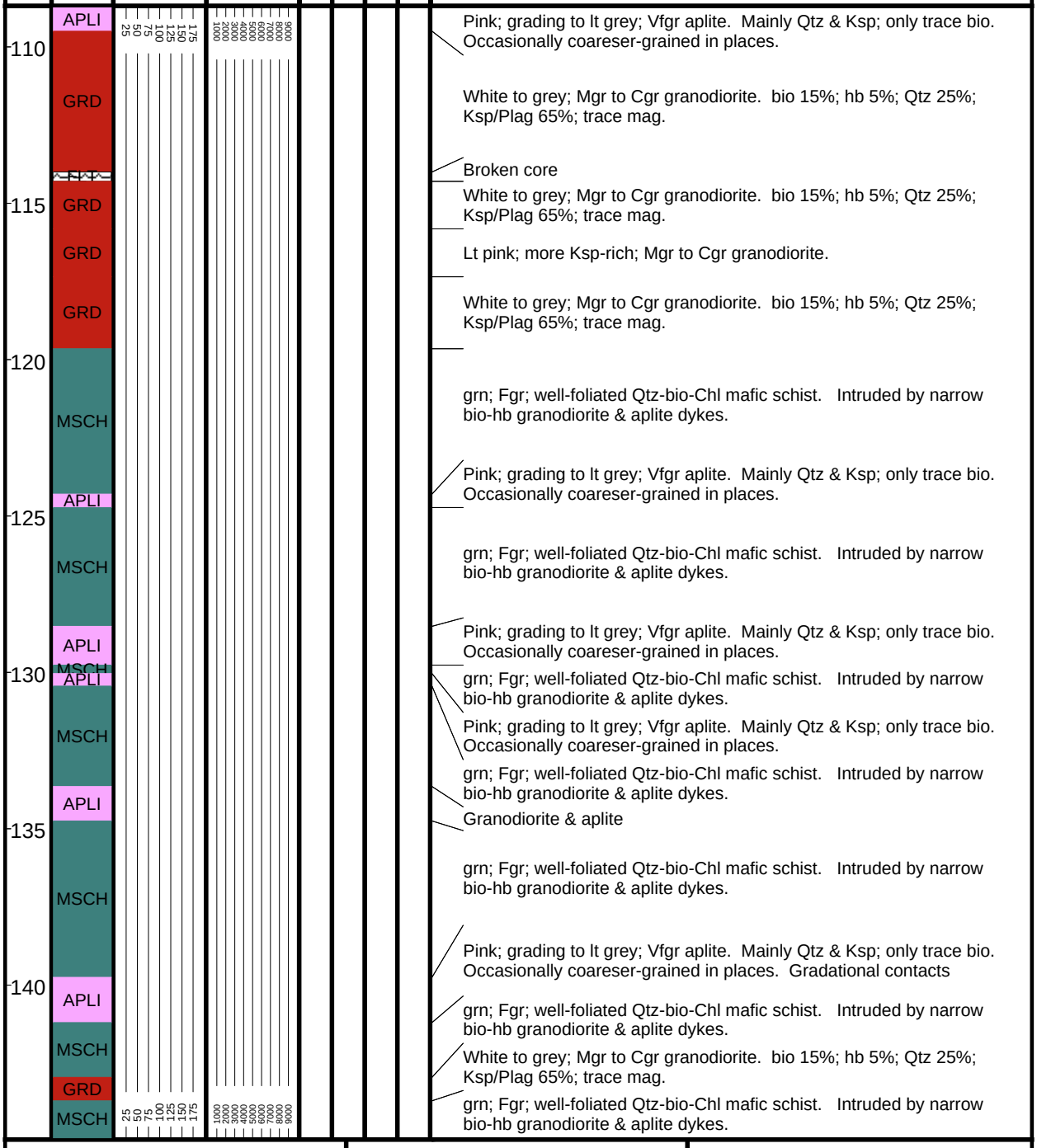

Scale 1:200	Date: May 03, 2009	Hole Page 4 of 7

BCGold Corp. - Carmacks Project

Hole Name :WS-07-05	Hole Length :217.93			
Collar X :414753.00	Collar Y :6910415.00	Collar Z :857.00	Azm :230	Dip :-50

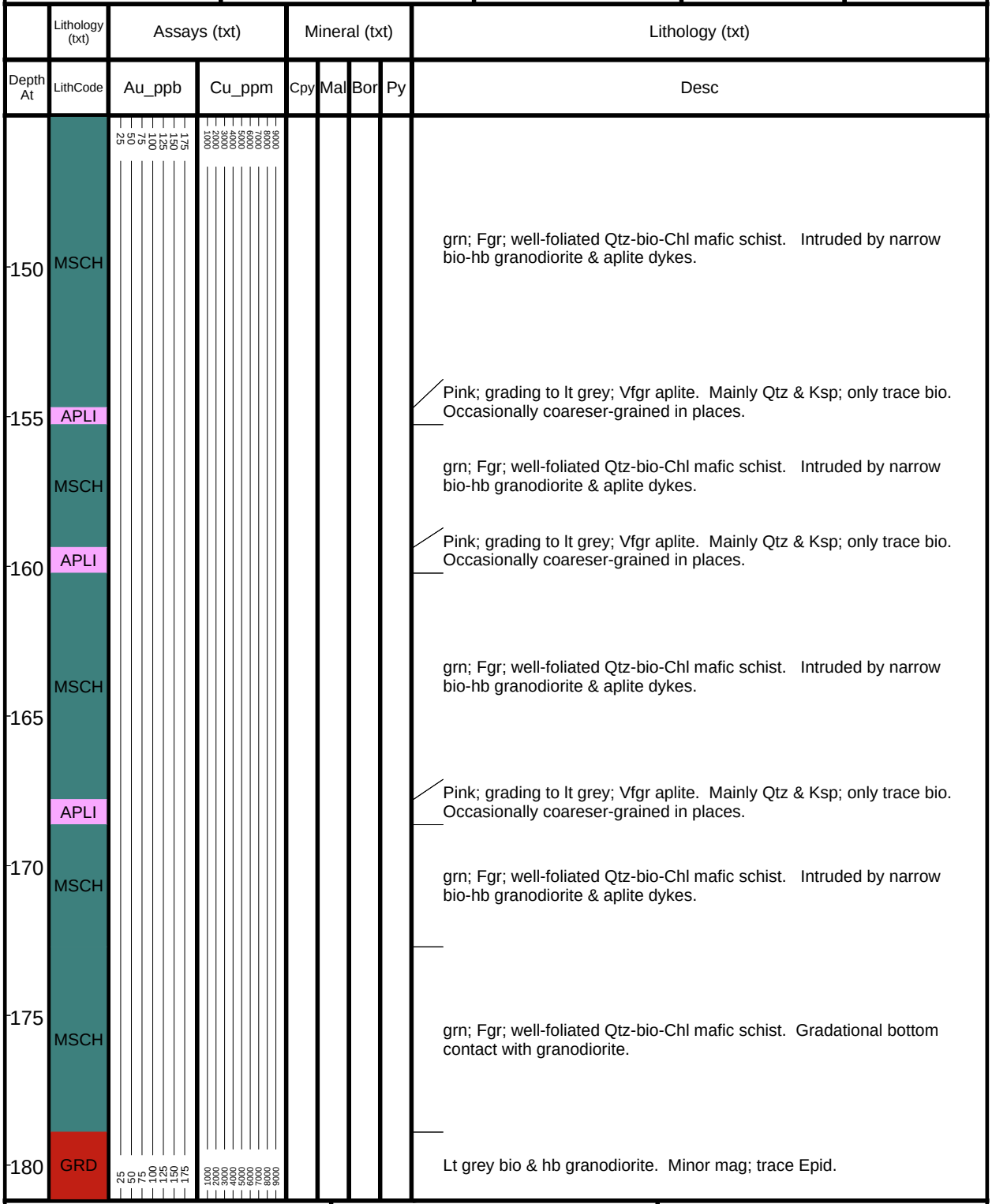

BCGold Corp. - Carmacks Project

Hole Name :WS-07-05		Hole Length :217.93		
Collar X :414753.00	Collar Y :6910415.00	Collar Z :857.00	Azm :230	Dip :-50

	Lithology (txt)	Assays (txt)		Mineral (txt)				Lithology (txt)
Depth At	LithCode	Au_ppb	Cu_ppm	Cpy	Mal	Bor	Py	Desc
185								
190								
195		15	50					
200	GRD							Lt grey bio & hb granodiorite. Minor mag; trace Epid.
205								
210								
215								

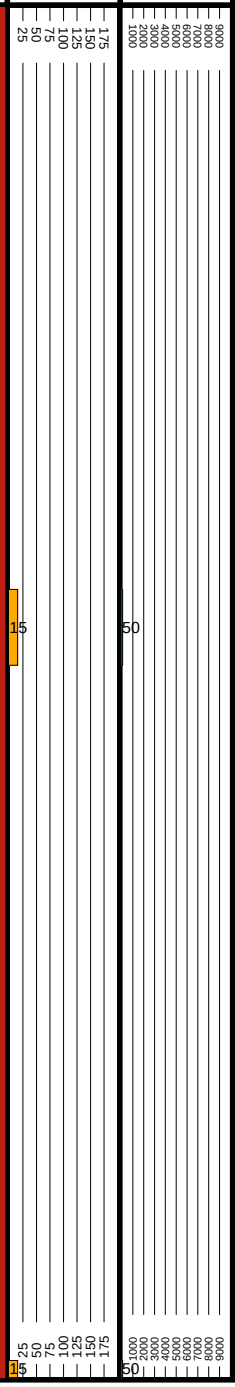

Scale 1:200	Date: May 03, 2009	Hole Page 6 of 7

BCGold Corp. - Carmacks Project

Hole Name :WS-07-05		Hole Length :217.93		
Collar X :414753.00	Collar Y :6910415.00	Collar Z :857.00	Azm :230	Dip :-50

	Lithology (txt)	Assays (txt)		Mineral (txt)				Lithology (txt)
Depth At	LithCode	Au_ppb	Cu_ppm	Cpy	Mal	Bor	Py	Desc
	GRD	1 5 25 50 75 100 125 150 175	50 1000 2000 3000 4000 5000 6000 7000 8000 9000					Lt grey bio & hb granodiorite. Minor mag; trace Epid.
220								
225								
230								
235								
240								
245								
250								

BCGold Corp. - Carmacks Project

Hole Name :WS-07-06		Hole Length :141.12		
Collar X :414947.00	Collar Y :6910319.00	Collar Z :833.00	Azm :230	Dip :-50

Depth At	Lithology (txt) LithCode	Assays (txt) Au_ppb	Assays (txt) Cu_ppm	Mineral (txt) Cpy	Mal	Bor	Py	Lithology (txt) Desc
5	OVBN	25 50 75 100 125 150 175	1000 2000 3000 4000 5000 6000 7000 8000 9000					Sandy clay with occasional rock fragments. Peat moss. Coarse mafic pebbles @ top of hole.
10	GRD							Lt grey to white Cgr granodiorite. Locally Ksp-megacrystic. Deeply weathered rubbly zone; locally oxidized orange-brown.
15	GRD							Lt grey to white Cgr granodiorite. Locally Ksp-megacrystic.
	PEG							Qtz-Ksp pegmatite vein
	FLT							Weathered rubble
20	GRD							Lt grey to white Cgr granodiorite. Locally Ksp-megacrystic.
25	GRD							Lt grey to white Cgr granodiorite. Locally Ksp-megacrystic. Blocky; fractured interval. Dull grey-brown weathering of hb. Weakly magnetic locally.
30	FLT							Broken rubble
	GRD							Lt grey to white Cgr granodiorite. Locally Ksp-megacrystic.
35	GRD	25 50 75 100 125 150 175	1000 2000 3000 4000 5000 6000 7000 8000 9000					Lt grey to white Cgr granodiorite. Locally Ksp-megacrystic. 15-20% bio.

BCGold Corp. - Carmacks Project

Hole Name :WS-07-06		Hole Length :141.12		
Collar X :414947.00	Collar Y :6910319.00	Collar Z :833.00	Azm :230	Dip :-50

	Lithology (txt)	Assays (txt)		Mineral (txt)				Lithology (txt)
Depth At	LithCode	Au_ppb	Cu_ppm	Cpy	Mal	Bor	Py	Desc
40	GRD							Lt grey to white Cgr granodiorite. Locally Ksp-megacrystic. 15-20% bio.
45								
50								
55	GRD							Lt grey to white Cgr granodiorite. Locally Ksp-megacrystic.
60								
65	MSCH							Mafic schist
	GRD							Lt grey to white Cgr granodiorite. Locally Ksp-megacrystic. Increasing modal% of coarse bio 9after hb?) towards lower contact.
70	MSCH							Grey-grn to black mafic schist. modly schistosity @ 70 degrees TCA.

BCGold Corp. - Carmacks Project

Hole Name :WS-07-06	Hole Length :141.12			
Collar X :414947.00	Collar Y :6910319.00	Collar Z :833.00	Azm :230	Dip :-50

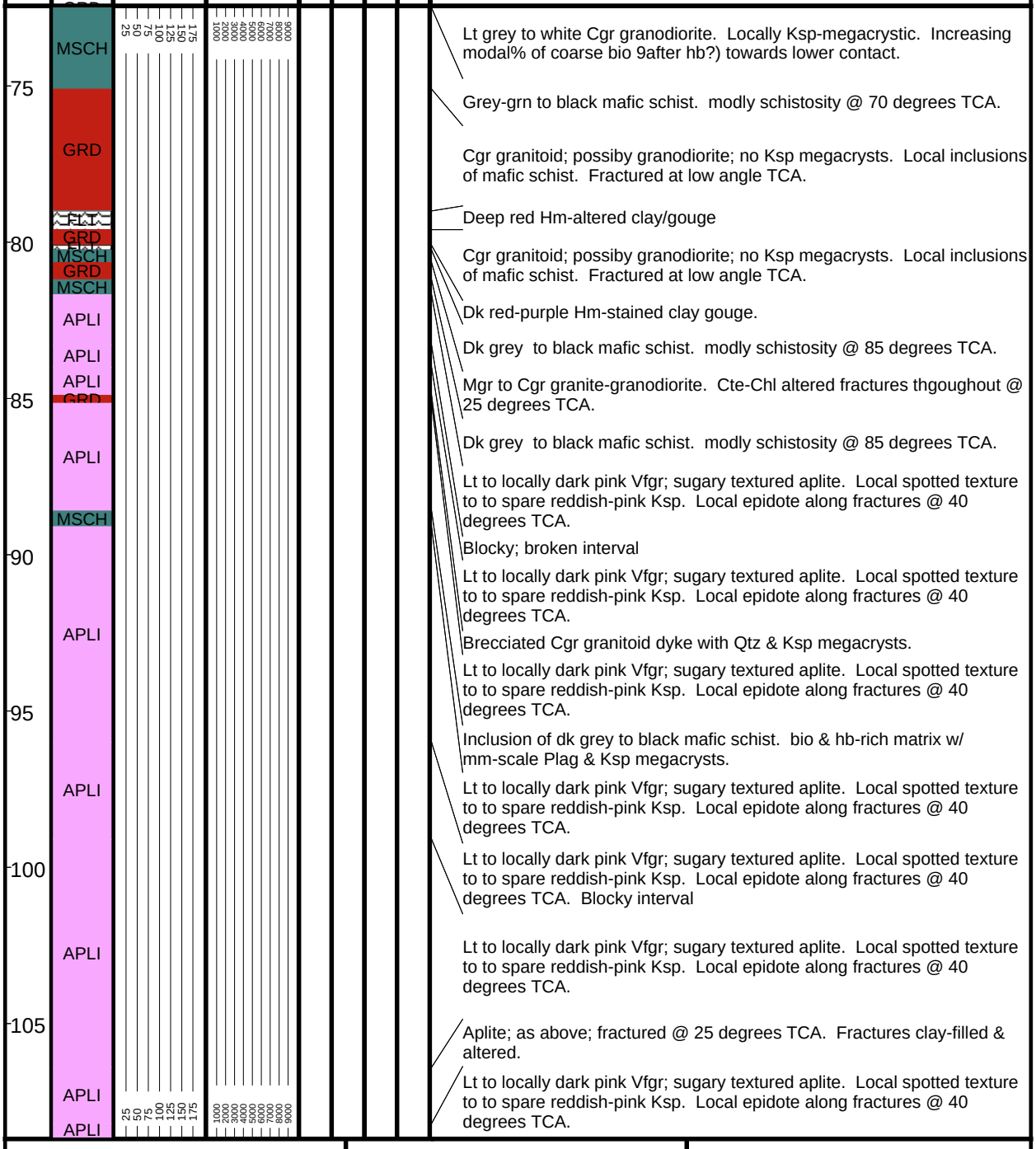

Scale 1:200	Date: May 03, 2009	Hole Page 3 of 4

BCGold Corp. - Carmacks Project

Hole Name :WS-07-06	Hole Length :141.12			
Collar X :414947.00	Collar Y :6910319.00	Collar Z :833.00	Azm :230	Dip :-50

	Lithology (txt)	Assays (txt)		Mineral (txt)				Lithology (txt)
Depth At	LithCode	Au_ppb	Cu_ppm	Cpy	Mal	Bor	Py	Desc
110	APLI							Lt to locally dark pink Vfgr; sugary textured aplite. Local spotted texture to to spare reddish-pink Ksp. Local epidote along fractures @ 40 degrees TCA.
	APLI							Mafic inclusion. Possibly recrystllized mafic schist. hb-bio matrix with 20% coarse Ksp megacrysts
	APLI							Lt to locally dark pink Vfgr; sugary textured aplite. Local spotted texture to to spare reddish-pink Ksp. Local epidote along fractures @ 40 degrees TCA. Blocky interval
115	GRD							Granodiorite fragment inclusion.
	APLI							Lt to locally dark pink Vfgr; sugary textured aplite. Local spotted texture to to spare reddish-pink Ksp. Local epidote along fractures @ 40 degrees TCA.
120	APLI							Lt to locally dark pink Vfgr; sugary textured aplite. Local spotted texture to to spare reddish-pink Ksp. Local epidote along fractures @ 40 degrees TCA.
125	APLI							Lt to locally dark pink Vfgr; sugary textured aplite. Local spotted texture to to spare reddish-pink Ksp. Local epidote along fractures @ 40 degrees TCA. Blocky; fractured inerval.
	APLI							Lt to locally dark pink Vfgr; sugary textured aplite. Local spotted texture to to spare reddish-pink Ksp. Local epidote along fractures @ 40 degrees TCA. Blocky; fractured inerval.
	APLI							Lt to locally dark pink Vfgr; sugary textured aplite. Local spotted texture to to spare reddish-pink Ksp. Local epidote along fractures @ 40 degrees TCA.
130	GRD							Mgr granodiorite with minor local aplite.
	PEG							Qtz-Ksp pegmatite
	GRD							Mgr granodiorite with minor local aplite.
	FLT							Clay gouge
	GRD							Mgr granodiorite with minor local aplite.
135	GRD							Carb-sricite altered vein. Locally strong Hm; strong Ksp halo.
	GRD							Mgr granodiorite with minor local aplite.
	GRD							Lt to locally dark pink Vfgr; sugary textured aplite. Local spotted texture to to spare reddish-pink Ksp. Blocky; with local epidote along fractures @ 40 degrees TCA.
140	APLI							

Scale 1:200	Date: May 03, 2009	Hole Page 4 of 4

BCGold Corp. - Carmacks Project

Hole Name :WS-07-07		Hole Length :141.73		
Collar X :414970.00	Collar Y :6909932.00	Collar Z :846.00	Azm :230	Dip :-50

Depth At	Lithology (txt) LithCode	Assays (txt) Au_ppb	Assays (txt) Cu_ppm	Mineral (txt) Cpy	Mal	Bor	Py	Lithology (txt) Desc
0	OVBN	25 50 75 100 125 150 175	1000 2000 3000 4000 5000 6000 7000 8000 9000					Overburden
5	FBGR	15	800					Foliated bio granodiorite. Foliation @ 80 degrees TCA
	APLI	15	100					Aplite dyke with Cgr Ksp
	FBGR	15	50 1330					Foliated bio granodiorite. bio >20%. Fractures @ 20 degrees TCA
10								
15								
20	GRD							Masive biotite granodiorite
25								
30								
35		25 50 75 100 125 150 175	1000 2000 3000 4000 5000 6000 7000 8000 9000					

BCGold Corp. - Carmacks Project

Hole Name :WS-07-07		Hole Length :141.73		
Collar X :414970.00	Collar Y :6909932.00	Collar Z :846.00	Azm :230	Dip :-50

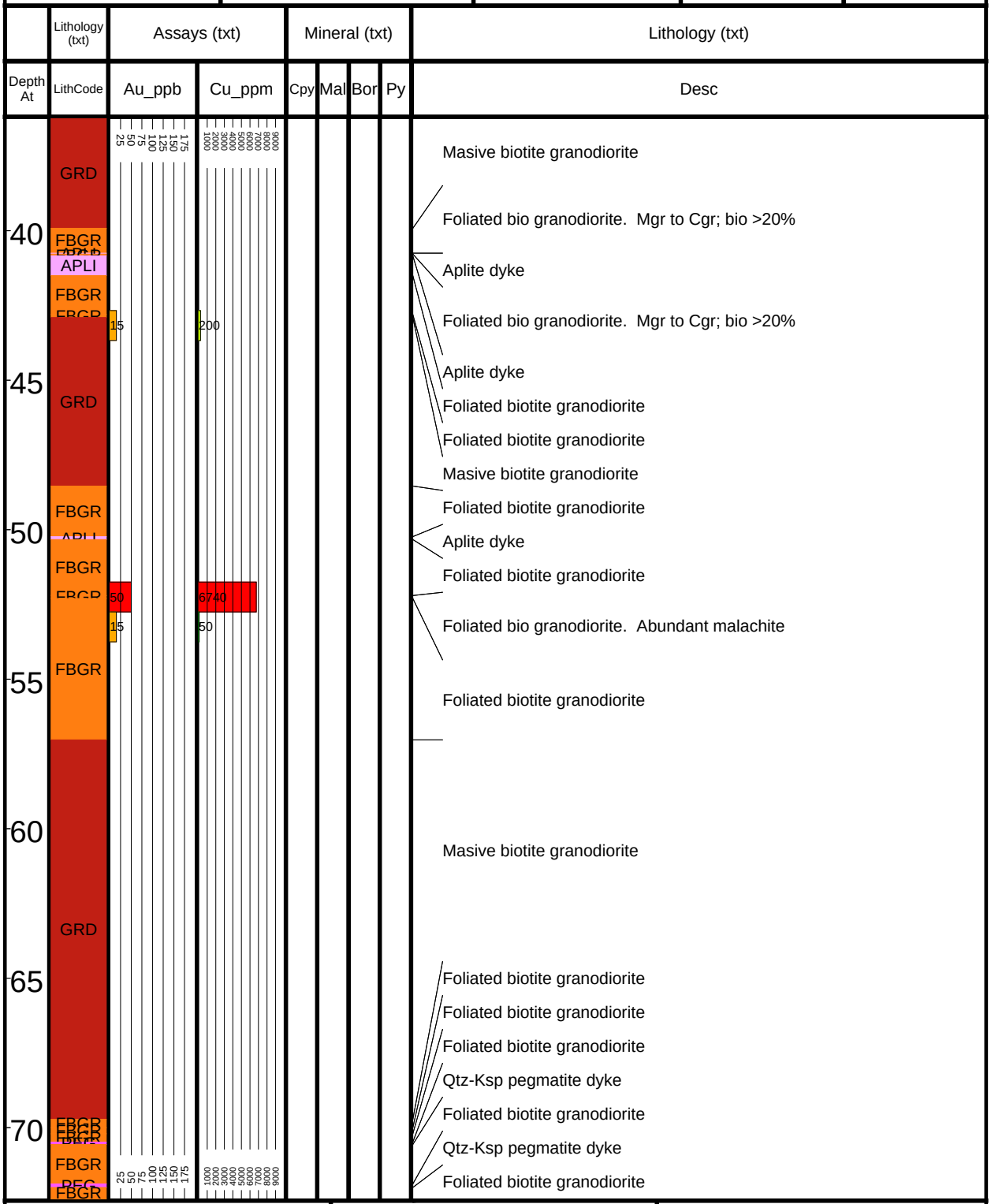

Scale 1:200	Date: May 03, 2009	Hole Page 2 of 4

BCGold Corp. - Carmacks Project

Hole Name :WS-07-07		Hole Length :141.73		
Collar X :414970.00	Collar Y :6909932.00	Collar Z :846.00	Azm :230	Dip :-50

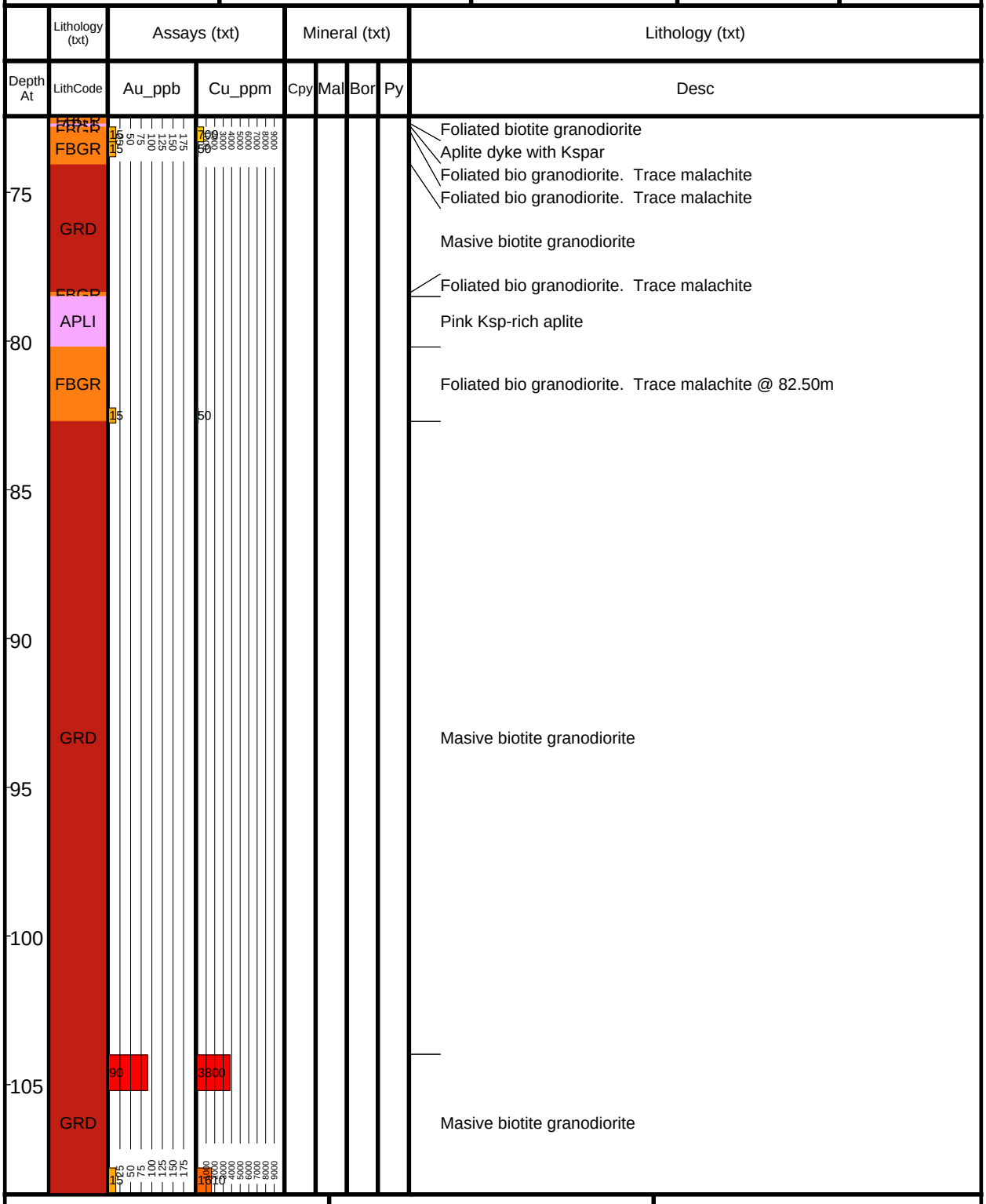

Scale 1:200	Date: May 03, 2009	Hole Page 3 of 4

BCGold Corp. - Carmacks Project

Hole Name :WS-07-07		Hole Length :141.73		
Collar X :414970.00	Collar Y :6909932.00	Collar Z :846.00	Azm :230	Dip :-50

	Lithology (txt)	Assays (txt)		Mineral (txt)				Lithology (txt)
Depth At	LithCode	Au_ppb	Cu_ppm	Cpy	Mal	Bor	Py	Desc
110	GRD	15	1540					Masive biotite granodiorite
		60	2130					
115		170	2670					
		15	120					
120								
125								
130								
135								
140								

Scale 1:200	Date: May 03, 2009	Hole Page 4 of 4

BCGold Corp. - Carmacks Project

Hole Name :WS-08-08		Hole Length :292.60		
Collar X :413890.00	Collar Y :6911242.00	Collar Z :855.00	Azm :230	Dip :-50

Depth At	Lithology (txt) LithCode	Assays (txt) Au_ppb	Assays (txt) Cu_ppm	Mineral (txt) Cpy	Mal	Bor	Py	Lithology (txt) Desc
0	OVBN	25 50 75 100 125 150 175	1000 2000 3000 4000 5000 6000 7000 8000 9000					Overburden. Mainly crumbly KMG/GRD with a gradational contact with solid bedrock.
5								
10								Lt grey pink Ksp-megacrystic CGr Qtz-Plag-bio granodiorite. Minor mag. Rare Chl replacing bio. Minor vuggy patches with increased modal bio. Minor aplite & pegmatite felsic dykes (<10cm thick) throughout. Very crumbly with broken patches throughout.
15	KMG							Pink VCGr Qtz-Plag-Ksp dyke with <5% Fgr bio in patches <1cm wide & trace WM.
20	PEG							Lt gy pk Ksp-mcrystic CGr Qtz-Plag-bio GC. Minor mag. Rare Chl replacing bio. Minor aplite & pegmatite felsic dykes (<10cm thick). Very crumbly with broken patches. Flt at lwr contact with 30cm of broken rock & Hm-Chl altrd gouge.
25	KMG							Med grey Mgr granodiorite dyke. Chilled margin at upper contact lower contact faulted. 15% bio minor hb & mag. Minor Hm & Chl staining along fractures.
30	GRD							Lt grey pink Ksp-mcrystic CGr Qtz-Plag-bio GD. Minor mag. Rare Chl replacing bio. Minor aplite & pegmatite felsic dykes (<10cm thick) throughout. Very crumbly with broken patches throughout to ±38m then becoming more competent. Solid & competent from ±45m on.
35	KMG	25 50 75 100 125 150 175	1000 2000 3000 4000 5000 6000 7000 8000 9000					

BCGold Corp. - Carmacks Project

Hole Name :WS-08-08		Hole Length :292.60		
Collar X :413890.00	Collar Y :6911242.00	Collar Z :855.00	Azm :230	Dip :-50

	Lithology (txt)	Assays (txt)		Mineral (txt)				Lithology (txt)
Depth At	LithCode	Au_ppb	Cu_ppm	Cpy	Mal	Bor	Py	Desc

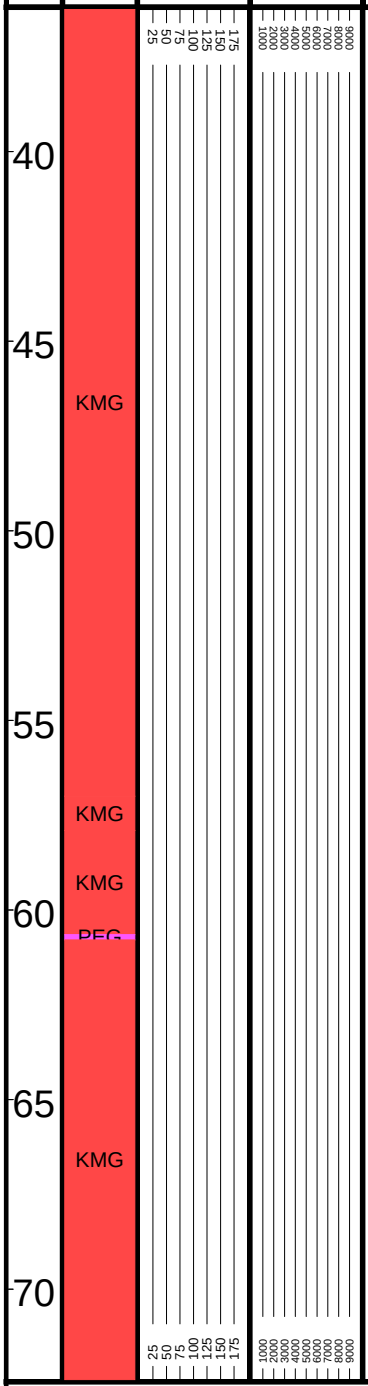

Lt grey pink Ksp-mcrystic CGr Qtz-Plag-bio GD. Minor mag. Rare Chl replacing bio. Minor aplite & pegmatite felsic dykes (<10cm thick) throughout. Very crumbly with broken patches throughout to ±38m then becoming more competent. Solid & competent from ±45m on.

Very leucocratic coarser-grained patch of KMG.

Lt grey pink Ksp-mcrystic CGr Qtz-Plag-bio GD. Minor mag. Rare Chl replacing bio. Minor aplite & pegmatite felsic dykes (<10cm thick) throughout. Very crumbly with broken patches throughout to ±38m then becoming more competent. Solid & competent from ±45m on.

Pink VCGr Qtz-Plag-Ksp dyke with <5% Fgr bio in patches <1cm wide & trace WM.

Lt grey pink Ksp-megacrystic CGr Qtz-Plag-bio granodiorite. Minor mag. Rare Chl replacing bio. Minor vuggy patches with increased modal bio. Minor aplite & pegmatite felsic dykes (<10cm thick) throughout.

BCGold Corp. - Carmacks Project

Hole Name :WS-08-08		Hole Length :292.60		
Collar X :413890.00	Collar Y :6911242.00	Collar Z :855.00	Azm :230	Dip :-50

	Lithology (txt)	Assays (txt)		Mineral (txt)				Lithology (txt)
Depth At	LithCode	Au_ppb	Cu_ppm	Cpy	Mal	Bor	Py	Desc
75	KMG	2	2.78					Lt grey pink Ksp-megacrystic CGr Qtz-Plag-bio granodiorite. Minor mag. Rare Chl replacing bio. Minor vuggy patches with increased modal bio. Minor aplite & pegmatite felsic dykes (<10cm thick) throughout.
80		2	2.6					
85		2	3.4					
90		2	2.98					
95		2	2.79					
100		2	2.98					
105		2	3.05					
		2	3.26					
		2	3.79					
		2	3.25					
		2	2.97					

Scale 1:200	Date: May 03, 2009	Hole Page 3 of 9

BCGold Corp. - Carmacks Project

Hole Name :WS-08-08		Hole Length :292.60		
Collar X :413890.00	Collar Y :6911242.00	Collar Z :855.00	Azm :230	Dip :-50

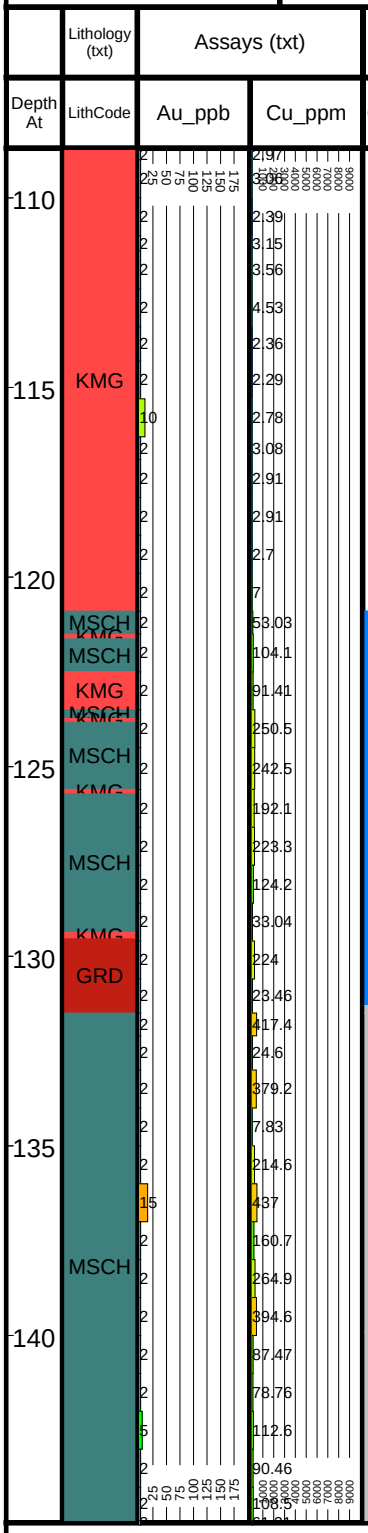

Lithology (txt)

Desc

Lt grey pink Ksp-megacrystic CGr Qtz-Plag-bio granodiorite. Minor mag. Rare Chl replacing bio. Minor vuggy patches with increased modal bio. Minor aplite & pegmatite felsic dykes (<10cm thick) throughout.

foliated bio schist cross cut by mm vnlts of KMG; MSCH (40% Hb; 5% Bio

foliated bio schist; mg to cg; cross cut by mm stgrs of KMG; finer grained at contacts; 10% Qtz; 25-30% Hb;10% bio; 3-5% K-fld; 3% Plag: 3% Mag;

foliated bio schist; mg to cg; cross cut by mm stgrs of KMG; finer grained at contacts; 10% Qtz; 25-30% Hb;10% bio; 3-5% K-fld; 3% Plag: 3% Mag;

well foliated; grey with mm patches of pink alteration halos, 15-20% % qtz; 35% Bio;45-50% Feldspars generally cut by lighter coloured vns. Both units are coarse grained and equigranular; silver coloured platy mineral overprinting bio could be muscovite; 1% py

well-modly foliated; grn with pink hem stained patches; 50% Plag (<2mm); rest is very fine grained mafics (pyx bio and hb?) that have been chloritized; hem staining carb on the fracs along with occasional ep

Scale 1:200	Date: May 03, 2009	Hole Page 4 of 9

BCGold Corp. - Carmacks Project

Hole Name :WS-08-08		Hole Length :292.60		
Collar X :413890.00	Collar Y :6911242.00	Collar Z :855.00	Azm :230	Dip :-50

Depth At	Lithology (txt) LithCode	Assays (txt) Au_ppb	Assays (txt) Cu_ppm	Mineral (txt) Cpy	Mal	Bor	Py	Lithology (txt) Desc
150	MSCH	2	61.34					well-modly foliated; grn with pink hem stained patches; 50% Plag (<2mm); rest is very fine grained mafics (pyx bio and hb?) that have been chloritized; hem staining carb on the fracs along with occasional ep
		5	376					
		2	109.3					
		10	365.2					
		2	115.4					
		2	156.4					
		5	274.1					
		2	166.2					
		2	7.97					
155		2	3.99					
		2	3.49					
		2	3.99					
		2	4.03					
		2	4.97					
160		2	5.05					
		2	3.71					
		2	2.56					
165		2	4.01					
	KMG	2	4.38					40% Qtz; 15% k-fld; 25 % Hb; 15% Bio; 2% Plag; 3% (mag hem); Cg equigranular Hb-bio (alkali) Gr. Subangular K-fld up to 5 cm; 70% of mafics alt to chl. Wk to mod magnetic; sub angular rip up clasts of MSCH within the KMG near the contact
		2	3.28					
		2	4.28					
170								
175								
180								

Scale 1:200	Date: May 03, 2009	Hole Page 5 of 9

BCGold Corp. - Carmacks Project

Hole Name :WS-08-08		Hole Length :292.60		
Collar X :413890.00	Collar Y :6911242.00	Collar Z :855.00	Azm :230	Dip :-50

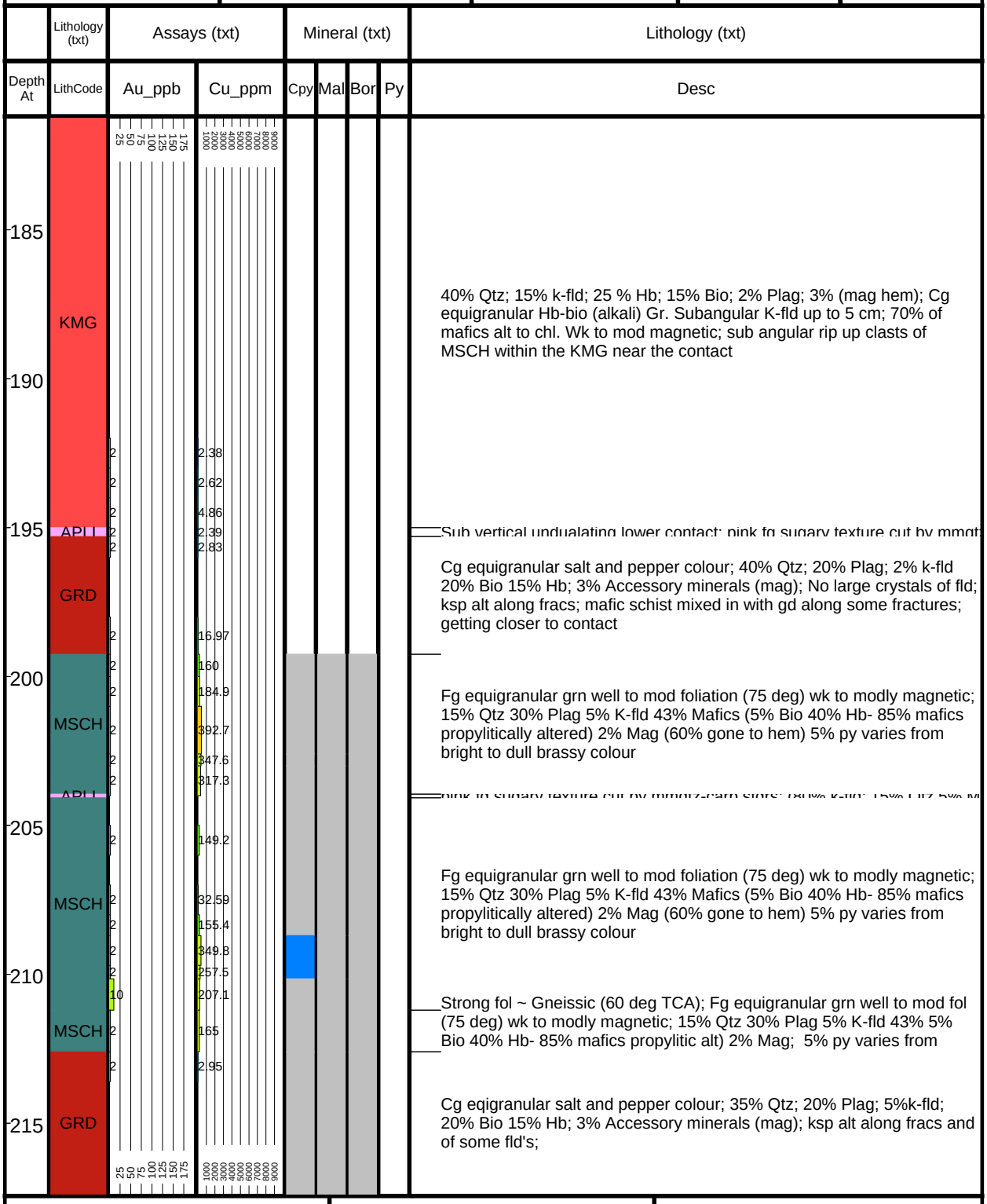

Lithology (txt)

Desc

40% Qtz; 15% k-fld; 25 % Hb; 15% Bio; 2% Plag; 3% (mag hem); Cg equigranular Hb-bio (alkali) Gr. Subangular K-fld up to 5 cm; 70% of mafics alt to chl. Wk to mod magnetic; sub angular rip up clasts of MSCH within the KMG near the contact

Sub vertical undualating lower contact; pink fg sugary texture cut by mmgt

Cg equigranular salt and pepper colour; 40% Qtz; 20% Plag; 2% k-fld 20% Bio 15% Hb; 3% Accessory minerals (mag); No large crystals of fld; ksp alt along fracs; mafic schist mixed in with gd along some fractures; getting closer to contact

Fg equigranular grn well to mod foliation (75 deg) wk to modly magnetic; 15% Qtz 30% Plag 5% K-fld 43% Mafics (5% Bio 40% Hb- 85% mafics propylitically altered) 2% Mag (60% gone to hem) 5% py varies from bright to dull brassy colour

Fg equigranular grn well to mod foliation (75 deg) wk to modly magnetic; 15% Qtz 30% Plag 5% K-fld 43% Mafics (5% Bio 40% Hb- 85% mafics propylitically altered) 2% Mag (60% gone to hem) 5% py varies from bright to dull brassy colour

Strong fol ~ Gneissic (60 deg TCA); Fg equigranular grn well to mod fol (75 deg) wk to modly magnetic; 15% Qtz 30% Plag 5% K-fld 43% 5% Bio 40% Hb- 85% mafics propylitic alt) 2% Mag; 5% py varies from

Cg eqigranular salt and pepper colour; 35% Qtz; 20% Plag; 5%k-fld; 20% Bio 15% Hb; 3% Accessory minerals (mag); ksp alt along fracs and of some fld's;

Scale 1:200	Date: May 03, 2009	Hole Page 6 of 9

BCGold Corp. - Carmacks Project

Hole Name :WS-08-08		Hole Length :292.60		
Collar X :413890.00	Collar Y :6911242.00	Collar Z :855.00	Azm :230	Dip :-50

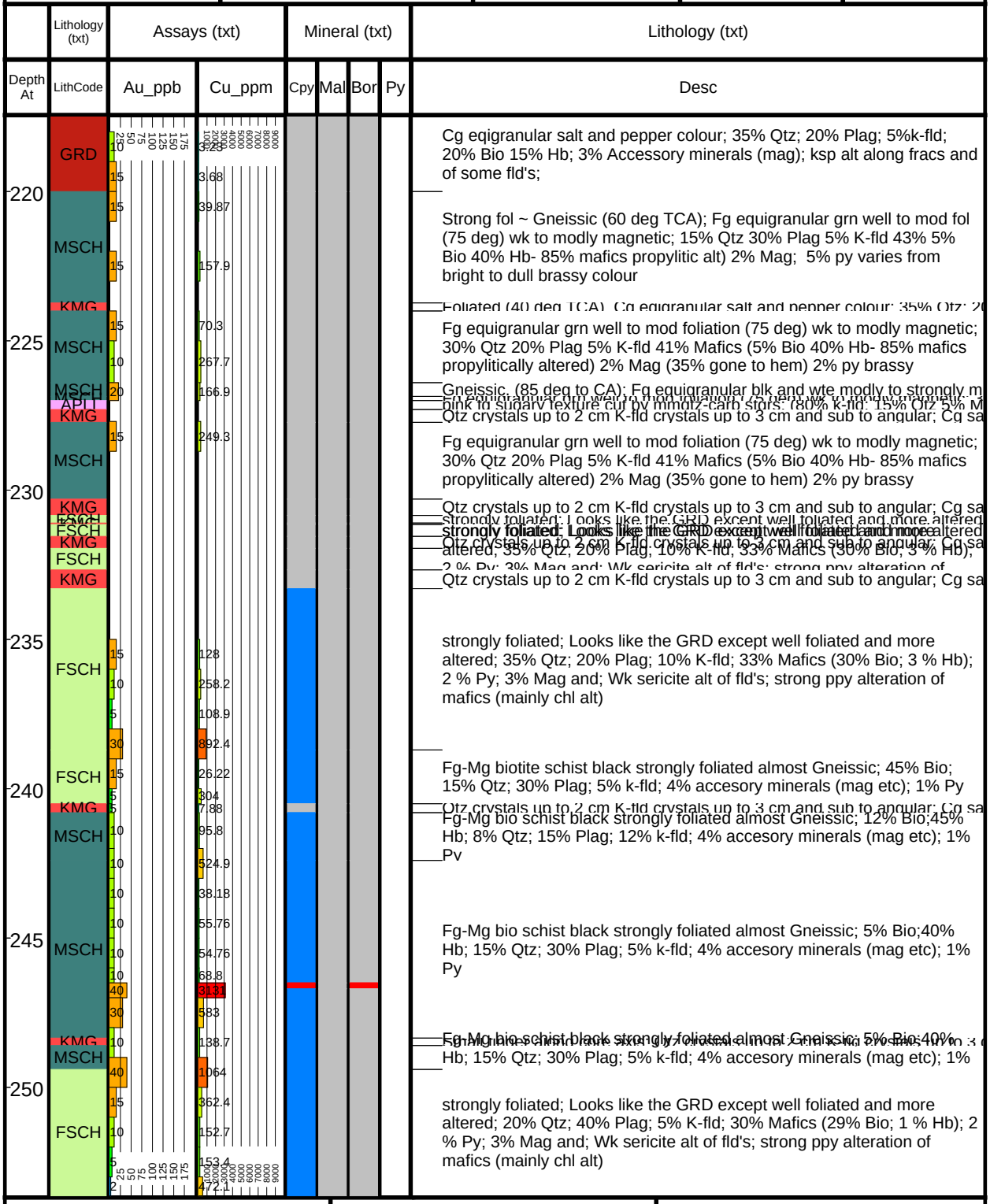

Scale 1:200	Date: May 03, 2009	Hole Page 7 of 9

BCGold Corp. - Carmacks Project

Hole Name :WS-08-08		Hole Length :292.60		
Collar X :413890.00	Collar Y :6911242.00	Collar Z :855.00	Azm :230	Dip :-50

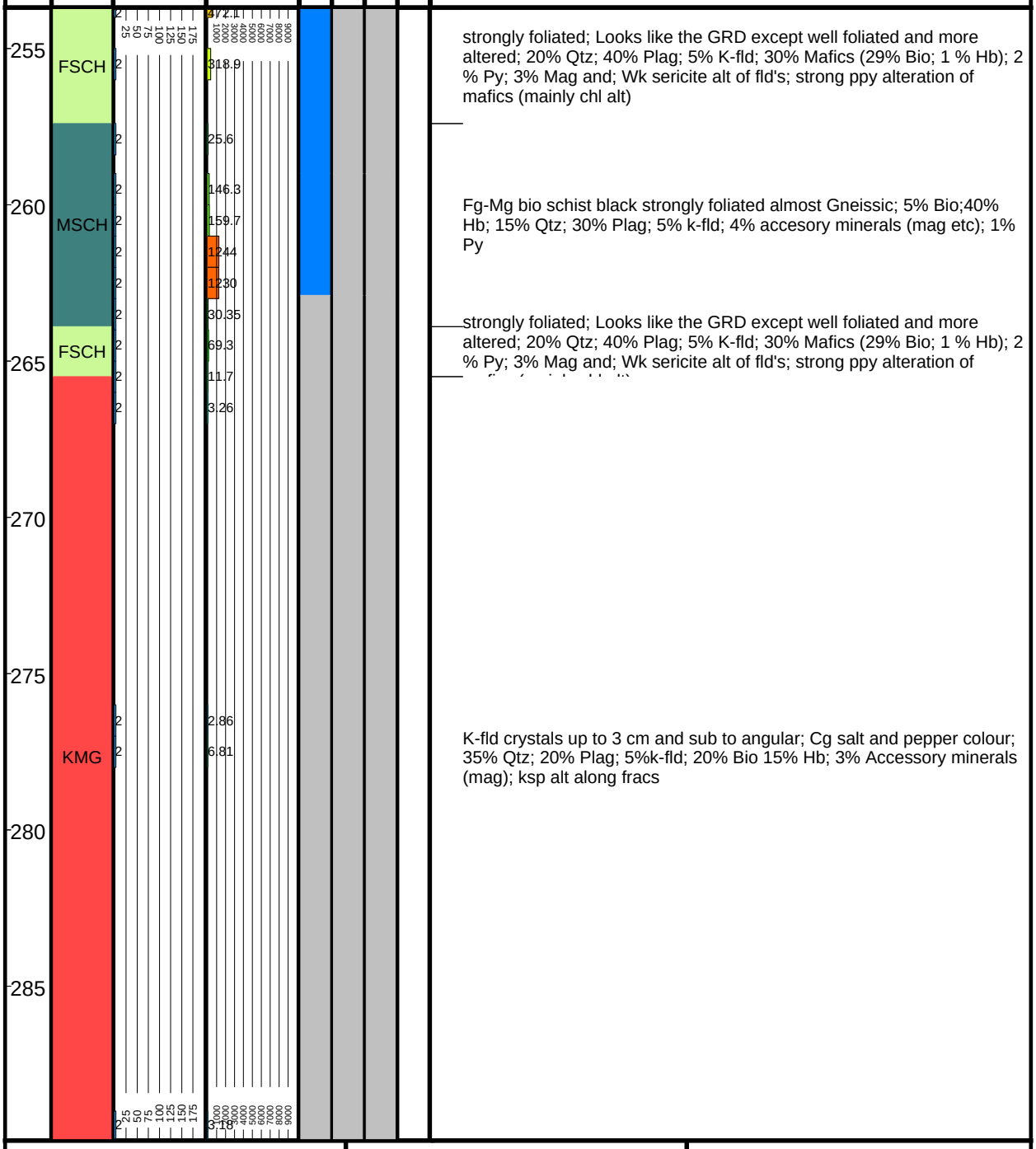

Lithology (txt) — Desc

strongly foliated; Looks like the GRD except well foliated and more altered; 20% Qtz; 40% Plag; 5% K-fld; 30% Mafics (29% Bio; 1 % Hb); 2 % Py; 3% Mag and; Wk sericite alt of fld's; strong ppy alteration of mafics (mainly chl alt)

Fg-Mg bio schist black strongly foliated almost Gneissic; 5% Bio;40% Hb; 15% Qtz; 30% Plag; 5% k-fld; 4% accesory minerals (mag etc); 1% Py

strongly foliated; Looks like the GRD except well foliated and more altered; 20% Qtz; 40% Plag; 5% K-fld; 30% Mafics (29% Bio; 1 % Hb); 2 % Py; 3% Mag and; Wk sericite alt of fld's; strong ppy alteration of

K-fld crystals up to 3 cm and sub to angular; Cg salt and pepper colour; 35% Qtz; 20% Plag; 5%k-fld; 20% Bio 15% Hb; 3% Accessory minerals (mag); ksp alt along fracs

BCGold Corp. - Carmacks Project

Hole Name :WS-08-08		Hole Length :292.60		
Collar X :413890.00	Collar Y :6911242.00	Collar Z :855.00	Azm :230	Dip :-50

	Lithology (txt)	Assays (txt)		Mineral (txt)				Lithology (txt)
Depth At	LithCode	Au_ppb	Cu_ppm	Cpy	Mal	Bor	Py	Desc
	KMG	2	3,31					K-fld crystals up to 3 cm and sub to angular; Cg salt and pepper colour; 35% Qtz; 20% Plag; 5%k-fld; 20% Bio 15% Hb; 3% Accessory minerals (mag); ksp alt along fracs
295								
300								
305								
310								
315								
320								
325								

Scale 1:200	Date: May 03, 2009	Hole Page 9 of 9

BCGold Corp. - Carmacks Project

Hole Name :WS-08-09		Hole Length :33.86		
Collar X :414156.00	Collar Y :6911632.00	Collar Z :850.00	Azm :230	Dip :-50

	Lithology (txt)	Assays (txt)		Mineral (txt)				Lithology (txt)
Depth At	LithCode	Au_ppb	Cu_ppm	Cpy	Mal	Bor	Py	Desc
5	OVBN	25 50 75 100 125 150 175	1000 2000 3000 4000 5000 6000 7000 8000 9000					Overburden. Mainly crumbly KMG/GRD with a gradational contact with solid bedrock.
10								
15								
20	KMG							Lt gy pk Ksp-mcrystic cg Qtz-Plag-bio GD.Minor mag. Rare Chl replacing bio. Minor vuggy patches with increased modal bio.Minor aplite & pegmatite felsic dykes (<10cm thick) throughout.Crumbly & broken @ top of interval;more competent after 9.1m.
25								
30								
35								

Scale 1:200	Date: May 03, 2009	Hole Page 1 of 1

BCGold Corp. - Carmacks Project

Hole Name :WS-08-09A		Hole Length :33.86		
Collar X :414156.00	Collar Y :6911632.00	Collar Z :850.00	Azm :230	Dip :-53

	Lithology (txt)	Assays (txt)		Mineral (txt)				Lithology (txt)
Depth At	LithCode	Au_ppb	Cu_ppm	Cpy	Mal	Bor	Py	Desc
5	OVBN	25 50 75 100 125 150 175	1000 2000 3000 4000 5000 6000 7000 8000 9000					Overburden. Mainly crumbly KMG/GRD with a gradational contact with solid bedrock.
10	KMG							Lt grey pk Ksp-mcrystic.Cg Qtz-Plag-bio GD.Minor mag.Rare Chl replacing bio.Minor vuggy patches with increased modal bio.Minor aplite & pegmatite felsic dykes (<10cm thick) throughout. Core starts to impinge on DDH WS-08-09 hole @ 14.2m.
15								
20								
25								
30								
35								

Scale 1:200	Date: May 03, 2009	Hole Page 1 of 1

BCGold Corp. - Carmacks Project

Hole Name :WS-08-09B		Hole Length :294.13		
Collar X :414156.00	Collar Y :6911632.00	Collar Z :850.00	Azm :230	Dip :-60

Depth At	Lithology (txt) LithCode	Assays (txt) Au_ppb	Assays (txt) Cu_ppm	Mineral (txt) Cpy	Mal	Bor	Py	Lithology (txt) Desc
5	KMG							White and black cg subhederal to euhedral; 10% Qtz; 40% Plag; 25% k-fld; 20% Bio; 3% Musc; 1% Hb; 1% Mag: K-fld grains up to 4 cm
10		2	8.1					
15		2	13.34					
20		2	3.94					Very coarse grained almost pegmatitic; White and black cg equigranular subhederal to euhedral; 10% Qtz; 40% Plag; 25% k-fld; 20% Bio; 3% Musc; 1% Hb; 1% Mag
25	KMG							White and black cg subhederal to euhedral; 10% Qtz; 40% Plag; 25% k-fld; 20% Bio; 3% Musc; 1% Hb; 1% Mag; K-fld grains up to 4cm
30	KMG	2	8.68					White and black cg subhederal to euhedral; 10% Qtz; 40% Plag; 25% k-fld; 20% Bio; 3% Musc; 1% Hb; 1% Mag; K-fld grains up to 4cm
35	KMG							White and black cg equigranular subhederal to euhedral; 10% Qtz; 40% Plag; 25% k-fld; 20% Bio; 3% Musc; 1% Hb; 1% Mag

BCGold Corp. - Carmacks Project

Hole Name :WS-08-09B		Hole Length :294.13		
Collar X :414156.00	Collar Y :6911632.00	Collar Z :850.00	Azm :230	Dip :-60

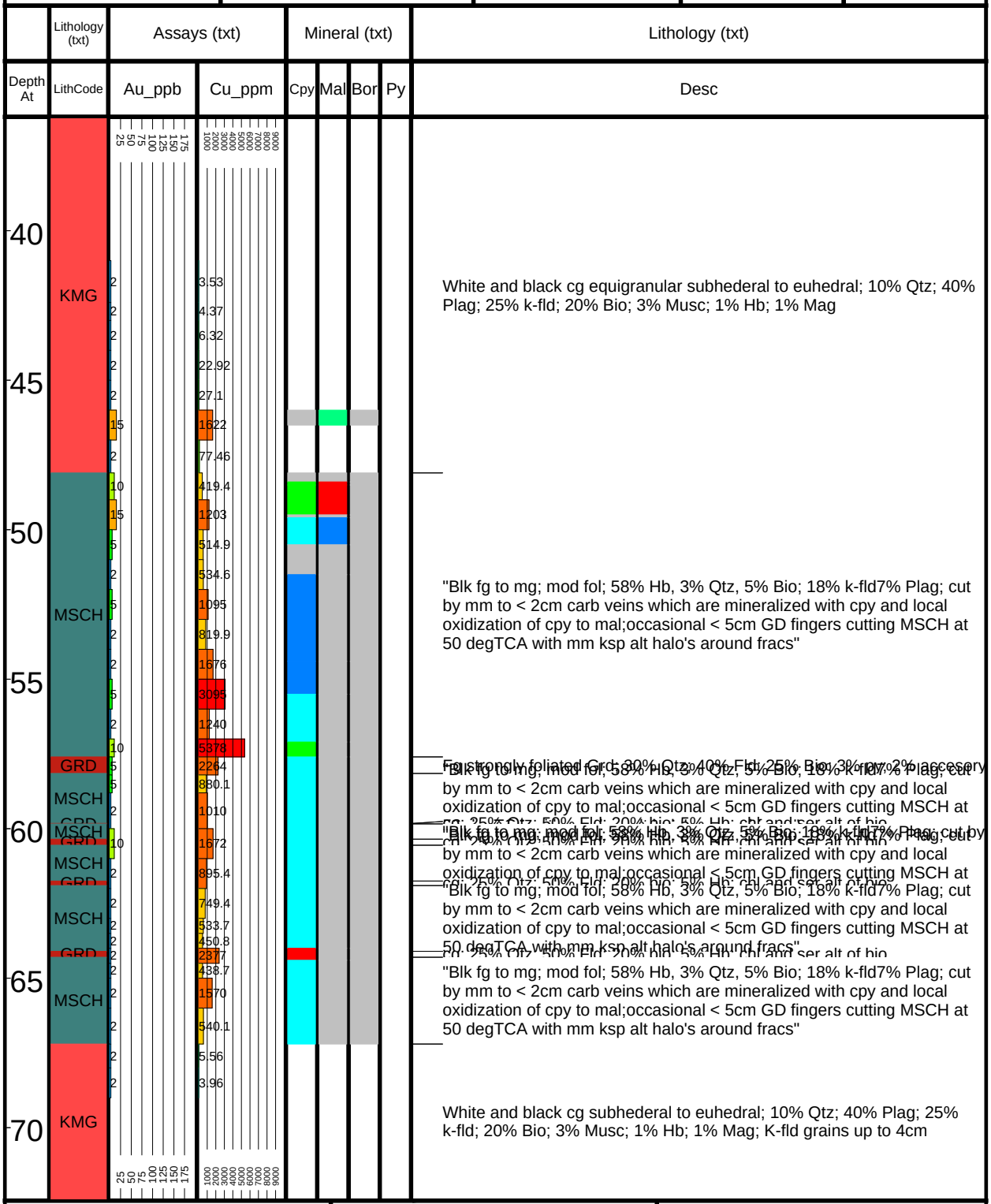

Scale 1:200	Date: May 03, 2009	Hole Page 2 of 9

BCGold Corp. - Carmacks Project

Hole Name :WS-08-09B		Hole Length :294.13		
Collar X :414156.00	Collar Y :6911632.00	Collar Z :850.00	Azm :230	Dip :-60

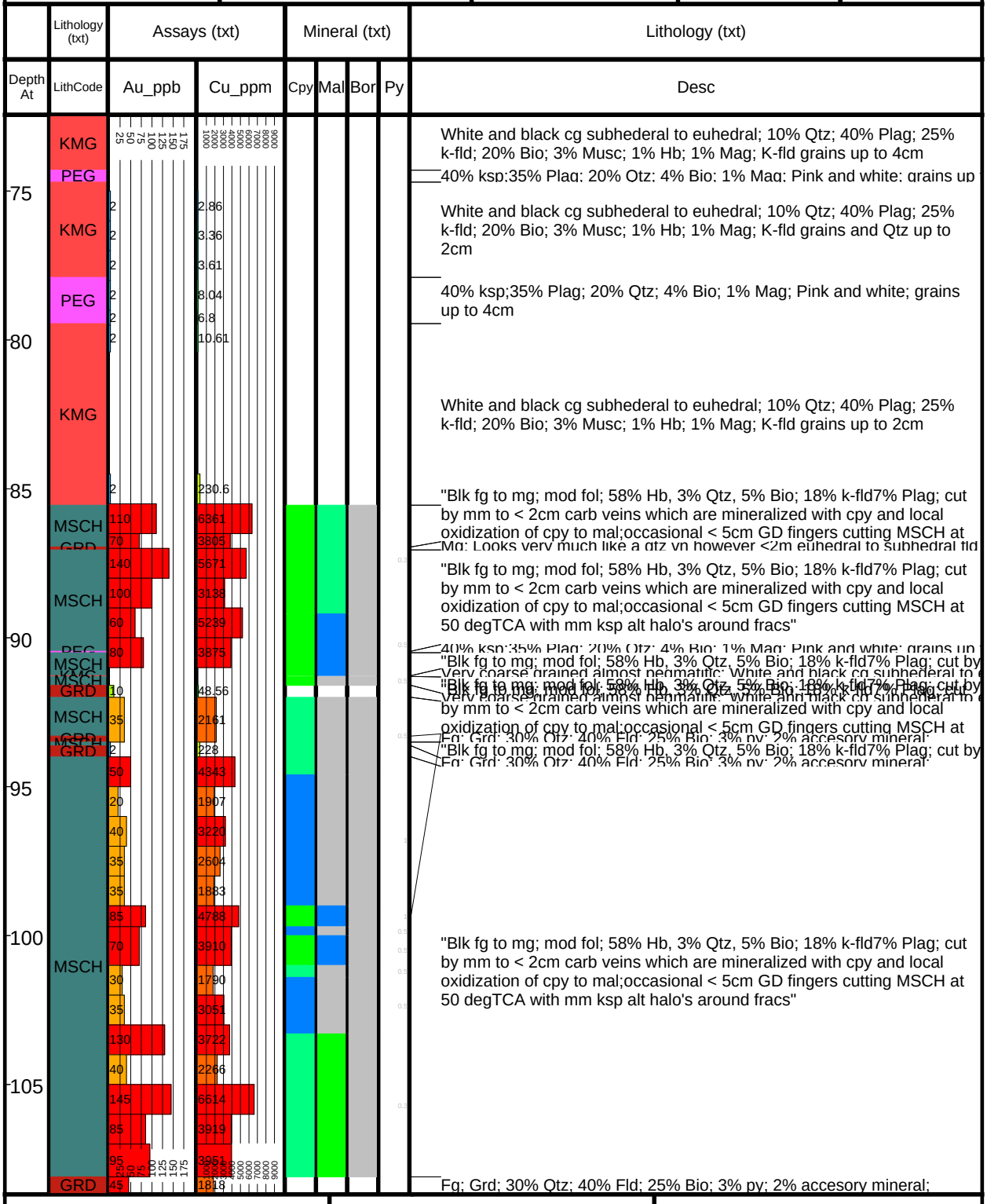

Scale 1:200	Date: May 03, 2009	Hole Page 3 of 9

BCGold Corp. - Carmacks Project

Hole Name :WS-08-09B		Hole Length :294.13		
Collar X :414156.00	Collar Y :6911632.00	Collar Z :850.00	Azm :230	Dip :-60

	Lithology (txt)	Assays (txt)		Mineral (txt)				Lithology (txt)
Depth At	LithCode	Au_ppb	Cu_ppm	Cpy	Mal	Bor	Py	Desc
110	GRD	45 2 2 2 5 5	18 46.69 45.54 69.93 18.52					Fg; Grd; 30% Qtz; 40% Fld; 25% Bio; 3% py; 2% accesory mineral;
115								
120	KMG PEG							White and black cg subhederal to euhedral; 10% Qtz; 40% Plag; 25% k-fld; 20% Bio; 3% Musc; 1% Hb; 1% Mag; K-fld grains up to 4cm 40% ksp;35% Plag; 20% Qtz; 4% Bio; 1% Mag; Pink and white; grains up to 5cm
125								
130								
135	KMG							White and black cg subhederal to euhedral; 10% Qtz; 40% Plag; 25% k-fld; 20% Bio; 3% Musc; 1% Hb; 1% Mag; K-fld grains up to 4cm
140		2	2.89					

BCGold Corp. - Carmacks Project

Hole Name :WS-08-09B		Hole Length :294.13		
Collar X :414156.00	Collar Y :6911632.00	Collar Z :850.00	Azm :230	Dip :-60

	Lithology (txt)	Assays (txt)		Mineral (txt)				Lithology (txt)
Depth At	LithCode	Au_ppb	Cu_ppm	Cpy	Mal	Bor	Py	Desc
150	KMG	5	29					White and black cg subhederal to euhedral; 10% Qtz; 40% Plag; 25% k-fld; 20% Bio; 3% Musc; 1% Hb; 1% Mag; K-fld grains up to 4cm
	PEG							40% ksp;35% Plag; 20% Qtz; 4% Bio; 1% Mag; Pink and white; grains up to 5cm
155	KMG							White and black cg subhederal to euhedral; 10% Qtz; 40% Plag; 25% k-fld; 20% Bio; 3% Musc; 1% Hb; 1% Mag; K-fld grains up to 4cm
	PEG							40% ksp;35% Plag; 20% Qtz; 4% Bio; 1% Mag; Pink and white; grains up to 5cm
160								
165								
170	KMG	2	7121					White and black cg subhederal to euhedral; 10% Qtz; 40% Plag; 25% k-fld; 20% Bio; 3% Musc; 1% Hb; 1% Mag; K-fld grains up to 4cm
		2	3999					
		2	2541					
		2	2391					
		2	2861					
175								
180								

Scale 1:200	Date: May 03, 2009	Hole Page 5 of 9

BCGold Corp. - Carmacks Project

Hole Name :WS-08-09B		Hole Length :294.13		
Collar X :414156.00	Collar Y :6911632.00	Collar Z :850.00	Azm :230	Dip :-60

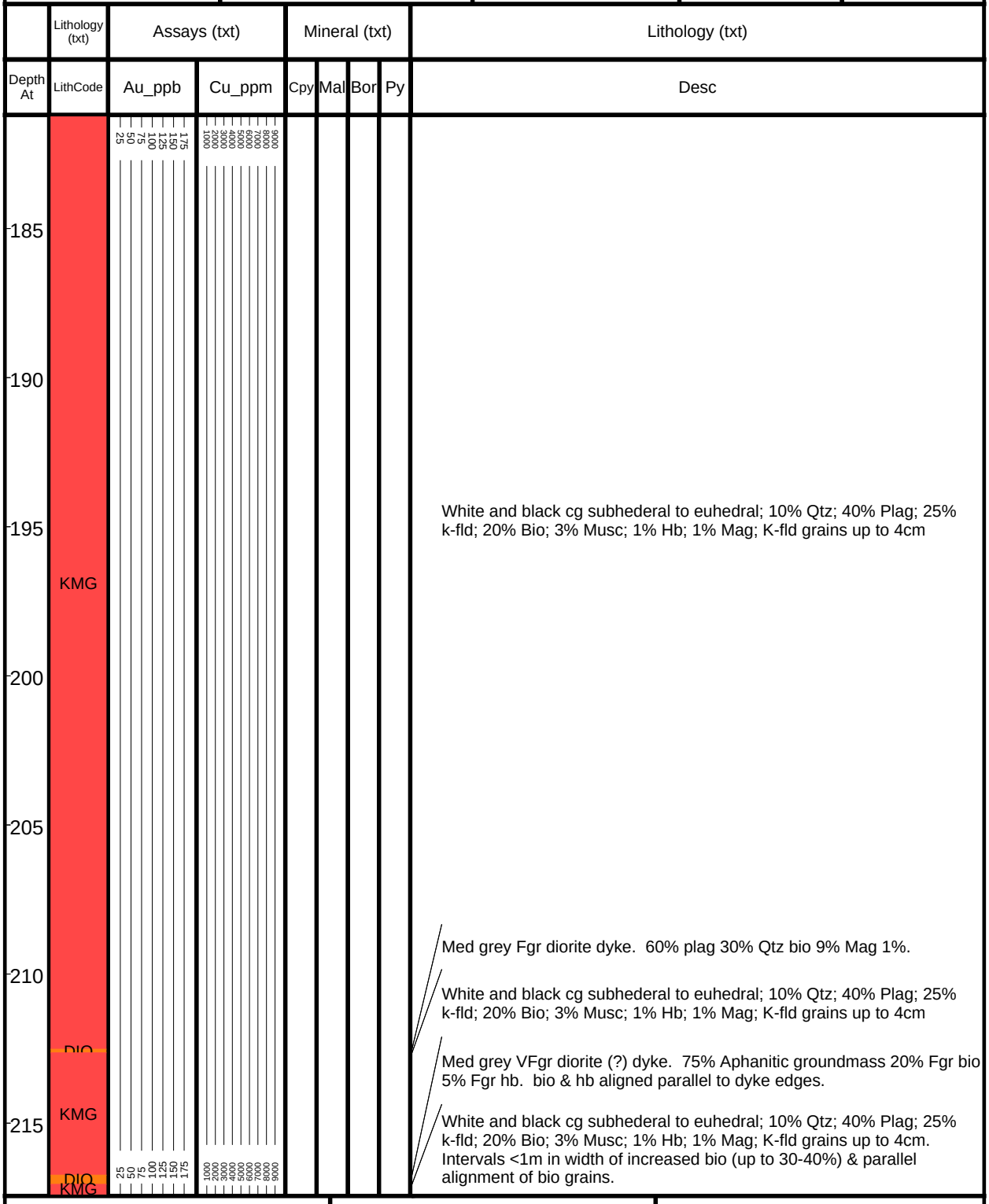

BCGold Corp. - Carmacks Project

Hole Name :WS-08-09B		Hole Length :294.13		
Collar X :414156.00	Collar Y :6911632.00	Collar Z :850.00	Azm :230	Dip :-60

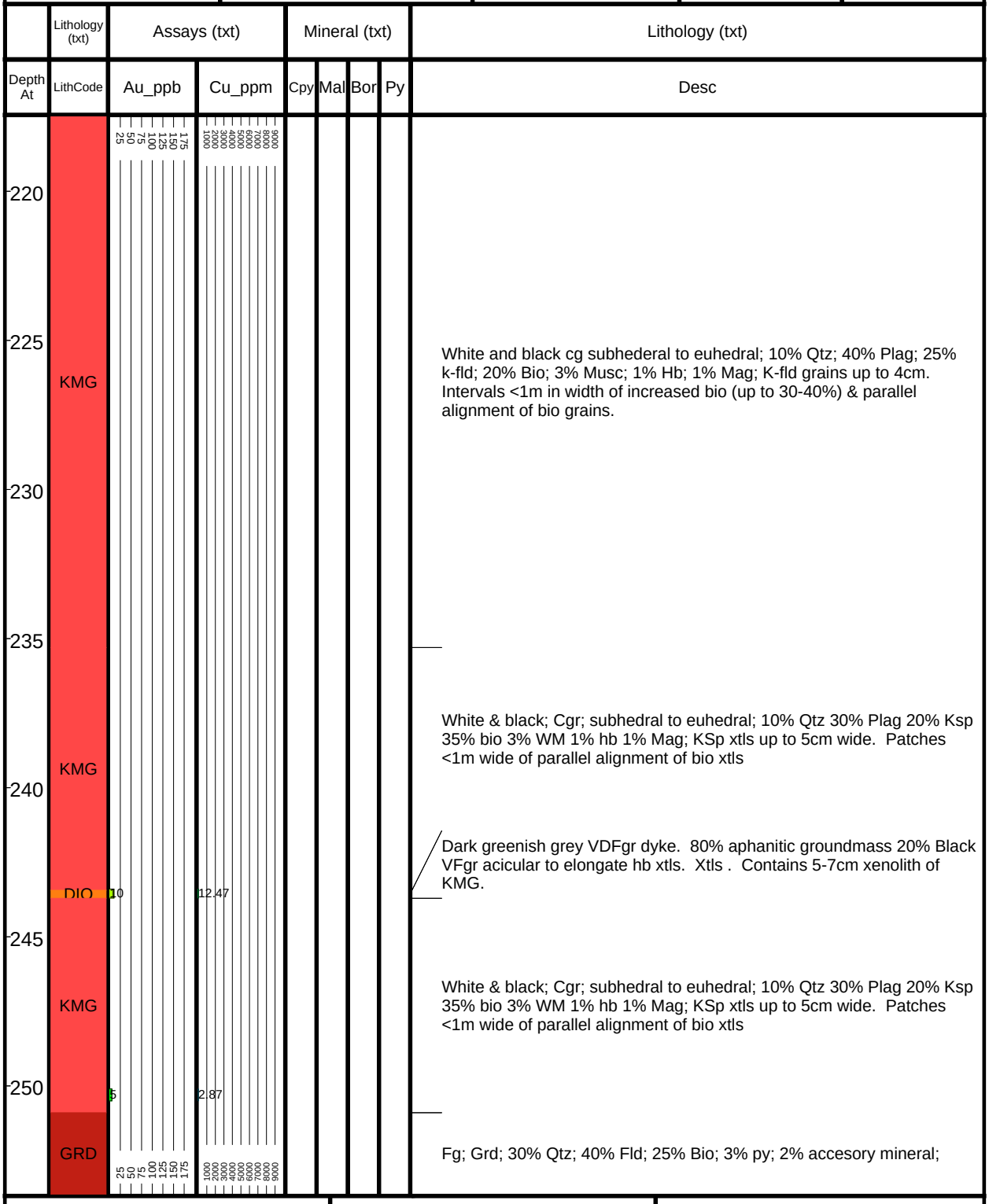

Scale 1:200	Date: May 03, 2009	Hole Page 7 of 9

BCGold Corp. - Carmacks Project

Hole Name :WS-08-09B		Hole Length :294.13		
Collar X :414156.00	Collar Y :6911632.00	Collar Z :850.00	Azm :230	Dip :-60

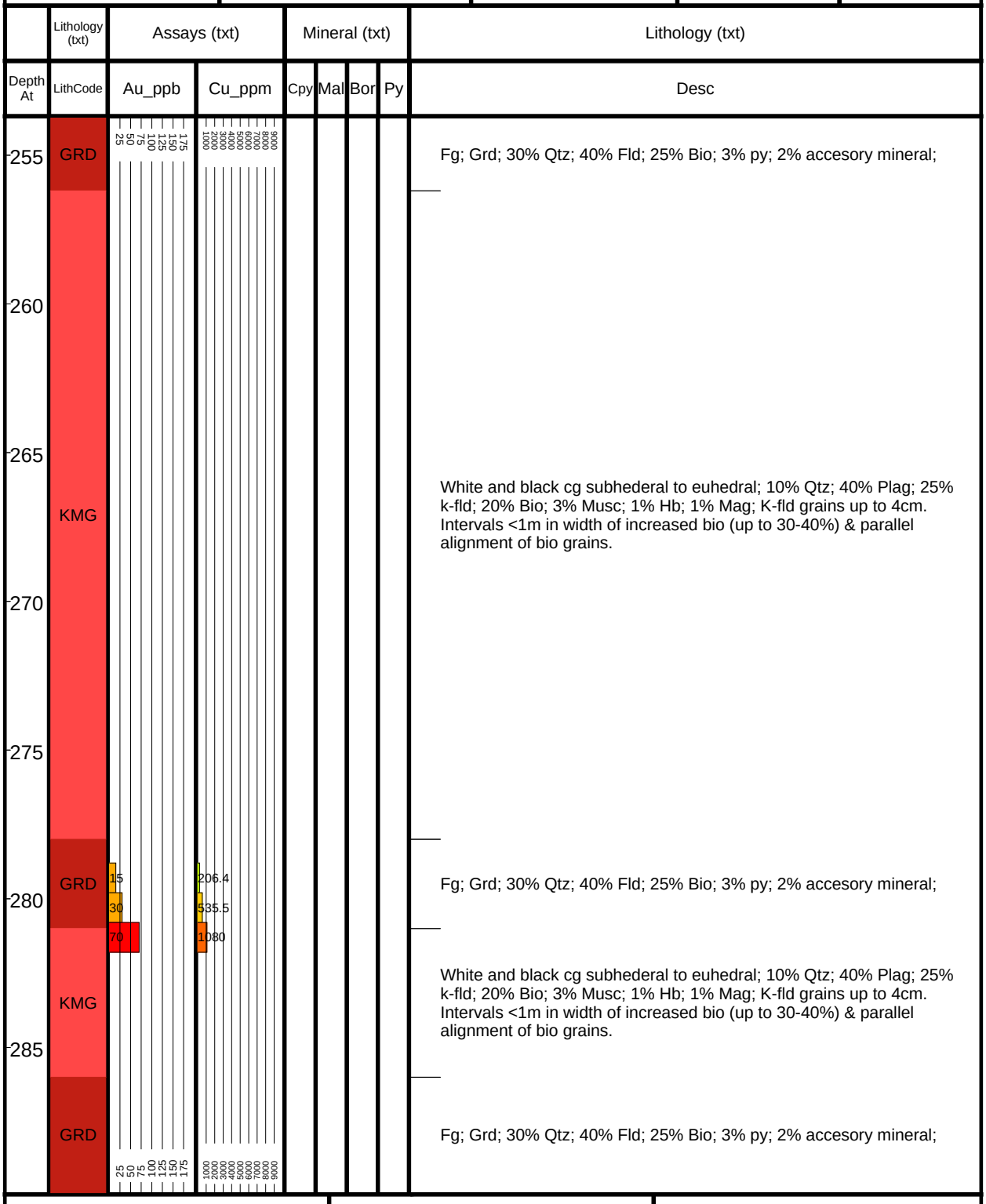

BCGold Corp. - Carmacks Project

Hole Name :WS-08-09B			Hole Length :294.13	
Collar X :414156.00	Collar Y :6911632.00	Collar Z :850.00	Azm :230	Dip :-60

	Lithology (txt)	Assays (txt)		Mineral (txt)				Lithology (txt)
Depth At	LithCode	Au_ppb	Cu_ppm	Cpy	Mal	Bor	Py	Desc
	GRD	25 50 75 100 125 150 175	1000 2000 3000 4000 5000 6000 7000 8000 9000					Fg; Grd; 30% Qtz; 40% Fld; 25% Bio; 3% py; 2% accesory mineral;
295								
300								
305								
310								
315								
320								
325		25 50 75 100 125 150 175	1000 2000 3000 4000 5000 6000 7000 8000 9000					

Scale 1:200	Date: May 03, 2009	Hole Page 9 of 9

BCGold Corp. - Carmacks Project

Hole Name :WS-08-10		Hole Length :224.94		
Collar X :414378.00	Collar Y :6911949.00	Collar Z :892.00	Azm :230	Dip :-60

Depth At	Lithology (txt) LithCode	Assays (txt) Au_ppb	Assays (txt) Cu_ppm	Mineral (txt) Cpy	Mal	Bor	Py	Lithology (txt) Desc
0	OVBN	25 50 75 100 125 150 175	1000 2000 3000 4000 5000 6000 7000 8000 9000					Rubble
5								
10								
15	CLT							Lt gn gy lapilli-tuff. 85%.15% rnded plag-phyric Andt/Bas clasts.GM is coarse ash & gy-gn lapilli.Lithic clasts are subangular to rounded 5-50mm;70% dk gn aphanitic gm 25%;2-5mm elongate wte Plag 5% 1-3mm elongate blk aug/hb.~10% of clasts are Hm-stained
20								
25								Lt gn gy lapilli-tuff. 85%.15% rnded plag-phyric Andt/Bas clasts.GM is coarse ash & gy-gn lapilli.Lithic clasts are subangular to rounded 5-50mm;70% dk gn aphanitic gm 25%;2-5mm elongate wte Plag 5% 1-3mm elongate blk aug/hb.~10% of clasts are Hm-stained
30	CLT							White and black cg subhederal to euhedral; 10% Qtz; 40% Plag; 25% k-fld; 20% Bio; 3% Musc; 1% Hb; 1% Mag; K-fld grains up to 4cm
35	KMG	25 50 75 100 125 150 175	1000 2000 3000 4000 5000 6000 7000 8000 9000					

Scale 1:200	Date: May 03, 2009	Hole Page 1 of 7

BCGold Corp. - Carmacks Project

Hole Name :WS-08-10		Hole Length :224.94		
Collar X :414378.00	Collar Y :6911949.00	Collar Z :892.00	Azm :230	Dip :-60

	Lithology (txt)	Assays (txt)		Mineral (txt)				Lithology (txt)
Depth At	LithCode	Au_ppb	Cu_ppm	Cpy	Mal	Bor	Py	Desc
40	KMG	25 50 75 100 125 150 175	1000 2000 3000 4000 5000 6000 7000 8000 9000					
45								
50								White and black cg subhederal to euhedral; 10% Qtz; 40% Plag; 25% k-fld; 20% Bio; 3% Musc; 1% Hb; 1% Mag; K-fld grains up to 4cm
55								
60								
65								Dk green mafic dyke. 98% dk green aphanitc groundmass 2% randomly-oriented black acicular to elongated Xtls (hb?)
70	CHB KMG	5	20 58					White and black cg subhederal to euhedral; 10% Qtz; 40% Plag; 25% k-fld; 20% Bio; 3% Musc; 1% Hb; 1% Mag; K-fld grains up to 4cm

BCGold Corp. - Carmacks Project

Hole Name :WS-08-10		Hole Length :224.94		
Collar X :414378.00	Collar Y :6911949.00	Collar Z :892.00	Azm :230	Dip :-60

	Lithology (txt)	Assays (txt)		Mineral (txt)				Lithology (txt)
Depth At	LithCode	Au_ppb	Cu_ppm	Cpy	Mal	Bor	Py	Desc
75	KMG	5	3.23					White and black cg subhederal to euhedral; 10% Qtz; 40% Plag; 25% k-fld; 20% Bio; 3% Musc; 1% Hb; 1% Mag; K-fld grains up to 4cm
80		10	2.84					
		5	2.77					
		40	2.71					
85		20	2.82					
		15	3.21					
90								
95								
100								
105								

Scale 1:200	Date: May 03, 2009	Hole Page 3 of 7

BCGold Corp. - Carmacks Project

Hole Name :WS-08-10		Hole Length :224.94		
Collar X :414378.00	Collar Y :6911949.00	Collar Z :892.00	Azm :230	Dip :-60

	Lithology (txt)	Assays (txt)		Mineral (txt)				Lithology (txt)
Depth At	LithCode	Au_ppb	Cu_ppm	Cpy	Mal	Bor	Py	Desc
110	KMG	25 50 75 100 125 150 175	1000 2000 3000 4000 5000 6000 7000 8000 9000					White and black cg subhederal to euhedral; 10% Qtz; 40% Plag; 25% k-fld; 20% Bio; 3% Musc; 1% Hb; 1% Mag; K-fld grains up to 4cm
115								
120								
125								
130								
135								
140								

BCGold Corp. - Carmacks Project

Hole Name :WS-08-10		Hole Length :224.94		
Collar X :414378.00	Collar Y :6911949.00	Collar Z :892.00	Azm :230	Dip :-60

	Lithology (txt)	Assays (txt)		Mineral (txt)				Lithology (txt)
Depth At	LithCode	Au_ppb	Cu_ppm	Cpy	Mal	Bor	Py	Desc
150	KMG	5	1.81					White and black cg subhederal to euhedral; 10% Qtz; 40% Plag; 25% k-fld; 20% Bio; 3% Musc; 1% Hb; 1% Mag; K-fld grains up to 4cm
		5	2.55					
		5	4.22					
155								
160								
165								
170								
175								
180								

BCGold Corp. - Carmacks Project

Hole Name :WS-08-10		Hole Length :224.94		
Collar X :414378.00	Collar Y :6911949.00	Collar Z :892.00	Azm :230	Dip :-60

Depth At	Lithology (txt) LithCode	Assays (txt) Au_ppb	Assays (txt) Cu_ppm	Mineral (txt) Cpy	Mal	Bor	Py	Lithology (txt) Desc
185	KMG	25 50 75 100 125 150 175	1000 2000 3000 4000 5000 6000 7000 8000 9000					
190								White and black cg subhederal to euhedral; 10% Qtz; 40% Plag; 25% k-fld; 20% Bio; 3% Musc; 1% Hb; 1% Mag; K-fld grains up to 4cm
195								
200	PEG							40% ksp;35% Plag; 20% Qtz; 4% Bio; 1% Mag; Pink and white; grains up to 4cm
205								
210	KMG							White and black cg subhederal to euhedral; 10% Qtz; 40% Plag; 25% k-fld; 20% Bio; 3% Musc; 1% Hb; 1% Mag; K-fld grains up to 4cm
215								

BCGold Corp. - Carmacks Project

Hole Name :WS-08-10		Hole Length :224.94		
Collar X :414378.00	Collar Y :6911949.00	Collar Z :892.00	Azm :230	Dip :-60

	Lithology (txt)	Assays (txt)		Mineral (txt)				Lithology (txt)
Depth At	LithCode	Au_ppb	Cu_ppm	Cpy	Mal	Bor	Py	Desc
220	KMG	25 50 75 100 125 150 175	1000 2000 3000 4000 5000 6000 7000 8000 9000					White and black cg subhederal to euhedral; 10% Qtz; 40% Plag; 25% k-fld; 20% Bio; 3% Musc; 1% Hb; 1% Mag; K-fld grains up to 4cm
225								
230								
235								
240								
245								
250								

Scale 1:200	Date: May 03, 2009	Hole Page 7 of 7

BCGold Corp. - Carmacks Project

Hole Name :WS-08-11		Hole Length :188.98		
Collar X :413419.00	Collar Y :6910982.00	Collar Z :921.00	Azm :50	Dip :-50

Depth At	Lithology (txt) LithCode	Assays (txt) Au_ppb	Assays (txt) Cu_ppm	Mineral (txt) Cpy	Mal	Bor	Py	Lithology (txt) Desc
0	OVBN							No recovery
0	KMG							White and black cg subhederal to euhedral; 10% Qtz; 40% Plag; 25% k-fld; 20% Bio; 3% Musc; 1% Hb; 1% Mag; K-fld grains up to 4cm
15	KMG							White and black cg subhederal to euhedral; 10% Qtz; 40% Plag; 25% k-fld; 20% Bio; 3% Musc; 1% Hb; 1% Mag; K-fld grains up to 2cm
25	CHB	10	2.65					Dk green mafic dyke. 98% dk green aphanitc groundmass 2% randomly-oriented black acicular to elongated Xtls (hb?)
25	CHB	5	41.12					
25	CHB	5	37.97					
25	CHB	10	2.62					
30	KMG							White and black cg subhederal to euhedral; 10% Qtz; 40% Plag; 25% k-fld; 20% Bio; 3% Musc; 1% Hb; 1% Mag; K-fld grains up to 4cm

BCGold Corp. - Carmacks Project

Hole Name :WS-08-11		Hole Length :188.98		
Collar X :413419.00	Collar Y :6910982.00	Collar Z :921.00	Azm :50	Dip :-50

	Lithology (txt)	Assays (txt)		Mineral (txt)				Lithology (txt)
Depth At	LithCode	Au_ppb	Cu_ppm	Cpy	Mal	Bor	Py	Desc
40	KMG	25 50 75 100 125 150 175	1000 2000 3000 4000 5000 6000 7000 8000 9000					White and black cg subhederal to euhedral; 10% Qtz; 40% Plag; 25% k-fld; 20% Bio; 3% Musc; 1% Hb; 1% Mag; K-fld grains up to 4cm
45								
50								
55								
60								
65								
70								

BCGold Corp. - Carmacks Project

Hole Name :WS-08-11		Hole Length :188.98		
Collar X :413419.00	Collar Y :6910982.00	Collar Z :921.00	Azm :50	Dip :-50

	Lithology (txt)	Assays (txt)		Mineral (txt)				Lithology (txt)
Depth At	LithCode	Au_ppb	Cu_ppm	Cpy	Mal	Bor	Py	Desc
75	KMG	25 50 75 100 125 150 175	1000 2000 3000 4000 5000 6000 7000 8000 9000					White and black cg subhederal to euhedral; 10% Qtz; 40% Plag; 25% k-fld; 20% Bio; 3% Musc; 1% Hb; 1% Mag; K-fld grains up to 4cm
80								
85								
90								
95								
100	PEG							40% ksp;35% Plag; 20% Qtz; 4% Bio; 1% Mag; Pink and white; grains up to 4cm
	KMG							White and black cg subhederal to euhedral; 10% Qtz; 40% Plag; 25% k-fld; 20% Bio; 3% Musc; 1% Hb; 1% Mag; K-fld grains up to 4cm
	PEG							40% ksp;35% Plag; 20% Qtz; 4% Bio; 1% Mag; Pink and white; grains up to 4cm
105	KMG							White and black cg subhederal to euhedral; 10% Qtz; 40% Plag; 25% k-fld; 20% Bio; 3% Musc; 1% Hb; 1% Mag; K-fld grains up to 4cm

BCGold Corp. - Carmacks Project

Hole Name :WS-08-11		Hole Length :188.98		
Collar X :413419.00	Collar Y :6910982.00	Collar Z :921.00	Azm :50	Dip :-50

	Lithology (txt)	Assays (txt)		Mineral (txt)				Lithology (txt)
Depth At	LithCode	Au_ppb	Cu_ppm	Cpy	Mal	Bor	Py	Desc
110	KMG	25 50 75 100 125 150 175	1000 2000 3000 4000 5000 6000 7000 8000 9000					White and black cg subhederal to euhedral; 10% Qtz; 40% Plag; 25% k-fld; 20% Bio; 3% Musc; 1% Hb; 1% Mag; K-fld grains up to 4cm
115								
120								
125								
130								
135								
140								

BCGold Corp. - Carmacks Project

Hole Name :WS-08-11		Hole Length :188.98		
Collar X :413419.00	Collar Y :6910982.00	Collar Z :921.00	Azm :50	Dip :-50

	Lithology (txt)	Assays (txt)		Mineral (txt)				Lithology (txt)
Depth At	LithCode	Au_ppb	Cu_ppm	Cpy	Mal	Bor	Py	Desc
150	KMG	25 50 75 100 125 150 175	1000 2000 3000 4000 5000 6000 7000 8000 9000					White and black cg subhederal to euhedral; 10% Qtz; 40% Plag; 25% k-fld; 20% Bio; 3% Musc; 1% Hb; 1% Mag; K-fld grains up to 4cm
155								
160								
165								
170								
175								
180								

BCGold Corp. - Carmacks Project

Hole Name :WS-08-11		Hole Length :188.98		
Collar X :413419.00	Collar Y :6910982.00	Collar Z :921.00	Azm :50	Dip :-50

	Lithology (txt)	Assays (txt)		Mineral (txt)				Lithology (txt)
Depth At	LithCode	Au_ppb	Cu_ppm	Cpy	Mal	Bor	Py	Desc
185	KMG	25 50 75 100 125 150 175	1000 2000 3000 4000 5000 6000 7000 8000 9000					White and black cg subhederal to euhedral; 10% Qtz; 40% Plag; 25% k-fld; 20% Bio; 3% Musc; 1% Hb; 1% Mag; K-fld grains up to 4cm
190								
195								
200								
205								
210								
215								

Scale 1:200	Date: May 03, 2009	Hole Page 6 of 6

BCGold Corp. - Carmacks Project

Hole Name :WS-08-12		Hole Length :231.04		
Collar X :413174.00	Collar Y :6910768.00	Collar Z :952.00	Azm :50	Dip :-50

	Lithology (txt)	Assays (txt)		Mineral (txt)				Lithology (txt)
Depth At	LithCode	Au_ppb	Cu_ppm	Cpy	Mal	Bor	Py	Desc
0	OVBN	25 50 75 100 125 150 175	1000 2000 3000 4000 5000 6000 7000 8000 9000					Rubble
5								
10								
15								
20	KMG							40% Qtz; 15% k-fld; 25 % Hb; 15% Bio; 2% Plag; 3%; Cg equigranular Hb-bio (alkali) granite. Subangular K-fld up to 5 cm; 20% of mafics altered to chl. Sub angular rip up clasts of MSCH within the KMG near the contact
25								
30								
35		25 50 75 100 125 150 175	1000 2000 3000 4000 5000 6000 7000 8000 9000					

BCGold Corp. - Carmacks Project

Hole Name :WS-08-12		Hole Length :231.04		
Collar X :413174.00	Collar Y :6910768.00	Collar Z :952.00	Azm :50	Dip :-50

Depth At	Lithology (txt) LithCode	Assays (txt) Au_ppb	Assays (txt) Cu_ppm	Mineral (txt) Cpy	Mal	Bor	Py	Lithology (txt) Desc
40	KMG	25 50 75 100 125 150 175	1000 2000 3000 4000 5000 6000 7000 8000 9000					40% Qtz; 15% k-fld; 25 % Hb; 15% Bio; 2% Plag; 3%; Cg equigranular Hb-bio (alkali) granite. Subangular K-fld up to 5 cm; 20% of mafics altered to chl. Sub angular rip up clasts of MSCH within the KMG near the contact
45	KMG							Pink VFgr sugary texture. bio aligned parallel to dyke margins & often chloritized
50	KMG							40% Qtz; 15% k-fld; 25 % Hb; 15% Bio; 2% Plag; 3%; Cg equigranular Hb-bio (alkali) granite. Subangular K-fld up to 5 cm; 20% of mafics altered to chl. Sub angular rip up clasts of MSCH within the KMG near the contact
55	PEG KMG							Pink VCGr Qtz-Plag-Ksp dyke with <5% Fgr bio in patches <1cm wide & trace WM.
60	APLI KMG							40% Qtz; 15% k-fld; 25 % Hb; 15% Bio; 2% Plag; 3%; Cg equigranular Hb-bio (alkali) granite. Subangular K-fld up to 5 cm; 20% of mafics altered to chl. Sub angular rip up clasts of MSCH within the KMG near the contact
65	KMG							Pink VFgr sugary texture. bio aligned parallel to dyke margins & often chloritized
70	KMG							40% Qtz; 15% k-fld; 25 % Hb; 15% Bio; 2% Plag; 3%; Cg equigranular Hb-bio (alkali) granite. Subangular K-fld up to 5 cm; 20% of mafics altered to chl. Sub angular rip up clasts of MSCH within the KMG near the contact

BCGold Corp. - Carmacks Project

Hole Name :WS-08-12		Hole Length :231.04		
Collar X :413174.00	Collar Y :6910768.00	Collar Z :952.00	Azm :50	Dip :-50

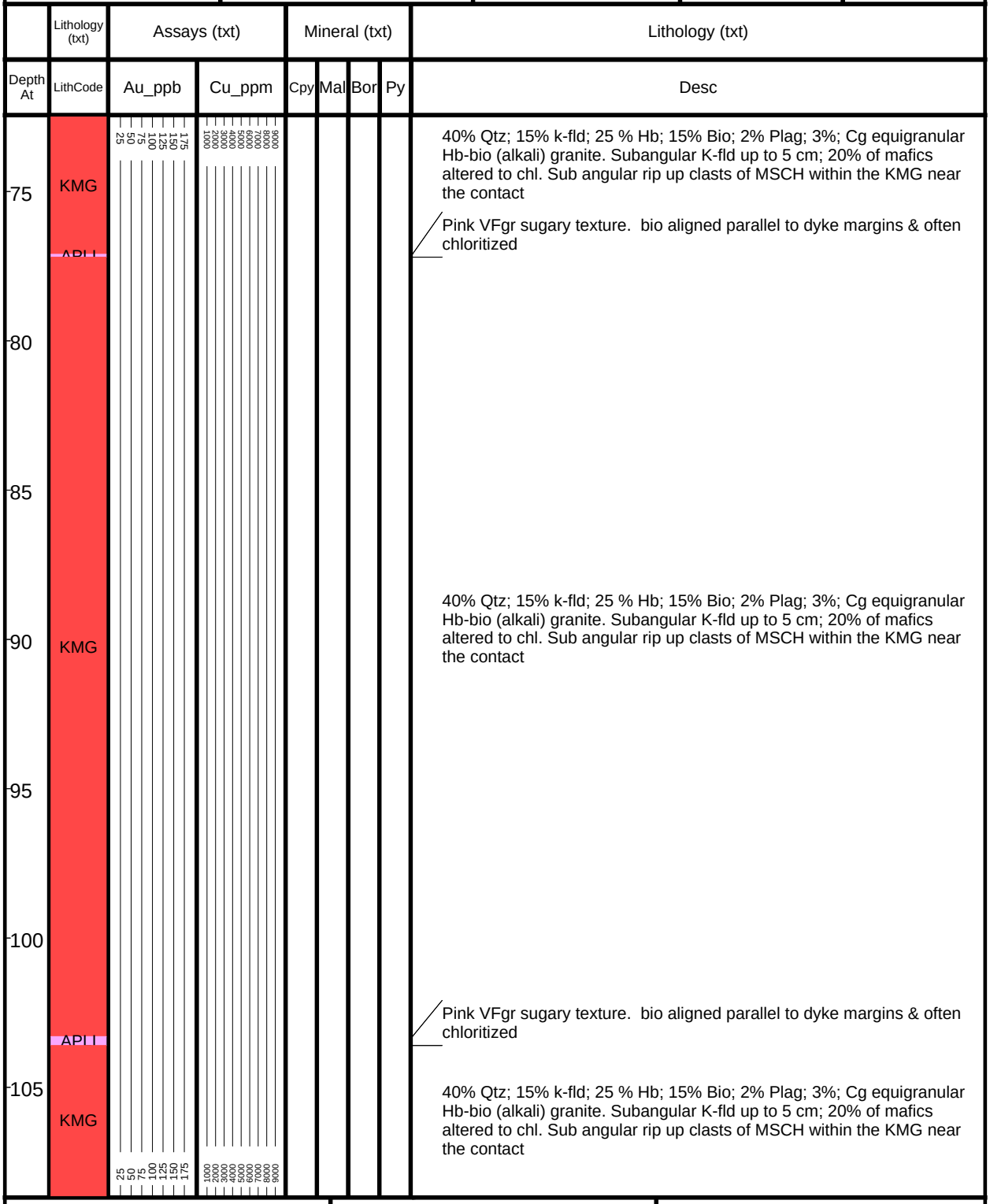

Scale 1:200	Date: May 03, 2009	Hole Page 3 of 7

BCGold Corp. - Carmacks Project

Hole Name :WS-08-12		Hole Length :231.04		
Collar X :413174.00	Collar Y :6910768.00	Collar Z :952.00	Azm :50	Dip :-50

	Lithology (txt)	Assays (txt)		Mineral (txt)				Lithology (txt)
Depth At	LithCode	Au_ppb	Cu_ppm	Cpy	Mal	Bor	Py	Desc
110	KMG	25 50 75 100 125 150 175	1000 2000 3000 4000 5000 6000 7000 8000 9000					40% Qtz; 15% k-fld; 25 % Hb; 15% Bio; 2% Plag; 3%; Cg equigranular Hb-bio (alkali) granite. Subangular K-fld up to 5 cm; 20% of mafics altered to chl. Sub angular rip up clasts of MSCH within the KMG near the contact
115								
120								
125								
130								
135								
140								

BCGold Corp. - Carmacks Project

Hole Name :WS-08-12		Hole Length :231.04		
Collar X :413174.00	Collar Y :6910768.00	Collar Z :952.00	Azm :50	Dip :-50

	Lithology (txt)	Assays (txt)		Mineral (txt)				Lithology (txt)
Depth At	LithCode	Au_ppb	Cu_ppm	Cpy	Mal	Bor	Py	Desc
150	KMG							40% Qtz; 15% k-fld; 25 % Hb; 15% Bio; 2% Plag; 3%; Cg equigranular Hb-bio (alkali) granite. Subangular K-fld up to 5 cm; 20% of mafics altered to chl. Sub angular rip up clasts of MSCH within the KMG near the contact
155								
160								
165	FSCH							Sharp contacts: KMG immediately above & below FSCH is unfoliated no gradual increase. FSCH is strongly foliated; Looks like the GRD except well foliated and more altered; 35% Qtz; 20% Plag; 10% K-fld; 33% Mafics (30% Bio; 3 % Hb); 2 % Py; 3% Mag
170	KMG							40% Qtz; 15% k-fld; 25 % Hb; 15% Bio; 2% Plag; 3%; Cg equigranular Hb-bio (alkali) granite. Subangular K-fld up to 5 cm; 20% of mafics altered to chl. Sub angular rip up clasts of MSCH within the KMG near the contact
175								
180								

BCGold Corp. - Carmacks Project

Hole Name :WS-08-12		Hole Length :231.04		
Collar X :413174.00	Collar Y :6910768.00	Collar Z :952.00	Azm :50	Dip :-50

	Lithology (txt)	Assays (txt)		Mineral (txt)				Lithology (txt)
Depth At	LithCode	Au_ppb	Cu_ppm	Cpy	Mal	Bor	Py	Desc
185	KMG	25 50 75 100 125 150 175	1000 2000 3000 4000 5000 6000 7000 8000 9000					40% Qtz; 15% k-fld; 25 % Hb; 15% Bio; 2% Plag; 3%; Cg equigranular Hb-bio (alkali) granite. Subangular K-fld up to 5 cm; 20% of mafics altered to chl. Sub angular rip up clasts of MSCH within the KMG near the contact
190								
195								
200								
205								
210								
215	APLI	25 50 75 100 125 150 175	1000 2000 3000 4000 5000 6000 7000 8000 9000					Pink VFgr sugary texture. bio aligned parallel to dyke margins & often chloritized

BCGold Corp. - Carmacks Project

Hole Name :WS-08-12		Hole Length :231.04		
Collar X :413174.00	Collar Y :6910768.00	Collar Z :952.00	Azm :50	Dip :-50

	Lithology (txt)	Assays (txt)		Mineral (txt)				Lithology (txt)
Depth At	LithCode	Au_ppb	Cu_ppm	Cpy	Mal	Bor	Py	Desc
220	APLI	25 50 75 100 125 150 175	1000 2000 3000 4000 5000 6000 7000 8000 9000					Pink VFgr sugary texture. bio aligned parallel to dyke margins & often chloritized
225	KMG							40% Qtz; 15% k-fld; 25 % Hb; 15% Bio; 2% Plag; 3%; Cg equigranular Hb-bio (alkali) granite. Subangular K-fld up to 5 cm; 20% of mafics altered to chl. Sub angular rip up clasts of MSCH within the KMG near the contact
230								
235								
240								
245								
250								